Improving the detection and estimation of birds’ collision risk with energy infrastructure using new and emerging tracking technologies

A thesis submitted in fulfilment of the requirements of the University of East Anglia,
for the award of Doctor of Philosophy

Jethro George Gauld

December 2022

Student Number: 100247442

DECLARATION

I hereby declare that the work presented in this thesis has not been submitted for any other degree or professional qualification, and that it is the result of my own independent work.

Word count of main manuscript including all tables, captions, figures, and references: 75,976

Jethro George Gauld

December 2022

ABSTRACT

The dual crises of biodiversity loss and climate change require swift action to protect ecosystems and transition away from fossil fuels. Halting climate change will require global wind energy generation capacity to more than quadruple compared to 2021. Expanding renewable energy will also require significant investment in transmission power lines. European bird populations have declined by approximately 600 million individuals since 1980, it is vital that the clean energy expansion does not further exacerbate this. Migratory soaring birds are among the most susceptible to collision mortality associated with renewable energy infrastructure. Conservation of these species in the context of the expansion of renewable energy requires assessment of collision risks across the whole flyway. This thesis focuses on how data from new and emerging satellite tracking technologies can help better understand where and when birds are most at risk of collision.

Analysing tracking data sets representing over 1,400 individual birds, identified collision risk hotspots within Europe and North Africa. Many of the hotspots identified were within migratory bottleneck regions where mitigation to reduce collision risks could have conservation benefits across the flyway. For both soaring and flapping species environmental variables such as thermal uplift were found to accurately predict how likely birds were to fly at heights where they risk collision with energy infrastructure. This research showed tracking data can inform estimates of sensitivity to collision risks for areas which are not, at present, well represented in the tracking data.

Through testing a new low cost, light weight GPS-LoRa tracking technology my research helped fill data gaps and improve our understanding of the movement behaviour of birds in relation to energy infrastructure. The devices were found to be able to collect and transmit accurate, high frequency GNSS/GPS location information over long distances (up to 53km). Lab tests revealed their potential to help validate collision risk maps by remotely detecting when and where bird collisions occur. This thesis generated important information to support development of renewables while minimizing impacts on biodiversity.

ACKNOWLEDGEMENTS

This PhD project was funded by UKRI (United Kingdom Research and Innovation) as part of the NEXUSS (Next Generation Unmanned Systems Science) centre for doctoral training programme. This included a capital grant of £35,000 toward the cost of developing, testing, and deploying new tracking devices. During my PhD I also received grant funding if £2000 from the BOU (British Ornithologists' Union) in the form of a small research grant, a training and travel grant of £450 from the British Ecological Society and £700 toward the cost of attending the 2022 Wind Energy and Wildlife conference from the school of environmental science travel support fund at the University of East Anglia.

Special thanks go to my supervisory team Aldina Franco, Joao P. Silva, and Phil Atkinson for their support during my PhD journey. Words cannot fully express how valuable their advice and technical input has been throughout the project. Aldina leads a supportive and engaging research group at UEA and her enthusiasm for the project was really motivating. The opportunities provided by João to gain experience tagging Little Bustards during my first year along with hosting me at his home on numerous occasions and the collaborations Phil facilitated with his colleagues at BTO (British Trust for Ornithology) were invaluable.

I would also like to thank Inés Catry, Marta Acácio, Bruno Martins, Rita Ramos and Karolina Zalewska for their assistance with assembly and deployment of the Movetech-50 stork tags. The training from Inés, Marta and Bruno to fit GPS tags on storks was top class. Also thanks to Carlos Pacheco from CIBIO, along with Eduardo Realinho and Hugo Blanco for their invaluable assistance with fieldwork to capture and deploy tags on

Griffon Vultures. Along with Miguel González for arranging for us to mount a LoRaWAN Gateway at the Cazalla Observatory in Tarifa, Spain and Catia Marques and Rui Constantino at LPN for allowing me to stay at the LPN centre and for their assistance deploying a LoRa gateway at the Vale Gonçalinho nature reserve.

For the technical assistance they provided, I would like to thank Nick Griffin, Gareth Flowerdew, David Ciplic and Nicholas Garrard from the University of East Anglia electronics workshop for their assistance. For technical assistance with the LoRa devices, I thank Andreas Senn from Copernicus Technologies, Marcel Wapper and Simon Galli from Miromico-AG, Benedetta Dini from the University of Grenoble, Steven Drewett from Concept13™ and Miles Clark from the University of East Anglia. For assistance with using the Global Animal Movement Toolkit, I would like to thank Daniel Bird and Stephen Laycock.

I really appreciated the camaraderie among the other NEXUSS CDT students in my cohort and PhD students on other DTP programmes at UEA. I also thank Helena Bathala for her Portuguese lessons, without which, my field work in remote areas of Alentejo and Algarve would have been much more difficult.

I would like to make special mention of my family, particularly my parents Jane and Peter Gauld, for always encouraging me. Last but not least, I would like to express my gratitude to my wife Elena, particularly during the final few months of the project. You really supported me and, having been through the process yourself, provided sage advice throughout my PhD.

PUBLICATIONS ASSOCIATED WITH THIS RESEARCH

Research Articles

- Gauld, J. G. *et al.* (2022) 'Hotspots in the grid: Avian sensitivity and vulnerability to collision risk from energy infrastructure interactions in Europe and North Africa', *Journal of Applied Ecology*, (May 2021), pp. 1–17. doi: 10.1111/1365-2664.14160.
- Gauld, J.G. *et al.* (2019) 'The fourth grand challenge in the science of wind energy: minimizing biodiversity impacts'; Science, eLetters (November 2019). https://www.science.org/do/10.1126/comment.734538/full/
- Gauld, J., Atkinson, P.W., Silva, J.P. et al. (2023) Characterisation of a new lightweight LoRaWAN GPS bio-logger and deployment on griffon vultures *Gyps fulvus*. Animal Biotelemetry 11, 17. https://doi.org/10.1186/s40317-023-00329-y
-

Photo 1: Juvenile storks tagged with Movetech-50 loggers during the Spring 2021 field season (Photo credit, J. Gauld 2021).

TABLE OF CONTENTS

CHAPTER 1: GENERAL INTRODUCTION

Photo 2: Transmission powerlines and windfarms within an important migratory bottleneck area in south west Portugal , (J.Gauld, October 2021)

1.1. THESIS CONTEXT AND MOTIVATION

Wildlife conservation in the 21st century faces several rapidly evolving challenges and pressures. While land use, illegal hunting, pollution and overexploitation of natural resources continue to be the main drivers of the rapid decline in avian populations (Birdlife International, 2022). The climate crisis places new pressures on species and human society (Birdlife International, 2022; IPCC, 2022a). For birds, climate impacts on their populations through multiple processes including changes in availability of resources, breakdown of seasonal weather patterns and the expansion of natural barriers such as deserts (Jaffré *et al.*, 2013; Newson *et al.*, 2016; Buchan *et al.*, 2022)

Limiting warming to relatively safe levels, well below 2°C as set by UNFCCC (Paris agreement), will require a rapid transformation of the global energy system away from fossil fuels to one dominated by renewables over the course of the next two to three decades (IPCC, 2022c). As one of the most mature forms of low carbon electricity generation, wind energy is set to play a central role in the energy transition alongside an expansion of the electricity transmission network (IEA, 2020, 2022). However, the energy transition needs to proceed in tandem with appropriate ecological impact assessment and mitigation to reduce risks to birds from wind farms and power lines. Without these measures, impacts will continue to grow posing a threat to the conservation of wild bird populations (Kiesecker *et al.*, 2019). The potential impact of renewable energy expansion on wildlife, particularly birds, creates tension between our targets to halt biodiversity loss and our ambitions to limit climate change (Kiesecker *et al.*, 2019). The two challenges are also inter-dependent because conservation and restoration of healthy ecosystems play a vital role in sequestering carbon dioxide from the atmosphere (IPCC, 2022c) and failure to halt warming at well below 2°C will severely limit our ability to prevent extinctions and conserve ecosystems (Warren *et al.*, 2018).

The PhD project was funded as part of the NEXUSS CDT (Centre for Doctoral Training) with an emphasis on developing new technologies for monitoring environmental problems and finding solutions. As such this thesis focuses on how advances in animal tracking technology can help fill gaps in our understanding of where and when birds are most at risk of collision with wind farms and power lines. In turn helping target actions to reduce risks to birds from energy infrastructure. The thesis also investigates the potential for a new type of GPS-LoRa tracking device to help understand the movements of birds around energy infrastructure and detect collisions in near real time using accelerometery information.

1.1.1 CONTEXT: THE CLIMATE PROBLEM

Humanity is exerting unprecedented pressure on the natural world (Elias, 2018; Grooten and Almond, 2018). One symptom of this is rapid climate change resulting from our use of fossil fuels. Which, in turn, has increased the concentration of greenhouse gases in the earth's atmosphere. This anthropogenic change in greenhouse gas concentrations has resulted in a rapid temperature rise of approximately 1.2°C since the 19th century (IPCC, 2018, 2022b). On our current emissions trajectory the Earth's climate is likely to warm by approximately 2.7°C (2.4 – 2.9°C) by 2100 with severe consequences for ecosystems, habitats and human society (IPCC, 2022c). Climate change is increasing the likelihood of extreme weather events such as floods, storms and extended periods of drought (IPCC, 2014; Newell *et al.*, 2015).

Climate change has potentially dire implications for biodiversity. One impact will be that on our current climate trajectory, by 2099, between 15 and 29% of all vertebrate species will regularly experience temperature extremes beyond what they are adapted to cope with (Murali *et al.*, 2023). Whereas rapid emissions reductions in line with the Paris agreement would limit this form of climate impact to 6.1% of vertebrate species (Murali *et al.*, 2023). Climate change is also changing seasonal weather patterns, one of the main ways in which these impacts on bird populations is in the form of a phenological mismatches between trophic levels. For many species, this means that the breeding season and the peak food availability are increasingly becoming mismatched (Lameris, van der Jeugd, *et al.*, 2018; Santangeli *et al.*, 2018). In turn this reduces breeding success and increases mortality. In Europe, those migratory species which are less able to adjust their migratory behaviour and timing have experienced some of the fastest population declines (Møller, Rubolini and Lehikoinen, 2008; Panuccio *et al.*, 2017). Short distance migrants appear to be most vulnerable to climatic changes affecting the breeding season (Buchan *et al.*, 2022). Whereas long distance migrants are threatened by climate induced changes to the size of natural barriers such as deserts, the increasing frequency of extreme weather events and changing suitability of stopover sites (Hewson *et al.*, 2016). Climate change is creating winners and losers among migratory species. The migratory species and individuals within those species, which have responded to climate change by advancing the timing of their arrival and departure from the breeding grounds are more successful (Panuccio *et al.*, 2017). One species which is exhibiting rapid change in migratory behaviour in response to climate and other anthropogenic environmental changes is the White Stork *Ciconia ciconia* (Gilbert, 2015; Acácio, Catry, *et al.*, 2022). While most first year juvenile birds are migratory, an increasing proportion of the population of adult White Storks in Iberia is now resident due to selective pressure in favour of remaining within Iberia all year or only undertaking a shorter migration to Northern Africa and foraging at landfill sites instead of foraging for natural food sources within the traditional wintering grounds (Gilbert, 2015; Acácio, Catry, *et al.*, 2022; Marcelino *et al.*, 2022).

To avoid climate change of greater than 1.5°C - 2°C above pre-industrial levels, the global economy needs to rapidly decarbonise energy, food production and transport systems by at latest mid-century with the majority of those reductions occurring before 2030 (Peters and Hausfather, 2020; IPCC, 2022c). Governments throughout Europe and North Africa have set ambitious targets for renewable electricity generation in a bid to phase out fossil fuels from the electricity supply (European Environment Agency, 2017). The renewable electricity generation sector is experiencing rapid growth. The EU is committed to reducing greenhouse gas emissions across all sectors by at least 55% by 2030 (European Commission, 2020). In 2022, in response to the energy crisis, the European Union published REPowerEU plan which includes a target of generating 45% of electricity from renewables by 2030 with the goal of accelerating emissions reductions and improving energy security (European Commission, 2022).

Some countries such as Scotland are aiming for even more ambitious targets with over 97% of electricity in Scotland now coming from low or zero carbon sources (Scottish Government, 2022). Meanwhile MENA (Middle East and North Africa) countries such as Morocco are building capacity to export renewable electricity to Europe via a series of interconnectors (Timmerberg *et al.*, 2019). Wind and solar power will provide the largest contribution to this growth in renewable electricity generation capacity (TPWind Advisory Council, 2006). To achieve net zero carbon emissions by 2050 and permit the phase out of fossil fuels, the International Energy Agency estimates that global wind energy generation capacity will need to reach 7,900 TWh compared to 1,870 TWh in 2021 alongside other measures such as improvements in energy efficiency (IEA, 2022).

To support this growth in renewable electricity generation, electricity distribution grids will need to be upgraded. Including construction of new high voltage electricity transmission lines (60-750kV) and medium voltage distribution lines (1 - 60kV) (European Commission, 2018) to add to the existing network (Figure 1). Generating 80% of European power from renewables would require at least a fourfold increase in transmission grid capacity before 2050 compared to 2010 (Mckinsey & Company, 2010). Much of this build-up of capacity will be concentrated between Central and Western Europe (European Climate Foundation, 2018). This is largely due to the geographic disparity between European demand centres for electricity and the optimal locations for deploying new renewable electricity generators (for example wind speeds are generally more consistent in the North and West of Europe (Mckinsey & Company, 2010; European Commission, 2018). With transmission powerlines typically up to 60m tall (National Grid, 2014), onshore wind turbines up to approximately 135m (Thaxter, Ross-Smith, *et al.*, 2019) and newer wind turbines now exceeding 200m where legislation allows (Siemens Gamesa Renewables, 2022). The expansion of renewables represents a significant increase in the number of manmade objects birds and other volant animals will interact with as well as being another potentially large driver of land use change and habitat loss.

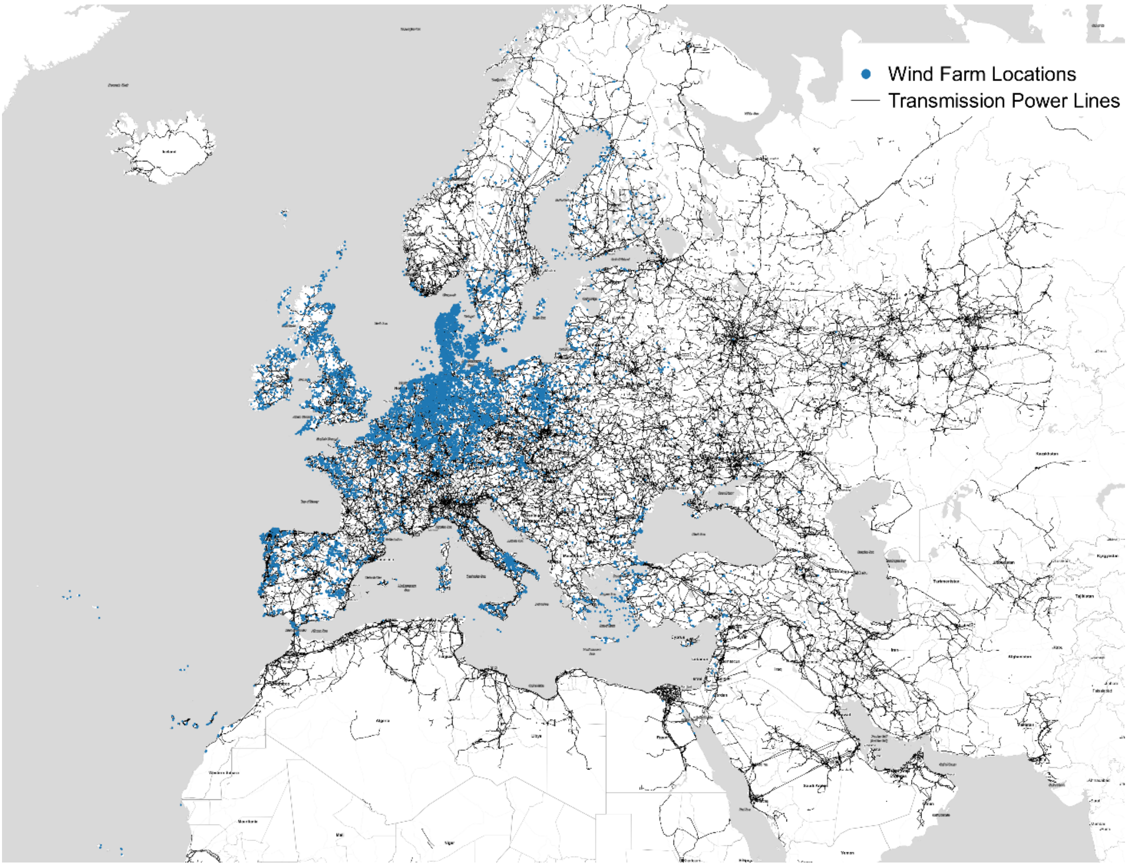

Figure 1: Current distribution of wind farms and power networks in Europe and North Africa. Map derived from wind turbine data compiled by (Dunnett *et al.*, 2020) *and transmission powerline data from the Open Infrastructure project* (Garret, 2018).

1.1.2 CONTEXT: BIODIVERSITY LOSS

Concurrent to climate change is a biodiversity crisis, WWF (World Wide Fund for Nature) refers to these two interlinked crises as “two sides of the same coin” (WWF, 2022). Human activity, predominantly land use change, invasive species and overexploitation of natural resources is resulting in a dramatic decline in both the abundance and diversity of wild species (Grooten and Almond, 2018; Leclère *et al.*, 2020). As ever more pressure is placed upon ecosystems, the biosphere is haemorrhaging species at as much as 1000 times the background rate observed in the geological record (Dellasala, Goldstein and Elias, 2018). Species loss is a direct consequence of shrinking populations of wild animals as the ecosystems they rely on are degraded. Humans have now altered and degraded over 75% of the Earth’s land surface (IPBES, 2019). As a result, wildlife populations are becoming smaller, since 1970 the populations of monitored vertebrate species have declined by an average of 69% (95% CI = 63% - 75%) (WWF, 2022). European bird populations have shrunk by over 600 million birds since 1980 (Burns *et al.*, 2021) and one in eight bird species are now considered to be threatened with extinction globally (Birdlife International, 2022).

What happens this decade will determine the extent to which we are able to halt and restore biodiversity (Leclère *et. al.* 2020). At the UNEP Convention on Biological Diversity COP15 summit in Montreal, the governments of the world committed to halt and reverse biodiversity loss (Ainsworth, Collins and D'Amico, 2022). It is therefore imperative that our efforts to combat climate change and de-carbonise our energy system do not have a detrimental impact on the global effort to halt biodiversity loss and restore ecosystems. "we should not rob Peter to pay Paul" (Kiesecker *et. al.* 2019).

All forms of human infrastructure or energy generation have the potential to impact negatively on wildlife, wind turbines and power lines are no exception from this (Scott R. Loss, 2016). Wind farms and power lines can impact on bird populations via direct mortality (collision and electrocution), barrier effects, habitat loss and disturbance (Bernardino *et al.*, 2018a; Heuck *et al.*, 2019a; Kiesecker *et al.*, 2019). In raw numbers, (Scott R. Loss, 2016) estimated that combined mortality from wind turbines in the US and Canada is currently in the region of 140,000 – 328,000 birds per year. When compared with 16 – 42 million due to collision with buildings this suggests that the overall impact is currently relatively minor. However, as clean energy investment accelerates in the absence of mitigation to reduce risks to birds, these impacts are likely to increase (Scott R. Loss, 2016). In some regions such as Latin America where ecological research on the topic has lagged behind the pace of development that the impacts of wind energy and power line development are thought to be underestimated (Agudelo *et al.*, 2021). Relative to their population size, migratory species within Europe are declining faster than non-migrants (Burns *et al.*, 2021) and direct mortality such as collision with wind farms and powerlines exacerbates the effects of other drivers of population decline such as land use change (Buchan *et al.*, 2022). This is particularly a problem where energy development occurs within migratory bottlenecks or where wind energy competes for wind resources with soaring birds creating an ecological trap (Oloo, Safi and Aryal, 2018; Marques *et al.*, 2020a). Collision with wind turbines and powerlines is one of the most common causes of anthropogenic mortality in White Storks, Egyptian Vultures and Griffon Vultures (Oppel *et al.*, 2020; Marcelino *et al.*, 2021; Ferrer *et al.*, 2022).

Within Europe, the EU birds and habitats directives provide a statutory framework within which member states operate (2009/147/EC, 2010). Under these directives member states are required to have their own devolved legislation for protecting birds, habitats to prevent declines in the populations of wild species. Alongside this, there are numerous international declarations of intent between countries and non-governmental bodies to protect migratory birds. For example, seventy-eight countries across Africa, Asia, Europe and North America have ratified the Agreement on the Conservation of African-Eurasian Migratory Waterbirds (AWEA) (UNEP AEWA Secretariat, 2018). Under the agreement, ratified nations are obliged to implement conservation action to protect the population status of 255 migratory species within the Eurasian-African flyways. This agreement includes efforts to reduce the risk posed by power infrastructure (Prinsen *et al.*, 2012). As such, power companies operating within Europe and Northern Africa are obliged to ensure that any new or existing energy developments do not adversely impact upon the population status of wild birds.

Typically, the potential impact of energy infrastructure developments on birds are assessed on a project-by-project, site-by-site basis. The single site focus of the assessment process can struggle to keep pace with the pace of change required in our energy system to effectively mitigate climate change (Diesendorf and Elliston, 2018; IPCC, 2018). Nor do such approaches fully assess the landscape level effects upon birds of new energy infrastructure developments (Bernardino *et al.*, 2018b). It is therefore an urgent conservation priority to advance research in this area to help facilitate a more targeted, efficient approach to mitigation of mortality risk for birds (Bernardino *et al.*, 2018b). New tracking technologies such as GPS loggers are providing an unprecedented volume of data about the movements of birds and in turn have the potential to allow for assessment of the potential effects of energy infrastructure on birds at the landscape and flyway scale (Masden *et al.*, 2010; Silva *et al.*, 2014).

If we do not manage to halt climate change, it threatens to undermine much of the conservation work done today and make efforts to halt biodiversity loss much more difficult because changes in climatic conditions will in turn cause changes to ecosystems (Murali *et al.*, 2023). To limit the impacts of climate change, investment in clean energy at scale is vital and urgent because, even factoring in potential societal and behavioural changes which may also reduce emissions, a zero carbon electricity grid is fundamental to decarbonising other sectors (IPCC, 2022c). However the expansion of renewables and the power line infrastructure required to support them is in itself a potential threat to biodiversity, particularly voilant animals like birds, which will have an additive effect on the other threats species are facing (Ferreira *et al.*, 2019; McManamay, Vernon and Jager, 2021). A 2019 study highlighted that within Europe there is approximately 17 times the potential capacity for onshore wind than is required to meet the European Union clean energy targets for 2050 (Ryberg *et al.*, 2019). Therefore, there is flexibility in where we build onshore wind meaning that more sensitive areas can be avoided. It is therefore vital that we improve our understanding of where and when birds are most sensitive to renewable energy developments and where conflicts may already exist so that measures and planning policies to reduce or eliminate the potential risks associated with wind farm or power lines can be implemented.

1.2 A REVIEW OF THE IMPACT OF ENERGY INFRASTRUCTURE ON BIRDS

To assess the current state of knowledge in relation to the impacts of wind energy and power lines upon birds, Science Direct and Google Scholar were used to search for journal articles relating to the topic of mortality risk for birds associated with energy infrastructure. Search terms included “Power lines” or “Wind farms” in combination with the following terms: “collision risk”, “electrocution”, “disturbance”, “displacement”, “gps tagging”, “species susceptibility to collision”, “spatial distribution of collision risk”, “energy infrastructure” and “mitigation”, “GPS”, “Collision detection”. Reports available on the websites of governmental and non-governmental organisations (NGOs) such as power line companies, industry guidance bodies and conservation bodies were also consulted. Relevant publications about bats were also included in the study as there is significant overlap between the study of bats and birds in relation to collision risk (Thaxter *et al.*, 2017). Other non-peer reviewed literature consulted during the literature search included relevant book chapters and MSc or PhD theses available on university websites. This search was undertaken between October 2018 and March 2019 and then updated during a subsequent literature search for new scientific papers on these topics was undertaken between May and July of 2022. During the update, 100 results per page were displayed, sorted by relevance and the first ten pages searched for relevant articles.

In total 234 relevant studies were found; keywords and the content of the articles was used to classify them by main topic and two sub-topics. The geographic focus and main research topic of these publications is summarised in Photo 3. This summary highlights how much of the research to date has originated from Europe and focussed on the impact of wind turbines (Photo 3a and Photo 3Photo 3b). Of the included studies, 80 focus on the issue of collision risk as their main topic (Photo 3c), 21 focus on electrocution, 19 focus on mitigation and 12 publications focus on disturbance (predominantly in relation to wind farms or other energy generation). Wind turbines were the focus of more publications (126) than papers about power lines (64); 22 papers involved study of other infrastructure in relation to mortality risk for birds (such as windows or oil platforms) and only 12 papers explicitly covered both power lines and wind farms. The remaining publications covered several related topics including (but not limited to) bird behaviour and advances in tracking technology. Alongside published articles, statutory guidance documents or reports from NGOs and Governments were also consulted such as the AWEA Guidance for mitigating power line impacts on birds (Prinsen *et al.*, 2012). Research published in the last ten years was prioritised however some older studies were also included if considered relevant, the earliest paper included dates from 1978.

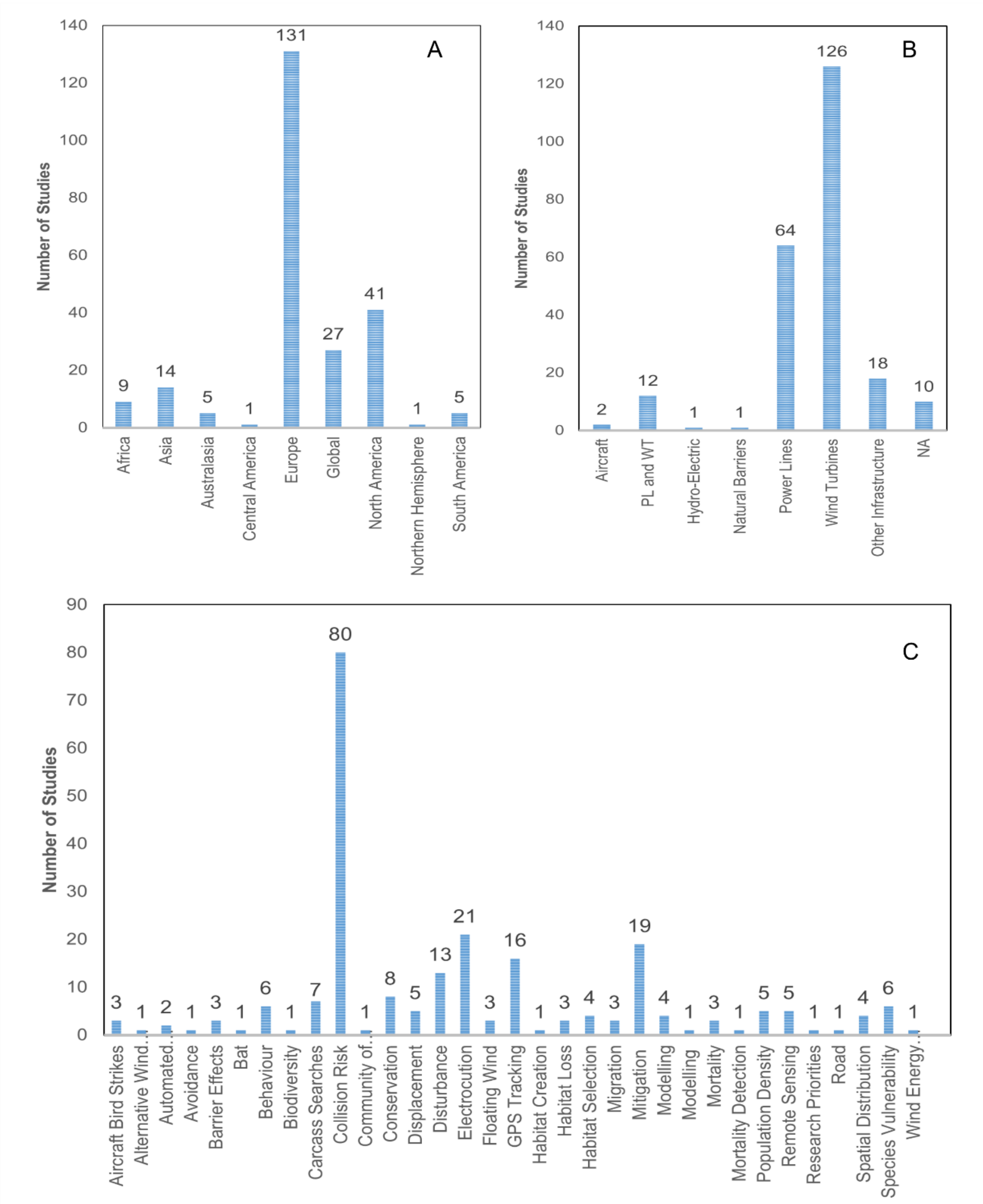

Photo 3: Summary of the geographical focus and topics of the relevant studies found during the literature search. A: Summarises the geographical focus of the studies, B. The type of infrastructure the study refers to, the category "PL and WT"represents studies which look at the impacts of both power lines and wind turbines. C. Summarises the main topics of all the studies.

One caveat to this literature review was the focus on studies which had used GPS to understand bird movements, we recognise that additional search terms such as “Habitat Loss”, “Avoidance”, “Barrier Effects”, “Displacement”, “Habitat Creation”, “Habitat Loss” may have yielded further studies on those specific topics. In the context of wind energy, Tethys Knowledge Base have compiled a list of 5,942 studies including peer reviewed papers and reports in the grey literature about the different impacts of wind energy (Tethys 2023). This data base highlights biases in the literature toward birds (1,666 studies) and collision risk as the most studies impact of wind energy (970 studies) compared to Habitat Change (778 studies), Noise (580 studies), Avoidance (329) and Displacement (260 studies). In agreement with the literature review performed for this thesis, the Tethys data base also highlights significant geographical biases in studies looking at the impacts of wind energy with 36% (2,119) of all studies in the Tethys wind energy impacts data base originating from just five countries: The United States of America (n= 1,162), United Kingdom (n = 462), Germany (n = 225), Denmark (n = 151) and the Netherlands (n = 119). Whereas only 52 studies originate from all of Latin America.

1.2.1 LETHAL AND SUB-LETHAL IMPACTS OF ENERGY INFRASTRUCTURE ON BIRDS

Wind turbines are effectively point features on the landscape with fast moving blades typically deployed in clusters across a given area, whereas power lines are large linear features in the land consisting of poles or towers with thin wires between them. Despite these differences in form, the way these infrastructures pose a risk to birds is similar. Direct effects on birds include the injuries sustained as a result of collision with wind turbines and both collision and electrocution arising from interactions with power lines.

Indirect effects arise from habitat loss, barrier effects and disturbance (Smith and Dwyer, 2016; May *et al.*, 2021; Husby and Pearson, 2022). When these effects become large enough, they can result in population level impacts on the species.

1.2.2 COLLISION

The most direct impact of wind turbines and power lines on birds is mortality from collision. Collision occurs when a bird hits one of these structures; such an event usually results in death or serious injury for the individual and often causes significant damage to electricity grids (Polat *et al.*, 2016). Near misses can also harm birds, Jiguet *et al.*, (2021), documented a near collision that they detected from GPS tracking and accelerometery of a Curlew *Numenius arquata* which was grounded for several hours after being caught in the turbulence from a wind turbine during migration. Collisions occur because power lines and wind turbines act as novel (in an evolutionary sense) barriers to the movement of birds; the nature of these structures consisting of thin wires or moving blades can make them next to invisible for birds owing to their poor ability to perceive contrast (Potier, Mitkus and Kelber, 2018).

While there remains, high uncertainty surrounding global or flyway scale estimates of the total number of bird deaths caused by collision, they point to it being a significant and growing source of mortality for wild birds. For wind turbines, (Scott R. Loss, 2016), estimated that between 140,000–328,000 birds are killed by collision with wind turbines each year in USA and a study of collision mortality of migratory soaring birds in southern Spain, estimated that wind turbines resulted in 0.3 dead soaring birds per MW per year (Martín *et al.*, 2018). For power lines, (Rioux, Savard and Gerick, 2013) estimated that between 2.5 and 25.6 million birds are killed by collision with power lines in Canada alone while (Loss, Will and Marra, 2014) placed the estimate at between 8 and 57 million birds killed by collision with power lines in the USA. The uncertainty surrounding these estimates arises from two factors. Firstly, the methods used for this monitoring such as carcass searches or vantage point survey are typically very labour intensive and prone to bias depending on the terrain, vegetation and level of carcass removal by predators (Travers *et al.*, 2021). Secondly post construction monitoring is not always stipulated as a planning requirement so the few global estimates which have been made arise from a relatively small number of published studies at specific wind farms and power lines. For example, (Krijgsveld *et al.*, 2009) found significant variation in the number of bird collisions both within and between three wind farms in the Netherlands, 19–68 collisions per turbine per year. Whereas a review by (Sovacool, 2009) showed that estimates varied between 0 and 38.2 collisions per turbine per year. The geographic bias in these studies (Photo 3a) also means that collision mortality from wind turbines and power lines is likely to be under reported in South America, Africa and Asia where very few studies of collision mortality have been undertaken (Aswal *et al.*, 2022).

For some species such as Little Bustard *Tetrax tetrax* collision risk from power lines is considered to be a major threat to the conservation status of the population in Western Europe (Silva *et al.*, 2014; Moreira *et al.*, 2018) and has resulted in localised extinctions for species such as the Eagle Owl *Bubo bubo* (Bassi *et al.*, 2002). In South Africa approximately 4,000 – 11,900 Ludwigs' Bustards *Neotis ludwigii* are killed annually by collision with power lines (Jenkins *et al.*, 2011) and in Norway approximately 5.3 ptarmigan are thought to collide per kilometre of transmission power line per year

(Bevanger and Brøseth, 2004). Where energy infrastructure is constructed in proximity to migratory bottlenecks such as the Strait of Gibraltar and the Bosporous region of Turkey, collision mortality associated with wind turbines and power lines can impact on populations of migratory species across the whole flyway (Thaxter, Ross-Smith, *et al.*, 2019; Oppel *et al.*, 2021b; Mattsson *et al.*, 2022).

1.2.3 ELECTROCUTION

Electrocution occurs when a bird touches two separate conductors, or a conductor and an uninsulated component connected to the ground. The design of power distribution infrastructure, particularly the low and medium tension lines of less than 60,000v, has a significant impact upon the risk posed to perching birds (Lehman, Kennedy and Savidge, 2007; Prinsen *et al.*, 2011). These lower voltage lines are more dangerous because they are less likely to be insulated in the same way as high voltage lines and the individual conductors tend to be closer together (Lehman, Kennedy and Savidge, 2007; Hernández-matías *et al.*, 2015; Guil *et al.*, 2017). Inclement weather can further increase this risk; birds tend to perch more often during periods of rainfall and wet feathers increase conductivity and there for the risk of electrocution (Lehman, Kennedy and Savidge, 2007).

For some species, particularly raptors and perching water birds with slower reproduction strategies (K-selected), electrocution of individual birds on power lines occurs frequently enough for it to be considered a significant population level impact (Sergio *et al.*, 2004; Guil, Colomer and Moreno-opo, 2015; Moreira *et al.*, 2018). For example electrocution on power lines accounted for over 50% of anthropogenic mortality in the population of Eagle Owl *Bubo bubo* in the Italian Alps (Bassi *et al.*, 2002).

Vultures and eagles are thought to be among the most susceptible; severe declines attributed to electrocution mortalities have been observed in a number of species including but not limited to Griffon Vultures *Gyps fulvus* (Donázar *et al.*, 2002), Egyptian Vulture *Neophron pernopterus* (Angelov, Hashim and Oppel, 2013; Phipps *et al.*, 2013; Oppel *et al.*, 2021b), Bonelli's Eagle *Hieraaetus fasciatus* (Rollan *et al.*, 2010), Spanish Imperial Eagle *Aquila adalberti* (López-López *et al.*, 2011).

Collateral impacts of bird electrocutions include wildfires and regional blackouts; such events incur a significant economic cost to power operators. In Spain, between 2005 and 2012 it is estimated that wildfires originating from an animal being electrocuted on a power line cost the operator €170,000 per year in direct repair costs and resulted in an additional annual release of 1,400 tons of CO_2 (Guil *et al.*, 2017).

1.2.4 DISTURBANCE AND DISPLACEMENT

Species vary in their sensitivity to new infrastructure developments (Bright *et al.*, 2008; Pearce-Higgins *et al.*, 2012; Astiaso Garcia *et al.*, 2015). Some species exhibit a pattern of temporary disturbance during the construction phase of a new wind farm or power line development with rapid re-colonisation post construction provided that habitats on site have been protected during the works (Astiaso Garcia *et al.*, 2015). Other species however, become permanently displaced in the wake of construction. This may occur when the displaced individuals fail to find enough food during the construction phase, therefore suffer mortality before construction is completed or they are impacted by the ongoing presence of power infrastructure or wind turbines in their habitat. This in effect results in a net loss of habitat for this species with resulting knock on effects for the population (Warwick-evans *et al.*, 2017; Cook *et al.*, 2018). For example (Peschko *et al.*,

2020) demonstrated a significant reduction in the density of Guillemots *Uria aalge* using the area in and around a newly constructed wind farm during spring with potential impacts on breeding success at nearby seabird colonies. Even relatively common generalist species such as Magpie *Pica pica* have been shown to have reduced breeding densities within and adjacent to wind farms (Song *et al.*, 2021).

1.2.5 ENERGY USED IN AVOIDANCE

The presence of new obstacles in the form of a power line or wind farm may result in barrier effects forcing the birds to fly further and for longer between feeding and roosting sites. This in turn results in an energetic cost for the affected individuals (Warwick-evans *et al.*, 2017; Cook *et al.*, 2018). At the fine scale, birds may expend more energy by avoiding individual turbines within a wind farm or by changing their altitude (C. Thaxter *et al.*, 2018).

1.3 CURRENT UNDERSTANDING OF TAXONOMIC DIFFERENCES AND THE SPATIAL DISTRIBUTION OF COLLISION RISK

1.3.1 TRAIT AND POPULATION DENSITY BASED APPROACHES

There has been a significant body of research undertaken on mortality risk associated with power lines (Pérez-García *et al.*, 2016; Bernardino *et al.*, 2018b) and wind farms (Johnston *et al.*, 2014; Köppel, 2015; Chris B Thaxter *et al.*, 2017; Chris B. Thaxter *et al.*, 2017). The ability to avoid collisions and the impact of collision mortality on populations varies significantly between species groups (Smith and Dwyer, 2016; Chris B. Thaxter *et al.*, 2017). A review by Thaxter et al. 2017 suggests the Acciptiformes (hawks, eagles & vultures), Bucerotiformes (hoopoes), Ciconiiformes (storks) and Charadriformes (shorebirds including Gulls and Waders) to be the most vulnerable to mortality associated with collision risk associate with wind farms based upon the traits of species within these groups (Thaxter et al., 2017). Relative to their population size, owls, raptors and large water birds (such as storks, herons, cranes, geese, swans and ducks) also suffer some of the highest mortality rates associated with power lines due to collision and electrocution (Bassi *et al.*, 2002; Donázar *et al.*, 2002; Rubolini *et al.*, 2005). A description of the risks from wind turbines and power lines posed to 85 species and 3 taxonomic grades of birds described in the literature is provided in the table in Appendix A, Supporting Information Table 1.

One reason that certain taxonomic groups are more susceptible to collision and electrocution risk is partly due to morphological and behavioural differences between species (Janss, 2000; Hull *et al.*, 2013). Key morphological factors are thought to be differences the visual system between species groups, flying ability linked to wing loading, wing shape and size and behaviour in terms of flying habits such as soaring vs. flapping flight and differing abilities to associate anthropogenic structures with danger (Bevanger, 1998; May *et al.*, 2014; Smith and Dwyer, 2016).

1.3.2 VISUAL DIFFERENCES

Birds have highly developed visual systems capable of distinguishing between colours in four or five bands compared allowing them to sense wavelengths beyond what our trichromatic vision will allow (Blackwell *et al.*, 2009; May *et al.*, 2014). However, this ability to visualise a greater range of the light spectrum appears to come at a cost. Based on the small number of bird species assessed it appears that birds detect contrast between 7 – 30 times less well than humans which is why they are less able to perceive objects such as wind turbine blades (Blary, 2022).

Most bird species also have eyes located on the side of their head with a single fovea (area of high density of light receptor cells on the retina) to favour a wide field of vision. This in turn means that they tend to have poor binocular vision (May *et al.*, 2014) and in some species such as storks and cranes, a blind spot directly ahead of them (Martin, 2011). This can inhibit their ability to detect manmade obstacles such as power lines or wind turbine blades encountered on their flight path (May *et al.*, 2014). Galliformes such as pheasants and grouse are particularly poor at avoiding obstacles because not only do they have poor depth perception but they also lack the visual acuity and efficient movement processing capabilities possessed by other birds (Blackwell *et al.*, 2009). In Norway alone, approximately 20,000 Capercaillie *Tetrao urogallus* and 26,000 Black Grouse T*etrao tetrix* are killed by collisions with power lines each year (Bevanger, 1995).

Despite excellent depth perception and visual acuity (Martin and Shaw, 2010; May *et al.*, 2014); raptors, owls and other hunting birds suffer from almost the opposite problem because their vision affords a very narrow field of view (in the region of 60°). This impedes their ability to detect obstacles immediately above or to the side of them, particularly when scanning the ground while hunting or while focussed on a prey item during a pursuit (Bevanger, 1978; Martin, 2011; May *et al.*, 2014).

The visual systems of birds also feed into their ability to associate human structures and activity with potential danger and avoid a collision (Blackwell *et al.*, 2009; Martin, 2011; Tyrrell and Fernández-Juricic, 2017). Some birds selectively change their flight route to avoid a wind farm or adjust their altitude on approach to either a power line or wind farm to avoid the danger zone completely (Macro and Meso Avoiders). These species and individuals are significantly less likely to collide than birds who fail to alter their behaviour ahead of time resulting in a need for emergency micro scale evasive action in close proximity to the power line or wind farm (May, 2015; C. B. Thaxter *et al.*, 2018). Some prey species exhibit an innate response however for the majority of species at risk of collision this is a learned response (Hernández-Pliego *et al.*, 2015; May, 2015).

This is partly why migratory species are thought to be at greater risk of collision than resident birds because they are more likely to encounter new energy infrastructure while on migration which they have not yet learned to anticipate (Skov *et al.*, 2016). They will also encounter numerous energy installations during each migrations meaning that they experience cumulative risks across the flyway (Thaxter, Ross-Smith, *et al.*, 2019). This is not always clear cut as some studies indicate that resident birds are more commonly recorded as collision victims of wind farms and flight behaviour was the key predictor of mortality risk (Barrios and Rodríguez, 2004). The link often made to migration may therefore instead be due to time of year and that many migratory species who are commonly recorded as collision victims use soaring flight. This flight method can bring them into direct conflict with wind infrastructure (Skov *et al.*, 2016; Oppel *et al.*, 2021a; Ferrer *et al.*, 2022). Regardless of the underlying mechanism, a major concern for practitioners working to conserve migratory species is, how, as the pace of renewables deployment increases, this is likely to significantly impact birds within the Afro-Palearctic flyways (Desholm, 2009; Prinsen *et al.*, 2011; Gyimesi and Prinsen, 2015).

1.3.3 FLYING ABILITY AND BEHAVIOUR

Wing loading, aerial manoeuvrability and behaviour influence both the frequency with which birds interact with power lines or wind turbines and how able they are to undertake evasive action to avoid collision with these structures (Janss, 2000; Rioux, Savard and Gerick, 2013; Smith and Dwyer, 2016). Wing loading is defined as the total area of wing relative to the mass and body size of the bird (Alerstam *et al.*, 2007); in general birds with higher wing loading are less agile (Santos *et al.*, 2016). In situations where birds enter a wind farm or encounter a power line in their flightpath, wing loading is considered to be one of the most important factors in determining whether that individual will be able to navigate their way to the other side without injury (Bevanger, 1998; Lucas *et al.*, 2012; May, 2015; Chris B Thaxter *et al.*, 2017). Collision with power lines, particularly around landfills, is one of the main causes of mortality for GPS tracked storks from Portuguese colonies (Marcelino *et al.*, 2021).

Poorly sited energy infrastructure can therefore cause significant mortality for soaring migrants. Especially at risk are juvenile birds who may not have learned to recognise the danger (Marques *et al.*, 2014a). Collision risk is further compounded when birds fly as a group. This is in part because birds flying toward the rear of the flock will be less aware of obstacles which lay ahead of them (Martin, 2011). There is also a strong desire for individuals in a flock to maintain course to avoid becoming separated, particularly for inexperienced birds (Rotics *et al.*, 2016). This desire to avoid separation from the group can delay avoidance action compared to birds flying alone, in turn increasing the chances of a collision (Croft, 2014).

Birds such as falcons, owls and hawks often use human structures as hunting perches. storks, eagles, ospreys and numerous other birds often nest on power line masts. This brings them into regular contact with these structures. As such power lines can act as ecological traps for certain species because this regular interaction significantly increases the risk of electrocution (Hernández-matías *et al.*, 2015; Moreira *et al.*, 2017; Dixon *et al.*, 2018; Uddin *et al.*, 2021a). In the region of Valencia in Spain a 2017 study found that over 80% of electrocution victims were either raptors or owls while storks represented 6.1% (Pérez-garcía *et al.*, 2017).

Other behavioural factors which bring birds into conflict with energy infrastructure include competition for wind resources (for soaring birds) and flocking behaviour. Wind turbines are most optimally located in areas with consistent high winds such as coast lines or upland ridges (Skov *et al.*, 2016). Where these are sited along key migratory routes or within close proximity to important breeding and wintering areas they can come into conflict with soaring birds such as large diurnal raptors, vultures, storks, cranes and other similar birds who utilise the uplift generated in these areas to fly efficiently (Lucas *et al.*, 2012; Skov *et al.*, 2016; Evan R Buechley *et al.*, 2018). Understanding the spatial and temporal patterns of orographic and thermal uplift can help us predict where soaring birds are more likely to fly at heights where they risk collision with wind turbines and power lines. For example in Norway (Hanssen, May and Nygård, 2020) demonstrated how uplift could be used to predict collision risk for White Tailed Eagles *Haliaeetus albicilla* within the Hitra wind farm and inform micro-siting of new turbines to minimise collision risk.

1.3.4 THE ROLE OF HABITAT IN COLLISION AND ELECTROCUTION RISK

Birds move in three dimensions; the height they are at when they encounter a wind farm or power line determines whether they are in danger of collision or not. In turn, ecological and physical factors play an important role in influencing the height at which an individual is flying (Péron *et al.*, 2017). These same factors such as habitat, also influence whether a bird decides to perch or build a nest on a power line (Hernández-matías *et al.*, 2015). These decisions by individual birds about where they move in relation to EI can have significant population level impacts (Janss, 2000). It is therefore important to understand how habitat, terrain and other bio-physical factors such as the weather and uplift influence mortality risk at EI installations to ensure we aren't creating ecological traps (Moreira *et al.*, 2018).

White Storks nest colonially and commonly use anthropogenic structures including pylons and towers for nesting (Mainwaring, 2015; Lines, 2022). Helicopter based surveys of the Portuguese transmission network identified stork nests in 7.7% of pylons in Portugal in June 2007 (Moreira *et al.*, 2018). The presence of rice fields or landfills within 30km of the pylon where there are abundant food resources for storks was found to be the single most important ecological predictor of stork nest density (Moreira *et al.*, 2018). Similarly opportunistic species such as the Osprey will also build their nests in pylons instead of tall trees (Prinsen *et al.*, 2011). Many raptors species will preferentially use pylons and distribution lines as hunting perches associated with suitable habitat for rodents such as rough grassland which is why kestrels are often killed by uninsulated power lines (Pérez-garcía *et al.*, 2017). Vegetation height and the terrain can strongly influence the height at which birds fly. Barn owls are often recorded as casualties of collision when crossing major roads because they tend to fly low while hunting; tall vegetation either side of these roads can force the birds to increase their altitude and avoid danger (Ramsden, 2003). A similar impact of vegetation, for example whether a development is surrounded by forest or not, can therefore be expected in other species in the context of wind farms and power lines (Pérez-garcía *et al.*, 2017).

Wind speed, weather conditions and the terrain influence flight height and avoidance rates of birds (Barrios and Rodríguez, 2004). This is particularly true of soaring birds such as vultures which use areas with higher orographic uplift associated with steeper slopes to gain altitude efficiently (Péron *et al.*, 2017). The variation in available uplift due to terrain features and wind speeds is therefore a significant influence upon the collision risk experienced by soaring species (Péron *et al.*, 2017). Birds tend to fly less often in inclement weather such as rain but moderate to strong winds and fog can reduce birds' ability to detect and avoid energy infrastructure resulting in greater collision risk (Furness, Wade and Masden, 2013).

1.3.5 SEASONAL VARIATION

For some species, particularly seabirds, colonially breeding species and long distance migrants, exposure to mortality risk from EI may be highly seasonal (Prinsen *et al.*, 2011; Palac *et al.*, 2016). This can simply be due to the birds not being present at certain times of year however in most species, including residents, there appears to be a significant seasonal variation in mortality risk. In the case of the Common Kestrel *Falco Columbus* higher mortality at EI installations is observed in summer when fledgling birds congregate prior to dispersal (Guil, Colomer and Moreno-opo, 2015). This is also true of other species including the White Stork *Ciconia ciconia* because juvenile birds fail to recognise the hazard (Martin and Shaw, 2010). The Common Tern *Sterna hirundo* is at greatest risk to collision with coastal wind farms during the breeding season when this species is concentrated around breeding colonies. During the peak of the breeding season between late May and June male mortality significantly increases (Stienen *et al.*, 2008). This is because males perform most of the foraging flights at this time of year (Stienen *et al.*, 2008). In the Spanish Imperial Eagle *Aquila aldaberti* this relationship is reversed with higher rates of mortality from power lines observed in females than males (Ferrer and Hiraldo, 1992).

1.3.6 MAPPING MORTALITY RISK

Under the ecological impact assessment (EcIA) framework; a preliminary assessment of the mortality risk for birds posed by a new EI development is most commonly achieved by using the proximity to important bird areas (IBAs) or special protected areas (SPAs) as a proxy for risk to sensitive bird species (SNH, 2006; CIEEM, 2018). This is often combined with a data search for records of sensitive species within the local area to assess whether the development is likely to cause adverse impacts upon the local, regional and national populations of any bird species found to be within 10km of the development site (CIEEM, 2018). Once a development passes the preliminary assessment stage, vantage point surveys are then performed on the proposed development site throughout the year (CIEEM, 2018). The data from these surveys is used to understand the movement of birds through the area and estimate collision risk using the band model (Band, 2012). While this provides an important insight into the potential impact of a wind or power line development on that particular site, it does little to help assess the cumulative impact of these developments at the national or regional scale. To address this knowledge gap for Scotland Bright *et al.*, 2008, used species distribution data in combination with information about species traits to map sensitivity to wind farm development for 16 priority species at a resolution of 2km x 2km (Table 1).

Using a similar approach, a 2017 study combined a population density approach with trait based analysis to estimate sensitivity to wind farm development at the global scale (Thaxter *et al.*, 2017). To date this appears to be the only truly global assessment of collision risk in relation to wind farms. This assessment first ranks species and species groups according to their susceptibility to collision. This metric is linked to physiological measurements such as wing loading which is known to be important in determining avoidance rates (Janss, 2000). This vulnerability assessment was then combines with a species distribution model to produce a global risk assessment at 5km resolution (Table 1). While this approach is informative, (Tikkanen *et al.*, 2018b; Vignali *et al.*, 2021) and others have highlighted how sensitivity mapping based purely on species distribution or buffering around breeding sites can exclude more area than necessary for development while not providing sufficient protection for collision prone species.

Until recently, relatively few studies have incorporated GPS telemetry data into their collision risk and sensitivity to collision risk assessments; the first to successfully demonstrate the potential offered is a 2014 study on little bustards (Silva *et al.*, 2014, Table 1). Since this study a number of others have been undertaken for individual taxa as summarised in Table 1. For example, the Birdlife sensitivity map combines species distribution information with GPS tracking data to provide a tool for practitioners to identify the species likely to be affected by a proposed development and the IBAs within close proximity to a proposed wind farm (BirdLife International, 2015a). This is draws on a number of data sources including movement data for soaring species from GPS tracking and bird observatories. One limitation of this tool is that it lacks information about whether birds flying through that area are spending significant time at collision height. Several studies have highlighted how GPS data can be used to help better understand the flight behaviour of birds in and around wind farms such as (Schaub *et al.*, 2020) and how terrain and environmental conditions such as Thermal and Orographic uplift can influence birds' flight height, speed and direction (Sage *et al.*, 2022). It is important that we start including this information in our sensitivity maps to help us prioritise areas for mitigating existing infrastructure and more effectively target pre-construction surveys for new developments (Prinsen *et al.*, 2011; Bernardino *et al.*, 2018b). This could facilitate better conservation outcomes while reducing uncertainty for developers about the project costs in relation to mitigation measures for wildlife (Bradbury *et al.*, 2014).

Study	Author(s)	Approach	Notes
Spatially explicit risk mapping reveals direct anthropogenic impacts on migratory birds	(Buchan *et al.* 2022)	Risk Mapping	Although not specific to energy infrastructure, this study looked at the key factors affecting migratory birds within the African-Eurasian flyways. The density of wind turbines and power lines was incorporated into an index of 16 different anthropogenic impacts on migratory birds. The study highlighted where these impacts were greatest and which species were most vulnerable to each kind of impact.
Birdlife International Sensitivity map tool: Red Sea Flyway	(BirdLife International, 2015a)	Combines species distribution based methods with satellite telemetry.	This web-based tool is the first to allow users to assess how sensitive an area is to wind farm development. It is designed to aid planners perform preliminary ecological impact assessments and desk studies. The tool combines population density data with spatial information about IBAs within a given distance of the area the user is interested in. Satellite tracking data is also incorporated into the tool but purely to identify which species fly over the area of interest rather than distinguishing how many birds spend time at danger height in the area.
Map of bird sensitivities to wind farms in Scotland: A tool	(Bright *et al.*, 2008)	Species Distribution based methods	This study produced for Scottish Natural Heritage (SNH) used data about known population densities to map the sensitivity of birds to wind farm developments. The source data was based upon national BBS in combination with other survey

Study	Author(s)	Approach	Notes
to aid planning and conservation			data collected during EIA assessments and a literature review of species traits.
Disentangling drivers of power line use by vultures: Potential to reduce electrocutions	Marina Garcia-Alfonso *et al.* 2012	Satellite Telemetry	Tracked 49 Canarian Egyptian Vultures *Neophron percnopterus majorensis* in Fuerteventura to understand the factors which make the use of power lines for perching more likely with a view to helping target mitigation to reduce electrocution and collision risk. Tracking data was used in conjunction with records of carcasses found under power lines over a period of 17 years. The study found season, proximity to territory, proximity to roads and proximity to food sources such as livestock and rubbish dumps to be key factors influencing the likelihood of the vultures using power lines. They also found that vultures were more likely to use power lines during the day than at night. The Authors concluded that installing mitigation at just 6% of the most utilised pylons could reduce mortalities by 50%.
Space–time trends in Spanish bird electrocution rates from alternative information sources	(Guil, Colomer and Moreno-opo, 2015)	Combined multiple sources of information to identify electrocution hotspots on the Spanish Electricity network.	This study analysed the sensitivity of 337 species known to breed in Spain to electrocution. The authors produced a density map of the transmission network (>66kV) as total power line length per 10 x 10 UTM grid square. This was then overlaid with data on the number of bird carcasses reported near power lines, proximity to protected areas, density of ornithologists (to measure survey effort) and population density data for each species. Data from ringing recoveries (in the context of ringing rates over the study period) were also used to assess how mortality from power lines has changed over time. Three models were produced for birds in general, raptors and large eagles. Three key factors were found to predict mortality for raptors: Rabbit population density, tree cover and power line density. Where there is high prey density and low tree cover it was found that raptors will preferentially use power lines as hunting perches resulting in higher electrocution mortality.
Drivers of power line use by White Storks: A case study of birds nesting on anthropogenic structures	(Moreira *et al.*, 2018)	Spatial generalised linear model	This study used helicopter surveys of the Portuguese transmission network (150–400 kV) to map the density of stork nests on power lines. The study highlighted how storks were attracted to pylons with a high density of other stork nests nearby. Other predictive factors included the distance to rice fields or landfills (within 30km) and the habitat mosaic within 1km of the pylon. The findings of this research can be used to predict stork usage of pylons for nesting in other parts of Iberia but stops short of providing a sensitivity map for the species.
Predicting migratory corridors of White Storks, ciconia ciconia, to enhance sustainablewind energy planning: A data-driven agent-based model	(Oloo, Safi and Aryal, 2018)	Satellite Telemetry	This study combined GNSS (Global Navigation Satellite System) tracking data with environmental data sets such as uplift, terrain roughness and landcover in an individual based modelling approach to predict the flight corridors of White Storks *Ciconia ciconia* in Tanzania. The authors then overlaid their results with the potential yield from wind energy development in the region to identify potential future conflict areas between wind farms and migratory soaring birds.
Using risk prediction models and species sensitivity maps for large-scale identification of	(Pérez-garcía *et al.*, 2017)	Species Distribution based methods	This study combined data on recorded electrocution mortality of birds in the Valencia region of Spain with the known population densities of sensitive bird species threatened by electrocution. The third step in the analysis was to validate the predicted sensitivity in the context of protected areas to identify the high priority areas. It is these areas where it is the most urgent conservation priority to

Study	Author(s)	Approach	Notes
infrastructure-related wildlife protection areas: The case of bird electrocution			install mitigation to reduce electrocutions. In areas where data was limited, these findings were then verified through field work. This study is among the first to map sensitivity to electrocution at a 1km resolution. At this resolution, conservation managers, power line companies and other stakeholders can rapidly identify mitigation priorities and complete preliminary assessments of how a new power line development may impact sensitive birds.
Do Power Lines and Protected Areas Present a Catch-22 Situation for Cape Vultures (Gyps coprotheres)?	(Phipps *et al.*, 2013)	Satellite Telemetry	Ten Cape vultures *Gyps coprotheres* were trapped in the Northwest Province of South Africa and fitted with Hawk105 GPS-GSM tags. Data on height above sea level, latitude, longitude, temperature, date, time, flight speed and direction of travel were recorded over a period of one year. This data was used to identify home range size of each individual and how this overlapped with the power line network. Stationary fixes within 50m of a power line were assumed to indicate the bird perching on a power line. The location of recorded vulture deaths at power lines form other monitoring work was also mapped. The research highlighted that vultures spend more than 50% of their time away from protected areas. Vultures appear to be attracted to transmission towers because they provide good alternative roosting sites in the absence of suitable cliff habitat. This preliminary study is therefore an important step toward assessing which sections of the transmission network in the region are to be prioritised for mitigation.
A spatially explicit approach to assess the collision risk between birds and overhead power lines: A case study with the little bustard	(Silva *et al.*, 2014)	Satellite Telemetry	One of the first studies to incorporate satellite telemetry into a risk assessment for birds in the context of transmission lines. Interpolated movement between GPS fixes for tagged little bustards *Tetrax tetrax* in 3d space to identify where the tracks of individuals intersected with the medium tension power line network (15kV – 60kV). Combining data from GPS tags with habitat data, terrain data and population density data allowed a regional map of collision risk to be produced for Alentejo in Portugal. This was then overlaid onto infrastructure data to identify problem power lines. High consistency was found between the model and carcass search data.
Bird and bat species' global vulnerability to collision mortality at wind farms revealed through a trait-based assessment	(Chris B. Thaxter *et al.*, 2017)	Species Distribution based methods	This paper is one of the first to have mapped the sensitivity of birds to wind farm developments at the global scale. The study identified the vulnerability of species and species groups according to recorded mortality at wind farms, wing loading, migration behaviour and a number of other eco-physiological factors. Bird orders were then ranked according to vulnerability to wind farms. The top five most susceptible orders are: Accipitriformes, Eurypygiformes, Bucerotiformes, Ciconiiformes and Charadriiformes. A Bayesian approach was then used to predict global collision risk for 9568 bird and bat species. These results were then mapped at the 5km resolution.
Avian vulnerability to wind farm collision through the year: Insights from lesser black-backed gulls (Larus fuscus) tracked from multiple breeding colonies	(Thaxter, Ross-Smith, *et al.*, 2019)	Risk Mapping	This study was among the first to use GPS tracking data to assess risk for a migratory bird species (Lesser black-backed gull, *Larus Fuscus*) from wind turbines at the flyway scale. The study highlighted risk areas around breeding colonies, along coastlines and within migratory bottlenecks. Defines clear terminology of "sensitivity" to highlight areas where birds could be put at risk by new wind farm development and "vulnerability" to highlight where risks caused by existing infrastructure already exist.

Study	Author(s)	Approach	Notes
Modelling golden eagle habitat selection and flight activity in their home ranges for safer wind farm planning	(Tikkanen *et al.* 2018)	Risk Mapping	This study used GPS data to produce a minimum convex polygons (MCP) of Golden Eagle *Aquila chrysaetos* territories in the Kaustinen region of Finland . These were then used in a resource selection modelling approach to identify which environmental and habitat factors best predicted which areas were most likely to be used by eagles and in which areas they were most likely to be flying at collision height for wind turbines and power lines. This approach could be applied to other areas and species to help identify potential conflicts with wind energy and power line developments.
Reconciling endangered species conservation with wind farm development: Cinereous vultures (Aegypius monachus) in south-eastern Europe	(Vasilakis *et al.*, 2016)	Satellite Telemetry	This study tracked vultures to investigate their flight behaviour and whether there was overlap between areas used by soaring species for thermaling behaviour and areas where wind farms are commonly constructed. The hypothesis being that there is competition between wind farms and soaring migrants. The study found that in moderate wind speeds, there is significant overlap in the 3D space used by vultures and coastal wind farms. Terrain and wind conditions were the key factors determining whether these birds were interacting with wind farms at the danger height.
Modelling the habitat selection of the bearded vulture to predict areas of potential conflict with wind energy development in the Swiss Alps	(Vignali *et al.* 2021)	Risk Mapping	Combined GPS tracking data with citizen science data (eBird observations) Bearded Vultures *Gypaetus barbatusi*. They used a species distribution modelling approach to identify current and potential future conflict areas with wind farm development in the Swiss Alps as the population recovers from a historic decline. The authors concluded that an approach using simple linear distances around nesting sites is both “insufficient and inefficient” as it overly restricts renewables development while not providing sufficient protection for the most suitable areas for Bearded Vultures.

Table 1: Examples of studies most relevant to sensitivity and risk mapping published in the literature as of July 2022. They highlight the increasing use of GPS tracking and citizen science data to complement other methods.

GPS DEVICES OFFER VALUABLE INFORMATION FOR SPATIAL PLANNING OF ENERGY INFRASTRUCTURE

1.4 TRACKING BIRD MOVEMENTS

Our ability to track the movements of birds using tagging, ringing, radio tracking, radar and satellite tag technology in combination with advances in molecular and genetic methods now allows us to study the movements of birds in great detail (Turbek, Scordato and Safran, 2018). Individual birds can be tracked for extended periods using data loggers or satellite tags small enough to attach to the bird's leg, as a backpack or tail feathers without impacting their wellbeing (Daunt *et al.*, 2014; Flack *et al.*, 2016; Fijn *et al.*, 2017; Acácio *et al.*, 2021). Data loggers can be used to record the location of the individual along with other environmental information such as altitude, temperature and movement allowing behaviour of the individual to be inferred (Cook *et al.*, 2014; Gilbert *et al.*, 2016). This behavioural information can in turn be used to identify important ecological areas for these birds such as feeding grounds or areas where birds roost in large numbers (Camphuysen *et al.*, 2012; Shariati *et al.*, 2017). Devices which store the data are often used for species with high site fidelity such as seabirds, or smaller species such as Nightjar where weight is a limiting factor (Evens *et al.*, 2018). This is because they require less power than loggers which transmit live location information so can be a good option where tag retrieval is possible (M. I. Bogdanova et al. 2011; Fijn et al. 2017; Widensaul, 2011). Using loggers can be less expensive compared to tags which send data via GSM or Satellite communications (Allan, Arnould, Martin, & Ritchie, 2013; Widensaul, 2011). This may change as new technologies emerge enabling low power, low-cost data transmission such as via LoRa (Mekki *et al.*, 2019).

There are three main types of bird mounted tracking device utilised in studying movement behaviour of birds: geologgers, VHF radio tags and satellite loggers/tags. Geolocation loggers measure light intensity to determine sunrise, sunset and noon in relation to GMT. This allows calculation of an approximate latitude and longitude (Harris et al. 2015; Widensaul, 2011). Once the logger has been retrieved and the data downloaded the location information can be processed to reveal the daily movements of the individual being studied to within approximately 186km (Widensaul, 2011). These loggers are lightweight and relatively inexpensive allowing large sample sizes and longer deployment to study birds for extended periods (M. I. Bogdanova et al. 2011; Widensaul, 2011). As such these loggers are typically deployed in large numbers to study bird movements over several years (Cook et al. 2014; Harris et al. 2015; Widensaul, 2011). However, they do not provide sufficient resolution to help understand bird movements in relation to wind farms or power lines.

VHF radio tags such as MOTUS do not store any data, they work by emitting a distinct radio signal several times per minute which can then be picked up by receivers. Using multiple receivers, the location of the tracked animal can be typically calculated to within a few kilometres using triangulation (Taylor *et al.*, 2017). Although new techniques are allowing radio tracking systems such as ATLAS (Advanced Tracking and Localisation of Animals in real- life Systems) to achieve position accuracies approaching that of GPS (Global Positioning System) (Beardsworth *et al.*, 2022). These devices allow the movements of animals to be monitored in near real time and the low energy requirements do not require a large battery pack. In turn this allows tags to weigh less than 0.21g (Taylor *et al.*, 2017).

Satellite data loggers utilise the signal from global positioning satellites (Typically ARGOS or GPS) to record accurate location and altitude data for the individual at pre-determined intervals. Satellite tags have improved accuracy over other types of loggers and are therefore more appropriate for studies requiring finer scale study of bird movements. GPS is accurate to within a few metres whereas ARGOS locations are usually only accurate to within a few hundred metres (Costa *et al.*, 2010). The power consumption of these systems can be a limitation, particularly when using GPRS or GSM to transmit the data. It is only with recent developments in solar panels, battery technology and the efficiency of GPS technology that small enough GPS loggers suitable for long term deployment on smaller birds such as lesser kestrel have been available (Limiñana *et al.*, 2012). Some tags simply store this information until such time that recovery is possibly while others transmit the data, permitting near real time tracking of individuals (Braham *et al.*, 2015; Fijn *et al.*, 2017). Typically the data is transmitted via GPRS or GSM over the mobile telephone network but can also be sent via satellite (Iridium, ARGOS) or short range UHF or Zigbee telemetry (typically <1km) such as Pathtrack™ and UVA-BiTs loggers (Bouten, 2018; Evens *et al.*, 2018). New technologies such as LoRaWAN (Long Range Wide Area Networks) are also emerging as low power, lightweight alternatives to GPS-GSM tags (Muteba, Djouani and Olwal, 2019; Dini *et al.*, 2021)

1.4.1 THE LIMITATIONS OF ESTABLISHED METHODS FOR ASSESSING MORTALITY RISK AT WIND FARMS AND POWER LINES

In general, the bulk of studies to date (particularly earlier studies) focus on the mechanics of bird mortality in relation to wind turbines and power lines using traditional survey techniques and retrospective empirical data. Our current understanding of the vulnerability of different species to collision or electrocution, such as a 2005 assessment of annual mortality rates in Italian bird species (Rubolini *et al.*, 2005), is based upon data acquired through labour intensive carcass count studies (Schutgens, Shaw and Ryan, 2014). Whereas knowledge of avoidance rates has been largely accumulated through detailed laboratory based study of bird physiology and behaviour in combination with modelling of data gathered through vantage point surveys looking at bird behaviour in relation to wind farm or power line installations (Johnston *et al.*, 2014). While the conclusions drawn from these studies are invaluable they require large inputs of time, money and personnel to perform on large enough spatial scales to allow the production of a sensitivity map at the continent scale at a useful spatial resolution (Bernardino *et al.*, 2018b).

For example, a study commissioned by Scottish Natural Heritage found that proximity to specially protected areas (SPAs for geese) was a predicting factor for whether flocks of geese were at danger height or not (Patterson, 2015). This was based upon data compiled from pre-construction vantage point surveys completed at proposed wind farms at varying distances (0 – 12km) from the nearest goose SPA as well as dedicated surveys on known flight routes between goose roosts and feeding sites. The study found that geese undertaking longer journeys in bigger flocks were more likely to be flying above the danger height associated with wind turbines (150m) whereas smaller flocks, travelling shorter distances of only a few kilometres between feeding and roosting sites were more likely to be flying at less than 150m. Geese were most vulnerable within the first few hundred metres from leaving the SPA where they were still gaining altitude and flying directly at rotor height for most commercial scale wind farms (Patterson, 2015).

The reliance upon data collected by observers in the field means that repeating this same study in another geographical location would be very labour-intensive, limiting the ability to replicate this at larger geographic scales or example to identify high risk areas across a whole flyway.

1.4.2 HOW GPS TECHNOLOGY CAN IMPROVE OUR SPATIAL UNDERSTANDING OF COLLISION RISK

Site focussed assessments using vantage point survey and breeding bird survey of new wind or power line developments will continue to be an important part of ecological impact assessments (CIEEM, 2018). However, as GPS and other remotely sensed data on bird movements such as radar become more available it has the potential to revolutionise how we perform the spatial planning and preliminary ecological assessments of energy infrastructure development proposals (Bernardino *et al.* 2018). This in turn will lead to better survey design and help conservation organisations better assess the risks associated with energy infrastructure at local and regional scales (Prinsen *et al.*, 2012). It can also help energy companies seeking to comply with wildlife legislation or reduce the damage cause to their infrastructure by interactions with birds through more targeted mitigation strategies (Guil *et al.*, 2017). For example, (García-Alfonso *et al.*, 2021) used GPS tracking data from 49 tagged Canarian Egyptian Vultures *Neophron percnopterus majorensis* to understand the environmental factors which make it more likely for vultures to perch on or collide with power lines. The results predicted actual mortality reasonably well and highlighted how installing mitigation at just 6% of the pylons could reduce mortality risk by 50% (García-Alfonso *et al.*, 2021).

Greater integration of GPS tracking data into sensitivity maps will help conservation agencies identify those areas where it is not appropriate to build new energy infrastructure (Bernardino *et al.*, 2018b). Examples include Tikkanen *et al*., 2018 to map golden eagle home ranges; Thaxter, Ross-Smith, *et al*., 2019 to map where birds are most sensitive to collision risk along their migratory route and Vignali *et al*., 2021 who combined GPS and citizen science data to forecast potential conflict areas between wind farm development and a recovering population of Bearded Vultures *Gypaetus barbatus* (Table 1). One feature of GPS data which, until recently, has been underutilised in the literature, is that it can help us distinguish between areas regularly used by birds at danger height from those areas where birds often fly over but rarely at danger height (Scacco *et al.*, 2019). In turn this can facilitate decisions about the most appropriate course of mitigation action for the existing or proposed energy development. (Santos *et al.*, 2017; Scacco *et al.*, 2019).

As outlined in the mitigation hierarchy (Figure 2) proposed by (Arnett and May, 2016) most effective mitigation option is to adjust the location of the development to avoid the most sensitive areas (Hernández-Pliego *et al.*, 2015). In some cases it might be appropriate to bury cables (Silva *et al.*, 2010) or pursue a strategy of micro-siting of individual turbines or pylons to reduce collision risk (Hanssen, May and Nygård, 2020). Where these options are not feasible, or where the infrastructure already exists we can implement marking of power lines and turbines to make the cables and rotor blades more visible and insulate the conductors on power line masts (Frost, 2008; Dixon *et al.*, 2018; May, Nygård, Falkdalen, Åström, Hamre and Bård G. Stokke, 2020). It is also possible to pursue a strategy of habitat modification to encourage birds to nest and forage away from power lines (Polat *et al.*, 2016) or in some cases it may be beneficial to install dedicated nesting platforms or perches which can be of benefit to bird populations (López-López *et al.*, 2011; Moreira *et al.*, 2017). In the case of wind farms, active mitigation strategies are now being investigated to reduce the risk to birds (Köppel, 2015). These autonomous monitoring systems use radar, cameras or LIDAR can detect birds and automatically slow or stop the turbine blades until the flock has safely passed through the wind farm (Fijn *et al.*, 2015; McClure, Martinson and Allison, 2018; McClure *et al.*, 2021). In southern Portugal and Spain where shutdown systems have been used for several years, they have significantly reduced collision mortality of large soaring birds such as Griffon Vultures *Gyps fulvus*, particularly during the Autumn migration (Ferrer *et al.*, 2022).

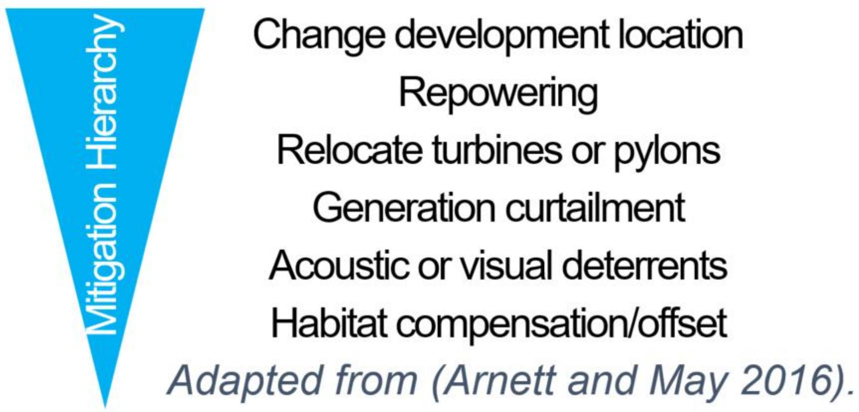

Figure 2: The mitigation hierarchy for energy infrastructure developments, adapted from the table in Arnett and May 2016.

1.4.3 LIVE DETECTION OF COLLISIONS

The next step in using GPS loggers is to detect mortality events using on board accelerometer technology however this work is still at an experimental stage (Sergio *et al.*, 2018). This is of interest to ecologists working on migration behaviour as well as those working to deter illegal shooting of raptors and waterfowl. In the context of energy infrastructure, the live detection of collisions in real time would help verify model based predictions about where birds are most at risk from collision or electrocution (Bernardino *et al.*, 2018b). A similar approach has been used to help detect landslides and boulder movements using accelerometer triggering whereby a force above a given threshold activates the tag which then records and sends the movement signature captured by the accelerometer (Dini *et al.*, 2021).

1.5 CONCLUSIONS AND KNOWLEDGE GAPS

We now have a good understanding of which species groups are most vulnerable to energy infrastructure, particularly in relation to collision risks (Janss, 2000; Péron *et al.*, 2013; Chris B Thaxter *et al.*, 2017). We broadly understand the distributions of these species. Therefore we are able to provide approximate estimates of collision risk in relation to where these vulnerable species or species groups are present in high numbers (Thaxter *et al.*, 2017). We have also developed robust methods for assessing impacts at the site level (May *et al.*, 2010; Kleyheeg-Hhartman *et al.*, 2018; Kettel *et al.*, 2022). However, to date, relatively few studies have assessed the potential cumulative impact of wind and power line developments at the flyway scale. Or utilised GPS tracking data to understand birds' movements in relation to proposed and existing developments as demonstrated by (Santos *et al.*, 2017; Hanssen, May and Nygård, 2020; Therkildsen *et al.*, 2021) and others. GPS telemetry is potentially a powerful tool to help pinpoint with more precision where birds are at most risk of mortality over larger geographical areas than is possible with survey based (Silva *et al.*, 2014; Thaxter, Ross-Smith, *et al.*, 2019). As the pace of renewable energy deployment accelerates it is vital that we begin to map sensitivity to mortality risk for birds at finer resolutions and at greater spatial scales to help proactively target mitigation and spatial planning of renewable energy developments. Failure to do so could lead to renewables development occurring in highly sensitive areas without sufficient mitigation. As highlighted by Tikkanen *et al*., 2018 and Vignali *et al.*, 2021 among others, a simple approach of excluding development within a certain distance of breeding sites is both inefficient in terms of excluding large areas from development while providing insufficient protection for the birds.

The use of GPS technology and other new methods for monitoring mortality risk at EI installations is vital if we are to keep pace with the growing renewable energy sector (Soanes *et al.*, 2013). There are already several hundred GPS tracking studies of birds published on Movebank (Movebank, 2019); researchers should be encouraged to share their GPS data on this platform to enable other researchers to make use of it. Work will also be needed to ground truth spatial models of bird sensitivity to power line and wind farm developments. Current work to detect mortality using satellite telemetry and on–board accelerometer data in combination with traditional field surveys is likely to help ground truth these sensitivity maps. There is a strong bias in the tracking data toward larger species of bird because GPS loggers were too heavy to deploy on smaller species up until recently (Bridge *et al.*, 2011). Advances in tracking methods to reduce the power requirements of loggers can help us to better understand the behaviour of birds in relation to wind farms and power lines (Santos *et al.*, 2017; C. B. Thaxter *et al.*, 2018).

Another issue is the lack of a central database for transmission and distribution network data and many power companies fail to make their information available to researchers. In countries such as the UK, Netherlands, Spain and Portugal it would be possible to obtain detailed spatial data on the power line network but in Northern Africa and large parts of Europe this data is lacking. Data sources such as OpenStreetMap (Garret, 2018) can be used however the rate at which this is updated is often significantly behind the rate at which new energy infrastructure is constructed (Brovelli and Zamboni, 2018). There are also significant gaps and inaccuracies in the data available to researchers about the location and status of wind turbines, particularly outside of Europe. The methods used by Dunnett *et al.*, 2020 to compile a data set of wind turbine locations provides a potential solution however this relies heavily on OpenStreetMap data rather than data from energy grid operators.

1.6 MOTIVATION AND RATIONALE OF THESIS DATA CHAPTERS

The central aim of NEXUSS (Next Generation Unmanned Systems Science) CDT programme was to determine how emerging autonomous technologies can help understand and find solutions to environmental problems (UKRI, 2017). To achieve this, NEXUSS CDT PhD candidates were encouraged to foster interdisciplinary approaches and collaborations between environmental scientists and engineers. This PhD project was funded in response to calls from the wider research community to help understand how to make use of GPS tracking data to better understand collision risks from renewables (Bernardino *et al.*, 2018b) and the need to develop and test new tracking solutions for birds and other animals (Ripperger *et al.*, 2020; Acácio *et al.*, 2021; Wild *et al.*, 2022).

Chapter 2: Hotspots in the grid: avian sensitivity and vulnerability to collisions risk from energy infrastructure interactions in Europe and North Africa

By combining GPS tracking data with altitude information available on Movebank for 27 species and using sensitivity mapping approaches we aimed to identify areas where wind turbines and power lines pose the greatest threat, in terms of collision risk to birds.

In turn these sensitivity maps can help developers avoid potential collision risk hotspots, inform preliminary ecological impact assessments, and guide the deployment of targeted mitigation measures to reduce risks where conflicts already exist.

Chapter 3: In the Danger Zone: Predictive Modelling of Sensitivity to Collision Risk

This chapter investigates how environmental variables, particularly uplift and land cover information, can be used to predict the likelihood of birds being present at danger height for wind turbines and power lines. These models were built for two case studies, to produce a predicted sensitivity to collision risk surface for White Storks *Ciconia ciconia* and Little Bustards *Tetrax tetrax* within their know breeding, migration and wintering distributions.

Chapter 4: Characterisation of a new lightweight LoRaWAN GPS biologger and deployment on Griffon Vultures *Gyps fulvus*

This chapter describes a new bird tracking system developed during this PhD. It describes the performance and potential applications of a new type of GPS tracker which uses LoRa (long range) to transmit data over long distances via LoRaWAN (a long-range wide area network) which together form a type of LPWA (low power, wide area) system for sending and receiving data over large distances. This method of data transmission uses less energy than other methods such as GSM (global system for mobile communication) allowing for smaller batteries and therefore tags (<5g). In turn this allows a greater range of species to be tracked over large areas without the need to physically retrieve the device from the animal. LoRa is also very inexpensive in terms of data costs. This chapter describes the results of a series of tests to evaluate the performance of the GPS-LoRa tags in terms of their GPS accuracy and transmission range. This has the potential to help fill gaps in the tracking data and begin to address the bias toward larger species in tracking studies.

Chapter 5: Bird Strike: remote sensing of bird collisions using accelerometer-based event triggering

This chapter tackles a technology gap: the ability to detect collisions in real time. It describes the results of experiments which test the ability of the GPS-LoRa tags to detect collisions using the onboard accelerometer. The results of these experiments can help inform other researchers who may wish to use accelerometery to remotely detect bird mortality. In the context of assessing the impact of the wider aims of the thesis, this has the potential to help validate collision risk maps and highlight problem areas where birds consistently collide with wind farms and power lines or are electrocuted on power lines.

1.7 REFERENCES

2009/147/EC, C.D. (2010) 'Directive 2009/147/EC of the European Parliament and of the Council on the conservation of wild birds', Official Journal of the European Union, L 20, pp. 7–25. Available at: https://doi.org/10.1126/science.aah3404.

Acácio, M. et al. (2021) Quantifying the performance of a solar GPS/GPRS tracking device: fix interval, but not deployment on birds, decreases accuracy and precision. University of East Anglia.

Acácio, M. et al. (2022) 'Timing is critical: consequences of asynchronous migration for the performance and destination of a long-distance migrant', Movement Ecology, 10(1), pp. 1–16. Available at: https://doi.org/10.1186/s40462-022-00328-3.

Agudelo, M.S. et al. (2021) 'Post-construction bird and bat fatality monitoring studies at wind energy projects in Latin America: A summary and review', Heliyon, 7(6), p. e07251. Available at: https://doi.org/10.1016/j.heliyon.2021.e07251.

Ainsworth, D., Collins, T. and D'Amico, F. (2022) 'Convention on Biological Diversity COP15: Nations Adopt Four Goals, 23 Targets for 2030 In Landmark UN Biodiversity Agreement', in. Montreal, Canada: United Nations. Available at: https://prod.drupal.www.infra.cbd.int/sites/default/files/2022-12/221219-CBD-PressRelease-COP15-Final_0.pdf.

Alerstam, T. et al. (2007) 'Flight Speeds among Bird Species: Allometric and Phylogenetic Effects', PLoS biology, 5(8), p. e197. Available at: https://doi.org/10.1371/journal.pbio.0050197.

Angelov, I., Hashim, I. and Oppel, S. (2013) 'Persistent electrocution mortality of Egyptian Vultures Neophron percnopterus over 28 years in East Africa', Bird Conservation International, 23(1), pp. 1–6. Available at: https://doi.org/10.1017/S0959270912000123.

Arnett, E.B. and May, R.F. (2016) 'Mitigating wind energy impacts on wildlife: Approaches for multiple taxa', Human-Wildlife Interactions, 10(1), pp. 28–41. Available at: https://doi.org/10.26077/1jeg-7r13.

Astiaso Garcia, D. et al. (2015) 'Analysis of wind farm effects on the surrounding environment : Assessing population trends of breeding passerines', Renewable Energy, 80, pp. 190–196. Available at: https://doi.org/10.1016/j.renene.2015.02.004.

Band, B. (2012) 'Using a collision risk model to assess bird collision risks for offshore windfarms', 02(March), p. 62. Available at: https://www.bto.org/sites/default/files/u28/downloads/Projects/Final_Report_SOSS02_Band1ModelGuidance.pdf.

Barrios, L. and Rodríguez, A. (2004) 'Behavioural and environmental correlates of soaring-bird mortality at on-shore wind turbines', Journal of Applied Ecology, 41(1), pp. 72–81. Available at: https://doi.org/10.1111/j.1365-2664.2004.00876.x.

Bassi, E. et al. (2002) 'Eagle Owl Bubo bubo and power line interactions in the Italian Alps', Bird Conservation International, 11(04), pp. 319–324. Available at: https://doi.org/10.1017/s0959270901000363.

Beardsworth, C.E. et al. (2022) 'Validating ATLAS: A regional-scale high-throughput tracking system', Methods in Ecology and Evolution, 13(9), pp. 1990–2004. Available at: https://doi.org/10.1111/2041-210X.13913.

Bernardino, J. et al. (2018a) 'Bird collisions with power lines: State of the art and priority areas for research', Biological Conservation, 222(March), pp. 1–13. Available at: https://doi.org/10.1016/j.biocon.2018.02.029.

Bernardino, J. et al. (2018b) 'Bird collisions with power lines: State of the art and priority areas for research', Biological Conservation, 222(March), pp. 1–13. Available at: https://doi.org/10.1016/j.biocon.2018.02.029.

Bevanger, K. (1978) 'Bird interactions with utility structures : collision and electrocution , causes and mitigating measures', IBIS, 136, pp. 412–425.

Bevanger, K. (1995) 'Estimates and population consequences of tetraonid mortality caused by collisions with high tension power lines in Norway', Journal of Applied Ecology, 32(4), pp. 745–753. Available at: https://doi.org/10.2307/2404814.

Bevanger, K. (1998) 'Biological and conservation aspects of bird mortality caused by electricity power lines: A review', Biological Conservation, 86(1), pp. 67–76. Available at: https://doi.org/10.1016/S0006-3207(97)00176-6.

Bevanger, K. and Brøseth, H. (2004) 'Impact of power lines on bird mortality in a subalpine area', Animal Biodiversity and Conservation, 27(2), pp. 67–77. Available at: https://doi.org/10.1021/cm101132g.

Birdlife International (2022) State of the world's birds. Cambridge, UK.

BirdLife International (2015) Migratory Soaring Birds Project: Soaring Bird Sensitivity Map. Available at: http://migratorysoaringbirds.undp.birdlife.org/en/sensitivity-map (Accessed: 3 November 2019).

Blackwell, B.F. et al. (2009) 'Avian visual system configuration and behavioural response to object approach', Animal Behaviour, 77(3), pp. 673–684. Available at: https://doi.org/10.1016/j.anbehav.2008.11.017.

Blary, C. (2022) 'Bird contrast sensitivity and wind turbines collisions', in CWW Wind Energy and Wildlife Conference. Egmond aan Zee. Available at: https://cww2022-live.org/livestream-tuesday-5-april-2022/#ROOM2.

Bouten, W. (2018) UvA-BiTS Bird Tracking System, University of Amsterdam. Available at: http://www.uva-bits.nl/.

Bradbury, G. et al. (2014) 'Mapping Seabird Sensitivity to offshore wind farms', PLoS ONE, 9(9). Available at: https://doi.org/10.1371/journal.pone.0106366.

Braham, M. et al. (2015) ‘Home in the heat: Dramatic seasonal variation in home range of desert golden eagles informs management for renewable energy development’, Biological Conservation, 186, pp. 225–232. Available at: https://doi.org/10.1016/j.biocon.2015.03.020.

Bridge, E.S. et al. (2011) ‘Technology on the move: Recent and forthcoming innovations for tracking migratory birds’, BioScience, 61(9), pp. 689–698. Available at: https://doi.org/10.1525/bio.2011.61.9.7.

Bright, J. et al. (2008) ‘Map of bird sensitivities to wind farms in Scotland: A tool to aid planning and conservation’, Biological Conservation, 141(9), pp. 2342–2356. Available at: https://doi.org/10.1016/j.biocon.2008.06.029.

Brovelli, M. and Zamboni, G. (2018) ‘A New Method for the Assessment of Spatial Accuracy and Completeness of OpenStreetMap Building Footprints’, ISPRS International Journal of Geo-Information, 7(8), p. 289. Available at: https://doi.org/10.3390/ijgi7080289.

Buchan, C. et al. (2022) ‘Spatially explicit risk mapping reveals direct anthropogenic impacts on migratory birds’, Global Ecology and Biogeography, (May), pp. 1–19. Available at: https://doi.org/10.1111/geb.13551.

Buechley, E.R. et al. (2018) ‘Identifying Critical Migratory Bottlenecks and High-Use Areas for an Endangered Migratory Soaring Bird Across Three Continents’, Journal of Avian Biology, e01629, pp. 1–13. Available at: https://doi.org/10.1111/jav.01629.

Burns, F. et al. (2021) ‘Abundance decline in the avifauna of the European Union reveals cross-continental similarities in biodiversity change’, Ecology and Evolution, 11(23), pp. 16647–16660. Available at: https://doi.org/10.1002/ece3.8282.

Camphuysen, K.C.J. et al. (2012) ‘Identifying ecologically important marine areas for seabirds using behavioural information in combination with distribution patterns’, Biological Conservation, 156, pp. 22–29. Available at: https://doi.org/10.1016/j.biocon.2011.12.024.

CIEEM (2018) Guidelines for Ecological Impact Assessment in the UK and Ireland. Winchester, Hampshire. Available at: https://www.cieem.net/data/files/ECIA Guidelines.pdf.

Cook, A.S.C.P. et al. (2014) 'Indicators of seabird reproductive performance demonstrate the impact of commercial fisheries on seabird populations in the North Sea', Ecological Indicators, 38, pp. 1–11. Available at: https://doi.org/10.1016/j.ecolind.2013.10.027.

Cook, A.S.C.P. et al. (2018) 'Quantifying avian avoidance of offshore wind turbines: Current evidence and key knowledge gaps', Marine Environmental Research, 140(March), pp. 278–288. Available at: https://doi.org/10.1016/j.marenvres.2018.06.017.

Costa, D.P. et al. (2010) 'Accuracy of ARGOS locations of pinnipeds at-sea estimated using fastloc GPS', PLoS ONE, 5(1). Available at: https://doi.org/10.1371/journal.pone.0008677.

Croft, S.A. (2014) Modelling collective motion and obstacle avoidance to assess avian collision risk with wind turbines. University of York.

D.K. Aswal , Ajay Singh, Shahswati Sen, Manmeet Kaur, C.S. Viswandham, G.L. Goswami, S.K.G. (2022) 'Power lines and birds: An overlooked threat in South America', Perspectives in Ecology and Conservation, In Press, pp. 1–11. Available at: https://doi.org/10.1016/j.pecon.2022.10.005.

Daunt, F. et al. (2014) 'Longitudinal bio-logging reveals interplay between extrinsic and intrinsic carry-over effects in a long-lived vertebrate', Ecology, 95(8), pp. 2077–2083. Available at: https://doi.org/10.1890/13-1797.1.

Dellasala, D.A., Goldstein, M.I. and Elias, S.A. (2018) 'Global Change Impacts on the Biosphere', Encyclopedia of the Anthropocene, pp. 81–94. Available at: https://doi.org/10.1016/B978-0-12-809665-9.09532-X.

Desholm, M. (2009) 'Avian sensitivity to mortality : Prioritising migratory bird species for assessment at proposed wind farms', Journal of Environmental Management, 90(8), pp. 2672–2679. Available at: https://doi.org/10.1016/j.jenvman.2009.02.005.

Diesendorf, M. and Elliston, B. (2018) 'The feasibility of 100% renewable electricity systems: A response to critics', Renewable and Sustainable Energy Reviews, 93(October 2017), pp. 318–330. Available at: https://doi.org/10.1016/j.rser.2018.05.042.

Dini, B. et al. (2021) 'Development of smart boulders to monitor mass movements via the Internet of Things: A pilot study in Nepal', Earth Surface Dynamics, 9(2), pp. 295–315. Available at: https://doi.org/10.5194/esurf-9-295-2021.

Dixon, A. et al. (2018) ‘Efficacy of a mitigation method to reduce raptor electrocution at an electricity distribution line in Mongolia’, Conservation Evidence, 15, pp. 50–53. Available at: https://www.conservationevidence.com/individual-study/6861.

Donázar, J.A. et al. (2002) ‘Conservation status and limiting factors in the endangered population of Egyptian vulture (Neophron percnopterus) in the Canary Islands’, Biological Conservation, 107(1), pp. 89–97. Available at: https://doi.org/10.1016/S0006-3207(02)00049-6.

Dunnett, S. et al. (2020) ‘Harmonised global datasets of wind and solar farm locations and power’, Scientific Data, 7(1), p. 130. Available at: https://doi.org/10.1038/s41597-020-0469-8.

Elias, S.A. (2018) ‘Global Change Impacts on The Biosphere’, Encyclopedia of the Anthropocene, 2, pp. 81–94. Available at: https://doi.org/10.1016/B978-0-12-809665-9.09532-X.

European Climate Foundation (2018) ‘Net Zero by 2050: From whether to how - Zero emission Pathways to the Europe we want’, (September), p. 66.

European Commission (2018) Guidance on Energy Transmission Infrastructure and EU nature legislation. Available at: http://ec.europa.eu/environment/nature/natura2000/management/docs/Energy guidance and EU Nature legislation.pdf.

European Commission (2020) ‘Stepping up Europe’s 2030 climate ambition Investing in a climate-neutral future for the benefit of our people’, Journal of Chemical Information and Modeling, 53(9), pp. 1689–1699. Available at: https://knowledge4policy.ec.europa.eu/publication/communication-com2020562-stepping-europe’s-2030-climate-ambition-investing-climate_en#:~:text=17 September 2020-,Communication COM%2F2020%2F562%3A Stepping up Europe’s 2030 climate,the benefit of our peopl.

European Commission (2022) Communication from the Commission to the European Parliament, the European Council, The Cuncil, The European economic and social committee and the committee of the regions. Belgium. Available at: https://eur-lex.europa.eu/legal-content/EN/TXT/?uri=COM%3A2022%3A230%3AFIN&qid=1653033742483.

European Environment Agency (2017) Trends and projections in Europe 2017. Tracking progress towards Europe’s climate and energy targets, EEA Report 6/2014. Available at: https://doi.org/10.1016/j.watres.2007.01.052.

Evens, R. et al. (2018) ‘An effective, low-tech drop-off solution to facilitate the retrieval of data loggers in animal-tracking studies’, Ringing and Migration, 33(1), pp. 10–18. Available at: https://doi.org/10.1080/03078698.2018.1521116.

Ferreira, D. et al. (2019) ‘Is wind energy increasing the impact of socio-ecological change on Mediterranean mountain ecosystems? Insights from a modelling study relating wind power boost options with a declining species’, Journal of Environmental Management, 238(October 2018), pp. 283–295. Available at: https://doi.org/10.1016/j.jenvman.2019.02.127.

Ferrer, M. et al. (2022) ‘Significant decline of Griffon Vulture collision mortality in wind farms during 13-year of a selective turbine stopping protocol’, Global Ecology and Conservation, 38(June), p. e02203. Available at: https://doi.org/10.1016/j.gecco.2022.e02203.

Ferrer, M. and Hiraldo, F. (1992) ‘Man-induced sex-biased mortality in the Spanish imperial eagle’, Biological Conservation, 60(1), pp. 57–60. Available at: https://doi.org/10.1016/0006-3207(92)90799-S.

Fijn, R.C. et al. (2015) ‘Bird movements at rotor heights measured continuously with vertical radar at a Dutch offshore wind farm’, Ibis, 157(3), pp. 558–566. Available at: https://doi.org/10.1111/ibi.12259.

Fijn, R.C. et al. (2017) ‘GPS-tracking and colony observations reveal variation in offshore habitat use and foraging ecology of breeding Sandwich Terns’, Journal of Sea Research, 127, pp. 203–211. Available at: https://doi.org/10.1016/j.seares.2016.11.005.

Flack, A. et al. (2016) ‘Costs of migratory decisions: A comparison across eight white stork populations’, Science Advances, 2(1), pp. e1500931–e1500931. Available at: https://doi.org/10.1126/sciadv.1500931.

Frost, D. (2008) ‘The use of “flight diverters” reduces mute swan Cygnus olor collision with power lines at Abberton Reservoir, Essex, England’, Conservation Evidence, 5, pp. 83–91. Available at: www.ConservationEvidence.com.

Furness, R.W., Wade, H.M. and Masden, E.A. (2013) ‘Assessing vulnerability of marine bird populations to offshore wind farms’, Journal of Environmental Management, 119, pp. 56–66. Available at: https://doi.org/10.1016/j.jenvman.2013.01.025.

García-Alfonso, M. et al. (2021) ‘Disentangling drivers of power line use by vultures: Potential to reduce electrocutions’, Science of the Total Environment, 793(2021), p. 148534. Available at: https://doi.org/10.1016/j.scitotenv.2021.148534.

Garret, R. (2018) The Open-source Infrastructure Project, OpenInfra. Available at: https://openinframap.org (Accessed: 5 November 2018).

Gilbert, N.I. (2015) Movement and foraging ecology of partially migrant birds in a changing world. University of East Anglia. Available at: https://ueaeprints.uea.ac.uk/59626/1/N_Gilbert_PhD_Thesis_Movement_and_foraging_ecology_of_partially_migrant_birds_in_a_changing_world.pdf.

Gilbert, N.I. et al. (2016) ‘Are white storks addicted to junk food? Impacts of landfill use on the movement and behaviour of resident white storks (Ciconia ciconia) from a partially migratory population’, Movement Ecology, 4(1), p. 7. Available at: https://doi.org/10.1186/s40462-016-0070-0.

Grooten, M. and Almond, R.E.A. (2018) Living Planet Report 2018 : Aiming higher (Full Report). Gland, Switzerland. Available at: https://www.zsl.org/sites/default/files/Living Planet Report 2018 - Full Report.pdf.

Guil, F. et al. (2017) ‘Wildfires as collateral effects of wildlife electrocution: An economic approach to the situation in Spain in recent years’. Available at: https://doi.org/10.1016/j.scitotenv.2017.12.242.

Guil, F., Colomer, M.À. and Moreno-opo, R. (2015) ‘Space–time trends in Spanish bird electrocution rates from alternative information sources’, Global Ecology and Conservation, 3, pp. 379–388. Available at: https://doi.org/10.1016/j.gecco.2015.01.005.

Gyimesi, A. and Prinsen, H.A.M. (2015) ‘Guidance on appropriate means of impact assessment of electricity power grids on migratory soaring birds in the Rift Valley / red Sea Flyway - Final Report’, p. 56.

Hanssen, F., May, R. and Nygård, T. (2020) ‘High-Resolution Modeling of Uplift Landscapes can Inform Micrositing of Wind Turbines for Soaring Raptors’, Environmental Management, 66(3), pp. 319–332. Available at: https://doi.org/10.1007/s00267-020-01318-0.

Hernández-matías, A. et al. (2015) ‘Electrocution threatens the viability of populations of the endangered Bonelli’s eagle (Aquila fasciata) in Southern Europe’, BIOC, 191, pp. 110–116. Available at: https://doi.org/10.1016/j.biocon.2015.06.028.

Hernández-Pliego, J. et al. (2015) ‘Effects of wind farms on Montagu’s harrier (Circus pygargus) in southern Spain’, Biological Conservation, 191, pp. 452–458. Available at: https://doi.org/10.1016/j.biocon.2015.07.040.

Heuck, C. et al. (2019) ‘Wind turbines in high quality habitat cause disproportionate increases in collision mortality of the white-tailed eagle’, Biological Conservation, 236(August 2018), pp. 44–51. Available at: https://doi.org/10.1016/j.biocon.2019.05.018.

Hewson, C.M. et al. (2016) ‘Population decline is linked to migration route in the Common Cuckoo’, Nature Communications, 7, pp. 1–8. Available at: https://doi.org/10.1038/ncomms12296.

Hull, C.L. et al. (2013) ‘Avian collisions at two wind farms in Tasmania, Australia: Taxonomic and ecological characteristics of colliders versus non-colliders’, New Zealand Journal of Zoology, 40(1), pp. 47–62. Available at: https://doi.org/10.1080/03014223.2012.757243.

Husby, M. and Pearson, M. (2022) ‘Wind Farms and Power Lines Have Negative Effects on Territory Occupancy in Eurasian Eagle Owls (Bubo bubo)’, Animals, 12(9), pp. 1–13. Available at: https://doi.org/10.3390/ani12091089.

IEA (2020) Onshore Wind: Tracking Report. Paris. Available at: https://www.iea.org/reports/onshore-wind.

IEA (2022) Wind Electricity Technological Outlook. Paris. Available at: https://www.iea.org/reports/wind-electricity.

IPBES (2019) The global assessment report on Biodiversity and Ecosystems. Edited by E.S. Brondízio, J. Settele, and N. H., T. Bonn, Germany: IPBES secretariat. Available at: https://zenodo.org/record/6417333#.Y8niUBXP02w.

IPCC (2014) Climate Change 2014: Synthesis Report, Contribution of Working Groups I, II and III to the Fifth Assessment Report of the Intergovernmental Panel on Climate Change. Available at: https://doi.org/10.1017/CBO9781107415324.

IPCC (2018) ‘IPCC special report on the impacts of global warming of 1.5 °C - Summary for policy makers’, (October 2018). Available at: http://www.ipcc.ch/report/sr15/.

IPCC (2022a) Summary for Policy Makers Climate Change 2022: Impacts, Adaptation, and Vulnerability. Contribution of Working Group II to the Sixth Assessment Report of the Intergovernmental Panel on Climate Change. Cambridge. Available at: https://www.ipcc.ch/report/ar6/wg2/about/how-to-cite-this-report/.

IPCC (2022b) Summary for Policymakers: The Physical Science Basis. Contribution of Working Group I to the Sixth Assessment Report of the Intergovernmental Panel on Climate Change, Cambridge University Press. Cambridge, UK. Available at: https://doi.org/10.1017/CBO9781139177245.003.

IPCC (2022c) Summary for Policymakers. In: Climate Change 2022: Mitigation of Climate Change. Contribution of Working Group III to the Sixth Assessment Report of the Intergovernmental Panel on Climate Change, Cambridge University Press. Cambridge, UK. Available at: https://www.ipcc.ch/report/ar6/wg3/about/how-to-cite-this-report.

Jaffré, M. et al. (2013) ‘Long-term phenological shifts in raptor migration and climate’, PLoS ONE, 8(11), pp. 8–15. Available at: https://doi.org/10.1371/journal.pone.0079112.

Janss, G.F.E. (2000) ‘Avian mortality from power lines: A morphologic approach of a species-specific mortality’, Biological Conservation, 95(3), pp. 353–359. Available at: https://doi.org/10.1016/S0006-3207(00)00021-5.

Jenkins, A.R. et al. (2011) ‘Estimating the impacts of power line collisions on Ludwig"s Bustards Neotis ludwigii’, Bird Conservation International, 21(3), pp. 303–310. Available at: https://doi.org/10.1017/S0959270911000128.

Jiguet, F. et al. (2021) ‘GPS tracking data can document wind turbine interactions: Evidence from a GPS-tagged Eurasian curlew’, Forensic Science International: Animals and Environments, 1, p. 100036. Available at: https://doi.org/10.1016/j.fsiae.2021.100036.

Johnston, A. et al. (2014) ‘Modelling flight heights of marine birds to more accurately assess collision risk with offshore wind turbines’, Journal of Applied Ecology, 51(1), pp. 31–41. Available at: https://doi.org/10.1111/1365-2664.12191.

Kettel, E.F. et al. (2022) ‘Better utilisation and transparency of bird data collected by powerline companies’, Journal of Environmental Management, 302(PA), p. 114063. Available at: https://doi.org/10.1016/j.jenvman.2021.114063.

Kiesecker, J. et al. (2019) 'Hitting the Target but Missing the Mark: Unintended Environmental Consequences of the Paris Climate Agreement', Frontiers in Environmental Science, 7(October). Available at: https://doi.org/10.3389/fenvs.2019.00151.

Kleyheeg-Hhartman, J.C. et al. (2018) 'Predicting bird collisions with wind turbines: Comparison of the new empirical Flux Collision Model with the SOSS Band model', Ecological Modelling, 387(March), pp. 144–153. Available at: https://doi.org/10.1016/j.ecolmodel.2018.06.025.

Köppel, J. (2015) Wind Energy and Wildlife Interactions: Presentations from the CWW2015 Conference, Wind Energy and Wildlife Interactions. Cham, Switzerland: Springer. Available at: https://doi.org/10.1007/978-3-319-51272-3.

Krijgsveld, K.L. et al. (2009) 'Collision Risk of Birds with Modern Large Wind Turbines', Ardea, 97(3), pp. 357–366. Available at: https://doi.org/10.5253/078.097.0311.

Lameris, T.K. et al. (2018) 'Arctic Geese Tune Migration to a Warming Climate but Still Suffer from a Phenological Mismatch', Current Biology, pp. 2467–2473. Available at: https://doi.org/10.1016/j.cub.2018.05.077.

Leclère, D. et al. (2020) 'Bending the curve of terrestrial biodiversity needs an integrated strategy', Nature, 585(October 2018). Available at: https://doi.org/10.1038/s41586-020-2705-y.

Lehman, R.N., Kennedy, P.L. and Savidge, J.A. (2007) 'The state of the art in raptor electrocution research: A global review', Biological Conservation, 135(4), pp. 459–474. Available at: https://doi.org/10.1016/j.biocon.2006.10.039.

Limiñana, R. et al. (2012) 'Mapping the Migratory Routes and Wintering Areas of Lesser Kestrels Falco naumanni : New Insights from Satellite Telemetry', Ibis, 154, pp. 389–399.

Lines, P. (2022) 'Power Lines and Birds : Drivers of Conflict-Prone Use of Pylons by Nesting White Storks (Ciconia ciconia)', pp. 1–13.

López-López, P. et al. (2011) 'Solving man-induced large-scale conservation problems: The Spanish Imperial Eagle and power lines', PLoS ONE, 6(3). Available at: https://doi.org/10.1371/journal.pone.0017196.

Loss, S.R. (2016) 'Avian interactions with energy infrastructure in the context of other anthropogenic threats', The Condor, 118(2), pp. 424–432. Available at: https://doi.org/10.1650/condor-16-12.1.

Loss, S.R., Will, T. and Marra, P.P. (2014) 'Refining estimates of bird collision and electrocution mortality at power lines in the United States', PLoS ONE, 9(7), pp. 26–28. Available at: https://doi.org/10.1371/journal.pone.0101565.

Lucas, M. De et al. (2012) 'Griffon vulture mortality at wind farms in southern Spain: Distribution of fatalities and active mitigation measures', Biological Conservation, 147(1), pp. 184–189. Available at: https://doi.org/10.1016/j.biocon.2011.12.029.

Mainwaring, M.C. (2015) 'The use of man-made structures as nesting sites by birds: A review of the costs and benefits', Journal for Nature Conservation, 25, pp. 17–22. Available at: https://doi.org/10.1016/j.jnc.2015.02.007.

Marcelino, J. et al. (2021) 'Flight altitudes of a soaring bird suggest landfill sites as power line collision hotspots', Journal of Environmental Management, 294(May). Available at: https://doi.org/10.1016/j.jenvman.2021.113149.

Marcelino, J. et al. (2022) 'Anthropogenic food subsidies reshape the migratory behaviour of a long-distance migrant', Science of The Total Environment, 858(October 2022), p. 159992. Available at: https://doi.org/10.1016/j.scitotenv.2022.159992.

Marques, A.T. et al. (2014) 'Understanding bird collisions at wind farms: An updated review on the causes and possible mitigation strategies', Biological Conservation, 179, pp. 40–52. Available at: https://doi.org/10.1016/j.biocon.2014.08.017.

Marques, A.T. et al. (2020) 'Wind turbines cause functional habitat loss for migratory soaring birds', Journal of Animal Ecology, 89(1), pp. 93–103. Available at: https://doi.org/10.1111/1365-2656.12961.

Martín, B. et al. (2018) 'Impact of wind farms on soaring bird populations at a migratory bottleneck', European Journal of Wildlife Research, 64(3). Available at: https://doi.org/10.1007/s10344-018-1192-z.

Martin, G.R. (2011) 'Understanding bird collisions with man-made objects : a sensory ecology approach', Ibis, (153), pp. 239–254.

Martin, G.R. and Shaw, J.M. (2010) 'Bird collisions with power lines: Failing to see the way ahead?', Biological Conservation, 143, pp. 2695–2702. Available at: https://doi.org/10.1016/j.biocon.2010.07.014.

Masden, E.A. et al. (2010) 'Cumulative impact assessments and bird / wind farm interactions : Developing a conceptual framework', Environmental Impact Assessment Review, 30(1), pp. 1–7. Available at: https://doi.org/10.1016/j.eiar.2009.05.002.

Mattsson, B.J. et al. (2022) ‘Enhancing monitoring and transboundary collaboration for conserving migratory species under global change: The priority case of the red kite’, Journal of Environmental Management, 317(February), p. 115345. Available at: https://doi.org/10.1016/j.jenvman.2022.115345.

May, R. et al. (2010) Collision risk in white-tailed eagles. Modelling collision risk using vantage point observations in Smøla wind-power plant, NINA Report. Available at: https://doi.org/ISSN: 1504-3312\nISBN: 978-82-426-2219-8.

May, R. et al. (2014) ‘Mitigating wind-turbine induced avian mortality: Sensory, aerodynamic and cognitive constraints and options’, Renewable and Sustainable Energy Reviews, 42, pp. 170–181. Available at: https://doi.org/10.1016/j.rser.2014.10.002.

May, R. et al. (2020) ‘Paint it black: Efficacy of increased wind turbine rotor blade visibility to reduce avian fatalities’, Ecology and Evolution, (June), pp. 1–9. Available at: https://doi.org/10.1002/ece3.6592.

May, R. et al. (2021) ‘Life-cycle impacts of wind energy development on bird diversity in Norway’, Environmental Impact Assessment Review, 90(July), p. 106635. Available at: https://doi.org/10.1016/j.eiar.2021.106635.

May, R.F. (2015) ‘A unifying framework for the underlying mechanisms of avian avoidance of wind turbines’, Biological Conservation, 190, pp. 179–187. Available at: https://doi.org/10.1016/j.biocon.2015.06.004.

McClure, C.J.W. et al. (2021) ‘Eagle fatalities are reduced by automated curtailment of wind turbines’, Journal of Applied Ecology, 58(3), pp. 446–452. Available at: https://doi.org/10.1111/1365-2664.13831.

McClure, C.J.W., Martinson, L. and Allison, T.D. (2018) ‘Automated monitoring for birds in flight: Proof of concept with eagles at a wind power facility’, Biological Conservation, 224(April), pp. 26–33. Available at: https://doi.org/10.1016/j.biocon.2018.04.041.

Mckinsey & Company (2010) Transformation of Europe’s power system until 2050 Including specific considerations for Germany Electric Power and Natural Gas Practice. Düsseldorf. Available at: https://www.mckinsey.com/~/media/mckinsey/dotcom/client_service/epng/pdfs/transformation_of_europes_power_system.ashx.

McManamay, R.A., Vernon, C.R. and Jager, H.I. (2021) ‘Global Biodiversity Implications of Alternative Electrification Strategies Under the Shared Socioeconomic Pathways’, Biological Conservation, 260(December 2020), p. 109234. Available at: https://doi.org/10.1016/j.biocon.2021.109234.

Mekki, K. et al. (2019) ‘A comparative study of LPWAN technologies for large-scale IoT deployment’, ICT Express, 5(1), pp. 1–7. Available at: https://doi.org/10.1016/j.icte.2017.12.005.

Møller, A.P., Rubolini, D. and Lehikoinen, E. (2008) ‘Populations of Migratory Bird Species That Did Not Show a Phenological Response to Climate Change are Declining’, PNAS, 105(42), pp. 16195–16200. Available at: https://doi.org/10.1073/pnas.0803825105.

Moreira, F. et al. (2017) ‘Wired: impacts of increasing power line use by a growing bird population’, Environmental Research Letters, 12(2), p. 024019. Available at: https://doi.org/10.1088/1748-9326/aa5c74.

Moreira, F. et al. (2018) ‘Drivers of power line use by white storks: A case study of birds nesting on anthropogenic structures’, Journal of Applied Ecology, 55(5), pp. 2263–2273. Available at: https://doi.org/10.1111/1365-2664.13149.

Movebank (2019) Movebank Data Repository. Available at: https://www.movebank.org/ (Accessed: 1 October 2018).

Murali, G. et al. (2023) ‘Future temperature extremes threaten land vertebrates’, Nature, In Press(September 2021), p. 8. Available at: https://doi.org/10.1038/s41586-022-05606-z.

Muteba, F., Djouani, K. and Olwal, T. (2019) ‘A comparative survey study on LPWA IoT technologies: Design, considerations, challenges and solutions’, Procedia Computer Science, 155, pp. 636–641. Available at: https://doi.org/10.1016/j.procs.2019.08.090.

National Grid (2014) Design Drawings 132kV Overhead Lines: Hinkley Point C Connection Project Application Reference EN020001.

Newell, M. et al. (2015) ‘Effects of an extreme weather event on seabird breeding success at a North Sea colony’, Marine Ecology Progress Series, 532, pp. 257–268. Available at: https://doi.org/10.3354/meps11329.

Newson, S.E. et al. (2016) ‘Long-term changes in the migration phenology of UK breeding birds detected by large-scale citizen science recording schemes’, Ibis, 158(3), pp. 481–495. Available at: https://doi.org/10.1111/ibi.12367.

Oloo, F., Safi, K. and Aryal, J. (2018) ‘Predicting migratory corridors of white storks, ciconia ciconia, to enhance sustainablewind energy planning: A data-driven agent-based model’, Sustainability (Switzerland), 10(5). Available at: https://doi.org/10.3390/su10051470.

Oppel, S. et al. (2020) ‘Major threats to a migratory raptor vary geographically along the eastern Mediterranean flyway’, bioRxiv [Preprint], (February). Available at: https://doi.org/10.1101/2020.12.16.422983.

Oppel, S. et al. (2021a) ‘Major threats to a migratory raptor vary geographically along the eastern Mediterranean flyway’, Biological Conservation, 262(August 2020). Available at: https://doi.org/10.1016/j.biocon.2021.109277.

Oppel, S. et al. (2021b) ‘Major threats to a migratory raptor vary geographically along the eastern Mediterranean flyway’, Biological Conservation, 262(February). Available at: https://doi.org/10.1016/j.biocon.2021.109277.

Palac, C. et al. (2016) ‘Changes in bird-migration patterns associated with human-induced mortality’, Conservation Biology, 31(1), pp. 106–115. Available at: https://doi.org/10.1111/cobi.12758.

Panuccio, M. et al. (2017) ‘Long-term changes in autumn migration dates at the Strait of Gibraltar reflect population trends of soaring birds’, Ibis, 159(1), pp. 55–65. Available at: https://doi.org/10.1111/ibi.12420.

Patterson, I.J. (2015) ‘Goose flight activity in relation to distance from SPAs in Scotland, including an analysis of flight height distribution’, Scottish Natural Heritage Commissioned Report, 735(735).

Pearce-Higgins, J.W. et al. (2012) ‘Greater impacts of wind farms on bird populations during construction than subsequent operation: Results of a multi-site and multi-species analysis’, Journal of Applied Ecology, 49(2), pp. 386–394. Available at: https://doi.org/10.1111/j.1365-2664.2012.02110.x.

Pérez-garcía, J.M. et al. (2017) ‘Using risk prediction models and species sensitivity maps for large-scale identification of infrastructure-related wildlife protection areas : The case of bird electrocution’, Biological Conservation, 210(August 2016), pp. 334–342. Available at: https://doi.org/10.1016/j.biocon.2017.04.033.

Pérez-García, J.M. et al. (2016) ‘Selecting indicator species of infrastructure impacts using network analysis and biological traits: Bird electrocution and power lines’, Ecological Indicators, 60, pp. 428–433. Available at: https://doi.org/10.1016/j.ecolind.2015.07.020.

Péron, G. et al. (2013) ‘Estimation of bird and bat mortality at wind-power farms with superpopulation models’, Journal of Applied Ecology, 50(4), pp. 902–911. Available at: https://doi.org/10.1111/1365-2664.12100.

Péron, G. et al. (2017) ‘The energy landscape predicts flight height and wind turbine collision hazard in three species of large soaring raptor’, Journal of Applied Ecology, 54(6), pp. 1895–1906. Available at: https://doi.org/10.1111/1365-2664.12909.

Peschko, V. et al. (2020) ‘Effects of offshore windfarms on seabird abundance: Strong effects in spring and in the breeding season’, Marine Environmental Research, 162, p. 105157. Available at: https://doi.org/10.1016/j.marenvres.2020.105157.

Peters, G.P. and Hausfather, Z. (2020) ‘Emissions - the “business as usual” story is misleading’, Nature, 577, pp. 618–620.

Phipps, W.L. et al. (2013) ‘Do Power Lines and Protected Areas Present a Catch-22 Situation for Cape Vultures (Gyps coprotheres)?’, PLoS ONE, 8(10). Available at: https://doi.org/10.1371/journal.pone.0076794.

Polat, Ö. et al. (2016) ‘An Overview of Bird Related Issues in Electrical Power Systems’, Materials Science and Engineering, 161, pp. 1–9. Available at: https://doi.org/10.1088/1757-899X/161/1/012091.

Potier, S., Mitkus, M. and Kelber, A. (2018) ‘High resolution of colour vision, but low contrast sensitivity in a diurnal raptor’, Proceedings of the Royal Society B: Biological Sciences, 285(1885). Available at: https://doi.org/10.1098/rspb.2018.1036.

Prinsen, H.A.M. et al. (2011) Guidelines on How to Avoid or Mitigate Impact of Electricity Power Grids on Migratory Birds in the African-Eurasian Region. Bonn, Germany. Available at: https://doi.org/10.3354/dao02488.

Prinsen, H.A.M. et al. (2012) ‘Guidelines on how to avoid or mitigate impact of electricity power grids on migratory birds in the African-Eurasian region.’, CMS Technical Series No. 29, AEWA Technical Series No. 50 , CMS Raptors MOU Technical Series No. 3., 9(UNEP/CMS/Conf.10.30/Rev.2), pp. 1–43. Available at: https://doi.org/10.1111/j.1461-0248.2006.00968.x.

Ramsden, D.J. (2003) Barn Owls and Major Roads, The Barn Owl Trust. Exeter.

Rioux, S., Savard, J.-P.L. and Gerick, A.A. (2013) ‘Avian mortalities due to transmission line collisions : a review of current estimates and field methods with an emphasis on applications to the Canadian electric network Mortalité aviaire attribuable aux collisions avec les lignes de transport d ’ électri’, Avian Conservation and Ecology, 8(2). Available at: http://www.ace-eco.org/vol8/iss2/art7/.

Ripperger, S.P. et al. (2020) ‘Thinking small: Next-generation sensor networks close the size gap in vertebrate biologging’, PLoS Biology, 18(4), pp. 1–25. Available at: https://doi.org/10.1371/journal.pbio.3000655.

Rollan, À. et al. (2010) ‘Modelling the risk of collision with power lines in Bonelli’s Eagle Hieraaetus fasciatus and its conservation implications’, Bird Conservation International, 20(3), pp. 279–294. Available at: https://doi.org/10.1017/S0959270910000250.

Rotics, S. et al. (2016) ‘The challenges of the first migration: Movement and behaviour of juvenile vs. adult white storks with insights regarding juvenile mortality’, Journal of Animal Ecology [Preprint], (June). Available at: https://doi.org/10.1111/1365-2656.12525.

Rubolini, D. et al. (2005) ‘Birds and powerlines in Italy: An assessment’, Bird Conservation International, 15(2), pp. 131–145. Available at: https://doi.org/10.1017/S0959270905000109.

Ryberg, D.S. et al. (2019) ‘The future of European onshore wind energy potential: Detailed distribution and simulation of advanced turbine designs’, Energy, 182, pp. 1222–1238. Available at: https://doi.org/10.1016/j.energy.2019.06.052.

Sage, E. et al. (2022) ‘Built up areas in a wet landscape are stepping stones for soaring flight in a seabird’, Science of The Total Environment, 852(May), p. 157879. Available at: https://doi.org/10.1016/j.scitotenv.2022.157879.

Santangeli, A. et al. (2018) ‘Stronger response of farmland birds than farmers to climate change leads to the emergence of an ecological trap’, Biological Conservation, 217(October 2017), pp. 166–172. Available at: https://doi.org/10.1016/j.biocon.2017.11.002.

Santos, C.D. et al. (2017) ‘Match between soaring modes of black kites and the fine-scale distribution of updrafts’, Scientific Reports, 7(1), pp. 1–10. Available at: https://doi.org/10.1038/s41598-017-05319-8.

Santos, S.M. et al. (2016) ‘Avian trait-mediated vulnerability to road traffic collisions’, Biological Conservation, 200, pp. 122–130. Available at: https://doi.org/10.1016/j.biocon.2016.06.004.

Scacco, M. et al. (2019) ‘Static landscape features predict uplift locations for soaring birds across Europe’, Royal Society Open Science, 6(1), pp. 1–12. Available at: https://doi.org/10.1098/rsos.181440.

Schaub, T. et al. (2020) ‘Collision risk of Montagu’s Harriers Circus pygargus with wind turbines derived from high-resolution GPS tracking’, Ibis, 162(2), pp. 520–534. Available at: https://doi.org/10.1111/ibi.12788.

Schutgens, M., Shaw, J.M. and Ryan, P.G. (2014) ‘Estimating scavenger and search bias for collision fatality surveys of large birds on power lines in the Karoo, South Africa’, Ostrich, 85(1), pp. 39–45. Available at: https://doi.org/10.2989/00306525.2014.888691.

Scottish Government (2022) Climate Change Plan: Monitoring Report. Edinburgh, UK. Available at: https://www.gov.scot/binaries/content/documents/govscot/publications/progress-report/2022/05/climate-change-plan-monitoring-reports-2022/documents/climate-change-plan-monitoring-reports-2022/climate-change-plan-monitoring-reports-2022/govscot%3Adocument/c.

Sergio, F. et al. (2004) ‘Electrocution alters the distribution and density of a top predator, the eagle owl Bubo bubo’, Journal of Applied Ecology, 41(5), pp. 836–845. Available at: https://doi.org/10.1111/j.0021-8901.2004.00946.x.

Sergio, F. et al. (2018) ‘Reliable methods for identifying animal deaths in GPS- and satellite-tracking data: Review, testing, and calibration’, Journal of Applied Ecology [Preprint], (November). Available at: https://doi.org/10.1111/1365-2664.13294.

Shariati, M. et al. (2017) ‘Expert system for modelling stopover site selection by barnacle geese’, Ecological Modelling, 359, pp. 398–405. Available at: https://doi.org/10.1016/j.ecolmodel.2017.06.018.

Siemens Gamesa Renewables (2022) Siemens Gamesa SG 6.6 - 155 Onshore Wind Turbine Specifications. Available at: https://www.siemensgamesa.com/products-and-services/onshore/wind-turbine-sg-5-8-155 (Accessed: 1 April 2022).

Silva, J.P. et al. (2010) ‘Estimating the influence of overhead transmission power lines and landscape context on the density of little bustard Tetrax tetrax breeding populations', Ecological Modelling, 221(16), pp. 1954–1963. Available at: https://doi.org/10.1016/j.ecolmodel.2010.03.027.

Silva, J.P. et al. (2014) 'A spatially explicit approach to assess the collision risk between birds and overhead power lines: A case study with the little bustard', Biological Conservation, 170, pp. 256–263. Available at: https://doi.org/10.1016/j.biocon.2013.12.026.

Skov, H. et al. (2016) 'Patterns of migrating soaring migrants indicate attraction to marine wind farms', Biology Letters, 12(12). Available at: https://doi.org/10.1098/rsbl.2016.0804.

Smith, J.A. and Dwyer, J.F. (2016) 'Avian interactions with renewable energy infrastructure: An update', The Condor, 118(2), pp. 411–423. Available at: https://doi.org/10.1650/CONDOR-15-61.1.

SNH (2006) Assessing significance of impacts from onshore windfarms on birds outwith designated areas. Edinburgh, UK. Available at: http://www.snh.org.uk/pdfs/strategy/renewable/Significance of bird impacts July 06.pdf.

Soanes, L.M. et al. (2013) 'Individual consistency in the foraging behaviour of Northern Gannets: Implications for interactions with offshore renewable energy developments', Marine Policy, 38, pp. 507–514. Available at: https://doi.org/10.1016/j.marpol.2012.08.006.

Song, N. et al. (2021) 'Effects of wind farms on the nest distribution of magpie (Pica pica) in agroforestry systems of Chongming Island, China', Global Ecology and Conservation, 27, p. e01536. Available at: https://doi.org/10.1016/j.gecco.2021.e01536.

Sovacool, B.K. (2009) 'Contextualizing avian mortality: A preliminary appraisal of bird and bat fatalities from wind, fossil-fuel, and nuclear electricity', Energy Policy, 37(6), pp. 2241–2248. Available at: https://doi.org/10.1016/j.enpol.2009.02.011.

Stienen, E.W.M. et al. (2008) 'Sex-Biased Mortality of Common Terns in Wind Farm Collisions', The Condor, 110(1), pp. 154–157. Available at: https://doi.org/10.1525/cond.2008.110.1.154.

Taylor, P.D. et al. (2017) 'The Motus Wildlife Tracking System: a collaborative research network', Avian Conservation and Ecology, 12(1), p. 8.

Tethys (2023) 'Knowledge Base: Wind Energy content', Available at: https://tethys.pnnl.gov/knowledge-base-wind-energy?f%5B0%5D=technology%3A430 accessed 20/05/2023

Thaxter, C. et al. (2018) 'Dodging the blades: new insights into three-dimensional space use of offshore wind farms by lesser black-backed gulls Larus fuscus', Marine Ecology Progress Series, 587, pp. 247–253. Available at: https://doi.org/10.3354/meps12415.

Thaxter, Chris B. et al. (2017) 'Bird and bat species' global vulnerability to collision mortality at wind farms revealed through a trait-based assessment', Proceedings of the Royal Society B: Biological Sciences, 284(1862). Available at: https://doi.org/10.1098/rspb.2017.0829.

Thaxter, Chris B et al. (2017) 'Bird and bat species ' global vulnerability to collision mortality at wind farms revealed through a trait-based assessment'.

Thaxter, C.B. et al. (2018) 'Dodging the blades: New insights into three-dimensional space use of offshore wind farms by lesser black-backed gulls Larus fuscus', Marine Ecology Progress Series, 587(3), pp. 247–253. Available at: https://doi.org/10.3354/meps12415.

Thaxter, C.B., Ross-Smith, V.H., et al. (2019) ' Avian vulnerability to wind farm collision through the year: Insights from lesser black-backed gulls (Larus fuscus) tracked from multiple breeding colonies ', Journal of Applied Ecology, (July), pp. 1–13. Available at: https://doi.org/10.1111/1365-2664.13488.

Thaxter, C.B., Ross-Smith, V.H., et al. (2019) 'Avian vulnerability to wind farm collision through the year: Insights from lesser black-backed gulls (Larus fuscus) tracked from multiple breeding colonies', Journal of Applied Ecology, 56(11), pp. 2410–2422. Available at: https://doi.org/10.1111/1365-2664.13488.

Therkildsen, O.R. et al. (2021) 'Changes in flight paths of large-bodied birds after construction of large terrestrial wind turbines', Journal of Environmental Management, 290(April 2020). Available at: https://doi.org/10.1016/j.jenvman.2021.112647.

Tikkanen, H. et al. (2018) 'Modelling golden eagle habitat selection and flight activity in their home ranges for safer wind farm planning', Environmental Impact Assessment Review, 71(September 2017), pp. 120–131. Available at: https://doi.org/10.1016/j.eiar.2018.04.006.

Timmerberg, S. et al. (2019) ‘Renewable electricity targets in selected MENA countries – Assessment of available resources, generation costs and GHG emissions’, Energy Reports, 5, pp. 1470–1487. Available at: https://doi.org/10.1016/j.egyr.2019.10.003.

TPWind Advisory Council (2006) ‘Wind Energy : A Vision for Europe in 2030’, p. 21. Available at: https://etipwind.eu/files/reports/TPWind-Vision-for-Europe.pdf.

Travers, M.S. et al. (2021) ‘Post-collision impacts, crippling bias, and environmental bias in a study of newell’s shearwater and hawaiian petrel powerline collisions’, Avian Conservation and Ecology, 16(1). Available at: https://doi.org/10.5751/ACE-01841-160115.

Turbek, S.P., Scordato, E.S.C. and Safran, R.J. (2018) ‘The Role of Seasonal Migration in Population Divergence and Reproductive Isolation’, Trends in Ecology and Evolution, 33(3), pp. 164–175. Available at: https://doi.org/10.1016/j.tree.2017.11.008.

Tyrrell, L.P. and Fernández-Juricic, E. (2017) ‘Avian binocular vision: It’s not just about what birds can see, it’s also about what they can’t’, PLoS ONE, 12(3), pp. 1–14. Available at: https://doi.org/10.1371/journal.pone.0173235.

Uddin, M. et al. (2021) ‘High bird mortality due to power lines invokes urgent environmental mitigation in a tropical desert’, Biological Conservation, 261(July), p. 109262. Available at: https://doi.org/10.1016/j.biocon.2021.109262.

UKRI (2017) NEXUSS CDT Next Generation Unmanned Systems Science. Available at: https://www.southampton.ac.uk/nexuss/index.page (Accessed: 1 October 2018).

UNEP AEWA Secretariat (2018) The Agreement on the Conservation of African-Eurasian Migratory Waterbirds The Agreement on the Conservation of African-Eurasian Migratory Waterbirds. Durban, South Africa.

Vasilakis, D.P. et al. (2016) ‘Reconciling endangered species conservation with wind farm development: Cinereous vultures (Aegypius monachus) in south-eastern Europe’, Biological Conservation, 196, pp. 10–17. Available at: https://doi.org/10.1016/j.biocon.2016.01.014.

Vignali, S. et al. (2021) ‘Modelling the habitat selection of the bearded vulture to predict areas of potential conflict with wind energy development in the Swiss Alps’, Global Ecology and Conservation, 25. Available at: https://doi.org/10.1016/j.gecco.2020.e01405.

Warren, R. et al. (2018) ‘The implications of the United Nations Paris Agreement on climate change for globally significant biodiversity areas’, Climatic Change, 147(3–4), pp. 395–409. Available at: https://doi.org/10.1007/s10584-018-2158-6.

Warwick-evans, V. et al. (2017) ‘Predicting the impacts of wind farms on seabirds : An individual-based model’, Journal of Applied Ecology, (August), pp. 1–13. Available at: https://doi.org/10.1111/1365-2664.12996.

Wild, T.A. et al. (2022) ‘Internet on animals: Wi-Fi-enabled devices provide a solution for big data transmission in biologging’, Methods in Ecology and Evolution, 2022(August 2021), pp. 1–16. Available at: https://doi.org/10.1111/2041-210X.13798.

WWF (2022) Living Planet Report 2022. Gland, Switzerland. Available at: https://www.wwf.org.uk/sites/default/files/2022-10/lpr_2022_full_report.pdf.

CHAPTER 2: HOTSPOTS IN THE GRID: AVIAN SENSITIVITY AND VULNERABILITY TO COLLISIONS RISK FROM ENERGY INFRASTRUCTURE INTERACTIONS IN EUROPE AND NORTH AFRICA

Photo 4: Juvenile storks fitted with Movetech GPS-GSM tags during the 2021 fieldwork season. (Photo Credit, J. Gauld 2021)

This chapter has been published as a paper in Journal of Applied Ecology (DOI: 10.1111/1365-2664.14160). Some minor editorial changes have been made for the purposes of the thesis, but the main text, figures and tables remain as they are in the published work. The only significant change relates to the supporting information, a table summarising a literature review of susceptibility to collision with energy infrastructure has been removed to avoid repetition of the literature review chapter.

2.1 ABSTRACT

1. Wind turbines and power lines can cause bird mortality due to collision or electrocution. The biodiversity impacts of energy infrastructure (EI) can be minimised through effective landscape-scale planning and mitigation. The identification of high-vulnerability areas is urgently needed to assess potential cumulative impacts of EI while supporting the transition to zero carbon energy.

2. We collected GPS location data from 1,454 birds from 27 species susceptible to collision within Europe and North Africa and identified areas where tracked birds are most at risk of colliding with existing EI. Sensitivity to EI development was estimated for wind turbines and power lines by calculating the proportion of GPS flight locations at heights where birds were at risk of collision and accounting for species' specific susceptibility to collision. We mapped the maximum collision sensitivity value obtained across all species, in each 5 × 5 km grid cell, across Europe and North Africa. Vulnerability to collision was obtained by overlaying the sensitivity surfaces with density of wind turbines and transmission power lines.

3. Results: Exposure to risk varied across the 27 species, with some species flying consistently at heights where they risk collision. For areas with sufficient tracking data within Europe and North Africa, 13.6% of the area was classified as high sensitivity to wind turbines and 9.4% was classified as high sensitivity to transmission power lines. Sensitive areas were concentrated within important migratory corridors and along coastlines. Hotspots of vulnerability to collision with wind turbines and transmission power lines (2018 data) were scattered across the study region with highest concentrations occurring in central Europe, near the strait of Gibraltar and the Bosporus in Turkey.

4. Synthesis and applications. We identify the areas of Europe and North Africa that

are most sensitive for the specific populations of birds for which sufficient GPS tracking data at high spatial resolution were available. We also map vulnerability hotspots where mitigation at existing EI should be prioritised to reduce collision risks. As tracking data availability improves our method could be applied to more species and areas to help reduce bird-EI conflicts.

2.2 INTRODUCTION

The transition to zero carbon energy is essential to avoid runaway climate change (IPCC, 2018). However, the expansion of renewable energy infrastructure (EI) required to achieve this poses a challenge to wildlife conservation due to collision and electrocution risks, particularly for birds and other aerial taxa (Marques *et al.*, 2014b; Bernardino *et al.*, 2018b; Kiesecker *et al.*, 2019). European, onshore wind energy capacity is projected to grow from approximately 169 GW in 2018 to between 262 GW and 760 GW by 2050 with enough economically viable wind turbine locations (approximately 3.4 million) for up to 13.4 TW of capacity (Ryberg *et al.*, 2019). Countries in the Middle East and North Africa also have targets to increase the share of electricity supply from onshore wind with Morocco and Tunisia aiming for 100% renewable electricity by 2050 (Timmerberg *et al.*, 2019). Huge investment in the electricity transmission network will accompany this expansion of renewables, with an estimated fivefold increase in transmission capacity required between 2010 and 2050 (Mckinsey & Company, 2010). However, when poorly designed or situated, wind farms and power lines can result in increased mortality of susceptible birds such as large water birds, gulls, ibis, storks, owls, vultures and other raptors (Janss, 2000; Chris B Thaxter *et al.*, 2017; Oppel *et al.*, 2021a).

Organisations, such as energy companies, charged with supporting the rollout of renewable energy generation are obliged by national, European legal (2009/147/EC, 2010) and pan-flyway voluntary (Horns and Şekercioğlu, 2018) frameworks to mitigate risks to birds (Gyimesi and Prinsen, 2015). Methods to evaluate and mitigate these impacts are relatively well understood at project-specific and local scales (Schaub *et al.*, 2020; Serrano *et al.*, 2020). However, such assessments often occur after a development site has already been selected because the initial feasibility studies for energy projects tend to focus on the economic viability of the development over other factors. The scale and pace of new development requires greater integration of high-level assessments of the potential cumulative impact at regional and flyway scales into these feasibility studies to highlight areas where additional EI development is likely to significantly increase the risk to bird populations (Eichhorn, Tafarte and Thrän, 2017; Loss, Dorning and Diffendorfer, 2019; Thaxter, Ross-Smith, *et al.*, 2019). This is particularly important for migratory bird species who may experience the impact of multiple developments in operation within key migration routes, stopover sites, wintering grounds and breeding sites (Gove *et al.*, 2013; Bernardino *et al.*, 2018b).

Bird sensitivity maps can be developed to illustrate the relative risk associated with EI development for sensitive bird species (Vasilakis *et al.*, 2016; Warwick-evans *et al.*, 2017). The distribution and behaviour of birds inferred from GPS tracking of individuals can be used to create a spatio-temporal measure of the potential impact of new EI developments, by identifying where and when birds would be most exposed to potential collision risks from EI developments (Ross-Smith *et al.*, 2016; Warwick-evans *et al.*, 2017; Thaxter, Ross-Smith, *et al.*, 2019). For areas with sufficient tracking data, combining sensitivity maps with other inputs, such as the available wind resources, can help planners optimise new wind farm and power line locations by avoiding high sensitivity areas during the site selection stage of the development process (Kiesecker *et al.*, 2019). This, in turn, can reduce mitigation costs and produce better wildlife outcomes compared with site-based assessments alone (Bright *et al.*, 2008; Bradbury *et al.*, 2014).

Sensitivity mapping is particularly useful for assessing the potential for negative interactions between birds and energy infrastructure at the level of migratory flyways. For example, a wind farm sensitivity map created for the Red Sea flyway estimates the potential collision risks for soaring migratory birds at the flyway scale (BirdLife International, 2015a). This tool enables preliminary impact assessment of wind farms by viewing protected areas and raw GPS tracks of susceptible bird species. However, it does not account for all dimensions related with collision risk, such as the height at which birds fly, which in turn may vary depending on landscape, meteorological, seasonal and species-specific factors (Kleyheeg-Hartman *et al.*, 2018; Marques *et al.*, 2020a). In the terrestrial context, other sensitivity mapping studies largely rely on trait-based analysis in relation to population densities of susceptible bird species (Chris B Thaxter *et al.*, 2017; Amico *et al.*, 2019).

In this context sensitivity is a measure of potential collision risk identifying areas where the tracked birds could collide if wind turbines or powerlines are present (Thaxter, Ross-Smith, *et al.*, 2019). We calculated this by combining susceptibility traits with GPS location and altitude data for individuals from 27 species, including resident and migratory birds in Europe and Northern Africa, to describe where and when the tracked birds are most sensitive to collision risks from terrestrial EI. Within the areas for which we obtained sufficient high spatial resolution GPS tracking data; this allows us to identify sensitivity hotspots where future onshore EI development should be discouraged. However, our work cannot reveal 'safe' areas where EI development could be encouraged. We then overlay this sensitivity surface onto the density of existing EI to identify vulnerability hotspots where the tracked individuals are most exposed to collision risks due to the presence of wind turbines and powerlines. Similar approaches using GPS tracking data have been applied to assess the impacts of proposed offshore windfarm developments where survey logistics are more challenging (Bradbury *et al.*, 2014; Cleasby *et al.*, 2015; Lees, Guerin and Masden, 2016; Ross-Smith *et al.*, 2016; Thaxter, Ross-Smith, *et al.*, 2019). Our work also highlights the spatial variation in GPS tagging effort and data availability which helps identify priority areas for future tracking studies and the need to increase data sharing via online platforms such as Movebank to help fill in the gaps in the existing tracking data where sensitivity assessment is not currently feasible using publicly available GPS tracking data.

2.3 MATERIALS AND METHODS

2.3.1 DATA ACQUISITION

An overview diagram of the methods is presented in Appendix A1, section 1. We sourced bird movement data via the Movebank data repository, a web-based online platform for sharing data from animal tracking studies (Movebank, 2019), with a view to maximising coverage of Europe and North Africa. In November of 2018, we identified 254 bird GPS-tracking studies on Movebank within Europe, the Mediterranean and North Africa. A literature search undertaken between October 2018 and April 2019 was used to assess whether the species in these GPS tracking studies were susceptible to mortality associated with EI. We did not request data from tracking studies with less than five individuals unless multiple individuals of the same species were tracked in other Movebank studies. Data managers were contacted between October 2018 and January 2019 to request access to their data sets with a response deadline of the end of April 2019. Studies using ARGOS Doppler tags (insufficient spatial accuracy) (Thompson *et al.* 2017), captive birds, lab-based tests of GPS devices, lacking altitude data or tracking predominantly pelagic species were not included. In total, we obtained permission to use data from 65 suitable GPS tracking studies (Figure 3), representing 27 species and 1,454 individual birds. This included some data hosted on the University of Amsterdam Bird-tracking system database (UvA-BiTS, Bouten 2018), offered for inclusion in this analysis by managers of some of the requested Movebank data sets. To our knowledge, all fieldwork associated with the movement data sets included in this study was undertaken with permission from the relevant licensing authority, further details of each dataset are provided in the Data References section of this paper and Appendix A, section 2. The earliest tag deployment within any of the data sets was 2006, while the latest deployment date is 2018; the mean deployment duration was 2.7 ± 1.8 SD years.

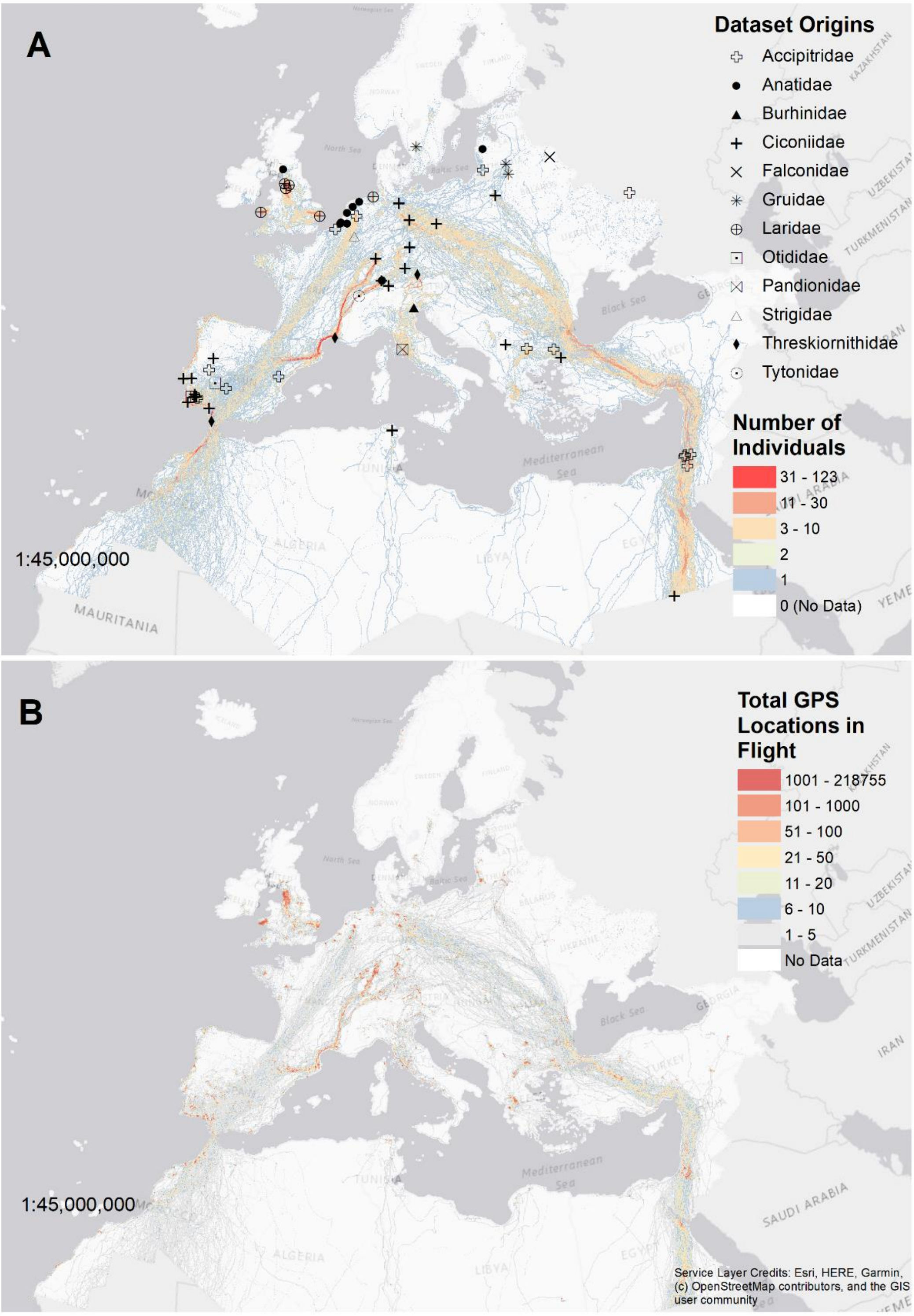

Figure 3: A: The location of the first GPS location of each dataset included in the analysis and the flux of individual birds through each 5 x 5 km grid cell (not controlled for year) for all areas for which we could source GPS tracking data. B. The density of GPS locations in flight per 5 x 5 km grid cell for all GPS tracking studies included in this study.

Infrastructure and terrain data were processed in QGIS and ArcGIS (ESRI, 2019; QGIS Development Team, 2019). We sourced transmission power line data from the open infrastructure project (Garret, 2018; OpenStreetMap, 2018). OpenStreetMap defines transmission lines as >50kV (OpenStreetMap, 2019). Flights between 10 – 60 m above ground were here taken as being within the danger height for transmission power lines (Figure 4) where birds risk collision (Infante and Peris, 2003; Harker, 2018). We intersected the data with a fishnet grid consisting of 554,993 individual 5x5 km grid cells representing a total area of 13.9 million square kilometres. Power line density is the total length in kilometres per grid cell, normalised onto a 0 – 100 scale.

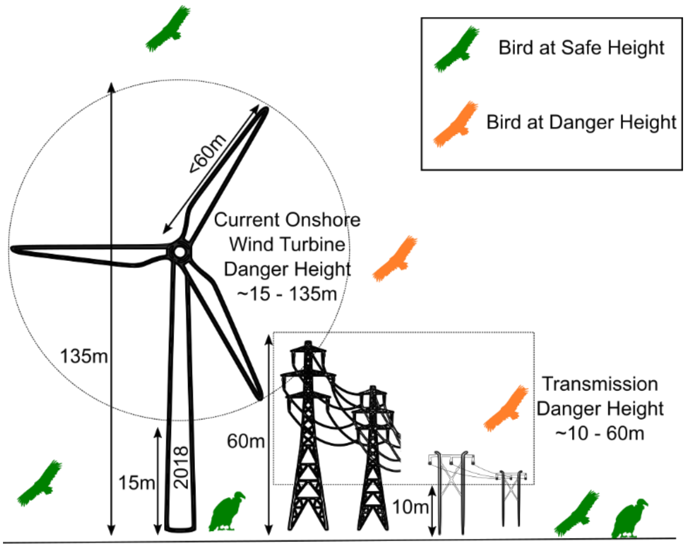

Figure 4: Danger height band definitions for energy infrastructure within which birds could be vulnerable to collision. The majority of transmission power lines (66kV and over) range from 10m to 60m in height (National Grid, 2014). For current onshore wind turbines, we derive a rotor swept zone ranging from 15m to 135m above ground (Pierrot, 2018; Thaxter et al., 2019).

Data on the location and size of onshore wind farms was downloaded from windpower.net (Pierrot, 2018). This data set contained centroid coordinates and information for 18,681 wind farms within Europe and North Africa. We used this to map the relative density of turbines on a 0 – 100 scale for each 5 x 5 km grid cell. Density was highest toward the North and West of Europe. From the hub heights and blade lengths in this data set, we derived a danger height (sometimes known as the rotor swept zone) of 15 – 135m for wind turbines (Figure 4), further details in appendix B section 3. To our knowledge, all tracking data sets used were collected in line with relevant guidance and licensing requirements of national ethical committees.

2.3.2 MOVEMENT DATA ANALYSIS

Measures of GPS accuracy were not uniformly indicated across all studies. Where the number of satellites was provided, only GPS locations associated with >=5 visible satellites were included (Morris and Conner, 2017). Duplicate GPS locations were removed. We used the raster package (R version 4.0.5, Hijmans 2019) to append elevation data from two 30m horizontal and 5m vertical accuracy digital surface models (DSM), STRM-GL1 and STRM-GL1-Ellipsoidal from the OpenTopography Portal (NGA and NASA, 2000; National Science Foundation, 2019) to each GPS location. For the small number of GPS locations at latitudes greater than 60° latitude an ALOS 30m DSM was used instead (JAXA, 2016). Further details of these DSM surfaces are in appendix A1 section 5. Height above ground in metres was calculated by subtracting the elevation of the ground from the altitude of the bird. Where bird altitude is in height above ellipsoid, ellipsoidal height of the land surface is used. Where altitude is relative to sea level, orthometric height of the land surface is used (Péron *et al.*, 2020). In some datasets, such as some Lesser Black-backed Gull studies, bespoke correction to obtain orthometric height had already been estimated in the database (Thaxter, Ross-Smith, *et al.*, 2019). GPS locations for each study were classified as breeding or non-breeding (including the migratory period) season by plotting week against latitude, (appendix A section 5).

Because instantaneous speed was not available across all data sets, we estimated speed in metres per second (m/s) using the time and distance between subsequent GPS locations derived with the anytime and geosphere R packages (Hijmans, Williams and Vennes, 2015; Eddelbuettel, 2018). All GPS locations within the 95% confidence interval for heights relative to ground level and greater than 10m above ground or associated with speeds greater than or equal to 1.39m/s (~5km/h) were classified as in flight. This approach accounts for the vertical error given by many GPS devices and excludes locations where the bird is likely to be stationary on the ground. The vertical position error associated with GPS tracking devices is typically in the range of 1.5m but can be as large as 31m due to the combined error of the GPS device and the DSM surface (Marques *et al.*, 2020). We categorised each flying GPS location as within each danger height band or not (Figure 4).

Some data sets contained bursts of high frequency GPS measurements (up to 1hz). Because the heights recorded in these bursts are not likely to be independent, the data were filtered to remove this potential source of bias by ensuring a minimum of 1 minute between subsequent GPS locations resulting in a total sample size of 18.0 million GPS locations. We then summarised the proportion of GPS locations in flight (6.6 million) observed at each danger height within each grid cell for each species in the data set.

Due to the nature of data obtained from tracking studies, the distribution of studies and individuals was heterogeneous across the study region (Figure 3), hence we considered cells with more tracking data to have more reliable estimates of the proportion of GPS locations in flight (Péron *et al.*, 2017; Silva *et al.*, 2017). We accounted for this at the species level using the Wilson's score (Reichensdörfer, Odenthal and Wollherr, 2017) whereby the lower bound of the Wilson confidence interval (WCI), calculated using the binconf function in the 'Hmisc' R package (Harrell, 2018), was used in place of the percentage (Lewis and Sauro, 2006; Lott and Reiter, 2020). Compared to a raw proportion, at low sample sizes, this has the effect of reducing the value assigned to grid cells where uncertainty is higher. For example, if a grid cell contained only three GPS locations, the Wilson Score (WS) tended toward zero due to the large WCI around the central point estimate of the proportion of GPS locations at danger height, as sample size increased ($n > 50$) and the WCI converged toward zero, the WS became comparable to a percentage (Cao, 2018). See further information in Appendix A, section 6.

We weighed this proportion of flying GPS locations to account for the collision susceptibility of different species using a morpho-behavioural risk index (MBRI) based on the method utilised in D'Amico *et al.*, 2019 and morphology data provided by Storchová and Hořák, 2018. Wing area and aspect in relation to weight is an important factor in avoidance ability as species with higher wing load are less able to take evasive action (Bevanger, 1998; Janss, 2000; May, 2015). Because wing area values were not available for all species, we simplified the shape of a bird as a rhombus and calculated a simplified area using the wingspan (WS) and body length (BL) in metres using data from Svensson, Mullarney and Zetterström, 2016 or Storchová and Hořák, 2018. Comparing this with wing area data available for 17 of the 27 species (Hedenström and Strandberg, 1993) using linear regression ($R^2 = 0.61$, $F_{1,15} = 23.44$, $p < 0.001$) suggests that it is a good proxy for assessing relative differences between species and an improvement on using wingspan alone ($R^2 = 0.46$, $F_{1,15} = 14.38$, $p < 0.001$), further details are provided in

Appendix A1, section 7. We then estimated a wing loading proxy by dividing the body mass (BM) in kilograms by wing area (m^2) as per equation 1:

$$WBMR = \frac{BM}{(WS * BL) \div 2} \quad (1)$$

We combined this wing-body-mass-ratio (WBMR) with several other factors scored as either 1 or 2 associated with avoidance ability (D'Amico *et al.*, 2019). These factors include flight style (FS), flapping (1) vs. soaring (2) because soaring species are less capable of making sudden changes in trajectory to avoid collision compared to flapping species (May, 2015); whether the species has binocular vision (BV) (1) or peripheral vision (2) (Martin and Shaw, 2010; D'Amico *et al.*, 2019); whether the species is a flocking species (FL) (2) or not (1) and whether the species flies frequently at night (ND) (2) or not (1). This definition of MBRI is the similar to D'Amico et al. 2019 apart from the flight style because D'Amico et al. 2019 use flight style as a proxy for flight height whereas we use flight style to help infer manoeuvrability (May, 2015). To account for the impact of mortality on the population of each species, this MBRI was then combined with European conservation status (Least Concern = 1, Other categories = 2) to produce a morpho-behavioural risk conservation status index (MBRCI) as per equation 2:

$$MBRCI = CI * \frac{(WBMR * FS * BV * FL * ND)}{5} \quad (2)$$

MBRCI was then normalised onto a scale between zero and one by calculating the ratio between the MBRCI for each species and the maximum value across all species. MBRCI for each species is detailed in the table in Appendix A, section 8. Sensitivity at the species level for each grid cell was then calculated as the proportion of tracking locations at danger height (quantified by the Wilson Score WS) multiplied by the MBRCI to produce a value between 0 and 1. The final sensitivity across all species is then defined as the maximum sensitivity of any species present in each grid cell. For example, if two species were present and species A was associated with a sensitivity score of 0.2 and species B was associated with a score of 0.4 the sensitivity for species B would be used for that grid cell. Alternative approaches using the raw proportion of flight locations at danger height, the Wilson score proportion or weighting the Wilson score proportion by conservation status did not alter our conclusions significantly and are provided in (Appendix A, section 9).

2.3.3 Vulnerability to Collision for GPS Tracked Birds

Vulnerability is a measure of how exposed individuals are to the presence of EI in horizontal and vertical space and how sensitive they are to the collision risks posed by this infrastructure (Thaxter *et al.*, 2019). We calculated vulnerability associated with existing infrastructure, for each grid cell, by multiplying the relative density of each EI type (0 – 100 scale) by the sensitivity value at the relevant height band for each 5x5km grid cell at the species level resulting in a value between 0 and 100. As per equation 3:

$$vulnerability = sensitivity * \ EI\ density\ (3)$$

A score of zero indicates that either no EI is present or sensitivity is zero whereas vulnerability of 100 would require relative density of EI to equal 100 and sensitivity to equal 1. Combined vulnerability is the sum of vulnerability for each height band. The final vulnerability across all species for each infrastructure is then defined as the maximum value of any species present in each grid cell.

2.3.4 DEFINING SENSITIVITY AND VULNERABILITY CATEGORIES

To ensure classification of sensitivity and risk was driven by the data (Gouhier and Pillai, 2020), we defined categories using the 25th, 75th and 97.5th percentiles for all grid cells where the sensitivity (or vulnerability) for a given height band was greater than zero. Grid cells scoring greater than zero but less than the 25th percentile are “Low”, scores between the 25th and 75th percentile are "Moderate", Scores greater than the 75th percentile are "High" and cells in the top 2.5% of observations are "Very High". All other cells are classified as "Very Low" if there are GPS locations but none at danger height resulting in a score of zero or "No Data" if data was lacking. We emphasize, therefore, that our method can only identify areas where a high risk of EI exists, but that the absence of a high vulnerability score in our analysis cannot be interpreted as indicative of low impact of EI due to the potential for other bird or bat populations (for which no data were available in our study) to be affected.

2.4 RESULTS

2.4.1 BIRD SENSITIVITY TO WIND FARM AND POWER LINE DEVELOPMENT

We mapped movements of 1,454 individual birds of 27 species (Figure 3). The study species travel across the continent and converge along key migratory routes. As expected, we observed a high flux of individuals through the bottlenecks of the European-African Flyway, such as Southern Iberia, Sinai, the Gulf of Iskenderun and the Bosporus in Turkey. Important gaps existed in the tracking data in North Spain, Scotland, Scandinavia, Italy, Eastern Europe and central North Africa (Figure 3). The median number of individuals tracked per species was 21, the species with the most tracked individuals was the White Stork *Ciconia ciconia* (n = 491) (Appendix A, section 2).

In total, 99,641 of the 554,993 5x5km grid cells in the study area (18%) contained at least one GPS location in flight. Sensitivity to wind turbines was greater than zero in 54.9% (n = 54,703) of these grid cells (Fig. 3a). 13.57% (n = 13,516, 337,900 km^2) of these cells were classified as high sensitivity i.e. they were in the upper quartile of sensitivity scores (>0.11). There was significant variability in sensitivity between species (ANOVA $F_{26, 59,592}$

= 432.4, p <0.001) with Eurasian eagle owl *Bubo bubo*, whooper swan *Cygnus cygnus*, eurasian spoonbill *Platalea leucorodia*, common crane *Grus grus* and white-fronted goose *Anser albifrons* exhibiting the greatest sensitivity to wind turbines across the grid cells where data are available for these species (Table 2). Sensitivity to transmission power lines (10 – 60m height band) was greater than zero in 37.64% (n = 37,509) of grid cells (Figure 5b). Across Europe and North Africa 9.41% (n = 9,375, 234,375 km^2) of these cells are classified as high sensitivity i.e. they are in the upper quartile of sensitivity scores (>0.14). Eurasian spoonbill *Platalea leucorodia*, European eagle owl *Bubo bubo*, whooper swan *Cygnus cygnus*, Iberian imperial eagle *Aquila adalberti* and white stork *Ciconia ciconia* are the five species which exhibited the greatest sensitivity at the transmission power line danger height band (Table 2).

Species	Common Name	Number of Grid Cells where Sensitivity >0 for Wind Turbines	Number of Grid Cells where Grid Cells Sensitivity >0 for Power Lines	Number of High Vulnerability Grid Cells (Vulnerability Hotspots) Associated with Wind Turbines	Number of High Vulnerability Grid Cells (Vulnerability Hotspots) Associated with Power Lines	Mean Combined Vulnerability ± SD
Anas platyrhynchos	Mallard	176	132	0	5	0.22 ± 0.28
Anser albifrons	White-fronted goose	20	27	0	5	0.74 ± 0.85
Aquila adalberti	Iberian imperial eagle	1734	1530	9	270	0.83 ± 1.05
Branta leucopsis	Barnacle goose	291	208	1	4	0.12 ± 0.29

Bubo bubo	Eurasian eagle owl	10	11	0	6	1.44 ± 1.32
Burhinus oedicnemus	Eurasian stone curlew	11	12	0	0	0.21 ± 0.26
Buteo lagopus	Rough-legged buzzard	815	766	0	88	0.49 ± 0.72
Buteo rufinus	Long-legged buzzard	455	296	0	8	0.23 ± 0.35
Ciconia ciconia	White stork	27401	17772	323	5361	2.14 ± 3.62
Ciconia nigra	Black stork	226	136	1	11	0.37 ± 0.9
Circaetus gallicus	Short-toed snake eagle	553	285	0	0	0.20 ± 0.25
Circus aeruginosus	Western marsh harrier	1063	780	0	1	0.10 ± 0.147
Circus pygargus	Montagu’s harrier	555	303	0	0	0.04 ± 0.08
Clanga clanga x pomarina	Hybrid spotted eagle	2711	1425	17	127	0.43 ± 0.68
Cygnus cygnus	Whooper swan	90	97	3	29	1.63 ± 1.98
Falco peregrinus	Peregrine falcon	347	300	0	0	0.09 ± 0.15
Geronticus eremita	Northern bald ibis	3830	2695	7	217	0.34 ± 0.57
Grus grus	Common crane	2794	1482	85	362	1.30 ± 2.56

Gyps fulvus	Griffon vulture	2019	1407	3	71	0.38 ± 0.63
Larus fuscus	Lesser black-backed gull	7227	5955	26	122	0.22 ± 0.31
Mareca penelope	Eurasian wigeon	276	232	0	0	0.09 ± 0.11
Neophron percnopterus	Egyptian vulture	792	477	4	81	1.01 ± 1.36
Pandion haliaetus	Osprey	524	325	0	48	0.59 ± 0.99
Pernis apivorus	European honey buzzard	5384	2966	53	440	0.62 ± 1.016
Platalea leucorodia	Eurasian spoonbill	19	19	0	5	1.02 ± 1.12
Tetrax tetrax	Little bustard	256	259	0	60	0.78 ± 0.73
Tyto alba	Barn owl	40	41	0	0	0.052 ± 0.04

Table 2: Sensitivity and vulnerability across all seasons and grid cells for which sufficient GPS data was obtained: summarised by species and infrastructure type, sorted according to species name in alphabetical order. Vulnerability Hotspots are defined as the upper quartile of the vulnerability scores obtained separately for vulnerability to collision with wind turbines and power lines. Mean combined vulnerability across all grid cells with sufficient data for that species is also described here.

Sensitivity was determined separately for breeding and non-breeding seasons (Appendix B section 1). Although the proportions are similar between seasons, during the breeding season we observed fewer overall high sensitivity grid cells at danger height than during the non-breeding season (Appendix C section 1). This clustered pattern is a product of sampling effort and is also indicative of the smaller scale movements of the tagged birds during the breeding season, which are centred on breeding locations. In the non-breeding season, birds move away from their breeding areas and we observe high sensitivity along coastlines and within major migratory routes. Notable sensitivity hotspots include the Western Mediterranean coast of France and Southern Spain, Eastern Romania, the Moroccan Coast, the Sinai Peninsula and the Baltic coast of Germany. Taxon specific maps of sensitivity are provided in Appendix C section 2, these can be used to compare with previous studies (see discussion) and highlight taxon specific gaps in the tracking data available on Movebank.

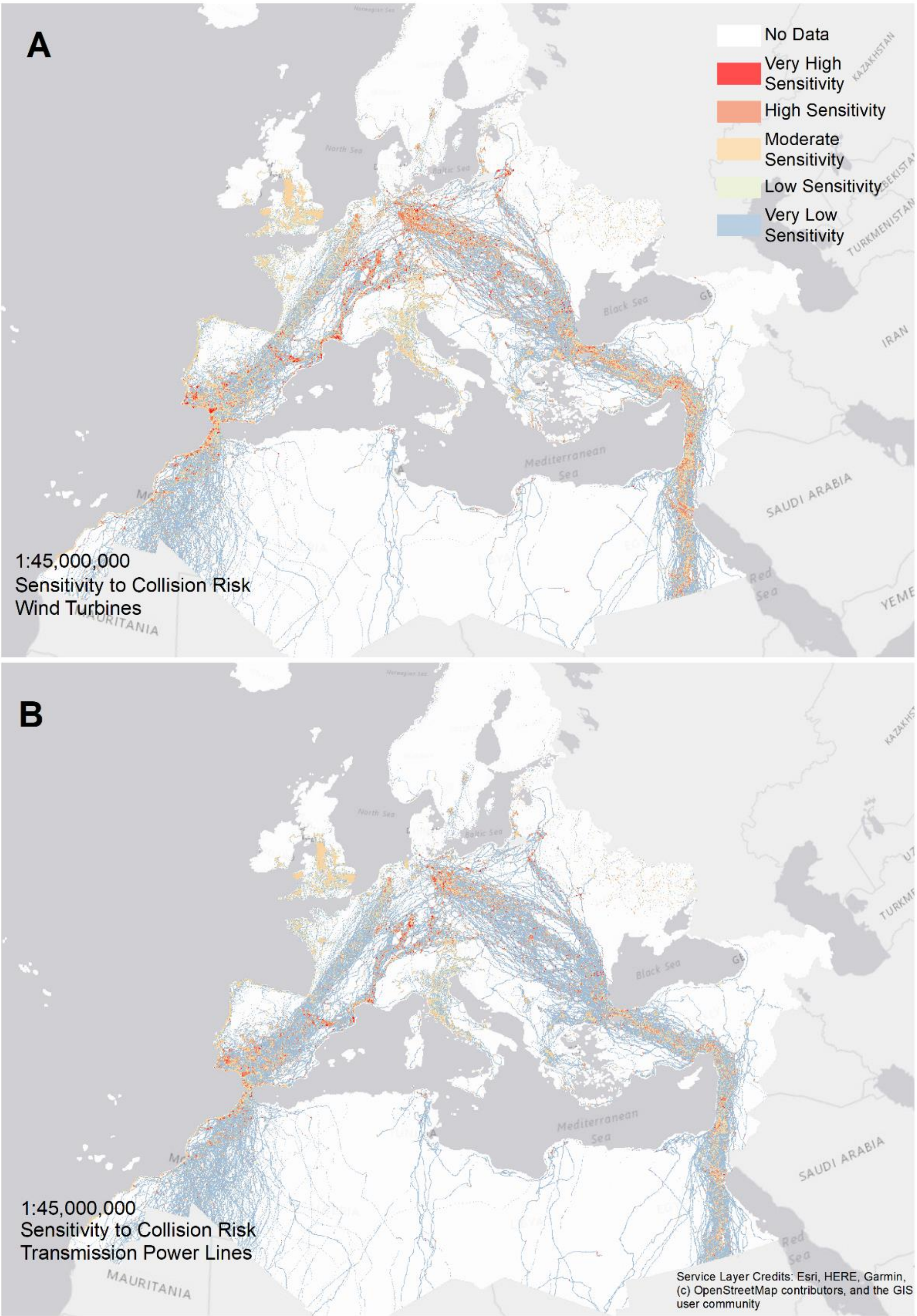

Figure 5: A. year-round sensitivity to wind turbines across all species (n=27) and areas for which we could obtain suitable GPS tracking data, B. year-round sensitivity to transmission power lines across all species using GPS tracking data (n=27) and areas for which we could obtain suitable GPS tracking data. Sensitivity at the species level for each grid cell was then calculated as the proportion of tracking locations at danger height (quantified by the Wilson Score WS) multiplied by the MBRCI to produce a value between 0 and 1. The final sensitivity across all species is then defined as the maximum sensitivity of any species present in each grid cell. Maps for breeding and non-breeding seasons are provided in Appendix B. Basemap from (OpenStreetMap, 2019b).

For some taxa such as cranes, as represented by common crane *Grus grus* in our data set, this highlights how individuals may travel long distances at altitudes where they are unlikely to collide with EI resulting in highly localised sensitivity hotspots.

2.4.2 VULNERABILITY OF TRACKED BIRDS TO ENERGY INFRASTRUCTURE RISKS

We plotted the combined vulnerability score as the sum of vulnerability from wind turbines and power lines present in each grid cell (Figure 6a). The tagged birds experience some degree of vulnerability in 28.2% (n = 28,051) of the grid cells with at least one GPS location in flight. 7.0% of these grid cells (n = 7,013) are high-vulnerability with values in the upper quartile of vulnerability scores (>1.13) and 1.7% (n = 702) are very high-vulnerability as they fall in the upper 2.5 percentile (>9.03). Fewer high vulnerability grid cells are associated with wind turbines (n =483, Figure 6b) compared with transmission lines (n = 6,861, Figure 6c). This suggests that transmission power lines are currently a more ubiquitous source of potential collision risks than wind turbines.

High-vulnerability areas were not distributed evenly across the study area (Figure 6a): just five countries (Germany, Spain, France, Turkey and Poland) accounted for 50.5% (n = 3,539) of the high-vulnerability grid cells. Measuring this relative to the percentage area of each country, the five countries with the most high-vulnerability grid cells were Liechtenstein (14.2%, n = 1), Germany (7.2%, n = 1028), Israel (5.8%, n = 48), Lebanon (5.4%, n = 22) and Portugal (5.0%, n = 176) (Appendix C, Section 3). However, it must be noted that this ranking will at least be partly influenced by the distribution of available tracking data. In the case of Turkey, Spain, Israel, Lebanon and Portugal, this indicated high densities of EI within important migratory bottlenecks where there is high flux of tracked birds at danger heights. On the other hand, for Central Europe, this high vulnerability is likely associated with the high density of wind turbines. Germany alone accounted for 55.2% (n = 267) of the 483 grid cells associated with a high vulnerability from wind turbines (Figure 6b). There were marked differences in vulnerability between species, with mean combined vulnerability ranging from 0.042 ± 0.081 SD for western marsh harrier *Circus pygargus* to 2.14 ± 3.62 SD for white stork (Table 2).

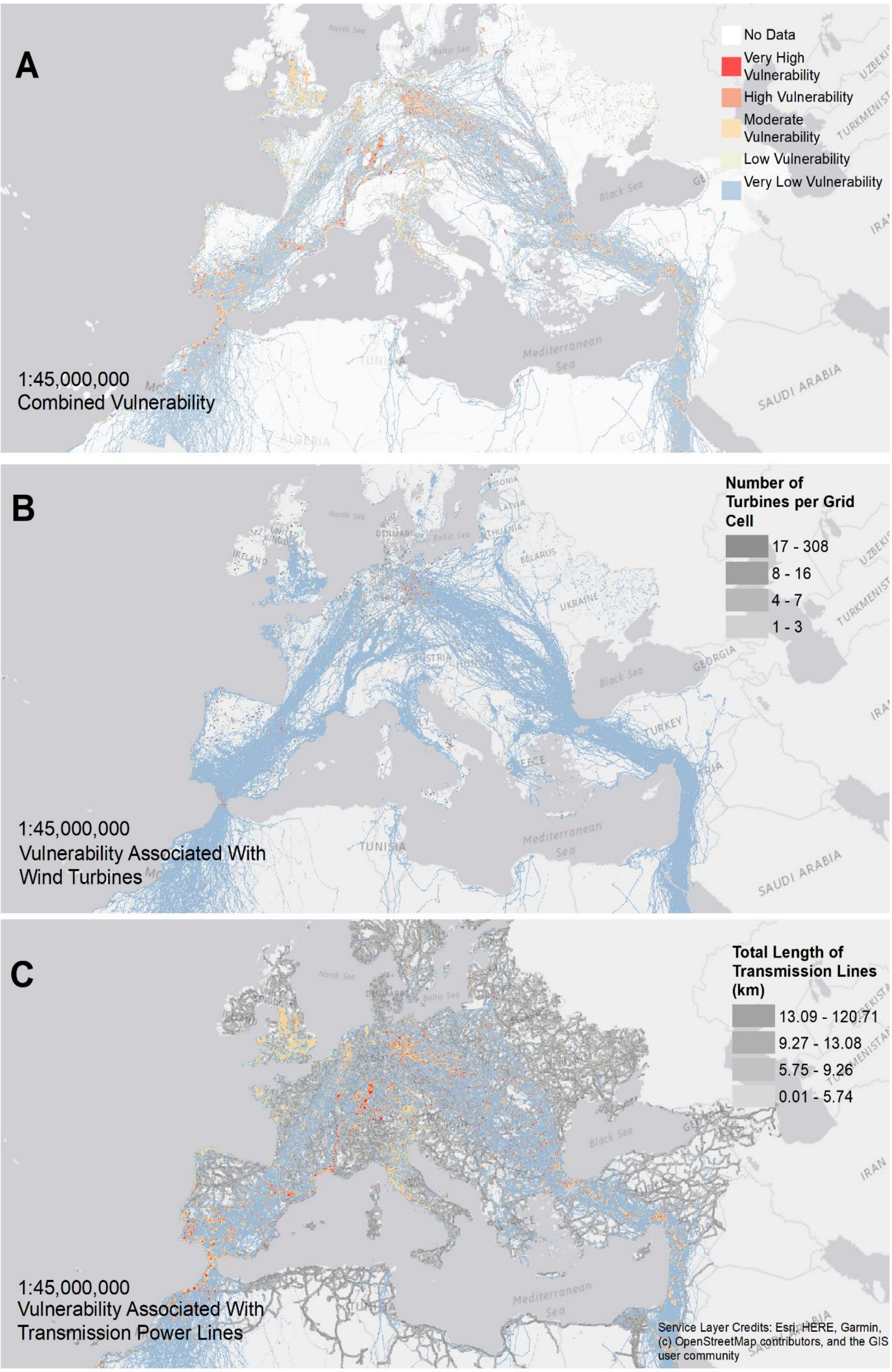

Figure 6: A. Vulnerability hotspots for wind farms where the GPS tracked birds (N= 1,454) are most likely to interact with wind turbines at danger height, white grid cells represent areas currently lacking sufficient GPS tracking data to assess vulnerability. B. Hotspots where the GPS tracked birds (N= 1,454) are most vulnerable to risks associated with transmission power lines. Grey grid cells in panels B and C represent the density of EI in grid cells for which we do not have sufficient tracking data and as such represent areas of unknown vulnerability. Vulnerability categories are symbolised as per the legend in panel A. Basemap from (OpenStreetMap, 2019b).

2.5 DISCUSSION

For areas with sufficient tracking data (currently 18% of the study area), our sensitivity surface identifies sensitivity hotspots associated with different height bands for wind turbines and transmission power lines (Figure 6). These are the areas where the tracked individuals are most sensitive to collision with EI. While not replacing the need for environmental impact assessment at more local and site-specific scales of relevance to local bird populations, our analysis successfully identified, areas where wind turbine and transmission powerline development should be minimised to protect the integrity of the flyway. As expected, many of these areas coincide with key migratory bottlenecks, such as the coasts of either side of the Strait of Gibraltar (Martín *et al.*, 2018), the Bosporus Strait, Gulf of Iskenderun, and the southern Sinai Peninsula (Evan R. Buechley *et al.*, 2018). This supports the idea that further development of EI within these migratory bottlenecks where species fly at danger height is likely to exacerbate existing anthropogenic mortality risks. Rigorous ecological impact assessment, spatial planning and mitigation at the local scales are needed within these bottleneck areas, as highlighted in other studies (Martín *et al.*, 2018; De Pascalis *et al.*, 2020). Comparing our results for the Laridae species included in our analysis (lesser black-backed gull *Larus fuscus*) with previous work by Thaxter *et al.*, 2019, which differed in methodology but utilised many of the same *L. fuscus* datasets, reveals similar patterns in sensitivity across the region for this species, supporting the validity of our approach (Appendix C, section 2).

Our results also highlighted differences in sensitivity to EI between species and which type of EI poses the most risk to each species (Table 2). It is beyond the scope of this study to provide specific ecological explanations for this observed variation as this is an ongoing topic of research in of itself, however, this is likely a product of ecological and morphological factors such as flight style (flapping versus soaring), migratory behaviour, habitat preference and how foraging strategy influences flight heights relative to the danger height bands (Martin and Shaw, 2010; Chris B Thaxter *et al.*, 2017; Bernardino *et al.*, 2018b).

Despite efforts to obtain as complete coverage of the study region as possible, we acknowledge gaps were present in the available GPS tracking data, particularly within areas such as northern France, northern Spain, Scandinavia, Algeria and Libya. These gaps reflect geographical and seasonal variation in the availability of bird telemetry data (Bouten *et al.*, 2013). As such, our results successfully highlight where sensitivity and vulnerability to collision with EI occurs but cannot indicate where vulnerability does not occur. Our sample includes only a subset of the most susceptible species, most of which are larger birds with a body mass of 350g or more, and only a subset of populations of these species, leading to sampling-related bias which is most evident during the breeding season (Appendix C, section 4). These sampling-related biases are a common issue in ecology, and collision risk cannot be inferred for areas where information is not available (Brotons *et al.*, 2004). Despite these limitations, the approach used, based on existing tracking data, accounting for species susceptibility to collision and the proportion of GPS records at danger height, provides a simple way to assess risk in the areas where data are available. As more tracking data become available, this analysis can be updated using data from (Movebank, 2019). This study highlights the benefits of data sharing and we expect data availability to increase significantly in the near future as GPS telemetry becomes more affordable and miniaturisation enables tracking devices to be fitted to smaller bird species (Bouten *et al.*, 2013). Advances in sensor technology may also soon allow collision mortality to be detected in real time (O'Donoghue and Rutz, 2016). One priority to aid future research is to help fill these gaps by improving data sharing via platforms such as Movebank or UvA-BiTS, promotion of new bird tracking studies in under-represented areas and taxonomic groups, improved standardisation of bio-logging data sets and deployment of loggers outwith the breeding season (Sequeira *et al.*, 2021). Other methods to address these data gaps may include the use of GPS data to model the relationship between flight heights and spatio-temporal factors such as weather, time of year, topography and land cover. However, such an analysis is beyond the scope of this paper.

Overlaying sensitivity with the existing wind farms and transmission lines identified a number of vulnerability hotspots where the tracked birds are vulnerable to collision with EI (Figure 6). While it is beyond the scope of this paper to evaluate the effectiveness of different mitigation options, we suggest that for areas with sufficient GPS tracking data, the vulnerability map can help identify priority areas for mitigation of impacts of EI, to reduce risks to birds. For existing power lines this could include line marking to increase visibility, burying cables or altering routes to avoid high sensitivity areas (Jenkins, Smallie and Diamond, 2010). For wind turbines, options include repowering with fewer larger turbines (Arnett and May, 2016), marking blades (May, Nygård, Falkdalen, Åström, Hamre and Bård G Stokke, 2020), temporary shutdown periods during the peak of the migratory season (Lucas *et al.*, 2012) which is already a requirement in some countries such as Jordan (Tomé *et al.*, 2017). Another option is to retrofit radar or camera-based systems to monitor bird movements and automatically shut down turbines during periods of high migratory movement (McClure, Martinson and Allison, 2018). Future analyses could be improved if official, multi-country, energy network spatial data sets were composed and made available to researchers. This would enable consideration of lower voltage distribution power lines which are under-represented in open-source data and are associated with electrocution, which was not considered in this study, as a major cause of injury and mortality (Garret, 2018; Hernández-Lambraño, Sánchez-Agudo and Carbonell, 2018). In a European study with Northern Bald Ibises 45% of the losses were caused by electrocution (Fritz, 2018). As with collision, there are several options such as retrofitting insulators or perches to reduce electrocution risk (Dixon *et al.*, 2019),but the problem could be entirely avoided by constructing safe poles that eliminate electrocution risk in the first place (Prinsen *et al.*, 2012).

2.5.1 IMPLICATIONS FOR MANAGEMENT AND CONSERVATION

To our knowledge, this is the first time that an assessment of this kind has been undertaken at the flyway scale across multiple species to highlight potential conflicts between renewable energy development and birds within Europe and the MENA nations which have ambitious targets for wind energy expansion. Our methodology provides a readily transferable approach to assess sensitivity and vulnerability for other species and areas as more GPS tracking data becomes available. The results presented here do not preclude the need for detailed local environmental impact assessment of the potential ecological impacts of EI on birds and other wildlife combined with post-construction monitoring to assess the risks due to disturbance, habitat loss, electrocution as well as collision which was the focus of this paper (Gove *et al.*, 2013; Bernardino *et al.*, 2018b). However, for areas with sufficient GPS tracking data, our sensitivity maps can inform where new wind farms and power lines should not be constructed and help include consideration of these impacts early in the site selection process for developments. Moreover, the vulnerability maps can help more effectively target areas for surveys to identify specific locations where mitigation of existing wind farms and power lines should be implemented. In our race to tackle the climate crisis, it is vital that we do not neglect the biodiversity crisis (Vasilakis *et al.*, 2016), sensitivity and vulnerability maps derived from GPS tracking data will be an important tool to help protect wildlife as our energy system transitions to zero carbon.

2.5.2 DATA AVAILABILITY STATEMENT

The raw data sets associated with this analyis are available for download on request via (Movebank, 2019), many of these data sets relate to sensitive or protected species and therefore permission from the managers of these data sets may be required prior to download. The processed data sets used to produce the sensitivity and vulnerability surfaces in this paper, including shapefiles of the final sensitivity surfaces and the density of energy infrastructure are available via the Dryad Digital Repository (Gauld *et al.*, 2022a) (https://doi.org/10.5061/dryad.jm63xsjcw)

2.5.3 DATA SOURCES

Carrapato, C. (2016) Iberian Imperial Eagle movement ecology 2014 – 2015, available on request from: https://www.movebank.org/cms/webapp?gwt_fragment=page=studies,path=study28407489; fieldwork undertaken with permission from the Portuguese national authority on nature conservation, Instituto da Conservação da Natureza e das Florestas, under permits issued by that authority.

Carrapato, C. (2016) Iberian Imperial Eagle movement ecology 2016, available on request from: https://www.movebank.org/cms/webapp?gwt_fragment=page=studies,path=study163340351; fieldwork undertaken with permission from the Portuguese national authority on nature conservation, Instituto da Conservação da Natureza e das Florestas, under permits issued by that authority.

Carrapato, C. (2017) Iberian Imperial Eagle movement ecology 2017, available on request from: https://www.movebank.org/cms/webapp?gwt_fragment=page=studies,path=study292890255; fieldwork undertaken with permission from the Portuguese national authority on nature conservation, Instituto da Conservação da Natureza e das Florestas, under permits issued by that authority.

Champagnon, J. (2017) Eurasian spoonbill – Tour du Valat – Camargue (France), available on request from: https://www.movebank.org/cms/webapp?gwt_fragment=page=studies,path=study311803430;

Clewley, G.C., Thaxter, C.B., Scragg, E. & Burton, N. (2015) BTO – Bowland 2015 - Lesser Black-backed Gull. Movebank study ID: 74375353, available on agreement and request from: www.movebank.org.

Clewley, G.C., Thaxter, C.B., Scragg, E. & Burton, N. (2017) BTO – Bowland 2017 - Lesser Black-backed Gull. Movebank study ID: 277843980, available on agreement and request from: www.movebank.org.

Clewley,G.C., Thaxter, C.B., Scragg, E. & Burton, N. (2017) BTO – Ribble Estuary 2017 - Lesser Black-backed Gull. Movebank study ID: 277841852, available on agreement and request from: www.movebank.org.

Clewley, G.C., Thaxter, C.B., Scragg, E. & Burton, N. (2018) BTO – Ribble Estuary 2018 - Lesser Black-backed Gull. Movebank study ID: 482136485, available on agreement and request from: www.movebank.org.

Anselin, A., Desmet, P., Milotic, T., Janssens, K., T'Jollyn, F., De Bruyn, L., & Bouten, W. (2019). MH_WATERLAND - Western marsh harriers (Circus aeruginosus, Accipitridae) breeding near the Belgium-Netherlands border [Data set]. Zenodo. http://doi.org/10.5281/zenodo.3826591

Duriez, O., Sforzi, A. & Monti, F. (2018) Osprey in Mediterranean (Corsica, Italy, Balearics), Data From:

a) Monti, F., Grémillet, D., Sforzi, A., Sammuri, G., Dominici, J.M., Triay Bagur, R., Muñoz Navarro, A., Fusani, L., Duriez, O. (2018a). Migration and wintering strategies in vulnerable Mediterranean Osprey populations. Ibis. https://doi.org/10.1111/ibi.12567.

b) Monti, F., Grémillet, D., Sforzi, A., Dominici, J.M., Triay Bagur, R., Muñoz Navarro, A., Fusani, L., Klaassen, R.H.G., Alerstam, T., Duriez, O. (2018b). Migration distance affects stopover use but not travel speed: contrasting patterns between long- and short distance migrating ospreys. J. Avian Biol. 49, e01839. https://doi.org/10.1111/jav.01839.

c) Duriez, O., Péron, G., Grémillet, D., Sforzi, A., Monti, F. (2018) Migrating ospreys use thermal uplifts over the open sea. Biology Letters 14(12).

https://doi.org/10.1098/rsbl.2018.0687, available on request from: www.movebank.org

Exo, K.M. and Griffin, L. (2006) Migration timing in barnacle geese (Svalbard) (data from Kölzsch et al. and Shariatinajafabadi et al. 2014), available on request from: https://www.movebank.org/cms/webapp?gwt_fragment=page=studies,path=study20039459

Exo, K.M. (2008) Migration timing in barnacle geese (Barents Sea) (data from Kölzsch et al. and Shariatinajafabadi et al. 2014), available on request from: https://www.movebank.org/cms/webapp?gwt_fragment=page=studies,path=study29799425

Fiedler, W. (2017) LifeTrack Lake Constance Ducks, available on request from: https://www.movebank.org/cms/webapp?gwt_fragment=page=studies,path=study236953686

Fiedler, W. & Wikelski, M. (2011) MPIO Lake Constance Mallards GPS, available on request from: https://www.movebank.org/cms/webapp?gwt_fragment=page=studies,path=study446579

Fiedler, W. (2013) Lifetrack White Stork Greece Evros Delta, available on request from: https://www.movebank.org/cms/webapp?gwt_fragment=page=studies,path=study10449535

Fiedler, W. (2013) Lifetrack White Stork Loburg, available on request from: https://www.movebank.org/cms/webapp?gwt_fragment=page=studies,path=study10449318

Fiedler, W. & Wilkelsi, M. (2013) Lifetrack White Stork Poland, available on request from: https://www.movebank.org/cms/webapp?gwt_fragment=page=studies,path=study10763606

Fiedler, W. (2014) Lifetrack White Stork Poland ECG, available on request from: https://www.movebank.org/cms/webapp?gwt_fragment=page=studies,path=study25166516

Fiedler, W. (2014) Lifetrack White Stork Bavaria, available on request from: https://www.movebank.org/cms/webapp?gwt_fragment=page=studies,path=study24442409

Fiedler, W. (2015) Lifetrack White Stork Rheinland-Pfalz, available on request from: https://www.movebank.org/cms/webapp?gwt_fragment=page=studies,path=study76367850

Fiedler, W., Blas J., Wilkelsi, M. (2013) Lifetrack White Stork Spain Donana, available on request from: https://www.movebank.org/cms/webapp?gwt_fragment=page=studies,path=study2988357

Fiedler, W. (2013) Lifetrack White Stork Tunisia, available on request from: https://www.movebank.org/cms/webapp?gwt_fragment=page=studies,path=study10157679

Fiedler, W. (2016) Lifetrack White Stork Bulgaria, available on request from: https://www.movebank.org/cms/webapp?gwt_fragment=page=studies,path=study128184877

Fiedler, W. (2016) Lifetrack White Stork Vorarlberg, available on request from:

https://www.movebank.org/cms/webapp?gwt_fragment=page=studies,path=study173641633

Fiedler, W. (2017) Lifetrack Black Stork, available on request from: https://www.movebank.org/cms/webapp?gwt_fragment=page=studies,path=study291047293

Flack A, Fiedler W, Wikelski M (2017) Fall migration of white storks in 2014, Data from: Wind estimation based on thermal soaring of birds. Movebank Data Repository. doi:10.5441/001/1.bj96m274

Franco, A.M.A. (2014) White Stork Juveniles 2014 UEA, available on request from: https://www.movebank.org/cms/webapp?gwt_fragment=page=studies,path=study83544657

Franco, A.M.A. (2016) White Stork Adults and Juveniles 2016, available on request from: https://www.movebank.org/cms/webapp?gwt_fragment=page=studies,path=study159302811

Franco, A.M.A. (2017) White Stork Juveniles (2017), available on request from: https://www.movebank.org/cms/webapp?gwt_fragment=page=studies,path=study279646867

Franco, A.M.A., Acacio, M. S., Rogerson, K., (2017) White Stork Adults 2017, available on request from: https://www.movebank.org/cms/webapp?gwt_fragment=page=studies,path=study229412850

Franco, A.M.A., Acacio, M. S. (2018) White Stork Adults 2018, available on request from: https://www.movebank.org/cms/webapp?gwt_fragment=page=studies,path=study451464940

Franco, A.M.A., Acacio, M. S. (2018) White Stork Juveniles 2018, available on request from: https://www.movebank.org/cms/webapp?gwt_fragment=page=studies,path=study495405707

Franco, A.M.A., Acacio, M. S. (2018) Black Storks Portugal 2018, available on request from: https://www.movebank.org/cms/webapp?gwt_fragment=page=studies,path=study518635174

Friedemann, G. (2011) Movements of long-legged buzzards and short-toed eagles, available on request from: https://www.movebank.org/cms/webapp?gwt_fragment=page=studies,path=study34551859

Fritz, J., Wikelski, M. & Pixner, E. (2018) Bald Ibis Waldrappteam 2, available on request from: https://www.movebank.org/cms/webapp?gwt_fragment=page=studies,path=study18957668

Garthe, S. (2016) FTZ: Foraging in lesser black-backed gulls; Data from Garthe S, Schwemmer P, Paiva VH, Corman A-M, Fock HO, Voigt CC, Adler S (2016) Terrestrial and marine foraging strategies of an opportunistic seabird species breeding in the Wadden Sea. PLoS ONE 11(8): e0159630; with DOI:10.5441/001/1.nk286sc0, available on request from: https://www.movebank.org/cms/webapp?gwt_fragment=page=studies,path=study82452206

Giunchi, D. (2015) Eurasian stone curlew Italy, Data from: Giunchi, D., Caccamo, C., Mori, A., Fox, J. W., Rodríguez-Godoy, F., Baldaccini, N. E., & Pollonara, E. (2015). Pattern of non-breeding movements by Stone-curlews Burhinus oedicnemus breeding in North Italy. Journal of Ornithology, 1-8 available on request from: https://www.movebank.org/cms/webapp?gwt_fragment=page=studies,path=study12883793

Hollerbach, S. (2016) Ciconia ciconia sudewiesen, available on request by contacting: storkenkate@gmx.de

Jansen, R. (2010) Eagle owls - 3 breeding pairs - Southern Part The Netherlands, available on request from https://www.movebank.org/cms/webapp?gwt_fragment=page=studies,path=study4502577

Kölzsch A, Bauer S, de Boer R, Griffin L, Cabot D, Exo K-M, van der Jeugd HP, Nolet BA (2014) Forecasting spring from afar? Timing of migration and predictability of phenology along different migration routes of an avian herbivore. Journal of Animal Ecology. doi:10.1111/1365-2656.12281

Kölzsch A (2015) Foraging by white-fronted geese after disturbance (data from Nolet et al. 2016) DOI: 10.5441/001/1.7tp81b7b., available on request from: https://www.movebank.org/cms/webapp?gwt_fragment=page=studies,path=study163020445

Lameris, T. K., Bouten, W. (2018) Barnacle Geese – Netherlands and North-Western Russia DOI https://doi.org/10.1016/j.cub.2018.05.077 & DOI: 10.1007/A10336-012-0908-1

López-López, P. (2007) Egyptian vulture EB Terra Natura UA Spain, available on request from: https://www.movebank.org/cms/webapp?gwt_fragment=page=studies,path=study20106351

Milotić, T. et al. (2020) ‘Gps tracking data of western marsh harriers breeding in Belgium and the Netherlands’, ZooKeys, 2020(947), pp. 143–155. doi: 10.3897/zookeys.947.52570. Movebank study: https://www.movebank.org/cms/webapp?gwt_fragment=page=studies,path=study604806671

Nathan, R. & Harel, R. (2016) Eurasian Griffon Vultures 1 Hz HUJ (Israel), available on request from: https://www.movebank.org/cms/webapp?gwt_fragment=page=studies,path=study16924201

Nathan, R. & Harel, R. (2012) Soaring flight in Eurasian griffon vultures (HUJ) (data from Harel and Nathan, 2018) DOI: 10.5441/001/1.46t5141d available on request from: https://www.movebank.org/cms/webapp?gwt_fragment=page=studies,path=study467005392

Nathan, R. (2012) Eastern flyway spring migration of adult white storks (data from Rotics et al. 2018) DOI 10.5441/001/1.v8d24552, available on request from: https://www.movebank.org/cms/webapp?gwt_fragment=page=studies,path=study560041066

Oppel, S. & Nikolov, S. (2018) Neophron percnopterus Bulgaria/Greece LIFE+ "The return of the Neophron" - LIFE10 NAT/BG/000152 available on request from:

https://www.movebank.org/cms/webapp?gwt_fragment=page=studies,path=study15869951

Peshev, H. (2016) Gyps fulvus Griffon vulture FWFF Kresna Gorge, available on request from: https://www.movebank.org/cms/webapp?gwt_fragment=page=studies,path=study305278048

Pokrovsky, I. (2015) LifeTrack Peregrine Falcon, available on request from: https://www.movebank.org/cms/webapp?gwt_fragment=page=studies,path=study103426553

Pokrovsky, I. (2016) LifeTrack rough-legged buzzards, available on request from: https://www.movebank.org/cms/webapp?gwt_fragment=page=studies,path=study9493874

Séchaud, R. (2016) Barn owl (Tyto alba) available on request from: https://www.movebank.org/cms/webapp?gwt_fragment=page=studies,path=study231741797

Silva, J., P., (2015) Little Bustard Movement Ecology 2015 - 2016 available on request from: https://www.movebank.org/cms/webapp?gwt_fragment=page=studies,path=study56464970

Silva, J., P., (2017) Little Bustard Movement Ecology 2017 - 2018 available on request from: https://www.movebank.org/cms/webapp?gwt_fragment=page=studies,path=study253940991

Silva, J., P., (2018) Little Bustard Movement Ecology 2018 - 2019 available on request from: https://www.movebank.org/cms/webapp?gwt_fragment=page=studies,path=study461568973

Thaxter, C.B., Ross-Smith, V.H., Bouten, W. and Burton, N.H.K. (2011) Lesser Black-backed Gull Orford Ness, available with agreement on request from www.uva-bits.nl

Thaxter, C.B., Ross-Smith, V.H., Bouten, W. and Burton, N.H.K. (2014) Lesser Black-backed Gull Walney, available with agreement on request from www.uva-bits.nl

Thaxter, C.B., Ross-Smith, V.H., Bouten, W. and Burton, N.H.K. (2014) Lesser Black-backed Gull Skokholm, available with agreement on request from www.uva-bits.nl

Thaxter, C.B., Clewley, G.C., Scragg, E. & Burton, N. (2016) BTO – North West England 2016 - Lesser Black-backed Gull. Movebank study ID: 167983392, available on agreement and request from: www.movebank.org.

Van Toor, M. & Waldenström, J. (2018) Eurasian wigeons spring 2018, available on request from: https://www.movebank.org/cms/webapp?gwt_fragment=page=studies,path=study412700082

Vansteelant, W. (2008) Honey_Buzzard_NL, data from: https://doi.org/10.1111/jav.00457 & https://doi.org/10.1111/1365-2656.12593

Lopez-Vazquez, J., M., (2013) Proyecto Eremita Geronticus eremita Reintroduction in Andalusia (Spain) available on request from: https://www.movebank.org/cms/webapp?gwt_fragment=page=studies,path=study463673774

Vornweg, B. & Fiedler, W. (2016) Lifetrack Circus pygargus, available on request from: https://www.movebank.org/cms/webapp?gwt_fragment=page=studies,path=study166943336

Wikelski, M. (2015) LifeTrack Whooper Swan Latvia, available on request from: https://www.movebank.org/cms/webapp?gwt_fragment=page=studies,path=study92261778

Žydelis, R. (2015) Hybrid Spotted Eagles Lithuania GPS 2015 – 2017, available on request from: https://www.movebank.org/cms/webapp?gwt_fragment=page=studies,path=study150764908

Žydelis, R. & Dagys, M. (2015) Common Crane Lithuania GPS, 2015-2016, available on request from: https://www.movebank.org/cms/webapp?gwt_fragment=page=studies,path=study146932094

Žydelis, R. & Dagys, M (2016) Common Crane Lithuania GPS, 2016, available on request from: https://www.movebank.org/cms/webapp?gwt_fragment=page=studies,path=study195375760

Žydelis, R. & Desholm, M. (2013) GPS telemetry of Common Cranes, Sweden, available on request from: https://www.movebank.org/cms/webapp?gwt_fragment=page=studies,path=study10722328

2.6 REFERENCES

2009/147/EC, C. D. (2010) ‘Directive 2009/147/EC of the European Parliament and of the Council on the conservation of wild birds’, Official Journal of the European Union, L 20, pp. 7–25. doi: 10.1126/science.aah3404.

Anselin, A., Desmet, P., Milotic, T., Janssens, K., T'Jollyn, F., De Bruyn, L., & Bouten, W. (2019). MH_WATERLAND - Western marsh harriers (Circus aeruginosus, Accipitridae) breeding near the Belgium-Netherlands border [Data set]. Zenodo. http://doi.org/10.5281/zenodo.3826591

AEWA. 2012. Guidelines on how to avoid or mitigate impact of electricity power grids on migratory birds in the African-Eurasian Region., United Nations Environment Programme, Bonn, Germany.

Bernardino, J. et al. (2018a) ‘Bird collisions with power lines: State of the art and priority areas for research’, Biological Conservation, 222(March), pp. 1–13. doi: 10.1016/j.biocon.2018.02.029.

Bernardino, J. et al. (2018b) ‘Bird collisions with power lines: State of the art and priority areas for research’, Biological Conservation. Elsevier, 222(March), pp. 1–13. doi: 10.1016/j.biocon.2018.02.029.

Bevanger, K. (1998) ‘Biological and conservation aspects of bird mortality caused by electricity power lines: A review’, Biological Conservation, 86(1), pp. 67–76. doi: 10.1016/S0006-3207(97)00176-6.

Birdlife International (2019) Bird Life Data Zone. Available at: http://datazone.birdlife.org/species (Accessed: 7 June 2019).

BirdLife International (2015) Migratory Soaring Birds Project: Soaring Bird Sensitivity Map. Available at: http://migratorysoaringbirds.undp.birdlife.org/en/sensitivity-map (Accessed: 3 November 2019).

Bouten, W. et al. (2013) ‘A flexible GPS tracking system for studying bird behaviour at multiple scales’, Journal of Ornithology, 154(2), pp. 571–580. doi: 10.1007/s10336-012-0908-1.

Bouten, W. (2018) UvA-BiTS Bird Tracking System, University of Amsterdam. Available at: http://www.uva-bits.nl/.

Bradbury, G. et al. (2014) ‘Mapping Seabird Sensitivity to offshore wind farms’, PLoS ONE, 9(9). doi: 10.1371/journal.pone.0106366.

Bright, J. et al. (2008) 'Map of bird sensitivities to wind farms in Scotland: A tool to aid planning and conservation', Biological Conservation, 141(9), pp. 2342–2356. doi: 10.1016/j.biocon.2008.06.029.

Buechley, E. R. et al. (2018) 'Identifying Critical Migratory Bottlenecks and High-Use Areas for an Endangered Migratory Soaring Bird Across Three Continents', Journal of Avian Biology, e01629, pp. 1–13. doi: 10.1111/jav.01629.

Cao, X. (2018) 'Improved Online Wilson Score Interval Method for Community Answer Quality Ranking', (April), pp. 1–8.

Cerritelli, G. et al. (2020) 'Simpler methods can outperform more sophisticated ones when assessing bird migration starting date', Journal of Ornithology. Springer Berlin Heidelberg, 161(3), pp. 901–907. doi: 10.1007/s10336-020-01770-z.

Cleasby, I. R. et al. (2015) 'Three-dimensional tracking of a wide-ranging marine predator: Flight heights and vulnerability to offshore wind farms', Journal of Applied Ecology, 52(6), pp. 1474–1482. doi: 10.1111/1365-2664.12529.

D'Amico, M, Martins, RC, Álvarez-Martínez, JM, Porto, M, Barrientos, R, Moreira, F. Bird collisions with power lines: Prioritizing species and areas by estimating potential population-level impacts. Divers Distrib. 2019; 25: 975– 982. https://doi.org/10.1111/ddi.12903.

De Pascalis, F. et al. (2020). Shift in diversity and distribution of the proximate causes of mortality in large migratory raptors over a century. Biological Conservation, 251:108793

Dixon, A. et al. (2019) 'Mitigation techniques to reduce avian electrocution rates', Wildlife Society Bulletin, 43(3), pp. 476–483. doi: 10.1002/wsb.990.

Eddelbuettel, D. (2018) 'Anytime: An R Package for working with "POSIXct" (or 'Date') objects'. Available at: http://dirk.eddelbuettel.com/code/anytime.html.

Eichhorn, M., Tafarte, P. and Thrän, D. (2017) 'Towards energy landscapes – "Pathfinder for sustainable wind power locations"', Energy, 134, pp. 611–621. doi: 10.1016/j.energy.2017.05.053.

ESRI (2019) 'ArcGIS Release 10.6.1'. Redlands, CA: Environmental Systems Research Institute.

Fritz J, Unsoeld M & Voelkl B (2019) Back into European Wildlife: The Reintroduction of the Northern Bald Ibis (Geronticus eremita). Bookchapter in: Scientific Foundations of Zoos and Aquariums: Their Role in Conservation and Research (Kaufman AB, Bashaw M, Maple T Edtrs.), Cambridge University Press; ISBN 978-1-316-64865-0. DOI: 10.1017/9781108183147.014

Garret, R. (2018) The Open-source Infrastructure Project, OpenInfra. Available at: https://openinframap.org (Accessed: 5 November 2018).

Gauld et al. (2022): Data from: Hotspots in the grid: avian sensitivity and vulnerability to collision risk from energy infrastructure interactions in Europe and North Africa, available from Dryad repository: https://doi.org/10.5061/dryad.jm63xsjcw

Gouhier, T. C. and Pillai, P. (2020) 'Avoiding Conceptual and Mathematical Pitfalls When Developing Indices to Inform Conservation', Frontiers in Ecology and Evolution, 8(September), pp. 1–5. doi: 10.3389/fevo.2020.00263.

Gove, B. et al. (2013) Wind farms and birds: an updated analysis of the effects of wind farms on bird, and best practice guidance on integrated planning and impact assessement T-PVS/Inf, Council of Europe. Strasbourg.

Gyimesi, A. and Prinsen, H. A. M. (2015) 'Guidance on appropriate means of impact assessment of electricity power grids on migratory soaring birds in the Rift Valley / red Sea Flyway - Final Report', p. 56.

Harker, K. (2018) 'Overhead line design', High Voltage Power Network Construction, pp. 123–150. doi: 10.1049/pbpo110e_ch6.

Hedenström, D. and Strandberg, A. (1993) 'Protocol S1 Supplementary list of flight speeds and biometry of bird species', Pennycuick Greenewalt Hedenström, 135(1), pp. 1–4.

Hijmans, R. J., Williams, E. and Vennes, C. (2015) 'Geosphere: spherical trigonometry'. R. Available at: url: https://CRAN. R-project. org/package= geosphere.

Hijmans, R. J. (2019) 'Raster: An R Package for working with raster data'. Available at: https://www.rspatial.org/.

Horns, J. J. and Şekercioğlu, Ç. H. (2018) 'Conservation of migratory species', Current Biology, 28(17), pp. R980–R983. doi: 10.1016/j.cub.2018.06.032.

Infante, O. and Peris, S. (2003) 'Bird nesting on electric power supports in northwestern Spain', Ecological Engineering, 20(4), pp. 321–326. doi: 10.1016/S0925-8574(03)00013-2.

Janss, G. F. E. (2000) ‘Avian mortality from power lines: A morphologic approach of a species-specific mortality’, Biological Conservation, 95(3), pp. 353–359. doi: 10.1016/S0006-3207(00)00021-5.

JAXA (2016) ALOS Global Digital Surface Model (AW3D30), OpenTopography. Available at: http://opentopo.sdsc.edu/raster?opentopoID=OTALOS.112016.4326.2 (Accessed: 1 February 2019).

Kiesecker, J. et al. (2019) ‘Hitting the Target but Missing the Mark: Unintended Environmental Consequences of the Paris Climate Agreement’, Frontiers in Environmental Science, 7(October). doi: 10.3389/fenvs.2019.00151.

Kleyheeg-hartman, J. C. et al. (2018) ‘Predicting bird collisions with wind turbines: Comparison of the new empirical Flux Collision Model with the SOSS Band model’, Ecological Modelling. Elsevier, 387(March), pp. 144–153. doi: 10.1016/j.ecolmodel.2018.06.025.

Lees, K. J., Guerin, A. J. and Masden, E. A. (2016) ‘Using kernel density estimation to explore habitat use by seabirds at a marine renewable wave energy test facility’, Marine Policy. Elsevier, 63, pp. 35–44. doi: 10.1016/j.marpol.2015.09.033.

Lewis, J. and Sauro, J. (2006) ‘When 100% really isn’t 100%: improving the accuracy of small-sample estimates of completion rates’, Journal of Usability Studies, 1(3), pp. 136–150.

Loss, S. R., Dorning, M. A. and Diffendorfer, J. E. (2019) ‘Biases in the literature on direct wildlife mortality from energy development’, BioScience, 69(5), pp. 348–359. doi: 10.1093/biosci/biz026.

Lott, A. and Reiter, J. P. (2020) ‘Wilson Confidence Intervals for Binomial Proportions with Multiple Imputation for Missing Data’, American Statistician. Taylor & Francis, 74(2), pp. 109–115. doi: 10.1080/00031305.2018.1473796.

Marques, A. T. et al. (2014) ‘Understanding bird collisions at wind farms: An updated review on the causes and possible mitigation strategies’, Biological Conservation. Elsevier Ltd, 179, pp. 40–52. doi: 10.1016/j.biocon.2014.08.017.

Marques, A. T. et al. (2020) ‘Wind turbines cause functional habitat loss for migratory soaring birds’, Journal of Animal Ecology, 89(1), pp. 93–103. doi: 10.1111/1365-2656.12961.

Martin, G. R. and Shaw, J. M. (2010) ‘Bird collisions with power lines: Failing to see the way ahead?’, Biological Conservation, 143, pp. 2695–2702. doi: 10.1016/j.biocon.2010.07.014.

May, R. F. (2015) ‘A unifying framework for the underlying mechanisms of avian avoidance of wind turbines’, Biological Conservation. Elsevier Ltd, 190, pp. 179–187. doi: 10.1016/j.biocon.2015.06.004.

Mckinsey & Company (2010) Transformation of Europe’s power system until 2050 Including specific considerations for Germany Electric Power and Natural Gas Practice. Düsseldorf. Available at: https://www.mckinsey.com/~/media/mckinsey/dotcom/client_service/epng/pdfs/transformation_of_europes_power_system.ashx.

Morris, G. and Conner, L. M. (2017) ‘Assessment of accuracy, fix success rate, and use of estimated horizontal position error (EHPE) to filter inaccurate data collected by a common commercially available GPS logger’, PLoS ONE, 12(11), pp. 1–12. doi: 10.1371/journal.pone.0189020.

Movebank (2019) Movebank Data Repository. Available at: https://www.movebank.org/ (Accessed: 1 October 2018).

National Grid (2014) Design Drawings 132kV Overhead Lines: Hinkley Point C Connection Project Application Reference EN020001.

National Science Foundation (2019) Open Topography Data Portal, OpenTopography. Available at: https://opentopography.org/news/three-new-global-topographic-datasets-available-srtm-ellipsoidal-alos-world-3d-gmrt (Accessed: 1 February 2019).

NGA and NASA (2000) Shuttle Radar Topography Mission (SRTM GL1) Global 30m Ellipsoidal, OpenTopography. Available at: http://opentopo.sdsc.edu/raster?opentopoID=OTSRTM.082016.4326.1 (Accessed: 1 February 2019).

Oppel, S., A. D. Ruffo, S. Bakari, M. Tesfaye, S. Mengistu, M. Wondafrash, A. Endris, C. Pourchier, A. Ngari, V. Arkumarev, and S. C. Nikolov. 2021. Pursuit of ‘sustainable’ development may contribute to vulture crisis in East Africa. Bird Conservation International in press. doi:10.1017/S0959270921000307

OpenStreetMap (2018) Classification of Power Lines, OpenStreetMap Wiki. Available at: https://wiki.openstreetmap.org/wiki/Classification_of_power_lines (Accessed: 15 October 2018).

OpenStreetMap (2019a) Guidance for Digitising Power Line Data into OpenStreetMap, OpenStreetMap Wiki. Available at: https://wiki.openstreetmap.org/wiki/Power_lines (Accessed: 10 March 2019).

OpenStreetMap (2019b) OpenStreetMap World Light Gray Base, ESRI Web Map Service. Available at: http://goto.arcgisonline.com/maps/World_Light_Gray_Base.

Péron, G. et al. (2017) 'The energy landscape predicts flight height and wind turbine collision hazard in three species of large soaring raptor', Journal of Applied Ecology, 54(6), pp. 1895–1906. doi: 10.1111/1365-2664.12909.

Pierrot, M. (2018) The Wind Power: Wind Energy Market Intelligence. Tournefeuille, France. Available at: https://www.thewindpower.net.

QGIS Development Team (2019) 'QGIS Geographic Information System'. Open-source Geospatial Foundation Project.

Ross-Smith, V. H. et al. (2016) 'Modelling flight heights of lesser black-backed gulls and great skuas from GPS: a Bayesian approach', Journal of Applied Ecology, 53(6), pp. 1676–1685. doi: 10.1111/1365-2664.12760.

Ryberg, D. S. et al. (2019) 'The future of European onshore wind energy potential: Detailed distribution and simulation of advanced turbine designs', Energy. Elsevier Ltd, 182, pp. 1222–1238. doi: 10.1016/j.energy.2019.06.052.

Sequeira, A. M. M. et al. (2021) 'A standardisation framework for bio-logging data to advance ecological research and conservation', Methods in Ecology and Evolution, Accepted Author Manuscript, pp. 2041–210. doi: 10.1111/2041-210X.13593.

Silva, R. et al. (2017) 'Seasonal and circadian biases in bird tracking with solar GPS-tags', PLoS ONE, 12(10), pp. 1–19. doi: 10.1371/journal.pone.0185344.

Storchová, L. and Hořák, D. (2018) 'Life-history characteristics of European birds', Global Ecology and Biogeography, 27(4), pp. 400–406. doi: 10.1111/geb.12709.

Svensson, L., Mullarney, K. and Zetterström, D. (2016) Collins Bird Guide. 2nd edn. Harper Collins Publishers.

Tanferna, A. et al. (2012) ‘Different Location Sampling Frequencies by Satellite Tags Yield Different Estimates of Migration Performance: Pooling Data Requires a Common Protocol’, PLoS ONE, 7(11). doi: 10.1371/journal.pone.0049659.

Thaxter, C. B. et al. (2017) ‘Bird and bat species’ global vulnerability to collision mortality at wind farms revealed through a trait-based assessment’, Proceedings of the Royal Society B: Biological Sciences, 284(1862). doi: 10.1098/rspb.2017.0829.

Thaxter, C. B. et al. (2019) ‘Avian vulnerability to wind farm collision through the year: Insights from lesser black-backed gulls (Larus fuscus) tracked from multiple breeding colonies’, Journal of Applied Ecology, 56(11), pp. 2410–2422. doi: 10.1111/1365-2664.13488.

Thomson, J. A. et al. (2017) ‘Implications of location accuracy and data volume for home range estimation and fine-scale movement analysis: comparing Argos and Fastloc-GPS tracking data’, Marine Biology. Springer Berlin Heidelberg, 164(10), pp. 1–9. doi: 10.1007/s00227-017-3225-7.

Tikkanen, H. et al. (2018) ‘Modelling golden eagle habitat selection and flight activity in their home ranges for safer wind farm planning’, Environmental Impact Assessment Review. Elsevier, 71(September 2017), pp. 120–131. doi: 10.1016/j.eiar.2018.04.006.

Timmerberg, S. et al. (2019) ‘Renewable electricity targets in selected MENA countries – Assessment of available resources, generation costs and GHG emissions’, Energy Reports. Elsevier Ltd, 5, pp. 1470–1487. doi: 10.1016/j.egyr.2019.10.003.

Vasilakis, D. P. et al. (2016) ‘Reconciling endangered species conservation with wind farm development: Cinereous vultures (Aegypius monachus) in south-eastern Europe’, Biological Conservation, 196, pp. 10–17. doi: 10.1016/j.biocon.2016.01.014.

Warwick-Evans , V. et al. (2017) ‘Predicting the impacts of wind farms on seabirds : An individual-based model’, Journal of Applied Ecology, (August), pp. 1–13. doi: 10.1111/1365-2664.12996.

CHAPTER 3: FLYING IN THE DANGER ZONE: PREDICTIVE MODELLING OF BIRD SENSITIVITY TO WIND FARMS AND POWER LINES

This chapter is yet to be submitted for publication.

Photo 5: White Stork Ciconia ciconia during the breeding season near Castro Verde, Portugal

Photo 6: Two male Little bustards foraging in May of 2021 near Castro Verde, Portugal. (Photos Credit, J. Gauld 2021)

3.1 ABSTRACT

1. The global energy system is likely to become dominated by renewables before 2050 as countries seek to reduce their use of fossil fuels. Poor spatial planning of wind turbines and power lines can negatively affect bird populations by increasing the risk of mortality from collision. It is therefore vital that we minimise potential conflicts between renewable energy infrastructure and bird conservation. One tool to help identify potential conflicts between birds and energy infrastructures are sensitivity maps. These highlight where birds are most likely to be at risk of collision with wind turbines and power lines.
2. Here we refine previous work on sensitivity mapping by combining GPS tracking data with environmental variables, namely thermal and orographic uplift, terrain roughness and landcover to model the relationship between these variables and flight height for White Stork *Ciconia ciconia* and Little Bustard *Tetrax tetrax*. The output of the GLMM (generalised linear mixed model) was then applied to a random points surface to estimate the proportion of flights at danger height for transmission power lines (10 – 60m) and wind turbines (15m – 135m). This was combined with species distribution data to estimate sensitivity to collision risks within the European breeding distribution of each species.
3. For White Stork, thermal uplift, orographic uplift, and migration season were significantly related to the probability of flying at danger height. For Little Bustard, temperature, precipitation and terrain roughness were most influential on the likelihood of flying at danger height during the breeding season. For White Storks landcover was a significant factor, with "Built Area" increasing the likelihood of the birds flying at danger height and a small but significant negative effect of migration. With regard to uplift, there was strong negative effect of

thermal uplift and a positive effect of orographic uplift on the probability of storks flying at danger height. The predictive models for white stork performed well with high (AUC >0.8) whereas the models for Little Bustard behaved poorly (AUC ~0.6) limiting our ability to predict sensitivity for Little Bustard.

4. Our results suggest that our approach is likely to be useful for other soaring bird species but not for flapping species. The sensitivity maps produced as a result of the analysis in this study help provides the high-level spatial information required for developers to avoid further energy infrastructure development in the most sensitive areas for these species, representing <2% of the study area. This information can also be used to target further survey and analysis at a local level to mitigate existing conflicts between energy infrastructure and birds.

3.2 INTRODUCTION

With the ongoing, rapid expansion of renewable energy, there is a danger that the biodiversity crisis may be neglected in the name of solving the climate crisis (Kiesecker *et al.*, 2019). The global energy system is likely to become dominated by renewables before 2050 as countries seek to reduce their use of fossil fuels in response to climate change (IEA, 2020; IPCC, 2022c). Wind power, as one of the more mature renewable energy technologies, is set to play an ever more important role in our energy mix as we seek to phase out fossil fuels (Ryberg *et al.*, 2019). The expansion of wind and solar energy will also require significant investments in the electricity transmission and distribution network. One way in which poor spatial planning of wind turbines and power lines can negatively affect bird populations is by increasing the risk of mortality from collision (Kiesecker *et al.*, 2019).

It is most optimal to consider potential wildlife impacts at the site selection and scoping stages of new wind farm developments as this can help avoid additional costs related to mitigation later in the development pipeline and public perception of the project (Kiesecker *et al.*, 2019; May *et al.*, 2019). Analysis of GPS and GNSS tracking data to produce bird sensitivity maps can fill this knowledge gap by helping us understand where and when birds are most at risk from new developments at the flyway or landscape scale (Bernardino *et al.*, 2018; Tikkanen *et al.*, 2018; Gauld *et al.*, 2022). Sensitivity maps are therefore a potentially important tool in the hierarchy of assessment used to optimise renewable energy development alongside home range analysis of the most vulnerable species to aid final site selection and site-based surveys to inform the layout of the development and any specific mitigation requirements. One limitation to this approach is the availability of tracking data which can result in gaps as highlighted in (Gauld *et al.*, 2022). While costs of GNSS loggers are becoming more economical, other costs associated with deploying loggers such as labour, data costs, training and time are likely to remain significant barriers (Hofman *et al.*, 2019). There are also ethical considerations for tracking studies as the potential impact on individual birds in terms of welfare needs to be balanced against the potential conservation benefits and advancements in our understanding of bird movement ecology arising from the use of bird mounted loggers. This will differ for each species, population, and the mounting method (leg loop, backpack or feather mounted). As such alternative approaches are likely to always be needed to estimate sensitivity to wind energy development in areas where tracking data is not available.

Other studies have highlighted how the likelihood of birds flying within the rotor swept zone (RSZ) of wind turbines (Hanssen, May and Nygård, 2020) is influenced by uplift conditions and how landscape factors can influence flight heights (Scacco *et al.*, 2019; Sage *et al.*, 2022). Here we model bird flight height (Thaxter *et al.*, 2019; Gauld *et al.*, 2022) combining GNSS/GPS tracking data with static landscape features and temporally dynamic variables factors such as uplift. We seek to demonstrate how this approach can be used to predict sensitivity to development of energy infrastructure (including wind farms and power lines) within the European breeding range of two bird species with different flight and migratory strategies. The two model species are sensitive to energy infrastructure, the White Stork *Ciconia ciconia*, is a soaring bird species for which collision with wind turbines and power lines is one of the single largest sources of anthropogenic mortality (Oloo, Safi and Aryal, 2018; Marcelino *et al.*, 2021); the Little Bustard *Tetrax tetrax*, is a flapping species with poor avoidance capabilities which is particularly vulnerable to collision with power lines (Silva *et al.*, 2014).

We aim to determine the influence of landscape and weather-related factors on the probability of birds flying at danger height across their entire distributions. This in turn will allow us to estimate sensitivity to new wind and power line developments and the risk posed by existing infrastructure for areas which lack coverage from GNSS tracking studies. To assess this, we seek to answer three research questions: How do landscape, seasonal and weather factors influence the likelihood of a bird flying at collision risk height? Can we combine this with a measure of the known breeding density of each species to predict sensitivity to the presence of energy infrastructure within the known range of each species? Can we use this information to identify potential conflicts between birds and energy infrastructure? In answering these research questions, we will improve the understanding of where and when birds are most likely to be at danger height for collision with wind turbines and power lines and identify priority areas for mitigation of existing infrastructure and protection from future development.

3.3 METHODS

3.3.1 DATA SEARCH

We sourced bird telemetry data via Movebank (Movebank, 2019) for White Stork *Ciconia ciconia* and Little Bustard *Tetrax tetrax* . The known distribution of these species in Europe and North Africa is well represented by GNSS tracking studies which include flight altitude. We used data from a total of 19 White Stork and 5 Little bustard datasets (Figure 7; Appendix D, Supporting Information Table 8), including 328 white storks and 39 little bustards, in the model relating flight behaviour to landscape and environmental factors. We use data from (Dunnett *et al.*, 2020) and the Open Infrastructure project (Garret, 2018) to create the infrastructure density layer. Terrain variables including slope, aspect and terrain roughness index were derived from the STRM digital surface model (NGA and NASA, 2000) using the Raster package in R (Hijmans, 2019). Sentinel-2 Landcover data for Europe and Africa was downloaded for the year 2020 (ESRI, 2021).

3.3.2 DATA HANDLING

Environmental, terrain and bird movement data sets used in this analysis are summarised in Table 3. Bird tracking data was prepared for analysis in R using the Tidyverse package to check for duplicates, filter out lower precision GNSS locations and remove GNSS locations outside the study area (Hadley Wickham *et al.*, 2015). Terrain and energy infrastructure layers were prepared using the geoprocessing and mosaic to new raster tools in Arc GIS (ESRI, 2019, 2020). The meteorological variables (temperature at 2m, temperature at altitude, land surface pressure, wind U, wind V), precipitation and cloud cover were downloaded and appended to the tracking data from Copernicus using the Global Animal Movement Toolkit R package (Bird and Laycock, 2019; European Commission; *et al.*, 2021; Muñoz Sabater, 2021). The summary funciton in R was used to check each meterological variable for erroneous values. This highlighted that the ERA5.Land.2m.Temperature data appended to the stork dataset included some values which were below the -58.1°C minimum recorded surface temperature for Europe and Africa (ASU 2023) and therefore highly likely to be erronous. These values (n = 615) were excluded from the final data set used to build the model. Height of the land surface was derived from the STRM digital surface model (DSM) available to download in height above ellipsoid (HAE) from the Opentopography Portal (NGA and NASA, 2000; National Science Foundation, 2019) and height above sea level from (CGIAR, 2022).

The DSM data along with other variables derived from it such as slope, terrain roughness index (TRI), ruggedness and aspect were appended to each GNSS fix using the Raster Package (Hijmans, 2019). Distance from the coast was calculated using the st_distance function (Pebesma, 2018). Displacement between GNSS locations was calculated using the Geosphere package (Hijmans, Williams and Vennes, 2015). We calculated height above ground by subtracting the height of the ground from the altitude for each GNSS location. We only did this for locations over land to avoid including large negative terrain height values in the analysis. Where this is in HAE (height above ellipsoid), we use a DSM in that reference. Where the altitude is measured relative to ASL (above sea level) we used a DSM in ASL (Péron *et al.*, 2017).

3.3.3 AUTOCORRELATION

One potential issue with analysing movement data from GPS tracking studies is autocorrelation due to the sequential nature of how the data is collected (Boyce *et. al.* 2010, Dormann *et. al.* 2007). It is therefore important to evalutate the importance of any inherent autocorrelation in the data set relative to the influence of external environmental factors such as habitat or weather conditions which also tend to be autocorrelated in time and space (Boyce *et. al.* 2010). The median interval between positions in the stork dataset was 17.4 minutes (ranging from 13 seconds to 87 days) whereas for little bustards the median fix interval was 30.2 minutes (ranging between 5 minutes and 106 days). This highlights how tags on some birds in the stork dataset appear to have been programmed to record high intensity bursts of GPS which could intorduce significant bias into the analysis due to a high volume of data being collected in a relatively small area. As an initial control for this, the data was filtered to a minimum 5-minute fix interval to match that of the little bustard dataset before further analysis was performed. Long intervals between positions being recorded can indicate a malfunctioning tag, to control for this locations associated with a fix interval of more than one week were also excluded from the stork (n = 321) and bustard (n = 49) data sets.

To further understand the influence of spatial autocorrelation on the flight height values observed in the data (as measured by metres relative to ground level), Moran's I was calculated for each data set using the "Moran.I" function in the "ape" package for R (Paradis *et al.* 2019). Observed values of Moran's I range between 0 and 1, values close to zero indicate low autocorrelation i.e. the values in the data are randomly dispersed whereas values approaching 1 indicate strong autocorrelation associated with highly clustered data. For the stork dataset, the observed value of Moran's I was 0.194 compared with an expected value of $-5.44*10^{-4}$, a standard deviation of $1.179*10^{-3}$ and $p < 0.001$. For the Bustard dataset, the observed value of Moran's I was 0.147 compared with an expected value of $-5.88*10^{-5}$, a standard deviation of $8.64*10^{-3}$ and $p < 0.001$. In both datasets the observed value of Moran's I was less than 0.2 but larger than the expected value suggesting weak but significant spatial autocorrelation or put another way weak clustering of flight heights in space (Bivand 2022, Dormann *et al.* 2007). As per Ramos *et al.* 2023 and Crase *et al.* 2012, the presence of autocorrelation in the data was controlled for by calculating a spatial autocovariate term (RAC). RAC was calculated from the residuals in the final model for each species and danger height (section 3.3.7) using the spdep and ape R packages (Bivand 2022).

DATA SET NAME	SPATIAL RESOLUTION	TEMPORAL RESOLUTION	UNITS	SOURCE	USAGE
STRM-30 -GL1 ELLIPSOIDAL	30m pixels	N/A	metres	(NGA and NASA, 2000)	height above ground calculation
SRTM 90M DEM VERSION 4	90m pixels	N/A	metres	(CGIAR, 2022)	height above ground calculation
SLOPE	90m pixels	N/A	metres	From STRM 90m (CGIAR, 2022)	orographic uplift
ASPECT	90m pixels	N/A	metres	From STRM 90m (CGIAR, 2022)	orographic uplift
TRI (TERRAIN ROUGHNESS INDEX)	120m pixels	N/A	metres	From STRM 90m (CGIAR, 2022)	in Bustard models
ERA5 LAND WIND U	0.1° x 0.1° (~9km)	Hourly	$m\,s^{-1}$	Copernicus Climate Data Store (Muñoz Sabater, 2021)	orographic uplift
ERA5 LAND WIND V	0.1° x 0.1° (~9km)	Hourly	$m\,s^{-1}$	Copernicus Climate Data Store (Muñoz Sabater, 2021)	orographic uplift
ERA5 LAND SURFACE PRESSURE	0.1° x 0.1° (~9km)	Hourly	Pa	Copernicus Climate Data Store (Muñoz Sabater, 2021)	thermal uplift
ERA5 LAND TEMP	0.1° x 0.1° (~9km)	Hourly	Kelvin	Copernicus Climate Data Store (Muñoz Sabater, 2021)	thermal uplift
ERA5 TEMPERATURE (5000M ASL)	0.1° x 0.1° (~9km)	Hourly	Kelvin	Copernicus Climate Data Store (Muñoz Sabater, 2021)	thermal uplift
ERA5 TOTAL CLOUD COVER	0.1° x 0.1° (~9km)	Hourly	%	Copernicus Climate Data Store (Muñoz Sabater, 2021)	tested in model
ERA5 TOTAL PRECIPITATION	0.1° x 0.1° (~9km)	Hourly	Metres	Copernicus Climate Data Store (Muñoz Sabater, 2021)	tested in model
SENTINAL-2 LANDCOVER 2020	10m (downscaled to 100m)	Yearly	N/A	Sentinel-2 Download Portal (ESRI, 2021)	in Stork models

Table 3 Summary of environmental and landscape variables used in the analysis. Rows labelled "tested in model" describe variables which were tested for significance in terms of predicting presence at danger height but were not included in the final models for either species. TRI was at 120m resolution because of how it calculates terrain roughness from the 30m DSM, the sentinal landcover data was downscaled to 100m due to the size of the orignial being too large to process.

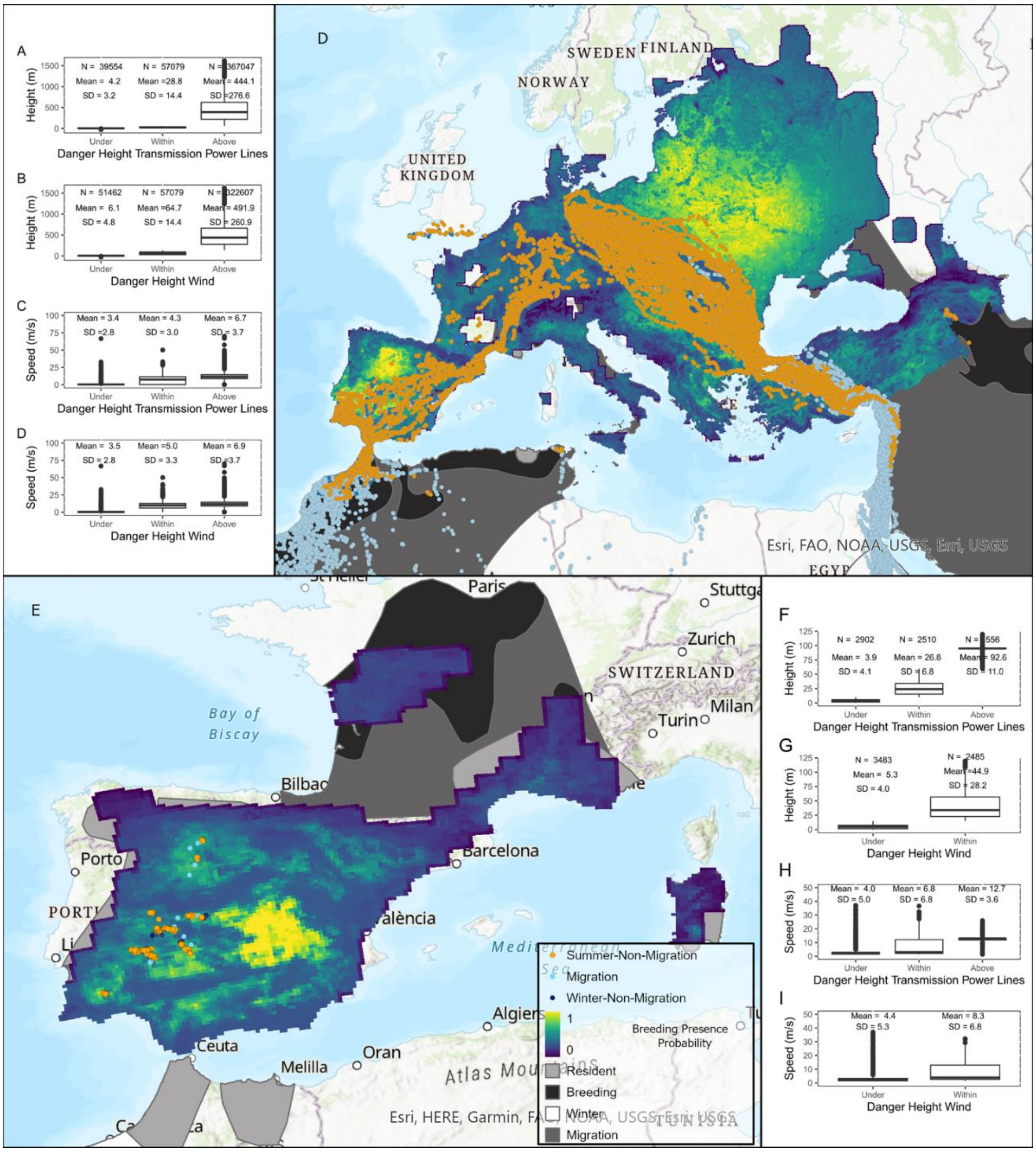

Figure 7: The plots use data included in the final models. A. Distribution of Stork flight heights under, within and above danger height for transmission powerlines, B. Distribution of Stork flight heights under, within and above danger height for wind turbines. C. Distribution of Stork flight speeds under, within and above danger height for Transmission Power Lines. D. Locations in flight for White Stork symbolised by season with the EBBA2 probability of presence in the breeding season and the bird life 2014 species distribution of white stork. E. Locations in flight for Little Bustard symbolised by season with the EBBA2 probability of presence in the breeding season and the bird life 2014 species distribution of Little Bustard. F. Distribution of Little Bustard flight heights under, within and above danger height for transmission powerlines, G. Distribution of Little Bustard heights under, within and above danger height for wind turbines. H. Distribution of Little Bustard flight speeds under, within and above danger height for Transmission Power Lines.

3.3.4 DEFINING FLIGHT

There are numerous, methods used to determine whether a bird is in flight or not. These generally rely on some measure of the bird's behaviour such as flight height or speed at the time a GNSS fix is recorded. In defining a fix as in flight we need to acknowledge the potential errors associated with measuring speed and altitude above the ground (Poessel *et al.*, 2018a). These errors are related to the number and position of satellites used by the GNSS device to measure altitude this vertical error given by many GNSS devices is typically in the region of 1.5m but can be as large as 31m (Marques *et al.*, 2020b; Acácio, Atkinson, *et al.*, 2022). There is additional error arising from the DSM (±5m) used to determine the height of the ground surface (Péron *et al.*, 2020). This can result in erroneously negative GNSS locations relative to the ground which are more likely to occur when the bird is perched or flying near the ground (Péron *et al.*, 2020). With improved computing power, state space models (SSM) have been used in post processing to reduce these error sources however, they can introduce circularity into models used to better understand the relationship between biophysical factors and bird flight behaviour so are not applicable here (Poessel *et al.*, 2018a). Speed was used to classify each fix as in flight (1) or not (0). For White Storks, instantaneous speed provided by the tag was not available across all studies, as such step speed was calculated for each fix per individual bird by dividing the distance between GNSS locations in metres by the time in seconds to yield a speed estimate in m/s. For little bustards, tag speed was present in the dataset for all individuals so this was used to classify whther a given location was in flight or not. Locations associated with speeds greater than a threshold of 1.39 m/s (5kmh) (Marcelino *et al.*, 2021). Then outlier GNSS locations which fall outwith the 95% confidence interval for height relative to ground were then removed from the data set. This does not eliminate all GNSS locations with a negative flight height. However, many of these GNSS locations will be associated with low altitude flights near ground level and are therefore of relevance to understanding where and when birds are most likely to be at danger height. We then classified all GNSS locations in flight at heights between 15m and 135m as within the danger height range for collision with modern onshore wind turbines, and transmission power lines danger height range of 10m – 60m (National Grid, 2014; Thaxter *et al.*, 2019; Gauld *et al.*, 2022). After removing non flying locations, final data sets used to construct the GLMM (generalised linear mixed model) for Little Bustard *Tetrax tetrax* consisted of 5,964 locations in flight. For White Stork, there were 463,680 locations in flight within the original data set, of these 104,661 locations were included in the final model after excluding points associated with NAs for any variable or located outwith the study area.

3.3.5 DEFINING MIGRATION

Season, namely Breeding, Migration and Non-Breeding, can influence the flight behaviour of birds, particularly migratory birds. In the breeding season, birds behaviour becomes focused around the breeding areas with more regular "commuting" flights between the nesting and foraging grounds. Whereas during migration birds may consistently fly long distances (tens or hundreds of kilomtres) each day (Soriano-Redondo *et al.*, 2021; Acácio, Catry, *et al.*, 2022). In the non-breeding season, migratory birds may move in response to changing weather condistions as they are less tied to a particular location than in the breeding season (Fandos *et al.*, 2020). As such, it is important to capture the effect of season in our analysis, even though the focus of this study is on predicting ssensitivity to collision for the breeding season.

Each GNSS location was classified as being “summer non migratory period”, “winter non-migratory period” and “migration”. For storks, a spatial thresholding approach was used whereby days were classified as migratory if the daily displacement exceeded 60km or the locations were between 18°N and 36°N as per (Soriano-Redondo *et al.*, 2020). For Little Bustard, there is a less well defined latitudinal or longitudinal threshold for defining migration, so a simpler method was used to classify each day as migratory if the daily displacement exceeded 8 km/day (Garcia et al. 2015).

3.3.6 OROGRAPHIC AND THERMAL UPLIFT

Orographic uplift describes the vertical deflection of horizontal wind by topography whereas thermal uplift describes the vertical movement of warm air generated by solar heating of the ground surface (Bohrer et al., 2012). Topographical inputs to the uplift calculation (Slope and Aspect) were derived from 90m resolution derived from STRM-GL1 30m DSM (CGIAR, 2022), meteorological input variables, namely wind U, wind V, temperature and air pressure were derived from the Copernicus ERA5 reanalysis (Muñoz Sabater, 2021) as detailed in Table 3**.** Once the environmental and terrain variables were appended to the bird movement data, orographic and thermal uplift estimates were calculated for each GNSS location using the method described in (Bohrer et al., 2012; Hanssen, May and Nygård, 2020; Santos et al., 2020). Orographic uplift ωo is calculated using the wind speed, direction in degrees relative to north, terrain aspect and slope as per $\omega o = vC\alpha$ (1) whereby v is the horizontal ground wind speed and $C\alpha$ describes the updraft resulting from the slope θ and aspect β of the terrain relative to the wind speed and direction as per: $C\alpha = \mathrm{Sin}(\theta)\mathrm{Cos}(\alpha - \beta)$. Where dz/dx and dz/dy are the slope components relative to east and north respectively, θ = arctan[(dz/dx)2 + (dz/dy)2]1/2 (3) and asp(β) = arctan[(dz/dx)/(dz/dy)] (4). All negative orographic uplift values were reclassified as zeroes (Bohrer *et al.*, 2012). Thermal uplift was estimated using w* = [gzH/T]1/3 (5) where g is the gravitational acceleration, z is the flight height, ABL is the atmospheric boundary layer, T is the temperature in kelvin, H is the surface sensible heat flux and w* is proportional to the mean uplift at a given height in the ABL (Bohrer *et al.*, 2012).

3.3.7 FLIGHT HEIGHT BEHAVIOUR IN RELATION TO LANDSCAPE FACTORS

To understand how biophysical factors in the landscape influence the likelihood of a bird flying at danger height or each species, we use a generalised linear mixed model (GLMM) approach (Fong, Rue and Wakefield, 2010) with the lme4 package in R. We modelled presence at danger height (1) or not (0) for each danger height band as a binomial distribution using a randomly selected sample containing 70% of the data. To select candidate input variables to the model and control for autocorrelation we used a custom R function to produce a Pearson-rank correlation matrix for all potential predictor variables along with presence at danger height and flight height (Supporting Information Figure 1). This allowed us to identify variables which were correlated with flight height and presence at danger height while eliminating variables which were strongly correlated with each other such as cloud cover which was strongly related to precipitation.

The distribution of each potential input variable was analysed, where appropriate a log transformation $(Log(x) + 1)$ was applied to continuous variables. Which were then centred using the scale function (Seidel and Wickham, 2022) and rescaled to 0 – 1 using $(x - min(x)) / (max(x) - min(x))$ (6). We also eliminated variables used to calculate thermal and orographic uplift such as wind speed, surface pressure and temperature from the modelling procedure due to autocorrelation. In the initial model for storks we included the following variables as fixed effects: thermal uplift, orographic uplift, landcover, terrain roughness index (TRI), precipitation and migration period. Migration period was included to account for flight behaviours varying between seasons, for example in the breeding season we would expect a greater number of low altitude flights around nesting sites. For little bustards, thermal uplift was replaced with surface temperature in the initial because flapping species are not reliant on thermal Uplift (Hernández-Pliego *et al.* 2015). Little Bustards are sensitive to extremes of temperature; therefore, it is a more ecologically relevant factor influencing their movement behaviour Ramos *et. al.* 2023. Orographic uplift was retained in the initial model because flapping species have been observed to make use of orographic uplift to gain altitude during flight (Sage *et al.* 2019, Scott *et. al.* 2015). For storks, Individual ID was nested within study was included as a random effect to account for potential variation in tagging methods and individual variation in flight behaviour. Whereas for Little Bustards, inter-study variation in methodology was less of a concern because the tagging studies were undertaken by the same team in consecutive years. Only Individual ID was included as a random effect to account for behavioural variation between individuals and the potential for tags from different manufacturers to have been used.

We then used the dredge function in the MuMin package (Barton, 2014) to rank candidate models with different combinations of the input variables by Akaike information criterion (AIC). This allowed us to identify which variables were in the top performing models. In each case, the best model with the lowest AIC was selected. The best models were validated using the validation sample (remaining 30% subset of the data) not included in the model. Model validation was achieved by calculating the sensitivity and specificity of the model to calculate the area under the curve (AUC) i.e. how well the model predicted presence at danger height for each data set (Silva et al., 2014; Rolek et al., 2022). Once a final model was selected, the model was re-run including the RAC term (described in section 3.3.3) to account for spatial autocorrelation and the dredge procedure repeated on this to determine whether it improved model performance. If the model did not appear to improve model performance, measured by Delta AIC, it was not included in the final model. For predicting the conditions under which White Storks would be in flight at danger height for wind turbines (Table 4a) included precipitation, landcover, migration period, terrain roughness Index (TRI) orographic uplift and thermal uplift as fixed effects. Whereas the final model for predicting flight at danger height for transmission power lines (Table 4b) did not include precipitation. Both models included individual ID nested within study name as a random effect to account for potential variation between tracking methodology such as tag type, GNSS sampling interval and mounting method which can impact upon GNSS accuracy (Silva et al., 2017; Acácio et al., 2021). Including study as a random effect also helps account for the behaviour of stork populations originating in different geographic regions of Europe and North Africa. For storks, including RAC to account for spatial autocorrelation was not found to improve either of the final models (Table 5).

ID	(Intercept)	ERA5 Total Precipitation	Landcover Category	Migration Period Group	Orographic Uplift	Thermal Uplift	TRI	df	logLik	AICc	Delta AIC	weight
					(A) White Stork Danger Height 15 - 135m							
64	0.986	0.479	+	+	0.869	-8.24	0.126	14	-98287.845	196603.692	0	0.862
32	1.016	0.485	+	+	0.877	-8.238	NA	13	-98291.004	196608.009	4.316	0.1
63	0.991	NA	+	+	0.869	-8.251	0.128	13	-98292.059	196610.12	6.428	0.035
31	1.021	NA	+	+	0.878	-8.249	NA	12	-98295.32	196614.64	10.948	0.004
60	0.937	0.531	+	NA	0.882	-8.225	0.162	12	-98311.568	196647.138	43.446	0
					(B) White Stork Danger Height 10 - 60m							
63	1.104	NA	+	+	0.909	-7.991	0.18	13	-27951.973	55929.952	0	0.468
64	1.101	0.237	+	+	0.907	-7.986	0.181	14	-27951.68	55931.366	1.414	0.231
31	1.146	NA	+	+	0.92	-7.987	NA	12	-27953.823	55931.65	1.698	0.2
32	1.143	0.241	+	+	0.92	-7.981	NA	13	-27953.516	55933.037	3.086	0.1
59	1.069	NA	+	NA	0.922	-7.988	0.21	11	-27960.481	55942.966	13.015	0.001

Table 4: Model Comparison Table for White Storks in relation to presence at danger height; the final model selection for each height band and species is highlighted in yellow. All numeric input variables for these models were normalised as described in the methods. The top model from each dredge was re-run including the RAC term to account fo spatial autocorrelation. The models with and without the RAC term were then validated using AUC and compared to determine if there was a difference between them in terms of their predictive power.

ID	(Intercept)	ERA5 Total Precipitation	Landcover Category	Migration Period Group	Orographic Uplift	Thermal Uplift	TRI	Autocorrelation (RAC)	df	logLik	AICc	Delta AIC	weight
					(A) White Stork Danger Height 10 - 60m								
28	1.191	NA	+	+	0.909	-7.991	0.18	NA	13	-27951.97	55929.952	0	0.468
26	1.296	NA	+	+	0.907	-7.986	0.181	NA	14	-27951.68	55931.366	1.414	0.231
20	1.31	NA	+	+	0.92	-7.987	NA	NA	12	-27953.82	55931.65	1.698	0.2
18	1.41	NA	+	+	0.92	-7.981	NA	NA	13	-27953.52	55933.037	3.086	0.1
27	0.826	NA	+	NA	0.922	-7.988	0.21	NA	11	-27960.48	55942.966	13.015	0.001
					(B) White Stork Danger Height 15 - 135m								
120	0.99	0.48	+	+	0.87	-8.24	0.13	NA	14	-98291.81	196611.63	0	0.86
56	1.02	0.48	+	+	0.88	-8.24	NA	NA	13	-98294.96	196615.92	4.29	0.1
119	0.99	NA	+	+	0.87	-8.25	0.13	NA	13	-98295.99	196617.98	6.35	0.04
55	1.02	NA	+	+	0.88	-8.25	NA	NA	12	-98299.23	196622.46	10.83	0
116	0.94	0.53	+	NA	0.88	-8.23	0.16	NA	12	-98315.34	196654.69	43.05	0

Table 5: Model Comparison Table for White Storks in relation to presence at danger height; the final model selection for each height band and species is highlighted in yellow. All numeric input variables for these models were normalised as described in the methods. The top model from each dredge was re-run including the RAC term to account fo spatial autocorrelation. The models with and without the RAC term were then validated using AUC and compared to determine if there was a difference between them in terms of their predictive power.

ID	Intercept	ERA5.Land.2m.Temperature	ERA5.Total.Precipitation	Landcover Category	Migration Period Group	Oro graphic Uplift	TRI	df	logLik	AICc	Delta AIC	weight
(A) Little Bustard Danger Height 10 - 60m (Power Lines)												
64	11.222	-0.566	1.725	+	+	0.396	5.274	13	-2295.077	4616.252	0	0.696
63	11.038	NA	1.957	+	+	0.384	5.44	12	-2297.268	4618.619	2.367	0.213
48	11.225	-0.539	1.858	+	+	+	5.277	12	-2298.434	4620.951	4.7	0.066
47	11.019	NA	2.074	+	+	+	5.435	11	-2300.43	4622.93	6.679	0.025
62	11.52	-0.866	NA	+	+	0.48	4.743	12	-2304.305	4632.694	16.442	0
(B) Little Bustard Danger Height 15 - 135m (Wind Turbines)												
63	-2.053	NA	1.794	+	+	0.304	6.445	12	-2505.397	5034.869	0	0.478
64	-1.911	-0.262	1.693	+	+	0.309	6.381	13	-2504.896	5035.879	1.01	0.288
47	-2.051	NA	1.891	+	+	+	6.448	11	-2507.566	5037.195	2.326	0.149
48	-1.922	-0.243	1.799	+	+	+	6.389	12	-2507.133	5038.341	3.471	0.084
62	-1.6	-0.548	NA	+	+	0.393	5.856	12	-2514.642	5053.36	18.49	0

Table 6: Model Comparison Table for Little Bustards in relation to presence at danger height; the final model selection for each height band is highlighted in yellow. All numeric input variables for these models were normalised as described in the methods. Where the model performance in the top models was similar (<2 delta AIC), the simplest model with the lowest AIC was selected.

Prior to controlling for spatial autocorrelation, the best model for predicting the likelihood of little bustards flying at danger height for transmission power lines (Table 6a) danger band included terrain roughness index (TRI), migration period, temperature and orographic uplift as fixed effects. While for predicting flight at danger height for wind turbines (Table 6b), temperature did not feature in the best performing model. Individual ID was included as a random effect in both models to account for differences in individual bird behaviour and tag type used to track each individual. Study ID was not included as a random effect because the tracking data originated from studies in the same geographical region which used the same methods between years (Figure 7; Supporting Information Table 1). Models which included an RAC term to account for autocorrelation were found to outperform those which did not account for autocorrelation Table 7. As such the final model for predicting the likelihood of Little Bustards flying at danger height for transmission power lines included precipitation, landcover, migration period, TRI and an RAC term while for the wind turbine danger height band (Table 7), the final model also included orographic uplift.

ID	(Intercept)	ERA5.Land.2m.Temperature	ERA5.Total.Precipitation	Landcover Category	Migration Period Group	Orographic Uplift	TRI	Autocorrelation (RAC)	df	logLik	AICc	Delta AIC	weight
(A) Little Bustard Danger Height 10 - 60m (Power Lines)													
96	10.588	-0.675	1.799	+	+	0.666	NA	6.156	12	-1330.687	2685.52	0	0.336
128	10.599	-0.686	1.744	+	+	0.687	0.178	6.138	13	-1330.29	2686.751	1.231	0.182
95	10.378	NA	2.075	+	+	0.753	NA	6.373	11	-1332.518	2687.159	1.639	0.148
80	10.509	-0.771	1.826	+	+	NA	NA	6.211	11	-1332.603	2687.33	1.81	0.136
127	10.382	NA	2.03	+	+	0.774	0.164	6.36	12	-1332.177	2688.499	2.98	0.076
(B) Little Bustard Danger Height 15 - 135m (Wind Turbines)													
127	-2.043	NA	1.873	+	+	0.301	6.527	-0.405	13	-2504.17	5034.43	0	0.264
111	-2.053	NA	1.794	+	+	0.304	6.445	NA	12	-2505.4	5034.87	0.436	0.213
128	-1.903	-0.257	1.774	+	+	0.306	6.463	-0.403	14	-2503.69	5035.48	1.05	0.156
112	-1.911	-0.262	1.693	+	+	0.309	6.381	NA	13	-2504.9	5035.88	1.445	0.128
95	-2.041	NA	1.971	+	+	NA	6.532	-0.413	12	-2506.3	5036.67	2.234	0.087

Table 7: Model Comparison Table for Little Bustards in relation to presence at danger height; the final model selection for each height band is highlighted in yellow. All numeric input variables for these models were normalised as described in the methods. Where the model performance in the top models was similar (<2 delta AIC), the simplest model with the lowest AIC was selected. The top model from the dredge in Table 5 was re-run including the RAC term to account for spatial autocorrelation to determine if this was significant (B). The final model was then validated using AUC and compared to determine if there was a difference between them in terms of their predictive power.

3.3.8 SENSITIVITY SURFACE

To demonstrate how the approach described here can be used to map sensitivity to collision risks, we used the output from the binomial GLMM to predict the proportion of GNSS locations at danger height for each grid cell for each season within the study area. To achieve this, we constructed a matrix of random points at a density of 50 points per 0.045° x 0.045° grid cell (~25km2 at the equator, Coordinate reference system: WGS 1984). We appended the final variables used in the model to these points using the Global Animal Movement Toolkit (Bird and Laycock, 2019), which was developed at UEA for using GPU (graphics processor unit) to speed up the processing and visualisation of animal movement data using parallel processing. Because the timestamps of the 50 points spanned the whole month, they provided a representative sample of the ERA5 data for each month in 2020.

The aim of this study was to estimate sensitivity to collision risks within the European breeding distribution for Little Bustards and White Storks. To extract the random points associated with migration, the mean migration start and end dates (Supporting Information Table 9) for each species across the study area were used to classify the season for the timestamp associated with each random point. Classifying the random points by season allowed us to then group the monthly point datasets into the migratory periods derived from the tracking data for each species and extract the breeding season points from each month. Points which contained predictor values outwith the range observed in the bird tracking data were removed from the random points surface. For the remaining points in the dataset, the likelihood of each point being at danger height as a binomial probability between zero and one was calculated for each height band. We then calculated the mean value across all points in each grid cell to provide a prediction of the proportion of flights likely to be present at danger height for a given grid cell in a given month for 2020.

To estimate sensitivity to collision risk surfaces for each species, it was insufficient simply to predict the likelihood of being at danger height or not for each grid cell, we also needed to include a measure of breeding density for each grid square. For each of the two species, we appended the probability (0 – 1) of breeding presence provided by the European Breeding Bird Atlas project (EBBA2) to all 50 random points within each 5km x 5km grid cell which is closely related to breeding density for each species (Keller et al., 2020, Table 1). Sensitivity for each grid cell (S_G) was calculated by calculating the mean sensitivity across all points in each grid cell. Sensitivity for each point was calculated by summing predicted probability of each point being in flight at danger height (DH) with the breeding presence (BP) value and dividing by two to yield a sensitivity value for each point (S_P) for a given danger height band (for wind turbines or for power lines) according to equation 7:

$$S_P = \frac{\mathrm{DH+BP}}{2} \quad (7)$$

For areas where the species is not present in either the EBBA2 or birdlife species distributions, the resulting sensitivity value was then set to zero. For each grid cell (G), the random points had randomly assigned time stamps spanning the duration of each month, as such Sp results in from Equation 7 is actually the value for that point in a specific month (Spm). Using the timestamp associated with each point, all points were assigned a season using the mean start and end dates for the migration periods for each species. The Spm values associated with all points within each month (M) associated with the breeding season, within each grid cell were then averaged to produce the mean value for each grid cell for that month ($\bar{x}$G,M). The mean breeding season sensitivity (SG) for each grid cell was then calculated across all months within that season as per equation 8:

$$S_G = \sum_m^M \frac{\bar{x}_{G,M}}{M} = \sum_m^N \frac{S_{pmn}}{n} \quad (8)$$

The same process was undertaken to calculate the mean value of probability of flying at danger height for each height band and the mean values of thermal and orographic uplift for each grid cell across the breeding season. For the purposes of this paper the prediction surfaces were produced for 2020 only to match the Landcover data set (ESRI, 2021) and for the Breeding season only to match the coverage of the EBBA2 breeding distribution data set (Keller et al., 2020, Supporting Information Figure 55). To aid interpretation, sensitivity was categorised using quantiles whereby “Negligible” <= 2.5th quantile, “Very Low” <=25th quantiles, “Low” <= 50th quantile, “Moderate” 75th quantile, “High” <= 97.5th and “Very High” > 97.5th quantile, values associated with sensitivity values of zero were classified as “No Sensitivity” and grid cells outwith the extent of the EBBA2 data set were classified as NA.

3.4 RESULTS

Environmental, terrain and landcover data (Figure 7) was appended to GNSS tracking data representing 398 White Storks, and 39 Little Bustards from studies available for download from Movebank (Supporting Information Table 8, Movebank, 2019). The locations within each tracking data set were classified as in flight at danger height (1) or not (0) for wind turbines and transmission power lines. For the 463,680 in flight locations in the White Stork data set, 12.3% were within the collision risk height band for transmission power lines and 19.3% were within the danger height band for wind turbines (Figure 7). Of the 5,968 locations in flight locations included in the final data set for Little Bustard, 42.1% were within the collision risk height band for transmission power lines and 41.6% were within the danger height band for collision with wind turbines. No locations in flight at heights greater than the upper bound of the wind turbine danger height band were present in the little bustard dataset indicating that this species generally flies near to the ground. Flight speeds were also generally higher within, and above the danger height bands for both species (Figure 7).

3.4.1 PREDICTORS OF FLYING AT DANGER HEIGHT

A binomial GLMM procedure was used to understand which environmental variables were important for determining how likely the birds were to fly at danger height. Although there were interspecies differences, the intraspecies results were similar across danger heights. For both species the proportion of flights at danger height present in the tracking data varied significantly among individuals, (Little Bustard, $F(36, 5931) = 16.46$, $p = < 0.001$), (White Stork, $F(398, 463281) = 72.13$, $p = < 0.001$) and for white storks there was significant variation between study was also found to be significant (White Stork, $F(398, 463281) = 1497$, $p = < 0.001$). Highlighting the importance of capturing this variation between individuals and data originating from disparate geographical locations. This variation can arise from methodical difference between years and regions and behavioural differences between populations of the same species. Variation in methodology includes the tag type deployed, sampling rate and attachment method (backpack harness vs. leg loop) which can all impact upon the GNSS position accuracy and the also influence the behaviour of the birds (Kölzsch *et al.*, 2016; Lameris, Müskens, *et al.*, 2018).

3.4.1.1 Little Bustard

For Little Bustard, all models performed poorly in terms of predicting how likely the birds were to fly at danger height. The likelihood of flying at danger height for collision with transmission power lines in this model (Adjusted-R^2 = 0.183, AUC = 0.658) was positively associated with terrain roughness (TRI) (Estimate = 0.49, SE = 0.161, Z = 3.02, P = 0.003), precipitation (Estimate = 1.799, SE = 0.557, Z = , P <0.001) and negatively correlated with temperature (Estimate = -0675, SE = 0.353, Z = , P = 0.056). The birds were more likely to fly at danger height in the summer (Estimate = 0.403, SE = 0.145, Z = 2.78, P = 0.05) and winter (Estimate = 0.94, SE = 0.13, Z = 7.3, P <0.001) non-migratory periods. There was no clear pattern in the landcover data. The likelihood of flying at danger height for collision with wind turbines in this model (Adjusted-R^2 = 0.179, AUC = 0.658) was positively associated with TRI (Estimate = 0.944, SE = 0.129, Z = 7.303, P <0.001) and the birds were more likely to fly at danger height for wind turbines within the summer (Estimate = 0.485, SE = 0.161, Z = 3.02, P = 0.003) and winter (Estimate = 1.02, SE = 0.14, Z = 7.3, P <0.001) non-migratory periods. Whereas temperature is negatively correlated with flight at danger height for collision with power lines (Estimate = 1.02, SE = 0.14, Z = 7.3, P <0.001). The random variance between individuals was (0.305 ± 0.553, groups = 36, n = 2347). The random variance between individuals was (0.251 ± 501, groups = 36, n = 2149) for the transmission power line model and (0.305 ± 0.553, groups = 36, n = 2347) for the wind turbine model. These results from the Little Bustard analysis are summarised in **Error! Reference source not found.**Table 7, Figure 9 and Figure 8. Although orographic uplift and landcover were not significant, landcover was included in the final model for power lines and both variables were included in the final model for wind turbines because models containing these predictors performed best in the dredge procedure (Table 7). Given the tendency of this species to fly near to the ground (Figure 7), the GLMM is effectively predicting the conditions under which the birds increase their flight altitude sufficiently to enter the danger height band. These results suggest that terrain roughness and weather conditions (precipitation and temperature) are the most important factors influencing whether the birds are likely to fly at collision height or not and that landscape factors are less important. The seasonal differences observed in the results align well with what is expected given that little bustards nest on the ground and the males spend a considerable proportion of their time performing territorial flights during the lekking season particularly during spring and early summer (Alonso *et al.*, 2019). However, neither model appears to be sufficiently robust to allow for reliable prediction of flight at danger height, as such we do not map the results for Little Bustard within this thesis. Spatial autocorrelation was significant in both models which could explain why AUC was low when the models were validated against the probability of flying at danger height in the 30% validation subset used to test the model.

Little Bustard Presence Within Danger Height Band for Transmission Power Lines					**Little Bustard Presence Within Danger Height Band for Wind Turbines**				
Predictors	*Estimate*	*SE*	*Z*	*p*	*Predictors*	*Estimate*	*SE*	*Z*	*p*
(Intercept)	10.5877	36.3872	0.291	0.77107	(Intercept)	-1.867	1.476	-1.265	0.206
ERA5.Land.2m.Temperature_norm	-0.675	0.353	-1.909	0.056	ERA5 Total Precipitation	-0.296	1.488	-0.199	0.842
ERA5 Total Precipitation	1.799	0.557	3.23	0.001	Landcover Category [Built Area]	0.11	1.46	0.076	0.94
Landcover Category [Built Area]	-12.214	36.391	-0.336	0.737	Landcover Category [Crops]	-0.576	2.113	-0.273	0.785
Landcover Category [Crops]	-11.838	36.388	-0.325	0.745	Landcover Category [Flooded Vegetation]	-0.59	1.462	-0.403	0.687
Landcover Category [Flooded Vegetation]	-12.337	36.412	-0.339	0.735	Landcover Category [Rangeland and Grassland]	-13.825	52.262	-0.265	0.791
Landcover Category [Rangeland and Grassland]	-12.627	36.389	-0.347	0.729	Landcover Category [Trees]	0.124	0.191	0.65	0.516
Landcover Category [Trees]	-12.214	36.391	-0.336	0.737	Landcover Category [Water]	7.243	0.911	7.954	<0.001
Landcover Category [Water]	-11.838	36.388	-0.325	0.745	Orographic Uplift norm	0.403	0.145	2.779	0.5
TRI normalised	0.485	0.161	3.015	0.003	TRI normalised	0.944	0.129	7.303	<0.001
Migration Period Group [Summer-Non-Migration]	1.018	0.142	7.173	<0.001	Migration Period Group [Summer-Non-Migration]	0.665	0.211	3.148	0.002
Migration Period Group [Winter-Non-Migration]	6.156	0.952	6.465	<0.001	Migration Period Group [Winter-Non-Migration]	-1.867	1.476	-1.265	0.206
Autocorrelation Term (RAC)	0.666	0.342	1.949	0.051	Autocorrelation Term (RAC)	1.944	0.519	3.744	<0.001
Random Effects					**Random Effects**				
σ^2				3.29	σ^2				3.29
$\tau_{00\ individual\_id}$				0.27	$\tau_{00\ individual\_id}$				0.31
ICC				0.08	ICC				0.12
$N_{individual\_id}$				36	$N_{individual\_id}$				35
Observations				2149	Observations				2374
Marginal R^2 / Conditional R^2				0.117 / 0.183	Marginal R^2 / Conditional R^2				0.122 / 0.197
AIC				2685.519895	AIC				2685.4
AUC				0.658	AUC				0.658

Table 8: Final GLMM model summaries for Little Bustard. Summary table produced using the tabmodel function from the R package sjPlot (CRAN, 2022) *All variables included in the final models were log transformed log(x+1) and centred and scaled to normalise them onto a 0 – 1 scale*

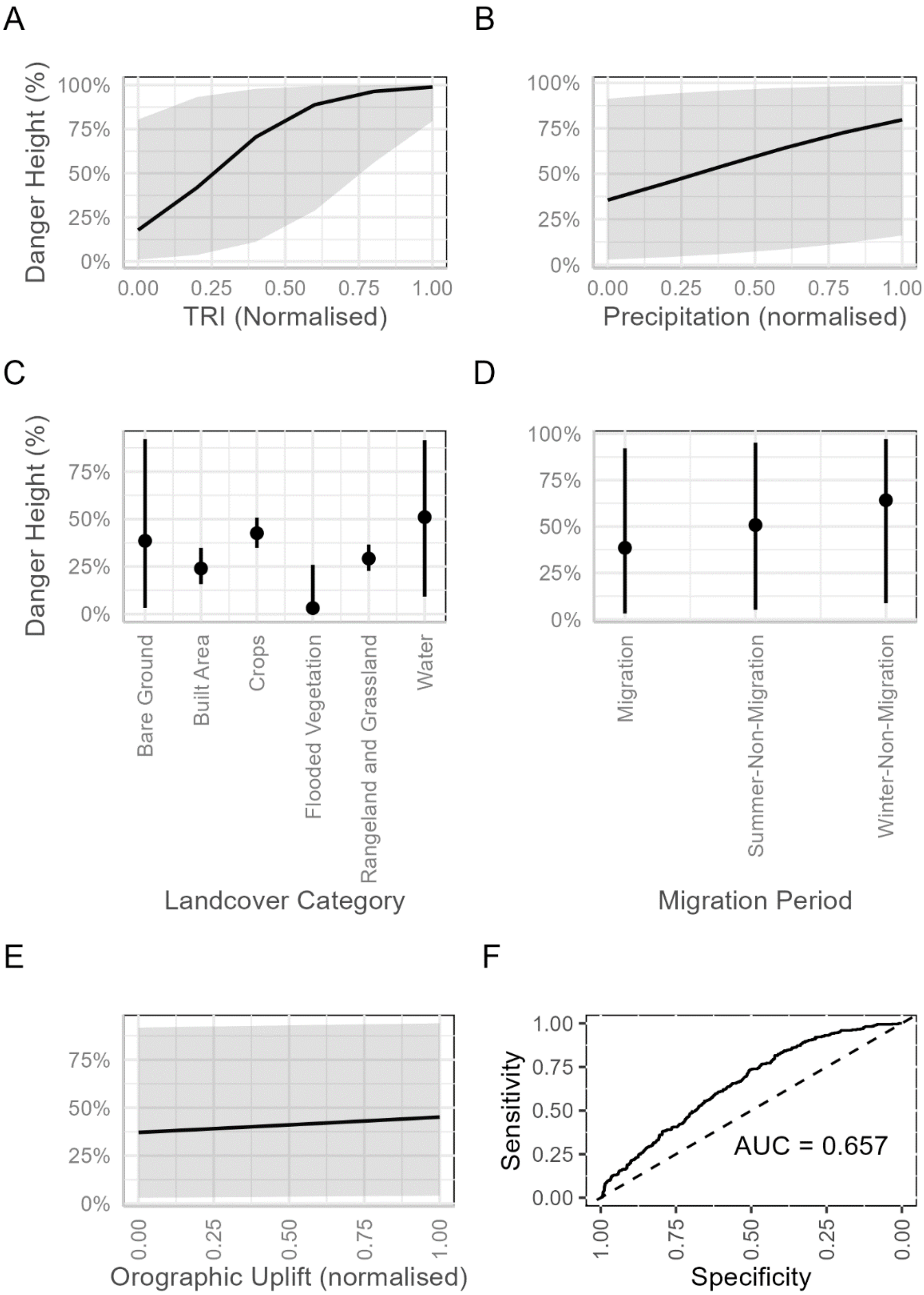

Figure 8: Predictors of presence at danger height for collision with wind turbines 15 – 135m for Little Bustard Tetrax tetrax. The model includes an RAC term to account for spatial autocorrelation. A. displays the relationship between Terrain Roughness and liklihood of flying at danger height. B. Describes the relationship between precipitation and presence at danger height, C. displays the effect of migration period, D. displays the effect of landcover and E. describes the weak positive correlation between orographic uplift and presence at danger height. F describes the model fit as measured by AUC.

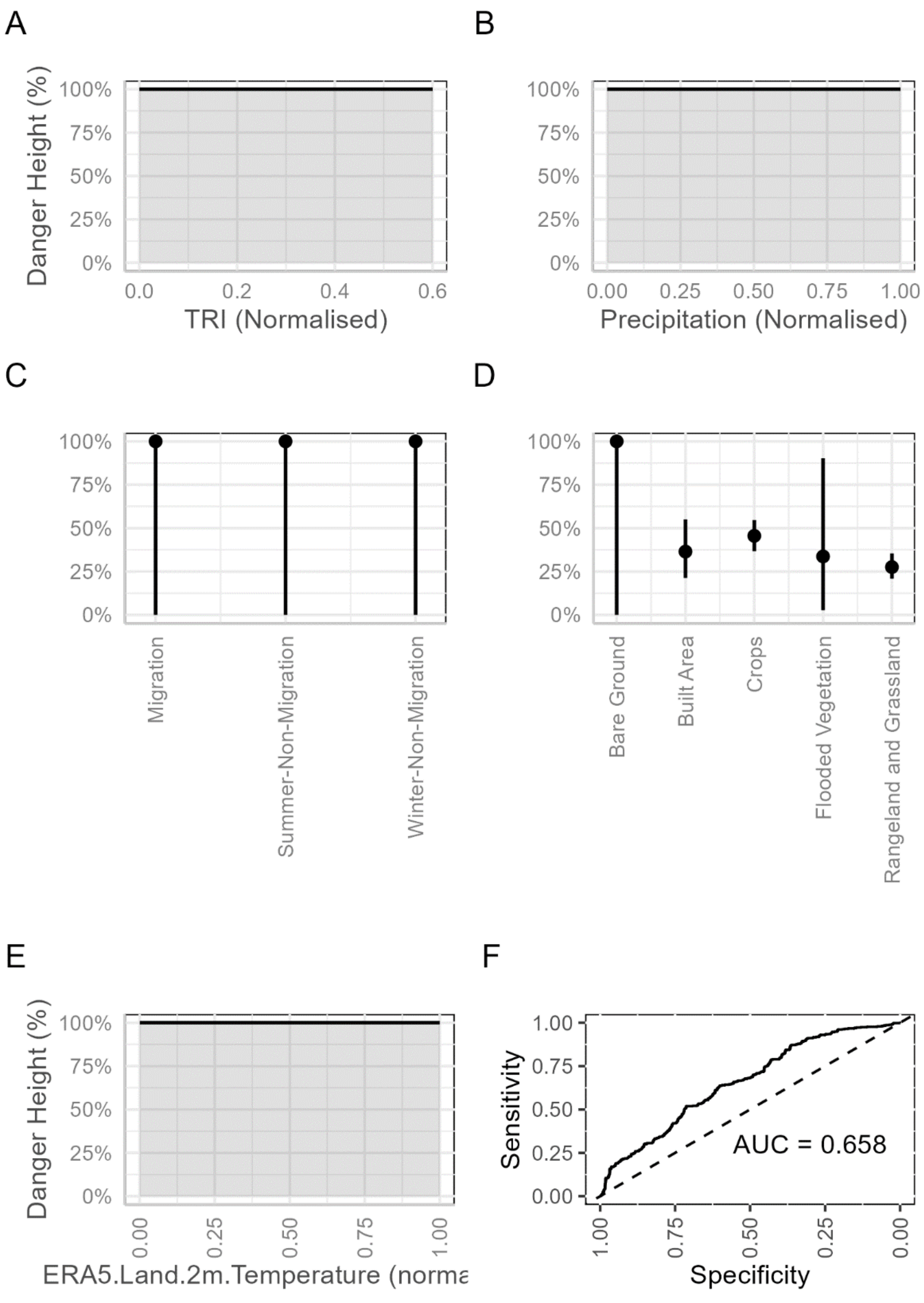

Figure 9: Predictors of presence at danger height for collision with transmission power lines 10m - 60m for Little Bustard Tetrax tetrax. The model includes an RAC term to account for spatial autocorrelation. A. Terrain Roughness B. Describes the relationship between precipitation and presence at danger height, C. displays the effect of migration period, D. displays the effect of landcover and E. describes the weak positive correlation between orographic uplift and presence at danger height. F describes the model fit as measured by AUC (0.658). The predictive power of this model is poor.

3.4.1.2 White Stork

For White Stork, the likelihood of flying within the danger height band for transmission power lines in this model (Adjusted-R^2 = 0.565, AUC = 0.898, Table 9) was positively correlated with orographic uplift (Estimate = 1.08, SE = 0.05, Z = 21.28, P <0.001) and negatively correlated with thermal uplift (Estimate = -11.379, SE = 0.0.07, Z = -166.8, P <0.001). Relative to migration, the probability of flying at danger height was higher during the breeding season (summer non-migratory period) than (Estimate = 0.22, SE = 0.02, Z = 8082, P <0.001) and the winter non-migratory period (Estimate = 0.17, SE = 0.03, Z = 6.44, P <0.001). Landcover was also found to be influential on the likelihood of storks flying at danger height, of the landcover categories present in the model, the category “Built Area” was the only landcover type to be positively correlated with flying at danger height for transmission power lines (Estimate = 0.22, SE = 0.03, Z = 6.87, P <0.001); the other landcover types were negatively associated with flying at danger height (Table 6). This is in line with other studies such as (Marcelino *et al.*, 2021) which demonstrated that storks are likely to fly at collision risk height in and around areas which have been heavily modified by humans such as landfills. The variance attributed to random effects was (0.21 ± 0.46, groups = 13_{study}:$397_{Individual}$, n = 3792). These results are summarised in Figure 10, and Table 6. A similar patter was observed in the final model for predicting flight at danger height for wind turbines (Adjusted-R^2 = 0.389, AUC = 0.838, Table 9) although this also included Precipitation (Estimate = 0.479, SE = 0.164, Z = -5.914, P <0.012); and Terrain Roughness Index (TRI) (Estimate = 0.126, SE = 0.05, Z = 2.514, P <0.003); which were both significant and positively correlated with flying at danger height in relation to wind turbines. Given that the majority of flights in the data set are at heights greater than the upper bound of the danger height band (Figure 7), the GLMMs for White Storks are highlighting the conditions under which the bird fly at lower heights than they would under different conditions. The high AUC and R^2 values indicate that the variables included in these models are good predictors of how likely White Storks are to fly at danger height. As a soaring species, White Storks are dependent upon uplift to gain altitude and sustain flight. In conditions of higher orographic uplift, they may utilise this by flying closer to the terrain where the uplift effect will be strongest, whereas in conditions of high thermal uplift, the birds are more likely to soar at higher altitudes to make use of the thermal eddies which occur as warmer air rises (Oloo, Safi and Aryal, 2018). The results also suggest that the birds are likely to be flying above danger height during migration, whereas during the breeding and non-breeding seasons they tend to undertake more frequent, lower altitude flights to find food (Soriano-Redondo *et al.*, 2021). When the outputs of the model were applied to the random points surface, the maximum proportion of flights at danger height in any grid cell for White Stork was 30% (Figure 12).

White Stork Presence Within Danger Height Band for Transmission Power Lines					White Stork Presence Within Danger Height Band for Wind Turbines				
Predictors	*Estimate*	*Standard Error*	*Z*	*p*	*Predictors*	*Estimate*	*Standard Error*	*Z*	*p*
(Intercept)	1.175	0.045	26.131	<0.001	(Intercept)	0.986	0.036	27.528	<0.001
Landcover Category [Built Area]	0.219	0.032	6.867	<0.002	Landcover Category [Built Area]	0.205	0.026	8.047	<0.001
Landcover Category [Crops]	-0.659	0.029	-22.564	<0.003	Landcover Category [Crops]	-0.218	0.022	-9.757	<0.001
Landcover Category [Flooded Vegetation]	-0.56	0.133	-4.217	<0.004	Landcover Category [Flooded Vegetation]	-0.078	0.109	-0.716	0.474
Landcover Category [Rangeland and Grassland]	-0.649	0.029	-22.278	<0.005	Landcover Category [Rangeland and Grassland]	-0.336	0.022	-15.363	<0.001
Landcover Category [Trees]	-0.736	0.042	-17.588	<0.006	Landcover Category [Trees]	-0.245	0.03	-8.272	<0.001
Landcover Category [Water]	-0.644	0.061	-10.493	<0.007	Landcover Category [Water]	-0.094	0.049	-1.911	0.056
Orographic Uplift	1.079	0.051	21.282	<0.008	Orographic Uplift norm	0.869	0.039	22.074	<0.001
Thermal Uplift	-11.805	0.071	-166.83	<0.009	Thermal Uplift norm	-8.24	0.047	-174.83	<0.001
Migration Period Group [Summer-Non-Migration]	0.218	0.025	8.82	<0.010	Migration Period Group [Summer-Non-Migration]	-0.023	0.018	-1.271	0.204
Migration Period Group [Winter-Non-Migration]	0.165	0.026	6.437	<0.011	Migration Period Group [Winter-Non-Migration]	-0.111	0.019	-5.914	0
Terrain Roughness Index (TRI)	0.071	0.065	1.088	0.276	Terrain Roughness Index (TRI)	0.126	0.05	2.514	0.012
					ERA5 total Precipitation	0.479	0.164	2.925	0.003
Random Effects					**Random Effects**				
σ^2				3.29	σ^2				3.29
$\tau_{00\ Study\_Group\_Name:individual\_id}$				0.21	$\tau_{00\ Study\_Group\_Name:individual\_id}$				0.14
ICC				0.06	ICC				0.04
$N_{Study\_Group\_Name}$				13	$N_{Study\_Group\_Name}$				13
$N_{individual\_id}$				392	$N_{individual\_id}$				392
Observations				256763	Observations				256763
Marginal R^2 / Conditional R^2				0.537/0.565	Marginal R^2 / Conditional R^2				0.363 / 0.389
AIC				55929.95	AIC				196611.63
AUC				0.89	AUC				0.838

Table 9: Final GLMM model summaries for white stork. Summary table produced using the tabmodel function from the R package sjPlot (CRAN, 2022) *All variables included in the final models were log transformed log(x+1) and centred and scaled to normalise them onto a 0 – 1 scale*

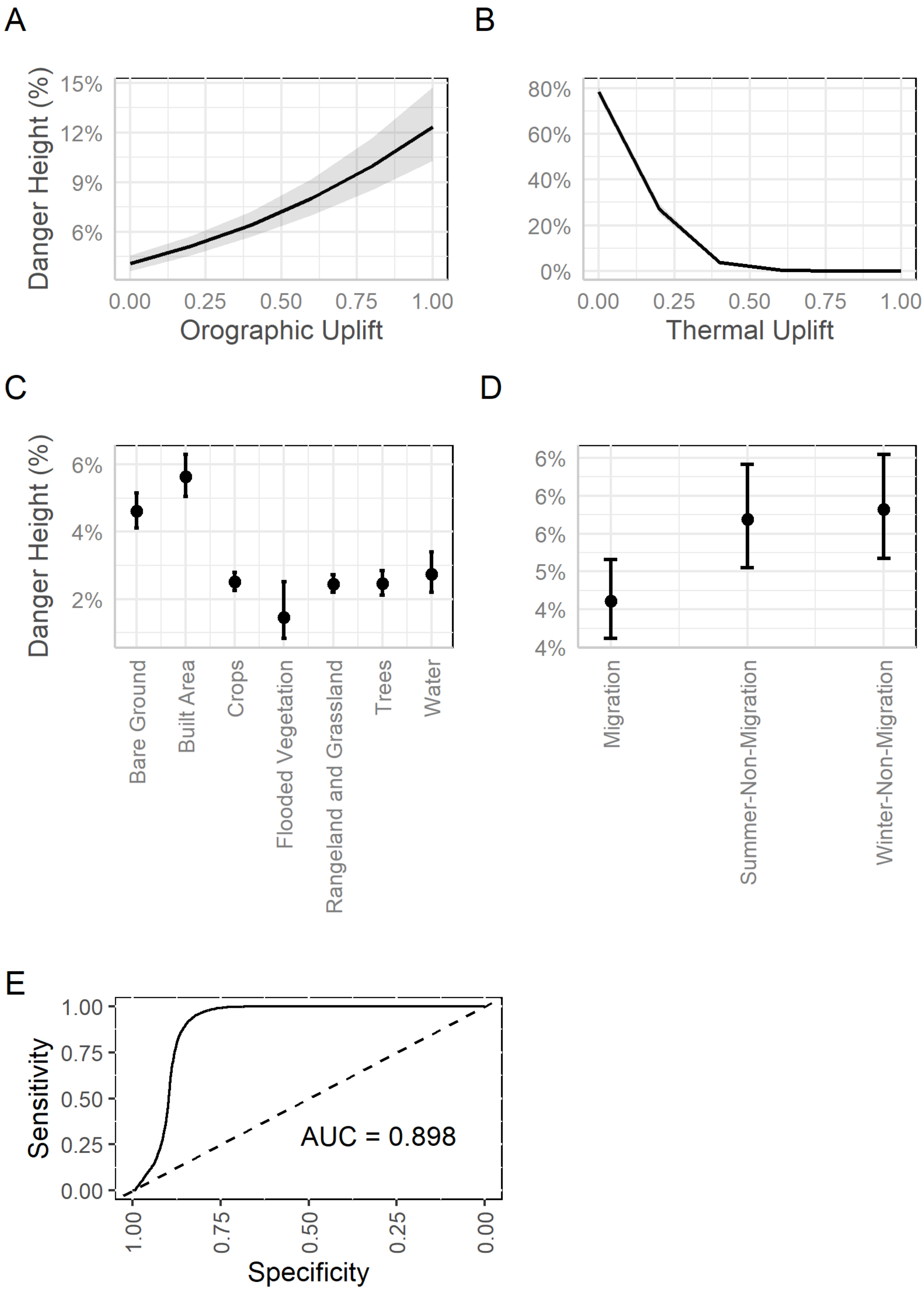

Figure 10: Plots describing the relationship between predictor variables in the final model for predicting flight at danger height for collision with collision power lines in white storks. A. describes the positive effect of orographic uplift, B. describes the negative effect of thermal uplift, C. displays the probabilty of flying at danger height in the context of different land cover types, D. displays the weak but significant effect of season, E. displays the AUC curve which describes a good fit betweenthe model predictions and the values in the validation data set.

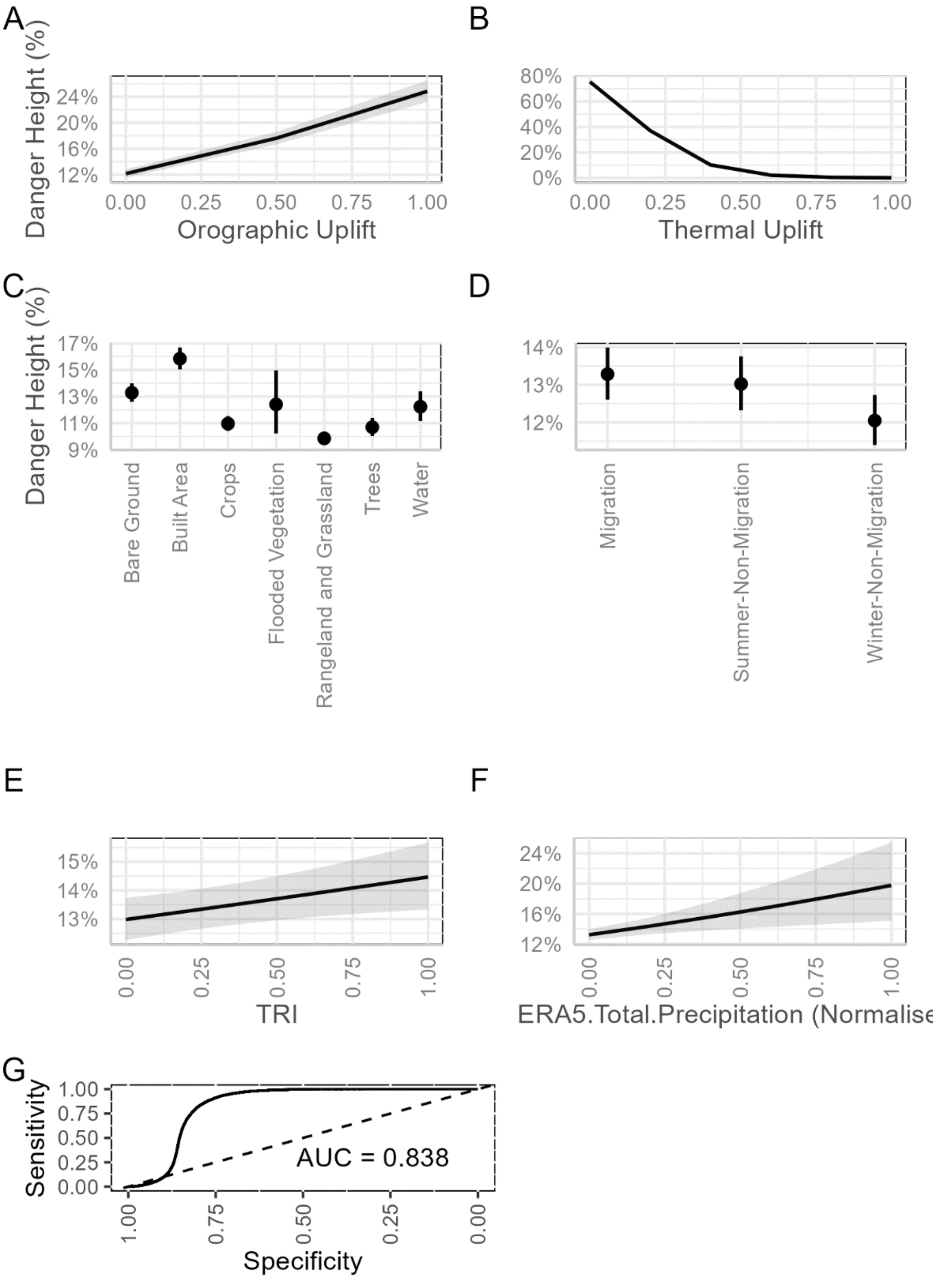

Figure 11: Plots describing the relationship between predictor variables in the final model for predicting flight at danger height for collision with wind turbines in white storks. A. describes the positive effect of orographic uplift, B. describes the negative effect of thermal uplift, C. displays the probabilty of flying at danger height in the context of different land cover types, D. displays the weak but significant effect of season, E. describes the positive relationship between TRI and flying at danger height and F. describes the effect of precipitation. G. displays the AUC curve which describes a good fit betweenthe model predictions and the values in the validation data set.

3.4.2 MAPPING SENSITIVITY TO COLLISION RISKS

The breeding season sensitivity to collision risks from transmission power lines and wind turbines derived from the predictive model for white storks is presented in Figure 13. Sensitivity to collision risk was categorised into seven categories, ranging from "No Sensitivity" associated with sensitivity values of zero to "Very High" associated with the highest sensitivity values in the final data set for each species. Grid cells associated with very high sensitivity are the cells where the birds are most likely to fly at danger height within their breeding distribution and therefore where the construction of new power lines and wind farms would have the greatest effect in terms of direct mortality from collision. The total number of grid cells in each sensitivity category within the EBBA2 and the proportion of the total area assessed for each species represented by each category is summarised in Table 10. This highlights that less than 2% of the total area assessed for each species would need to be avoided by wind farm and power line development and helps highlight the high and moderate sensitivity areas where more detailed surveys could be prioritised to identify potential conflicts between birds and energy infrastructure developments. This estimate, although influenced by the EBBA2 data, is useful for spatial planning of wind and power line developments because rather than simply mapping the distribution of each species, as done previously by (Chris B Thaxter *et al.*, 2017), it also takes into account the predicted proportion of flights at danger height within each 5km x 5km grid cell.

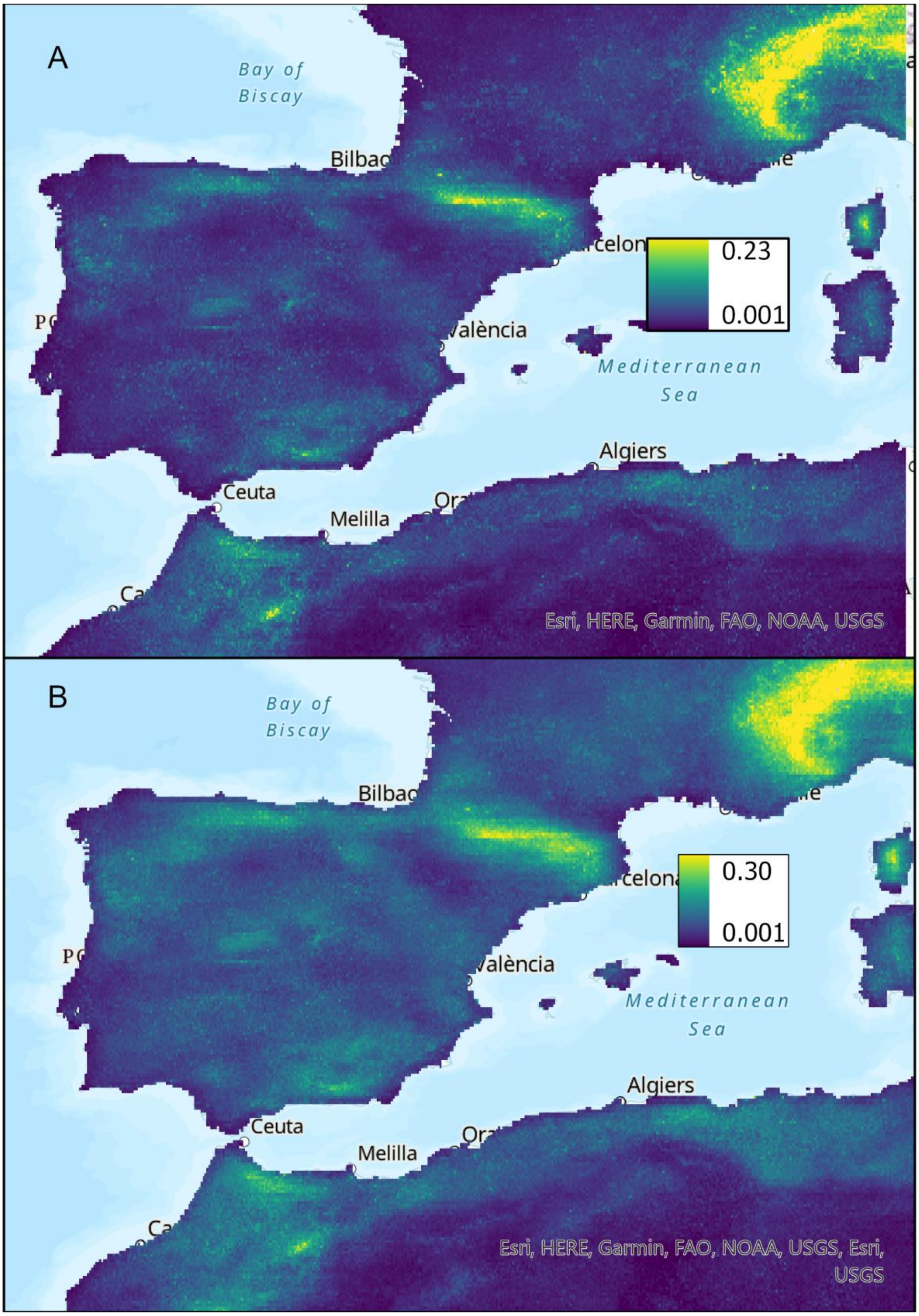

Figure 12: Predicted probability of flying at danger height for white storks in relation to (A) transmission powerlines and (B) wind turbines. This figure does not illustrate where the birds are sensitive to collision but rather how likely it would be for the birds to fly at danger height if they fly in a given grid suqare. Resolution 0.045 x 0.045 decimal degrees.

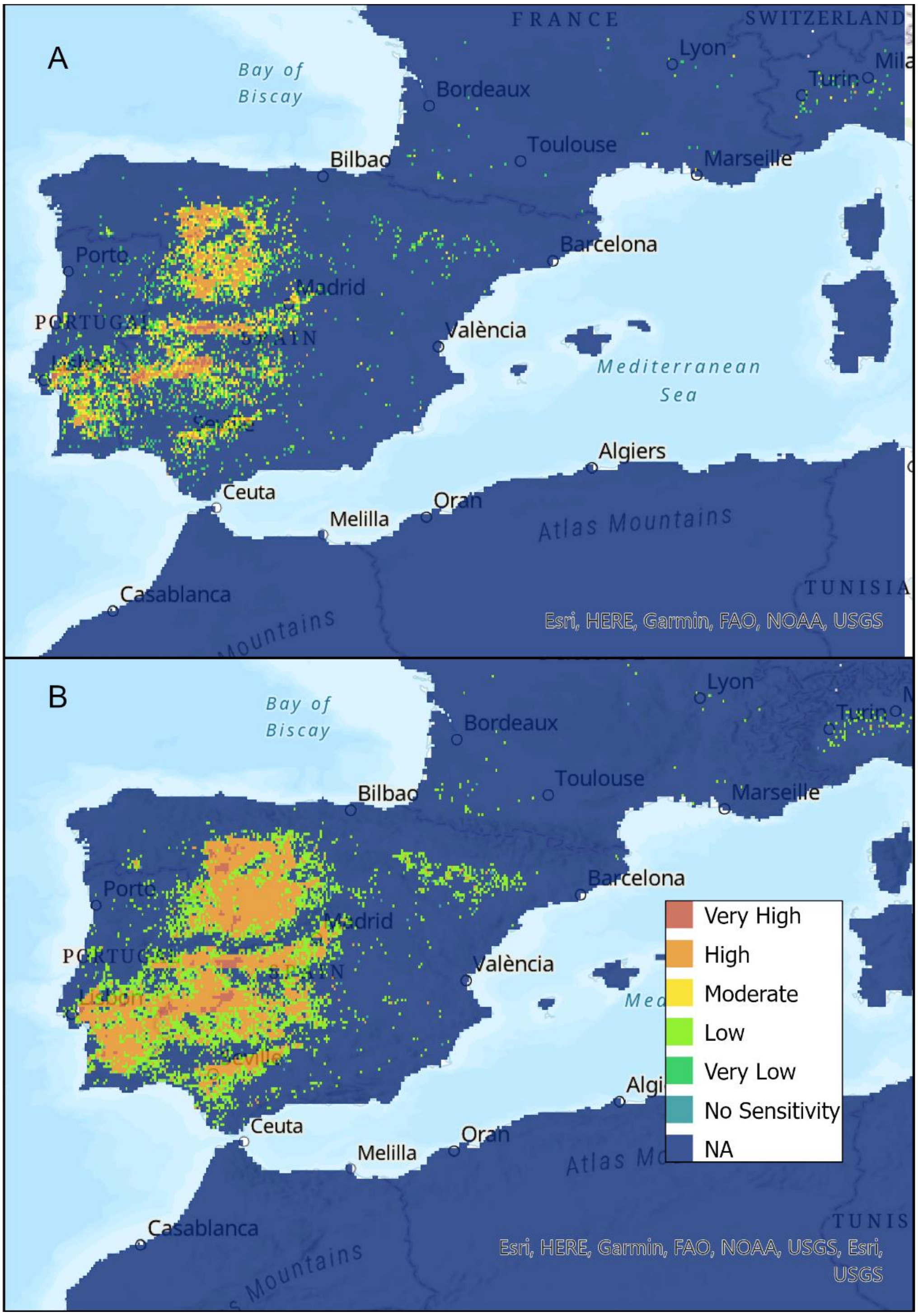

Figure 13: Breeding season sensitivity to transmission power lines for White Stork Ciconia ciconia (A) displays sensitivity to collision risks for the transmission powerline height band (10 – 60m) and (B) sensitivity within the danger height band for onshore wind turbines (15 – 135m) at a resolution of 0.045 x 0.045 decimal degrees (~5x5km) within the EBBA2 distribution. Data was classified into 6 numerical sensitivity categories as described in the methods section.

Species	Species Name	EI Type	Category	Count	Approximate Area (km^2)	Percentage of Area Assessed
White Stork	Ciconia ciconia	Transmission Sensitivity	Very High	138	3450	2.51
White Stork	Ciconia ciconia	Transmission Sensitivity	High	1229	30725	22.36
White Stork	Ciconia ciconia	Transmission Sensitivity	Moderate	1325	33125	24.11
White Stork	Ciconia ciconia	Transmission Sensitivity	Low	1217	30425	22.14
White Stork	Ciconia ciconia	Transmission Sensitivity	Very Low	1388	34700	25.25
White Stork	Ciconia ciconia	Transmission Sensitivity	Negligible	199	4975	3.62
White Stork	Ciconia ciconia	Wind Sensitivity	Very High	235	5875	2.51
White Stork	Ciconia ciconia	Wind Sensitivity	High	2109	52725	22.5
White Stork	Ciconia ciconia	Wind Sensitivity	Moderate	2335	58375	24.91
White Stork	Ciconia ciconia	Wind Sensitivity	Low	2331	58275	24.87
White Stork	Ciconia ciconia	Wind Sensitivity	Very Low	2080	52000	22.19
White Stork	Ciconia ciconia	Wind Sensitivity	Negligible	284	7100	3.03

Table 10: Percentage of the total area assessed for white stork by sensitivity category. This excludes grid cells where the sensitivity value is zero due to being outwith the EBBA2 or Birdlife breeding range for this species.

3.5 DISCUSSION

Using a binomial GLMM approach to determine the environmental conditions and landscape features which increase the likelihood of birds flying at danger height for collision with energy infrastructure for a soaring (White Stork) and a flapping species (Little Bustard).

For White Stork, the best performing models identified in the model optimisation procedure (Table 5) found thermal uplift, orographic uplift and migratory period were significant predictors of flight at danger height. The high AUC values (>0.8) for both the White Stork GLMMs indicate that the final models are good predictors of the conditions under which storks are most likely to fly at heights where they could collide with wind turbines or power lines. The majority of white stork flights at or above the upper bound of the danger height band for collision risk (Figure 7a). As such, the model is essentially highlighting the conditions under which storks are more likely to fly at lower heights (i.e. when uplift is weaker) (Figure 10 and Figure 11). Our results from the binomial GLMM showed a strong negative relationship between flight at danger height and the strength of thermal uplift. This aligns with work by (Santos *et al.*, 2017; and Scacco *et al.*, 2019) which showed a strong positive relationship between flight height and thermal uplift in migratory soaring birds (Black Kite *Milvus migrans* and White Stork).

Whereas for Little Bustard temperature, precipitation, migratory period, terrain roughness and landcover were important factors (Table 6). The importance of meteorological variables in our results aligns with the sensitivity of this species to weather extremes. For example, Little Bustards show a strong positive effect of Temperature on their activity levels whereas in the breeding season when the birds are more likely to experience heat stress, their activity tends to decrease with temperature (Silva *et al.*, 2015). This change in activity levels in response to weather conditions could partially explain the seasonal variation in how likely it is the birds are to fly at danger height for wind turbines Figure 8. The majority of Little Bustard flights were at or below danger height (Figure 7) because the binomial model (Table 14) is, in effect, predicting the conditions under which bustards increase their flight height sufficiently to enter the danger height band such as when the birds fly over areas with greater terrain roughness (Figure 8) or during migratory flights. The high proportion of flights within the two danger heigh bands used in this analysis is likely why the models produced have such poor predictive power (AUC <0.7 and R^2 <0.2). Therefore sensitivity to collision risks is likely to be more directly related to density of this species than for a soaring bird such as White Stork.

Here we sought to combine approaches in previous studies which have used GPS tracking data to understand collision risk at the continental scale such as (Thaxter, Ross-Smith, *et al.*, 2019) with modelling approaches which use environmental and terrain information to predict the flight height of birds such as (Santos *et al.*, 2017; Hanssen, May and Nygård, 2020). Combining the predicted proportion of flights at danger for each grid cell (Figure 13) with the EBBA2 species distribution data (Figure 7) allowed us to estimate sensitivity to collision risks across the 2020 European breeding distribution for White Stork at a resolution of 0.045 x 0.045 decimal degrees (Figure 13). This overcomes one of the limitations highlighted in previous work by (Gauld *et al.*, 2022 and Thaxter *et al.* 2019) which is that the use of GPS tracking data to estimate sensitivity to collision risks is limited to areas with sufficient coverage of GPS tracking data. As yet, GPS tracking data for most species does not provide sufficient coverage to map sensitivity at large scales, except for within migratory bottlenecks and in and around breeding sites (Gauld *et al.*, 2022). Another limitation to this analysis is the vertical position accuracy of the GPS/GNSS which is typically within ±10m accuracy (Marcelino et al., 2021). Grouping the data into height bands rather than modelling changes in continuous flight height meant that our analysis was less sensitive to the effect of position error, we further controlled for this by excluding locations that were stationary or associated with extreme positive or negative height values from the final model. As highlighted by (Poessel *et al.*, 2018), state space modelling approaches can be used to adjust position error in bird tracking studies however, they were not used here because they risk introducing circularity to any models which later use this data to model flight height related responses of birds to environmental conditions (Marcelino *et al.*, 2021).

By incorporating a method for estimating the proportion of flights at danger height for a given grid cell and season, the approach outlined in this study represents a potentially useful method for refining global and continental estimates of sensitivity to collision risk derived from species distribution data such as (Chris B. Thaxter *et al.*, 2017). In our analysis, the EBBA2 data provided a measure of relative utilisation for each grid square. Currently, only presence/absence data appears to be available for the migratory and winter periods of the annual cycle which doesn't provide sufficient detail about how likely birds of a given species are to use a given area at a particular time of year. One possible solution to expand the analysis to other seasons would be to combine our method for predicting flight at danger height with the approach outlined by (Vignali *et al.*, 2021). In that study, citizen science data from eBird was combined with GPS tracking data in a habitat selection model to produce a seasonal probability of presence data set which would match the metric of utilisation used by EBBA2.

An example of how this sensitivity mapping approach can be applied is displayed in Figure 14a. Here, the final sensitivity value for each grid cell has been multiplied by the total length of transmission power lines (km) in each grid cell normalised onto the same 0 – 1 scale. This can be used to prioritise the sections of power line for further survey and the deployment of mitigation to reduce collision risks such as line markers which increase the visibility of the power line to birds (Pavón-Jordán *et al.*, 2020). As well as identifying existing conflicts between birds and energy infrastructure. Figure 14b displays predicted vulnerability to collision risks in relation to the density of wind turbines in the landscape derived from Dunnet *et al.* 2020. The sensitivity surface could also be applied to the potential future density of wind turbines and power lines to inform high level spatial planning of these infrastructures (Ryberg *et al.*, 2019). In turn, providing decision makers with the information required to incorporate sensitivity to collision risks into the spatial planning tools used to identify suitable sites for renewable energy development.

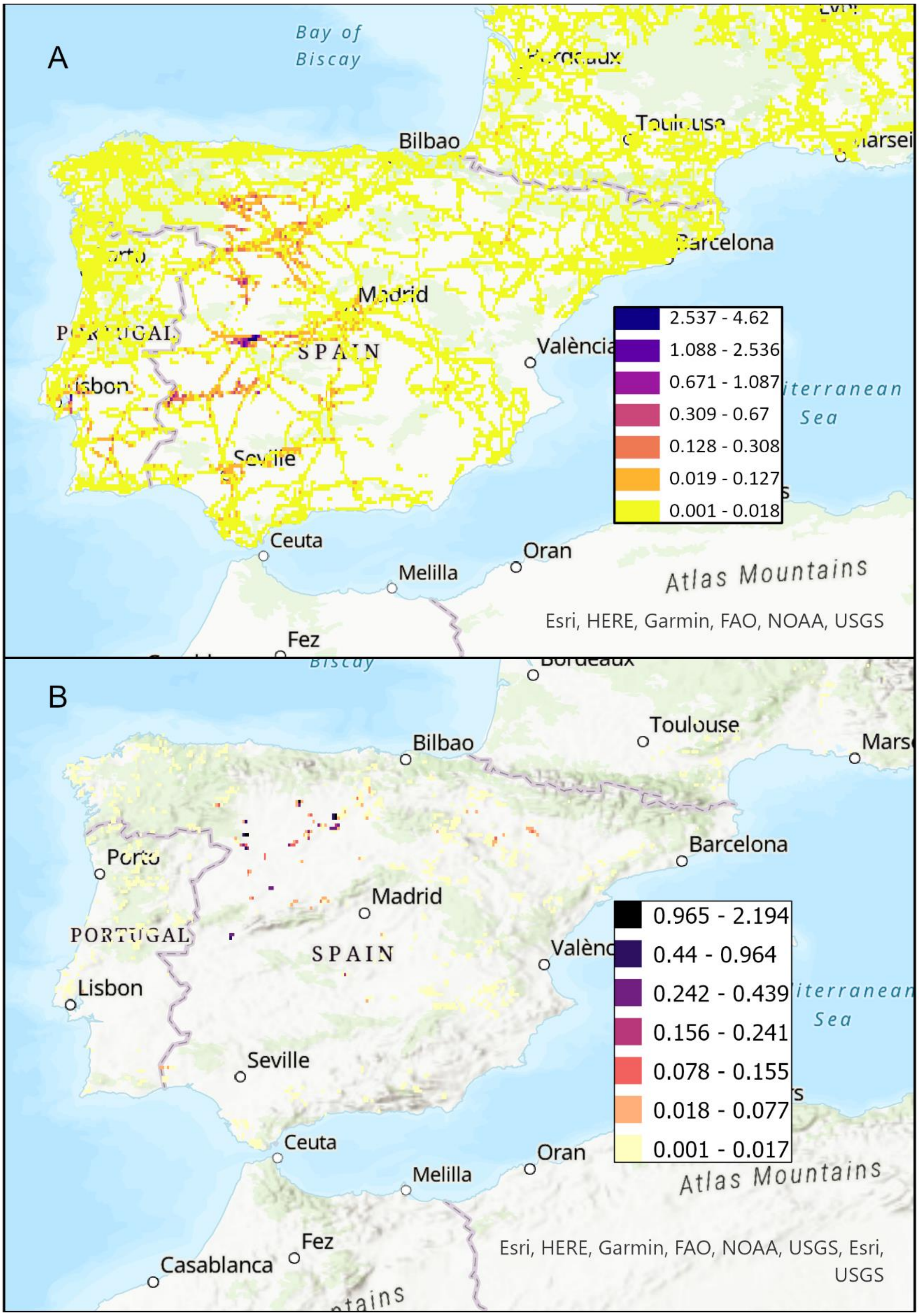

Figure 14: Vulnerability to Collision risk for White Stork in relation to the transmission powerline network in their western European Breeding distribution. A. The map highlights the section of power line where the predicted sensitivity to collision is highest i.e. where the birds are most likely to be present and more flying at danger height and therefore where potential conflicts may occur during the breeding season. B. Predicted vulnerability to collision with wind turbines. In both maps, higher values are associated with higher vulnerability to collision.

This analysis was limited to providing a snapshot of sensitivity to collision risk for the prevalent conditions during the 2020 breeding season within the extent of the EBBA2 species distribution data set for each species (Keller *et al.*, 2020). Given sufficient computing time and access to population density estimates for the non-breeding season, it would be possible to produce annual sensitivity maps for the migratory and winter non-migratory periods of the annual lifecycle of these species. Generating a new set of monthly timestamps for each point across multiple years could provide a multiyear average of the environmental conditions within each grid cell for each season.

Our approach could also be applied to other regions, such as South America where there is currently a poor understanding of the spatial distribution of collision risks for birds in relation to wind and power line development (Aswal *et al.*, 2022). The global animal movement toolkit (GAMT) developed by (Bird and Laycock, 2019) could facilitate the processing of the necessary environmental data sets because it allows global scale, high temporal resolution environmental data sets from Copernicus (Muñoz Sabater, 2021) and other global data stores of environmental data derived from satellite measurements to be processed relatively quickly on almost any computer equipped with an NVIDIA graphics card. Future climate data, such as that provided by Copernicus could also be used to project future sensitivity to collision risks in relation to the projected expansion of renewable energy development (Ryberg *et al.*, 2019; Wouters *et al.*, 2021). Analysis of potential future collision risks in relation to wind turbines may require increasing the upper bound of the wind turbine collision risk height band (15 – 135m) (Thaxter, Ross-Smith, *et al.*, 2019) to account for new developments in wind turbine technology. In an offshore context, wind turbines of greater than 200m blade tip height are now regularly deployed so it is likely that newly developed, larger turbines will also begin to be used onshore where local planning policy allows (Siemens Gamesa Renewables, 2022).

3.5.1 CONCLUSIONS AND CONSERVATION APPLICATION

In this study we demonstrated a method for using GPS tracking data to refine population distribution estimates of sensitivity to collision risks by determining the environmental, landscape and terrain factors which increase the likelihood of White Storks and Little bustards flying at danger height. Our results confirmed that thermal uplift and orographic uplift are important determinants of flight height for White Storks which is in line with previous studies which have identified a link between uplift and the flight height of soaring birds (Santos *et al.*, 2017; Hanssen, May and Nygård, 2020). For White Stork, the most sensitive areas to collision with transmission powerlines and wind turbines where further development should be discouraged, represented less than 3% of the total study area and the areas identified as high and moderate risk can help prioritise more localised survey work to prioritise mitigation actions to reduce risks from power lines and wind turbines. However, this approach is likely to be less useful for flapping species owing to the poor fit of the models produced for Little Bustard.

The outputs of the model predicted the maximum proportion of flights at danger height in any grid cell for White Stork to be 30%. Whereas for little bustard, the minimum predicted proportion of flights at danger height was 42%. This highlights a baseline differences in flight heights between species which in turn could help prioritise the application of our method to assess sensitivity to collision for other species. For low flying species which fly at, or near collision risk height the majority of the time, our approach may be less useful for identifying hotspots for sensitivity to collision risk. A simple two dimensional habitat selection approach as used by (Silva *et al.*, 2014; Tikkanen *et al.*, 2018b; Vignali *et al.*, 2021) and others, is likely to be sufficient for identifying the locations where these birds are most likely to fly at heights where they could collide with energy infrastructure. The main benefit of the approach outlined in this study, is likely to be for identifying collision risk sensitivity hotspots for large, soaring bird species which tend to fly at higher altitudes the majority of the time (Katzner *et al.*, 2012). As highlighted by our analysis for White Storks, the areas where they are likely to fly at heights where they risk collision with energy infrastructure are relatively localised (Figure 7). Potential priority species to apply this sensitivity mapping procedure to include could include Griffon Vulture *Gyps fulvus* and Egyptian Vulture *Neophron percnopterus* which both suffer high rates of mortality associated with collision with wind turbines and power lines (Lucas *et al.*, 2012; Angelov, Hashim and Oppel, 2013; Oppel *et al.*, 2021a). Also White Tailed Eagle *Haliaeetus albicilla* for which collision mortality arising from interaction with wind turbines and power lines is a potentially significant threat to the population (Heuck *et al.*, 2019b).

Data Availability Statement

The R scripts and final sensitivity layers are available for download from figshare via this link: https://tinyurl.com/5eevp5nz

3.6 REFERENCES

Acácio, M. et al. (2021) Quantifying the performance of a solar GPS/GPRS tracking device: fix interval, but not deployment on birds, decreases accuracy and precision. University of East Anglia.

Acácio, M., Atkinson, P.W., et al. (2022) ‘Performance of GPS/GPRS tracking devices improves with increased fix interval and is not affected by animal deployment’, Plos One, 17(3), p. e0265541. Available at: https://doi.org/10.1371/journal.pone.0265541.

Acácio, M., Catry, I., et al. (2022) ‘Timing is critical: consequences of asynchronous migration for the performance and destination of a long-distance migrant’, Movement Ecology, 10(1), pp. 1–16. Available at: https://doi.org/10.1186/s40462-022-00328-3.

Alonso, H. et al. (2019) ‘Male Post-Breeding Movements and Stopover Habitat Selection of an Endangered Short-Distance Migrant, the Little Bustard Tetrax tetrax’, Ibis, 162, pp. 202–216. Available at: https://doi.org/10.1111/ibi.12706.

Angelov, I., Hashim, I. and Oppel, S. (2013) ‘Persistent electrocution mortality of Egyptian Vultures Neophron percnopterus over 28 years in East Africa’, Bird Conservation International, 23(1), pp. 1–6. Available at: https://doi.org/10.1017/S0959270912000123.

ASU 2023 ‘WMO Region VI (Europe, Continent only): Lowest Temperature’, World Meteorological Organization's World Weather & Climate Extremes Archive, Arizona State University, available at: https://wmo.asu.edu/content/europe-lowest-temperature (accessed 24/05/2023).

Aswal, D.K. et al. (2022) ‘Power lines and birds: An overlooked threat in South America’, Perspectives in Ecology and Conservation, In Press, pp. 1–11. Available at: https://doi.org/10.1016/j.pecon.2022.10.005.

Barton, K. (2014) ‘Package “MuMIn”: model selection and model av-erage based on information criteria (AICc and alike).’, CRAN R Project., (1), p. 46. Available at: http://cran.r-project.org/web/ pack-ages/MuMIn/MuMIn.pdf.

Bernardino, J. et al. (2018) ‘Bird collisions with power lines: State of the art and priority areas for research’, Biological Conservation, 222(March), pp. 1–13. Available at: https://doi.org/10.1016/j.biocon.2018.02.029.

Bird, D. and Laycock, S. (2019) ‘GPGPU acceleration of environmental and movement datasets’, in ACM SIGGRAPH 2019. Available at: https://doi.org/10.1145/3306214.3338584.

Roger Bivand (2022). “R Packages for Analyzing Spatial Data: A Comparative Case Study with Areal Data.” Geographical Analysis, 54(3), 488-518. doi:10.1111/gean.12319.

Bohrer, G. et al. (2012) ‘Estimating updraft velocity components over large spatial scales: Contrasting migration strategies of golden eagles and turkey vultures’, Ecology Letters, 15(2), pp. 96–103. Available at: https://doi.org/10.1111/j.1461-0248.2011.01713.x.

Boyce MS, Pitt J, Northrup JM, Morehouse AT, Knopff KH, Cristescu B, Stenhouse GB. Temporal autocorrelation functions for movement rates from global positioning system radiotelemetry data. Philos Trans R Soc Lond B Biol Sci. 2010 Jul 27;365(1550):2213-9. doi: 10.1098/rstb.2010.0080

Burnham, K.P. and Anderson, D.R. (2002) Model selection and multimodel inference: a practical -theoretical approach. 2nd edn, Journal of Wildlife Management. 2nd edn. New York: Springer. Available at: https://doi.org/10.1007/b97636.

CGIAR (2022) SRTM 90m Digital Elevation Data Consortium for Spatial Information (CGIAR-CSI) Download Portal. Available at: https://srtm.csi.cgiar.org/ (Accessed: 26 September 2022).

CRAN (2022) ‘sjPlot Data Visualisation for Social Statistics’. Available at: https://cran.r-project.org/package=sjPlot.

Dormann, F., McPherson C., M., Araújo J., B., Bivand, Bolliger, M., R., Carl, J., Davies, G., G., Hirzel, R., Jetz, A., Kissling, D. W., Kühn, W., Ohlemüller, I., Peres-Neto, R., R., Reineking, P., Schröder, B., Schurr, F. and Wilson, R. (2007), Methods to account for spatial autocorrelation in the analysis of species distributional data: a review. Ecography, 30: 609-628. https://doi.org/10.1111/j.2007.0906-7590.05171.x

Dunnett, S. et al. (2020) ‘Harmonised global datasets of wind and solar farm locations and power’, Scientific Data, 7(1), p. 130. Available at: https://doi.org/10.1038/s41597-020-0469-8.

ESRI (2019) ‘ArcGIS Release 10.6.1’. Redlands, CA: Environmental Systems Research Institute.

ESRI (2020) ‘Arc GIS Pro 3.0.1’. Available at: https://www.esriuk.com/en-gb/arcgis/products/arcgis-pro/overview.

ESRI (2021) Sentinel-2 10-Meter Land Use/Land Cover. Available at: https://livingatlas.arcgis.com/landcover/ (Accessed: 5 November 2022).

European Commission; et al. (2021) ERA5 hourly data on single levels from 1979 to present. Available at: https://doi.org/10.24381/cds.adbb2d47.

Fandos, G. et al. (2020) ‘Seasonal niche tracking of climate emerges at the population level in a migratory bird’, Proceedings. Biological sciences, 287(1935), p. 20201799. Available at: https://doi.org/10.1098/rspb.2020.1799.

Fong, Y., Rue, H. and Wakefield, J. (2010) ‘Bayesian inference for generalized linear mixed models’, Biostatistics, 11(3), pp. 397–412. Available at: https://doi.org/10.1093/biostatistics/kxp053.

Garret, R. (2018) The Open Source Infrastructure Project, OpenInfra. Available at: https://openinframap.org (Accessed: 5 November 2018).

Gauld, J.G. et al. (2022a) ‘Hotspots in the grid: Avian sensitivity and vulnerability to collision risk from energy infrastructure interactions in Europe and North Africa, Dryad, Dataset’, Dryad Digital Repository [Preprint]. Available at: https://doi.org/10.5061/dryad.jm63xsjcw.

Gauld, J.G. et al. (2022b) ‘Hotspots in the grid: Avian sensitivity and vulnerability to collision risk from energy infrastructure interactions in Europe and North Africa’, Journal of Applied Ecology, (May 2021), pp. 1–17. Available at: https://doi.org/10.1111/1365-2664.14160.

Hadley Wickham et al. (2015) ‘DPLYR’. RStudio. Available at: https://dplyr.tidyverse.org/.

Hanssen, F., May, R. and Nygård, T. (2020) ‘High-Resolution Modeling of Uplift Landscapes can Inform Micrositing of Wind Turbines for Soaring Raptors’, Environmental Management, 66(3), pp. 319–332. Available at: https://doi.org/10.1007/s00267-020-01318-0.

Hernández-Pliego J, Rodríguez C, Bustamante J. Why Do Kestrels Soar? PLoS One. 2015 Dec 21;10(12):e0145402. doi: 10.1371/journal.pone.0145402. PMID: 26689780; PMCID: PMC4687047.

Heuck, C. et al. (2019) ‘Wind turbines in high quality habitat cause disproportionate increases in collision mortality of the white-tailed eagle’, Biological Conservation, 236(May), pp. 44–51. Available at: https://doi.org/10.1016/j.biocon.2019.05.018.

Hijmans, R.J. (2019) ‘Raster: An R Package for working with raster data’. Available at: https://www.rspatial.org/.

Hijmans, R.J., Williams, E. and Vennes, C. (2015) ‘Geosphere: spherical trigonometry’. R. Available at: url: https://CRAN. R-project. org/package= geosphere.

Hofman, M.P.G. et al. (2019) ‘Right on track? Performance of satellite telemetry in terrestrial wildlife research’, PLoS ONE, 14(5), pp. 1–26. Available at: https://doi.org/10.1371/journal.pone.0216223.

IEA (2020) Onshore Wind: Tracking Report. Paris. Available at: https://www.iea.org/reports/onshore-wind.

Iñigo, A. and Barov, B. (2010) Action plan for the little bustard Tetrax tetrax in the European Union. Available at: https://ec.europa.eu/environment/nature/conservation/wildbirds/action_plans/docs/tetrax_tetrax.pdf.

IPCC (2022) Summary for Policymakers. In: Climate Change 2022: Mitigation of Climate Change. Contribution of Working Group III to the Sixth Assessment Report of the Intergovernmental Panel on Climate Change, Cambridge University Press. Cambridge, UK. Available at: https://www.ipcc.ch/report/ar6/wg3/about/how-to-cite-this-report.

Katzner, T.E. et al. (2012) 'Topography drives migratory flight altitude of golden eagles: Implications for on-shore wind energy development', Journal of Applied Ecology, 49(5), pp. 1178–1186. Available at: https://doi.org/10.1111/j.1365-2664.2012.02185.x.

Keller, V. et al. (2020) European Breeding Bird Atlas 2: Distribution, Abundance and Change. Barcelona: European Bird Census Council & Lynx Edicions. Available at: https://ebba2.info.

Kiesecker, J. et al. (2019) 'Hitting the Target but Missing the Mark: Unintended Environmental Consequences of the Paris Climate Agreement', Frontiers in Environmental Science, 7(October). Available at: https://doi.org/10.3389/fenvs.2019.00151.

Kölzsch, A. et al. (2016) 'Neckband or backpack? Differences in tag design and their effects on GPS/accelerometer tracking results in large waterbirds', Animal Biotelemetry, 4(1), p. 13. Available at: https://doi.org/10.1186/s40317-016-0104-9.

Lameris, T.K. et al. (2018) 'Effects of harness-attached tracking devices on survival, migration, and reproduction in three species of migratory waterfowl', Animal Biotelemetry, 6(1), pp. 4–11. Available at: https://doi.org/10.1186/s40317-018-0153-3.

Lucas, M. De et al. (2012) 'Griffon vulture mortality at wind farms in southern Spain: Distribution of fatalities and active mitigation measures', Biological Conservation, 147(1), pp. 184–189. Available at: https://doi.org/10.1016/j.biocon.2011.12.029.

Maisonneuve, C. et al. (2011) 'Estimating updraft velocity components over large spatial scales: contrasting migration strategies of golden eagles and turkey vultures', Ecology

Letters, 15(2), pp. 96–103. Available at: https://doi.org/10.1111/j.1461-0248.2011.01713.x.

Marcelino, J. et al. (2021) ‘Flight altitudes of a soaring bird suggest landfill sites as power line collision hotspots’, Journal of Environmental Management, 294(May). Available at: https://doi.org/10.1016/j.jenvman.2021.113149.

Marques, A.T. et al. (2020) ‘Wind turbines cause functional habitat loss for migratory soaring birds’, Journal of Animal Ecology, 89(1), pp. 93–103. Available at: https://doi.org/10.1111/1365-2656.12961.

May, R. et al. (2019) ‘Considerations for upscaling individual effects of wind energy development towards population-level impacts on wildlife’, Journal of Environmental Management, 230(January 2018), pp. 84–93. Available at: https://doi.org/10.1016/j.jenvman.2018.09.062.

Movebank (2019) Movebank Data Repository. Available at: https://www.movebank.org/ (Accessed: 1 October 2018).

Muñoz Sabater, J. (2021) ERA5-Land hourly data from 1981 to present, Copernicus Climate Change Service (C3S). Available at: 10.24381/cds.e2161bac (Accessed: 1 February 2022).

National Grid (2014) Design Drawings 132kV Overhead Lines: Hinkley Point C Connection Project Application Reference EN020001.

National Science Foundation (2019) Open Topography Data Portal, OpenTopography. Available at: https://opentopography.org/news/three-new-global-topographic-datasets-available-srtm-ellipsoidal-alos-world-3d-gmrt (Accessed: 1 February 2019).

NGA and NASA (2000) Shuttle Radar Topography Mission (SRTM GL1) Global 30m Ellipsoidal, OpenTopography. Available at: http://opentopo.sdsc.edu/raster?opentopoID=OTSRTM.082016.4326.1 (Accessed: 1 February 2019).

Oloo, F., Safi, K. and Aryal, J. (2018) ‘Predicting migratory corridors of white storks, ciconia ciconia, to enhance sustainablewind energy planning: A data-driven agent-based model’, Sustainability (Switzerland), 10(5). Available at: https://doi.org/10.3390/su10051470.

Oppel, S. et al. (2021) ‘Major threats to a migratory raptor vary geographically along the eastern Mediterranean flyway’, Biological Conservation, 262(August 2020). Available at: https://doi.org/10.1016/j.biocon.2021.109277.

Paradis E, Schliep K (2019). “ape 5.0: an environment for modern phylogenetics and evolutionary analyses in R.” Bioinformatics, 35, 526-528. doi:10.1093/bioinformatics/bty633

Pavón-Jordán, D. et al. (2020) ‘Do birds respond to spiral markers on overhead wires of a high-voltage power line? Insights from a dedicated avian radar’, Global Ecology and Conservation, 24. Available at: https://doi.org/10.1016/j.gecco.2020.e01363.

Pebesma, E.. (2018) ‘Simple Features for R: Standardized Support for Spatial Vector Data.’, The R Journal, 10(1), pp. 439–446. Available at: https://doi.org/https://doi.org/10.32614/RJ-2018-009.

Péron, G. et al. (2017) ‘The energy landscape predicts flight height and wind turbine collision hazard in three species of large soaring raptor’, Journal of Applied Ecology, 54(6), pp. 1895–1906. Available at: https://doi.org/10.1111/1365-2664.12909.

Péron, G. et al. (2020) ‘The challenges of estimating the distribution of flight heights from telemetry or altimetry data’, Animal Biotelemetry, 8(5), pp. 1–13. Available at: https://doi.org/10.1101/751271.

Poessel, S.A. et al. (2018) ‘Improving estimation of flight altitude in wildlife telemetry studies’, Journal of Applied Ecology, 55(4), pp. 2064–2070. Available at: https://doi.org/10.1111/1365-2664.13135.

Ramos, R.F., Franco, A.M.A., Gilroy, J.J. et al. Combining bird tracking data with high-resolution thermal mapping to identify microclimate refugia. Sci Rep 13, 4726 (2023). https://doi.org/10.1038/s41598-023-31746-x

Rolek, B.W. et al. (2022) ‘Flight characteristics forecast entry by eagles into rotor-swept zones of wind turbines’, Ibis, pp. 968–980. Available at: https://doi.org/10.1111/ibi.13076.

Ryberg, D.S. et al. (2019) ‘The future of European onshore wind energy potential: Detailed distribution and simulation of advanced turbine designs’, Energy, 182, pp. 1222–1238. Available at: https://doi.org/10.1016/j.energy.2019.06.052.

Sage, E., Bouten, W., Hoekstra, B. *et al.* Orographic lift shapes flight routes of gulls in virtually flat landscapes. *Sci Rep* **9**, 9659 (2019). https://doi.org/10.1038/s41598-019-46017-x

Sage, E. et al. (2022) 'Built up areas in a wet landscape are stepping stones for soaring flight in a seabird', Science of The Total Environment, 852(May), p. 157879. Available at: https://doi.org/10.1016/j.scitotenv.2022.157879.

Santos, C.D. et al. (2017) 'Match between soaring modes of black kites and the fine-scale distribution of updrafts', Scientific Reports, 7(1), pp. 1–10. Available at: https://doi.org/10.1038/s41598-017-05319-8.

Santos, C.D. et al. (2020) 'The gateway to Africa: What determines sea crossing performance of a migratory soaring bird at the Strait of Gibraltar?', Journal of Animal Ecology, 89(6), pp. 1317–1328. Available at: https://doi.org/10.1111/1365-2656.13201.

Scacco, M. et al. (2019) 'Static landscape features predict uplift locations for soaring birds across Europe', Royal Society Open Science, 6(1), pp. 1–12. Available at: https://doi.org/10.1098/rsos.181440.

Scott GR, Hawkes LA, Frappell PB, Butler PJ, Bishop CM, Milsom WK. How bar-headed geese fly over the Himalayas. Physiology (Bethesda). 2015 Mar;30(2):107-15. doi: 10.1152/physiol.00050.2014. PMID: 25729056; PMCID: PMC4346704.

Seidel, D. and Wickham, H. (2022) 'Scales 1.2.1.9000 R package for rescaling data'. CRAN 1.2.1. Available at: https://scales.r-lib.org/.

Shariati-Najafabadi, M. et al. (2016) 'Environmental parameters linked to the last migratory stage of barnacle geese en route to their breeding sites', Animal Behaviour, 118, pp. 81–95. Available at: https://doi.org/10.1016/j.anbehav.2016.05.018.

Siemens Gamesa Renewables (2022) Siemens Gamesa SG 6.6 - 155 Onshore Wind Turbine Specifications. Available at: https://www.siemensgamesa.com/products-and-services/onshore/wind-turbine-sg-5-8-155 (Accessed: 1 April 2022).

Silva, J.P. et al. (2014) 'A spatially explicit approach to assess the collision risk between birds and overhead power lines: A case study with the little bustard', Biological Conservation, 170, pp. 256–263. Available at: https://doi.org/10.1016/j.biocon.2013.12.026.

Silva, J.P. et al. (2015) ‘Freezing heat: Thermally imposed constraints on the daily activity patterns of a free-ranging grassland bird’, Ecosphere, 6(7). Available at: https://doi.org/10.1890/ES14-00454.1.

Silva, R. et al. (2017) ‘Seasonal and circadian biases in bird tracking with solar GPS-tags’, PLoS ONE, 12(10), pp. 1–19. Available at: https://doi.org/10.1371/journal.pone.0185344.

Soriano-Redondo, A. et al. (2020) ‘Testing alternative methods for estimation of bird migration phenology from GPS tracking data’, Ibis, 162(2), pp. 581–588. Available at: https://doi.org/10.1111/ibi.12809.

Soriano-Redondo, A. et al. (2021) ‘Flying the extra mile pays-off: Foraging on anthropogenic waste as a time and energy-saving strategy in a generalist bird’, Science of the Total Environment, 782, p. 146843. Available at: https://doi.org/10.1016/j.scitotenv.2021.146843.

STHDA (2017) Corstars Function: Elegant correlation table using xtable R package. Available at: http://www.sthda.com/english/wiki/elegant-correlation-table-using-xtable-r-package (Accessed: 2 October 2018).

Thaxter, Chris B. et al. (2017) ‘Bird and bat species’ global vulnerability to collision mortality at wind farms revealed through a trait-based assessment’, Proceedings of the Royal Society B: Biological Sciences, 284(1862). Available at: https://doi.org/10.1098/rspb.2017.0829.

Thaxter, Chris B et al. (2017) ‘Bird and bat species ’ global vulnerability to collision mortality at wind farms revealed through a trait-based assessment’.

Thaxter, C.B. et al. (2019) ‘Avian vulnerability to wind farm collision through the year: Insights from lesser black-backed gulls (Larus fuscus) tracked from multiple breeding colonies’, Journal of Applied Ecology, 56(11), pp. 2410–2422. Available at: https://doi.org/10.1111/1365-2664.13488.

Tikkanen, H. et al. (2018a) ‘Modelling golden eagle habitat selection and flight activity in their home ranges for safer wind farm planning’, Environmental Impact Assessment Review, 71(April), pp. 120–131. Available at: https://doi.org/10.1016/j.eiar.2018.04.006.

Tikkanen, H. et al. (2018b) ‘Modelling golden eagle habitat selection and flight activity in their home ranges for safer wind farm planning’, Environmental Impact Assessment

Review, 71(September 2017), pp. 120–131. Available at: https://doi.org/10.1016/j.eiar.2018.04.006.

Vignali, S. et al. (2021) ‘Modelling the habitat selection of the bearded vulture to predict areas of potential conflict with wind energy development in the Swiss Alps’, Global Ecology and Conservation, 25. Available at: https://doi.org/10.1016/j.gecco.2020.e01405.

Wouters, H. et al. (2021) Downscaled bioclimatic indicators for selected regions from 1950 to 2100 derived from climate projections, version 1.0, Copernicus Climate Change Service (C3S) Climate Data Store (CDS). Available at: doi: 10.24381/cds.0ab27596 (Accessed: 15 November 2022).

TRACKING DATA REFERENCES

Fiedler, W. & Wilkelsi, M. (2013) Lifetrack White Stork Poland, available on request from: https://www.movebank.org/cms/webapp?gwt_fragment=page=studies,path=study10763606

Fiedler, W. (2013) Lifetrack White Stork Tunisia, available on request from: https://www.movebank.org/cms/webapp?gwt_fragment=page=studies,path=study10157679

Fiedler, W. (2014) Lifetrack White Stork Armenia, available on request from: https://www.movebank.org/cms/webapp?gwt_fragment=page=studies,path=study10236270

Fiedler, W. (2014) Lifetrack White Stork Bavaria, available on request from: https://www.movebank.org/cms/webapp?gwt_fragment=page=studies,path=study24442409

Fiedler, W. & Wilkelsi, M. (2013) Lifetrack White Stork Poland, available on request from: https://www.movebank.org/cms/webapp?gwt_fragment=page=studies,path=study10763606

Fiedler, W., Blas J., Wilkelsi, M. (2013) Lifetrack White Stork Spain Donana, available on request from: https://www.movebank.org/cms/webapp?gwt_fragment=page=studies,path=study2988357

Fiedler, W. (2016) Lifetrack White Stork Bulgaria, available on request from: https://www.movebank.org/cms/webapp?gwt_fragment=page=studies,path=study128184877

Fiedler, W. (2016) Lifetrack White Stork Vorarlberg, available on request from: https://www.movebank.org/cms/webapp?gwt_fragment=page=studies,path=study173641633

Flack A, Fiedler W, Wikelski M (2017) Fall migration of white storks in 2014, Data from: Wind estimation based on thermal soaring of birds. Movebank Data Repository. doi:10.5441/001/1.bj96m274

Franco, A.M.A. (2014) White Stork Juveniles 2014 UEA, available on request from: https://www.movebank.org/cms/webapp?gwt_fragment=page=studies,path=study83544657

Franco, A.M.A. (2016) White Stork Adults and Juveniles 2016, available on request from: https://www.movebank.org/cms/webapp?gwt_fragment=page=studies,path=study159302811

Franco, A.M.A. (2017) White Stork Juveniles (2017), available on request from: https://www.movebank.org/cms/webapp?gwt_fragment=page=studies,path=study279646867

Franco, A.M.A., Acacio, M. S., Rogerson, K., (2017) White Stork Adults 2017, available on request from: https://www.movebank.org/cms/webapp?gwt_fragment=page=studies,path=study229412850

Franco, A.M.A., Acacio, M. S. (2018) White Stork Adults 2018, available on request from: https://www.movebank.org/cms/webapp?gwt_fragment=page=studies,path=study451464940

Franco, A.M.A., Acacio, M. S. (2018) White Stork Juveniles 2018, available on request from: https://www.movebank.org/cms/webapp?gwt_fragment=page=studies,path=study495405707

Nathan, R. (2012) Eastern flyway spring migration of adult white storks (data from Rotics et al. 2018) DOI 10.5441/001/1.v8d24552, available on request from: https://www.movebank.org/cms/webapp?gwt_fragment=page=studies,path=study560041066

Silva, J., P., (2015) Little Bustard Movement Ecology 2015 - 2016 available on request from: https://www.movebank.org/cms/webapp?gwt_fragment=page=studies,path=study56464970

Silva, J., P., (2017) Little Bustard Movement Ecology 2017 - 2018 available on request from: https://www.movebank.org/cms/webapp?gwt_fragment=page=studies,path=study253940991

Silva, J., P., (2018) Little Bustard Movement Ecology 2018 - 2019 available on request from: https://www.movebank.org/cms/webapp?gwt_fragment=page=studies,path=study461568973

Silva, J., P., (2019) Little Bustard Movement Ecology 2019 - 2020 available on request from: https://www.movebank.org/cms/webapp?gwt_fragment=page=studies,path=study769933377

Silva, J., P., (2020) Little Bustard Movement Ecology 2020 - 2021 available on request from: https://www.movebank.org/cms/webapp?gwt_fragment=page=studies,path=study1083249254

Silva, J., P., (2021) Little Bustard Movement Ecology 2021 - 2022 available on request from: https://www.movebank.org/cms/webapp?gwt_fragment=page=studies,path=study1471129898

CHAPTER 4: CHARACTERISATION OF A NEW LIGHTWEIGHT LORAWAN GPS BIOLOGGER AND DEPLOYMENT ON GRIFFON VULTURES *GYPS FULVUS*

This chapter has been published in the Journal of Animal Biotelemetry. Some minor editorial changes have been made for the purposes of the thesis, but the main text, figures and tables remain as they are in the submitted paper. For the purposes of the thesis the tables, images of the tags under test and one figure from the supporting information for the paper has been included in the main body of the text here.

Photo 7: Griffon Vultures Gyps fulvus flying in close proximity to powerlines in south west Portugal during fieldwork to deploy the GPS-LoRa tags.(Photo Credit, J. Gauld 2021)

4.1 ABSTRACT

1. Information provided by tracking studies using remote telemetry is providing ecologists with invaluable new insights into animal behaviour and movement strategies. Here we describe a new type of GNSS (Global Navigation Satellite System) tracking device currently under development and nearing commercialisation, which transmits data via LoRaWAN (long range wide area network) gateways. These tags have the potential to be a low weight and power consumption solution for tracking the movement of animals at high resolution.

2. We characterise the position accuracy and data transmission range, including uplinks and downlinks, for the tracker using a series of ground-based field tests. Data transmission range was tested by visiting locations with line of sight to the LoRaWAN Gateway at distances up to 75km and recording whether data transmission was completed successfully from each location. These tests were complemented by a trial deployment of six devices on Griffon Vultures *Gyps fulvus*.

3. These LoRa tags reliably provided accurate position estimates, particularly on more frequent acquisition cycles. At one-minute intervals the GNSS location bias was 4.71m in the horizontal plane and 5m in the vertical plane while precision, measured by standard deviation, was 3.9m in horizontal space and 7.7m in vertical space. Ground based range tests confirmed data transmission from a maximum distance of 40.7km. Initial results from a deployment on Griffon Vultures yielded useful information about flight speeds, altitude, and transmission range (up to 53.4km).

4. With consistent GNSS position accuracy and the ability to transmit data over tens of kilometres, the LoRa tags demonstrated potential for monitoring animal movement over large areas. The small size and power needs of the device allow for flexibility in which combination of battery, solar panel, and housing they are paired with. The tags can be

assembled in housing formats ranging in size from less than 5g for deployment on Kestrel sized birds to 80g for deployment on large birds such as Vultures. The devices are particularly suitable for philopatric (site-faithful) species because LoRa gateways can be installed near breeding sites to maximise opportunities for data transmission. Our findings are informative for studies seeking to use LoRa for tracking birds and other animals using the miro-Nomad or a different type of GPS-LoRa logger.

4.2 INTRODUCTION

Advances in biologging technology are allowing ecologists to collect data about animal movements and behaviour at unprecedented high spatial and temporal resolution. GNSS (Global Navigation Satellite Systems), of which GPS (Global Positioning System) is one of four main systems alongside GLONASS , Galileo, and Beidou, provide positional information accurate to within a few metres (Ossi, Urbano and Cagnacci, 2019b; Acácio *et al.*, 2021). This level of detail allows researchers to remotely monitor the location and movement behaviour (speed, flight height, direction of movement, energy expenditure and dwell times). Alongside location information, some bio-loggers record data from accelerometers and other sensors which can be used to categorise behaviours (resting, feeding, flying or walking for example) and measure environmental variables such as temperature and air pressure (Ossi, Urbano and Cagnacci, 2019a; Perona, Urios and López-López, 2019; Williams *et al.*, 2021). Many trackers are now able to combine information from these sensors to change the quantity of data recorded depending upon what the animal is doing for example recording a burst of GNSS/GPS or accelerometery data when a bird commences flapping or gliding during flight (Spivey, Stansfield and Bishop, 2014).

The data from tracking studies is providing new insights into animal movement and ecology (e.g. Rotics *et al.* 2021, Williams et al. 2021). High resolution tracking data can be paired with environmental variables such as climate, weather, season, terrain and landcover to help understand the drivers of animal movement. Using this approach, the flight paths and height above ground of Black Kites *Milvus migrans* were shown to be predicted by the strength of Orographic Upflift (caused by terrain diverting wind currents vertically) and Thermal Uplift (cause by the temperature differential between the ground and the atmosphere) (Santos *et al.*, 2017). Tracking data can also be used to assess the importance of human impacts such as disturbance, land use change and the availability of artificial food sources upon the movement behaviour of birds. For example, the availability of food at landfills is changing the movement and migratory behaviour of White Storks *Ciconia ciconia* in Portugal (Gilbert *et al.*, 2016). Another application is to better understand conflicts between wildlife and human activities such as renewable energy development as demonstrated by Schaub et al. 2020 who used high resolution tracking behaviour to better understand the avoidance behaviour of Montagu's Harriers around wind turbines in the Netherlands.

To date, the major factors which have limited the wider use of biologging technology have been the financial cost of purchasing the devices (Kauth *et al.*, 2020), data costs associated with sending the data via mobile phone networks (GSM or GPRS) or satellite systems (Iridium) which can cost hundreds of euros per year per device and device size and weight (Bridge *et al.*, 2011). For animal welfare reasons, tags should not exceed 3-5% of the animal's weight (Bridge *et al.*, 2011; Rodríguez *et al.*, 2012) and lower weights are recommended to make sure the devices do not affect animal behaviour or fitness (Rodríguez *et al.*, 2012; Kölzsch *et al.*, 2016). To reduce energy requirements, tracking devices suitable for smaller species often rely on the physical recovery of the device from the tracked animal or, as is the case with devices which utilise UHF download of GNSS/GPS location data from within a few hundred metres of the animal (Stienen *et al.*, 2016; Evens *et al.*, 2018; Ossi, Urbano and Cagnacci, 2019a). The requirement to physically retrieve the tag or get close to the animal to receive the data can be labour intensive, cause disturbance to the animal and losing data is a significant risk if the animal dies or the device falls off before retrieval (Recio *et al.*, 2011; Evens *et al.*, 2018). Transmitting data remotely, over long distances, is a better solution since it can provide near real time understanding of an animal's movements and reduces the risk of losing data (Evens *et al.*, 2018; Ripperger *et al.*, 2020). Most remote tracking systems capable of sending data over long distances do so via GSM (Global System for Mobile communications), ARGOS or Iridium satellites (Ossi, Urbano and Cagnacci, 2019a). However, the financial cost associated with data transmission subscriptions needed for these methods (Supporting Information A1: Table 1) can place a constraint upon sample sizes and the high energy consumption biases tracking studies towards larger species because of the need for larger, heavier, batteries and solar panels (Bridge *et al.*, 2011; Silva *et al.*, 2017; Ripperger *et al.*, 2020). Currently the lightest solar powered GPS-GSM biologgers for birds weigh over 6g while others weigh over 8g (Interex, 2022; Lotek, 2022) (Table 15). New low-cost, light weight technologies with the capability to remotely record and send data at high frequencies are needed to help expand the use of satellite telemetry to a wider range of species and applications.

As highlighted by (Mekki *et al.*, 2019), open-source low power wide area networks (LPWAN) offer a potential alternative solution to GSM for transmitting data from GPS/GNSS tags over long distances. LoRa (long range communications) is a type of unlicensed LPWAN (low-power wide area network system) communications protocol within the IOT (Internet of Things) architecture alongside Sigfox (now unsupported) and the proprietary NB-IoT. Under this architecture the devices, often referred to as Nodes, are connected to the internet by transmitting data to a LoRaWAN (long range wide area network) gateway which in turn forwards the data to a server via a GSM, WIFI or Ethernet internet connection. A data subscription is only needed for each gateway which can provide connectivity for hundreds of LoRa devices meaning the total annual data cost per tag can be reduced to almost zero (TTN, 2016; Mekki *et al.*, 2019; LORIOT, 2021). The low energy consumption of LoRa, typically ~28mA, with a maximum of ~118mA during data transmission, compares favourably with more energy intensive methods of data transmission such as GSM, typically 240 – 360mA but can exceed 1000mA during data transmission (Finnegan and Brown, 2020; Quectel, 2021; Semtech, 2021). This allows LoRa to efficiently send data over long distances, typically 3km in cluttered environments and over 25km with clear line of sight (Mekki *et al.*, 2019; Finnegan and Brown, 2020; Multi-Tech Systems Inc., 2021; Semtech, 2021). However, the low energy requirement does have a drawback in terms of the rate of data transmission. LoRa data payloads are limited to less than 243 bytes and the maximum data rate is 50kbps (kilobits per second) which is approximately one third of the speed of the 3G GSM transmission typically used by GPS-GSM tracking devices and approximately 1/2000th the speed of 4G (100 Mbps) (Muteba, Djouani and Olwal, 2019).

Data transmission speed for LoRa also varies depending on the spreading factor (SF), which is effectively a measure of the duration of the transmission, usually referred to as a CHIRP (Compressed High-Intensity Radar Pulse), required to send a given unit of data (Mekki *et al.*, 2019). LoRa uses six spreading factors SF7 to SF12 which are adaptively used depending on factors such as proximity to the LoRaWAN gateway which affect the transmission duration. Higher spreading factors are used when more time and energy is required to send a packet of data whereas a lower spreading factor is used when less energy and time is required to send the data (Mekki *et al.*, 2019). Within Europe where LoRa devices use the 868 MHz frequency band with a bandwidth of either 125hHz or

250kHz data transmission speeds range from 250bps (bits per second) at SF12 to a maximum of 11,000bps at SF7 (IoT, 2022). To put that in context a typical location or ACC (acceleration) payload sent by the Nomad tracker consisting of 160bits would take approximately 13ms (milliseconds) to be sent at SF7 compared to approximately 640ms at SF12. To ensure compliance with the LoRa fair usage policy (TTN, 2016) most LoRa devices use an adaptive data rate system to ensure the advised maximum air time of 30 seconds per 24 hours isn't exceeded. As such it is important when planning the deployment of LoRa devices to understand if the animals being studied are likely to spend a significant amount of time away from transmission range to a LoRaWAN Gateway and plan data acquisition and transmission rates that account for connectivity availability.

In this paper, we describe the characteristics of the miro-Nomad GPS tracker, a new type of logger developed in partnership between the University of East Anglia, Movetech and Miromico to provide a lower cost, lightweight, high resolution tracking solution. The logger uses LoRa to transmit data stored on the device and has the capability to recording high accuracy, high frequency, location data alongside other measurements (Dini *et al.*, 2021). The device has been used extensively to monitor for landslides and other geohazards (Dini *et al.*, 2021) and is now being applied to study the movement of birds and mammals. While it is important to contextualise the use of LoRa with the performance of other technologies, several other studies have already performed similar comparisons (Mekki *et al.*, 2019; Application and Singh, 2020; Finnegan and Brown, 2020). This study specifically aims to describe the characteristics of a new LoRa miniaturised device in terms of the GNSS position accuracy, data transmission range, and post deployment performance to assess its viability for animal tracking studies and provide recommendations for using LoRa in the context of animal biotelemetry.

4.3 METHODS

4.3.1 DESCRIPTION OF THE NOMAD GPS -LORAWAN DEVICES

The miro-Nomad GPS-LoRa logger equipped with a ZOE GNSS chip (Figure 15; Figure 16), referred to as “Nomad” hereafter, used in this study has been developed under a NERC Proof-of-concept project led by University of East Anglia in a collaborative project between Movetech Telemetry and Miromico (UK Research and Innovation, 2016; Miromico AG, 2021). The Nomad PCB (printed circuit board) module measures 23mm by 13mm, weighs 0.9g alone and less than 1.5g when paired with wire LoRa and GNSS antennas (Figure 16a, c). Where weight is less of a constraint, other types of antenna can be used, such as ceramic (Figure 16a), to suit the study species’ needs. The devices are capable of recording GNSS measurements up to every second (1Hz) independently of the other sensors which include two accelerometers, a gyroscope, a magnetometer, a barometer, and thermometer. The 9-axis sensor can capture acceleration measurements at resolutions ranging from 10Hz to 200Hz, and can be programmed alongside the gyroscope and magnetometer, with each sensor able to record data at the same or different rates. As with the location data, data form the 9-axis sensor is then processed and stored by the tag until it is in contact with a LoRaWAN gateway for sufficient time for the data to be sent via LoRa. The device also measures battery voltage and temperature so battery health can be monitored and reprogrammed remotely as needed using the downlink function on LORIOT. Although the devices can protect the battery from being discharged, for configurations which use solar, a harvester is recommended to help regulate energy consumption and protect the battery from overcharging. A version of the Nomad PCB with built in harvester is currently in development which will allow for smaller housings and additional weight savings during tag assembly.

Data is sent via LoRa to a LoRaWAN gateway (Figure 15), which then forwards the data via the internet to an Internet of Things network server such as LORIOT (LORIOT, 2021) or The Things Network (TTN, 2021) which in turn can forward the data to a data repository such as Movebank or IoT Wonderland (Movebank, 2019; IoT Wonderland, 2022) (Figure 15). Where good coverage provided by gateways registered on the open TTN network is available, typically in urban centres (TTN Mapper, 2022), using a TTN server can be a low cost option for deploying new LoRa devices. However, in southern Portugal and Spain, TTN coverage remains limited, as such we deployed gateways and GPS-LoRa devices registered on a private LORIOT server. LORIOT can provide greater control over the number of devices using the LoRaWAN Gateways deployed by the account holder along with scalability to allow for hundreds of gateways and nodes on one account along with technical support to help users integrate their devices with different platforms and data servers. The gateways used fall into two broad categories: Fixed Position ‘Outdoor’ Gateways (Figure 15a – e) and mobile gateways, sometimes referred to as 'indoor' or 'mobile’ gateways (Figure 17G). The cost of LoRaWAN Gateway systems range from less than 100 euros for a simple ethernet or WiFi connected ‘indoor’ LoRaWAN Gateway up to 2000 – 3000 euros for a fully autonomous, solar powered outdoor gateway system with LTE (*long-term evolution*)/GSM connectivity.

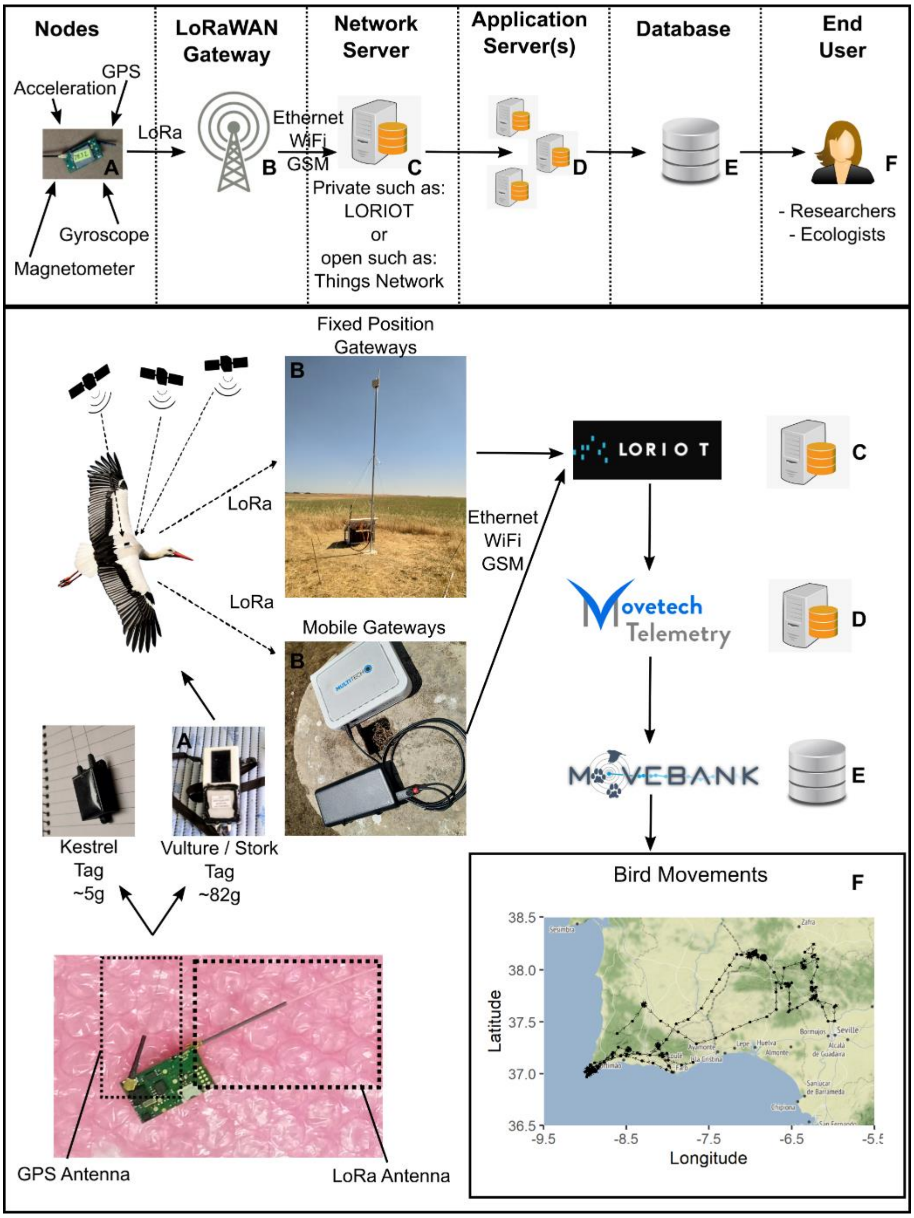

Figure 15: An overview of the LoRa system. The data is sent via LoRa [A] to a gateway [B] which in turn forwards the data to a network server such as LORIOT or TTN [C] via an internet connection such as GSM, WiFi or Ethernet. The network server then forwards the data onto one or multiple application servers [D] which decode and store the data. From the application server, data can either directly downloaded or re-formatted and forwarded to a publicly accessible data base such as Movebank [E] where the data can be downloaded for analysis by multiple users [F]. Fixed position gateways can be indoors, mounted to a building or standalone solar powered systems. Mobile gateways can be powered by a portable power bank and carried in a car, on foot or flown on a drone to maximise coverage. The lower panel highlights how these tags are used in practice to track animals.

The Nomad tracker software allows users to tailor the data collection to the research question depending on study species and battery size. GNSS position and acceleration can be recorded at regular intervals or to trigger recording of higher intensity data based on trigger parameters detected by one of the accelerometers. For example, when the force measured by the accelerometer exceeds a pre-programmed force threshold. This allows for live detection of collisions between birds and human infrastructure and more intensive sampling when the bird is moving. The tags used in the tests described in this study can store up to 60,000 data records in the onboard memory, newer versions can store up to 100,000 records. Each record represents a single data payload in containing either a welcome message, status message, location information (GNSS), Acceleration data, Magnetometer data or Gyroscope data. Users have the option of deciding whether to transmit this data in chronological order or to receive the most recent data first by changing the data buffer mode. With a migratory bird it might be useful to ensure the most recent locations are sent first whenever the bird is in range of the gateway whereas for a more sedentary species which is likely to remain within gateway range most of the time sending the data in chronological order may be preferable.

Figure 16: A: GPS-LoRa tag configured for vultures prior to assembly using a ceramic GNSS antenna, molex flexible LoRa antenna and a 1100mah LiPo battery. During assembly the housing was re-inforced with potting epoxy. B: The GPS-LoRa tag deployed on a vulture, photo taken immediately prior to the bird flying away. C. The PCB which can be paired with different types of GNSS/GPS and LoRA antenna depending on weight requirements, with wire or flexible antennas it weighs 1.5g. D. GPS-LoRa tag configured for kestrels with a total weight of 4.5-5g including housing, solar panel, antennae and 40mah battery. E. Tag deployed on a common kestrel Falco tinniculus. F: 10g GPS-LoRa tag configured with a solar harvester and 30mah battery prior to assembly. G. The 10g GPS-LoRa tag used for the position accuracy tests.

When a device is in range of a gateway it will try to transmit on a user-specified duty cycle (usually one payload every 15 – 20 seconds or up to 180 – 220 payloads per hour). The device detects when it is in range of a gateway because an acknowledgement message is sent by the LoRaWAN Gateway once the data has been successfully forwarded to the server. The acknowledgement ensures that each message stored on the payload buffer on the device is only deleted from memory after it has been successfully forwarded to the server by the LoRaWAN Gateway. This confirmation feature also facilitates the remote programming of device settings and ensures data not received by a gateway, is not lost. If an acknowledgement message is not received, data is kept in the buffer and the device switches to a User-Specified longer interval forced transmission duty cycle (usually 30 - 60 minutes) once the payload is sent and an acknowledgement is received the device restarts transmitting data more frequently according to the standard duty cycle.

Animals may move away from the range of existing gateways (or may be in landscapes with signal obstructions) and in these cases the data transmission alternates between TX and TXF cycles to save energy. The TX cycle is used when the tag is in contact with the gateway whereas the TXF cycle is used when out of gateway range to force the tag to attempt to make contact with the gateway at a user specified interval. Weaker signals are associated with a high spreading factor and reduced data transmission speed. Meaning the acknowledgement from the gateway that a given payload has been successfully forwarded to the server is less likely to be received by the device within the required timeframe, designated as the RX1 (usually 1-second) or RX2 (usually 2-seconds) window (TTN, 2021). Where confirmation is not received within the RX1 or RX2 windows the data is stored until contact with a gateway is re-established. Transmission speed decreases by a factor of two as spreading factor (SF) increases. SF also influences the data rate. This is because the devices have an adaptive data rate (ADR) feature to ensure compliance with the LoRa fair use policy (TTN, 2016; Miromico AG, 2022). The NOMAD devices do this by measuring the spreading factor (SF). As with other LoRa devices, in practice this means that at a lower spreading factor the user specified transmission cycle will be closely followed whereas when the device is further from the gateway or there's interference resulting in a high spreading factor the data rate may drop to just a few messages per hour to avoid breaching the fair use policy and conserve power (Kim, Lee and Jeon, 2020).

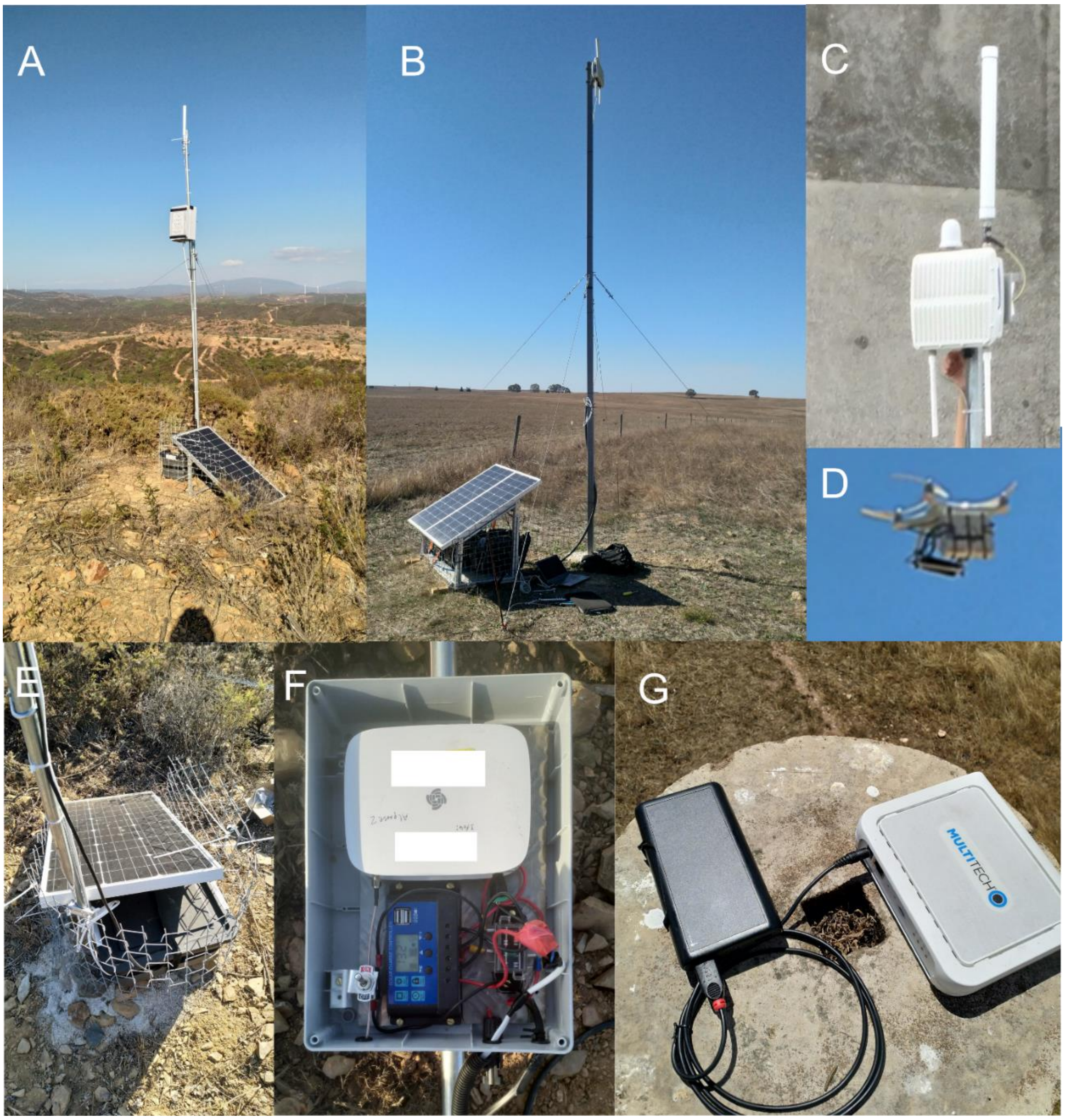

Figure 17:Examples of LoRaWAN Gateway configurations. A. Custom LoRaWAN Gateway solar system constructed by ruggedising a RAK 'indoor' LoRaWAN Gateway, total materials cost at the time (2021) was approximately £500. B. LoRaWAN Gateway solar system with a 24v solar system and MultiTech IP67 gateway (Multi-Tech Systems Inc., 2021)*, total system cost approximately £2500. C. Close up of the IP67 MultiTech LoRaWAN Gateway. D. A proof of concept UAV (unmanned aerial vehicle) flight with the mobile gateway. E. View of the solar and battery set up for the 12v system to supply the adapted RAK indoor gateway. F: Inner workings of the ruggedised gateway solution put together using off the shelf components. G. A mobile LoRaWAN Gateway powered by a USB power bank.*

4.3.2 QUANTIFYING POSITION ACCURACY

The devices use a ZOE GNSS chip capable of communicating with GPS, Glonass, Navstar and Beidou satellites to determine the spatial co-ordinates and altitude of the tag. The accuracy of GNSS measurements was tested under different fix acquisition rates (1, 30 and 60 minutes) by leaving a tag in position on a geographical marker (Figure 18) with known co-ordinates (37.7481317, -8.0403338), a clear view of the sky and altitude above sea level (221m) for sufficient time to acquire at least 300 locations (358 locations at 60-minute intervals, 367 locations at 30-minute intervals and 767 locations at one-minute intervals). The location and altitude of the geographical marker was derived from google maps using aerial imagery and the altitude was derived from a terrain model and measuring the height of the geographic marker in the field. The device was set up with a wire-type GNSS antenna (typically used for deployments on smaller species) and the GNSS sampling interval was adjusted remotely via the downlink feature in LORIOT. Total device weight including housing, solar panel, harvester, epoxy and batter was 11g. During the 60-minute cycle test the tag was in sight of a mean of 11.7 ± 1.3 sd (standard deviation) GLONASS and 7.4 ± 1.5sd Galileo GNSS satellites, for the 30-minute cycle this was 10.6 ± 1.7sd GLONASS and 7.9 ± 1.6sd Galileo satellites and for the 1-minute cycle this was 12.9 ± 1.3sd GLONASS and 5.7 ± 1.4sd Galileo satellites. No Navstar or Beidou satellites were observed by the tag during the tests.

Figure 18: GPS-LoRa device on test during GPS accuracy field trials on the 8g configuration. Garmin GPS for scale.

Accuracy for each location estimate was calculated by calculating the distance between the horizontal and vertical co-ordinates with the known location of the geographic marker. These horizontal distances were calculated using the ‘distHaversine’ function from the Geosphere package in R version 4.0.5 (Hijmans, Williams and Vennes, 2015). Accuracy encompasses two components, bias and precision (Walther and Moore, 2005). Bias was calculated as the mean location error relative to the true location to inform us about the magnitude of systematic over or underestimation of the true position resulting from the GNSS measurements and the standard deviation was used to quantify the precision i.e. the random spread of the error relative to the true value (Walther and Moore, 2005). A one-way ANOVA and post-hoc Tukey’s HSD significance test was used to determine whether there was a significant difference in accuracy between different GNSS acquisition cycles in terms of horizontal and vertical location estimation.

4.3.3 QUANTIFYING LORA TRANSMISSION RANGE

The documented estimates of maximum transmission range of long-range wireless vary considerably in the available literature. Data transmission for a mobile gateway model (MultiTech Conduit MTCAP-LEU1-868-001A) can range from 17km with clear line-of-sight and 2-3km in more cluttered environments (Multi-Tech Systems Inc., 2021) but it has also referred to be up to 40km with clear line of sight for LPWAN data transmission (Mekki et al., 2019). The world record for data transmission between a node and a LoRaWAN Gateway with LoRaWAN within the Earth's atmosphere of 766km was set in 2019 using a weather balloon at high altitude (The Things Network, 2019). The record highlights the potential of this technology to send data long distances however, this kind of transmission distance is not realistic under most usage scenarios.

The main focus of the range tests was on data transmission from a NOMAD node to a Multi-Tech IP67 outdoor gateway (Concept 13 Limited, 2022) located at co-ordinates 37.731°, -8.029°, mounted on a mast 5.5m above the ground (Figure 19b). During the range tests gateways other than the target gateway were switched off. Four Nomad devices with different antenna types (flexi, gold-plated wire, brass wire, and silver-plated wire) were set to record and transmit GNSS locations and status messages at least every 15 minutes. Acceleration and other sensors were disabled.

The devices were taken to locations of known distance away from the gateway ranging from <1km to ~70km. Test locations were identified using viewshed analysis in QGIS (QGIS Development Team, 2019) to determine locations with line of sight to the gateway. The viewshed analysis assumed that both device and gateway were at 5 metres above ground level. To achieve this, the devices were placed in anti-static bags and suspended vertically with antennae pointing toward the sky from a frame elevated using a telescopic pole to a height of 5 metres at all test locations (Figure 19a). At each location, the data stream from the gateway was monitored using a web browser interface on a smartphone and the devices left in position until either all four devices had successfully transmitted data, or half an hour had elapsed to allow for transmissions on a 15-minute TXF cycle. Transmission was deemed successful from a given location if at least one device was able to contact the gateway for sufficient time to allow for multiple data packets (Status and/or Location) to be sent. Transmissions consisting only of the initial 'welcome' message data packet used to confirm communication with the gateway was not classed as a successful transmission. The range test was also repeated at the locations in (Figure 19c) with two Nomad devices using a portable Multitech™ Mobile Gateway (MTCAP2-L4E1-868-002A-POE) up to 17km. All range tests were conducted under field conditions in Portugal during May and June of 2021 on calm, dry days with minimal cloud cover.

4.3.4 CASE STUDY WITH GRIFFON VULTURES

In October of 2021, six devices were deployed on Griffon Vultures *Gyps fulvus* as a trial deployment to test the GNSS and Accelerometer features of the loggers. Here we report on the location information acquired during this trial deployment and the data transmission performance. The GPS-LoRa Modules were assembled in a solar powered configuration including an integrated solar-panel and harvester, 1100mah lithium-polymer battery, ceramic "high gain" GNSS antenna using a Movetech flyway-50 housing (Figure 16a-b). Griffon Vultures have powerful beaks, to increase tag durability the top half of the housing was re-enforced with several layers of potting epoxy prior to assembly and additional plastic was mounted on the exterior of the housing to help increase durability of the device. As such, the final device weight was 83g, which equates to approximately 1% of the body mass of the tagged birds. The component cost for assembling the device was approximately £350 in 2020 although this does not account for the labour costs involved in tag assembly. The final price once commercialised will likely be similar to that of GSM tags with similar capabilities.

The devices were programmed to record a GPS/GNSS location every 30 minutes and one second burst of Acceleration measurements at a frequency of 50Hz whenever a force exceeding 3.2g was detected with a view to detecting avoidance or collision events. The loggers were deployed in Southern Portugal under licence from CNF – Instituto da Conservação da Natureza e das Florestas, on the 23rd and 24th of October 2021 using a backpack style harness with a weak link consisting of cotton designed to degrade over time to ensure the loggers fall off after a few years (typically 1- 3 years) without harming the bird. Four of the tagged birds were caught and tagged near Bensafrim, north of Sagres in Southwest Portugal on the 23rd of October and the remaining two birds were rehabilitated birds. The rehabilitated birds were released near Mertola, in Southeast Portugal. To support the vulture tracking work, an additional three fixed position LoRaWAN gateways within important areas for bird migration in Southern Portugal and Spain (Figure 21e) to complement the Multitech IP67 gateway deployed near Castro Verde in April of 2021. The three additional gateway systems used RAK Wisgate Edge Lite indoor gateways housed within a weatherproof IP56 rated plastic junction box and paired with a 3dbi outdoor rated gateway (Figure 17a, e, f). Each system was powered by a single 100w solar panel and 60ah 12v battery using a generic

30a solar charge controller. There are plans to deploy more gateways to cover the main migration route between Portugal and Tarifa. Data were processed in R version 4.0.5 (R Core Team, 2019) and maps were produced using the ggmap and patchwork packages (Wickham, 2016; Pedersen, 2020).

Here we report the initial results from tracking data received during the first two weeks after tag deployment allowing us to understand the performance of the tags under real world conditions including data transmission range and GNSS performance. Data transmission range was assessed using the pointDistance function in the raster package in R (Hijmans, 2019) to measure the distance between the nearest LoRaWAN Gateway and the GNSS location of the bird. Transmission success was coded as a binary variable with 0 representing locations where transmission was not possible and 1 representing locations where the GNSS position was successfully sent to a gateway within 1-minute of the GNSS location being recorded. Transmission success was then modelled in a binomial generalised linear model (GLM) with a logit link to identify whether any factors aside from distance to the nearest gateway significantly influenced transmission success. The initial model included distance to the nearest LoRaWAN Gateway (km), height of the bird above ground (m), roughness of the terrain as measured by the terrain roughness index (TRI) (Riley, DeGloria and Elliot, 1999; Evans;, Murphy; and Ram, 2021) and landcover associated with each GNSS location (ESRI, 2021). Landcover was investigated because features in the landscape such as buildings and trees may impact upon transmission, however including landcover in the model was found to introduce significant bias because the birds favoured certain habitats over others. As such it was not possible to meaningfully assess the impact of landcover and therefore it was not included in the final model. Co-linearity was checked using the ggpairs function (Schloerke *et al.*, 2021); non-significant variables were sequentially eliminated from the model in a stepwise fashion until the most parsimonious model with the lowest AIC value was established. Model outputs were then plotted using the ggeffects function (Lüdecke *et al.*, 2022).

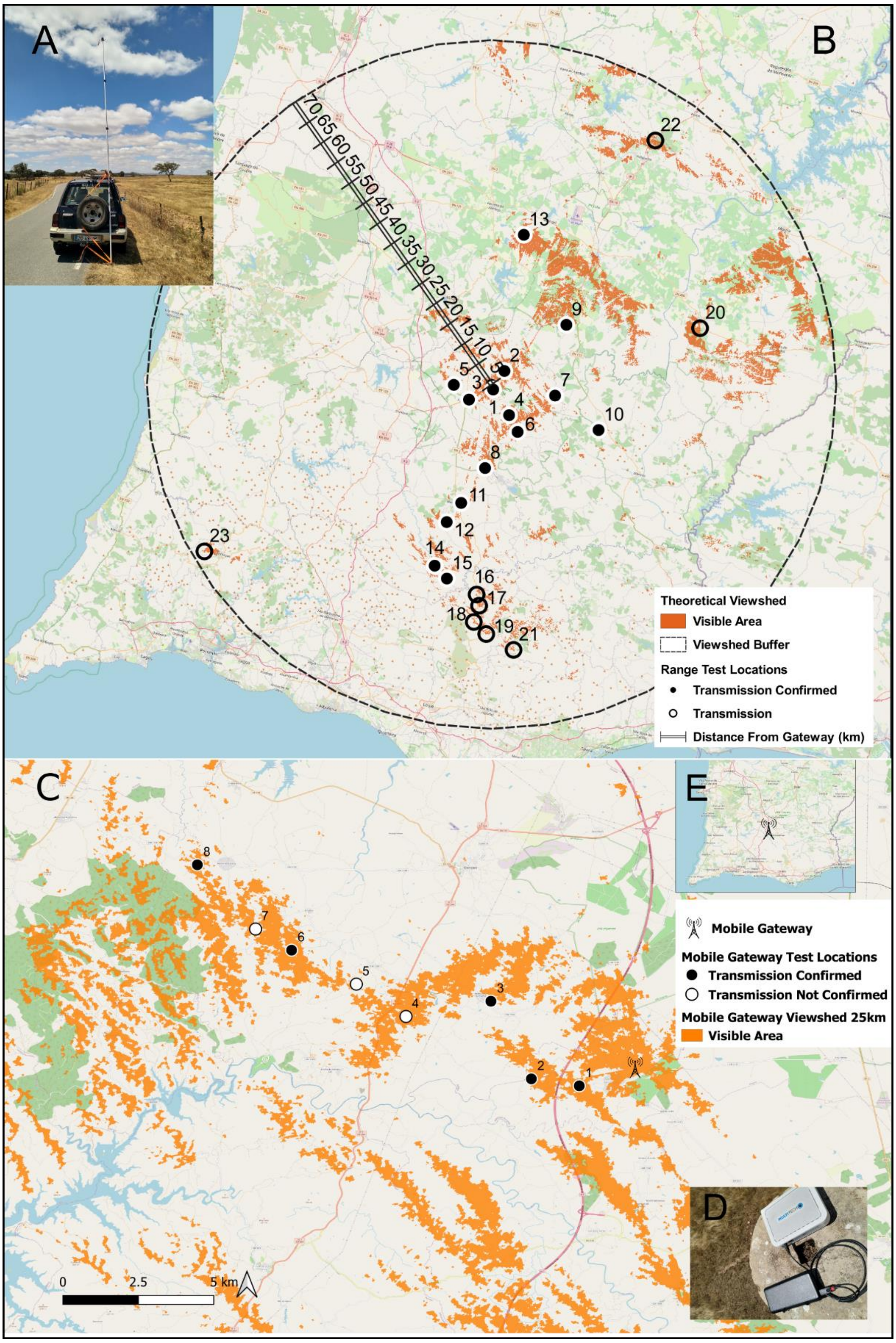

Figure 19: A: Pole used to elevate the NOMAD devices to 5m at each location. B: Ground based range test locations for the fixed position LoRaWAN Gateway. C. Ground based range test locations for the mobile LoRaWAN Gateway. D. the mobile gateway used. E. The location in Portugal where the mobile gateway was tested. Hollow circles represent locations where data transmission from the devices to the gateway was not confirmed, filled circles represent locations where data transmission was confirmed. The Orange areas represent areas with line of sight to the gateway at 5m above ground, this was calculated in QGIS using the viewshed analysis tools and a 30m digital surface model from (QGIS Development Team, 2019).

4.4 RESULTS

4.4.1 POSITION ACCURACY FROM GNSS

Location bias relative to the true location in horizontal space (Figure 20a, Table 11) ranged between 4.71m for the 1-minute cycle, 6.63m for the half-hourly cycle and 8.44m for the 60-minute cycle. Significant differences between cycles were detected in terms of horizontal precision (Figure 16a), ANOVA ($F(2, 1486) = 19.62$, $p < 0.01$). Location precision was highest in the 1-minute cycle (3.88m precision) and lowest the 60-minute cycle (18m precision) (2.79, p = <0.01 , 95% C.I. = [1.68, 3.90]). Errors greater than 100m only occurred on three occasions representing 0.2% of recorded locations and were associated with the hourly GPS position cycle.

Cycle	Total Locations	Horizontal Bias	Min Horizontal Error	Max Horizontal Error	SD	Horizontal 2.5 Percentile	Horizontal 97.5 Percentile	Horizontal CI 95%	Vertical Bias	Min Vertical Error	Max Vertical Error	SD	Vertical 2.5 Percentile	Vertical 97.5 Percentile	Vertical CI 95%
1 minute	767	4.71	0.35	21.9	3.88	0.53	15	14.4	5	-18	43.1	7.77	-10.4	21	20.5
30 minute	367	6.63	0.35	39.5	6.91	0.53	27.5	27	2.03	-78.3	102	15.3	-26.4	36.4	35.9
60 minute	358	8.44	0.35	224	18	0.35	34.7	34.3	2.99	-138	349	27.4	-40.2	42.8	42.4

Table 11: GPS position error (bias) and precision (standard deviation) in horizontal and vertical space for different transmission schedules.

Location bias relative to the true position in vertical space (Figure 20b, Table 11) ranged between 2-5m for the three acquisition cycles used. Vertical precision was significantly different between GPS acquisition cycles (Figure 16), ANOVA ($F(2, 1486) = 12.72$, $p < 0.01$), with the post hoc TUKEY-HSD test confirming the significant differences between the 60-minute cycle (28m precision) and the 1-minute cycle (7m precision) (-3.44, $p < 0.01$, 95% C.I. = [-5.37, -1.52]) as well as the 30-minute (15.3m precision) and 1-minute cycles (-3.25, p < 0.01, 95% C.I. = [-5.16, -1.34]) but not the 60-minute and 30-minute cycles (-0.19, p = 0.98, 95% C.I. = [-2.43, 2.04]). These results indicate a slight overestimation of altitude relative to the true position across cycles with reduced position bias observed in the 30-minute and 60-minute cycles than with the 1-minute cycle. A small but significant reduction in both horizontal and vertical precision at lower frequency cycles (30-minute and 60-minute) was also detected which manifests in a greater spread of position estimates compared to the 1-minute cycle (Figure 20a and Figure 20c, Table 11).

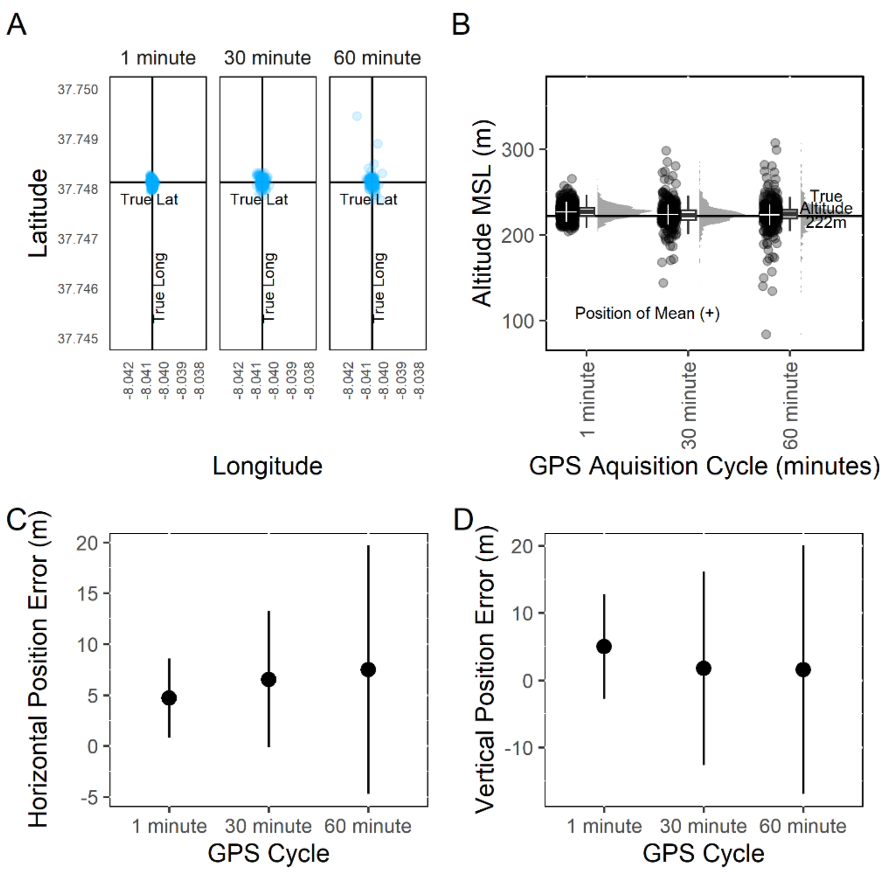

Figure 20: A: Distribution of horizontal GPS locations relative to the true position under different GPS acquisition cycles. The mean position in all instances is similar, however the precision of the altitude is best under a 1-minute GPS acquisition cycle. B: The distribution of GPS position estimates relative to the true position in vertical space. C: Horizontal position error under a 1-minute, 30-minute and 60-minute GPS acquisition cycle, error bars represent the standard deviation from the mean. D: Vertical position error under a 1-minute, 30-minute and 60-minute GPS acquisition cycle, error bars represent the standard deviation from the mean. As expected, both bias and precision was best under the 1-minute cycle.

4.4.2 QUANTIFYING LORA TRANSMISSION RANGE

Ground based range tests in locations with theoretical line of sight to the “Castro Verde” gateway (Figure 19) confirmed the ability of these tags to transmit data reliably at all locations at distances less than 40km from the gateway (Figure 19b). The successful transmission of a single data payload from over 62km to the North of the LoRaWAN Gateway Mendro (Test location 22) suggests that the devices can send data over that distance. However, the latency may be too great for the tag to receive acknowledgement of the payload, or the gateway detects that the signal is weak and therefore fails to send the acknowledgement back to the device. Without an acknowledgement the tag will not send further data which is why this was not categorised as a successful transmission.

The tags used during these tests had different types of wire antenna namely, flexible plastic-coated wire, brass wire, silver wire and gold-plated wire but it was not part of the objectives of this study to determine whether this affected transmission range, transmission success was confirmed for all antenna types. This is broadly in line with findings by another study which investigated transmission range and data transmission speed in low power wireless networks which indicated a maximum transmission range of between 20km and 40km (Mekki *et al.*, 2019). Furthermore, we performed range tests using a LoRa device and a mobile gateway. These tests were performed in areas which did not have line of sight to the fixed position Castro Verde gateway and ranged from 2km to 17km (Figure 19c). These tests demonstrated successful data transmission at 17km from the gateway which is in line with the manufacturer claiming a range of 800m in cluttered environments, 15km with line of sight (Multi-Tech Systems Inc., 2022).

The tests also highlighted how transmission from ground level can be impeded by terrain and vegetation because data transmission was not successful at 7km, 9km and 14km where there was higher tree cover.

ID	Location	Long	Lat	Distance from Gateway (km)	Date	Start Time	Finish Time	EE5E (Flexi-Antennas)	C311 (Silver Antennas, in housing)	3751 (Brass antennas)	1653 (Gold antennas)
1	Kestrel Tower	-8.02931	37.73124	1.1	06/05/2021	10:30	11:00	Status and Location Sent	Status and Location Sent	Status and Location Sent	Status and Location Sent
2	Entradas	-8.013	37.7693	4.2	06/06/2021	9:35	10:05	Status and Location Sent	Status and Location Sent	No transmission (Battery Issue)	No transmission
3	Castro Verde A	-8.079033363	37.70283228	5.5	06/06/2021	14:00	14:30	Status and Location Sent	Status and Location Sent	Status and Location Sent	Status and Location Sent
4	Ermida do Sao Pedro	-8.036109912	37.67798892	5.8	07/06/2021	14:50	15:20	Status and Location Sent	Status and Location Sent	Status and Location Sent	Status and Location Sent
5	Gateguinha Grande	-7.9813	37.69231	8	06/06/2021	13:15	13:45	Status and Location Sent	No transmission	Status and Location Sent	No transmission
6	Castro Verde B	-8.11996	37.72259	9.6	07/06/2021	13:50	14:20	Status and Location Sent	Not present	Status and Location Sent	Status and Location Sent
7	Rolão	-7.95425	37.66597	12.2	06/06/2021	14:45	15:15	Status and Location Sent	Status and Location Sent	Status and Location Sent	Status and Location Sent
8	Lancadoiras	-8.00979	37.58738	17.1	06/06/2021	15:25	15:55	Status sent	Status sent	Status and Location Sent	Status sent
9	Trinidade	-7.89594	37.87849	21.9	06/06/2021	10:35	11:05	No transmission	Status and Location Sent	Status and Location Sent	No transmission
10	Navarro	-7.773514	37.704042	22	06/06/2021	11:45	12:10	No transmission	Status sent	Status and Location Sent	Status and Location Sent
11	Almodovar	-8.04661	37.51468	25	07/06/2021	16:00	16:30	No transmission	No transmission	Status and Location Sent	Status
12	Monte Acharrua	-8.06982	37.47419	29.7	07/06/2021	17:15	17:45	Status sent	No transmission	No transmission	No transmission (Had sent status from here during previous test)
13	Mombeja	-8.03513	38.02106	31.3	21/05/2021	19:15	19:45	Multiple status and location messages sent successfully	No transmission	Multiple status and location messages sent successfully	N/A
14	Miro	-8.07578	37.39103	38.9	24/05/2021	9:20	9:50	Multiple status and location messages sent successfully	Multiple status and location messages sent successfully	Multiple status and location messages sent successfully	N/A
15	Transmission Lines Santa Cruz	-8.04242	37.37326	40.7	24/05/2021	10:05	10:35	Status message sent	No transmission	Multiple status and location	N/A

										messages sent succesfully	
16	Ameixal	-7.96843	37.35752	43	24/05/2021	11:15	11:45	No transmission	No transmission	No transmission	N/A
17	Texageiras	-7.95754	37.33858	45	24/05/2021	12:00	12:30	No transmission	No transmission	No transmission	N/A
18	Pelados	-7.9616	37.30718	48.7	24/05/2021	12:50	13:20	No transmission	No transmission	No transmission	N/A
19	Vale do Rosa	-7.92825	37.2909	51	31/05/2021	18:10	18:40	No transmission	N/A	No transmission	No transmission
20	Guadalupe	-7.59355	37.92932	53.4	09/06/2021	16:45	17:15	No transmission	No transmission	No transmission	No transmission
21	Feiteira	-7.85983	37.2742	55.2	24/05/2021	19:10	19:40	No transmission	N/A	No transmission	No transmission
22	Mendro - high peak to north overlooking plain.	-7.78385	38.24621	62.8	01/06/2021	9:45	10:45	No transmission	No transmission	Welcome Messages Sent	No transmission
	Foia_Mountain_Monchique	-8.59644	37.3156	78	17/05/2021	15:00	15:30	No transmission	No transmission	No transmission	No transmission

Table 12: Detailed description of range test results between the LoRa-GPS devices and the IP67 gateway located at the LPN reserve to the north of Castro Verde (Gateway A9_f6_Castro_Verde).

4.4.3 PERFORMANCE DURING DEPLOYMENT

Initial data from the deployed tags provided some useful insights into their performance; location data was obtained for two of the six birds which stayed within the vicinity of the LoRaWAN Gateways allowing full data download to occur, the other four tags provided accelerometer data only. This provided 2,208 GNSS locations which allowed us to plot the post tagging movements along with daily height and speed for two of the six vultures (Figure 21). A daily summary of the movements is provided in Table 13 for each bird. Both birds exhibited a high daily variation in movement behaviour in terms of mean daily speed (0 – 2.65 m/s), height (-24.9m – 450.9m) and total daily displacement of (0.06km – 209.3km). The low average step-speed across both birds of 0.26 ± 0.52 SD m/s during this period suggests they may have spent a significant proportion of their flight time circling on thermals.

The wild caught bird, 9012_Eduardo, flew to the Extremadura region of Spain near the Portuguese border prior to returning to the area around Sagres, southwest Portugal. The tag on this bird was last seen by a LoRaWAN Gateway on 08/11/2021 as it was travelling west to east along the southern coast of Portugal toward Spain. The rehabilitated bird, 7DA6_Marta, stayed close to the release site near Mertola, Portugal before heading to the Southwest point of Portugal (Figure 21b). The final location received from this tag was over the Atlantic to the south of Lagos, Portugal at 15:40 on the 6^{th} of November (36.88323, -9.01409). This vulture lost altitude over the hour preceding the final GNSS record obtained (1474m down to 583m above sea level). Had the individual returned to the Algarve, one of the gateways would have picked up the signal from the tag suggesting that, most likely, this individual failed to return to land and likely drowned.

The devices of the other four individuals only sent acceleration but no location data. Despite this it was possible to follow the birds' movements by monitoring which gateways received data from them and when. Data were most recently received from two of the birds on 08/11/2021 and 07/11/2021 by the 3C_F4_Tarifa gateway near the southern tip of Spain suggesting that two birds attempted to migrate to Africa. This is a total minimum distance of approximately 480km from where they were tagged in southwest Portugal. Two of the six tags deployed appear to have stopped sending data within 48 hours after deployment and it is unclear whether this is because the birds moved out of range of the gateway or some other issue. In both cases, the payload buffer on the tag was clearly filled by acceleration recording being erroneously triggered numerous times suggesting an issue with the user defined accelerometer settings. We do not summarise acceleration data further as it is beyond the scope of this paper.

Bird ID	Gateway Range	Count	Minimum Distance (Km)	Mean Distance (Km)	Max Distance (Km)	Standard Deviation Distance (Km)	Percent
Eduardo_9012	N	283	14.8	81.8	106	32.4	94.6
Eduardo_9012	Y	16	8.6	29.6	50.2	9.21	5.4
Marta_7DA6	N	1625	9.3	34.5	54.2	13.9	85.1
Marta_7DA6	Y	284	4.1	21.5	53.4	6.99	14.9

Table 13: Locations obtained within range of a gateway (Y) and their distance in kilometres to the nearest LoRa gateway and locations which were recorded by the device while out of gateway range (N) which were transmitted a posteriori.

(Intercept)	1.53 ***
	(0.26)
Minimum_Distance_to_Gateway_km	-0.13 ***
	(0.01)
Height_Above_Ground	0.003 ***
	(0.00)
AIC	1282.66
BIC	1299.85
Log Likelihood	-638.33
Deviance	1276.66
Num. obs.	2277

Table 14: summary of final binomial GLM relating the probability of successful data transmission to the height above ground (m) and distance of the logger (km) from the gateway.

Locations within range of a gateway ($n = 300$, 13.2%) obtained at the time they were transmitted, ranged between 4.1 – 53.4km from the nearest LoRaWAN Gateway. Whereas locations which were recorded but not immediately transmitted ($n = 1{,}908$) ranged from 9.3 – 106km from a gateway, (Table 13,Figure 22). A binomial GLM confirmed distance from the nearest gateway in kilometres has a significant negative relationship with transmission success (-0.135, $DF = 2270$, $SE = 0.011$, $P < 0.001$, $Z = 11.98$) and height above ground in metres was found to have a significant positive effect on transmission success (0.003, $DF = 2270$, $SE = 0.0002$, $P < 0.001$, $Z = 8.84$). A univariate model in which only height relative to ground was included as a predictor of transmission success was performed less well ($AIC = 1357$) compared to the model containing both distance and height ($AIC = 1276$). No significant difference was found between tags and there was no significant effect of terrain roughness detected by the model, this is likely because during flight the birds will generally be above any features on the ground which could obstruct line of sight to the gateway. Plotting the output of the binomial GLM using the ggeffects package (Lüdecke et al. 2022) suggests the probability of successful transmission drops below 50% at approximately 15km from the nearest gateway and that transmission range from these devices during deployment is limited to 53.4km (Figure 22).

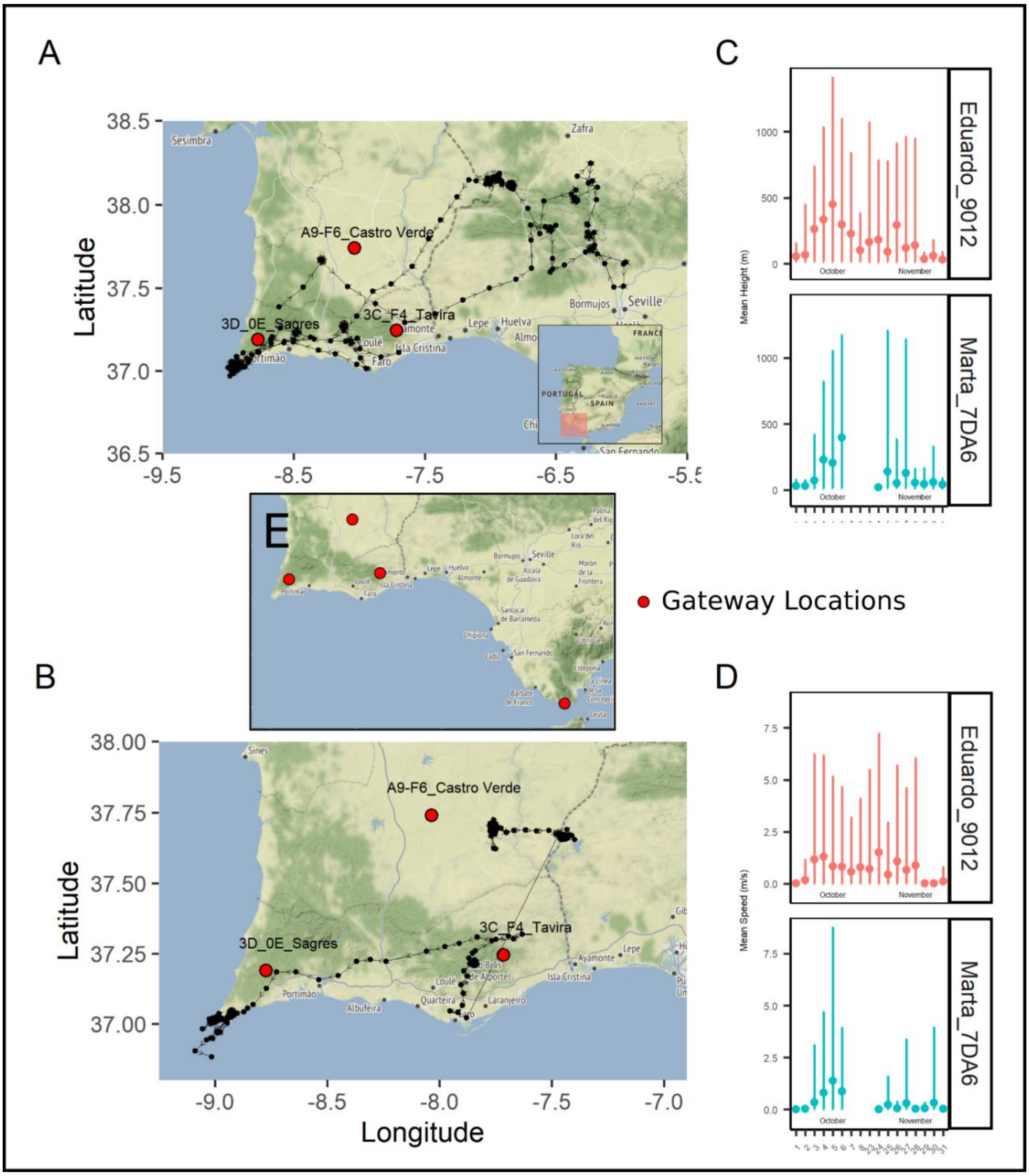

4266 *Figure 21: Panels A and B show the movements of the two tracked vultures. All locations shown are in flight. Panel C:*
4267 *mean height of the birds above ground and the 95% confidence interval. Panel D: mean speed of the birds along with*
4268 *the 95% confidence interval and panel E: location of the four LoRa gateways deployed for this project.*

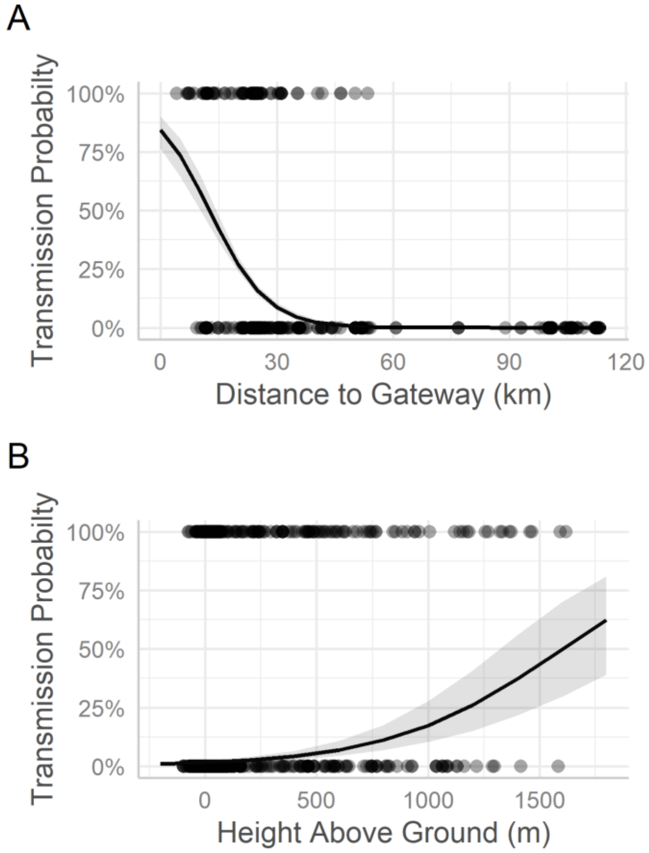

Figure 22: Relationship of the likelihood of successful data transmission with distance from a LoRa gateway (A) and height above ground(B).

4.5 DISCUSSION

Our tests of tag performance revealed the GNSS position data provided by the miro-Nomad is sufficiently accurate for high resolution animal tracking studies such as those seeking to evaluate the fine scale movement of birds in relation to weather, habitat and landscape factors (Scacco *et al.*, 2019). Horizontal bias was <9m with precision <18m and vertical bias was <5m with precision of <28m (Figure 20) on up to one hour location acquisition cycles. Accuracy was improved at higher frequency of GNSS position acquisition. LoRa is a promising technology for animal movement studies. Especially for colonial species that frequently return to the same locations and for smaller species because of the possibility to assemble devices weighing less than 5g. Ground based tests confirmed data transmission up to 40.7km from the gateway and data from deployed tags indicates a maximum data transmission range of 53.4km. This confirms that GPS-LoRa devices can perform similarly to devices using GSM while offering advantages in terms of reduced data costs and energy consumption. The ability to send data over tens of kilometres also offers a clear advantage over alternative lightweight GNSS loggers using shorter range transmission methods for data download to a basestation (e.g. UHF download or ZigBee). While these other devices perform similarly in terms of GNSS position accuracy, they generally require the animal to pass within a few hundred metres of a receiver in the case of UHF download or within a few kilometres (<8km) for download via Zigbee (Bouten *et al.*, 2013; Stienen *et al.*, 2016; Evens *et al.*, 2018; Ripperger *et al.*, 2020). Whereas GSM devices' need for larger batteries and solar panels places a constraint on tag weight, the smallest available GPS-GSM tags are currently over 6g (Table 15).

Logger Type	*Data Transmission Method*	*Smallest Tag Weight (g)*	*Manufacturer stated typical data cost per logger per year (Euros)*	*Source*
EOBS	GSM	15.0	50 – 150	Marc Büntjen (2021), Personal communication, marc.buentjen@e-obs.de
Interex	GSM (2G)	6.2	Unknown	Interrex Website 2022: https://interrex-tracking.com/mini/
LOTEK	GSM/Iridium/ARGOS	6.6	100 (GSM) / 324 (Iridium)	Sarah Deans (2021), Personal communication, sdeans@lotek.com
Movetech	GSM	18.0	50 - 70	Aldina Franco (2021), Personal communication, a.franco@uea.ac.uk; Movetech Telemetry (2021) https://movetech-telemetry.com/
Ornitela	GSM	9.0	70 – 90	Ramunas Zydelis (2021), Personal communication, zydelis@ornitela.eu
Pathtrack	GSM	8.0	Unknown	Pathtrack Website 2022: https://www.pathtrack.co.uk/products/nanofix-geo-gsm.html
UvA-BiTS	Zigbee	7.5	Effectively free	UvA-BiTS website: https://www.uva-bits.nl/system/
Miro Nomand GPS-LoRa Devices using a LORIOT private LoRa server	LoRa	<5g	~4 (Assumes a LORIOT subscription for up to 250 devices)	LORIOT 2022 https://www.loriot.io/professional-public-server.html

Table 15: Data cost estimates for different types of GPS logger as stated by the relevant manufacturer or data provider. Tag weights are for the smallest solar powered tag produced by that manufacturer with the capability to send data via GSM or via satellite. Data costs exclude purchase of equipment, for LoRa gateways this is a one off cost ranging from aproximately 100 – 3000 euros depending on manufacturer and gateway model.

4.5.1 POSITON ACCURACY FROM GNSS

Under all GNSS position acquisition cycles tested, horizontal position bias was less than 9m (4.71 – 8.44) relative to the true position of the tag with precision of 18 or less (±2.88 – ±18.0) as measured by the standard deviation from the mean (Figure 20, Table 11). This is comparable with other, commercially available GPS/GNSS devices and bio-loggers (Forin-Wiart *et al.*, 2015; Evens *et al.*, 2018; Acácio, Atkinson, *et al.*, 2022). The relationship between the GNSS position acquisition interval and accuracy indicates that where high position accuracy is a concern, a shorter interval between location acquisition can be adopted. The vertical position bias varied between +2 and +5m relative to the true position. Across all cases these results suggest a slight bias towards over-estimating altitude relative to the true position of the tag in vertical space (Figure 20d). Precision, as measured by the standard deviation from the mean (Table 11), was best for the 1-minute acquisition cycle (±7.77m) compared with the 30-minute (±15.3m) and 60-minute (±27.4m) cycles. The variation in accuracy between location acquisition cycles is likely due to the GNSS chip switching off or going to sleep between fixes whereas during the 1-minute cycle, the GNSS remains switched on constantly meaning it can maintain contact with a larger number of GNSS satellites. This relationship between GNSS accuracy and sampling interval in the Nomad tags is comparable to that observed in other GNSS tags (Evens *et al.*, 2018). It is important to be aware of these errors when planning deployment of these tracking devices, particularly where height data is used to assess the behaviour of the animal relative to anthropogenic hazards such as planes, powerlines or wind turbines (Katzner and Arlettaz, 2020).

4.5.2 LORA DATA TRANSMISSION RANGE

Our ground-based tests confirmed data transmission up to distances of 40.7km (Figure 19). While tags deployed on Griffon Vultures demonstrated data transmission up to approximately 53km is possible (Figure 22; Table 13). The probability of successful data transmission declines significantly in relation to distance from the gateway and proximity to the ground. This makes sense because at higher altitudes, the tags are more likely to have obstruction free line of sight to a gateway caused by rough terrain. Our results suggest that placing gateways approximately every 30 - 60km should provide sufficient coverage for tracking studies for birds, particularly when paired with the use of mobile gateways which may be temporarily deployed in the field at colonies, nest sites or known migratory stopover areas to complement the fixed position outdoor gateways.

Although we did not detect an effect of landcover or terrain roughness on the probability of successful data transmission in the vulture tracking data, this is likely because the birds tend to fly at heights where the presence of tree cover or large boulders is less influential. For mammals or species of bird which habitually fly very close to the ground, obstructions to line of sight are likely to be a more significant factor in inhibiting data transmission than was found for the Griffon Vultures. This effect of landcover was observed during the tests of data transmission to the mobile gateway (Figure 19c) at location 7 which was on a high point on a track surrounded by a Eucalyptus plantation. Depending on how mobile the study species is, to facilitate studies of mammal movements, the viewshed would likely be more limited than for birds. As such gateways would need to be placed within ~5-10km of each other to provide sufficient coverage of the study area. Alternative solutions such as regular drone flights or vehicle transects with a mobile gateway to download the data or deployment of gateways near den sites or known feeding areas could also help in areas where perfect coverage from static gateways is not possible to achieve. With the caveat that the use of drones or vehicles should be weighed against the potential impact of this extra disturbance on the animals.

4.5.3 POWER CONSUMPTION

It is difficult to assess power consumption in a standardized manner under field conditions because of daily variations in solar and temperature conditions and variations between batteries which make it difficult to fairly compare devices using different settings. There are other studies such as (Finnegan and Brown, 2020) which have compared the power consumption of different technologies such as GSM and LPWAN (LoRA, Sigfox, NB-IoT and others) under controlled laboratory conditions. As such, testing power consumption of the devices was not one of the core research questions of this research. What we can say based on the performance of the device used to assess GNSS accuracy is that even with a small 0.3mah battery paired with a solar harvester (Figure 18f-g), the device was able to recharge sufficiently during daylight hours to maintain continuous GNSS recording at the programmed schedules (1 minute, 30 minute and 60 minute), with data sent up to every 15 seconds, over a period of 6 weeks in May and June when solar conditions in Portugal are usually optimal (Figure 23). To inform potential future deployments of Nomad or other GPS-LoRa devices, a spreadsheet for estimating power consumption and battery longevity under different settings has been provided by the manufacturer and can be downloaded from here: https://tinyurl.com/bdz4rehv.

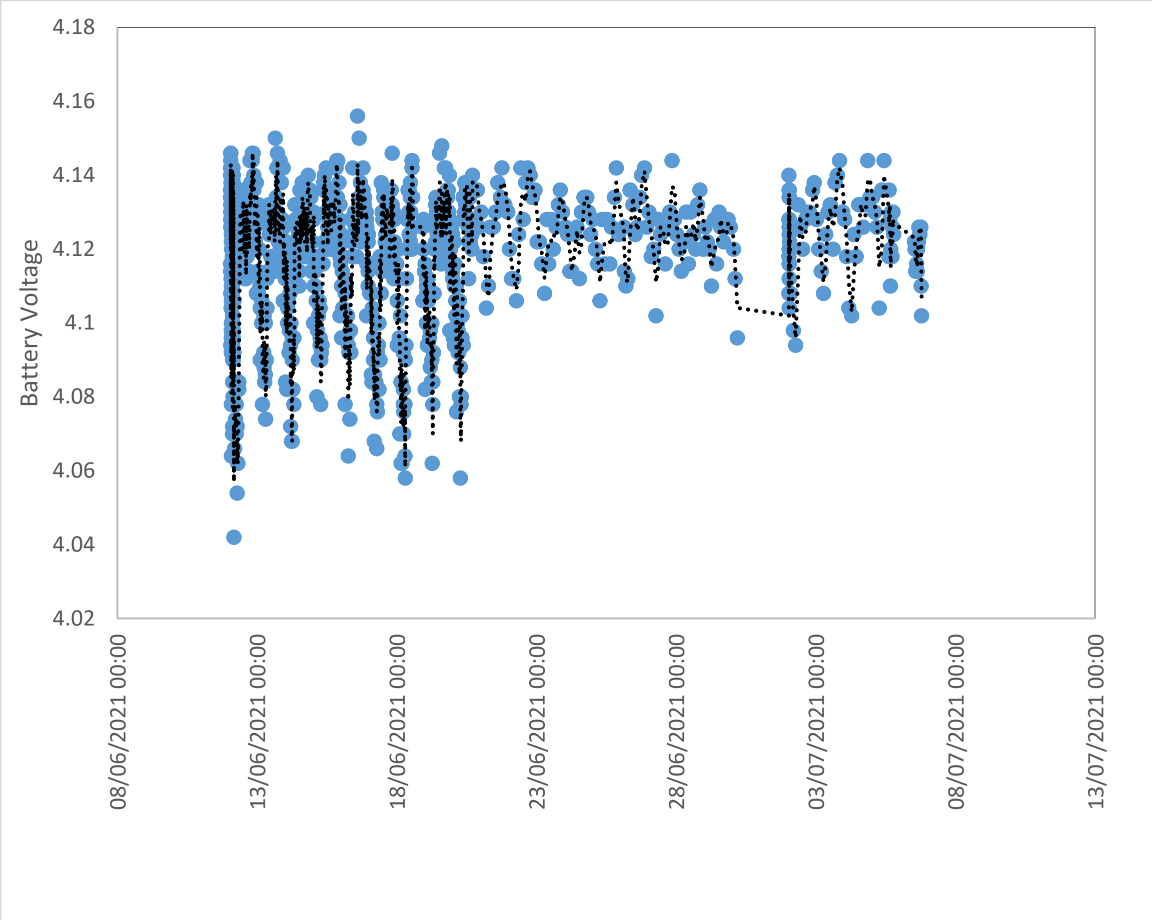

Figure 23: Battery voltage reported by the Status payloads sent by the tag during the GPS Accuracy Tests performed between June and July of 2021 in Portugal. The line follows the moving average of battery voltage over time.

4.5.4 DEPLOYMENT PERFORMANCE

Preliminary results from the trial deployment of the Nomad tags on Griffon Vultures confirmed that tracking data can be obtained over large areas. This study demonstrated this technology can be used to successfully follow the birds' daily movements (Figure 21), obtain information on the daily variability in flight speed, flight height relative to ground level and measure the daily displacement. This included the detection of a failed sea crossing attempt of one bird (Figure 21b). However, to date, we have only successfully received post-deployment location data for two of the six birds tagged so we are not able to comment on the long-term performance of the tags deployed on vultures.

Acceleration data was obtained for the remaining four vultures. Although we do not know the route taken by 9DF1_Jethro (total of 2,156 data payloads sent) and 6923_Carlos (2,047 data payloads sent) between southwest Portugal and Tarifa, the minimum possible distance travelled is approximately 480km. The data transmission pattern around the Tarifa gateways suggests that the birds were likely thermaling in vicinity of the gateway to gain altitude and then moved further away. Hence these birds likely attempted to cross the strait of Gibraltar, but this has not been confirmed. The tags for FB45_Benoit and 7E32_Aldina most likely moved to areas out of transmission range. Issues related to animals moving beyond transmission range will ease as the number and density of LoRaWAN gateways continues to increase. The vulture 9012_Eduardo was not detected by the LoRaWAN Gateway in Tarifa, suggesting that it did not migrate to Africa. Provided the tag was still on the bird, had it migrated, data would have been received by the gateway in Tarifa.

The capability of the NOMAD tags to record high resolution accelerometer data means they have the potential to record when birds collide with infrastructure such as wind turbines or if a bird is shot. To test this feature, the devices were programmed to trigger acceleration acquisition at 50Hz when forces exceeding a 3.2g threshold were detected. Using this feature, the GPS-LoRa tags have been successfully used to study movement of boulders where the accelerometer triggered events can be used to detect movement of objects in response to environmental factors (e.g. floods or heavy precipitation) (Dini et al. 2021). This threshold was exceeded for 4 birds during transport and deployment of the loggers resulting in large quantities of acceleration measurements being collected prior to the release of the birds, so clearing the memory buffer prior to the birds' release is recommended. Further work is required to refine the appropriate settings to avoid the 9-axis sensor from being erroneously triggered and preventing location data from being sent.

As with other gateway or antenna reliant systems, an important consideration for the settings on these tags is how often the bird or other study species is likely to be in range of a gateway. This will inform the sampling regime and the number of gateways deployed to collect the data. Using the upper limit of flight speeds recorded during the trial deployment on Griffon Vultures as a guide (Figure 21). A bird flying at 6 m/s (21.6 Km/h) will pass through the area in range of a mobile gateway (17km radius) in approximately 2,833 seconds (47 minutes) allowing up to a maximum of approximately 188 payloads to be sent. This is assuming perfect coverage and no obstacles to transmission. For a more powerful fixed position gateway, depending on terrain, the potential transmission radius is up to 53km meaning the bird could be in range for 17,666 seconds (4.9 hours) allowing for up to approximately 1,177 payloads to be sent depending on SF. These are theoretical values, in reality, a high SF when the device is further away from the gateway is likely to reduce the transmission rate to a few payloads per hour (TTN, 2016). For the data from the two devices for which we have GNSS location data, the mean number of locations recorded per day from each bird was 55.7 (range 2 -167). On days when the birds were in range of a gateway 184.5 (range 1- 749) locations were transmitted per day. One development which may assist with this is the use of Delta Compression which significantly reduces the size of individual payloads by "coding the difference between the actual acquired value and the previous acquired value” (Săcăleanu *et al.*, 2018). The Nomad tags are capable of this however further development is required to allow the application server (Figure 15) to decode delta compressed data packets.

4.6 CONCLUSIONS

This is an exciting time in the field of movement ecology, a diverse range of technologies are available to monitor the movements and behaviours of animals (Ripperger *et al.*, 2020). The tags described in this paper can currently be deployed in form factors weighing from 5g up to the 83g format deployed on Griffon Vultures as part of this study. Prior to commercialisation, further development of the tags and housing designs is ongoing with a view to further reduce the minimum weight of the fully assembled tag. This includes plans for a large-scale trial deployment of the 5g tag format with lesser kestrels and common kestrels in Portugal and the installation of additional LoRaWAN gateways.

Our tests of GNSS position accuracy, transmission range and deployment performance of the GPS-LoRa tags have demonstrated their potential as a viable alternative to other tracking technologies currently available. These results and the information provided in this paper will be informative for researchers seeking to use or develop tags which use LoRa to transmit data. The key advantage over tags which transmit via satellite or GSM is that LoRa uses less energy to send the data over long distances (tens of kilometres) (Finnegan and Brown, 2020). This affords the ability to use smaller batteries and solar panels compared to GSM devices which in turn has the potential to help increase the range of species we can track in near real time. While data costs for GPS-LoRa tags can be effectively zero when using open-source, publicly accessible, networks like TTN or when the cost of a paid for server such as LORIOT is spread across a large number of devices (LORIOT, 2021; TTN, 2021).

One disadvantage is that away from urban areas, LoRa coverage provided by publicly accessible gateways is currently limited. This means that, researchers would likely need to install their own gateway systems to provide coverage for the area of interest. As such, we would currently recommend the use of GPS-LoRa devices to monitor either resident or site-faithful species because gateways can be set up adjacent to breeding sites, along known migratory routes and near known foraging areas to download stored tracking data. This strategy would suit many long-distance migrants ranging from seabirds like Terns to colonial soaring migrants like Storks. Provided optimal placement of the LoRa gateway to allow for data transmission at low spreading factors. Upon the bird's return to the breeding site, it could take as little as one day to download a month's worth of tracking data accumulated at a rate of one location every half an hour without breaching the LoRa fair use guidance. For determining optimal gateway placement, we would advise the use of Viewshed analysis tools commonly available in GIS software such as QGIS and Arcmap (ESRI, 2018; QGIS Development Team, 2019). As gateway coverage improves, there will be less need for researcher to invest in their own gateway systems to receive data and the range of species that can effectively be tracked will increase. That said, the flexibility of LoRa to deploy new LoRaWAN gateways relatively inexpensively to receive data in situations where a lack of GSM coverage would prevent data being received from being received from GSM devices. There are also plans to launch LoRaWAN gateways into space which would provide global coverage and the ability to receive tracking data in real time via LoRa from almost anywhere on Earth (Lacuna, 2022).

ACKNOWLEDGEMENTS

We thank all those who have contributed to this research. Special thanks go to Carlos Pacheco from CIBIO, along with Eduardo Realinho and Hugo Blanco for their invaluable assistance with fieldwork to capture and deploy tags on the vultures. We also thank Miguel González for arranging for us to mount a LoRaWAN Gateway at the Cazalla Observatory in Tarifa, Spain. The team at STRIX (https://strixinternational.com/) kept us informed about the movements of large vulture flocks. The wildlife rescue organisations RIAS (https://riaswildliferescuecentre.wordpress.com/), CARAS (LPN, Alentejo) and SEPNA/GNR (https://www.gnr.pt/atrib_SPENA.aspx) for allowing us to deploy tags on rehabilitated birds. Nick Griffin, Gareth Flower Dew and David Ciplic from the University of East Anglia electronics workshop for their assistance. For technical assistance with the devices and LoRaWAN Gateways, we thank Marcel Wapper and Simon Galli from Miromico-AG, Benedetta Dini from the University of Grenoble, Steven Drewett from Concept13™ and Miles Clark from the University of East Anglia.

AVAILABILITY OF DATA AND MATERIALS

All data and R-scripts used to produce this work are available for download from Figshare here: https://tinyurl.com/bdz4rehv

ETHICS APPROVAL

All fieldwork with vultures was performed under license from CNF - Instituto da Conservação da Natureza e das Florestas (the Portuguese Government agency responsible for wildlife and forests) and Ethics approval was granted by the ethics committee of the University of East Anglia.

4.7 REFERENCES

Acácio, Marta, Philip W. Atkinson, João Paulo Silva, and Aldina M. A. Franco. 2021. “Quantifying the Performance of a Solar GPS/GPRS Tracking Device: Fix Interval, but Not Deployment on Birds, Decreases Accuracy and Precision.” University of East Anglia.

Application, Iot, and Ritesh Kumar Singh. 2020. “Energy Consumption Analysis of LPWAN Technologies and Lifetime Estimation For.” https://doi.org/10.3390/s20174794.

Bouten, Willem, Edwin W. Baaij, Judy Shamoun-Baranes, and Kees C.J. Camphuysen. 2013. “A Flexible GPS Tracking System for Studying Bird Behaviour at Multiple Scales.” Journal of Ornithology 154 (2): 571–80. https://doi.org/10.1007/s10336-012-0908-1.

Bridge, Eli S., Kasper Thorup, Melissa S. Bowlin, Phillip B. Chilson, Robert H. Diehl, René W. Fléron, Phillip Hartl, et al. 2011. “Technology on the Move: Recent and Forthcoming Innovations for Tracking Migratory Birds.” BioScience 61 (9): 689–98. https://doi.org/10.1525/bio.2011.61.9.7.

Concept 13 Limited. 2022. “Concept 13: Sensors-Gateways-LoRaWAN.” 2022. https://www.concept13.co.uk/.

Dini, Benedetta, Georgina L. Bennett, Aldina M.A. Franco, Michael R.Z. Whitworth, Kristen L. Cook, Andreas Senn, and John M. Reynolds. 2021. “Development of Smart Boulders to Monitor Mass Movements via the Internet of Things: A Pilot Study in Nepal.” Earth Surface Dynamics 9 (2): 295–315. https://doi.org/10.5194/esurf-9-295-2021.

ESRI. 2018. “ArcGIS Desktop: Release 10.6.1.” Redlands, CA: Environmental Systems Research Institute.

Evans;, Jeffrey S., Melanie A. Murphy;, and Karthik Ram. 2021. “SpatialEco: Spatial Analysis and Modelling Utilities.” cran-r. https://cran.r-project.org/web/packages/spatialEco/index.html.

Evens, Ruben, Natalie Beenaerts, Eddy Ulenaers, Nele Witters, and Tom Artois. 2018. “An Effective, Low-Tech Drop-off Solution to Facilitate the Retrieval of Data Loggers in Animal-Tracking Studies.” Ringing and Migration 33 (1): 10–18. https://doi.org/10.1080/03078698.2018.1521116.

Finnegan, Joseph, and Stephen Brown. 2020. “An Analysis of the Energy Consumption of LPWA-Based IoT Devices.” In 2018 International Symposium on Networks, Computers and Communications (ISNCC), 1–6. Maynooth: IEEE. https://doi.org/10.1109/ISNCC.2018.8531068.

Forin-Wiart, Marie Amélie, Pauline Hubert, Pascal Sirguey, and Marie Lazarine Poulle. 2015. “Performance and Accuracy of Lightweight and Low-Cost GPS Data Loggers According to Antenna Positions, Fix Intervals, Habitats and Animal Movements.” PLoS ONE 10 (6): 1–21. https://doi.org/10.1371/journal.pone.0129271.

Gilbert, Nathalie I., Ricardo A. Correia, João Paulo Silva, Carlos Pacheco, Inês Catry, Philip W. Atkinson, Jenny A. Gill, and Aldina M. A. Franco. 2016. “Are White Storks Addicted to Junk Food? Impacts of Landfill Use on the Movement and Behaviour of Resident White Storks (Ciconia Ciconia) from a Partially Migratory Population.” Movement Ecology 4 (1): 7. https://doi.org/10.1186/s40462-016-0070-0.

Hijmans, R. J., E. Williams, and C. Vennes. 2015. “Geosphere: Spherical Trigonometry.” R. url: https://CRAN. R-project. org/package= geosphere.

Hijmans, Robert J. 2019. “Raster: An R Package for Working with Raster Data.” https://www.rspatial.org/.

Interex. 2022. “Interex:Mini GPS-GSM-ACC.” 2022. https://interrex-tracking.com/mini/.

IoT. 2022. “Internet of Things: Airtime Calculator.” 2022. https://www.thethingsnetwork.org/airtime-calculator.

IoT Wonderland. 2022. “IoT Wonderland: Geo-Spacial Data Visualization.” 2022. https://www.iotwonderland.com/.

Katzner, Todd E., and Raphaël Arlettaz. 2020. “Evaluating Contributions of Recent Tracking-Based Animal Movement Ecology to Conservation Management.” Frontiers in Ecology and Evolution 7 (January). https://doi.org/10.3389/fevo.2019.00519.

Kauth, Hilary R., Robert C. Lonsinger, Adam J. Kauth, and Andrew J. Gregory. 2020. “Low-Cost DIY GPS Trackers Improve Upland Game Bird Monitoring.” Wildlife Biology 2020 (2). https://doi.org/10.2981/wlb.00653.

Kim, Seungku, Heonkook Lee, and Sungho Jeon. 2020. “An Adaptive Spreading Factor Selection Scheme for a Single Channel Lora Modem.” Sensors (Switzerland) 20 (4). https://doi.org/10.3390/s20041008.

Kölzsch, Andrea, Marjolein Neefjes, Jude Barkway, Gerhard J.D.M. Müskens, Frank van Langevelde, Willem F. de Boer, Herbert H.T. Prins, Brian H. Cresswell, and Bart A. Nolet. 2016. “Neckband or Backpack? Differences in Tag Design and Their Effects on GPS/Accelerometer Tracking Results in Large Waterbirds.” Animal Biotelemetry 4 (1). https://doi.org/10.1186/s40317-016-0104-9.

Lacuna. 2022. “Lacuna Space.” 2022. https://lacuna.space/.

LORIOT. 2021. “LORIOT Internet of Things LoRaWAN Server.” 2021. https://www.loriot.io/.

Lotek. 2022. “Lotek:PinPoint Cell.” 2022. https://www.lotek.com/wp-content/uploads/2020/06/PinPoint-Cell-Spec-Sheet.pdf.

Lüdecke, Daniel, Frederik Aust, Sam Crawley, and Mattan S. Ben-Shachar. 2022. “Ggeffects: Create Tidy Data Frames of Marginal Effects for ‘ggplot’ from Model Outputs.”

Mekki, Kais, Eddy Bajic, Frederic Chaxel, and Fernand Meyer. 2019. “A Comparative Study of LPWAN Technologies for Large-Scale IoT Deployment.” ICT Express 5 (1): 1–7. https://doi.org/10.1016/j.icte.2017.12.005.

Miromico AG. 2021. “MiroNomad Data Sheet: Ultra Lightweight LoRaWAN GPS Tracker.” 2021.

https://docs.miromico.ch/datasheets/_attachments/tracker/miro_Nomad_datasheet_V1_0.pdf.

Miromico AG. 2022. “Miromico Docs: Tracking Solutions Documentation.” Zurich. https://docs.miromico.ch/tracker/dev/index.html.

Movebank. 2019. “Movebank Data Repository.” 2019. https://www.movebank.org/.

Multi-Tech Systems Inc. 2021. “MultiTech Conduit IP67 Base Station 16-Channel v2.1 Geolocation EU686 for Europe.” 2021. https://www.multitech.com/documents/publications/data-sheets/86002223.pdf.

Multi-Tech Systems Inc.. 2022. “Multi-Tech DeviceHQ: Cloud-Based Application Store and IoT Device Management.” 2022. www.multitech.com.

Muteba, Franck, Karim Djouani, and Thomas Olwal. 2019. “A Comparative Survey Study on LPWA IoT Technologies: Design, Considerations, Challenges and Solutions.” Procedia Computer Science 155: 636–41. https://doi.org/10.1016/j.procs.2019.08.090.

Ossi, Federico, Ferdinando Urbano, and Francesca Cagnacci. 2019a. Biologging and Remote-Sensing of Behavior. Encyclopedia of Animal Behavior. Second Edi. Vol. 3. Elsevier. https://doi.org/10.1016/B978-0-12-809633-8.90089-X.

Pedersen, Thomas Lin. 2020. “Patchwork: The Composer of Plots.” https://patchwork.data-imaginist.com.

Perona, Arturo M., Vicente Urios, and Pascual López-López. 2019. “Holidays? Not for All. Eagles Have Larger Home Ranges on Holidays as a Consequence of Human Disturbance.” Biological Conservation 231 (July 2018): 59–66. https://doi.org/10.1016/j.biocon.2019.01.010.

QGIS Development Team. 2019. “QGIS Geographic Information System.” Open Source Geospatial Foundation Project.

Quectel. 2021. “Global IOT Solutions Provider IoT Modules and Antenna Catalogue.” Shanghai. https://www.quectel.com/wp-content/uploads/2022/10/Quectel_Product_Brochure_v7.2.pdf.

R Core Team. 2019. “R: A Language and Environment for Statistical Computing.” http://www.r-project.org/.

Recio, Mariano R, Renaud Mathieu, Richard Maloney, and Philip J Seddon. 2011. “Cost Comparisons between GPS- and VHF-Based Telemetry : Case Study of Feral Cats in New Zealand SHORT COMMUNICATION Cost Comparison between GPS- and VHF-Based Telemetry : Case Study of Feral Cats Felis Catus in New Zealand,” no. May 2014.

Riley, S.J., S.D. DeGloria, and R. Elliot. 1999. “A Terrain Ruggedness Index That Quantifies Topographic Heterogeneity.” Intermountain Journal of Sciences 5: 23–27.

Ripperger, Simon P., Gerald G. Carter, Rachel A. Page Supervision, Niklas Duda, Alexander Koelpin, Robert Weigel, Markus Hartmann, et al. 2020. “Thinking Small: Next-Generation Sensor Networks Close the Size Gap in Vertebrate Biologging.” PLoS Biology 18 (4): 1–25. https://doi.org/10.1371/journal.pbio.3000655.

Rodríguez, Airam, Juan J. Negro, Mara Mulero, Carlos Rodríguez, Jesús Hernández-Pliego, and Javier Bustamante. 2012. “The Eye in the Sky: Combined Use of Unmanned Aerial Systems and GPS Data Loggers for Ecological Research and Conservation of Small Birds.” PLoS ONE 7 (12). https://doi.org/10.1371/journal.pone.0050336.

Rotics, Shay, Sondra Turjeman, Michael Kaatz, Damaris Zurell, Martin Wikelski, Nir Sapir, Wolfgang Fiedler, et al. 2021. “Early-Life Behaviour Predicts First-Year Survival in a Long-Distance Avian Migrant.” Proceedings of the Royal Society B: Biological Sciences 288 (1942). https://doi.org/10.1098/rspb.2020.2670.

Săcăleanu, D I, R Popescu, I P Manciu, and L A Perișoară. 2018. “Data Compression in Wireless Sensor Nodes with LoRa.” In ECAI 2018 - International Conference – 10th Edition: Electronics, Computers and Artificial Intelligence, 5–8. Iasi, romania: IEEE. https://ieeexplore.ieee.org/stamp/stamp.jsp?tp=&arnumber=8679003.

Santos, Carlos D., Frank Hanssen, Antonio Román Muñoz, Alejandro Onrubia, Martin Wikelski, Roel May, and João P. Silva. 2017. “Match between Soaring Modes of Black Kites and the Fine-Scale Distribution of Updrafts.” Scientific Reports 7 (1): 1–10. https://doi.org/10.1038/s41598-017-05319-8.

Scacco, Martina, Andrea Flack, Olivier Duriez, Martin Wikelski, and Kamran Safi. 2019. “Static Landscape Features Predict Uplift Locations for Soaring Birds across Europe.” Royal Society Open Science 6 (1): 1–12. https://doi.org/10.1098/rsos.181440.

Schaub, Tonio, Raymond H.G. Klaassen, Willem Bouten, Almut E. Schlaich, and Ben J. Koks. 2020. “Collision Risk of Montagu’s Harriers Circus Pygargus with Wind Turbines Derived from High-Resolution GPS Tracking.” Ibis 162 (2): 520–34. https://doi.org/10.1111/ibi.12788.

Schloerke, Barret, Di Cook, Joseph Larmarange, Francois Briatte, Moritz Marbach, Edwin Thoen, Amos Elberg, et al. 2021. “GGally: Extension to ‘Ggplot2.’” cran-r. https://cran.r-project.org/package=GGally.

Semtech. 2021. “Datasheet: DS.SX1261-2 Long Range, Low Power, Sub-GHz RF Transceiver.” 2021. https://www.semtech.com/products/wireless-rf/lora-connect/sx1262.

Silva, Rafa, Isabel Afán, Juan A. Gil, and Javier Bustamante. 2017. “Seasonal and Circadian Biases in Bird Tracking with Solar GPS-Tags.” PLoS ONE 12 (10): 1–19. https://doi.org/10.1371/journal.pone.0185344.

Spivey, R. J., S. Stansfield, and C. M. Bishop. 2014. “Analysing the Intermittent Flapping Flight of a Manx Shearwater, Puffinus Puffinus, and Its Sporadic Use of a Wave-Meandering Wing-Sailing Flight Strategy.” Progress in Oceanography 125: 62–73. https://doi.org/10.1016/j.pocean.2014.04.005.

Stienen, Eric W.M., Peter Desmet, Bart Aelterman, Wouter Courtens, Simon Feys, Nicolas Vanermen, Hilbran Verstraete, et al. 2016. “GPS Tracking Data of Lesser Black-Backed Gulls and Herring Gulls Breeding at the Southern North Sea Coast.” ZooKeys 2016 (555): 115–24. https://doi.org/10.3897/zookeys.555.6173.

The Things Network. 2019. “LoRaWAN® Distance World Record Broken, Twice. 766 Km (476 Miles) Using 25mW Transmission Power.” 2019. https://www.thethingsnetwork.org/article/lorawan-distance-world-record.

TTN. 2016. “The Things Network Fair Usage Policy.” 2016. https://www.thethingsnetwork.org/forum/t/fair-use-policy-explained/1300.

TTN. 2021. “The Things Network LoRaWAN Server.” 2021. https://www.thethingsnetwork.org/.

TTN Mapper. 2022. “TTN Mapper: Interactive Map of TTN LoRa Gateways.” 2022. https://ttnmapper.org/heatmap/.

UK Research and Innovation. 2016. “Long Range Wireless Devices for High-Resolution Monitoring of Animal Movement.” 2016. https://gtr.ukri.org/projects?ref=NE%2FP003907%2F1.

Walther, Bruno A., and Joslin L. Moore. 2005. “The Concepts of Bias, Precision and Accuracy, and Their Use in Testing the Performance of Species Richness Estimators, with a Literature Review of Estimator Performance.” Ecography 28 (6): 815–29. https://doi.org/10.1111/j.2005.0906-7590.04112.x.

Wickham, H. 2016. “Ggplot2: Elegant Graphics for Data Analysis in R.”

Williams, H. J., J. Ryan Shipley, C. Rutz, M. Wikelski, M. Wilkes, and L. A. Hawkes. 2021. “Future Trends in Measuring Physiology in Free-Living Animals.” Philosophical Transactions of the Royal Society B: Biological Sciences 376 (1831). https://doi.org/10.1098/rstb.2020.0230.

CHAPTER 5: BIRD STRIKE: REMOTE SENSING OF BIRD COLLISIONS USING ACCELEROMETER-BASED EVENT TRIGGERING

The intention is to submit this chapter as a paper however, at the time of submission, it is yet to be submitted to a journal for peer review.

Photo 8: Whooper Swan Cygnus cygnus killed by collision with a medium tension power line near WWT Welney, Norfolk, UK. Photo Credit: Jethro Gauld

5.1 ABSTRACT

1. An ever-increasing number of birds are now subject to tracking studies using satellite telemetry due to a growing interest in using remote data for studying animal behaviour. The loggers used to gather location data usually contain additional sensors such as accelerometers which can measure the forces birds are exposed to. Here we demonstrate how collision events can be remotely detected using a new type of logger capable of using “event triggering” to record high frequency acceleration data.

2. We first analysed data from existing tracking studies to define the normal range of forces experienced by wild birds with body mass ranging from 0.44kg to 9.4kg to determine whether body mass and flight style could predict the magnitude of forces recorded by loggers deployed on different species. To help better understand the capability of the GPS-LoRa tags to detect collisions, lab-based collision tests were performed to determine the reliability of collision detection under different settings.

3. The analysis of accelerometery data from wild birds revealed a positive relationship between body mass, flapping flight and the mean magnitude of forces. However, no clear relationship was found between the upper range of forces (>99th percentile) experienced by the birds and body mass. The results of the lab tests indicate that setting the accelerometer to record at a rate of 25Hz is optimal for reliably detecting collision events with a LoRa tracking device.

4. While we did demonstrate that soaring flight and body mass were positively correlated with the forces measured by the loggers, the results were not sufficiently robust to support any recommendations to inform the trigger threshold settings for particular species. However, this work did demonstrate the potential to use accelerator enabled logger to remotely sense collision events and provide insight into the appropriate settings to use. The information presented here can inform the use of

biologging to identify where birds are killed by collision with power lines, wind turbines or due to illegal hunting.

5.2 INTRODUCTION

It is clear that power lines and wind farms are responsible for a significant number of bird deaths each year, primarily due to collision and electrocution (Loss, Will and Marra, 2014; Thaxter, Ross-Smith, *et al.*, 2019). In Canada collision with power lines accounts for the deaths of 2.5 million to 25.6 million birds each year (Rioux, Savard and Gerick, 2013). For some species, for example the Little Bustard (*Tetrax tetrax*) and many soaring birds such as White Stork (*Ciconia ciconia*) and Griffon Vulture (Gyps fulvus), collision with power lines and wind farms is one of the most significant anthropogenic sources or mortality resulting in population level impacts (Martin and Shaw, 2010; Silva et al., 2010; Lucas et al., 2012; Moreira et al., 2018). Bird collisions and electrocution events also come with an associated economic cost. In Spain the annual release cost of property, habitat and infrastructure damage caused by wildfires resulting from bird mortality on powerlines is between 7.6 and 12.4 million euros per year (Guil et al., 2017). There is, therefore, significant interest in retro-fitting these infrastructures with mitigation to reduce risks as well as minimising the impact of new energy infrastructure (Prinsen et al., 2012). Spatial analysis to identify high risk areas for birds in the context of both of these threats is becoming increasingly important to help target conservation actions to reduce bird deaths (Scott R Loss, 2016; Chris B Thaxter *et al.*, 2017).

There is large uncertainty in the absolute numbers of birds killed due to collision with energy infrastructure, (Rees, 2012; Gómez-Catasús *et al.*, 2021). Identifying mortality hotspots where large numbers of collisions occur can help validate the accuracy of sensitivity and risk maps and improve our understanding of the conditions under which collision events are most likely to occur (Evan R. Buechley *et al.*, 2018; Oloo, Safi and Aryal, 2018; Thaxter, Ross-Smith, *et al.*, 2019). Traditional carcass count surveys of wind farms and power lines are labour intensive which can result in significant under recording of bird mortality and limits the spatio-temporal scale of such studies (Huso and Dalthorp, 2014; Gómez-Catasús *et al.*, 2021). Unless the carcass can be recovered, researchers are often limited to determining where the bird died with limited understanding of the cause of mortality. This hampers the ability to definitively determine a bird has collided or died from other causes. Remote detection of collision events using accelerometery would help build up an evidence base to improve spatio-temporal modelling of collision sensitivity and identify priority areas for conservation actions to reduce bird mortality. There is also interest in remote detection of mortality events in tagged birds for reasons other than detecting collisions, such as identifying incidents of illegal killing of raptors (Whitfield and Fielding, 2017; Sergio *et al.*, 2018). This is important for wide ranging species and long-distance migrants where mortality of tracked birds often occurs in remote or inaccessible areas where physical recovery of the tag and inspection of the carcass can be impossible (Schutgens, Shaw and Ryan, 2014).

Previous animal behaviour studies have used accelerometer data in combination with data from the various other on-board sensors namely, temperature, atmospheric pressure, and gyroscope to remotely categorise bird behaviour (Ossi, Urbano and Cagnacci, 2019). This permits us to better understand how external factors such as weather or time of year influence the energy budgets of birds and therefore the time individuals spend foraging, flying, or sitting on the nest. In White Storks *Ciconia ciconia* this data has been used to help understand how the artificial availability of food in landfill sites is altering the timing of seasonal breeding behaviours (Gilbert et al., 2016) and in Griffon Vultures Gyps fulvus GPS tracking data in combination with barometric pressure and accelerometer sensors has been used to understand how these birds use thermals to minimise energy expenditure during flight (Harel and Nathan, 2018).

This study describes how a new type of GPS-LoRa tracking device equipped with high frequency accelerometers can be used to detect and alert researchers to bird collisions in near real time. These tags can be programmed to use “event triggering” to record bursts of high frequency acceleration data up to 200Hz when a user defined G-force is exceeded. This event triggering approach has already been used to detect hazards such as landslides and the movement of large boulders (Ren *et al.*, 2018; Dini *et al.*, 2021). The ability to record is of relevance as increasing numbers of satellite tags are being deployed on birds for the purposes of studying their behaviour, habitat preferences and how they are responding to anthropogenic change (Sergio et al., 2018). As the pace of renewable energy deployment increases (IEA, 2020), there is an increasing interest in using the information from these tags to help identify hotspots for collision with energy infrastructure (Bernardino *et al.*, 2018b). A key challenge is that the collision triggering threshold need to be high enough to avoid false alarms while being low enough to detect collisions across species of different masses. Here we demonstrate how this capability allows us to detect probable mortality events involving tagged birds in near real time by relating the information provided by the on-board sensors to the type of mortality event being recorded. Specifically, this paper aims to describe the optimal settings such as sampling frequency (Hz), trigger threshold (g-force) and recording duration that enable the detection of collision events using both existing accelerometery data collected by bird tracking devices and lab experiments with a new GPS long-range wireless (LoRa) device. Our findings are also applicable to help inform the methodology of studies using other types of tags with the capability to record bursts of high frequency acceleration measurements.

COMMON NAME	SPECIES	NUMBER OF INDIVIDUALS	START YEAR	BIRD WEIGHT (KG)	STUDY NAME	COUNTRY	DATA OWNER	MOVEBANK ID
GREYLAG GOOSE	*Anser anser*	10	2016	3.35	Greylag Goose Anser anser – Belfast	UK	Phil Atkinson	118192126
IBERIAN IMPERIAL EAGLE	*Aquila adalberti*	12	2014	3	Iberian Imperial Eagle movement ecology 2014 – 2015	Spain	Carlos Carrapato	28407489
EAGLE OWL	*Bubo bubo*	6	2010	2.29	Eagle owls – 3 breeding pairs – Southern Part The Netherlands	Netherlands	René Janssen	4502577
WHITE STORK	*Ciconia ciconia*	8	2018	3.25	White Stork Adults 2018	Portugal	Aldina Franco & Marta Serra Acacio	451464940
NORTHERN HARRIER	*Circus cyaneus*	5	2018	0.44	Northern Harrier (Breeding, Fledging and Wintering)	USA	Cory, T. Overton, Michael Casazza, Joshua Hull & Shannon Skalos	884046948
WHOOPER SWAN	*Cygnus cygnus*	12	2016	9.4	Whooper swans in Latvia 2016	Latvia	Wolfgang Fiedler	182459847
COMMON CRANE	*Grus grus*	2	2013	6.05	Common Crane Lithuania GPS, 2015-2016	Lithuania	Ramunas Zydelis & Mindaugas Dagys	146932094
GRIFFON VULTURE	*Gyps fulvus*	1	2016	9.25	LifeTrack Griffon Vulture Croatia	Croatia	Wolfgang Fiedler	154820583
EURASIAN WIGEON	*Mareca penelope*	20	2018	0.725	Eurasian wigeons spring 2018	Netherlands	Mariëlle Van Toor, Jonas Waldenström	412700082
EURASIAN SPOONBILL	*Platalea leucordia*	7	2016	1.87	Eurasian spoonbill – Tour du Valat	France	Jocelyn Champagnon	311803430
LITTLE BUSTARD	*Tetrax tetrax*	8	2018	0.9	Little Bustard Movement Ecology 2018 – 2019	Portugal	João P Silva	461568973

Table 16: Summary of studies used to determine the forces experienced during natural behaviour in medium and large size birds with different flight styles. Table sorted by species name.

5.3 METHODS

5.3.1 DETERMINING FORCES AND SPEEDS OBSERVED UNDER NORMAL BIRD BEHAVIOUR

To distinguish normal bird behaviour from a collision event we examined accelerometer data from existing satellite telemetry studies (Table 16). We examined the distribution of forces individual birds from 11 species were exposed to under normal conditions in wild birds. The data downloaded from (Movebank, 2019) represents species of birds ranging from a body mass of 440g for the Northern Harrier *Circus cyaenus* to 9.4kg for the Whooper Swan *Cygnus cygnus* (Table 16). These species represent the typical range in body size for birds studied using GPS loggers, they also represent different flight behaviours; the Little Bustard for example uses flapping flight and generally flies close to the ground (Alonso *et al.*, 2019) whereas the White Stork *Ciconia ciconia* and Griffon Vulture are large soaring species (Rotics *et al.*, 2016). All species included in the analysis are considered to be susceptible to collision with power lines or wind farms (SNH, 2010; BSG Ecological Consultants, 2011; Vanermen *et al.*, 2015; Moreira *et al.*, 2018). We obtained permission to use this data during a Movebank data search performed in early 2021, to our knowledge all data was collected under the appropriate licenses and country ethics guidelines for animal tracking studies. Each data set contains measurements of acceleration collected from multiple individuals using loggers deployed on each bird. While some of these data sets contained GPS locations, many were acceleration only therefore it was not possible to calculate speed in order to distinguish measurements recorded while the bird was in flight from other behaviours.

It was also not possible to control for tag type in the analysis because this was not detailed in the metadata for all studies.

This data was processed in R using the Tidyverse, DPLYR and ggplot packages (Hadley Wickham *et al.*, 2015; Wickham, 2016; R Core Team, 2019). Rows in the data frame which lacked acceleration data were removed. All data were centred by subtracting the median to account for biases relating to how the tag is mounted on different species and all values below zero were converted to positive using $\sqrt{x^2}$. Our analysis was focused on understanding the range of forces experienced by these birds rather than characterising a specific behavioural signature. As such, forces in the three axes were grouped by calculating the maximum force in any of the three axes associated with a given data point. This allowed us to summarise the mean, maximum, 95% and 99% confidence intervals of forces (G-force) cross three axes (X, Y and Z) for each individual and species. We used an ANOVA to test for differences between species and a generalised linear model GLM to determine whether there was a causal relationship between flight style, body mass and the forces experienced by the birds. To account for individual variation in behaviour and control for the potential for different tag types being used on different individuals, “Individual ID” was included as a random effect.

5.3.2 LAB BASED TRIALS WITH THE ACCELEROMETER

To determine whether the loggers can reliably detect collisions and determine the signature of a collision, we drew on experience of replicating bird strikes from other research in the fields of engineering and aerospace (Liu, Li and Gao, 2014; Allaeys *et al.*, 2017) to simulate the forces experienced by a bird during a collision event. Upon triggering, it is important that sufficient data is captured to record the collision signature and allow remote confirmation of a collision event. To determine the optimum settings in terms of the number of acceleration measurements recorded per second (Hz), the duration of this sampling and sample averaging a series of bench-based experiments with the devices was undertaken. This utilised a pendulum set up whereby the device was raised to a 90-degree angle and allowed to fall reaching a speed of 1.95 ± 0.12 m/s. This was repeated 20 - 30 times under each combination of settings (10hz, 25hz and 50hz). Tests with 1hz were also performed, however the tags were found to still record at 10hz, this appears to be their base level of ACC recording and some tests with 100hz were performed but this was found to require several hours to transmit the data accumulated from a small number of impacts highlighting one limitation of the slower transmission speeds via LoRa. The effect of duration of recording was also tested for by performing tests with a duration of 1.5 seconds and two seconds of acceleration recording. These timings were used because it was observed during initial trials that the pendulum continued to move after the initial impact and in (Jiguet *et al.*, 2021) the accelerometer peak, observed when a Eurasian Curlew *Numenius arquata* fell to the ground after narrowly avoiding collision with a wind turbine, lasted several seconds. Collision rate refers to the proportion of collision tests recorded by the tag and how many of the accelerometer bursts provide a clear collision signature when plotted compared to the number of tests undertaken. The collision signature from each test was plotted and the percentage of these plots with a clear collision signature was calculated for each setting used in the experiment.

5.3.3 DEVICES USED IN LAB EXPERIMENTS

specified interval (typically every 30 – 90 minutes) which, along with the number of visible satellites, battery voltage and temperature, records a single record of acceleration in the X, Y and Z axes. The flexibility of the onboard software allowed us to programme LoRa devices to sample GPS and acceleration at regular intervals to allow monitoring of normal bird movements. Accelerometer data can be used to continuously record bird movements between GPS positions with minimal additional drain on the battery using dead reckoning (Bidder et al., 2012). Alternatively, the devices can be set to trigger a burst of high frequency recording of acceleration when the force measured by the accelerometer exceeds a pre-programmed force threshold. We used data from previous bird tracking studies (Table 16) and a series of lab-based experiments to determine the optimum settings for the trigger threshold and frequency of data acquisition required for detecting collision events in real time. Upon triggering, the devices were programmed to record a burst of accelerometer measurements before transmitting this data to a LoRa gateway which in turn forwards the data to an online server. The duty cycle of each device was set to fifteen minutes, therefore unless triggered by an impact the GPS location and other measurements would be recorded and transmitted at this interval.

5.3.4 DETERMINING WHETHER BIRD MASS INFLUENCES THE MAGNITUDE OF FORCES RECORDED

We would expect collisions involving larger species to result in a greater magnitude impact force being recorded by the tags. We can estimate the likely force of impact by calculating the G-force resulting from sudden deceleration of an object of a known mass and velocity as per $\rho = MV$ (1), where momentum (ρ) is the product of multiplying mass by the velocity of the object. We can then calculate the net impact force using $F_{net} = (\Delta\rho)/\Delta t$ (2), where the net force on impact is the difference between the momentum of the object and the momentum at rest which for our purposes is treated as zero. This is then divided by the time taken for the object to come to rest (Δt) to produce the expected change in force. Video footage can be used to calculate (Δt). We can then compare this with the forces measured by the on-board accelerometer to determine how much of this energy is transferred to the device and whether this differs significantly between bird analogues of different masses. The bird analogues used in the "drop" and "zipline" tests were polythene sandbags representing birds of different masses. During the tests they were fitted with a GPS-LoRA device in a housing and the same backpack configuration used during deployment on real birds. These bird analogues were more appropriate for our purposes than the ballistics gel models used in the high velocity safety tests performed by the aircraft industry (LIU *et al.*, 2018) to determine the impact of bird strikes on airplanes.

To confirm whether the impact force and signature of collisions recorded by the tags varies depending on the birds' mass, we performed repeated tests using sandbags of different masses. These tests utilised two different experimental designs. The first test, henceforth referred to as the "drop" test, was undertaken by repeatedly dropping sandbags of different masses (0.3kg, 0.5kg, 1kg, 2kg and 4kg) from a known height (1.5m). This height was chosen to enable repeated drops without the use of a raised platform or other method involving working from height. The amplitude of forces was characterised for each mass. The velocity and duration of impact was estimated by videoing some of these drop tests and calculating the speed (2.85 m/s (2.81 – 3.0 m/s)) based upon how long it took to drop 1.5m and how long it took for the sandbag to come to rest for different masses.

The second experimental set up, henceforth referred to as the “zipline” test, aimed to closely replicate a collision signature from a bird in flight colliding with an object such as a wind turbine blade. The bird analogues were flown along a zipline consisting of a 3mm steel cable of known length (44m) and a pair of a LIXDA ZWA006 zip line trolleys with low friction rollers to collide with a wooden panel. The zipline (Appendix E) had a height difference of approximately 12m between the start of the zip line and where the bird collides with an object allowing for speeds of up to 6m/s to be achieved. The velocity and duration of impact was estimated in a similar manner as the drop tests. A subsample of the runs for each mass was filmed to allow for the time taken to travel between a marker 5m away and the collision point. Speeds ranged from 3.65 m/s to 5.95m/s. The zipline collision test was repeated for each mass of ‘bird’ (1kg, 2kg and 4kg) to determine whether the collision signature changed between collisions involving birds of different masses.

5.4 RESULTS

5.4.1 FORCES EXPERIENCED UNDER NORMAL BIRD BEHAVIOUR

Across all species analysed, the maximum forces recorded by the onboard accelerometer across for each species in the data ranged between 2.04g and 12.78g (Table 17; Figure 24). The mean forces recorded by the tags varied significantly between species ($F(10, 542{,}102) = [240{,}039]$, $p = < 0.001$). The single largest interspecies difference was between Eagle Owl *Bubo bubo* and Greylag Goose *Anser anser* (Appendix E). The GLM result suggests a weak but significant positive relationship between body mass and the mean forces experienced by the birds (Estimate = 0.056, t = 208.1, $P < 0.001$, Table 18). The GLMS also confirmed a significant difference between flight styles with soaring species exhibiting greater mean forces (Estimate = 0.229, t = 1114.5, $P < 0.001$, Table 18), than flapping species. Although the small R^2 value of 0.174 suggests that body mass and flight style alone do not fully explain the observed variation in forces recorded for different species.

Common Name	Species	Flight Style	Wing Length (cm)	Body Mass (g)	ACC 1th Percentile	ACC 2.5^{t} Percentile	ACC Mean	ACC 97.5th Percentile	ACC 99th Percentile	ACC Max	Count exceedance of 99th percentile	Expected Impact Force at 2.8m/s (G-Force)
Wigeon	Mareca penelope	flapping	25.9	725	0.03	0.04	0.29	1.42	1.95	3.05	5481	1.02
Little Bustard	Tetrax tetrax	flapping	24.7	900	0.04	0.05	0.27	0.54	0.59	4.41	1827	1.26
Spoonbill	Platalea leucorodia	flapping	38.2	1868	0.03	0.04	0.26	0.84	1.04	3.06	808	2.62
Eurasian Eagle Owl	Bubo bubo	flapping	46.3	2288	0.01	0.02	0.10	0.34	0.40	2.30	64058	3.2
Greylag Goose	Anser anser	flapping	45.4	3347	0.19	0.22	0.61	1.42	1.72	4.76	208	4.69
Whooper Swan	Cygnus cygnus	flapping	59.7	9400	0.21	0.24	0.38	0.55	0.63	2.04	1664	13.6
Northern Harrier	Circus cyaneus	soaring	35.7	436.5	0.02	0.03	0.29	0.99	1.20	2.16	442	0.42
Iberian Imperial Eagle	Aquila adalberti	soaring	61	3000	0.09	0.11	0.54	0.93	0.95	3.47	4416	4.2
White Stork	Ciconia ciconia	soaring	57	3245.5	0.08	0.06	0.32	0.89	0.96	12.78	89070	4.54
Common Crane	Grus grus	soaring	57.5	6055	0.08	0.08	0.60	1.90	1.98	4.48	993	8.48
Griffon Vulture	Gyps fulvus	soaring	73.9	9250	0.004	0.004	0.14	0.67	0.74	2.38	1669	12.95

Table 17: Summary of forces by species adjusted to centre around the median. Rows are sorted by flight style and body mass. Expected impact force assumes a collision duration of 2 seconds at a relatively slow flight speed of 2.8m/s (~10kmh), calculated as per formulas 1 & 2 in methods section 2.5. The table is sorted by body mass.

The upper range of forces experienced between species, as measured by the 99th percentile ranged between 0.4g and 1.98g (Table 17). The ANOVA confirmed a significant difference between species ($F(10, 63) = 7.86$, $p = < 0.001$) in the 99th percentile of forces between species but not the maximum force recorded ($F(10, 63) = 0.81$, $p = 0.62$). Analysis with a GLM suggests that the difference in the upper range of forces experienced by the birds was not explained by body mass (Estimate = 0.09, p = 0.676, t = 0.419, DF = 74), or the difference between flight styles (Estimate = 1.954, p = 0.21, t = 1.264, DF = 74). The results suggest significant inter-species variation in the forces experienced by different bird species that is not well explained by the factors tested here. As such our results do not allow guideline values for the trigger threshold to be defined for different species in relation to body mass or flight style.

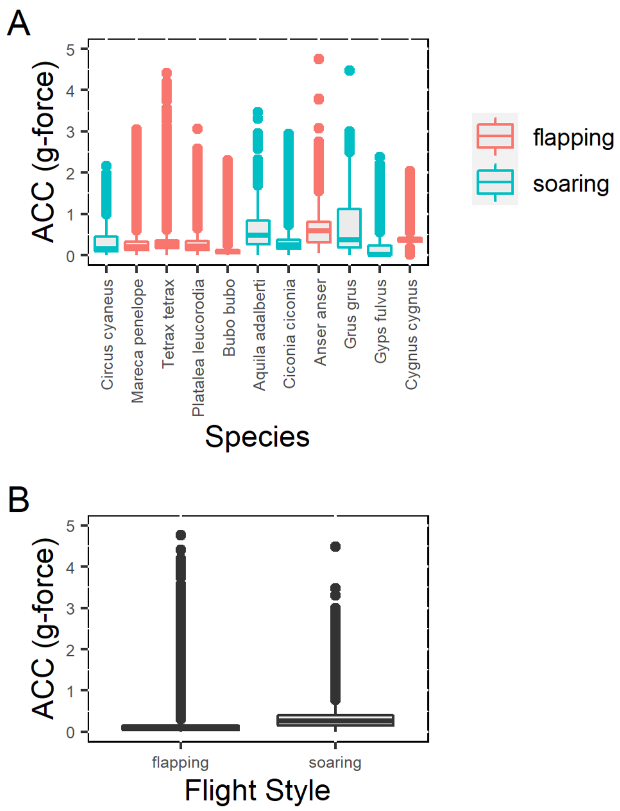

Figure 24: The median-adjusted range of forces recorded by tags on the eleven species for which were able to source accelerometer data via Movebank. A: The distribution of forces experienced by all species, B: Inter-Species differences in forces recorded by the tags, C: A comparison between flapping and soaring species, the x-axis is sorted by body mass.

	Estimate	**Standard Error**	**T Value**	**P-Value**
Mean Forces				
Intercept	0.56	0.02	269.8	<0.001
Log(Body Mass + 1) (g)	$3.38 * 10^{-5}$	0.0002	-208.1	<0.001
Flight Style (soaring	0.23	0.0002	1114.5	<0.001
Observations	16,584,343			
R^2	0.174			
Upper Bound of Forces (99th Percentile)				
Intercept	1.954	1.546	1.264	0.21
Log(Body Mass + 1) (g)	0.09	0.214	0.419	0.676
Flight Style (soaring	1.954	1.546	1.264	0.21
Observations	74			
R^2	0.002			

Table 18: Summary of GLM outputs for understanding interspecies differences; body mass and flight style appear to influence the mean forces recorded by tags mounted on free roaming birds; whereas only flight style was found to significantly influence the upper limit of forces (99th Percentile) recorded by the tags.

5.4.2 RELIABLY OF IMPACT DETECTION UNDER DIFFERENT SETTINGS

A one-way ANOVA revealed there to be significant differences in collision detection rates between acceleration recording ($F(3, 180) = [31.86]$, $p = < 0.001$) with 25Hz performing best (add detail of the others). Furthermore, recording duration (1.5 seconds or 2 seconds) was not found to influence this result. Example collision signatures from the pendulum tests (Figure 25) highlight the tags' ability to record changes in acceleration at very high frequencies. They also highlight that at 10hz the collision signature is much less well defined than at 25hz or above. The collision detection rate was also lower at 10hz when recording for 1.5 seconds (3% of collisions detected) and 2 seconds (16% of collisions detected). While more detail of the collision signatures is visible at higher frequencies, 25hz appears to be sufficient to reliably characterise collision events. Accelerometers recording collisions at 25Hz showed the highest success rate (89% collisions were detected) and recording at 25hz used half of the memory needed compared to recording at 50hz and therefore data transmission is faster (Table 19).

Recording Frequency (hz)	Recording Duration (s)	Sample Size	Collision Detection Rate (%)	Percentage of Expected Records Received from the Tag
10	1.5	32	3.125	100
10	2	32	15.625	96.875
25	1.5	19	89.474	100
25	2	28	60.714	96.429
50	1.5	13	69.231	88.259
50	2	18	77.778	95.0

Table 19: Percentage of collisions detected compared to number of records received and the percentage of tests for which data was received compared to the total number which were performed under different settings during pendulum tests.

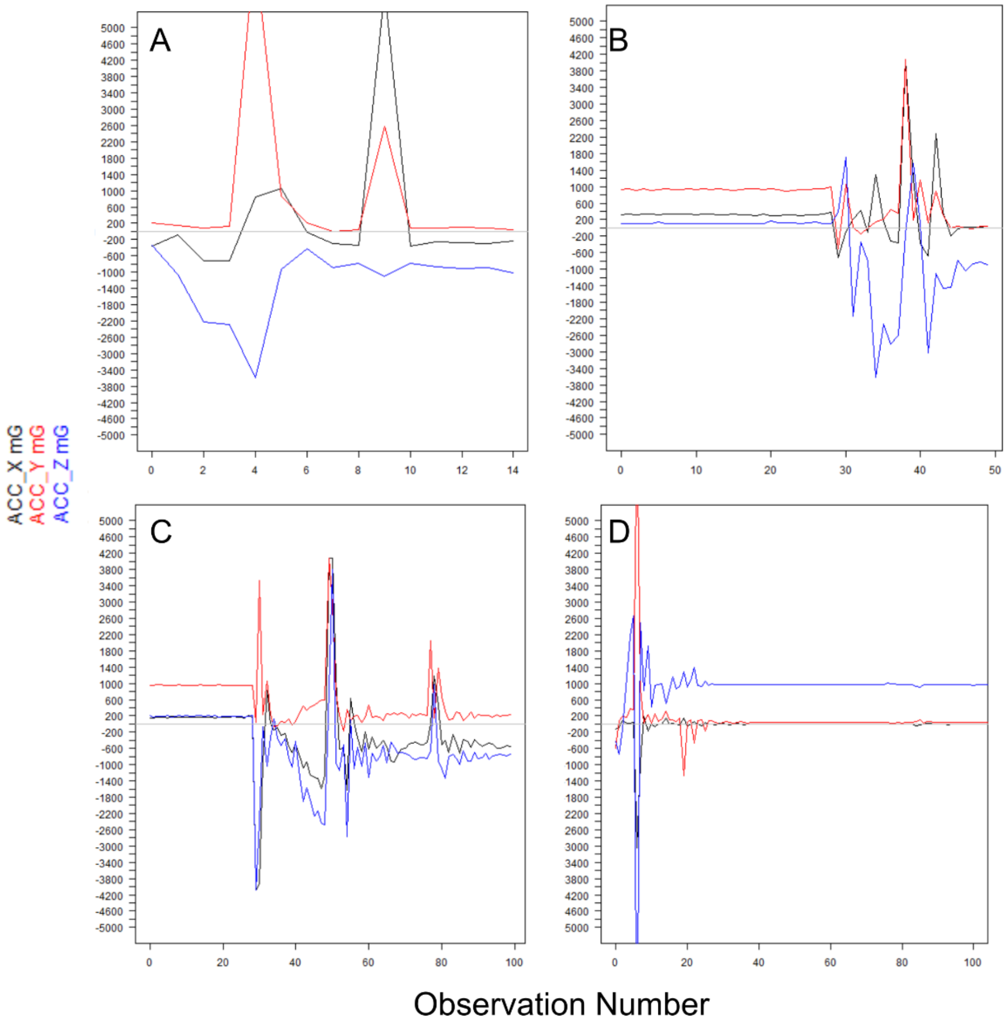

Figure 25: Comparison of collision signatures at 10, 25, 50 and 100hz from pendulum experiments. A. displays the signature recorded at 10hz, B. Displays the signature recorded at 25hz, C. Displays the signature at 50hz and D. Displays the signature at 100hz, the x-axis was limited to 100 observations i.e. 1 second.

5.4.3 HOW MASS INFLUENCES THE MAGNITUDE AND PATTERN OF IMPACT RECORDED BY THE LOGGER

The data from the drop tests suggest that during collision events, the tags record a similar range of forces regardless of the mass involved (0.3kg, 0.5kg, 1kg, 2kg or 4kg) (Figure 26a). There is a strong positive correlation between the mass and the upper bound of forces, represented here by the log of the 99th percentile, recorded by the tag during each collision event (0.85x + 4.90, $p < 0.001$, $R^2 = 0.13$, $F(1{:}62) = 10.33$) (Figure 26b). However, the low R^2 value suggests that mass alone does not explain the observed difference in impact forces. This could be because of how the smaller sandbags sometimes twisted during the drop tests. Thus, part of the tag may have directly collided with the ground rather than the impact being cushioned by the sandbag resulting in the tag perceiving a faster deceleration. Unfortunately, this was not possible to control for.

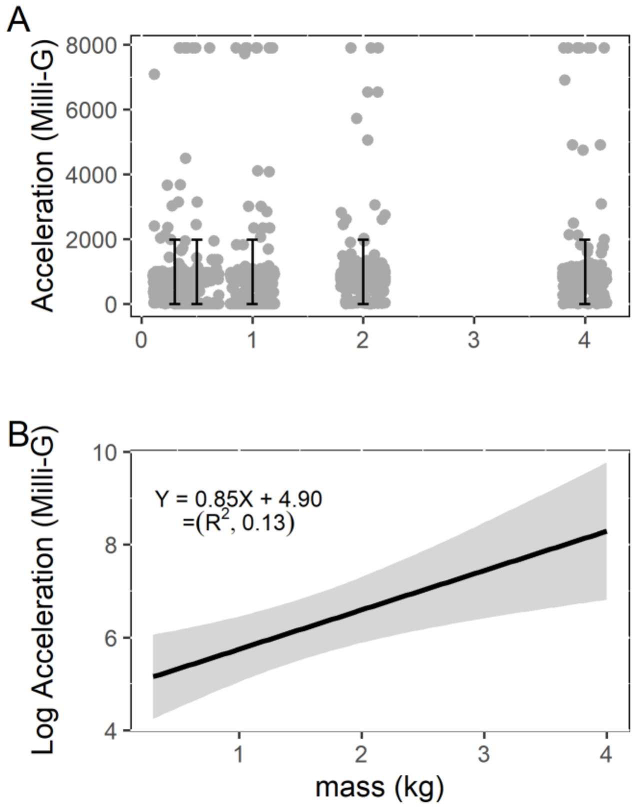

Figure 26: The range of forces observed during drop tests at 25hz using different masses for X (A), Y (B) and Z (C) axes. D displays the range of forces across all three axes for each drop test and E shows the relationship between mass and the 99^{th} percentile of forces observed during the drop tests. Error bars represent the 95% confidence interval around the mean.

As with the drop tests, the zipline tests results confirmed that the tags could reliably detect collisions in birds ranging from 1kg to 4kg. No major differences between masses were found in terms of the proportion of collisions registered by the tags. Approximately 80% of collisions detected at 1kg (n = 10), 90% at 2kg (n = 10) and 80% at 4kg (n = 20). Alongside these tests, a further 10 runs were performed with a 1kg mass starting from only 10m from the collision point, these allowing the devices to reach approximately walking pace speed. None of these “slow” runs were detected at the 3.2G threshold used for the zipline tests meaning that the devices were not activated to collect information. The collision signatures were also broadly similar across masses (Figure 27). The proportion of collisions where the maximum acceleration (8G) was detected was higher for the larger weights (4kg (6/20), 2kg (5/10) and 1kg (2/10)). However, no significant relationship emerged between mass and the forces recorded by the tags during the zipline collision tests.

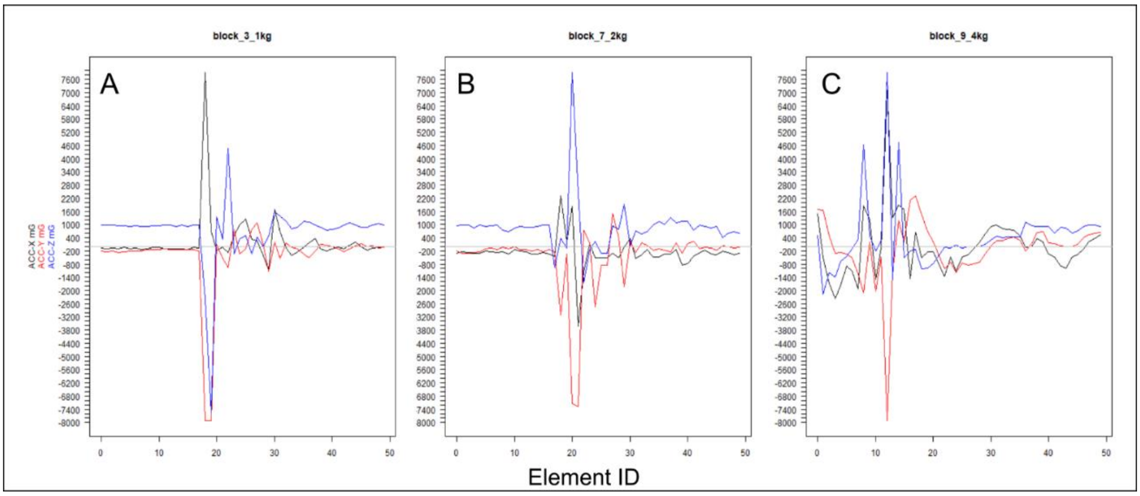

Figure 27: Example collison signatures recorded by the GPS-LoRa tag during zipline tests. A. is from a test performed with a 1kg sand bag, B. is from a test performed with a 2kg sand bag and C. is from a test with a 4kg sand bag.

5.5 DISCUSSION

To our knowledge, this is the first attempt to characterise how bird mounted tracking devices could be used to detect collisions and provide guidance for practitioners in how to use them. Some papers such as (Jiguet *et al.*, 2021) have used GPS tracking and accelerometery to understand the behaviour of a bird in the hours after a near-collision event but not to detect and document the actual event itself. The results of demonstrated how new accelerometer sensors on tracking devices allows us to remotely detect collisions in near real time. This capability could help practitioners better target mitigation to reduce the significant numbers of bird deaths which occur each year due to collision with energy infrastructure (Rioux, Savard and Gerick, 2013; Uddin *et al.*, 2021b). As technology allows us to track more species in this way at reduced costs, it is also important to consider any potential trade-offs between wellbeing of the individual bird and the benefits from the research to the species. Sensitivity to tagging can very significantly between similar species, research by Lameris *et al.* 2018 found that while tagging had a negligible impact on Barnacle Geese *Branta leucopsis*, Brent geese *Branta bernicla* and White-Fronted Geese *Answer albifrons* exhibited changes in behaviour which in turn, resulted in reduced breeding success. Therefore, in the context of collision detection for highlighting mortality from power lines and other human infrastructure, it would not be appropriate or feasible to tag a whole population. Deployment of tags should be targeted in populations where the risk of this type of mortality is thought to be high or in situations where evidence needs to be accumulated to secure mitigation actions at problematic power lines and wind farms.

Until recently, most bird telemetry data studies have focused on collecting bird position and movement data rather than accelerometer data. As such our data on a limited number of tracking data sets representing 11 different species is the first to consider differences in the magnitude of forces different wild bird species experience during normal behaviour. While this is a relatively small number of species, they do span a broad range of sizes (0.4kg – 9.2kg) including both flapping and soaring species enabling us to compare the influences of these variables on accelerometer signatures.

A source of potential bias was that most data sets did not specify the tag manufacturer, and some did not include the GPS locations which precluded the ability to categorise data points as in flight, walking or stationary. As such it was not possible to control for tag type or bird behaviour by excluding measurements associated with the birds being stationary. Although we attempted to account for different tag mounting methods by centring the observations from each species around the median. Tag type is likely to be influential because some tags are limited in terms of the range of forces they can record and tag design can also impact upon the results of accelerometer recording (Kölzsch *et al.*, 2016). There was a weak but significant positive correlation between the bird mass and the mean acceleration measured by the logger (Table 17 & Table 18). The data also suggests that soaring species experience greater extremes of forces during normal behaviour, which was counter to our expectations given that the highest forces recorded for any species (12.78g) was for Little Bustard (Table 18). The tags on the wild birds consistently measured greater G-forces than the expected collision force for some of the smaller species (described in Table 17). This has implications for the trigger threshold settings used to detect collisions because using the theoretical collision force as the trigger threshold could yield potentially thousands of false positives (Table 17). Unlike the mean forces, there was no clear correlation between the upper bound of forces measured by the tags and the body mass of the birds, as such it was not possible to define a rule to determine the correct trigger threshold to use for species of different masses or flight styles. It could also suggest that one single threshold could be used across all species. A possible starting point would be to use a threshold of 4.1g. This is the mean value of the maximum forces recorded across all species during normal behaviour. The exact threshold would depend on the number of false positives which could be tolerated in the dataset and the limitations in terms of data storage (100,000 rows on the miro Nomad GPS-LoRa logger) and data transmission time. This is particularly relevant for migratory species who may be out of range of a LoRaWAN gateway for several months.

The lab-based experiments yielded important information on the reliability of collision detection and the variation in forces recorded under different tag settings. The pendulum tests suggest that the optimum resolution of accelerometer recording for the Lora device used is 25hz (Table 19;Figure 25) as this yielded the highest success rate (100%) in terms of detecting collisions while keeping the data volume to a manageable level. The maximum LoRaWAN data transmission rate is approximately half that of 4G (Mekki *et al.*, 2019), as such the quantity of data accumulated is an important consideration. This is supported by the finding that at 50hz and 100hz, the larger quantities of data recorded during each collision may have prevented the data being recorded or sent through LoRaWAN during a small number of the collision tests (Table 19). This is potentially related to three factors. Firstly, the maximum data transmission speed over LoRa under optimal conditions is 50kbps (kilobits per second) which is approximately 1/2000th the speed of 4G (100 Mbps) (Muteba, Djouani and Olwal, 2019). Secondly, because LoRa is an open-source technology, reliant upon an unlicensed radio frequency (868MHz in Europe); the tags use an adaptive data rate system to ensure the daily maximum air time of 30 seconds advised in the LoRa fair use policy is not exceeded (TTN, 2016). The third factor could be that, when such large volumes of data are recorded it can take time for the device to process and store it ready for transmission. When multiple collisions are repeated within a few minutes of each other, there is a chance that triggering the accelerometer could interrupt the onboard data processing and data may not be correctly committed to the internal memory on the tag. This is unlikely to be a problematic issue in a deployment scenario because collisions or near misses which would trigger acceleration recording would be rare events.

The tags reliably detected collisions in both the drop tests with masses ranging from 300g to 4kg and the zipline tests with masses between 1kg and 4kg. Even with smaller masses involved (300g), the tags consistently recorded large acceleration values during collisions (Figure 26a). As observed in the bird telemetry data, the drop tests revealed a significant positive relationship between the mass and the impact force (Figure 26b). This relationship suggests that where the tags are to be deployed on larger species weighing 3kg or more, a higher threshold could be used to help reduce the frequency of false triggering events. The zipline experiments were more labour intensive than anticipated and we faced delays relating to a firmware update from the tag manufacturer which prevented data from some of the zipline tests being transmitted in a useful format. This resulted in a smaller sample size than planned for each mass used 1kg (n = 10) and 2kg tests (n = 10) compared to the 4kg tests (N = 20) and precluded additional masses being used in the analysis (500g and 8kg). The results highlighted the similarity in the collision signature between masses (Figure 27). At the speeds in the zipline tests (3.65 m/s to 5.95m/s) there was no clear relationship between mass and the G-forces recorded by the tag because max impact forces ranging from 1 – 8 G were recorded. The video footage of the zipline tests suggests that this could be because the larger sandbag (4kg) may have provided a cushioning effect compared to the smaller sandbag (1kg). It could also be an indicator that from the perspective of the tag, it is the velocity of impact and rate of deceleration that is more important than the mass of the bird to which it is attached.

5.6 CONCLUSIONS AND RECOMMENDATIONS

Our results highlight the potential for collisions to be remotely detected in near real time using new accelerometer enabled tracking devices. However, determining the correct trigger threshold to use for detecting collisions in bird tracking studies is considerably more complex than detecting when inanimate objects, which as usually stationary, are moved by earthquakes or landslides (Dini *et al.*, 2021). We found significant interspecies variation however the results arising from the wild bird data was not sufficiently robust to make recommendations about the correct threshold to use for birds of different sizes. One possible reason for this was that due to the lack of information about the body mass of each individual in the data set, a single value for body mass from (Hedenström and Strandberg, 1993) to be applied to each species. This prevented an assessment of whether intraspecies variation in the forces measured by the tags was related to body mass. As such, for real world deployments we would recommend making use of the capability of the miro-NOMAD tags to be remotely programmed. This could work by initially deploying the tags without high frequency acceleration recording activated and allowing time to accumulate "Status" messages from the tag which include low frequency acceleration measurements. Analysis of this data would allow the normal range of forces recorded for that species to be understood and in turn the appropriate trigger threshold to be defined to avoid large volumes of acceleration data from being accumulated. This could then be set remotely before activating the high frequency accelerometer. As these tags are applied to more species, a data set of the appropriate trigger thresholds for detecting collisions in different types of birds could be collated.

The pendulum tests revealed that the optimum frequency of acceleration recording is 25Hz and that the larger volumes of data collected when using higher frequencies (such as 50Hz) can affect the reliability of collision detection. This is likely due to data transmission speed limitations of LoRa. Altering the duration of the accelerometer recording between 1.5 and 2.0 seconds did not significantly alter the detection rate so this will depend on specific considerations for each deployment. Where it would be beneficial to capture the bird falling to the ground post collision a longer recording period of 2-seconds (~50 measurements at 25Hz) or more would be recommended. Whereas if minimising the data quantity involved is a concern, the 1.5 second duration (~37 measurements at 25Hz) could be used. Both the pendulum and zipline tests suggest that a shorter recording time may not reliably capture the whole collision signature (Figure 25; Figure 27). Next steps for this work would be to perform real world trials with the tags using the settings detailed here. Real world deployments of tags with this collision detection capability would likely help validate risk maps such as (Thaxter, Ross-Smith, *et al.*, 2019; Gauld *et al.*, 2022b). Other further work may include pairing these tags with a cloud based alert system which would recognise the collision signature and email the principal investigator of the tracking project to automatically alert them to a collision. This would be of particular interest to researchers investigating illegal persecution of raptors because rapidly identifying mortality events using location information alone is difficult (Sergio *et al.*, 2019).

AVAILABILITY OF DATA AND MATERIALS

Summaries of the data used from studies of wild birds are available to download from here:

https://figshare.com/articles/dataset/Data_for_BIRD_STRIKE_REMOTE_SENSING_OF_BIRD_COLLISIONS_USING_ACCELEROMETER_BASED_EVENT_TRIGGERING/21961352

5.7 REFERENCES

Allaeys, F. et al. (2017) 'Characterization of real and substitute birds through experimental and numerical analysis of momentum, average impact force and residual energy in bird strike on three rigid targets: A flat plate, a wedge and a splitter', International Journal of Impact Engineering, 99, pp. 1–13. Available at: https://doi.org/10.1016/j.ijimpeng.2016.08.009.

Alonso, H. et al. (2019) 'Male post-breeding movements and stopover habitat selection of an endangered short-distance migrant, the Little Bustard Tetrax tetrax', Ibis [Preprint]. Available at: https://doi.org/10.1111/ibi.12706.

Bernardino, J. et al. (2018) 'Bird collisions with power lines: State of the art and priority areas for research', Biological Conservation, 222(March), pp. 1–13. Available at: https://doi.org/10.1016/j.biocon.2018.02.029.

Bidder, O.R. et al. (2012) 'The need for speed : testing acceleration for estimating animal travel rates in terrestrial dead-reckoning systems', Zoology, 115(1), pp. 58–64. Available at: https://doi.org/10.1016/j.zool.2011.09.003.

BSG Ecological Consultants (2011) 'Bsg Technical Review: Bird collisions at onshore wind farms', in. Trondheim. Available at: http://www.bsg-ecology.com/wp-content/uploads/2015/03/Bird-Collisions-and-Wind-Farms.pdf.

Buechley, E.R. et al. (2018) 'Identifying critical migratory bottlenecks and high-use areas for an endangered migratory soaring bird across three continents', Journal of Avian Biology, 49(7), pp. 1–13. Available at: https://doi.org/10.1111/jav.01629.

Dini, B. et al. (2021) 'Development of smart boulders to monitor mass movements via the Internet of Things: A pilot study in Nepal', Earth Surface Dynamics, 9(2), pp. 295–315. Available at: https://doi.org/10.5194/esurf-9-295-2021.

Gauld, J.G. et al. (2022) 'Hotspots in the grid: Avian sensitivity and vulnerability to collision risk from energy infrastructure interactions in Europe and North Africa', Journal of Applied Ecology, (May 2021), pp. 1–17. Available at: https://doi.org/10.1111/1365-2664.14160.

Gómez-Catasús, J. et al. (2021) ‘Factors Affecting Differential Underestimates of Bird Collision Fatalities at Electric Lines: A Case Study in the Canary Islands’, Ardeola, 68(1), pp. 71–94. Available at: https://doi.org/10.13157/arla.68.1.2021.ra5.

Guil, F. et al. (2017) ‘Wildfires as collateral effects of wildlife electrocution: An economic approach to the situation in Spain in recent years’. Available at: https://doi.org/10.1016/j.scitotenv.2017.12.242.

Hadley Wickham et al. (2015) ‘DPLYR’. RStudio. Available at: https://dplyr.tidyverse.org/.

Hedenström, D. and Strandberg, A. (1993) ‘Protocol S1 Supplementary list of flight speeds and biometry of bird species’, Pennycuick Greenewalt Hedenström, 135(1), pp. 1–4.

Huso, M.M.P. and Dalthorp, D. (2014) ‘Accounting for unsearched areas in estimating wind turbine-caused fatality’, Journal of Wildlife Management, 78(2), pp. 347–358. Available at: https://doi.org/10.1002/jwmg.663.

IEA (2020) Onshore Wind: Tracking Report. Paris. Available at: https://www.iea.org/reports/onshore-wind.

Jiguet, F. et al. (2021) ‘GPS tracking data can document wind turbine interactions: Evidence from a GPS-tagged Eurasian curlew’, Forensic Science International: Animals and Environments, 1, p. 100036. Available at: https://doi.org/10.1016/j.fsiae.2021.100036.

Kölzsch, A. et al. (2016) ‘Neckband or backpack? Differences in tag design and their effects on GPS/accelerometer tracking results in large waterbirds’, Animal Biotelemetry, 4(1), p. 13. Available at: https://doi.org/10.1186/s40317-016-0104-9.

LIU, J. et al. (2018) ‘Design of aircraft structures against threat of bird strikes’, Chinese Journal of Aeronautics, 31(7), pp. 1535–1558. Available at: https://doi.org/10.1016/j.cja.2018.05.004.

Lameris, T.K., Müskens, G.J.D.M., Kölzsch, A. *et al.* Effects of harness-attached tracking devices on survival, migration, and reproduction in three species of migratory waterfowl. Anim Biotelemetry 6, 7 (2018). https://doi.org/10.1186/s40317-018-0153-3

Liu, J., Li, Y. and Gao, X. (2014) ‘Bird strike on a flat plate: Experiments and numerical simulations’, International Journal of Impact Engineering, 70, pp. 21–37. Available at: https://doi.org/10.1016/j.ijimpeng.2014.03.006.

Loss, S.R. (2016) ‘Avian interactions with energy infrastructure in the context of other anthropogenic threats’, The Condor, 118(2), pp. 424–432. Available at: https://doi.org/10.1650/CONDOR-16-12.1.

Loss, S.R., Will, T. and Marra, P.P. (2014) ‘Refining estimates of bird collision and electrocution mortality at power lines in the United States’, PLoS ONE, 9(7), pp. 26–28. Available at: https://doi.org/10.1371/journal.pone.0101565.

Lucas, M. De et al. (2012) ‘Griffon vulture mortality at wind farms in southern Spain: Distribution of fatalities and active mitigation measures’, Biological Conservation, 147(1), pp. 184–189. Available at: https://doi.org/10.1016/j.biocon.2011.12.029.

Martin, G.R. and Shaw, J.M. (2010) ‘Bird collisions with power lines: Failing to see the way ahead?’, Biological Conservation, 143, pp. 2695–2702. Available at: https://doi.org/10.1016/j.biocon.2010.07.014.

Mekki, K. et al. (2019) ‘A comparative study of LPWAN technologies for large-scale IoT deployment’, ICT Express, 5(1), pp. 1–7. Available at: https://doi.org/10.1016/j.icte.2017.12.005.

Moreira, F. et al. (2018) ‘Drivers of power line use by white storks: A case study of birds nesting on anthropogenic structures’, Journal of Applied Ecology, 55(5), pp. 2263–2273. Available at: https://doi.org/10.1111/1365-2664.13149.

Movebank (2019) Movebank Data Repository. Available at: https://www.movebank.org/ (Accessed: 1 October 2018).

Muteba, F., Djouani, K. and Olwal, T. (2019) ‘A comparative survey study on LPWA IoT technologies: Design, considerations, challenges and solutions’, Procedia Computer Science, 155, pp. 636–641. Available at: https://doi.org/10.1016/j.procs.2019.08.090.

Oloo, F., Safi, K. and Aryal, J. (2018) ‘Predicting migratory corridors of white storks, ciconia ciconia, to enhance sustainablewind energy planning: A data-driven agent-based model’, Sustainability (Switzerland), 10(5). Available at: https://doi.org/10.3390/su10051470.

Prinsen, H.A.M. et al. (2012) ‘Guidelines on how to avoid or mitigate impact of electricity power grids on migratory birds in the African-Eurasian region.’, CMS Technical Series No. 29, AEWA Technical Series No. 50 , CMS Raptors MOU Technical Series No. 3., 9(UNEP/CMS/Conf.10.30/Rev.2), pp. 1–43. Available at: https://doi.org/10.1111/j.1461-0248.2006.00968.x.

R Core Team (2019) ‘R: A language and environment for statistical computing’. Available at: http://www.r-project.org/.

Rees, E.C. (2012) ‘Impacts of wind farms on swans and geese: A review’, Wildfowl, 62, pp. 37–72.

Ren, L. et al. (2018) ‘Enabling resilient distributed power sharing in networked microgrids through software defined networking’, Applied Energy, 210, pp. 1251–1265. Available at: https://doi.org/10.1016/j.apenergy.2017.06.006.

Rioux, S., Savard, J.-P.L. and Gerick, A.A. (2013) ‘Avian mortalities due to transmission line collisions: a review of current estimates and field methods with an emphasis on applications to the Canadian electric network Mortalité aviaire attribuable aux collisions avec les lignes de transport d ’ électri’, Avian Conservation and Ecology, 8(2). Available at: http://www.ace-eco.org/vol8/iss2/art7/.

Rotics, S. et al. (2016) ‘The challenges of the first migration: Movement and behaviour of juvenile vs. adult white storks with insights regarding juvenile mortality’, Journal of Animal Ecology [Preprint], (June). Available at: https://doi.org/10.1111/1365-2656.12525.

Schutgens, M., Shaw, J.M. and Ryan, P.G. (2014) ‘Estimating scavenger and search bias for collision fatality surveys of large birds on power lines in the Karoo, South Africa’, Ostrich, 85(1), pp. 39–45. Available at: https://doi.org/10.2989/00306525.2014.888691.

Sergio, F. et al. (2018) ‘Reliable methods for identifying animal deaths in GPS- and satellite-tracking data: Review, testing, and calibration’, Journal of Applied Ecology [Preprint], (November). Available at: https://doi.org/10.1111/1365-2664.13294.

Sergio, F. et al. (2019) ‘Reliable methods for identifying animal deaths in GPS- and satellite-tracking data: Review, testing, and calibration’, Journal of Applied Ecology, 56(3), pp. 562–572. Available at: https://doi.org/10.1111/1365-2664.13294.

Silva, J.P. et al. (2010) ‘Estimating the influence of overhead transmission power lines and landscape context on the density of little bustard Tetrax tetrax breeding populations’, Ecological Modelling, 221(16), pp. 1954–1963. Available at: https://doi.org/10.1016/j.ecolmodel.2010.03.027.

SNH (2010) Use of avoidance rates in the SNH wind farm collision risk model., SNH Avoidance Rate Information & Guidance Note. Available at:

http://scholar.google.com/scholar?hl=en&btnG=Search&q=intitle:Use+of+Avoidance+Rates+in+the+SNH+Wind+Farm+Collision+Risk+Model#1.

Thaxter, C.B. et al. (2017) ‘Bird and bat species ’ global vulnerability to collision mortality at wind farms revealed through a trait-based assessment’.

Thaxter, C.B., Ross-Smith, V.H., et al. (2019) ‘ Avian vulnerability to wind farm collision through the year: Insights from lesser black-backed gulls (Larus fuscus) tracked from multiple breeding colonies ’, Journal of Applied Ecology, (July), pp. 1–13. Available at: https://doi.org/10.1111/1365-2664.13488.

Thaxter, C.B., Ross-Smith, V.H., et al. (2019) ‘Avian vulnerability to wind farm collision through the year: Insights from lesser black-backed gulls (Larus fuscus) tracked from multiple breeding colonies’, Journal of Applied Ecology, 56(11), pp. 2410–2422. Available at: https://doi.org/10.1111/1365-2664.13488.

TTN (2016) The Things Network Fair Usage Policy. Available at: https://www.thethingsnetwork.org/forum/t/fair-use-policy-explained/1300 (Accessed: 23 September 2022).

Uddin, M. et al. (2021) ‘High bird mortality due to power lines invokes urgent environmental mitigation in a tropical desert’, Biological Conservation, 261(January), p. 109262. Available at: https://doi.org/10.1016/j.biocon.2021.109262.

UK Research and Innovation (2016) Long range wireless devices for high-resolution monitoring of animal movement. Available at: https://gtr.ukri.org/projects?ref=NE%2FP003907%2F1 (Accessed: 26 September 2019).

Vanermen, N. et al. (2015) ‘Seabird avoidance and attraction at an offshore wind farm in the Belgian part of the North Sea’, Hydrobiologia, 756(1), pp. 51–61. Available at: https://doi.org/10.1007/s10750-014-2088-x.

Whitfield, D.P. and Fielding, A.H. (2017) Analyses of the fates of satellite tracked golden eagles in Scotland. Edinburgh, UK. Available at: http://www.snh.org.uk/pdfs/publications/commissioned_reports/982.pdf.

Wickham, H. (2016) ‘ggplot2: Elegant Graphics for Data Analysis in R’.

DATA REFERENCES

Atkinson, P.W. (2016) Greylag Goose – *Anser anser* Belfast available on request from www.movebank.org, study ID 118192126

Carrapato, C. (2014) Iberian Imperial Eagle Movement Ecology 2014 – 2015, available on request from www.movebank.org, study ID 28407489

Champagnon, J. (2016) Eurasian Spoonbill – Tour du Valat, available on request from www.movebank.org, study ID 311803430

Janssen, J. (2010) Eagle Owls – 3 Breeding Pairs – Southern Part of the Netherlands, available on request from www.movebank.org, study ID 4502577

Fiedler, W. (2016) Whooper Swans in Latvia 2016, available on request from www.movebank.org, study ID 18259847

Fiedler, W. (2016) Lifetrack Griffon Vulture Croatia, available on request from www.movebank.org, study ID 154820583

Franco, A.M. A. & Acacio, M.S. (2018) White Stork Adults 2018, available on request from www.movebank.org, study ID 451464940

Overton, C. T., Casazza, M., Hull, J. and Skalos, S. (2018) Northern Harrier Breeding, Fledging, Wintering, available on request from www.movebank.org, study ID 884046948

Silva, J. P. (2018) Little Bustard Movement Ecology 2018 – 2019, available on request from www.movebank.org, study ID 461568973

Van Toor, M. and Waldenstrom, J. (2018) Eurasian Wigeons Spring 2018, available on request from www.movebank.org, study ID 412700082

Zydelis, R. and Dagys, M. (2013) Common Crane Lithuania 2015 – 2016, available on request from www.movebank.org, study ID 146932094

CHAPTER 6: GENERAL CONCLUSIONS

Photo 9: A wind farm in southern spain, near Cadiz, where blades have been painted black on some turbines to increase contrast and visibility for birds (October 2021).

Photo 10: A transmission powerline in Alentejo, north of Castro Verde where storks nest within the pylons (June 2021).

6.1 KEY FINDINGS

6.1.1 CHAPTER 2: USING GPS TRACKING DATA TO MAP SENSITIVITY AND VULNERABILITY TO MORTALITY RISKS FROM ENERGY INFRASTRUCTURE

This chapter demonstrated how tracking data could be used to describe where and when individual birds representing 27 different species from across the Afro-palearctic flyways in Europe and North Africa were most sensitive to collision with wind farms and power lines. For areas with sufficient tracking data within Europe and North Africa, 13.6% of the area was classified as high sensitivity to wind turbines and 9.4% was classified as high sensitivity to transmission power lines. The highest sensitivity areas were concentrated within important migratory corridors and along coastlines where the construction of new wind turbines and power lines would likely increase the mortality risk to birds. For example, either side of the Strait of Gibraltar in Southern Spain and Northern Morocco (Figure 28).

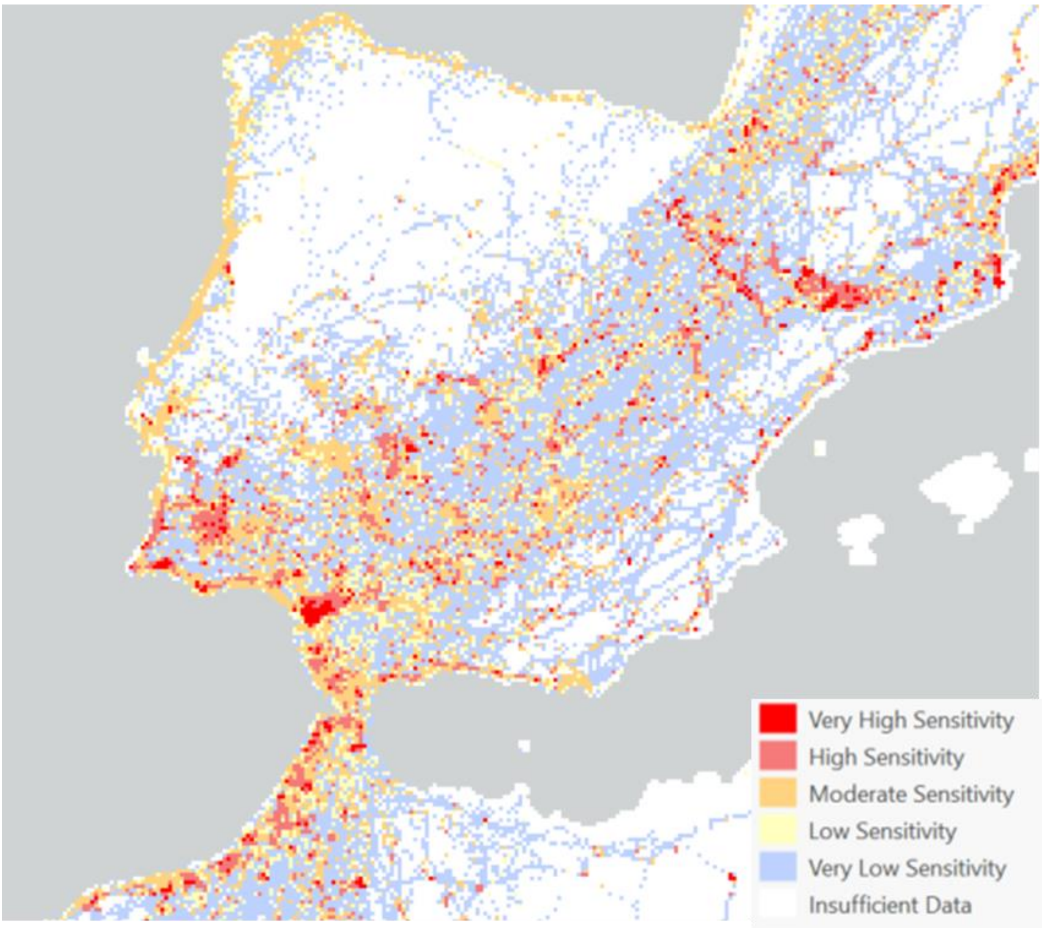

Figure 28: Sensitivity to colision risks in Iberia.

Overlaying the sensitivity surface with the available data on the known locations of wind farms and transmission power lines highlighted where conflicts exist between the birds in the tracking data and renewable energy infrastructure. For example, there has been extensive development of wind energy around the Strait of Gibraltar (Figure 29) where large numbers of vultures and other soaring birds has been documented (de Lucas *et al.*, 2012). Targeted deploying of mitigation, such as shutdown systems, marking power lines and painting wind turbine blades to increase their visibility to birds could have pan-flyway benefits to bird populations in Europe (Barrientos *et al.*, 2011; May, Nygård, Falkdalen, Åström, Hamre and Bård G Stokke, 2020; Ferrer *et al.*, 2022).

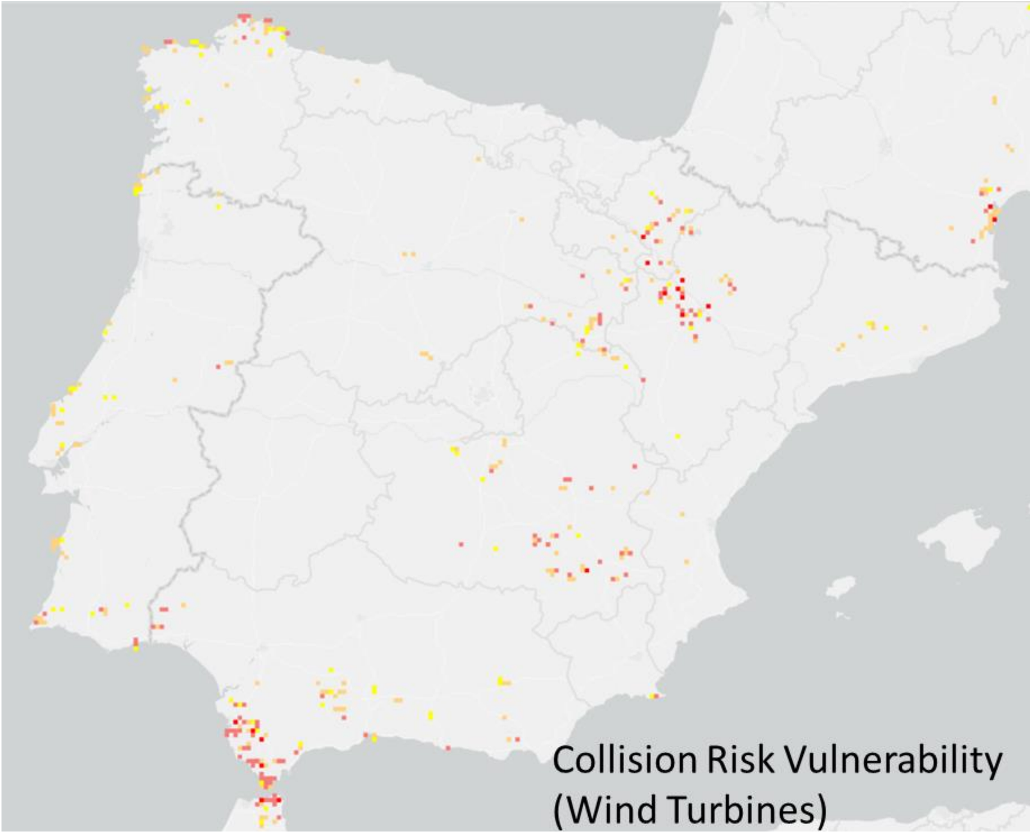

Figure 29: Vulnerability to collision risk associated with wind turbines in Iberia.

Although this analysis was restricted to the estimating sensitivity and vulnerability to collision risks for areas with sufficient tracking data it provided useful information about where the potential conflicts with renewable energy infrastructure exist and where they could arise. As more datasets are added to Movebank, it would be relatively simple to apply the assessment method to identify collision risk hotspots for other species. This study also highlighted how the lack of reliable information about the location of wind turbines and power lines, particularly medium voltage power lines (<60Kv), could inhibit conservation action to reduce collison risks.

6.1.2 CHAPTER 3: PREDICTIVE MODELLING OF BIRD SENSITIVITY TO WIND FARMS AND POWER LINES

This chapter built on the work of chapter two and results presented in other studies which identified a strong influence of thermal uplift, orographic uplift, terrain and landcover upon the flight height for a variety of bird species (Santos *et al.*, 2017; Oloo, Safi and Aryal, 2018; Scacco *et al.*, 2019; Hanssen, May and Nygård, 2020). Using a binomial GLMM model to relate presence in flight at danger height to these factors we were able to predict the likely presence in flight at danger height across the breeding range of White Stork *Ciconia ciconia* and Little Bustard *tetrax tetrax*.

The differences in how likely the two species respond to environmental factors in terms of likelihood of flying within the danger height bands is likely due to be due to the different flight behaviour. Storks, a soaring bird, tends to fly at higher altitudes than the flapping Bustard) which tends to fly close to the ground. The consequence of this is that when uplift conditions are strong, the likelihood of flying at danger height decreased with stronger uplift because it allows them to gain height pushing them out of the danger height band. For Little Bustard, the effect of terrain and weather conditions such as precipitation were more important predictors. Both species exhibited seasonal differences in flight behaviour and for White Storks landcover was a significant factor, with "Built Area" increasing the likelihood of the birds flying at danger height.

The sensitivity maps produced as a result of the analysis in this study help provide the high-level spatial information required for developers to avoid further energy infrastructure development in the most sensitive areas for these species, representing <3% of the study area. This information can also be used to target further survey and analysis at a local level to mitigate existing conflicts between energy infrastructure and birds such as at the high-risk sections of power line identified in Figure 14, chapter three. Given sufficient computing time and access to population density estimates for the non-breeding season, it would be possible to produce annual sensitivity maps across multiple years, which in turn could provide a multiyear average of sensitivity to collision risks within each grid cell for each season.

The main benefit of the approach outlined in this study, is likely to be for identifying collision risk sensitivity hotspots for large, soaring bird species which tend to fly at higher altitudes the majority of the time (Katzner *et al.*, 2012). As highlighted by our analysis for White Storks, the areas where they are likely to fly at heights where they risk collision with energy infrastructure are relatively localised (Figure 12). The predictive power of our model was quite poor (AUC ~ 0.6) for Little Bustard indicating that this approach is less useful for flapping species. For species which tend to fly at or below the danger height for collision the majority of the time, a resource selection modelling approach as outlined by Silva *et al.* 2014. which could incorporate other data sources such as citizen science species observations could be sufficient to help understand where and when birds are most sensitive to potential collision risks. The next steps for this work would be to apply this method to predicting presence in flight at danger height for other seasons and other soaring species such as the critically endangered Egyptian Vulture *Neophron percnopterus* (Oppel *et al.*, 2021a).

Photo 11: Griffon vultures observed during the October 2021 field work with the LoRa tags (Photo credit, J. Gauld 2021).

6.1.3 CHAPTERS 4 AND 5: THE ROLE OF NEW TRACKING TECHNOLOGIES IN ASSESSING COLLISION RISKS

The results of the work in these two chapters highlight the potential utility of an emerging GNSS (Global Navigation Satellite System) tracking technology which utilises LoRa to transmit the data recorded by the satellite logger over long distances (up to 53.4km). One of the key advantages of LoRa over equivalent devices which send data via GSM or satellite link is the low energy consumption used during data transmission (Mekki *et al.*, 2019). This allows for smaller batteries and solar panels to maintain high frequency GNSS position sampling. In turn this permits flexibility to deploy loggers on species ranging in size from Kestrels up to Griffon Vultures. LoRa is an open source technology, affording users the flexibility to either set up their own private network using a LORIOT (LORIOT, 2021) and deploying their own LoRaWAN gateway systems to receive the data. Or, depending on coverage, devices can be registered on the Things Network allowing the tags to send data via a growing number of publicly accessible ‘open’ LoRaWAN gateways (Muteba, Djouani and Olwal, 2019; TTN, 2021). So, while there can be high initial set up costs if new LoRa gateway systems, unlike systems which use a GSM subscription for each individual tag, there are minimal ongoing data costs associated with deploying new tracking devices. The trial deployment of six GPS-LoRa logger on vultures in October 2021 showed that these tags can be used to study the movements of a wide-ranging species. Work at UEA is ongoing to refine a smaller format <5g LoRa logger currently being used to track Common Kestrels *Falco tinicullus* and Lesser Kestrels *Falco naumanni* (Photo 12). Data gaps and a bias toward tracking larger species such as White Stork *Ciconia ciconia* in the currently available tracking data were highlighted in chapter two as a limitation for mapping sensitivity to collision risks(Movebank, 2019). By allowing a greater range of species to be tracked with high resolution GNSS, including altitude, these devices have the potential to contribute to addressing these gaps in the existing tracking data. Although this opens up another ethical consideration about what proportion of each population should be tracked and whether the benefits of the research outweigh the potential effects on the tracked individuals. Some species such as White Stork *Ciconia ciconia* seem to be fairly tolerant of GPS tracking whereas others like Barnacle Goose *Branta leucopsis* exhibit signs of discomfort and reduced breeding success Lameris *et al.* 2018.

Photo 12: Prototype kestrel GPS-LoRa tracking device deployed on a Lesser Kestrel Falco naumanni near Castro verde, Portugal in May 2021. This design was refined as a direct result of this trial deployment. (Photo credit, J. Gauld 2021).

The lab tests with these devices demonstrated their potential to reliably detect collision events remotely using the onboard accelerometer. The lab tests confirmed that the optimal frequency for detecting collisions for the LoRa devices was 25Hz. No clear guidance emerged from this work regarding the optimal force threshold to use to trigger the device to start recording high intensity acceleration measurements. This ability to detect collisions can help ground truth vulnerability to collision risk estimates by building up a picture of where birds collide with wind turbines and power lines, it could also be applied to studies of illegal hunting. Remotely inference of the cause of mortality, without requiring physical inspection of the carcass to confirm collisions the cause of death would be advantageous. Firstly it would avoid the bias associated with variable carcass disappearance rates in different locations (Schutgens, Shaw and Ryan, 2014) and allow detection of mortality in less accessible locations where it may not be possible to recover the device.

6.1.4 RECOMMENDATIONS FOR THE DEPLOYMENT OF LORA-GPS TRACKERS

Helping develop and test these GPS-LoRa tracking devices has been an enjoyable component of my PhD project. During this work I have acquired knowledge which could help inform future deployments of these devices for monitoring the movement behaviour of birds and other animals.

Data transmission over LoRa is very energy efficient, as discussed in chapter 4. It achieves this efficiency by using relatively slow data transfer speeds (<50kbps) which is approximately one third the speed of the 3G GSM bandwidths typically used by GPS-GSM loggers. This data rate can be slower depending on various factors such as distance from the nearest gateway. Data transmission speed is therefore likely to be more of a constraint on data rates than the quantity of data the tag is programmed to collect each day. It is important when deploying these tags to consider the behaviour of the study species and how often it is likely to be within transmission range of the available LoRa gateways. The tags can be remotely programmed, so it is advisable to initially deploy the tags with a conservative data rate which can then be varied after deployment depending on how often the deployed is in contact with the gateway. It may also be desirable to collect location data at higher frequency during the breeding season when the device is regularly in contact with the gateway and then implement a more conservative data rate for the non-breeding season.

For resident species, this is less problematic as they are likely to remain within gateway range for the majority of the time. Whereas for high site fidelity migrants such as White

Storks or Seabirds, it could be advantageous to deploy a LoRa gateway at the breeding colony to receive data when the birds return to the breeding grounds. Over a period of 6 months on a half hourly cycle the devices would record approximately 8600 locations. The devices can store up to 100,000 payloads so could potentially store multiple years' worth of data.

The same conservative approach to collection of accelerometer data is also advisable. In chapter four we advise that initially the devices should be deployed either with the accelerometer switched off or with a conservatively high trigger threshold to prevent large volumes of data accumulating in the device memory. For example, during the trial deployment of these devices on Griffon vultures, accelerometer triggering was active on four devices. It appears that the trigger threshold of 3.2g may have been too low because on at least two devices appeared to continuously collect high resolution accelerometery data. Once behaviour of the animal and range of acceleration values experienced by the logger collected as part of the tag "status" payloads is understood then accelerometer settings can be remotely changed accordingly.

As part of my PhD work, I designed and assembled three lower cost solar powered LoRa gateway systems. To enable other researchers to do this, the parts list and approximate price of components used to assemble them are described here in a Figshare folder along with a set up guide to aid programming the gateway and registering it on LORIOT: https://tinyurl.com/diygatewaysystem

6.2 CONCLUDING REMARKS

Resolving the dual crises of biodiversity loss and climate change requires swift action to protect ecosystems and transition away from fossil fuels (IPBES, 2019; IPCC, 2022c). The expansion of renewable energy infrastructure required to mitigate climate change poses a potential threat to bird populations, however, in the context of collision risks, this does not need to be the case. There is flexibility in where new wind farms and power lines are constructed as highlighted by (Ryberg *et al.*, 2019) who estimated that within Europe there is approximately 17 times the potential capacity for onshore wind energy generation than is needed to achieve European Union targets for renewable energy capacity by 2050. This means that the most sensitive areas for birds can be avoided while supporting a rapid transition toward a zero-carbon energy system. There is also a growing understanding of how to mitigate collision risk through measures such as line marking and automated shutdown of turbines (BirdLife International, 2015b).

The work in this thesis highlights the potential for data from emerging tracking technologies to inform the siting of wind farms and power lines through sensitivity mapping, identify potential conflict areas where mitigation should be prioritised and validate collision risk maps using accelerometery to remotely sense when and where collisions occur. Going forward key conservation priorities and future work arising from this include:

- Expanding sensitivity to collision risk mapping to more species and regions to provide the high-level spatial information needed to guide decisions about where to construct large infrastructure projects such as wind farms. Of particular importance are regions like South America where significant investment in renewable energy infrastructure is underway but the potential impacts are poorly understood (Aswal *et al.*, 2022).

- Building partnerships with energy companies and governments to create more accessible and accurate spatial data sets for energy infrastructure so we can more accurately assess where these infrastructures intersect with areas of high sensitivity to collision risk for birds to help target mitigation of collision risks.
- Improving the availability of tracking data through sharing platforms such as (Movebank, 2019) and work collaboratively to utilise new, low cost, light weight tracking technologies to increase the number and diversity of birds tracked with high resolution GNSS/GPS. Some refer to this as the "Internet of Animals" (Wild *et al.*, 2022).

Photo 13: Griffon vultures flying safely through a wind farm in Portugal after the blades were stopped until the birds passed through the wind farm. There are other wind farms in the area which do not operate shutdown systems where the risks to vultures during the Autumn migration are high (Photo credit, J. Gauld 2021).

6.3 REFERENCES

Aswal, D.K. et al. (2022) ‘Power lines and birds: An overlooked threat in South America’, Perspectives in Ecology and Conservation, In Press, pp. 1–11. Available at: https://doi.org/10.1016/j.pecon.2022.10.005.

Barrientos, R. et al. (2011) ‘Meta-Analysis of the Effectiveness of Marked Wire in Reducing Avian Collisions with Power Lines’, Conservation Biology, 25(5), pp. 893–903. Available at: https://doi.org/10.1111/j.1523-1739.2011.01699.x.

BirdLife International (2015) ‘Review and guidance on use of “shutdown-on-demand” for wind turbines to conserve migration soaring birds in the Rift Valley/Red Sea Flyway’, Regional Flyway Facility. Amman, Jordan., p. 49. Available at: http://migratorysoaringbirds.undp.birdlife.org/sites/default/files/msb_guidance_shutdown_on_demand.pdf.

Ferrer, M. et al. (2022) ‘Significant decline of Griffon Vulture collision mortality in wind farms during 13-year of a selective turbine stopping protocol’, Global Ecology and Conservation, 38(June), p. e02203. Available at: https://doi.org/10.1016/j.gecco.2022.e02203.

Hanssen, F., May, R. and Nygård, T. (2020) ‘High-Resolution Modeling of Uplift Landscapes can Inform Micrositing of Wind Turbines for Soaring Raptors’, Environmental Management, 66(3), pp. 319–332. Available at: https://doi.org/10.1007/s00267-020-01318-0.

IPBES (2019) The global assessment report on Biodiversity and Ecosystems. Edited by E.S. Brondízio, J. Settele, and N. H., T. Bonn, Germany: IPBES secretariat. Available at: https://zenodo.org/record/6417333#.Y8niUBXP02w.

IPCC (2022) Summary for Policymakers. In: Climate Change 2022: Mitigation of Climate Change. Contribution of Working Group III to the Sixth Assessment Report of the Intergovernmental Panel on Climate Change, Cambridge University Press. Cambridge, UK. Available at: https://www.ipcc.ch/report/ar6/wg3/about/how-to-cite-this-report.

Katzner, T.E. et al. (2012) ‘Topography drives migratory flight altitude of golden eagles: Implications for on-shore wind energy development’, Journal of Applied Ecology, 49(5), pp. 1178–1186. Available at: https://doi.org/10.1111/j.1365-2664.2012.02185.x.

LORIOT (2021) LORIOT Internet of Things LoRaWAN Server. Available at: https://www.loriot.io/.

de Lucas, M. et al. (2012) ‘Griffon vulture mortality at wind farms in southern Spain: Distribution of fatalities and active mitigation measures’, Biological Conservation, 147(1), pp. 184–189. Available at: https://doi.org/10.1016/j.biocon.2011.12.029.

May, R. et al. (2020) ‘Paint it black: Efficacy of increased wind turbine rotor blade visibility to reduce avian fatalities’, Ecology and Evolution, 00(February), pp. 1–9. Available at: https://doi.org/10.1002/ece3.6592.

Mekki, K. et al. (2019) ‘A comparative study of LPWAN technologies for large-scale IoT deployment’, ICT Express, 5(1), pp. 1–7. Available at: https://doi.org/10.1016/j.icte.2017.12.005.

Movebank (2019) Movebank Data Repository. Available at: https://www.movebank.org/ (Accessed: 1 October 2018).

Muteba, F., Djouani, K. and Olwal, T. (2019) ‘A comparative survey study on LPWA IoT technologies: Design, considerations, challenges and solutions’, Procedia Computer Science, 155, pp. 636–641. Available at: https://doi.org/10.1016/j.procs.2019.08.090.

Oloo, F., Safi, K. and Aryal, J. (2018) ‘Predicting migratory corridors of white storks, ciconia ciconia, to enhance sustainablewind energy planning: A data-driven agent-based model’, Sustainability (Switzerland), 10(5). Available at: https://doi.org/10.3390/su10051470.

Oppel, S. et al. (2021) ‘Major threats to a migratory raptor vary geographically along the eastern Mediterranean flyway’, Biological Conservation, 262(August 2020). Available at: https://doi.org/10.1016/j.biocon.2021.109277.

Ryberg, D.S. et al. (2019) ‘The future of European onshore wind energy potential: Detailed distribution and simulation of advanced turbine designs’, Energy, 182, pp. 1222–1238. Available at: https://doi.org/10.1016/j.energy.2019.06.052.

Santos, C.D. et al. (2017) ‘Match between soaring modes of black kites and the fine-scale distribution of updrafts’, Scientific Reports, 7(1), pp. 1–10. Available at: https://doi.org/10.1038/s41598-017-05319-8.

Scacco, M. et al. (2019) ‘Static landscape features predict uplift locations for soaring birds across Europe’, Royal Society Open Science, 6(1), pp. 1–12. Available at: https://doi.org/10.1098/rsos.181440.

Schutgens, M., Shaw, J.M. and Ryan, P.G. (2014) ‘Estimating scavenger and search bias for collision fatality surveys of large birds on power lines in the Karoo, South Africa’, Ostrich, 85(1), pp. 39–45. Available at: https://doi.org/10.2989/00306525.2014.888691.

TTN (2021) The Things Network LoRaWAN Server. Available at: https://www.thethingsnetwork.org/ (Accessed: 5 June 2021).

Wild, T.A. et al. (2022) ‘Internet on animals: Wi-Fi-enabled devices provide a solution for big data transmission in biologging’, Methods in Ecology and Evolution, 2022(August 2021), pp. 1–16. Available at: https://doi.org/10.1111/2041-210X.13798.

Photo 14:A Griffon Vultures flying through a wind farm and over a medium tension power lines as is comes in to roost with the rest of the flock in a field near Vila do Bispo, Algarve, Southwest Portugal (Photo credit, J. Gauld 2021).

BIBLIOGRAPHY

2009/147/EC, C.D. (2010) ‘Directive 2009/147/EC of the European Parliament and of the Council on the conservation of wild birds’, *Official Journal of the European Union*, L 20, pp. 7–25. Available at: https://doi.org/10.1126/science.aah3404.

Acácio, M. *et al.* (2021) *Quantifying the performance of a solar GPS/GPRS tracking device: fix interval, but not deployment on birds, decreases accuracy and precision*. University of East Anglia.

Acácio, M., Atkinson, P.W., *et al.* (2022) ‘Performance of GPS/GPRS tracking devices improves with increased fix interval and is not affected by animal deployment’, *Plos One*, 17(3), p. e0265541. Available at: https://doi.org/10.1371/journal.pone.0265541.

Acácio, M., Catry, I., *et al.* (2022) ‘Timing is critical: consequences of asynchronous migration for the performance and destination of a long-distance migrant’, *Movement Ecology*, 10(1), pp. 1–16. Available at: https://doi.org/10.1186/s40462-022-00328-3.

Agudelo, M.S. *et al.* (2021) ‘Post-construction bird and bat fatality monitoring studies at wind energy projects in Latin America: A summary and review’, *Heliyon*, 7(6), p. e07251. Available at: https://doi.org/10.1016/j.heliyon.2021.e07251.

Ainsworth, D., Collins, T. and D’Amico, F. (2022) ‘Convention on Biological Diversity COP15: Nations Adopt Four Goals, 23 Targets for 2030 In Landmark UN Biodiversity Agreement’, in. Montreal, Canada: United Nations. Available at: https://prod.drupal.www.infra.cbd.int/sites/default/files/2022-12/221219-CBD-PressRelease-COP15-Final_0.pdf.

Alerstam, T. *et al.* (2007) ‘Flight Speeds among Bird Species: Allometric and Phylogenetic Effects’, *PLoS biology*, 5(8), p. e197. Available at: https://doi.org/10.1371/journal.pbio.0050197.

Allaeys, F. *et al.* (2017) ‘Characterization of real and substitute birds through experimental and numerical analysis of momentum, average impact force and residual energy in bird strike on three rigid targets: A flat plate, a wedge and a splitter’, *International Journal of Impact Engineering*, 99, pp. 1–13. Available at: https://doi.org/10.1016/j.ijimpeng.2016.08.009.

Alonso, H. *et al.* (2019) ‘Male Post-Breeding Movements and Stopover Habitat Selection of an Endangered Short-Distance Migrant, the Little Bustard Tetrax tetrax’, *Ibis*, 162, pp. 202–216. Available at: https://doi.org/10.1111/ibi.12706.

Alonso, J.C., Alonso, J.A. and Mufioz-Pulido, R. (1994) *Mitigation of Bird Collisions with*

Transmission Lines through Groundwire Marking, *Biological Conservation*.

Amico, M.D. *et al.* (2019) ‘Bird collisions with power lines : Prioritizing species and areas by estimating potential population - level impacts’, (December 2018), pp. 1–8. Available at: https://doi.org/10.1111/ddi.12903.

Angelov, I., Hashim, I. and Oppel, S. (2013) ‘Persistent electrocution mortality of Egyptian Vultures Neophron percnopterus over 28 years in East Africa’, *Bird Conservation International*, 23(1), pp. 1–6. Available at: https://doi.org/10.1017/S0959270912000123.

Application, I. and Singh, R.K. (2020) ‘Energy Consumption Analysis of LPWAN Technologies and Lifetime Estimation for’. Available at: https://doi.org/10.3390/s20174794.

Arnett, E.B. and May, R.F. (2016) ‘Mitigating wind energy impacts on wildlife: Approaches for multiple taxa’, *Human-Wildlife Interactions*, 10(1), pp. 28–41. Available at: https://doi.org/10.26077/1jeg-7r13.

Astiaso Garcia, D. *et al.* (2015) ‘Analysis of wind farm effects on the surrounding environment : Assessing population trends of breeding passerines’, *Renewable Energy*, 80, pp. 190–196. Available at: https://doi.org/10.1016/j.renene.2015.02.004.

Aswal, D.K. *et al.* (2022) ‘Power lines and birds: An overlooked threat in South America’, *Perspectives in Ecology and Conservation*, In Press, pp. 1–11. Available at: https://doi.org/10.1016/j.pecon.2022.10.005.

Band, B. (2012) ‘Using a collision risk model to assess bird collision risks for offshore windfarms’, 02(March), p. 62. Available at: https://www.bto.org/sites/default/files/u28/downloads/Projects/Final_Report_SOSS02_Band1ModelGuidance.pdf.

Barn Owl Trust (2015) *Barn Owl Hazards: Electrocution and Wires*. Available at: https://www.barnowltrust.org.uk/hazards-solutions/electrocution-wires-barn-owls/ (Accessed: 1 March 2019).

Barrientos, R. *et al.* (2011) ‘Meta-Analysis of the Effectiveness of Marked Wire in Reducing Avian Collisions with Power Lines’, *Conservation Biology*, 25(5), pp. 893–903. Available at: https://doi.org/10.1111/j.1523-1739.2011.01699.x.

Barrios, L. and Rodríguez, A. (2004) ‘Behavioural and environmental correlates of soaring-bird mortality at on-shore wind turbines’, *Journal of Applied Ecology*, 41(1), pp. 72–81. Available at: https://doi.org/10.1111/j.1365-2664.2004.00876.x.

Bassi, E. *et al.* (2002) ‘Eagle Owl Bubo bubo and power line interactions in the Italian Alps’, *Bird Conservation International*, 11(04), pp. 319–324. Available at: https://doi.org/10.1017/s0959270901000363.

Beardsworth, C.E. *et al.* (2022) ‘Validating ATLAS: A regional-scale high-throughput tracking system’, *Methods in Ecology and Evolution*, 13(9), pp. 1990–2004. Available at: https://doi.org/10.1111/2041-210X.13913.

Bernardino, J. *et al.* (2018a) ‘Bird collisions with power lines: State of the art and priority areas for research’, *Biological Conservation*, 222(March), pp. 1–13. Available at: https://doi.org/10.1016/j.biocon.2018.02.029.

Bernardino, J. *et al.* (2018b) ‘Bird collisions with power lines: State of the art and priority areas for research’, *Biological Conservation*, 222(March), pp. 1–13. Available at: https://doi.org/10.1016/j.biocon.2018.02.029.

Bevanger, K. (1978) ‘Bird interactions with utility structures : collision and electrocution , causes and mitigating measures’, *IBIS*, 136, pp. 412–425.

Bevanger, K. (1995) ‘Estimates and population consequences of tetraonid mortality caused by collisions with high tension power lines in Norway’, *Journal of Applied Ecology*, 32(4), pp. 745–753. Available at: https://doi.org/10.2307/2404814.

Bevanger, K. (1998) ‘Biological and conservation aspects of bird mortality caused by electricity power lines: A review’, *Biological Conservation*, 86(1), pp. 67–76. Available at: https://doi.org/10.1016/S0006-3207(97)00176-6.

Bevanger, K. and Brøseth, H. (2004) ‘Impact of power lines on bird mortality in a subalpine area’, *Animal Biodiversity and Conservation*, 27(2), pp. 67–77. Available at: https://doi.org/10.1021/cm101132g.

Bird, D. and Laycock, S. (2019) ‘GPGPU acceleration of environmental and movement datasets’, in *ACM SIGGRAPH 2019*. Available at: https://doi.org/10.1145/3306214.3338584.

Birdlife International (2022) *State of the world’s birds*. Cambridge, UK.

BirdLife International (2015a) *Migratory Soaring Birds Project: Soaring Bird Sensitivity Map*. Available at: http://migratorysoaringbirds.undp.birdlife.org/en/sensitivity-map (Accessed: 3 November 2019).

BirdLife International (2015b) ‘Review and guidance on use of “shutdown-on-demand” for wind turbines to conserve migration soaring birds in the Rift Valley/Red Sea Flyway’, *Regional Flyway Facility. Amman, Jordan.*, p. 49. Available at:

http://migratorysoaringbirds.undp.birdlife.org/sites/default/files/msb_guidance_shutdown_on_demand.pdf.

Blackwell, B.F. *et al.* (2009) 'Avian visual system configuration and behavioural response to object approach', *Animal Behaviour*, 77(3), pp. 673–684. Available at: https://doi.org/10.1016/j.anbehav.2008.11.017.

Blary, C. (2022) 'Bird contrast sensitivity and wind turbines collisions', in *CWW Wind Energy and Wildlife Conference*. Egmond aan Zee. Available at: https://cww2022-live.org/livestream-tuesday-5-april-2022/#ROOM2.

Bohrer, G. *et al.* (2012) 'Estimating updraft velocity components over large spatial scales: Contrasting migration strategies of golden eagles and turkey vultures', *Ecology Letters*, 15(2), pp. 96–103. Available at: https://doi.org/10.1111/j.1461-0248.2011.01713.x.

Botha, J. *et al.* (2002) 'A comparison of anthropogenic and elephant disturbance on Acacia xanthophloea (fever tree) populations in the Lowveld , South Africa', 1.

Bouten, W. *et al.* (2013) 'A flexible GPS tracking system for studying bird behaviour at multiple scales', *Journal of Ornithology*, 154(2), pp. 571–580. Available at: https://doi.org/10.1007/s10336-012-0908-1.

Bouten, W. (2018) *UvA-BiTS Bird Tracking System*, *University of Amsterdam*. Available at: http://www.uva-bits.nl/.

Boyd, H. and Fox, A.D. (2008) 'Effects of climate change on the breeding success of White-fronted Geese Anser albifrons flavirostris in west Greenland', *Wildfowl*, 58(2008), pp. 55–70.

Bradbury, G. *et al.* (2014) 'Mapping Seabird Sensitivity to offshore wind farms', *PLoS ONE*, 9(9). Available at: https://doi.org/10.1371/journal.pone.0106366.

Braham, M. *et al.* (2015) 'Home in the heat: Dramatic seasonal variation in home range of desert golden eagles informs management for renewable energy development', *Biological Conservation*, 186, pp. 225–232. Available at: https://doi.org/10.1016/j.biocon.2015.03.020.

Bridge, E.S. *et al.* (2011) 'Technology on the move: Recent and forthcoming innovations for tracking migratory birds', *BioScience*, 61(9), pp. 689–698. Available at: https://doi.org/10.1525/bio.2011.61.9.7.

Bright, J. *et al.* (2008) 'Map of bird sensitivities to wind farms in Scotland: A tool to aid planning and conservation', *Biological Conservation*, 141(9), pp. 2342–2356. Available at: https://doi.org/10.1016/j.biocon.2008.06.029.

Bright, J. a *et al.* (2006) 'Bird sensitivity map to provide locational guidance for onshore wind farms in Scotland', *RSPB Research Report*, 20(20), pp. i–ii, 1–136.

Brotons, L. *et al.* (2004) 'Presence-absence versus presence-only modelling methods for predicting bird habitat suitability', *Ecography*, 27(4), pp. 437–448. Available at: https://doi.org/10.1111/j.0906-7590.2004.03764.x.

Brovelli, M. and Zamboni, G. (2018) 'A New Method for the Assessment of Spatial Accuracy and Completeness of OpenStreetMap Building Footprints', *ISPRS International Journal of Geo-Information*, 7(8), p. 289. Available at: https://doi.org/10.3390/ijgi7080289.

BSG Ecological Consultants (2011) 'Bsg Technical Review: Bird collisions at onshore wind farms', in. Trondheim. Available at: http://www.bsg-ecology.com/wp-content/uploads/2015/03/Bird-Collisions-and-Wind-Farms.pdf.

Buchan, C. *et al.* (2022) 'Spatially explicit risk mapping reveals direct anthropogenic impacts on migratory birds', *Global Ecology and Biogeography*, (May), pp. 1–19. Available at: https://doi.org/10.1111/geb.13551.

Buechley, Evan R. *et al.* (2018) 'Identifying critical migratory bottlenecks and high-use areas for an endangered migratory soaring bird across three continents', *Journal of Avian Biology*, 49(7), pp. 1–13. Available at: https://doi.org/10.1111/jav.01629.

Buechley, Evan R *et al.* (2018) 'Identifying Critical Migratory Bottlenecks and High-Use Areas for an Endangered Migratory Soaring Bird Across Three Continents', *Journal of Avian Biology*, e01629, pp. 1–13. Available at: https://doi.org/10.1111/jav.01629.

Burns, F. *et al.* (2021) 'Abundance decline in the avifauna of the European Union reveals cross-continental similarities in biodiversity change', *Ecology and Evolution*, 11(23), pp. 16647–16660. Available at: https://doi.org/10.1002/ece3.8282.

Camphuysen, K.C.J. *et al.* (2012) 'Identifying ecologically important marine areas for seabirds using behavioural information in combination with distribution patterns', *Biological Conservation*, 156, pp. 22–29. Available at: https://doi.org/10.1016/j.biocon.2011.12.024.

CGIAR (2022) *SRTM 90m Digital Elevation Data Consortium for Spatial Information (CGIAR-CSI) Download Portal*. Available at: https://srtm.csi.cgiar.org/ (Accessed: 26 September 2022).

Christel, I. *et al.* (2013) 'Seabird aggregative patterns: A new tool for offshore wind energy risk assessment', *Marine Pollution Bulletin*, 66(1–2), pp. 84–91. Available at:

https://doi.org/10.1016/j.marpolbul.2012.11.005.

CIEEM (2018) *Guidelines for Ecological Impact Assessment in the UK and Ireland*. Winchester, Hampshire. Available at: https://www.cieem.net/data/files/ECIA Guidelines.pdf.

Cleasby, I.R. *et al.* (2015) 'Three-dimensional tracking of a wide-ranging marine predator: Flight heights and vulnerability to offshore wind farms', *Journal of Applied Ecology*, 52(6), pp. 1474–1482. Available at: https://doi.org/10.1111/1365-2664.12529.

Concept 13 Limited (2022) *Concept 13: Sensors-Gateways-LoRaWAN*. Available at: https://www.concept13.co.uk/ (Accessed: 5 January 2022).

Cook, A.S.C.P. *et al.* (2014) 'Indicators of seabird reproductive performance demonstrate the impact of commercial fisheries on seabird populations in the North Sea', *Ecological Indicators*, 38, pp. 1–11. Available at: https://doi.org/10.1016/j.ecolind.2013.10.027.

Cook, A.S.C.P. *et al.* (2018) 'Quantifying avian avoidance of offshore wind turbines: Current evidence and key knowledge gaps', *Marine Environmental Research*, 140(March), pp. 278–288. Available at: https://doi.org/10.1016/j.marenvres.2018.06.017.

Costa, D.P. *et al.* (2010) 'Accuracy of ARGOS locations of pinnipeds at-sea estimated using fastloc GPS', *PLoS ONE*, 5(1). Available at: https://doi.org/10.1371/journal.pone.0008677.

CRAN (2022) 'sjPlot Data Visualisation for Social Statistics'. Available at: https://cran.r-project.org/package=sjPlot.

Croft, S.A. (2014) *Modelling collective motion and obstacle avoidance to assess avian collision risk with wind turbines*. University of York.

Daunt, F. *et al.* (2014) 'Longitudinal bio-logging reveals interplay between extrinsic and intrinsic carry-over effects in a long-lived vertebrate', *Ecology*, 95(8), pp. 2077–2083. Available at: https://doi.org/10.1890/13-1797.1.

Dellasala, D.A., Goldstein, M.I. and Elias, S.A. (2018) 'Global Change Impacts on the Biosphere', *Encyclopedia of the Anthropocene*, pp. 81–94. Available at: https://doi.org/10.1016/B978-0-12-809665-9.09532-X.

Denac, D., Schneider-Jacoby, M. and Stumberger, B. (2009) *Adriatic Flyway – Closing the gap in bird Conservation*. Edited by H. Ciglic. Schwarz d.o.o.

Desholm, M. (2009) 'Avian sensitivity to mortality : Prioritising migratory bird species for assessment at proposed wind farms', *Journal of Environmental Management*, 90(8), pp.

2672–2679. Available at: https://doi.org/10.1016/j.jenvman.2009.02.005.

Diesendorf, M. and Elliston, B. (2018) ‘The feasibility of 100% renewable electricity systems: A response to critics’, *Renewable and Sustainable Energy Reviews*, 93(October 2017), pp. 318–330. Available at: https://doi.org/10.1016/j.rser.2018.05.042.

Dini, B. *et al.* (2021) ‘Development of smart boulders to monitor mass movements via the Internet of Things: A pilot study in Nepal’, *Earth Surface Dynamics*, 9(2), pp. 295–315. Available at: https://doi.org/10.5194/esurf-9-295-2021.

Dixon, A. *et al.* (2018) ‘Efficacy of a mitigation method to reduce raptor electrocution at an electricity distribution line in Mongolia’, *Conservation Evidence*, 15, pp. 50–53. Available at: https://www.conservationevidence.com/individual-study/6861.

Dixon, A. *et al.* (2019) ‘Mitigation techniques to reduce avian electrocution rates’, *Wildlife Society Bulletin*, 43(3), pp. 476–483. Available at: https://doi.org/10.1002/wsb.990.

Donázar, J.A. *et al.* (2002) ‘Conservation status and limiting factors in the endangered population of Egyptian vulture (Neophron percnopterus) in the Canary Islands’, *Biological Conservation*, 107(1), pp. 89–97. Available at: https://doi.org/10.1016/S0006-3207(02)00049-6.

Dunnett, S. *et al.* (2020) ‘Harmonised global datasets of wind and solar farm locations and power’, *Scientific Data*, 7(1), p. 130. Available at: https://doi.org/10.1038/s41597-020-0469-8.

Eichhorn, M., Tafarte, P. and Thrän, D. (2017) ‘Towards energy landscapes – “Pathfinder for sustainable wind power locations”’, *Energy*, 134, pp. 611–621. Available at: https://doi.org/10.1016/j.energy.2017.05.053.

Elias, S.A. (2018) ‘Global Change Impacts on The Biosphere’, *Encyclopedia of the Anthropocene*, 2, pp. 81–94. Available at: https://doi.org/10.1016/B978-0-12-809665-9.09532-X.

ESRI (2018) ‘ArcGIS Desktop: Release 10.6.1’. Redlands, CA: Environmental Systems Research Institute.

ESRI (2019) ‘ArcGIS Release 10.6.1’. Redlands, CA: Environmental Systems Research Institute.

ESRI (2020) ‘Arc GIS Pro 3.0.1’. Available at: https://www.esriuk.com/en-gb/arcgis/products/arcgis-pro/overview.

ESRI (2021) *Sentinel-2 10-Meter Land Use/Land Cover*. Available at:

https://livingatlas.arcgis.com/landcover/ (Accessed: 5 November 2022).

European Climate Foundation (2018) 'Net Zero by 2050: From whether to how - Zero emission Pathways to the Europe we want', (September), p. 66.

European Commission; *et al.* (2021) *ERA5 hourly data on single levels from 1979 to present*. Available at: https://doi.org/10.24381/cds.adbb2d47.

European Commission (2018) *Guidance on Energy Transmission Infrastructure and EU nature legislation*. Available at: http://ec.europa.eu/environment/nature/natura2000/management/docs/Energy guidance and EU Nature legislation.pdf.

European Commission (2020) 'Stepping up Europe's 2030 climate ambition Investing in a climate-neutral future for the benefit of our people', *Journal of Chemical Information and Modeling*, 53(9), pp. 1689–1699. Available at: https://knowledge4policy.ec.europa.eu/publication/communication-com2020562-stepping-europe's-2030-climate-ambition-investing-climate_en#:~:text=17 September 2020-,Communication COM%2F2020%2F562%3A Stepping up Europe's 2030 climate,the benefit of our peopl.

European Commission (2022) *Communication from the Commission to the European Parliament, the European Council, The Cuncil, The European economic and social committee and the committee of the regions*. Belgium. Available at: https://eur-lex.europa.eu/legal-content/EN/TXT/?uri=COM%3A2022%3A230%3AFIN&qid=1653033742483.

European Environment Agency (2017) *Trends and projections in Europe 2017. Tracking progress towards Europe's climate and energy targets*, *EEA Report 6/2014*. Available at: https://doi.org/10.1016/j.watres.2007.01.052.

Evans;, J.S., Murphy;, M.A. and Ram, K. (2021) 'spatialEco: Spatial Analysis and Modelling Utilities'. cran-r. Available at: https://cran.r-project.org/web/packages/spatialEco/index.html.

Evens, R. *et al.* (2018) 'An effective, low-tech drop-off solution to facilitate the retrieval of data loggers in animal-tracking studies', *Ringing and Migration*, 33(1), pp. 10–18. Available at: https://doi.org/10.1080/03078698.2018.1521116.

Fandos, G. *et al.* (2020) 'Seasonal niche tracking of climate emerges at the population level in a migratory bird', *Proceedings. Biological sciences*, 287(1935), p. 20201799. Available at: https://doi.org/10.1098/rspb.2020.1799.

Ferreira, D. *et al.* (2019) ‘Is wind energy increasing the impact of socio-ecological change on Mediterranean mountain ecosystems? Insights from a modelling study relating wind power boost options with a declining species’, *Journal of Environmental Management*, 238(October 2018), pp. 283–295. Available at: https://doi.org/10.1016/j.jenvman.2019.02.127.

Ferrer, M. *et al.* (2022) ‘Significant decline of Griffon Vulture collision mortality in wind farms during 13-year of a selective turbine stopping protocol’, *Global Ecology and Conservation*, 38(June), p. e02203. Available at: https://doi.org/10.1016/j.gecco.2022.e02203.

Ferrer, M. and Hiraldo, F. (1992) ‘Man-induced sex-biased mortality in the Spanish imperial eagle’, *Biological Conservation*, 60(1), pp. 57–60. Available at: https://doi.org/10.1016/0006-3207(92)90799-S.

Fijn, R.C. *et al.* (2015) ‘Bird movements at rotor heights measured continuously with vertical radar at a Dutch offshore wind farm’, *Ibis*, 157(3), pp. 558–566. Available at: https://doi.org/10.1111/ibi.12259.

Fijn, R.C. *et al.* (2017) ‘GPS-tracking and colony observations reveal variation in offshore habitat use and foraging ecology of breeding Sandwich Terns’, *Journal of Sea Research*, 127, pp. 203–211. Available at: https://doi.org/10.1016/j.seares.2016.11.005.

Finnegan, J. and Brown, S. (2020) ‘An Analysis of the Energy Consumption of LPWA-based IoT Devices’, in *2018 International Symposium on Networks, Computers and Communications (ISNCC)*. Maynooth: IEEE, pp. 1–6. Available at: https://doi.org/10.1109/ISNCC.2018.8531068.

Flack, A. *et al.* (2016) ‘Costs of migratory decisions: A comparison across eight white stork populations’, *Science Advances*, 2(1), pp. e1500931–e1500931. Available at: https://doi.org/10.1126/sciadv.1500931.

Forin-Wiart, M.A. *et al.* (2015) ‘Performance and accuracy of lightweight and low-cost GPS data loggers according to antenna positions, fix intervals, habitats and animal movements’, *PLoS ONE*, 10(6), pp. 1–21. Available at: https://doi.org/10.1371/journal.pone.0129271.

Fritz, J. (2018) ‘Life Northern Bald Ibis Reintroduction of the Northern Bald Ibis in Europe Annual Report 2018’.

Frost, D. (2008) ‘The use of “flight diverters” reduces mute swan Cygnus olor collision with power lines at Abberton Reservoir, Essex, England’, *Conservation Evidence*, 5, pp.

83–91. Available at: www.ConservationEvidence.com.

Furness, R.W., Wade, H.M. and Masden, E.A. (2013) ‘Assessing vulnerability of marine bird populations to offshore wind farms’, *Journal of Environmental Management*, 119, pp. 56–66. Available at: https://doi.org/10.1016/j.jenvman.2013.01.025.

García-Alfonso, M. *et al.* (2021) ‘Disentangling drivers of power line use by vultures: Potential to reduce electrocutions’, *Science of the Total Environment*, 793(2021), p. 148534. Available at: https://doi.org/10.1016/j.scitotenv.2021.148534.

Garret, R. (2018) *The Open Source Infrastructure Project*, *OpenInfra*. Available at: https://openinframap.org (Accessed: 5 November 2018).

Gauld, J.G. *et al.* (2022a) ‘Hotspots in the grid: Avian sensitivity and vulnerability to collision risk from energy infrastructure interactions in Europe and North Africa, Dryad, Dataset’, *Dryad Digital Repository* [Preprint]. Available at: https://doi.org/10.5061/dryad.jm63xsjcw.

Gauld, J.G. *et al.* (2022b) ‘Hotspots in the grid: Avian sensitivity and vulnerability to collision risk from energy infrastructure interactions in Europe and North Africa’, *Journal of Applied Ecology*, (May 2021), pp. 1–17. Available at: https://doi.org/10.1111/1365-2664.14160.

Gilbert, N.I. (2015) *Movement and foraging ecology of partially migrant birds in a changing world*. University of East Anglia. Available at: https://ueaeprints.uea.ac.uk/59626/1/N_Gilbert_PhD_Thesis_Movement_and_foraging_ecology_of_partially_migrant_birds_in_a_changing_world.pdf.

Gilbert, N.I. *et al.* (2016) ‘Are white storks addicted to junk food? Impacts of landfill use on the movement and behaviour of resident white storks (Ciconia ciconia) from a partially migratory population’, *Movement Ecology*, 4(1), p. 7. Available at: https://doi.org/10.1186/s40462-016-0070-0.

Gómez-Catasús, J. *et al.* (2021) ‘Factors Affecting Differential Underestimates of Bird Collision Fatalities at Electric Lines: A Case Study in the Canary Islands’, *Ardeola*, 68(1), pp. 71–94. Available at: https://doi.org/10.13157/arla.68.1.2021.ra5.

Gouhier, T.C. and Pillai, P. (2020) ‘Avoiding Conceptual and Mathematical Pitfalls When Developing Indices to Inform Conservation’, *Frontiers in Ecology and Evolution*, 8(September), pp. 1–5. Available at: https://doi.org/10.3389/fevo.2020.00263.

Gove, B. *et al.* (2013) *Wind farms and birds: an updated analysis of the effects of wind farms on bird, and best practice guidance on integrated planning and impact* *assessement T-PVS/Inf*, *Council of Europe*. Strasbourg.

Griffin, L., Rees, E. and Hughes, B. (2010) *The Migration of Whooper Swans in Relation to Offshore Wind Farms*, *WWT Final Report to*. Available at: http://www.offshorewindfarms.co.uk/Assets/WWT Final Report to COWRIE Ltd (Whooper Swan tracking).pdf.

Grooten, M. and Almond, R.E.A. (2018) *Living Planet Report 2018 : Aiming higher (Full Report)*. Gland, Switzerland. Available at: https://www.zsl.org/sites/default/files/Living Planet Report 2018 - Full Report.pdf.

Guil, F. *et al.* (2017) 'Wildfires as collateral effects of wildlife electrocution: An economic approach to the situation in Spain in recent years'. Available at: https://doi.org/10.1016/j.scitotenv.2017.12.242.

Guil, F., Colomer, M.À. and Moreno-opo, R. (2015) 'Space–time trends in Spanish bird electrocution rates from alternative information sources', *Global Ecology and Conservation*, 3, pp. 379–388. Available at: https://doi.org/10.1016/j.gecco.2015.01.005.

Gyimesi, A. and Prinsen, H.A.M. (2015) 'Guidance on appropriate means of impact assessment of electricity power grids on migratory soaring birds in the Rift Valley / red Sea Flyway - Final Report', p. 56.

Hadley Wickham *et al.* (2015) 'DPLYR'. RStudio. Available at: https://dplyr.tidyverse.org/.

Hanssen, F., May, R. and Nygård, T. (2020) 'High-Resolution Modeling of Uplift Landscapes can Inform Micrositing of Wind Turbines for Soaring Raptors', *Environmental Management*, 66(3), pp. 319–332. Available at: https://doi.org/10.1007/s00267-020-01318-0.

Harker, K. (2018) *High Voltage Power Network Construction*. Hertfordshire, United Kingdom: The Institution of Engineering and Technology. Available at: https://digital-library.theiet.org/content/books/10.1049/pbpo110e_ch6.

Hedenström, D. and Strandberg, A. (1993) 'Protocol S1 Supplementary list of flight speeds and biometry of bird species', *Pennycuick Greenewalt Hedenström*, 135(1), pp. 1–4.

Hernández-Lambraño, R.E., Sánchez-Agudo, J.Á. and Carbonell, R. (2018) 'Where to start? Development of a spatial tool to prioritise retrofitting of power line poles that are dangerous to raptors', *Journal of Applied Ecology*, 55(6), pp. 2685–2697. Available at:

https://doi.org/10.1111/1365-2664.13200.

Hernández-matías, A. *et al.* (2015) ‘Electrocution threatens the viability of populations of the endangered Bonelli’s eagle (Aquila fasciata) in Southern Europe’, *BIOC*, 191, pp. 110–116. Available at: https://doi.org/10.1016/j.biocon.2015.06.028.

Hernández-Pliego, J. *et al.* (2015) ‘Effects of wind farms on Montagu’s harrier (Circus pygargus) in southern Spain’, *Biological Conservation*, 191, pp. 452–458. Available at: https://doi.org/10.1016/j.biocon.2015.07.040.

Heuck, C. *et al.* (2019a) ‘Wind turbines in high quality habitat cause disproportionate increases in collision mortality of the white-tailed eagle’, *Biological Conservation*, 236(August 2018), pp. 44–51. Available at: https://doi.org/10.1016/j.biocon.2019.05.018.

Heuck, C. *et al.* (2019b) ‘Wind turbines in high quality habitat cause disproportionate increases in collision mortality of the white-tailed eagle’, *Biological Conservation*, 236(May), pp. 44–51. Available at: https://doi.org/10.1016/j.biocon.2019.05.018.

Hewson, C.M. *et al.* (2016) ‘Population decline is linked to migration route in the Common Cuckoo’, *Nature Communications*, 7, pp. 1–8. Available at: https://doi.org/10.1038/ncomms12296.

Hijmans, R.J. (2019) ‘Raster: An R Package for working with raster data’. Available at: https://www.rspatial.org/.

Hijmans, R.J., Williams, E. and Vennes, C. (2015) ‘Geosphere: spherical trigonometry’. R. Available at: url: https://CRAN. R-project. org/package= geosphere.

Hofman, M.P.G. *et al.* (2019) ‘Right on track? Performance of satellite telemetry in terrestrial wildlife research’, *PLoS ONE*, 14(5), pp. 1–26. Available at: https://doi.org/10.1371/journal.pone.0216223.

Horns, J.J. and Şekercioğlu, Ç.H. (2018) ‘Conservation of migratory species’, *Current Biology*, 28(17), pp. R980–R983. Available at: https://doi.org/10.1016/j.cub.2018.06.032.

Hötker, H., Thomsen, K.-M. and Jeromin, H. (2006) ‘Impacts on biodiversity of exploitation of renewable energy sources: the example of birds and bats - facts, gaps in knowledge, demands for further research, and ornithological guidelines for the development of renewable energy exploitation.’, *Michael-Otto-Institut im NABU, Berghusen*, pp. 1–65.

Hull, C.L. *et al.* (2013) ‘Avian collisions at two wind farms in Tasmania, Australia:

Taxonomic and ecological characteristics of colliders versus non-colliders', *New Zealand Journal of Zoology*, 40(1), pp. 47–62. Available at: https://doi.org/10.1080/03014223.2012.757243.

Husby, M. and Pearson, M. (2022) 'Wind Farms and Power Lines Have Negative Effects on Territory Occupancy in Eurasian Eagle Owls (Bubo bubo)', *Animals*, 12(9), pp. 1–13. Available at: https://doi.org/10.3390/ani12091089.

Huso, M.M.P. and Dalthorp, D. (2014) 'Accounting for unsearched areas in estimating wind turbine-caused fatality', *Journal of Wildlife Management*, 78(2), pp. 347–358. Available at: https://doi.org/10.1002/jwmg.663.

IEA (2020) *Onshore Wind: Tracking Report*. Paris. Available at: https://www.iea.org/reports/onshore-wind.

IEA (2022) *Wind Electricity Technological Outlook*. Paris. Available at: https://www.iea.org/reports/wind-electricity.

Infante, O. and Peris, S. (2003) 'Bird nesting on electric power supports in northwestern Spain', *Ecological Engineering*, 20(4), pp. 321–326. Available at: https://doi.org/10.1016/S0925-8574(03)00013-2.

Interex (2022) *Interex:Mini GPS-GSM-ACC*. Available at: https://interrex-tracking.com/mini/ (Accessed: 16 December 2022).

IoT (2022) *Internet of Things: Airtime Calculator*. Available at: https://www.thethingsnetwork.org/airtime-calculator (Accessed: 15 December 2022).

IoT Wonderland (2022) *IoT Wonderland: Geo-spacial Data Visualization*. Available at: https://www.iotwonderland.com/ (Accessed: 6 October 2022).

IPBES (2019) *The global assessment report on Biodiversity and Ecosystems*. Edited by E.S. Brondízio, J. Settele, and N. H., T. Bonn, Germany: IPBES secretariat. Available at: https://zenodo.org/record/6417333#.Y8niUBXP02w.

IPCC (2014) *Climate Change 2014: Synthesis Report*, *Contribution of Working Groups I, II and III to the Fifth Assessment Report of the Intergovernmental Panel on Climate Change*. Available at: https://doi.org/10.1017/CBO9781107415324.

IPCC (2018) 'IPCC special report on the impacts of global warming of 1.5 °C - Summary for policy makers', (October 2018). Available at: http://www.ipcc.ch/report/sr15/.

IPCC (2022a) *Summary for Policy Makers Climate Change 2022: Impacts, Adaptation, and Vulnerability. Contribution of Working Group II to the Sixth Assessment Report of the Intergovernmental Panel on Climate Change*. Cambridge. Available at:

https://www.ipcc.ch/report/ar6/wg2/about/how-to-cite-this-report/.

IPCC (2022b) *Summary for Policymakers: The Physical Science Basis. Contribution of Working Group I to the Sixth Assessment Report of the Intergovernmental Panel on Climate Change*, *Cambridge University Press*. Cambridge, UK. Available at: https://doi.org/10.1017/CBO9781139177245.003.

IPCC (2022c) *Summary for Policymakers. In: Climate Change 2022: Mitigation of Climate Change. Contribution of Working Group III to the Sixth Assessment Report of the Intergovernmental Panel on Climate Change*, *Cambridge University Press*. Cambridge, UK. Available at: https://www.ipcc.ch/report/ar6/wg3/about/how-to-cite-this-report.

Jaffré, M. *et al.* (2013) 'Long-term phenological shifts in raptor migration and climate', *PLoS ONE*, 8(11), pp. 8–15. Available at: https://doi.org/10.1371/journal.pone.0079112.

Janss, G.F.E. (2000) 'Avian mortality from power lines: A morphologic approach of a species-specific mortality', *Biological Conservation*, 95(3), pp. 353–359. Available at: https://doi.org/10.1016/S0006-3207(00)00021-5.

Janss, G.F.E. and Ferrer, M. (2000) 'Common crane and great bustard collision with power lines: collision rates and risk exposure', *Wildlife Society Bulletin*, 28(September), pp. 675–680. Available at: https://doi.org/10.2307/3783619.

JAXA (2016) *ALOS_30m Digital Terrain Model WGS84 ellipsoidal vertical datum*, *OpenTopography*. Available at: http://opentopo.sdsc.edu/raster?opentopoID=OTALOS.082017.4326.1 (Accessed: 1 February 2019).

Jenkins, A.R. *et al.* (2011) 'Estimating the impacts of power line collisions on Ludwig"s Bustards Neotis ludwigii', *Bird Conservation International*, 21(3), pp. 303–310. Available at: https://doi.org/10.1017/S0959270911000128.

Jenkins, A.R., Smallie, J.J. and Diamond, M. (2010) 'Avian collisions with power lines: A global review of causes and mitigation with a South African perspective', *Bird Conservation International*, 20(3), pp. 263–278. Available at: https://doi.org/10.1017/S0959270910000122.

Jiguet, F. *et al.* (2021) 'GPS tracking data can document wind turbine interactions: Evidence from a GPS-tagged Eurasian curlew', *Forensic Science International: Animals and Environments*, 1, p. 100036. Available at: https://doi.org/10.1016/j.fsiae.2021.100036.

Johnston, A. *et al.* (2014) 'Modelling flight heights of marine birds to more accurately assess collision risk with offshore wind turbines', *Journal of Applied Ecology*, 51(1), pp. 31–41. Available at: https://doi.org/10.1111/1365-2664.12191.

Katzner, T.E. *et al.* (2012) 'Topography drives migratory flight altitude of golden eagles: Implications for on-shore wind energy development', *Journal of Applied Ecology*, 49(5), pp. 1178–1186. Available at: https://doi.org/10.1111/j.1365-2664.2012.02185.x.

Katzner, T.E. and Arlettaz, R. (2020) 'Evaluating Contributions of Recent Tracking-Based Animal Movement Ecology to Conservation Management', *Frontiers in Ecology and Evolution*, 7(January). Available at: https://doi.org/10.3389/fevo.2019.00519.

Kauth, H.R. *et al.* (2020) 'Low-cost DIY GPS trackers improve upland game bird monitoring', *Wildlife Biology*, 2020(2). Available at: https://doi.org/10.2981/wlb.00653.

Keller, V. *et al.* (2020) *European Breeding Bird Atlas 2: Distribution, Abundance and Change*. Barcelona: European Bird Census Council & Lynx Edicions. Available at: https://ebba2.info.

Kelsey, E.C. *et al.* (2018) 'Collision and displacement vulnerability to offshore wind energy infrastructure among marine birds of the Pacific Outer Continental Shelf', *Journal of Environmental Management*, 227(August), pp. 229–247. Available at: https://doi.org/10.1016/j.jenvman.2018.08.051.

Kettel, E.F. *et al.* (2022) 'Better utilisation and transparency of bird data collected by powerline companies', *Journal of Environmental Management*, 302(PA), p. 114063. Available at: https://doi.org/10.1016/j.jenvman.2021.114063.

Kiesecker, J. *et al.* (2019) 'Hitting the Target but Missing the Mark: Unintended Environmental Consequences of the Paris Climate Agreement', *Frontiers in Environmental Science*, 7(October). Available at: https://doi.org/10.3389/fenvs.2019.00151.

Kim, S., Lee, H. and Jeon, S. (2020) 'An adaptive spreading factor selection scheme for a single channel lora modem', *Sensors (Switzerland)*, 20(4). Available at: https://doi.org/10.3390/s20041008.

Kleyheeg-Hartman, J.C. *et al.* (2018) 'Predicting bird collisions with wind turbines: Comparison of the new empirical Flux Collision Model with the SOSS Band model', *Ecological Modelling*, 387(March), pp. 144–153. Available at: https://doi.org/10.1016/j.ecolmodel.2018.06.025.

Kleyheeg-Hhartman, J.C. *et al.* (2018) 'Predicting bird collisions with wind turbines: Comparison of the new empirical Flux Collision Model with the SOSS Band model', *Ecological Modelling*, 387(March), pp. 144–153. Available at: https://doi.org/10.1016/j.ecolmodel.2018.06.025.

Kölzsch, A. *et al.* (2016) 'Neckband or backpack? Differences in tag design and their effects on GPS/accelerometer tracking results in large waterbirds', *Animal Biotelemetry*, 4(1), p. 13. Available at: https://doi.org/10.1186/s40317-016-0104-9.

Köppel, J. (2015) *Wind Energy and Wildlife Interactions: Presentations from the CWW2015 Conference*, *Wind Energy and Wildlife Interactions*. Cham, Switzerland: Springer. Available at: https://doi.org/10.1007/978-3-319-51272-3.

Krijgsveld, K.L. *et al.* (2009) 'Collision Risk of Birds with Modern Large Wind Turbines', *Ardea*, 97(3), pp. 357–366. Available at: https://doi.org/10.5253/078.097.0311.

Lacuna (2022) *Lacuna Space*. Available at: https://lacuna.space/ (Accessed: 4 August 2022).

Lameris, T.K., van der Jeugd, H.P., *et al.* (2018) 'Arctic Geese Tune Migration to a Warming Climate but Still Suffer from a Phenological Mismatch', *Current Biology*, pp. 2467–2473. Available at: https://doi.org/10.1016/j.cub.2018.05.077.

Lameris, T.K., Müskens, G.J.D.M., *et al.* (2018) 'Effects of harness-attached tracking devices on survival, migration, and reproduction in three species of migratory waterfowl', *Animal Biotelemetry*, 6(1), pp. 4–11. Available at: https://doi.org/10.1186/s40317-018-0153-3.

Larsen, J.K. and Guillemette, M. (2007) 'Effects of wind turbines on flight behaviour of wintering common eiders: implications for habitat use and collission risk', *Journal of Applied Ecology*, 44, pp. 516–522. Available at: https://doi.org/10.1111/j.1365-2664.2007.1303.x.

Leclère, D. *et al.* (2020) 'Bending the curve of terrestrial biodiversity needs an integrated strategy', *Nature*, 585(October 2018). Available at: https://doi.org/10.1038/s41586-020-2705-y.

Lees, K.J., Guerin, A.J. and Masden, E.A. (2016) 'Using kernel density estimation to explore habitat use by seabirds at a marine renewable wave energy test facility', *Marine Policy*, 63, pp. 35–44. Available at: https://doi.org/10.1016/j.marpol.2015.09.033.

Lehman, R.N., Kennedy, P.L. and Savidge, J.A. (2007) 'The state of the art in raptor electrocution research: A global review', *Biological Conservation*, 135(4), pp. 459–474. Available at: https://doi.org/10.1016/j.biocon.2006.10.039.

Limiñana, R. *et al.* (2012) 'Mapping the Migratory Routes and Wintering Areas of Lesser

Kestrels Falco naumanni : New Insights from Satellite Telemetry', *Ibis*, 154, pp. 389–399.

Lines, P. (2022) 'Power Lines and Birds : Drivers of Conflict-Prone Use of Pylons by Nesting White Storks (Ciconia ciconia)', pp. 1–13.

LIU, J. *et al.* (2018) 'Design of aircraft structures against threat of bird strikes', *Chinese Journal of Aeronautics*, 31(7), pp. 1535–1558. Available at: https://doi.org/10.1016/j.cja.2018.05.004.

Liu, J., Li, Y. and Gao, X. (2014) 'Bird strike on a flat plate: Experiments and numerical simulations', *International Journal of Impact Engineering*, 70, pp. 21–37. Available at: https://doi.org/10.1016/j.ijimpeng.2014.03.006.

López-López, P. *et al.* (2011) 'Solving man-induced large-scale conservation problems: The Spanish Imperial Eagle and power lines', *PLoS ONE*, 6(3). Available at: https://doi.org/10.1371/journal.pone.0017196.

LORIOT (2021) *LORIOT Internet of Things LoRaWAN Server*. Available at: https://www.loriot.io/.

Loss, Scott R. (2016) 'Avian interactions with energy infrastructure in the context of other anthropogenic threats', *The Condor*, 118(2), pp. 424–432. Available at: https://doi.org/10.1650/condor-16-12.1.

Loss, Scott R (2016) 'Avian interactions with energy infrastructure in the context of other anthropogenic threats', *The Condor*, 118(2), pp. 424–432. Available at: https://doi.org/10.1650/CONDOR-16-12.1.

Loss, S.R., Dorning, M.A. and Diffendorfer, J.E. (2019) 'Biases in the literature on direct wildlife mortality from energy development', *BioScience*, 69(5), pp. 348–359. Available at: https://doi.org/10.1093/biosci/biz026.

Loss, S.R., Will, T. and Marra, P.P. (2014) 'Refining estimates of bird collision and electrocution mortality at power lines in the United States', *PLoS ONE*, 9(7), pp. 26–28. Available at: https://doi.org/10.1371/journal.pone.0101565.

Lotek (2022) *Lotek:PinPoint Cell*. Available at: https://www.lotek.com/wp-content/uploads/2020/06/PinPoint-Cell-Spec-Sheet.pdf (Accessed: 17 December 2022).

de Lucas, M. *et al.* (2012) 'Griffon vulture mortality at wind farms in southern Spain: Distribution of fatalities and active mitigation measures', *Biological Conservation*, 147(1), pp. 184–189. Available at: https://doi.org/10.1016/j.biocon.2011.12.029.

Lucas, M. De *et al.* (2012) 'Griffon vulture mortality at wind farms in southern Spain: Distribution of fatalities and active mitigation measures', *Biological Conservation*, 147(1), pp. 184–189. Available at: https://doi.org/10.1016/j.biocon.2011.12.029.

Lüdecke, D. *et al.* (2022) ‘ggeffects: Create Tidy Data Frames of Marginal Effects for “ggplot” from Model Outputs’.

Mainwaring, M.C. (2015) ‘The use of man-made structures as nesting sites by birds: A review of the costs and benefits’, *Journal for Nature Conservation*, 25, pp. 17–22. Available at: https://doi.org/10.1016/j.jnc.2015.02.007.

Maisonneuve, C. *et al.* (2011) ‘Estimating updraft velocity components over large spatial scales: contrasting migration strategies of golden eagles and turkey vultures’, *Ecology Letters*, 15(2), pp. 96–103. Available at: https://doi.org/10.1111/j.1461-0248.2011.01713.x.

Marcelino, J. *et al.* (2021) ‘Flight altitudes of a soaring bird suggest landfill sites as power line collision hotspots’, *Journal of Environmental Management*, 294(May). Available at: https://doi.org/10.1016/j.jenvman.2021.113149.

Marcelino, J. *et al.* (2022) ‘Anthropogenic food subsidies reshape the migratory behaviour of a long-distance migrant’, *Science of The Total Environment*, 858(October 2022), p. 159992. Available at: https://doi.org/10.1016/j.scitotenv.2022.159992.

Marques, A.T. *et al.* (2014a) ‘Understanding bird collisions at wind farms: An updated review on the causes and possible mitigation strategies’, *Biological Conservation*, 179, pp. 40–52. Available at: https://doi.org/10.1016/j.biocon.2014.08.017.

Marques, A.T. *et al.* (2014b) ‘Understanding bird collisions at wind farms: An updated review on the causes and possible mitigation strategies’, *Biological Conservation*, 179, pp. 40–52. Available at: https://doi.org/10.1016/j.biocon.2014.08.017.

Marques, A.T. *et al.* (2020a) ‘Wind turbines cause functional habitat loss for migratory soaring birds’, *Journal of Animal Ecology*, 89(1), pp. 93–103. Available at: https://doi.org/10.1111/1365-2656.12961.

Marques, A.T. *et al.* (2020b) ‘Wind turbines cause functional habitat loss for migratory soaring birds’, *Journal of Animal Ecology*, 89(1), pp. 93–103. Available at: https://doi.org/10.1111/1365-2656.12961.

Martín, B. *et al.* (2018) ‘Impact of wind farms on soaring bird populations at a migratory bottleneck’, *European Journal of Wildlife Research*, 64(3). Available at: https://doi.org/10.1007/s10344-018-1192-z.

Martin, G.R. (2011) ‘Understanding bird collisions with man-made objects : a sensory ecology approach’, *Ibis*, (153), pp. 239–254.

Martin, G.R. and Shaw, J.M. (2010) ‘Bird collisions with power lines: Failing to see the way ahead?’, *Biological Conservation*, 143, pp. 2695–2702. Available at: https://doi.org/10.1016/j.biocon.2010.07.014.

Masden, E.A. *et al.* (2010) ‘Cumulative impact assessments and bird / wind farm interactions : Developing a conceptual framework’, *Environmental Impact Assessment Review*, 30(1), pp. 1–7. Available at: https://doi.org/10.1016/j.eiar.2009.05.002.

Mattsson, B.J. *et al.* (2022) ‘Enhancing monitoring and transboundary collaboration for conserving migratory species under global change: The priority case of the red kite’, *Journal of Environmental Management*, 317(February), p. 115345. Available at: https://doi.org/10.1016/j.jenvman.2022.115345.

May, R. *et al.* (2010) *Collision risk in white-tailed eagles. Modelling collision risk using vantage point observations in Smøla wind-power plant*, *NINA Report*. Available at: https://doi.org/ISSN: 1504-3312\nISBN: 978-82-426-2219-8.

May, R. *et al.* (2014) ‘Mitigating wind-turbine induced avian mortality: Sensory, aerodynamic and cognitive constraints and options’, *Renewable and Sustainable Energy Reviews*, 42, pp. 170–181. Available at: https://doi.org/10.1016/j.rser.2014.10.002.

May, R. *et al.* (2019) ‘Considerations for upscaling individual effects of wind energy development towards population-level impacts on wildlife’, *Journal of Environmental Management*, 230(January 2018), pp. 84–93. Available at: https://doi.org/10.1016/j.jenvman.2018.09.062.

May, R., Nygård, T., Falkdalen, U., Åström, J., Hamre, Ø. and Stokke, Bård G. (2020) ‘Paint it black: Efficacy of increased wind turbine rotor blade visibility to reduce avian fatalities’, *Ecology and Evolution*, (June), pp. 1–9. Available at: https://doi.org/10.1002/ece3.6592.

May, R., Nygård, T., Falkdalen, U., Åström, J., Hamre, Ø. and Stokke, Bård G (2020) ‘Paint it black: Efficacy of increased wind turbine rotor blade visibility to reduce avian fatalities’, *Ecology and Evolution*, 00(February), pp. 1–9. Available at: https://doi.org/10.1002/ece3.6592.

May, R. *et al.* (2021) ‘Life-cycle impacts of wind energy development on bird diversity in Norway’, *Environmental Impact Assessment Review*, 90(July), p. 106635. Available at: https://doi.org/10.1016/j.eiar.2021.106635.

May, R.F. (2015) ‘A unifying framework for the underlying mechanisms of avian avoidance of wind turbines’, *Biological Conservation*, 190, pp. 179–187. Available at:

https://doi.org/10.1016/j.biocon.2015.06.004.

McClure, C.J.W. *et al.* (2021) 'Eagle fatalities are reduced by automated curtailment of wind turbines', *Journal of Applied Ecology*, 58(3), pp. 446–452. Available at: https://doi.org/10.1111/1365-2664.13831.

McClure, C.J.W., Martinson, L. and Allison, T.D. (2018) 'Automated monitoring for birds in flight: Proof of concept with eagles at a wind power facility', *Biological Conservation*, 224(April), pp. 26–33. Available at: https://doi.org/10.1016/j.biocon.2018.04.041.

Mckinsey & Company (2010) *Transformation of Europe's power system until 2050 Including specific considerations for Germany Electric Power and Natural Gas Practice*. Düsseldorf. Available at: https://www.mckinsey.com/~/media/mckinsey/dotcom/client_service/epng/pdfs/transformation_of_europes_power_system.ashx.

McManamay, R.A., Vernon, C.R. and Jager, H.I. (2021) 'Global Biodiversity Implications of Alternative Electrification Strategies Under the Shared Socioeconomic Pathways', *Biological Conservation*, 260(December 2020), p. 109234. Available at: https://doi.org/10.1016/j.biocon.2021.109234.

Mekki, K. *et al.* (2019) 'A comparative study of LPWAN technologies for large-scale IoT deployment', *ICT Express*, 5(1), pp. 1–7. Available at: https://doi.org/10.1016/j.icte.2017.12.005.

Miromico AG (2021) *miroNomad Data Sheet: Ultra Lightweight LoRaWAN GPS Tracker*. Available at: https://docs.miromico.ch/datasheets/_attachments/tracker/miro_Nomad_datasheet_V1_0.pdf (Accessed: 1 October 2021).

Miromico AG (2022) 'Miromico Docs: Tracking Solutions Documentation'. Zurich. Available at: https://docs.miromico.ch/tracker/dev/index.html.

Møller, A.P., Rubolini, D. and Lehikoinen, E. (2008) 'Populations of Migratory Bird Species That Did Not Show a Phenological Response to Climate Change are Declining', *PNAS*, 105(42), pp. 16195–16200. Available at: https://doi.org/10.1073/pnas.0803825105.

Moreira, F. *et al.* (2017) 'Wired: impacts of increasing power line use by a growing bird population', *Environmental Research Letters*, 12(2), p. 024019. Available at: https://doi.org/10.1088/1748-9326/aa5c74.

Moreira, F. *et al.* (2018) 'Drivers of power line use by white storks: A case study of birds nesting on anthropogenic structures', *Journal of Applied Ecology*, 55(5), pp. 2263–2273. Available at: https://doi.org/10.1111/1365-2664.13149.

Morris, G. and Conner, L.M. (2017) 'Assessment of accuracy, fix success rate, and use of estimated horizontal position error (EHPE) to filter inaccurate data collected by a common commercially available GPS logger', *PLoS ONE*, 12(11), pp. 1–12. Available at: https://doi.org/10.1371/journal.pone.0189020.

Movebank (2019) *Movebank Data Repository*. Available at: https://www.movebank.org/ (Accessed: 1 October 2018).

Multi-Tech Systems Inc. (2021) *MultiTech Conduit IP67 Base Station 16-Channel v2.1 Geolocation EU686 for Europe*. Available at: https://www.multitech.com/documents/publications/data-sheets/86002223.pdf.

Multi-Tech Systems Inc. (2022) *Multi-Tech DeviceHQ: Cloud-based Application Store and IoT Device Management*. Available at: www.multitech.com (Accessed: 5 January 2022).

Muñoz Sabater, J. (2021) *ERA5-Land hourly data from 1981 to present*, *Copernicus Climate Change Service (C3S)*. Available at: 10.24381/cds.e2161bac (Accessed: 1 February 2022).

Murali, G. *et al.* (2023) 'Future temperature extremes threaten land vertebrates', *Nature*, In Press(September 2021), p. 8. Available at: https://doi.org/10.1038/s41586-022-05606-z.

Muteba, F., Djouani, K. and Olwal, T. (2019) 'A comparative survey study on LPWA IoT technologies: Design, considerations, challenges and solutions', *Procedia Computer Science*, 155, pp. 636–641. Available at: https://doi.org/10.1016/j.procs.2019.08.090.

National Grid (2014) *Design Drawings 132kV Overhead Lines: Hinkley Point C Connection Project Application Reference EN020001*.

National Science Foundation (2019) *Open Topography Data Portal*, *OpenTopography*. Available at: https://opentopography.org/news/three-new-global-topographic-datasets-available-srtm-ellipsoidal-alos-world-3d-gmrt (Accessed: 1 February 2019).

New, L. *et al.* (2015) 'A collision risk model to predict avian fatalities at wind facilities: An example using golden eagles, Aquila chrysaetos', *PLoS ONE*, 10(7), pp. 1–12. Available at: https://doi.org/10.1371/journal.pone.0130978.

Newell, M. *et al.* (2015) 'Effects of an extreme weather event on seabird breeding success at a North Sea colony', *Marine Ecology Progress Series*, 532, pp. 257–268. Available at: https://doi.org/10.3354/meps11329.

Newson, S.E. *et al.* (2016) ‘Long-term changes in the migration phenology of UK breeding birds detected by large-scale citizen science recording schemes’, *Ibis*, 158(3), pp. 481–495. Available at: https://doi.org/10.1111/ibi.12367.

NGA and NASA (2000) *Shuttle Radar Topography Mission (SRTM GL1) Global 30m Ellipsoidal*, *OpenTopography*. Available at: http://opentopo.sdsc.edu/raster?opentopoID=OTSRTM.082016.4326.1 (Accessed: 1 February 2019).

O’Donoghue, P. and Rutz, C. (2016) ‘Real-time anti-poaching tags could help prevent imminent species extinctions’, *Journal of Applied Ecology*, 53(1), pp. 5–10. Available at: https://doi.org/10.1111/1365-2664.12452.

Oloo, F., Safi, K. and Aryal, J. (2018) ‘Predicting migratory corridors of white storks, ciconia ciconia, to enhance sustainablewind energy planning: A data-driven agent-based model’, *Sustainability (Switzerland)*, 10(5). Available at: https://doi.org/10.3390/su10051470.

OpenStreetMap (2018) *Classification of Power Lines*, *OpenStreetMap Wiki*. Available at: https://wiki.openstreetmap.org/wiki/Classification_of_power_lines (Accessed: 15 October 2018).

OpenStreetMap (2019) *Guidance for Digitising Power Line Data into OpenStreetMap*, *OpenStreetMap Wiki*. Available at: https://wiki.openstreetmap.org/wiki/Power_lines (Accessed: 10 March 2019).

Oppel, S. *et al.* (2020) ‘Major threats to a migratory raptor vary geographically along the eastern Mediterranean flyway’, *bioRxiv* [Preprint], (February). Available at: https://doi.org/10.1101/2020.12.16.422983.

Oppel, S. *et al.* (2021a) ‘Major threats to a migratory raptor vary geographically along the eastern Mediterranean flyway’, *Biological Conservation*, 262(August 2020). Available at: https://doi.org/10.1016/j.biocon.2021.109277.

Oppel, S. *et al.* (2021b) ‘Major threats to a migratory raptor vary geographically along the eastern Mediterranean flyway’, *Biological Conservation*, 262(February). Available at: https://doi.org/10.1016/j.biocon.2021.109277.

Ossi, F., Urbano, F. and Cagnacci, F. (2019a) *Biologging and remote-sensing of behavior*. Second Edi, *Encyclopedia of Animal Behavior*. Second Edi. Elsevier. Available at: https://doi.org/10.1016/B978-0-12-809633-8.90089-X.

Ossi, F., Urbano, F. and Cagnacci, F. (2019b) *Biologging and Remote-Sensing of Behavior*.

Second Edi, *Encyclopedia of Animal Behavior*. Second Edi. Elsevier. Available at: https://doi.org/10.1016/b978-0-12-809633-8.90089-x.

Palac, C. *et al.* (2016) ‘Changes in bird-migration patterns associated with human-induced mortality’, *Conservation Biology*, 31(1), pp. 106–115. Available at: https://doi.org/10.1111/cobi.12758.

Palacin, C. *et al.* (2012) ‘The importance of traditional farmland areas for steppe birds : a case study of migrant female Great Bustards Otis tarda in Spain’, *Ibis*, 154, pp. 85–95.

Panuccio, M. *et al.* (2017) ‘Long-term changes in autumn migration dates at the Strait of Gibraltar reflect population trends of soaring birds’, *Ibis*, 159(1), pp. 55–65. Available at: https://doi.org/10.1111/ibi.12420.

De Pascalis, F. *et al.* (2020) ‘Shift in proximate causes of mortality for six large migratory raptors over a century’, *Biological Conservation*, 251(June), p. 108793. Available at: https://doi.org/10.1016/j.biocon.2020.108793.

Patterson, I.J. (2015) ‘Goose flight activity in relation to distance from SPAs in Scotland, including an analysis of flight height distribution’, *Scottish Natural Heritage Commissioned Report*, 735(735).

Pavón-Jordán, D. *et al.* (2020) ‘Do birds respond to spiral markers on overhead wires of a high-voltage power line? Insights from a dedicated avian radar’, *Global Ecology and Conservation*, 24. Available at: https://doi.org/10.1016/j.gecco.2020.e01363.

Pearce-Higgins, J.W. *et al.* (2009) ‘The distribution of breeding birds around upland wind farms’, *Journal of Applied Ecology*, 46(6), pp. 1323–1331. Available at: https://doi.org/10.1111/j.1365-2664.2009.01715.x.

Pearce-Higgins, J.W. *et al.* (2012) ‘Greater impacts of wind farms on bird populations during construction than subsequent operation: Results of a multi-site and multi-species analysis’, *Journal of Applied Ecology*, 49(2), pp. 386–394. Available at: https://doi.org/10.1111/j.1365-2664.2012.02110.x.

Pebesma, E.. (2018) ‘Simple Features for R: Standardized Support for Spatial Vector Data.’, *The R Journal*, 10(1), pp. 439–446. Available at: https://doi.org/https://doi.org/10.32614/RJ-2018-009.

Pedersen, T.L. (2020) ‘patchwork: The Composer of Plots’. Available at: https://patchwork.data-imaginist.com.

Pérez-garcía, J.M. *et al.* (2017) ‘Using risk prediction models and species sensitivity maps for large-scale identification of infrastructure-related wildlife protection areas : The case of bird electrocution', *Biological Conservation*, 210(August 2016), pp. 334–342. Available at: https://doi.org/10.1016/j.biocon.2017.04.033.

Pérez-García, J.M. *et al.* (2016) 'Selecting indicator species of infrastructure impacts using network analysis and biological traits: Bird electrocution and power lines', *Ecological Indicators*, 60, pp. 428–433. Available at: https://doi.org/10.1016/j.ecolind.2015.07.020.

Péron, G. *et al.* (2013) 'Estimation of bird and bat mortality at wind-power farms with superpopulation models', *Journal of Applied Ecology*, 50(4), pp. 902–911. Available at: https://doi.org/10.1111/1365-2664.12100.

Péron, G. *et al.* (2017) 'The energy landscape predicts flight height and wind turbine collision hazard in three species of large soaring raptor', *Journal of Applied Ecology*, 54(6), pp. 1895–1906. Available at: https://doi.org/10.1111/1365-2664.12909.

Péron, G. *et al.* (2020) 'The challenges of estimating the distribution of flight heights from telemetry or altimetry data', *Animal Biotelemetry*, 8(5), pp. 1–13. Available at: https://doi.org/10.1101/751271.

Perona, A.M., Urios, V. and López-López, P. (2019) 'Holidays? Not for all. Eagles have larger home ranges on holidays as a consequence of human disturbance', *Biological Conservation*, 231(July 2018), pp. 59–66. Available at: https://doi.org/10.1016/j.biocon.2019.01.010.

Peschko, V. *et al.* (2020) 'Effects of offshore windfarms on seabird abundance: Strong effects in spring and in the breeding season', *Marine Environmental Research*, 162, p. 105157. Available at: https://doi.org/10.1016/j.marenvres.2020.105157.

Peters, G.P. and Hausfather, Z. (2020) 'Emissions - the "business as usual" story is misleading', *Nature*, 577, pp. 618–620.

Phipps, W.L. *et al.* (2013) 'Do Power Lines and Protected Areas Present a Catch-22 Situation for Cape Vultures (Gyps coprotheres)?', *PLoS ONE*, 8(10). Available at: https://doi.org/10.1371/journal.pone.0076794.

Poessel, S.A. *et al.* (2018a) 'Improving estimation of flight altitude in wildlife telemetry studies', *Journal of Applied Ecology*, 55(4), pp. 2064–2070. Available at: https://doi.org/10.1111/1365-2664.13135.

Poessel, S.A. *et al.* (2018b) 'Improving estimation of flight altitude in wildlife telemetry studies', *Journal of Applied Ecology*, 55(4), pp. 2064–2070. Available at: https://doi.org/10.1111/1365-2664.13135.

Polat, Ö. *et al.* (2016) ‘An Overview of Bird Related Issues in Electrical Power Systems’, *Materials Science and Engineering*, 161, pp. 1–9. Available at: https://doi.org/10.1088/1757-899X/161/1/012091.

Potier, S., Mitkus, M. and Kelber, A. (2018) ‘High resolution of colour vision, but low contrast sensitivity in a diurnal raptor’, *Proceedings of the Royal Society B: Biological Sciences*, 285(1885). Available at: https://doi.org/10.1098/rspb.2018.1036.

Prinsen, H.A.M. *et al.* (2011) *Guidelines on How to Avoid or Mitigate Impact of Electricity Power Grids on Migratory Birds in the African-Eurasian Region*. Bonn, Germany. Available at: https://doi.org/10.3354/dao02488.

Prinsen, H.A.M. *et al.* (2012) ‘Guidelines on how to avoid or mitigate impact of electricity power grids on migratory birds in the African-Eurasian region.’, *CMS Technical Series No. 29, AEWA Technical Series No. 50 , CMS Raptors MOU Technical Series No. 3.*, 9(UNEP/CMS/Conf.10.30/Rev.2), pp. 1–43. Available at: https://doi.org/10.1111/j.1461-0248.2006.00968.x.

QGIS Development Team (2019) ‘QGIS Geographic Information System’. Open Source Geospatial Foundation Project.

Quectel (2021) *Global IOT Solutions Provider IoT Modules and Antenna Catalogue*. Shanghai. Available at: https://www.quectel.com/wp-content/uploads/2022/10/Quectel_Product_Brochure_v7.2.pdf.

R Core Team (2019) ‘R: A language and environment for statistical computing’. Available at: http://www.r-project.org/.

Ramsden, D.J. (2003) *Barn Owls and Major Roads*, *The Barn Owl Trust*. Exeter.

Recio, M.R. *et al.* (2011) ‘Cost comparisons between GPS- and VHF-based telemetry : case study of feral cats in New Zealand SHORT COMMUNICATION Cost comparison between GPS- and VHF-based telemetry : case study of feral cats Felis catus in New Zealand’, (May 2014).

Ramos, R.F., Franco, A.M.A., Gilroy, J.J. et al. Combining bird tracking data with high-resolution thermal mapping to identify microclimate refugia. Sci Rep 13, 4726 (2023). https://doi.org/10.1038/s41598-023-31746-x

Rees, E.C. (2012) ‘Impacts of wind farms on swans and geese: A review’, *Wildfowl*, 62, pp. 37–72.

Ren, L. *et al.* (2018) ‘Enabling resilient distributed power sharing in networked microgrids through software defined networking’, *Applied Energy*, 210, pp. 1251–1265.

Available at: https://doi.org/10.1016/j.apenergy.2017.06.006.

Riley, S.J., DeGloria, S.D. and Elliot, R. (1999) ‘A terrain ruggedness index that quantifies topographic heterogeneity’, *Intermountain Journal of Sciences*, 5, pp. 23–27.

Rioux, S., Savard, J.-P.L. and Gerick, A.A. (2013) ‘Avian mortalities due to transmission line collisions : a review of current estimates and field methods with an emphasis on applications to the Canadian electric network Mortalité aviaire attribuable aux collisions avec les lignes de transport d ’ électri’, *Avian Conservation and Ecology*, 8(2). Available at: http://www.ace-eco.org/vol8/iss2/art7/.

Ripperger, S.P. *et al.* (2020) ‘Thinking small: Next-generation sensor networks close the size gap in vertebrate biologging’, *PLoS Biology*, 18(4), pp. 1–25. Available at: https://doi.org/10.1371/journal.pbio.3000655.

Rodríguez, A. *et al.* (2012) ‘The Eye in the Sky: Combined Use of Unmanned Aerial Systems and GPS Data Loggers for Ecological Research and Conservation of Small Birds’, *PLoS ONE*, 7(12). Available at: https://doi.org/10.1371/journal.pone.0050336.

Rollan, À. *et al.* (2010) ‘Modelling the risk of collision with power lines in Bonelli’s Eagle Hieraaetus fasciatus and its conservation implications’, *Bird Conservation International*, 20(3), pp. 279–294. Available at: https://doi.org/10.1017/S0959270910000250.

Ross-Smith, V.H. *et al.* (2016) ‘Modelling flight heights of lesser black-backed gulls and great skuas from GPS: a Bayesian approach’, *Journal of Applied Ecology*, 53(6), pp. 1676–1685. Available at: https://doi.org/10.1111/1365-2664.12760.

Rotics, S. *et al.* (2016) ‘The challenges of the first migration: Movement and behaviour of juvenile vs. adult white storks with insights regarding juvenile mortality’, *Journal of Animal Ecology* [Preprint], (June). Available at: https://doi.org/10.1111/1365-2656.12525.

Rotics, S. *et al.* (2021) ‘Early-life behaviour predicts first-year survival in a long-distance avian migrant’, *Proceedings of the Royal Society B: Biological Sciences*, 288(1942). Available at: https://doi.org/10.1098/rspb.2020.2670.

Rubolini, D. *et al.* (2005) ‘Birds and powerlines in Italy: An assessment’, *Bird Conservation International*, 15(2), pp. 131–145. Available at: https://doi.org/10.1017/S0959270905000109.

Ruddock, M. and Whitfield, D.P. (2007) ‘A Review of Disturbance Distances in Selected Bird Species’.

Ryberg, D.S. *et al.* (2019) ‘The future of European onshore wind energy potential:

Detailed distribution and simulation of advanced turbine designs', *Energy*, 182, pp. 1222–1238. Available at: https://doi.org/10.1016/j.energy.2019.06.052.

Săcăleanu, D.I. *et al.* (2018) 'Data Compression in Wireless Sensor Nodes with LoRa', in *ECAI 2018 - International Conference – 10th Edition: Electronics, Computers and Artificial Intelligence*. Iasi, romania: IEEE, pp. 5–8. Available at: https://ieeexplore.ieee.org/stamp/stamp.jsp?tp=&arnumber=8679003.

Sage, E. *et al.* (2022) 'Built up areas in a wet landscape are stepping stones for soaring flight in a seabird', *Science of The Total Environment*, 852(May), p. 157879. Available at: https://doi.org/10.1016/j.scitotenv.2022.157879.

Santangeli, A. *et al.* (2018) 'Stronger response of farmland birds than farmers to climate change leads to the emergence of an ecological trap', *Biological Conservation*, 217(October 2017), pp. 166–172. Available at: https://doi.org/10.1016/j.biocon.2017.11.002.

Santos, C.D. *et al.* (2017) 'Match between soaring modes of black kites and the fine-scale distribution of updrafts', *Scientific Reports*, 7(1), pp. 1–10. Available at: https://doi.org/10.1038/s41598-017-05319-8.

Santos, C.D. *et al.* (2020) 'The gateway to Africa: What determines sea crossing performance of a migratory soaring bird at the Strait of Gibraltar?', *Journal of Animal Ecology*, 89(6), pp. 1317–1328. Available at: https://doi.org/10.1111/1365-2656.13201.

Santos, S.M. *et al.* (2016) 'Avian trait-mediated vulnerability to road traffic collisions', *Biological Conservation*, 200, pp. 122–130. Available at: https://doi.org/10.1016/j.biocon.2016.06.004.

Scacco, M. *et al.* (2019) 'Static landscape features predict uplift locations for soaring birds across Europe', *Royal Society Open Science*, 6(1), pp. 1–12. Available at: https://doi.org/10.1098/rsos.181440.

Schaub, M. (2012) 'Spatial distribution of wind turbines is crucial for the survival of red kite populations', *Biological Conservation*, 155, pp. 111–118. Available at: https://doi.org/10.1016/j.biocon.2012.06.021.

Schaub, T. *et al.* (2020) 'Collision risk of Montagu's Harriers Circus pygargus with wind turbines derived from high-resolution GPS tracking', *Ibis*, 162(2), pp. 520–534. Available at: https://doi.org/10.1111/ibi.12788.

Schloerke, B. *et al.* (2021) 'GGally: Extension to "ggplot2"'. cran-r. Available at: https://cran.r-project.org/package=GGally.

Schutgens, M., Shaw, J.M. and Ryan, P.G. (2014) 'Estimating scavenger and search bias for collision fatality surveys of large birds on power lines in the Karoo, South Africa', *Ostrich*, 85(1), pp. 39–45. Available at: https://doi.org/10.2989/00306525.2014.888691.

Scottish Government (2022) *Climate Change Plan: Monitoring Report*. Edinburgh, UK. Available at: https://www.gov.scot/binaries/content/documents/govscot/publications/progress-report/2022/05/climate-change-plan-monitoring-reports-2022/documents/climate-change-plan-monitoring-reports-2022/climate-change-plan-monitoring-reports-2022/govscot%3Adocument/c.

Seidel, D. and Wickham, H. (2022) 'Scales 1.2.1.9000 R package for rescaling data'. CRAN 1.2.1. Available at: https://scales.r-lib.org/.

Semtech (2021) *Datasheet: DS.SX1261-2 Long Range, Low Power, sub-GHz RF Transceiver*. Available at: https://www.semtech.com/products/wireless-rf/lora-connect/sx1262 (Accessed: 19 December 2022).

Sequeira, A.M.M. *et al.* (2021) 'A standardisation framework for bio-logging data to advance ecological research and conservation', *Methods in Ecology and Evolution, Accepted Author Manuscript*, pp. 2041–210. Available at: https://doi.org/10.1111/2041-210X.13593.

Sergio, F. *et al.* (2004) 'Electrocution alters the distribution and density of a top predator, the eagle owl Bubo bubo', *Journal of Applied Ecology*, 41(5), pp. 836–845. Available at: https://doi.org/10.1111/j.0021-8901.2004.00946.x.

Sergio, F. *et al.* (2018) 'Reliable methods for identifying animal deaths in GPS- and satellite-tracking data: Review, testing, and calibration', *Journal of Applied Ecology* [Preprint], (November). Available at: https://doi.org/10.1111/1365-2664.13294.

Sergio, F. *et al.* (2019) 'Reliable methods for identifying animal deaths in GPS- and satellite-tracking data: Review, testing, and calibration', *Journal of Applied Ecology*, 56(3), pp. 562–572. Available at: https://doi.org/10.1111/1365-2664.13294.

Serrano, D. *et al.* (2020) 'Renewables in Spain threaten biodiversity', *Science (New York, N.Y.)*, 370. Available at: https://doi.org/DOI: 10.1126/science.abf6509.

Shariati-Najafabadi, M. *et al.* (2016) 'Environmental parameters linked to the last migratory stage of barnacle geese en route to their breeding sites', *Animal Behaviour*, 118, pp. 81–95. Available at: https://doi.org/10.1016/j.anbehav.2016.05.018.

Shariati, M. *et al.* (2017) 'Expert system for modelling stopover site selection by barnacle geese', *Ecological Modelling*, 359, pp. 398–405. Available at: https://doi.org/10.1016/j.ecolmodel.2017.06.018.

Siemens Gamesa Renewables (2022) *Siemens Gamesa SG 6.6 - 155 Onshore Wind Turbine Specifications*. Available at: https://www.siemensgamesa.com/products-and-services/onshore/wind-turbine-sg-5-8-155 (Accessed: 1 April 2022).

Silva, J.P. *et al.* (2010) 'Estimating the influence of overhead transmission power lines and landscape context on the density of little bustard Tetrax tetrax breeding populations', *Ecological Modelling*, 221(16), pp. 1954–1963. Available at: https://doi.org/10.1016/j.ecolmodel.2010.03.027.

Silva, J.P. *et al.* (2014) 'A spatially explicit approach to assess the collision risk between birds and overhead power lines: A case study with the little bustard', *Biological Conservation*, 170, pp. 256–263. Available at: https://doi.org/10.1016/j.biocon.2013.12.026.

Silva, J.P. *et al.* (2015) 'Freezing heat: Thermally imposed constraints on the daily activity patterns of a free-ranging grassland bird', *Ecosphere*, 6(7). Available at: https://doi.org/10.1890/ES14-00454.1.

Silva, R. *et al.* (2017) 'Seasonal and circadian biases in bird tracking with solar GPS-tags', *PLoS ONE*, 12(10), pp. 1–19. Available at: https://doi.org/10.1371/journal.pone.0185344.

Skov, H. *et al.* (2016) 'Patterns of migrating soaring migrants indicate attraction to marine wind farms', *Biology Letters*, 12(12). Available at: https://doi.org/10.1098/rsbl.2016.0804.

Smith, J.A. and Dwyer, J.F. (2016) 'Avian interactions with renewable energy infrastructure: An update', *The Condor*, 118(2), pp. 411–423. Available at: https://doi.org/10.1650/CONDOR-15-61.1.

SNH (2006) *Assessing significance of impacts from onshore windfarms on birds outwith designated areas*. Edinburgh, UK. Available at: http://www.snh.org.uk/pdfs/strategy/renewable/Significance of bird impacts July 06.pdf.

SNH (2010) *Use of avoidance rates in the SNH wind farm collision risk model.*, *SNH Avoidance Rate Information & Guidance Note*. Available at: http://scholar.google.com/scholar?hl=en&btnG=Search&q=intitle:Use+of+Avoidance+Rates+in+the+SNH+Wind+Farm+Collision+Risk+Model#1.

SNH (2016) ‘Assessment and mitigation of impacts of power lines and guyed meteorological masts on birds’, (July 2016), pp. 1–11.

Soanes, L.M. *et al.* (2013) ‘Individual consistency in the foraging behaviour of Northern Gannets: Implications for interactions with offshore renewable energy developments’, *Marine Policy*, 38, pp. 507–514. Available at: https://doi.org/10.1016/j.marpol.2012.08.006.

Song, N. *et al.* (2021) ‘Effects of wind farms on the nest distribution of magpie (Pica pica) in agroforestry systems of Chongming Island, China’, *Global Ecology and Conservation*, 27, p. e01536. Available at: https://doi.org/10.1016/j.gecco.2021.e01536.

Soriano-Redondo, A. *et al.* (2020) ‘Testing alternative methods for estimation of bird migration phenology from GPS tracking data’, *Ibis*, 162(2), pp. 581–588. Available at: https://doi.org/10.1111/ibi.12809.

Soriano-Redondo, A. *et al.* (2021) ‘Flying the extra mile pays-off: Foraging on anthropogenic waste as a time and energy-saving strategy in a generalist bird’, *Science of the Total Environment*, 782, p. 146843. Available at: https://doi.org/10.1016/j.scitotenv.2021.146843.

Sovacool, B.K. (2009) ‘Contextualizing avian mortality: A preliminary appraisal of bird and bat fatalities from wind, fossil-fuel, and nuclear electricity’, *Energy Policy*, 37(6), pp. 2241–2248. Available at: https://doi.org/10.1016/j.enpol.2009.02.011.

Spivey, R.J., Stansfield, S. and Bishop, C.M. (2014) ‘Analysing the intermittent flapping flight of a Manx Shearwater, Puffinus puffinus, and its sporadic use of a wave-meandering wing-sailing flight strategy’, *Progress in Oceanography*, 125, pp. 62–73. Available at: https://doi.org/10.1016/j.pocean.2014.04.005.

STHDA (2017) *Corstars Function: Elegant correlation table using xtable R package*. Available at: http://www.sthda.com/english/wiki/elegant-correlation-table-using-xtable-r-package (Accessed: 2 October 2018).

Stienen, E.W.M. *et al.* (2008) ‘Sex-Biased Mortality of Common Terns in Wind Farm Collisions’, *The Condor*, 110(1), pp. 154–157. Available at: https://doi.org/10.1525/cond.2008.110.1.154.

Stienen, E.W.M. *et al.* (2016) ‘GPS tracking data of lesser black-backed gulls and herring gulls breeding at the southern north sea coast’, *ZooKeys*, 2016(555), pp. 115–124. Available at: https://doi.org/10.3897/zookeys.555.6173.

Taylor, P.D. *et al.* (2017) ‘The Motus Wildlife Tracking System: a collaborative research network’, *Avian Conservation and Ecology*, 12(1), p. 8.

Thaxter, C. *et al.* (2018) ‘Dodging the blades: new insights into three-dimensional space use of offshore wind farms by lesser black-backed gulls Larus fuscus’, *Marine Ecology Progress Series*, 587, pp. 247–253. Available at: https://doi.org/10.3354/meps12415.

Thaxter, C.B. *et al.* (2015) ‘Seabird-wind farm interactions during the breeding season vary within and between years: A case study of lesser black-backed gull Larus fuscus in the UK’, *Biological Conservation*, 186, pp. 347–358. Available at: https://doi.org/10.1016/j.biocon.2015.03.027.

Thaxter, Chris B. *et al.* (2017) ‘Bird and bat species’ global vulnerability to collision mortality at wind farms revealed through a trait-based assessment’, *Proceedings of the Royal Society B: Biological Sciences*, 284(1862). Available at: https://doi.org/10.1098/rspb.2017.0829.

Thaxter, Chris B *et al.* (2017) ‘Bird and bat species ’ global vulnerability to collision mortality at wind farms revealed through a trait-based assessment’.

Thaxter, C.B. *et al.* (2018) ‘Dodging the blades: New insights into three-dimensional space use of offshore wind farms by lesser black-backed gulls Larus fuscus’, *Marine Ecology Progress Series*, 587(3), pp. 247–253. Available at: https://doi.org/10.3354/meps12415.

Thaxter, C.B., Ross-Smith, V.H., *et al.* (2019) ‘ Avian vulnerability to wind farm collision through the year: Insights from lesser black-backed gulls (Larus fuscus) tracked from multiple breeding colonies ’, *Journal of Applied Ecology*, (July), pp. 1–13. Available at: https://doi.org/10.1111/1365-2664.13488.

Thaxter, C.B., Ross-Smith, V.H., *et al.* (2019) ‘Avian vulnerability to wind farm collision through the year: Insights from lesser black-backed gulls (Larus fuscus) tracked from multiple breeding colonies’, *Journal of Applied Ecology*, 56(11), pp. 2410–2422. Available at: https://doi.org/10.1111/1365-2664.13488.

The Things Network (2019) *LoRaWAN® distance world record broken, twice. 766 km (476 miles) using 25mW transmission power*. Available at: https://www.thethingsnetwork.org/article/lorawan-distance-world-record (Accessed: 16 February 2022).

Therkildsen, O.R. *et al.* (2021) ‘Changes in flight paths of large-bodied birds after construction of large terrestrial wind turbines’, *Journal of Environmental Management*, 290(April 2020). Available at: https://doi.org/10.1016/j.jenvman.2021.112647.

Tikkanen, H. *et al.* (2018a) ‘Modelling golden eagle habitat selection and flight activity in their home ranges for safer wind farm planning’, *Environmental Impact Assessment Review*, 71(April), pp. 120–131. Available at: https://doi.org/10.1016/j.eiar.2018.04.006.

Tikkanen, H. *et al.* (2018b) ‘Modelling golden eagle habitat selection and flight activity in their home ranges for safer wind farm planning’, *Environmental Impact Assessment Review*, 71(September 2017), pp. 120–131. Available at: https://doi.org/10.1016/j.eiar.2018.04.006.

Timmerberg, S. *et al.* (2019) ‘Renewable electricity targets in selected MENA countries – Assessment of available resources, generation costs and GHG emissions’, *Energy Reports*, 5, pp. 1470–1487. Available at: https://doi.org/10.1016/j.egyr.2019.10.003.

Tomé, R. *et al.* (2017) ‘Radar assisted shutdown on demand ensures zero soaring bird mortality at a wind farm located in a migratory flyway’, in J. Köppel (ed.) *Wind Energy and Wildlife Interactions: Presentations from the CWW2015 Conference*. Springer International Publishing, pp. 119–133. Available at: https://doi.org/https://doi.org/10.1007/978-3-319-51272-3_7.

TPWind Advisory Council (2006) ‘Wind Energy : A Vision for Europe in 2030’, p. 21. Available at: https://etipwind.eu/files/reports/TPWind-Vision-for-Europe.pdf.

Travers, M.S. *et al.* (2021) ‘Post-collision impacts, crippling bias, and environmental bias in a study of newell’s shearwater and hawaiian petrel powerline collisions’, *Avian Conservation and Ecology*, 16(1). Available at: https://doi.org/10.5751/ACE-01841-160115.

TTN (2016) *The Things Network Fair Usage Policy*. Available at: https://www.thethingsnetwork.org/forum/t/fair-use-policy-explained/1300 (Accessed: 23 September 2022).

TTN (2021) *The Things Network LoRaWAN Server*. Available at: https://www.thethingsnetwork.org/ (Accessed: 5 June 2021).

TTN Mapper (2022) *TTN Mapper: Interactive Map of TTN LoRa Gateways*. Available at: https://ttnmapper.org/heatmap/ (Accessed: 18 December 2022).

Turbek, S.P., Scordato, E.S.C. and Safran, R.J. (2018) ‘The Role of Seasonal Migration in Population Divergence and Reproductive Isolation’, *Trends in Ecology and Evolution*, 33(3), pp. 164–175. Available at: https://doi.org/10.1016/j.tree.2017.11.008.

Tyrrell, L.P. and Fernández-Juricic, E. (2017) ‘Avian binocular vision: It’s not just about what birds can see, it’s also about what they can’t’, *PLoS ONE*, 12(3), pp. 1–14. Available at: https://doi.org/10.1371/journal.pone.0173235.

Uddin, M. *et al.* (2021a) ‘High bird mortality due to power lines invokes urgent environmental mitigation in a tropical desert’, *Biological Conservation*, 261(July), p. 109262. Available at: https://doi.org/10.1016/j.biocon.2021.109262.

Uddin, M. *et al.* (2021b) ‘High bird mortality due to power lines invokes urgent environmental mitigation in a tropical desert’, *Biological Conservation*, 261(January), p. 109262. Available at: https://doi.org/10.1016/j.biocon.2021.109262.

UK Research and Innovation (2016) *Long range wireless devices for high-resolution monitoring of animal movement*. Available at: https://gtr.ukri.org/projects?ref=NE%2FP003907%2F1 (Accessed: 26 September 2019).

UKRI (2017) *NEXUSS CDT Next Generation Unmanned Systems Science*. Available at: https://www.southampton.ac.uk/nexuss/index.page (Accessed: 1 October 2018).

UNEP AEWA Secretariat (2018) *The Agreement on the Conservation of African-Eurasian Migratory Waterbirds The Agreement on the Conservation of African-Eurasian Migratory Waterbirds*. Durban, South Africa.

Vanermen, N. *et al.* (2015) ‘Seabird avoidance and attraction at an offshore wind farm in the Belgian part of the North Sea’, *Hydrobiologia*, 756(1), pp. 51–61. Available at: https://doi.org/10.1007/s10750-014-2088-x.

Vasilakis, D.P. *et al.* (2016) ‘Reconciling endangered species conservation with wind farm development: Cinereous vultures (Aegypius monachus) in south-eastern Europe’, *Biological Conservation*, 196, pp. 10–17. Available at: https://doi.org/10.1016/j.biocon.2016.01.014.

Vignali, S. *et al.* (2021) ‘Modelling the habitat selection of the bearded vulture to predict areas of potential conflict with wind energy development in the Swiss Alps’, *Global Ecology and Conservation*, 25. Available at: https://doi.org/10.1016/j.gecco.2020.e01405.

Walther, B.A. and Moore, J.L. (2005) ‘The concepts of bias, precision and accuracy, and their use in testing the performance of species richness estimators, with a literature review of estimator performance’, *Ecography*, 28(6), pp. 815–829. Available at: https://doi.org/10.1111/j.2005.0906-7590.04112.x.

Warren, R. *et al.* (2018) ‘The implications of the United Nations Paris Agreement on climate change for globally significant biodiversity areas’, *Climatic Change*, 147(3–4), pp.

395–409. Available at: https://doi.org/10.1007/s10584-018-2158-6.

Warwick-evans, V. *et al.* (2017) 'Predicting the impacts of wind farms on seabirds : An individual-based model', *Journal of Applied Ecology*, (August), pp. 1–13. Available at: https://doi.org/10.1111/1365-2664.12996.

Whitfield, D.P. and Fielding, A.H. (2017) *Analyses of the fates of satellite tracked golden eagles in Scotland*. Edinburgh, UK. Available at: http://www.snh.org.uk/pdfs/publications/commissioned_reports/982.pdf.

Wickham, H. (2016) 'ggplot2: Elegant Graphics for Data Analysis in R'.

Wild, T.A. *et al.* (2022) 'Internet on animals: Wi-Fi-enabled devices provide a solution for big data transmission in biologging', *Methods in Ecology and Evolution*, 2022(August 2021), pp. 1–16. Available at: https://doi.org/10.1111/2041-210X.13798.

Williams, H.J. *et al.* (2021) 'Future trends in measuring physiology in free-living animals', *Philosophical Transactions of the Royal Society B: Biological Sciences*, 376(1831). Available at: https://doi.org/10.1098/rstb.2020.0230.

Wouters, H. *et al.* (2021) *Downscaled bioclimatic indicators for selected regions from 1950 to 2100 derived from climate projections, version 1.0*, *opernicus Climate Change Service (C3S) Climate Data Store (CDS)*. Available at: doi: 10.24381/cds.0ab27596 (Accessed: 15 November 2022).

WWF (2022) *Living Planet Report 2022*. Gland, Switzerland. Available at: https://www.wwf.org.uk/sites/default/files/2022-10/lpr_2022_full_report.pdf.

APPENDIX A: LITERATURE REVIEW SUPPLEMENTARY MATERIAL

Species or Group	Latin Name	Conservation Status	Susceptible to Collision with wind farms	Susceptible to Collision with power lines	Susceptible to Electrocution	Population Level Impacts Observed from EI	Notes (Energy infrastructure abbreviated to EI)
Egyptian vulture	*Neophron percnopterus*	EN (Decreasing)	Y	Y	Y	Global	This soaring species is endangered throughout its range. It is prone to collision with wind farms (Hötker, Thomsen and Jeromin, 2006; Prinsen *et al.*, 2012; Gyimesi and Prinsen, 2015) and transmission lines but the major cause of mortality is electrocution associated with nesting and perching behaviour (Angelov, Hashim and Oppel, 2013).
Saker Falcon	*Falco cherrug*	EN (Decreasing)	Y	Y	Y	Regional	This raptor is infrequently recorded as a collision victim, however the endangered status of this species makes this cause of mortality important at the regional and global level (Gyimesi and Prinsen, 2015).
Steppe Eagle	*Aquila nipalensis*	EN (Decreasing)	Y	Y	Y	Global	This endangered eagle species is facing multiple conservation challenges. Collision associated with transmission infrastructure and wind farms is a major cause of mortality. Electrocution on lower voltage lines is also considered to impact this species at the population level across the species' range (Palacin *et al.*, 2012; Gyimesi and Prinsen, 2015).
Northern Bald Ibis	*Geronticus eremita*	EN	Y	Y	Y	Regional	This species is endangered throughout its range. Collision and electrocution are listed as major threats to conservation to its conservation status (Gyimesi and Prinsen, 2015; Bernardino *et al.*, 2018b).
Eastern Imperial Eagle	*Aquila heliaca*	VU (Decreasing)	Y	Y	Y	Global	As with other eagles, this species is highly susceptible to collision and electrocution. Low to medium tension lines appear to pose a significant electrocution problem for the close cousin if this species the Iberian Imperial Eagle (López-López *et al.*, 2011; Gyimesi and Prinsen, 2015).

Species or Group	Latin Name	Conservation Status	Susceptible to Collision with wind farms	Susceptible to Collision with power lines	Susceptible to Electrocution	Population Level Impacts Observed from EI	Notes (Energy infrastructure abbreviated to EI)
Great bustard	*Otis tarda*	VU (Decreasing)	Y	Y	Y	Global	Classified as a poor avoider; this species has high wing loading and poor perception of anthropogenic hazards. Collision risk is therefore a threat to the conservation status of this species across its known range (Janss and Ferrer, 2000; Hötker, Thomsen and Jeromin, 2006).
Greater Spotted Eagle	*Aquila clanga*	VU (Decreasing)	Y	Y	Y	Global	This species often uses human structures as hunting posts making it highly susceptible to electrocution and collisions. Mortality associated with EI is contributing to the ongoing decline in this species (Janss, 2000).
Kittiwake	*Rysa tridactyla*	VU (Decreasing)	Y	N	N	Regional	Offshore and coastal wind farms can result in increased collision and displacement impacts for this species (Vanermen *et al.*, 2015).
Turtle dove	*Streptopelia turtur*	VU (Decreasing)	N	N	Y	Regional	Land use change is the major driver of population decline in this species. Hunting and Electrocution are two other major mortality factors contributing to this decline across the range (Janss, 2000; Denac, Schneider-Jacoby and Stumberger, 2009; Gyimesi and Prinsen, 2015).
Iberian Imperial Eagle	*Aquila adalberti*	VU	Y	Y	Y	Global	This large raptor often comes into conflict with EI resulting in significant population level impacts across the species' range (Ferrer and Hiraldo, 1992; Janss, 2000; López-López *et al.*, 2011).
Black vulture	*Aegypius monachus*	NT (Decreasing)	Y	Y	Y	Global	Electrocution on medium tension lines is contributing to the global decline observed in this species (Janss, 2000; Prinsen *et al.*, 2011).
Curlew	*Numenius arquata*	NT (Decreasing)	Y	Y	Y	Local	Collision and electrocution associated with low voltage lines near wetlands and breeding sites is linked with local scale impacts on this species (SNH, 2010).
Herring Gull	*Larus argenatus*	NT (Decreasing)	Y	Y	Y	Local	Globally declining; this common species is prone

Species or Group	Latin Name	Conservation Status	Susceptible to Collision with wind farms	Susceptible to Collision with power lines	Susceptible to Electrocution	Population Level Impacts Observed from EI	Notes (Energy infrastructure abbreviated to EI)
							to collision with wind turbines (Hötker, Thomsen and Jeromin, 2006).
Lapwing	*Vanellus vanellus*	NT (Decreasing)	Y	Y	N	Local	This species is most prone to collision during the breeding season when territorial displays make it vulnerable to collision with power lines and wind farms (Hötker, Thomsen and Jeromin, 2006; SNH, 2010).
Little bustard	*Tetrax tetrax*	NT (Decreasing)	Y	Y	Y	Global	Bustards are poor fliers; collision with power lines is a major conservation concern for the Iberian population of this species. EI adjacent to known lekking sites and important feeding areas is a particular conservation concern (Janss, 2000; Silva *et al.*, 2010; Gyimesi and Prinsen, 2015).
Pallid Harrier	*Circus macrourus*	NT (Decreasing)	Y	Y	Y	Regional	This species is declining across much of its range. Electrocution mortality is thought to have regionally important negative impacts on the population of this species (Janss, 2000; Gyimesi and Prinsen, 2015).
Red kite	*Milvus milvus*	NT (Decreasing)	Y	Y	Y	Global	Kites are common victims of collision and electrocution. Mitigating the impacts of EI is therefore an urgent conservation priority for this species (SNH, 2010; Schaub, 2012).
Red-footed Falcon	*Falco vespertinus*	NT (Decreasing)	Y	N	Y	Local	This species is a commonly recorded victim of collision and electrocution resulting in localised impacts on the population (Janss, 2000; Guil, Colomer and Moreno-opo, 2015).
Bean Goose	*Anser fabalis*	LC (Decreasing)	Y	Y	N	Local	Poor siting of unmitigated EI can adversely impact this species at the local scale (SNH, 2016).
Black grouse	*Tetrao tetrix*	LC (Decreasing)	Y	Y	N	Regional	This poor flyer commonly collides with human structures. In Norway 47,000 black grouse are killed every year as a result of power line collisions (Bevanger, 1995).
Black-throated Diver	*Gavia arctica*	LC (Decreasing)	Y	Y	N	Local	A rare breeding bird across much of its range. It has been recorded as a collision victim however

Species or Group	Latin Name	Conservation Status	Susceptible to Collision with wind farms	Susceptible to Collision with power lines	Susceptible to Electrocution	Population Level Impacts Observed from EI	Notes (Energy infrastructure abbreviated to EI)
							the main impact for this species is disturbance (Botha *et al.*, 2002; Ruddock and Whitfield, 2007).
Bonelli's eagle	*Hieraaetus fasciatus*	LC (Decreasing)	Y	Y	Y	Global	Electrocution on medium tension lines is contributing to the global decline observed in this species (Rollan *et al.*, 2010; Hernández-matías *et al.*, 2015).
Capercaillie	*Tetrao urogallus*	LC (Decreasing)	Y	Y	N	Regional	Approximately 20,000 Capercaillie per year are killed by collisions with power lines in Norway. This large heavy bird has high wing loading and poor binocular vision (Bevanger, 1995).
Common kestrel	*Falco tinnunculus*	LC (Decreasing)	Y	N	Y	Local	This species often uses power lines as hunting perches increasing the risk of electrocution (Barrios and Rodríguez, 2004).
Dunlin	*Calidris alpina*	LC (Decreasing)	Y	N	Y	Local	EI constructed near wetland sites can cause significant collision mortality. Disturbance at breeding sites is another impact of poorly planned EI (SNH, 2010).
Eagle Owl	*Bubo bubo*	LC (Decreasing)	Y	Y	Y	Regional	Power line related mortality has significantly impacted the population of this species in the Italian Alps and has likely cause similar impacts elsewhere in its range (Sergio *et al.*, 2004).
Eurasian Wigeon	*Mareca penelope*	LC (Decreasing)	Y	Y	N	Regional	EI adjacent to wetlands can have significant impact on this duck species (Krijgsveld *et al.*, 2009; SNH, 2010).
European Honey-buzzard	*Pernis apivorus*	LC (Decreasing)	Y	Y	Y	Global	This migratory species suffers from collision and electrocution throughout its range (Janss, 2000; Jenkins, Smallie and Diamond, 2010; Gyimesi and Prinsen, 2015).
Hen harrier	*Circus cyaneus*	LC (Decreasing)	Y	Y	Y	Regional	The main threat to this species is illegal persecution. However collision with EI is a significant mortality factor (Pearce-Higgins *et al.*, 2009; SNH, 2010; Prinsen *et al.*, 2012).
Hobby	*Falco subbuteo*	LC (Decreasing)	Y	Y	Y	Local	This small migratory raptor often uses perches during

Species or Group	Latin Name	Conservation Status	Susceptible to Collision with wind farms	Susceptible to Collision with power lines	Susceptible to Electrocution	Population Level Impacts Observed from EI	Notes (Energy infrastructure abbreviated to EI)
							hunting making it prone to electrocution on low to medium voltage power lines (Janss, 2000; Guil, Colomer and Moreno-opo, 2015).
Hoopoe	*Upupa epops*	LC (Decreasing)	N	N	N	Negligible	Occasionally recorded as a collision victim however this species is not significantly impacted by EI (Janss, 2000).
Montagu's harrier	*Circus pygargus*	LC (Decreasing)	Y	Y	Y	Regional	Collision and electrocution are thought to have regionally important population level impacts on this migratory raptor (Hernández-Pliego *et al.*, 2015).
Red-throated Diver	*Gavia stellata*	LC (Decreasing)	Y	Y	N	Local	EI sited adjacent to breeding lochs poses a collision risk for this species. The main impact for divers is the disturbance generated during construction and operation of EI (Ruddock and Whitfield, 2007; Pearce-Higgins *et al.*, 2012).
Short-eared owl	*Asio flammeus*	LC (Decreasing)	Y	Y	Y	Local	Poorly constructed EI can result in localised population impacts through collision and electrocution mortality. Habitat and other environmental changes are thought to be of more significance for this species (Bright *et al.*, 2006; SNH, 2010).
Skylark	*Alauda arvensis*	LC (Decreasing)	Y	Y	Y	Local	This species is particularly vulnerable to collision with wind turbines and power lines during the breeding season when the males perform their aerial displays. EI in areas of high skylark density can therefore cause localised impacts on the population (Pearce-Higgins *et al.*, 2012).
Stone Curlew	*Burhinus oedicnemus*	LC (Decreasing)	Y	?	N	Local	Data is poor however this species is known to collide with fences and other human objects. It is therefore highly likely that this species is negatively impacted by the presence of unmitigated EI.
White Fronted Goose	*Anser albifrons*	LC (Decreasing)	Y	Y	N	Local	Climate change is thought to be the major driver in

Species or Group	Latin Name	Conservation Status	Susceptible to Collision with wind farms	Susceptible to Collision with power lines	Susceptible to Electrocution	Population Level Impacts Observed from EI	Notes (Energy infrastructure abbreviated to EI)
							population change for this species however collision with EI near overwintering sites and during passage is thought to have localised impacts on the population (Boyd and Fox, 2008).
Audouin's Gull	*Larus audouinii*	LC	Y	Y	N	Local	Poorly sited wind farms can result in greater collision risk for gulls (Christel *et al.*, 2013; Thaxter *et al.*, 2015).
Barnacle goose	*Branta leucopsis*	LC	Y	Y	N	Local	High wing loading increases the susceptibility of this species to collision (SNH, 2010; Patterson, 2015).
Barn Owl	*Tyto alba*	LC	Y	Y	Y	Local	Barn owls are often recorded as electrocution and collision victims. Poor mitigation of low voltage lines can therefore cause local level impacts on the population (Alonso, Alonso and Mufioz-Pulido, 1994; Hötker, Thomsen and Jeromin, 2006; Barn Owl Trust, 2015).
Black kite	*Milvus migrans*	LC	Y	Y	Y	Global	Common victim of collision and electrocution across the species range (Prinsen *et al.*, 2012; Gyimesi and Prinsen, 2015; Skov *et al.*, 2016; Sergio *et al.*, 2018).
Black stork	*Ciconia nigra*	LC	Y	Y	Y	Regional	Large numbers are killed or injured by interactions with power lines (Prinsen *et al.*, 2012).
Booted eagle	*Hieraaetus pennatus*	LC	Y	Y	Y	Regional	This species is infrequently recorded as a victim of collision with EI (Hötker) however it is prone to Electrocution on low to medium voltage lines (Janss, 2000).
Cattle egret	*Bubulcus ibis*	LC	Y	N	N	Negligible	A relatively common species; prone to collisions however this is not thought to have population level consequences (Janss, 2000).
Common buzzard	*Buteo buteo*	LC	Y	Y	Y	Local	This common raptor species often uses power lines as hunting perches increasing the risk of electrocution. It is also a commonly recorded collision victim at wind farms and power lines (Pearce-Higgins *et al.*, 2009).
Common crane	*Grus grus*	LC	Y	Y	N	Regional	This soaring species has poor binocular vision and

Species or Group	Latin Name	Conservation Status	Susceptible to Collision with wind farms	Susceptible to Collision with power lines	Susceptible to Electrocution	Population Level Impacts Observed from EI	Notes (Energy infrastructure abbreviated to EI)
							high wing loading. It often comes into conflict with EI constructed along ridgelines (Janss and Ferrer, 2000).
Common raven	*Corvus corax*	LC	Y	N	N	Negligible	Occasionally recorded as a collision victim however this species is not significantly impacted by EI (Hötker, Thomsen and Jeromin, 2006).
Eleonora's Falcon	*Falco eleonorae*	LC	Y	N	Y	Local	As with other falcons, this species is susceptible to electrocution because it uses human structures as hunting perches (Gyimesi and Prinsen, 2015).
Eurasian Sparrowhawk	*Accipiter nisus*	LC	Y	Y	Y	Local	This common and widespread raptor is susceptible to collision and electrocution resulting in localised impacts on the population (SNH, 2010; Prinsen *et al.*, 2012).
Golden eagle	*Aquila chrysaetos*	LC	Y	Y	Y	Regional	Widely reported as a victim of collision with power lines and wind farms. This species also falls victim to electrocution after perching on power lines and can be displaced from suitable breeding habitat by disturbance during wind farm construction (New *et al.*, 2015; Tikkanen *et al.*, 2018b).
Golden plover	*Pluvialis apricaria*	LC	Y	Y	N	Local	Occasionally recorded as a collision victim however this species is not significantly impacted by EI (SNH, 2010).
Goshawk	*Accipiter gentilis*	LC	Y	Y	Y	Regional	This species has a very narrow field of view making it susceptible to collision with manmade structures. These impacts are most closely associated with forest habitats (Janss, 2000; Hötker, Thomsen and Jeromin, 2006).
Greater Black-backed Gull	*Larus marinus*	LC	Y	Y	Y	Regional	Commonly recorded as a collision victim at coastal wind farms and power lines. Unmitigated and poorly planned EI can therefore cause a significant number of mortalities in this species (Hötker, Thomsen and Jeromin, 2006; Fijn *et al.*, 2015).

Species or Group	Latin Name	Conservation Status	Susceptible to Collision with wind farms	Susceptible to Collision with power lines	Susceptible to Electrocution	Population Level Impacts Observed from EI	Notes (Energy infrastructure abbreviated to EI)
Great spotted cuckoo	*Clamator glandarius*	LC	Y	N	Y	Local	This species has been recorded as a victim of electrocution and collision however the impact upon the global population is thought to be negligible (Gyimesi and Prinsen, 2015).
Greenshank	*Tringa nebularia*	LC	Y	Y	N	Local	EI adjacent to wetlands can significantly impact this species in overwintering areas at the local scale (Hötker, Thomsen and Jeromin, 2006).
Grey heron	*Ardea cinerea*	LC	Y	Y	Y	Local	A large water bird with limited capability to avoid collisions. Regularly recorded as a victim of EI however this is not thought to have a population level impact on this species (Janss, 2000; Rubolini *et al.*, 2005).
Greylag Goose	*Anser anser*	LC	Y	Y	N	Local	Poorly sited EI can result in greater collision risk for geese (Rees, 2012).
Griffon vulture	*Gyps fulvus*	LC	Y	Y	Y	Global	These vultures are poor avoiders and regularly build their nests on human structures bringing them into conflict with EI. Electrocution impacts this species at the global level (Lucas *et al.*, 2012).
Jackdaw	*Corvus monedula*	LC	N	N	Y	No	EI is not thought to have a significant impact on this species (Hötker, Thomsen and Jeromin, 2006).
Jay	*Garrulus glandarius*	LC	N	N	Y	Negligible	EI is not thought to have a significant impact on this species (Hötker, Thomsen and Jeromin, 2006).
Lanner Falcon	*Falco biarmicus*	LC	Y	Y	Y	Local	This small migratory raptor often uses perches during hunting making it prone to electrocution on low to medium voltage power lines (Gyimesi and Prinsen, 2015).
Lesser Black-backed gull	*Larus fuscus*	LC	Y	Y	Y	Regional	This species appears to exhibit a mesa avoidance strategy around EI which can make it vulnerable to collisions in poor weather (C. Thaxter *et al.*, 2018).
Lesser kestrel	*Falco naumanni*	LC	Y	Y	Y	Local	Like other falcons, this species often uses power lines as hunting perches. Electrocution and collision mortality is therefore considered to be a major human impact for this

Species or Group	Latin Name	Conservation Status	Susceptible to Collision with wind farms	Susceptible to Collision with power lines	Susceptible to Electrocution	Population Level Impacts Observed from EI	Notes (Energy infrastructure abbreviated to EI)
							species (Janss, 2000; Guil, Colomer and Moreno-opo, 2015).
Lesser Spotted Eagle	*Aquila pomarina*	LC	Y	Y	Y	Regional	Collision and Electrocution are commonly recorded in this species (Gyimesi and Prinsen, 2015).
Levant Sparrowhawk	*Accipiter brevipes*	LC	Y	Y	Y	Local	Electrocution mortality is the most common impact associate with EI for this species (Gyimesi and Prinsen, 2015).
Little egret	*Egretta garzetta*	LC	Y	Y	N	Negligible	Like other Herons, this species is vulnerable to collision but population level impacts are not thought to be a conservation concern for this species (Rubolini *et al.*, 2005).
Long-legged Buzzard	*Buteo rufinus*	LC	Y	Y	Y	Regional	Electrocution is the major mortality risk factor for this species associated with EI resulting in regional level impacts on the population (Gyimesi and Prinsen, 2015).
Magpie	*Pica pica*	LC	N	Y	Y	Negligible	Population level impacts are not observed in this species however it is often found during carcass counts (Janss, 2000) and reduced breeding density within wind farms has been observed (Song *et al.*, 2021).
Mallard	*Anas platyrhynchos*	LC	Y	Y	N	Local	Like other ducks, this species has high wing loading making it more susceptible to collision. Poorly sited EI can have local scale impacts on this species (Larsen and Guillemette, 2007).
Marsh harrier	*Circus aeruginosus*	LC	Y	Y	Y	Regional	This species does collide with EI but the major cause of mortality is electrocution on lower voltage power lines (Janss, 2000; Guil, Colomer and Moreno-opo, 2015; Gyimesi and Prinsen, 2015; Hernández-Pliego *et al.*, 2015).
Merlin	*Falco columbarius*	LC	Y	Y	Y	Local	Electrocution on medium and low voltage power lines results in localised impacts on this species (Janss, 2000).
Moorhen	*Gallinula chloropus*	LC	Y	Y	N	Negligible	As a poor flier this species is a common collision victim however mortality

Species or Group	Latin Name	Conservation Status	Susceptible to Collision with wind farms	Susceptible to Collision with power lines	Susceptible to Electrocution	Population Level Impacts Observed from EI	Notes (Energy infrastructure abbreviated to EI)
							from EI is relatively low compared with the population size.
Mute Swan	*Cynus olor*	LC	Y	Y	N	Local	Collision with EI is recorded relatively frequently in this species however it is not thought to have significant population level impacts (Frost, 2008).
Osprey	*Pandion haliaetus*	LC	Y	Y	Y	Regional	Although this species is recovering in some areas this migratory raptor is among the most susceptible species to collision and electrocution mortality (Janss, 2000; Guil, Colomer and Moreno-opo, 2015; Gyimesi and Prinsen, 2015).
Peregrine falcon	*Falco peregrinus*	LC	Y	Y	Y	Local	The global population of this species appears to be increasing as this falcon is able to utilise human structures for nesting. It is a commonly recorded victim of electrocution and collision; this is partly due to the narrow field of view of this species' visual system (Marques *et al.*, 2014a).
Pink-footed Goose	*Anser brachyrhynchus*	LC	Y	Y	Y	Local	This species is vulnerable to collision where EI is located adjacent to wintering roosts and feeding areas (Rees, 2012).
Rough Legged Buzzard	*Buteo lagopus*	LC	Y	Y	Y	Local	Electrocution is the major mortality risk factor for this species associated with EI resulting in localised impacts on the population (Janss, 2000).
Short-toed Snake Eagle	*Circaetus gallicus*	LC	Y	Y	Y	Regional	Electrocution is a major cause of mortality for this species, particularly for the Iberian population (Loss, Will and Marra, 2014; Gyimesi and Prinsen, 2015).
Spoonbill	*Platalea leucorodia*	LC	Y	Y	N	Regional	Spoonbills have poor binocular vision reducing their avoidance abilities. EI is therefore considered to have regional impacts on population soft this species (Prinsen *et al.*, 2012).
White Pelican	*Pelecanus onocrotalus*	LC	Y	Y	N	Local	Electrocution risk is negligible for this species however collision risk is a major mortality factor in some regions (Gyimesi and Prinsen, 2015).

Species or Group	Latin Name	Conservation Status	Susceptible to Collision with wind farms	Susceptible to Collision with power lines	Susceptible to Electrocution	Population Level Impacts Observed from EI	Notes (Energy infrastructure abbreviated to EI)
White stork	*Ciconia ciconia*	LC	Y	Y	Y	Global	This species regularly nests on power lines; therefore EI has the potential to benefit white storks. However most power lines have poor insulation resulting in high mortality arising from electrocution. Collision with power lines and wind farms is considered to be a major conservation challenge across this species' range however the problem is most acute in Iberia (Janss, 2000; Infante and Peris, 2003; Chris B. Thaxter *et al.*, 2017).
White-tailed Eagle	*Haliaeetus albicilla*	LC	Y	Y	Y	Global	Even compared to other eagles, this species has a poor avoidance rates (only 95% compared with 98% average for Golden Eagle) (SNH, 2010). Electrocution is also a major mortality factor for this species and poorly sited EI can result in displacement of breeding pairs which usually results in mortality (May *et al.*, 2010).
Whooper Swan	*Cygnus cygnus*	LC	Y	Y	N	Local	This species has high wing loading and poor binocular vision. Therefore, power lines sited adjacent to water bodies in northern Europe used by this species over winter pose a significant but localised threat to this species (Griffin, Rees and Hughes, 2010; Rees, 2012).
Wood pigeon	*Columba palumbus*	LC	N	N	Y	Negligible	This species is a common victim of electrocution linked to power lines however this is not thought to have significant population level impacts (Janss and Ferrer, 2000).
Yellow-legged Gull	*Larus michahellis*	LC	Y	Y	N	Local	Gulls appear to be attracted to wind farms which can put them at higher collision risk than other species. Low voltage power lines are also associated with high rates of collision and electrocution resulting in localised population level impacts (Furness, Wade and Masden, 2013; Chris B. Thaxter *et al.*, 2017).

Species or Group	Latin Name	Conservation Status	Susceptible to Collision with wind farms	Susceptible to Collision with power lines	Susceptible to Electrocution	Population Level Impacts Observed from EI	Notes (Energy infrastructure abbreviated to EI)
Passerformes			Y	Y	Y	Local	Passerines are generally not thought to be significantly impacted by collision with power lines and wind farms. Electrocution on low voltage power lines can result in localised declines in some passerine species. The main impact from EI is associated with disturbance and displacement from breeding habitat during the construction and operation phases (Pearce-Higgins *et al.*, 2012; Chris B. Thaxter *et al.*, 2017).
Skua (all species)	*Stercorarius spp.*		Y	Y	N	Local	EI which intersects with Skua colonies can cause displacement and increase collision risk. Electrocution is not considered to be a significant mortality factor for this genus (Janss, 2000; Ross-Smith *et al.*, 2016).
Tern (all species)			Y	Y	Y	Regional	EI adjacent to tern colonies has been shown to cause displacement and collision impacts. Sex-biased collision risk is observed in common terns during the breeding season (Stienen *et al.*, 2008; Kelsey *et al.*, 2018).

Supporting Information Table 1: This table summarises the relative vulnerability of different species or species groups based upon their conservation status, observed collision or electrocution rates and morphology Species and species groups are sorted first by conservation status and then by alphabetical order of the English common name for the species. Conservation status is ranked according to IUCN categories of Endangered (EI), Vulnerable (VU), Near Threatened (NT) and Least Concern (LC). The scale of impacts on each population were ranked according to impact categories used in ecological impact assessments namely: negligible, local (impact observed at the local scale only), regional (a major impact observed a the country or continent scale) or global (impacts are significant enough to negatively affect the global population of the species) (CIEEM, 2018).

APPENDIX B: CHAPTER 2 METHODS SUPPORTING INFORMATION

DOCUMENT DESCRIPTION

This document contains the supplementary material to supplement the methods of the paper “Hotspots in the grid: the avian sensitivity and vulnerability to collision risk form energy infrastructure interactions in Europe and North Africa”. This provides more detail and additional insights beyond what is possible within the word count of the journal. Section 1 provides a high-level summary of the methods. Section 2 summarises the datasets used in the analysis and the spatial distribution of these bird tracking data sets. Section 4 provides more detail on the validation process for the energy infrastructure data. Section 5 described the two digital surface models used in the analysis and how flight height relative to ground level was calculated. Section 6 describes the different methods considered for accounting for uncertainty in our estimates of the proportion of flights at danger height. This provides more background on the Wilson score and the justification for using this instead of the raw percentage or weighted average derived methods commonly deployed in meta-analyses. For the purposes of the thesis, the literature review summary featured in the supplementary material for the published paper is omitted because it is covered by the literature review section.

SECTION 1: OVERVIEW OF METHODS

The flow chart in Figure 1 provides a high-level summary of the methods and outputs in this paper and the supplementary material.

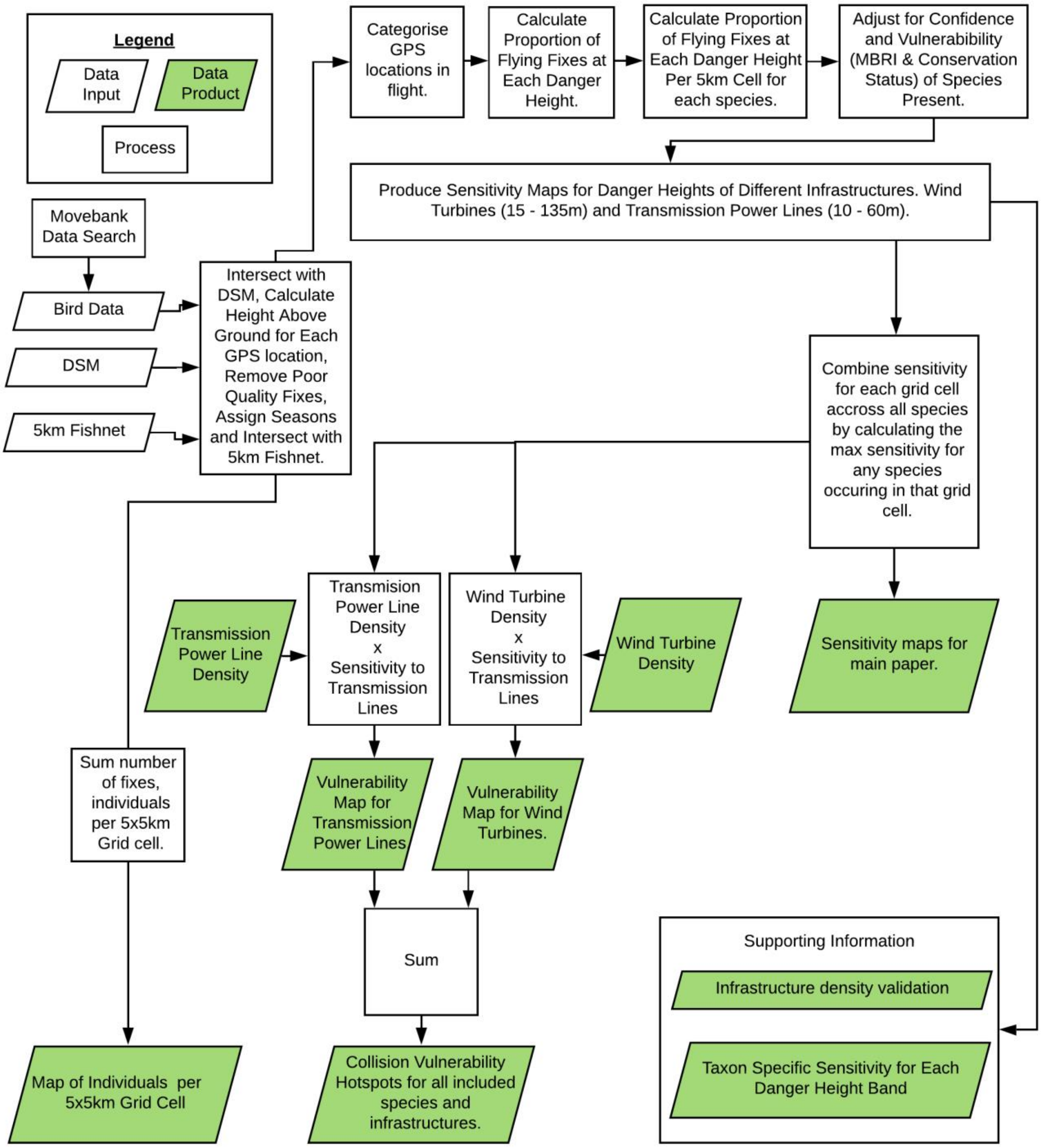

Supporting Information Figure 1: High-level overview of methods and outputs.

SECTION 2: MOVEBANK STUDIES INCLUDED IN THE ANALYSIS FOR CHAPTER 3

Map ID	Study Name	Common Name	Species	Individuals	Start Year	Duration	Number of GPS Points	Country	Authors	DOI (If available) or Movebank Study ID
1	MPIO Lake Constance Mallards GPS	Mallard	*Anas platyrhynchos*	45	2011	6	71992	Switzerland	Wolfgang Fiedler & Martin Wikelski	446579
2	LifeTrack Ducks Lake Constance	Mallard	*Anas platyrhynchos*	52	2017	2	207657	Switzerland	Wolfgang Fiedler	236953686
3	Foraging by white-fronted geese after disturbance (data from Nolet et al. 2016)	White-Fronted Goose	*Anser albifrons*	9	2015	<1	827	Netherland	Andrea Koelzsch	163020445
4	Iberian Imperial Eagle movement ecology 2014 - 2015	Iberian Imperial Eagle	*Aquila adalberti*	10	2016	2	90878	Portugal	Carlos Carrapato	28407489
5	Iberian Imperial Eagle movement ecology 2016	Iberian Imperial Eagle	*Aquila adalberti*	6	2016	1	44858	Portugal	Carlos Carrapato	163340351
6	Iberian Imperial Eagle movement ecology 2017	Iberian Imperial Eagle	*Aquila adalberti*	5	2017	2	94009	Portugal	Carlos Carrapato	292890255
7	Migration timing in barnacle geese (Barents Sea) (data from Kölzsch et al. and Shariatinajafabadi et al. 2014)	Barnacle Goose	*Branta leucopsis*	15	2008	3	2800	Netherland	Michael Exo	20039459
8	Migration timing in barnacle geese (Svalbard) (data from Kölzsch et al. and Shariatinajafabadi et al. 2014)	Barnacle Goose	*Branta leucopsis*	22	2006	5	4743	UK	Michael Exo & Larry Griffin	29799425
9	Barnacle Goose Netherlands	Barnacle Goose	*Branta leucopsis*	23	2015	4	144027	Netherlands	Thomas Lameris	https://doi.org/10.1016/j.cub.2018.05.077
10	Westplaat 6200-6229 2015-2017	Barnacle Goose	*Branta leucopsis*	8	2015	4	501720	Netherland	Thomas Lameris	https://doi.org/10.1016/j.cub.2018.05.077
11	Westplaat 6087-6135 2016-2017	Barnacle Goose	*Branta leucopsis*	10	2016	3	378511	Netherland	Thomas Lameris	https://doi.org/10.1016/j.cub.2018.05.077
12	Eagle owls - 3 breeding pairs - Southern Part The Netherlands	Eurasian Eagle Owl	*Bubo bubo*	6	2010	1	10475	Netherland	René Janssen	4502577

13	Eurasian stone curlew, Giunchi, Italy	Stone Curlew	*Burhinus oedicnemus*	23	2015	2	501720	Italy	Dimitri Giunchi	12883793
14	LifeTrack rough-legged buzzards	Rough Legged Buzzard	*Buteo lagopus*	27	2016	4	378511	Russia	Ivan Pokrovsky	9493874
15	Movements of long-legged buzzards and short-toed eagles	Long-Legged Buzzard	*Buteo rufinus*	13	2011	3	101301	Israel	Guilad Friedemann	34551859
16	Ciconia ciconia Sudewiesen	White Stork	*Ciconia ciconia*	8	2016	2	233031	Germany	Steffen Hollerbach	4502577
17	Eastern flyway spring migration of adult white storks (data from Rotics et al. 2018)	White Stork	*Ciconia ciconia*	36	2012	4	447304	Germany	Ran Nathan & Shay Rotics	560041066
18	Fall migration of white storks in 2014	White Stork	*Ciconia ciconia*	60	2014	<1	737503	Germany	Andrea Flack	doi:10.5441/001/1.bj96m274
19	LifeTrack White Stork Bavaria	White Stork	*Ciconia ciconia*	26	2014	4	903027	Germany	Wolfgang Fiedler	24442409
20	LifeTrack White Stork Greece Evros Delta	White Stork	*Ciconia ciconia*	10	2013	1	61261	Greece	Wolfgang Fiedler	10449535
21	LifeTrack White Stork Bulgaria	White Stork	*Ciconia ciconia*	5	2016	2	87808	Bulgaria /Greece	Wolfgang Fiedler	128184877
22	LifeTrack White Stork Loburg	White Stork	*Ciconia ciconia*	35	2013	5	1070913	Germany	Martin Wilkelski	10449318
23	LifeTrack White Stork Poland	White Stork	*Ciconia ciconia*	4	2013	1	35769	Poland	Martin Wilkelski & Wolfgang Fiedler	10763606
24	LifeTrack White Stork Poland ECG	White Stork	*Ciconia ciconia*	20	2014	1	217113	Poland	Wolfgang Fiedler	25166516
25	LifeTrack White Stork Rheinland-Pfalz	White Stork	*Ciconia ciconia*	82	2015	4	1138668	Germany	Wolfgang Fiedler	76367850
26	LifeTrack White Stork Spain Donana	White Stork	*Ciconia ciconia*	42	2013	2	482731	Spain	Martin Wilkelski & Julio Blas	2988357
27	LifeTrack White Stork Tunisia	White Stork	*Ciconia ciconia*	9	2013	1	80087	Tunisia	Andrea Flack	10157679
28	LifeTrack White Stork Vorarlberg	White Stork	*Ciconia ciconia*	4	2016	3	239994	Switzerland	Wolfgang Fiedler	173641633
29	White Stork Adults 2017	White Stork	*Ciconia ciconia*	19	2017	1	378395	Portugal	Aldina Franco & Marta Serra Acacio	279646867
30	White Stork Adults 2018	White Stork	*Ciconia ciconia*	8	2018	1	2483296	Portugal	Aldina Franco & Marta Serra Acacio	451464940
31	White Stork Adults and Juveniles 2016	White Stork	*Ciconia ciconia*	41	2016	3	674628	Portugal	Aldina Franco	159302811
32	White Stork Juveniles 2014 UEA	White Stork	*Ciconia ciconia*	14	2014	1	24535	Portugal	Aldina Franco	83544657

33	White Stork Juveniles 2017	White Stork	*Ciconia ciconia*	34	2017	2	162603	Portugal	Aldina Franco	279646867
34	White Stork Juveniles 2018	White Stork	*Ciconia ciconia*	34	2018	1	597728	Portugal	Aldina Franco & Marta Serra Acacio	495405707
35	Black Storks Portugal 2018	Black Stork	*Ciconia nigra*	7	2018	<1	32092	Portugal	Aldina Franco	518635174
36	LifeTrack Black Stork	Black Stork	*Ciconia nigra*	19	2017	2	5317	Germany	Wolfgang Fiedler	291047293
37	Movements of long-legged buzzards and short-toed eagles (short-toed Eagle)	Short-toed Eagle	*Circaetus gallicus*	11	2011	3	93477	Portugal	Guilad Friedemann	34551859
38	Western Marsh Harriers breeding near the Belgium-Netherlands border	Marsh Harrier	*Circus aeruginosus*	6	2013	5	312640	Belgium	Peter Desmet	http://doi.org/10.5281/zenodo.3826591
39	Lifetrack Circus pygargus	Montagu's Harrier	*Circus pygargus*	12	2016	2	23108	Spain	Bernd Vorneweg & Wolfgang Fiedler	166943336
40	Hybrid Spotted Eagles Lithuania GPS 2015-2017	Hybrid Spotted Eagle	*Clanga clanga x pomarina*	4	2015	3	246405	Lithuania	Ramunas Zydelis	150764908
41	LifeTrack Whooper Swan Latvia	Whooper Swan	*Cygnus cygnus*	9	2015	2	55461	Latvia	Martin Wikelski	92261778
42	LifeTrack Peregrine falcon	Peregrine Falcon	*Falco peregrinus*	15	2015	4	7165	Belarus	Ivan Pokrovsky	103426553
43	Bald Ibis Waldrappteam 2	Northern Bald Ibis	*Geronticus eremita*	148	2018	6	281120	Italy	Johannes Fritz, Martin Wikelski & Emanuel Pixner	https://doi.org/10.1111/izy.12163
44	Proyecto Eremita Geronticus eremita Reintroduction in Andalusia (Spain)	Northern Bald Ibis	*Geronticus eremita*	26	2013	1	1440825	Spain	Jose Manuel Lopez Vazquez	463673774
45	Common Crane Lithuania GPS, 2015-2016	Common Crane	*Grus grus*	2	2015	3	98967	Lithuania	Ramunas Zydelis & Mindaugas Dagys	146932094
46	Common Crane Lithuania GPS, 2016	Common Crane	*Grus grus*	1	2016	3	177316	Lithuania	Ramunas Zydelis & Mindaugas Dagys	195375760
47	GPS telemetry of Common Cranes, Sweden	Common Crane	*Grus grus*	19	2013	4	580929	Sweden	Ramunas Zydelis	10722328
48	Eurasian Griffon Vultures 1 Hz HUJ (Israel)	Griffon Vulture	*Gyps fulvus*	9	2014	<1	226588	Israel	Ran Nathan & Roi Harel	16924201
49	Gyps fulvus Griffon vulture FWFF Kresna Gorge - Bulgaria	Griffon Vulture	*Gyps fulvus*	17	2016	3	412459	Bulgaria	Hristo Peshev	305278048

50	Soaring flight in Eurasian griffon vultures (HUJ) (data from Harel and Nathan, 2018)	Griffon Vulture	*Gyps fulvus*	10	2012	1	1999314	Israel	Ran Nathan & Roi Harel	467005392
51	BTO Lesser Black-backed Gull Bowland	Lesser Black-backed Gull	*Larus fuscus*	27	2015	4	138331	United Kingdom	Gary Clewley, Emily Scragg, Chris Thaxter & Niall Burton	Movebank study IDs: 277843980 and 167983392
52	FTZ_Lesser_Black_Backed_Gull	Lesser Black-backed Gull	*Larus fuscus*	8	2010	<1	42552	Germany	Stefan Garthe	82452206
53	BTO Lesser Black-backed Gull Orford Ness	Lesser Black-backed Gull	*Larus fuscus*	23	2010	5	400600	United Kingdom	Chris Thaxter, Viola Ross-Smith, Willem Bouten and Niall Burton	http://www.uva-bits.nl
54	BTO Lesser Black-backed Gull Ribble	Lesser Black-backed Gull	*Larus fuscus*	28	2016	3	82452	United Kingdom	Gary Clewley, Emily Scragg, Chris Thaxter, Willem Bouten and Niall Burton	Movebank study IDs: 277841852 and 167983392; and http://www.uva-bits.nl
55	BTO Lesser Black-backed Gull Skokholm	Lesser Black-backed Gull	*Larus fuscus*	25	2014	3	2519264	United Kingdom	Chris Thaxter, Viola Ross-Smith, Willem Bouten and Niall Burton	http://www.uva-bits.nl
56	BTO Lesser Black-backed Gull Walney	Lesser Black-backed Gull	*Larus fuscus*	29	2014	4	1802192	United Kingdom	Gary Clewley, Emily Scragg, Chris Thaxter Willem Bouten and Niall Burton	http://www.uva-bits.nl; and Movebank study ID: 167983392
57	Eurasian wigeons spring 2018	Eurasian Wigeon	*Mareca penelope*	19	2018	1	343249	Netherland	Mariëlle Van Toor Jonas Waldenström	412700082
58	Egyptian vulture EB Terra Natura UA Spain	Egyptian Vulture	*Neophron percnopterus*	7	2007	6	7612	Spain	Pascual López-López	20106351
59	Neophron percnopterus Bulgaria/Greece	Egyptian Vulture	*Neophron percnopterus*	8	2018	1	142853	Bulgaria & Greece	Steffen Oppel, Stoyan Nikolov, Vladimir Dobrev, Volen Arkumarev, Elzbieta Kret, Victoria Saravia	15869951

60	Osprey in Mediterranean (Corsica, Italy, Balearics)	Osprey	*Pandion haliaetus*	13	2017	2	764213	Italy	Olivier Duriez, Flavio Monti, Andrea Sforzi	20039459
61	Honey_Buzzard_NL	Honey Buzzard	*Pernis apivorus*	29	2008	11	1070920	Netherlands	Wouter Vansteelant, Jan van Diermen, Willem van Maanen and Willem Bouten	https://doi.org/10.1111/jav.00457 & https://doi.org/10.1111/1365-2656.12593
62	Eurasian Spoonbill - Tour du Valat - Camargue (France)	Eurasian Spoonbill	*Platalea leucorodia*	3	2017	2	387	France	Jocelyn Champagnon	311803430
63	Little Bustard Movement Ecology 2015 - 2016	Little Bustard	*Tetrax tetrax*	7	2015	2	68979	Portugal	João P Silva	56464970
64	Little Bustard Movement Ecology 2017 - 2018	Little Bustard	*Tetrax tetrax*	11	2017	2	80200	Portugal	João P Silva	253940991
65	Little Bustard Movement Ecology 2018 - 2019	Little Bustard	*Tetrax tetrax*	8	2018	1	30976	Portugal	João P Silva	461568973
66	Barn owl (*Tyto alba*)	Barn Owl	*Tyto alba*	151	2016	1	2001600	Switzerland	Robin Séchaud	231741797

Supporting Information Table 2: This table provides a summary of the 65 studies included in the analysis and the main contact for each study. The study “Movements of long-legged buzzards and short-toed eagles (Short-toed Eagle)” is multispecies and therefore listed twice. The Eurasian spoonbill Platalea leucorodia data set was described on Movebank as containing 7 birds but only the 3 with height data were included in the analysis.

SECTION 3: ENERGY INFRASTRUCTURE DATA PREPARATION AND VALIDATION

Here we assess how the open-source Openinfra data set of power lines (Garret, 2018) and the paid for wind farm data (Pierrot, 2018) used in our analysis compares against official data sets for The Netherlands and Portugal (Supporting Information Figure 2). We recognise that single country validations are not representative of the whole continent, however in the absence of complete official data sets for other countries it does provide insight into how representative these data sets are. Both data sets were processed in ArcMap (ESRI, 2018).

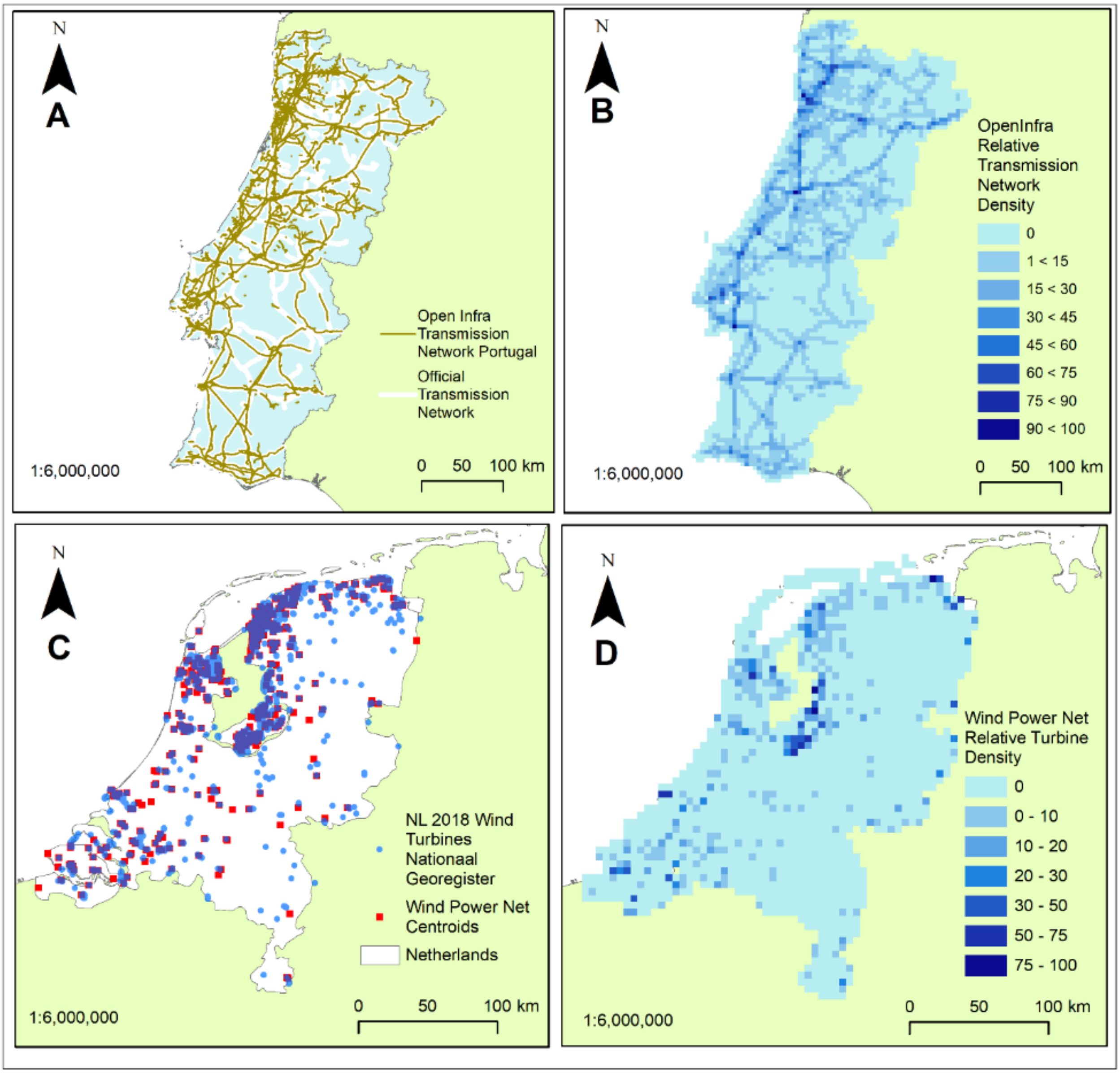

Supporting Information Figure 2: A. displays the raw data for the transmission power line network in Portugal overlaying the Open Infrastructure data set (brown) onto the official REN data set, B. maps the relative density of transmission power lines derived from the open infrastructure data, C. compares the official wind farm data with data derived from windpower.net for the Netherlands. The main differences arise from how the windpower.net maps windfarm centroids rather than individual turbines. D. displays the relative density of wind turbines derived from the windfarm.net dataset, this successfully reflects the broad patterns of high and low densities of wind turbines in the landscape.

Although there is guidance for digitisers (OpenStreetMap, 2018, 2019) the open-source nature of how OpenStreetMap data is collected results in inconsistencies in the attributes of each feature (Chilton, 2009). To resolve these issues, we reclassified all line features of the same voltage as one consistent numerical voltage. In some cases, voltage is inferred from the other data such as line type.

In OpenStreetMap terminology ‘minor lines’ are low or medium voltage (<50kV) whereas ‘lines’ are high voltage (>50kV) (OpenStreetMap, 2019). This differs from power companies who typically use 66kV as the cut off between medium and high-tension power lines (EDP Commercial, 2011). Representation of distribution power lines (under 50kV) is poor with significant gaps in several regions. To our knowledge, no alternative pan-European sets are available hence impacts relating to the distribution network (<50kV) could not be used in this study.

For transmission lines (>50kV) the Open Infra dataset has 13,286.89km of lines within Portugal, while the official data set has 17,472.99km, the overlap between the two is 10,813.72km, (62%) indicating an underestimate in total line length in the OpenInfra data set (Supporting Information Figure 2). In some areas, the OpenInfra data includes line features which do not feature in the official data set. This disparity also arises where some line features have been digitised in a slightly different location compared to the same feature in the official data set. As such when the two data sets are intersected, this excludes line sections in approximately the correct location, but which may be a few metres out from the corresponding line in the official data set. To measure power line density, we determined the total length of transmission lines in each 5km grid square and normalise this onto a 0 – 100 scale to give a relative density of transmission lines in any grid cell in Portugal. Using this relative measure of transmission power line density, there is high level of agreement between the relative density of power lines in each 5km grid square resulting from Open Infra and the official dataset for >50kV. Within Portugal, the mean difference in relative density between the two data sets per grid cell is calculated to be 0.44 with a standard deviation of 4.96. Relatively few grid squares (0.06%) contain a major over or under-estimates of transmission line density and overall, 81.04% (3304) of cells possess almost identical estimates of power line density (0 ± 5). This indicates that while there may be some gaps in the OpenInfra data set resulting in an underestimate of absolute line length for Portugal, when used to create the relative density surface it results in similar scores for the majority of grid cells and correctly identifies regions of higher transmission line density.

Some entries in the WindPower.net database lacked location information (n= 1424). Through a search for planning documents, we found co-ordinates for 171 of the 231 records with more than eight turbines which were missing co-ordinates. We excluded wind farms without spatial reference (n = 1253, 6.4% of entries). Where number of turbines was not available (n=602), the total power output was used as a proxy. The output for a standard commercial terrestrial turbine is currently in the region of 2000 - 2500kw (Komusanac, Fraile and Brindley, 2019). Wind farms with a power output of less than 2000kw were categorised as single turbines. We classified wind farms without power information as single turbines (n = 7). For the remaining wind farms (n = 595) with power information, we used this as a proxy for the number of wind turbines by dividing the total power output of the wind farm by 2000 and rounding to the nearest integer. We calculated the number of wind turbines per 5km x 5km grid cell using a spatial join to sum the total number of turbines within each cell. This was then normalised to a scale of 0 -100.

We determined the minimum height for each wind turbine by subtracting the radius of turbines within each wind farm from the hub height and the maximum height by summing the hub height and turbine radius. The height band was obtained by subtracting the standard deviation of minimum heights (12.78m) from the mean minimum height of the wind farm data set (32.51m) and rounding to the nearest 5m (15m). The upper bound of the height band was derived by summing the standard deviation of maximum wind turbine heights (23.83m) with the mean maximum height of wind turbines in the data set (113.37m) and rounding up to the nearest 5m (135m). A GPS location between 15 – 135m therefore indicates that the tracked bird is present at a height where there is potential risk of collision with a turbine.

We assess the validity of the WPN data set against that of the register of wind turbines for the Netherlands available on the Arc GIS web map service (Nationaal Georegister, 2018, ESRI 2019). This includes the locations of all commercial wind turbines installed as of 2018. There are some disparities related to how the WPN data set represents multiple turbines as a single point location instead of providing locations for individual turbines. This centroid may fall on one side or the other of a grid cell boundary. This is mainly an issue for larger wind farms which may extend of a larger area than a single 5km x 5km grid cell.

For wind turbines, we quantify the validity of the WPN data set by subtracting the relative density derived from the official data set for the Netherlands (Nationaal Georegister, 2018). For the 1702 grid cells in the Netherlands, the mean difference in relative density is -0.14 with a standard deviation of 5.4 for this difference score. 1480 grid cells (87%) have the same or similar relative density (within +/- 0.5 standard deviations from each other i.e. +/- 2.7). The main source of disparity between the two data sets is a product of the WPN data set representing multiple turbines as a single centroid, which may fall on one side or the other of a grid cell boundary. The official Nationaal Georegister data set plots the locations of individual turbines. As such, turbines belonging to the same wind farm may straddle several grid cells. Overall, our assessment is that the final density surface produced from the continent scale WPN data set provides a good representation of the spatial distribution of the density of wind energy infrastructure.

A recent publication, not available at the time of our analysis, has demonstrated how open-source data can be used to create a reliable spatial data resource for researchers working in fields related to renewable energy. Below in Supporting Information Figure 3 and Supporting Information Figure 4 we compare this newer data set from Dunnet *et al.* 2020 with the windpower.net data set used in our analysis. This shows that between 2018 and 2020 more wind turbines have been constructed meaning that the maximum number of wind turbines in one grid cell is now higher however the overall pattern of wind farm density is similar across both data sets suggesting that the Dunnet *et al.* 2020 would not represent a significant update relative to the windfarm.net data set. However, going forward, future analyses could make use of their R code to produce a more up to date wind turbine density surface from OpenStreetMap^{TM} data.

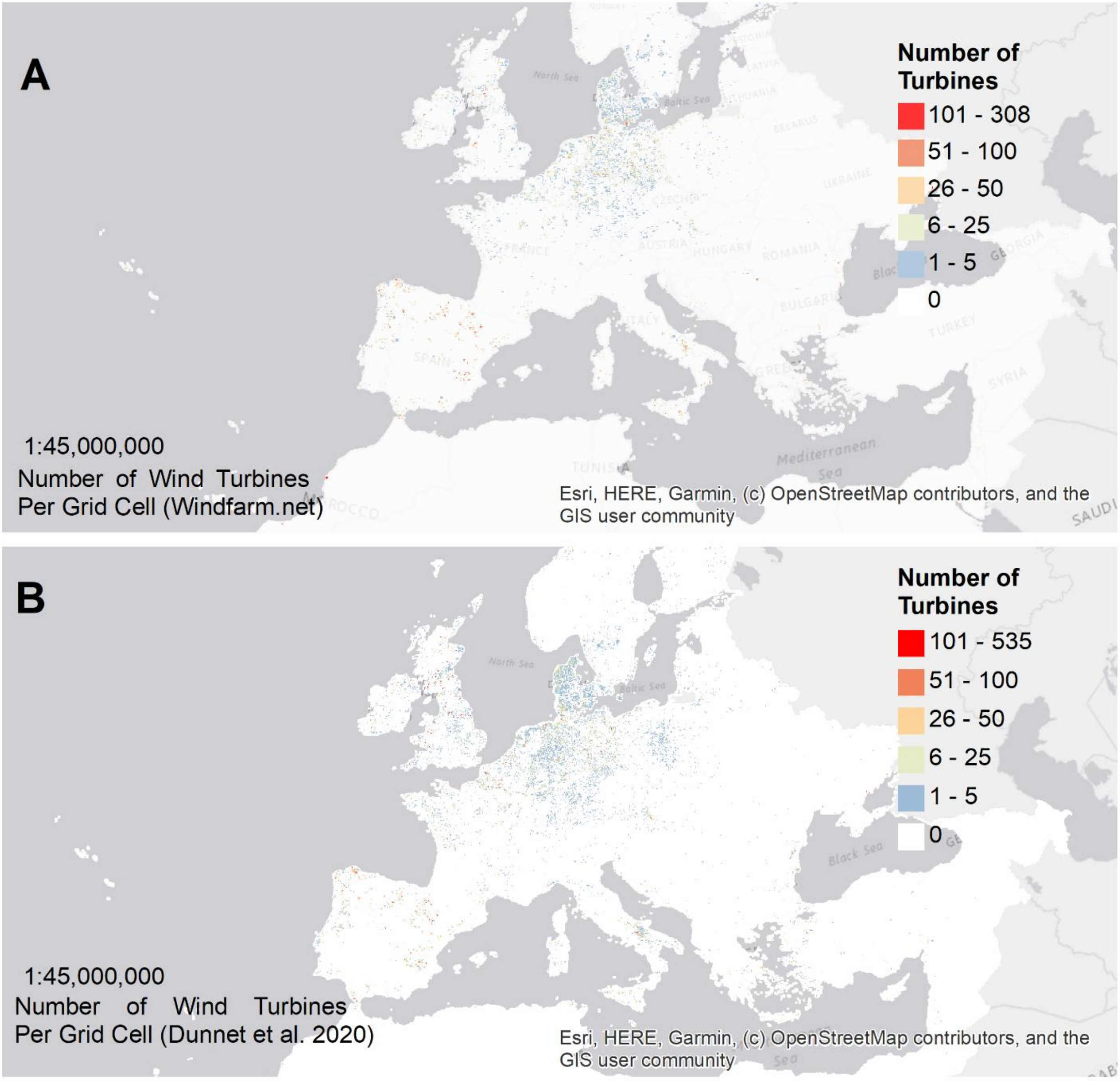

Supporting Information Figure 3: A comparison between the density of wind turbines as measured by the windfarm.net data set (Panel A) and the Dunnet et. al. 2020 data set (Panel B) highlighting how both result in similar patterns of wind turbine density across the study area with Germany and Northern Europe possessing the greatest coverage of wind farms.

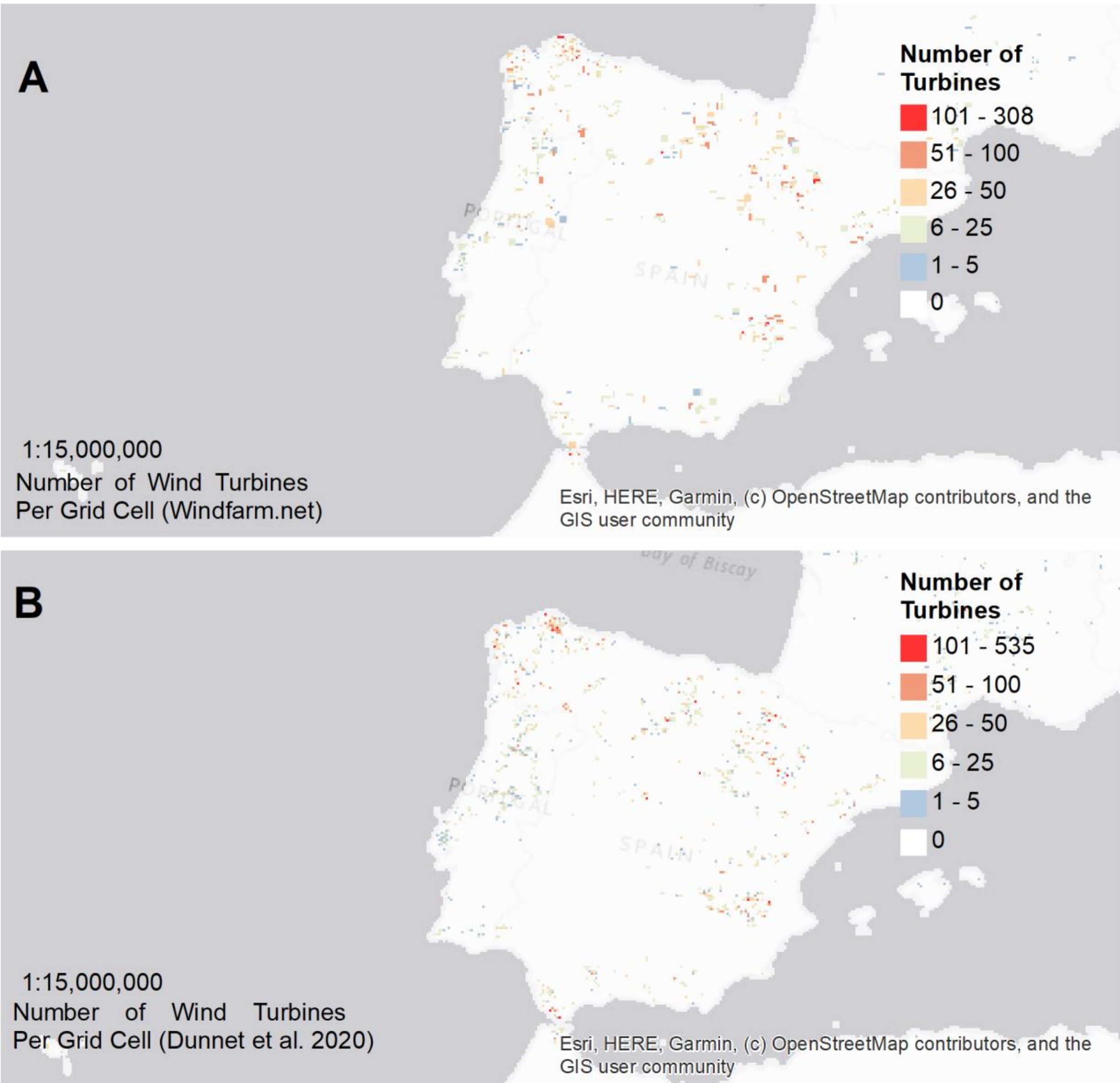

Supporting Information Figure 4: A comparison between the density of wind turbines as measured by the windfarm.net data set (Panel A) and the Dunnet et. al. 2020 data set (Panel B) highlighting how both result in similar patterns of wind turbine density across Iberia where a key migratory bottleneck exists in southern Spain.

SECTION 3 REFERENCES

Dunnett, S. *et al.* (2020) 'Harmonised global datasets of wind and solar farm locations and power', *Scientific Data*. Springer US, 7(1), p. 130. doi: 10.1038/s41597-020-0469-8.

ESRI (2018) 'ArcGIS Desktop: Release 10.6.1'. Redlands, CA: Environmental Systems Research Institute.

Garret, R. (2018) *The Open-source Infrastructure Project*, *OpenInfra*. Available at: https://opensourceinfra.org/ (Accessed: 5 November 2018).

Komusanac, I., Fraile, D. and Brindley, G. (2019) *Wind energy in Europe in 2018 - Trends and statistics*. Available at: policy@windeurope.org.

Nationaal Georegister (2018) *Wind Molens Nederland TOP.10.NL*, *ESRI Web Map Service*. Available at: http://www.nationaalgeoregister.nl/geonetwork/srv/dut/catalog.search#/metadata/07fc19de-369f-4b62-8eee-fabee3c89faa (Accessed: 20 July 2019).

Pierrot, M. (2018) *The Wind Power: Wind Energy Market Intelligence*. Tournefeuille, France. Available at: https://www.thewindpower.net.

SECTION 4: TERRAIN MODEL DATA AND FLIGHT HEIGHT CLASSIFICATION

To calculate height above ground, for each GPS location, we used two 5m vertical accuracy, 30m horizontal resolution Digital Surface Models (DSM) (Displayed in supplementary material A5). One surface, a 30m resolution height above ellipsoid surface model was constructed by combining tiles from the ALOS World 3D – 32 Bit 30m Ellipsoidal DSM (JAXA, 2016) and the Shuttle Radar Topography Mission (SRTM GL1) ellipsoid DSM in a mosaic to new raster operation. Both datasets are Global 32 Bit 30m Ellipsoidal terrain models available from the OpenTopography data portal (National Science Foundation, 2019). The second surface, a 30m resolution DSM with units in height above sea level, was created in the same manner by combining tiles from the ALOS World 3D – 32 Bit 30m resolution orthometric DSM. In both DSM models, it was necessary to use ALOS DSM tiles for all locations at latitudes greater than 60°N because STRM GL1 DSM data is not available at higher latitudes. Compared to the STRM-GL1 data, one disadvantage of the ALOS data is that the radar system used by the Japan Aerospace Exploration Agency (JAXA) to scan the Earth's surface suffers from interference due to cloud cover. As such, gaps occur in the DSM at higher latitudes in both the ellipsoidal and orthometric data sets (>60° Latitude), but these do not significantly affect the study area at more southerly latitudes where the STRM surface was used. Surface elevation data was appended to the bird tracking data using the Raster Package (Hijmans 2019). Bird height relative to ground level was then calculated by subtracting Elevation (relative to the Ellipsoid) from bird altitude relative to the ellipsoid, or where altitude was given relative to sea level, Elevation relative to sea level was used. Locations associated with outlier heights (outwith the 95% confidence interval) were removed from the data set and the resulting distribution of heights is displayed in Figure 5 and Figure 6. Across all GPS locations (including stationary GPS locations, n = 46.9 million), prior to further processing, the mean height relative to ground = 119.0m; descriptive statistics of flight height for each of the 27 species is provided in Supplementary Material S1 section 5. These negative altitude GPS locations are usually associated with periods when the bird is on the ground where line of sight to the satellites used to acquire a location may be obstructed by features on the landscape (Silva et al., 2017). The majority of flight heights observed in the data set are below 300m and we also observe variation in flight heights within and between species (Supporting Information Table 1). The proportion of negative altitude GPS locations appears to vary considerably between species. This is possibly linked to two factors. The first being body size and the resulting impact on the tag type which can be fitted to the bird which in turn can affect the position accuracy, in turn this influences the available power for the tag to keep the GPS activated (Poessel *et al.* 2018, Peron *et al.* 2019). The second is possibly in relation to the species-specific flight behaviour. For example, the Barn Owl *Tyto alba* tracking data is associated with a high proportion of negative altitude locations. This is a species which spends much of its flight time hunting in close proximity to the ground. Whereas Iberian Imperial Eagle *Aquila fasciata* is associated with only 1.4% negative altitude GPS locations, this species is a large soaring bird which tends to scan for prey from higher altitudes where there is less risk of line of sight being obstructed by near-ground objects. As a larger species, it is also capable of carrying a heavier device with a larger battery which in turn can enable to the GPS to remain switched on for longer periods to improve accuracy of the acquired position.

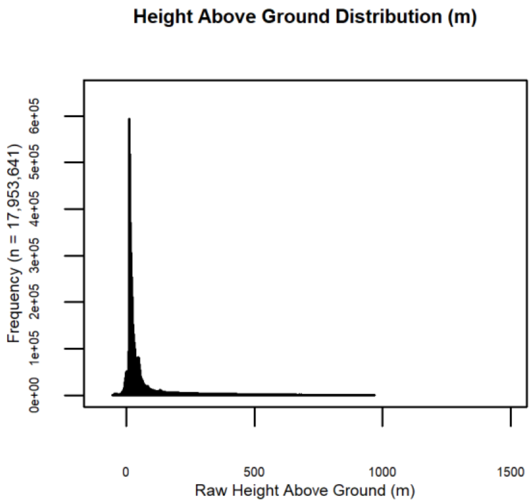

Supporting Information Figure 5 Frequency distribution of raw heights relative to ground for all GPS locations after subsampling the data set to a minimum GPS location interval of 1 minute and outlier GPS locations beyond the 95% confidence interval of heights were removed. The Majority of GPS locations are near ground level.

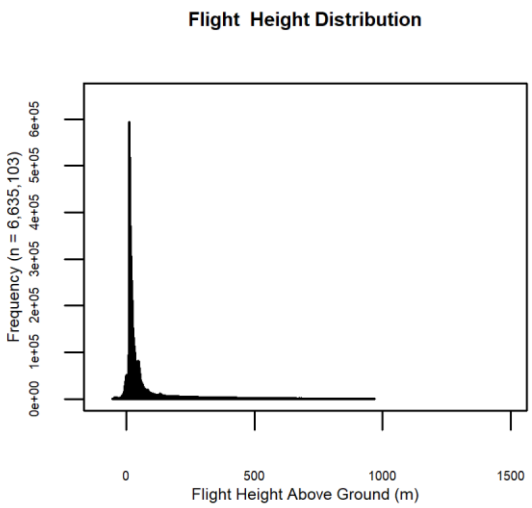

Supporting Information Figure 6: Distribution of heights relative to ground (m) for all GPS locations classified as in height using height and speed.

7023

Common Name	Species	Total GPS locations in Flight	Mean Flight Height (m)	SD	Minimum Flight Height (m)	Maximum Flight Height (m)	Percent at Danger Height for Transmission Lines	Percent at Danger Height for Wind Turbines	Percentage of Flight Locations associated with a Negative Altitude
Mallard	Anas platyrhynchos	13982	39.51	77.36	-53	927	74.2	57.45	6.69
White-fronted Goose	Anser albifrons	138	31.42	24.72	-10.88	153.11	82.61	57.97	3.62
Iberian Imperial Eagle	Aquila adalberti	92004	127.26	211.19	-53.4	968.39	65.21	40.42	1.39
Barnacle Goose	Branta leucopsis	15166	93.06	154.27	-53	948.36	16.77	23.06	39.54
Eurasian Eagle Owl	Bubo bubo	4433	29.18	33.32	-38.08	769.93	91.68	71.06	0.47
Stone Curlew	Burhinus oedicnemus	512	3.5	75.56	-53	864	35.35	30.86	50.59
Rough-legged Buzzard	Buteo lagopus	9637	37.13	76.31	-49.9	959.62	86.47	59.75	1.5
Long-legged Buzzard	Buteo rufinus	64703	91.55	136.06	-53.97	967.85	58.49	54.82	3.03
White stork	Ciconia ciconia	4027158	90.94	174.53	-53.95	968.6	71.9	52.85	2.03
Black Stork	Ciconia nigra	4014	305.95	278.89	-53.45	968.26	17.41	20.4	6.83
Short-toed Snake Eagle	Circaetus gallicus	84953	172.59	176.6	-53.65	968.44	36.57	39.88	1.88
Western Marsh Harrier	Circus aeruginosus	92156	46.17	109.67	-53	968	30.74	26.35	12.31
Montagu's Harrier	Circus pygargus	8097	264.73	273.3	-53.86	968.21	13.3	21.77	12.76

Hybrid Spotted Eagle	Clanga clanga x pomarina	71943	212.64	232.1	-53	968	34.52	37.67	1.83
Whooper Swan	Cygnus cygnus	5463	20.15	30.04	-48.02	755.28	86.82	44.06	4.7
Peregrine Falcon	Falco peregrinus	7280	47.44	69.42	-53.31	955.31	70.4	76.1	3.37
Northern Bald Ibis	Geronticus eremita	617011	50.62	80.35	-53.96	968	63.3	63.98	4.55
Common Crane	Grus grus	77749	81.58	171.24	-53.98	968	46.18	42.52	20.83
Griffon Vulture	Gyps fulvus	370953	185.99	225.13	-53.6	968.5	38.72	49.43	1.68
Lesser-black Backed Gull	Larus fuscus	745237	60.02	98.36	-53.9	968	53.21	57.04	7.01
Eurasian Wigeon	Mareca penelope	4996	45.7	92.11	-52	964	70.36	56.69	4.34
Egyptian Vulture	Neophron percnopterus	50174	128.37	209.7	-53	968	48.84	52.91	4.61
Osprey	Pandion haliaetus	18897	71.19	132.32	-51	966	66.21	56.7	1.94
Honey Buzzard	Pernis apivorus	222469	158.39	226.28	-53	968	45.29	39.39	2.59
Eurasian Spoonbill	Platalea leucorodia	54	39.75	50.59	10	305	64.81	59.26	0
Little Bustard	Tetrax tetrax	25216	23.86	27.63	-50.49	916.98	92.57	55	1.32
Barn Owl	Tyto alba	708	-3.66	65.41	-53.99	696.71	27.97	26.41	61.72

Supporting Information Table 3: Number of flying GPS locations and individuals by species and the percentage of these GPS locations within each danger height band. The table is sorted by each species in alphabetical order.

SECTION 4 REFERENCES

National Science Foundation (2019) *Open Topography Data Portal*, *OpenTopography*. Available at: https://opentopography.org/news/three-new-global-topographic-datasets-available-srtm-ellipsoidal-alos-world-3d-gmrt (Accessed: 1 February 2019).

Hijmans, R. J. (2019) ‘Raster: An R Package for working with raster data’. Available at: https://www.rspatial.org/.

Poessel, S. A. *et al.* (2018) ‘Improving estimation of flight altitude in wildlife telemetry studies’, *Journal of Applied Ecology*, 55(4), pp. 2064–2070. doi: 10.1111/1365-2664.13135.

Péron, G. *et al.* (2020) ‘The challenges of estimating the distribution of flight heights from telemetry or altimetry data’, *Animal Biotelemetry*. BioMed Central, 8(5), pp. 1–13. doi: 10.1101/751271.

SECTION 5: SUMMARY OF BREEDING SEASON CLASSIFICATION

For migratory species, there is variation within and between populations. To account for this, the breeding season was identified for each individual bird tracking data set used in the analysis by plotting the week of the year against latitude. This allowed the periods of stable latitude to be identified and classified. We use this to distinguish between the breeding season as the period of the year when birds are mostly constrained to breeding locations and the non-breeding season (including the migratory period). We do this because the impact of bias relating to the distribution of GPS tag deployment across the study area, which is mostly undertaken within the vicinity of breeding sites, is most evident during the breeding season. Examples of these plots are provided in Supporting Information Figure 7. Debate surrounding the most optimal approach to categorising breeding vs. non-breeding seasons is ongoing in the literature (Soriano-Redondo *et al.* 2020, Cerritelli *et al.* 2020). This simple approach allowed us to easily and transparently account for the large variation in movement behaviour and data structures between the 65 data sets.

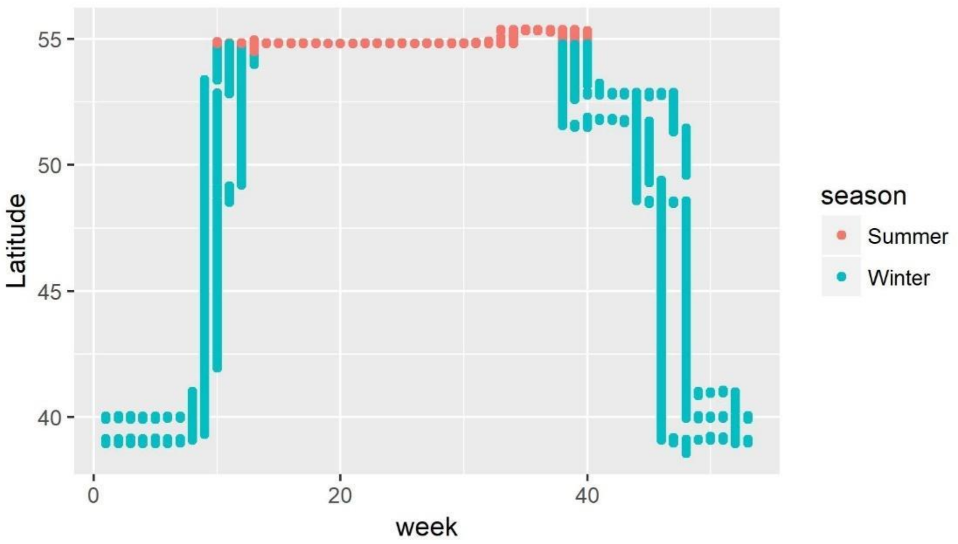

Supporting Information Figure 7: Example plot illustrating how the manual classification of the Breeding Season for Common Crane Gus grus was performed for the data set Žydelis, R. & Dagys, M. (2015) Common Crane Lithuania GPS, 2015-2016.

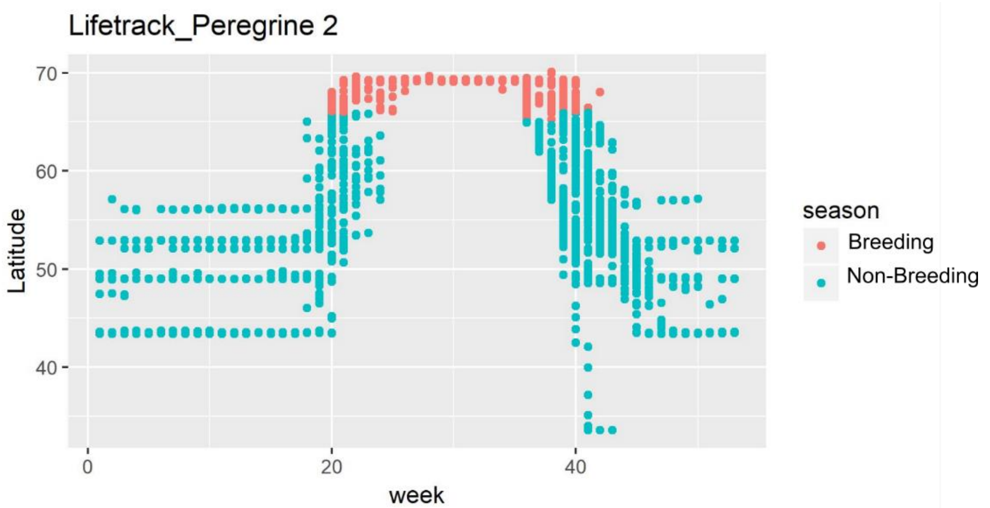

Supporting Information Figure 8: Classification of 'Breeding' and 'Non-Breeding' periods for Peregrine Falcon Falco peregrinus from the data set Pokrovsky, I. (2015) LifeTrack Peregrine Falcon, available on request from www.movebank.org.

Section 5 References

Cerritelli, G. *et al.* (2020) 'Simpler methods can outperform more sophisticated ones when assessing bird migration starting date', *Journal of Ornithology*. Springer Berlin Heidelberg, 161(3), pp. 901–907. doi: 10.1007/s10336-020-01770-z.elli

Soriano-Redondo, A. *et al.* (2020) 'Testing alternative methods for estimation of bird migration phenology from GPS tracking data', *Ibis*, 162(2), pp. 581–588. doi: 10.1111/ibi.12809.

SECTION 6: METHODS FOR INCLUDING OUR CONFIDENCE IN OUR ESTIMATE OF THE PROPORTION OF FLYING GPS LOCATIONS AT DANGER HEIGHT IN CELLS WITH VARYING SAMPLE SIZES

A central input to the analysis in this paper is the use of altitude data from GPS telemetry to estimate how sensitive birds recorded in each grid cell are to energy infrastructure developments. We do this by classifying each flying GPS location as at danger height (0) or not at danger height (1) for a given height band. Within each grid cell we then sum the total number of GPS locations in flight (n) and seek to estimate the proportion (P) of these GPS locations at danger height. As such we can think of this estimate as a binary proportion because we are essentially seeking to estimate the proportion of GPS locations in flight where danger height = TRUE. Simply calculating the percentage fails to provide us with any information about the certainty of our estimate in relation to the sample size. For example, in a cell with sample size n = 2 the observed binary proportion (*p*) is constrained to 0, 0.5 or 1. Therefore, by chance it is highly likely that unless we account for uncertainty, our analysis will classify a large number of grid cells with poor certainty with a higher sensitivity score than grid cells where we have higher certainty due to a large sample size. Ideally, we would suppress the scores of cells with poor certainty relative to other cells with high certainty for a given value of *p* as you would seek to reduce the influence of lower quality results on the estimated effect size in a meta-analysis (Stewart, Pullin and Coles, 2007; Doncaster and Spake, 2018).

There is a significant body of academic literature in statistics but also in other quantitative fields such as biosciences and computing about how to improve the accuracy of these point estimates. where the average is weighted to account for the variance or sample size (Stewart, Pullin and Coles, 2007; One such approach uses the Confidence interval (CI) to adjust the point estimate based upon the confidence in that sample (Brown, Cai and Das Gupta, 2001; Pobocikova, 2010) or in some cases the lower bound of the CI is used (Reichensdörfer, Odenthal and Wollherr, 2017). Here we outline how the Wilson’s confidence interval can be used to incorporate uncertainty into estimates of a proportion (Pobocikova, 2010).

Confidence intervals are a measure of our confidence in our estimate of P, small sample sizes are generally associated with reduced confidence and therefore larger confidence intervals (Wilson, 1927). This can help us understand and improve our point estimates for the true value of *p*. Here we present two different confidence intervals, evaluate how they impact the data and describe which approach is most suited to this analysis. We use the 'binconf' function from the R package 'Hmisc' to calculate these confidence intervals (Harrell, 2018).

<u>Wald</u>

The Wald interval, sometimes referred to as the normal approximation interval, is historically, one of the most commonly used approaches for calculating point estimates for binomial proportions (Agresti and Coull, 1998). This is because it is relatively simple to calculate:

$$\rho \ \pm z\sqrt{\frac{\rho(1-\ \rho)}{n}}$$

Where ρ is the point estimate of the proportion of GPS locations at danger height, n is the sample size i.e. the number of flying GPS locations and z is the desired confidence interval. However, several researchers have highlighted limitations of the Wald interval. Two issues are relevant to our analysis. The first issue is that the Wald interval performs poorly at sample sizes of 40 or less (Lewis and Sauro, 2006; Lott and Reiter, 2018) resulting in erratic point estimates. The second key issue is how the resulting lower and upper bounds of the 95% confidence interval are not constrained to between 0 and 1 as with other methods (Brown, Cai and Das Gupta, 2001; Pobocikova, 2010).

<u>Wilson</u>

The Wilson confidence interval is generally considered superior to the Wald interval (Pobocikova, 2010; Lott and Reiter, 2018; Park and Leemis, 2019).

$$\frac{\hat{p}}{1} \pm \frac{\frac{z^2}{2n}}{\frac{z^2}{n}} \sqrt{\frac{\hat{p}(1-\hat{p})}{n} + \frac{z^2}{4n^2}}$$

$\hat{p}$ = the observed proportion of observations at danger height, n = the sample size and z is the required confidence interval. For a 95% confidence interval, this would be 1.96. This estimate of the binomial confidence interval performs better than alternative intervals at low sample sizes while at larger sample sizes it yields broadly similar coverage (Lewis and Sauro, 2006; Lott and Reiter, 2018). As with the Wald interval, the distribution of the point estimate is broadly similar to that of the raw percentages of flights at danger height (visible in the next two plots).

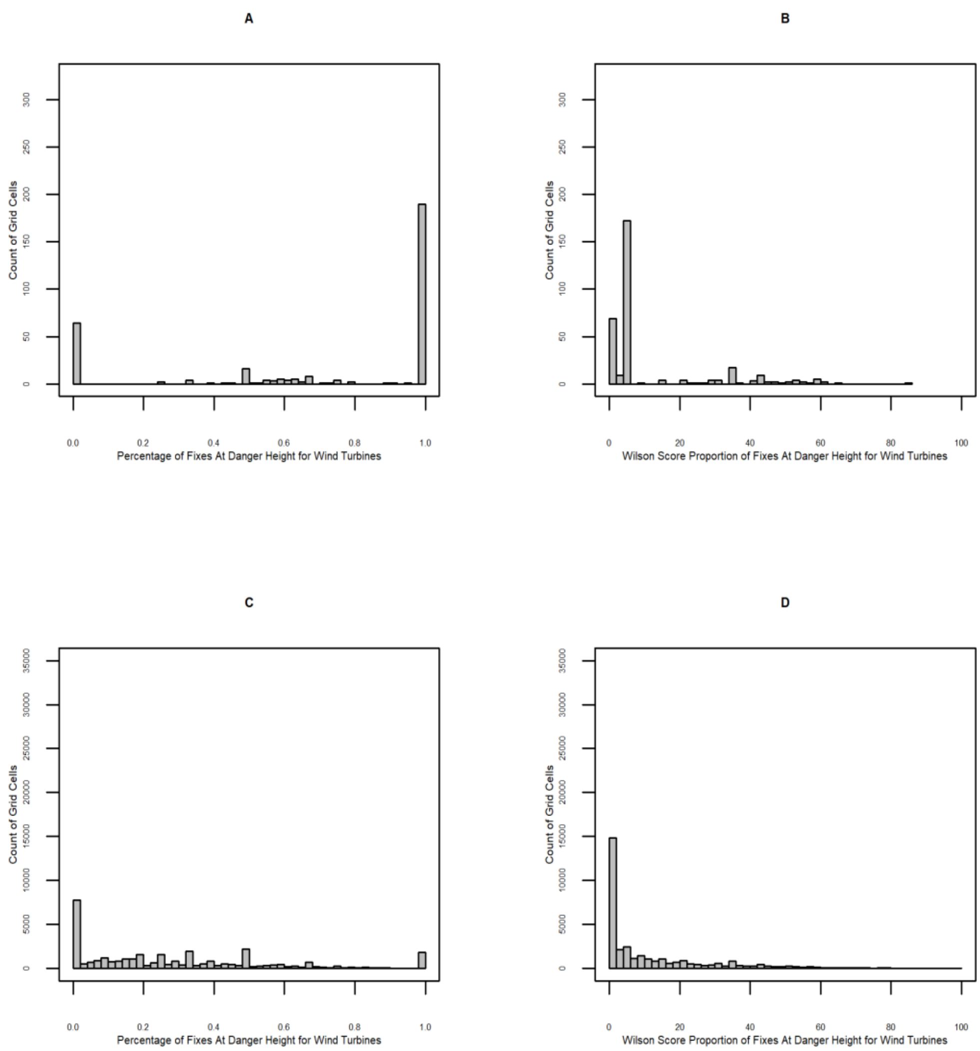

Supporting Information Figure 9: Plot A: the distribution of the percent of spoonbill P. leucordia flying GPS locations at danger height within each 5km x 5km grid cell. Plot B: the distribution of the proportion of flying GPS locations at danger height using the Wilson's score. C: the distribution of the percent of white stork C. ciconia flying GPS locations at danger height within each 5km x 5km grid cell. Plot D: the distribution of the proportion of white stork C. ciconia flying GPS locations at danger height within each 5km x 5km grid cell using the Wilson's score.

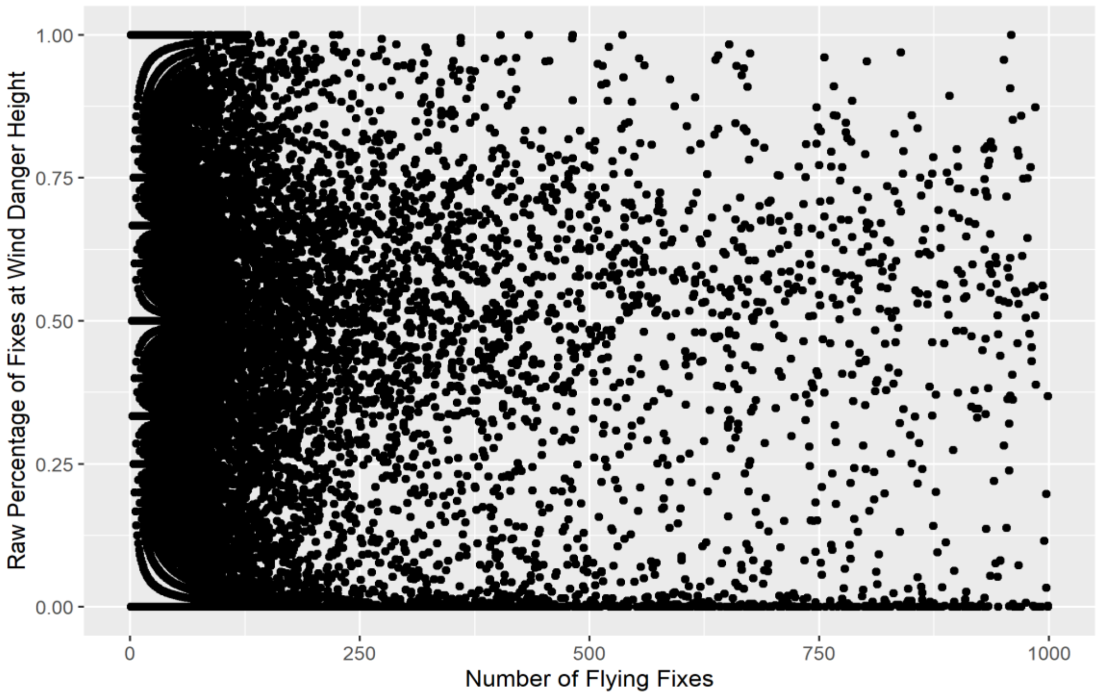

Supporting Information Figure 10: Plot of sample size against the raw proportion of flying GPS locations at danger height to demonstrate how probabilities become constrained at low sample sizes.

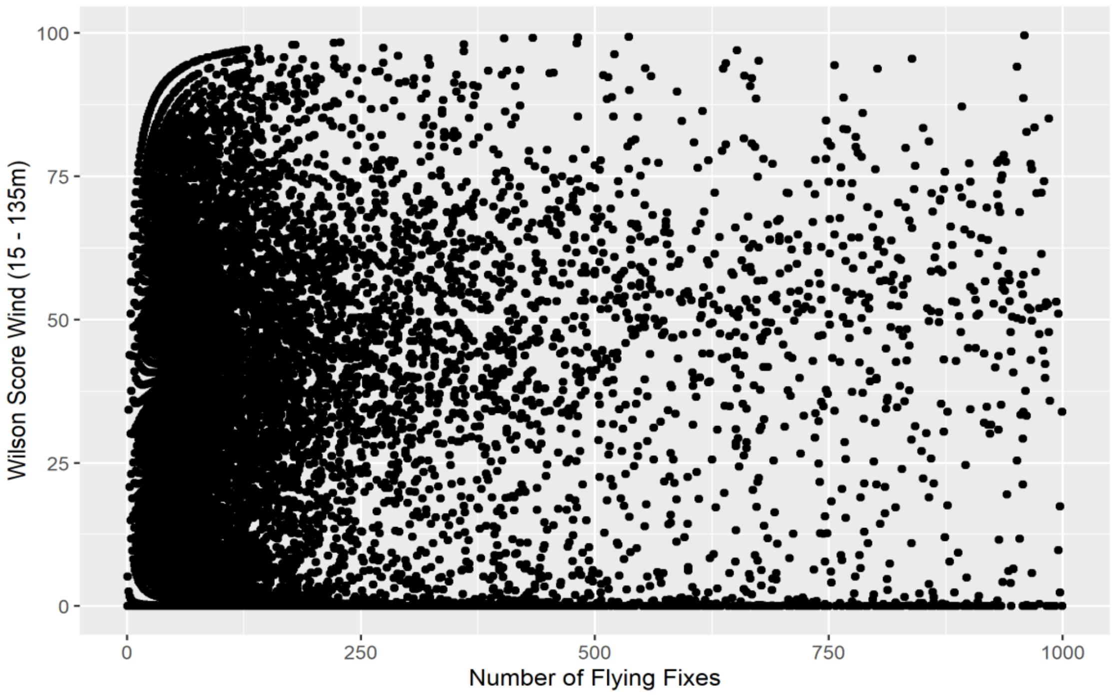

Supporting Information Figure 11: Proportion of GPS locations as represented by the Wilson score (lower bound of the Wilson's confidence interval) plotted against sample size to demonstrate how it behaves like a percentage at higher sample sizes while controlling for uncertainty at lower sample sizes.

The key difference (visible in Supporting Information Figure 10 and Supporting Information Figure 11) is that when the lower bound of the Wilson confidence interval is used, estimates of ρ are constrained to between 0 and 1 with no negative lower bound. When applied to the percentage of flying GPS locations at danger height in each cell, this results in proportions from 0 to 100. Where cells have a lower sample size and therefore reduced confidence, the uncertainty is reflected by not assigning high percentage scores. We also observe that as sample size increases (>200) the lower bound for high scoring cells (p > 0.9) converges on 100 as the size of the confidence interval shrinks toward zero in line with central limit theorem. This has not been widely used in ecology, however, in other disciplines such as computer sciences the lower bound of the Wilson interval, sometimes referred to as the Wilson score, is commonly used to rank the quality of observations while reflecting the magnitude of the effect observed (Wallis, 2013; Reichensdörfer, Odenthal and Wollherr, 2017; Cao, 2018).

Weighted average methods

Inverse-variance $1/\sigma^2_k$ weighting described by (Doncaster and Spake, 2018) is commonly used in meta-analyses to reflect sample size and to control for variance in samples from different studies (Stewart, Pullin and Coles, 2007). An assumption of these models is that each effect size is derived from a single population however, the data used in this analysis breaches that assumption. It can also introduce large biases where the sensitivity score of cells with larger sample sizes was artificially inflated even when the proportion of GPS locations at danger height was near zero and produced figures which no longer have a resemblance to the original percentages.

Maximum Likelihood Estimation (MLE)

MLE methods are an alternative frequentist approach to using a confidence interval to refine a point estimate based on observed data at large sample sizes p = X/N (Lewis and

Sauro, 2006). However, without additional techniques such as bootstrapping to artificially inflate the sample size (Dalitz, 2018), this method performs poorly and does not allow us to adjust for uncertainty in our sensitivity score for each grid cell.

Summary

In summary, the Wilson Score (the lower bound of the Wilson confidence interval) is a relatively simple yet effective solution which allows us to build certainty into our estimates of the percentage of flights at a given danger height within each Grid Cell. The Wilson interval behaves as we would expect with increased sample size and there is extensive literature supporting its use over that of alternatives such as the Wald interval. The Wilson Score also eliminates arbitrary weightings from the analysis which is historically a common problem in conservation priority setting (Game, Kareiva and Possingham, 2013).

SECTION 6 REFERENCES

Agresti, A. and Coull, B. A. (1998) 'Approximate is better than "Exact" for interval estimation of binomial proportions', *American Statistician*, 52(2), pp. 119–126. doi: 10.1080/00031305.1998.10480550.

Brown, L. D., Cai, T. T. and Das Gupta, A. (2001) 'Interval estimation for a binomial proportion', *Statistical Science*, 16(2), pp. 101–117. doi: 10.1214/ss/1009213286.

Cao, X. (2018) 'Improved Online Wilson Score Interval Method for Community Answer Quality Ranking', (April), pp. 1–8. Georgia Institute of Technology.

Dalitz, C. (2018) 'Construction of Confidence Intervals', pp. 15–28. Available at: http://arxiv.org/abs/1807.03582.

Doncaster, C. P. and Spake, R. (2018) 'Correction for bias in meta-analysis of little-replicated studies', *Methods in Ecology and Evolution*, 9(3), pp. 634–644. doi: 10.1111/2041-210X.12927.

Game, E. T., Kareiva, P. and Possingham, H. P. (2013) 'Six Common Mistakes in Conservation Priority Setting', *Conservation Biology*, 27(3), pp. 480–485. doi: 10.1111/cobi.12051.

Lewis, J. and Sauro, J. (2006) 'When 100% really isn't 100%: improving the accuracy of small-sample estimates of completion rates', *Journal of Usability Studies*, 1(3), pp. 136–150.

Lott, A. and Reiter, J. P. (2018) 'Wilson Confidence Intervals for Binomial Proportions With Multiple Imputation for Missing Data', *American Statistician*. Taylor & Francis, 1305. doi: 10.1080/00031305.2018.1473796.

Park, H. and Leemis, L. M. (2019) 'Ensemble confidence intervals for binomial proportions', *Statistics in Medicine*, 38(18), pp. 3460–3475. doi: 10.1002/sim.8189.

Pobocikova, I. (2010) 'Better confidence intervals for a binomial proportion', *Komunikacie*, 12(1), pp. 31–37.

Reichensdörfer, E., Odenthal, D. and Wollherr, D. (2017) 'Grammatical Evolution of Robust Controller Structures Using Wilson Scoring and Criticality Ranking', in McDermott, J. et al. (eds) *Genetic Programming: 20th European Conference, EuroGP 2017 Amsterdam, The Netherlands, April 19–21, 2017 Proceedings*. Amsterdam: Springer, pp. 194–209. doi: 10.1007/978-3-319-55696-3_19.

Wallis, S. (2013) 'Binomial confidence intervals and contingency tests: Mathematical fundamentals and the evaluation of alternative methods', *Journal of Quantitative Linguistics*, 20(3), pp. 178–208. doi: 10.1080/09296174.2013.799918.

Wilson, E. B. . (1927) ‘Probable Inference , the Law of Succession and Statistical Inference’, *Journal of the American Statistical Association*, 22(158), pp. 209–212. doi: 10.2307/2276774.

SECTION 7: MBRCI

MBRCI describes the Wing area values were not available for all species, as a proxy for wing area we simplify the shape of a bird as a rhombus and calculate a simplified area using the wingspan (WS) and body length (BL) in metres using data from Svensson, Mullarney and Zetterström, 2016 or Storchová and Hořák, 2018.

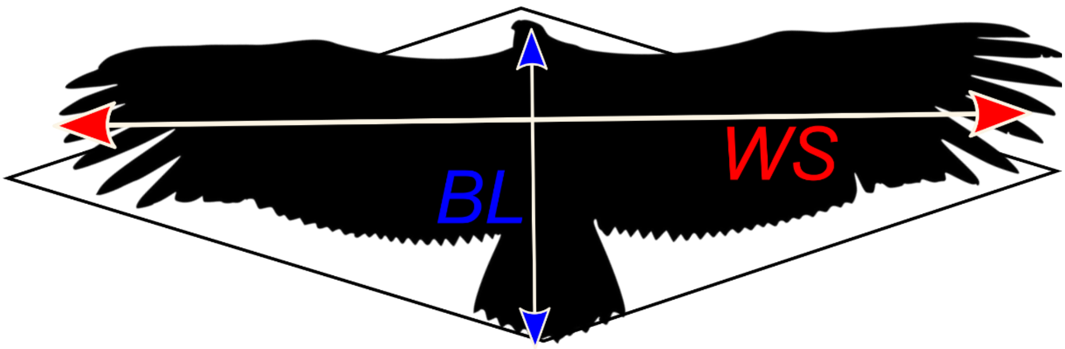

Supporting Information Figure 12: Approximation of wingspan and body size to substitute for wing area measurements.

Comparing this with wing area data available for 17 of the 27 species (Hedenström and Strandberg, 1993) using linear regression (R^2 = 0.61, F(1,15)=23.44, p = 2.16 * 10^{-5}, Supporting Information Figure 12) suggests that it is a good proxy for assessing relative differences between species. We then estimate wing loading by dividing this proxy area (m^2) body mass (BM) in kilograms as per:

$$WBMR = \frac{BM}{(WS * BL) \div 2}$$

We combine this wing-body-mass-ratio (WBMR) with a number of other factors scored as either 1 or 2 associated with avoidance ability (Amico *et al.*, 2019). Namely flight style (FS), flapping (1) vs. soaring (2) because soaring species are less able to make sudden changes in trajectory to avoid collision compared to flapping species (May, 2015), whether the species has binocular vision (BV) (1) or peripheral vision (2) (Martin and

Shaw, 2010; Amico *et al.*, 2019), whether the species is a flocking species (FL) (2) or not (1) and whether the species flies frequently at night (ND) (2) or not (1). This definition of MBRI is the similar Amico et al. 2019 apart from the flight style because Amico et al. 2019 use flight style as a proxy for flight height whereas we use flight style to help infer manouverability (May, 2015). This MBRI is then combined with European conservation status (Least Concern = 1, Other categories = 2) to produce a morpho-behavioural risk conservation status index (MBRCI) as per equation:

$$MBRCI = CI * \frac{(MBMR * FS * BV * FL * ND)}{5}$$

MBRCI is then normalised onto a scale between zero and one by calculating the ratio between the MBRCI for each species and the maximum value across all species as detailed in the table in section 8. Sensitivity at the species level is then defined as the WS multiplied by the MBRCI. The final sensitivity across all species is then defined as the maximum sensitivity of any species present in each grid cell.

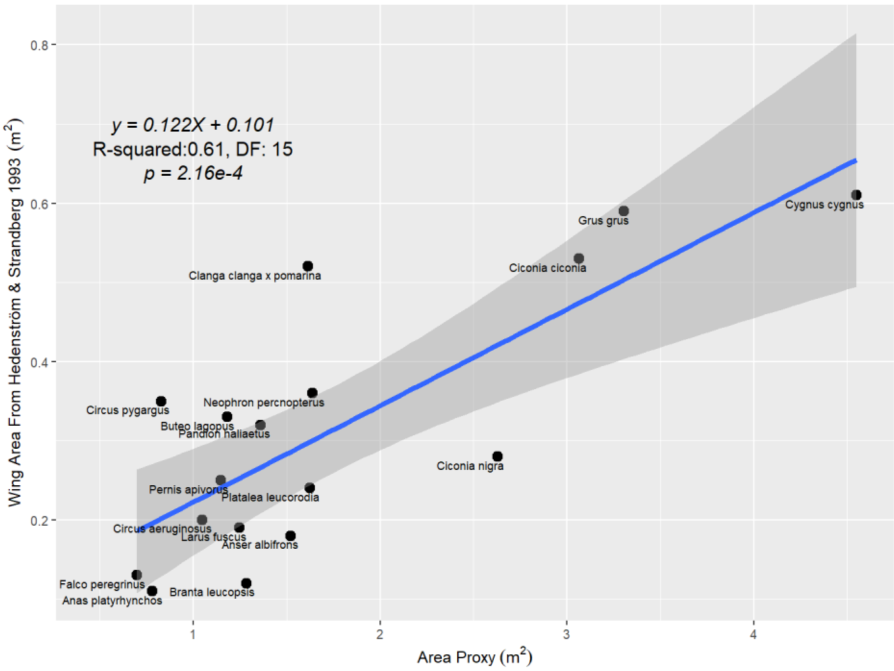

Supporting Information Figure 13: Relationship between proxy 'wing area' and wing area from museum specimens described in Hedenström and Strandberg 1993.

Common Name	Species	Family	Flight Style	Europe Red Lis t Status 2015	MBRCI Normalised	MBRCI Rank
Mallard	Anas platyrhynchos	Anatidae	Flapping	LC	0.118261	Moderate
White-fronted Goose	Anser albifrons	Anatidae	Flapping	LC	0.230179	Moderate
Iberian Imperial Eagle	Aquila adalberti	Accipitridae	Soaring	VU	0.369301	High
Barnacle Goose	Branta leucopsis	Anatidae	Flapping	LC	0.194057	Moderate
Eurasian Eagle Owl	Bubo bubo	Strigidae	Soaring	LC	0.236314	Moderate
Stone Curlew	Burhinus oedicnemus	Burhinidae	Flapping	LC	0.152756	Moderate
Rough-legged Buzzard	Buteo lagopus	Accipitridae	Soaring	LC	0.17862	Moderate
Long-legged Buzzard	Buteo rufinus	Accipitridae	Soaring	LC	0.090109	Low
White stork	Ciconia ciconia	Ciconiidae	Soraring	LC	0.926654	High
Black Stork	Ciconia nigra	Ciconiidae	Soaring	LC	0.397372	High
Short-toed Snake Eagle	Circaetus gallicus	Accipitridae	Soaring	LC	0.129	Moderate
Western Marsh Harrier	Circus aeruginosus	Accipitridae	Soaring	LC	0.079229	Low
Montagu's Harrier	Circus pygargus	Accipitridae	Soaring	LC	0.062694	Low
Hybrid Spotted Eagle	Clanga clanga x pomarina	Accipitridae	Soaring	EN	0.24417	Moderate
Whooper Swan	Cygnus cygnus	Anatidae	Flapping	LC	0.687836	High
Peregrine Falcon	Falco peregrinus	Falconidae	Soaring	LC	0.052798	Low
Northern Bald Ibis	Geronticus eremita	Threskiornithidae	Flapping	RE	0.141777	Moderate
Common Crane	Grus grus	Gruidae	Soaring	LC	1	High
Griffon Vulture	Gyps fulvus	Accipitridae	Soaring	LC	0.272226	Moderate
Lesser-black Backed Gull	Larus fuscus	Laridae	Flapping	LC	0.094368	Low
Eurasian Wigeon	Mareca penelope	Anatidae	Flapping	LC	0.046911	Low

Egyptian Vulture	Neophron percnopterus	Accipitridae	Soaring	EN	0.495425	High
Osprey	Pandion haliaetus	Pandionidae	Soaring	LC	0.205921	Moderate
Honey Buzzard	Pernis apivorus	Accipitridae	Soaring	LC	0.346798	Moderate
Eurasian Spoonbill	Platalea leucorodia	Threskiornithidae	Soaring	LC	0.982079	High
Little Bustard	Tetrax tetrax	Otididae	Flapping	VU	0.159074	Moderate
Barn Owl	Tyto alba	Tytonidae	Flapping	LC	0.037085	Low

Supporting Information Table 4:: Summary of the susceptibility to collision with EI for species included in the analysis.

SECTION 7 REFERENCES

Amico, M. D. *et al.* (2019) ‘Bird collisions with power lines: Prioritizing species and areas by estimating potential population-level impacts’, *Biodiversity Research*, 25, pp. 975–982. doi: 10.1111/ddi.12903.

Hedenström, D. and Strandberg, A. (1993) ‘Protocol S1 Supplementary list of flight speeds and biometry of bird species’, *Pennycuick Greenewalt Hedenström*, 135(1), pp. 1–4.

Martin, G. R. and Shaw, J. M. (2010) ‘Bird collisions with power lines: Failing to see the way ahead?’, *Biological Conservation*, 143, pp. 2695–2702. doi: 10.1016/j.biocon.2010.07.014.

May, R. F. (2015) ‘A unifying framework for the underlying mechanisms of avian avoidance of wind turbines’, *Biological Conservation*. Elsevier Ltd, 190, pp. 179–187. doi: 10.1016/j.biocon.2015.06.004.

Storchová, L. and Hořák, D. (2018) ‘Life-history characteristics of European birds’, *Global Ecology and Biogeography*, 27(4), pp. 400–406. doi: 10.1111/geb.12709.

Svensson, L., Mullarney, K. and Zetterström, D. (2016) *Collins Bird Guide*. 2nd edn. Harper Collins Publishers.

SECTION 8: COMPARISON OF DIFFERENT SENSITIVITY METRICS

The maps provided in this section describe how different layers of the analysis impact upon the final result. These show the raw proportion of flights at danger height for wind turbines in each grid cell (Supporting Information Figure 14a), the wilson score proportion of flights at danger height (Supporting Information Figure 14b) and the maximum value associated with this combined with just the IUCN status for the species present in each grid cell (Supporting Information Figure 14c) whereby 1 = least concern, and 2 = near threatened through to critically endangered, to allow this to be compared with the sensitivity maps produced using the MBCRI score as per the method described in the paper. As per the sensitivity maps, the data is symbolised by quantiles whereby for each metric, the lower quartile, upper quartile and 97.5th quantile is calculated for grid cells with a score greater than zero. Grid cells scoring greater than zero but less than the 25th percentile are “Low”, scores between the 25th and 75th percentile are “Moderate”, Scores greater than the 75th percentile are “High” and cells in the top 2.5% of observations are “Very High” all other cells are classified as “Very Low” if there are GPS locations but none at danger height resulting in a score of zero or “No Data” if data was lacking.

The main difference between these metrics is in the number of high and very high scoring grid cells, using the raw proportion of locations at danger height results in a much larger number of grid cells being categorised as very high (n = 6,986) compared to either the Wilson score (n = 1,309), the maximum value associated with any species present in each grid cell derived from multiplying the Wilson score by the conservation status (n = 1,338) or Very High Sensitivity cells as presented in the main paper and supporting information figure 15 (n = 1,368). This is because the raw proportion of locations in flight at danger height includes a large number of grid cells with very low sample sizes (<5 records) which happen to be at danger height whereas the Wilson score method would down weight the values in these cells due to the large confidence intervals around them. Overall the different components of the MBRCI score have a small impact on the results because the main determinant of the final sensitivity score is the Wilson score proportion of locations in flight at danger height.

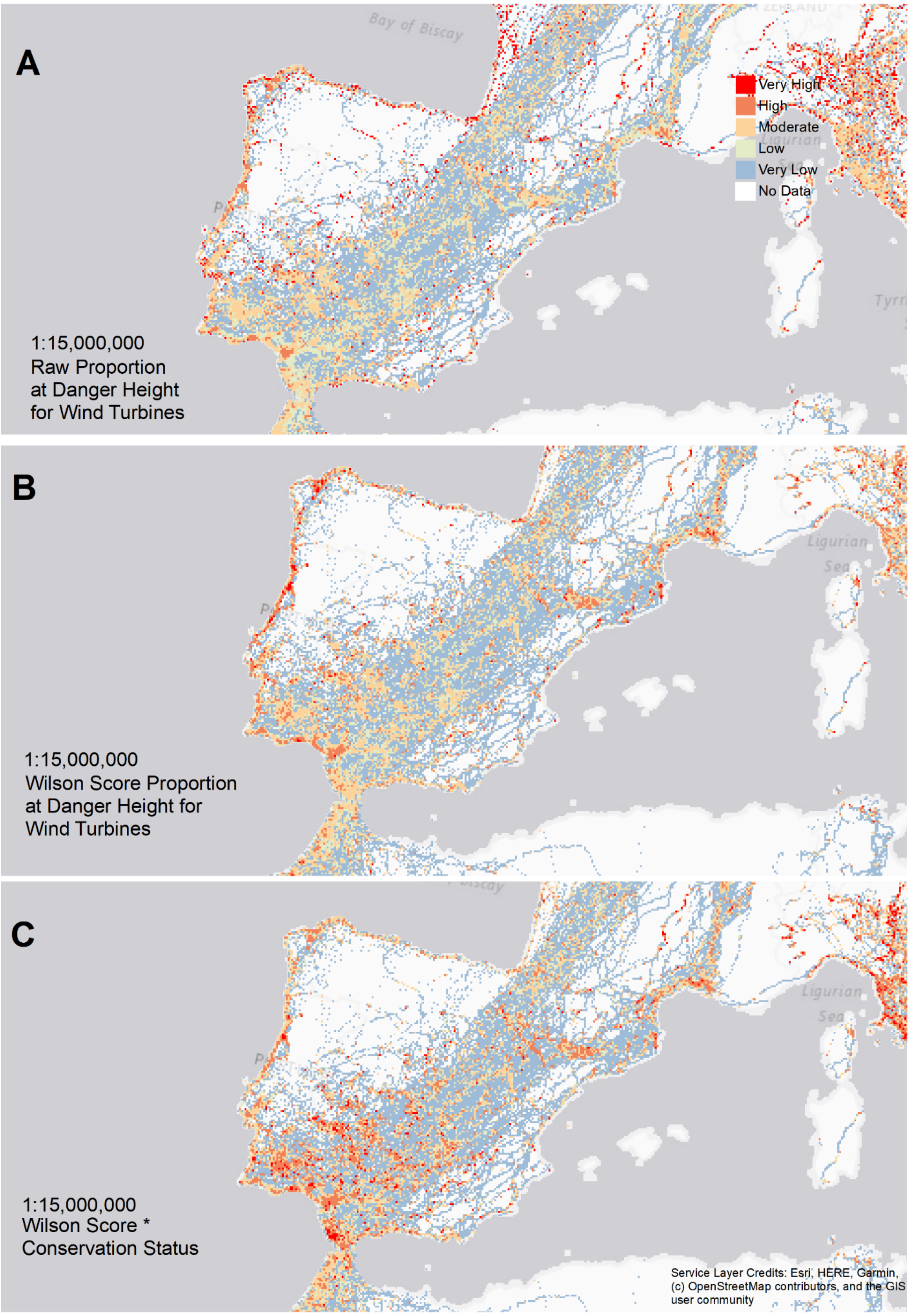

Supporting Information Figure 14: Panel A displays the raw proportion of locations in flight at danger height for wind turbines and regions where no GPS data is available. Panel B. displays the proportion of locations in flight at danger height for wind turbines as calculated using the Wilson Score which allows us to weight the final value by our confidence in that estimate and regions where no GPS data is available. Panel C displays the score resulting from weighting the Wilson score by the IUCN conservation status of species present in each grid cell and then displaying the maximum score associated with any of the tracked species present.

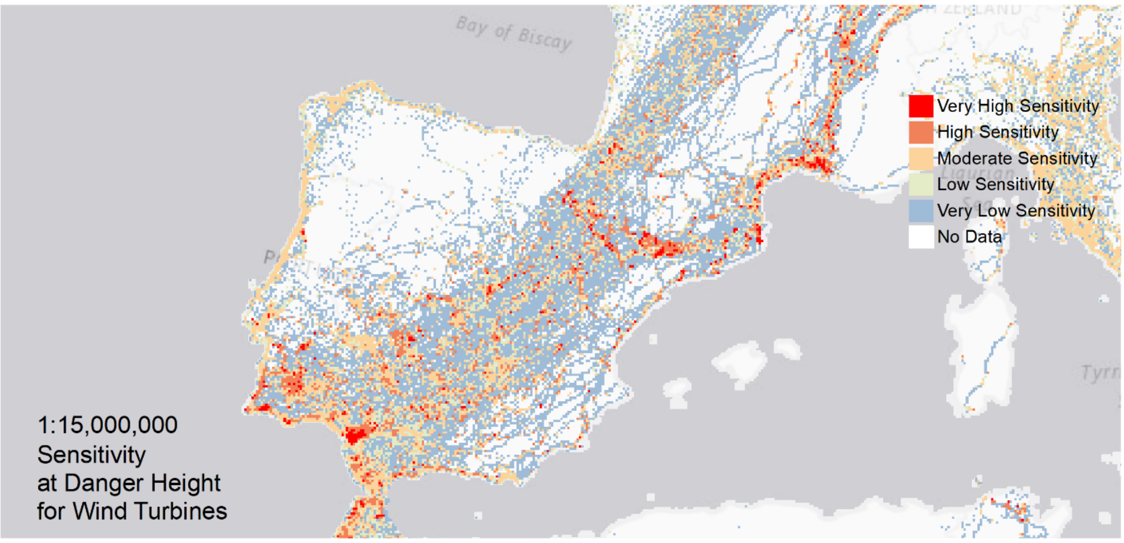

Supporting Information Figure 15: The final sensitivity score at danger height for wind turbines in the Iberian Peninsula.

APPENDIX C: CHAPTER 2 RESULTS SUPPORTING INFORMATION

DOCUMENT DESCRIPTION

This document contains the supplementary material to supplement the results of the paper “Hotspots in the grid: the avian sensitivity and vulnerability to collision risk form energy infrastructure interactions in Europe and North Africa”. Section 1 displays sensitivity plots by season. Section 2 displays plots of sensitivity to energy infrastructure by family and infrastructure type highlighting where additional EI development could increase risks to the tagged birds from each taxonomic group. Section 3 summarises the distribution of moderate, high and very high vulnerability grid cells by country to highlight where mitigation to reduce collision risk for the tagged birds could be prioritised. Section 4 contains maps of vulnerability to energy infrastructure by family.

SECTION 1: SENSITIVITY BY SEASON

The maps in this section plot the distribution of sensitivity to wind turbines and power lines for all 27 species in the breeding and non-breeding season. GPS locations were categorised as “breeding” representing the period when the birds and therefore potential conflicts with EI will be more constrained to a breeding territory or “non-breeding” when movements may be less concentrated within a breeding territory resulting in seasonal variation of the locations where conflicts with EI could occur (Tikkanen *et al.*, 2018). For each study (and species where studies featured multiple species), we plotted week against latitude to manually identify the start and finish of the breeding season, associated with a period of stable latitude and labelled all other observations as non-breeding (Buechley *et al.*, 2018; Cerritelli *et al.*, 2020). This allowed the observed variation within and between datasets to be accounted for. For the small number of non-migratory species, namely, barn owl *Tyto alba,* eurasian eagle owl *Bubo bubo*, and Iberian imperial eagle *Aquila adalberti*, we categorise GPS locations according to life-cycle information (Svensson, Mullarney and Zetterström, 2016; Birdlife International, 2019).

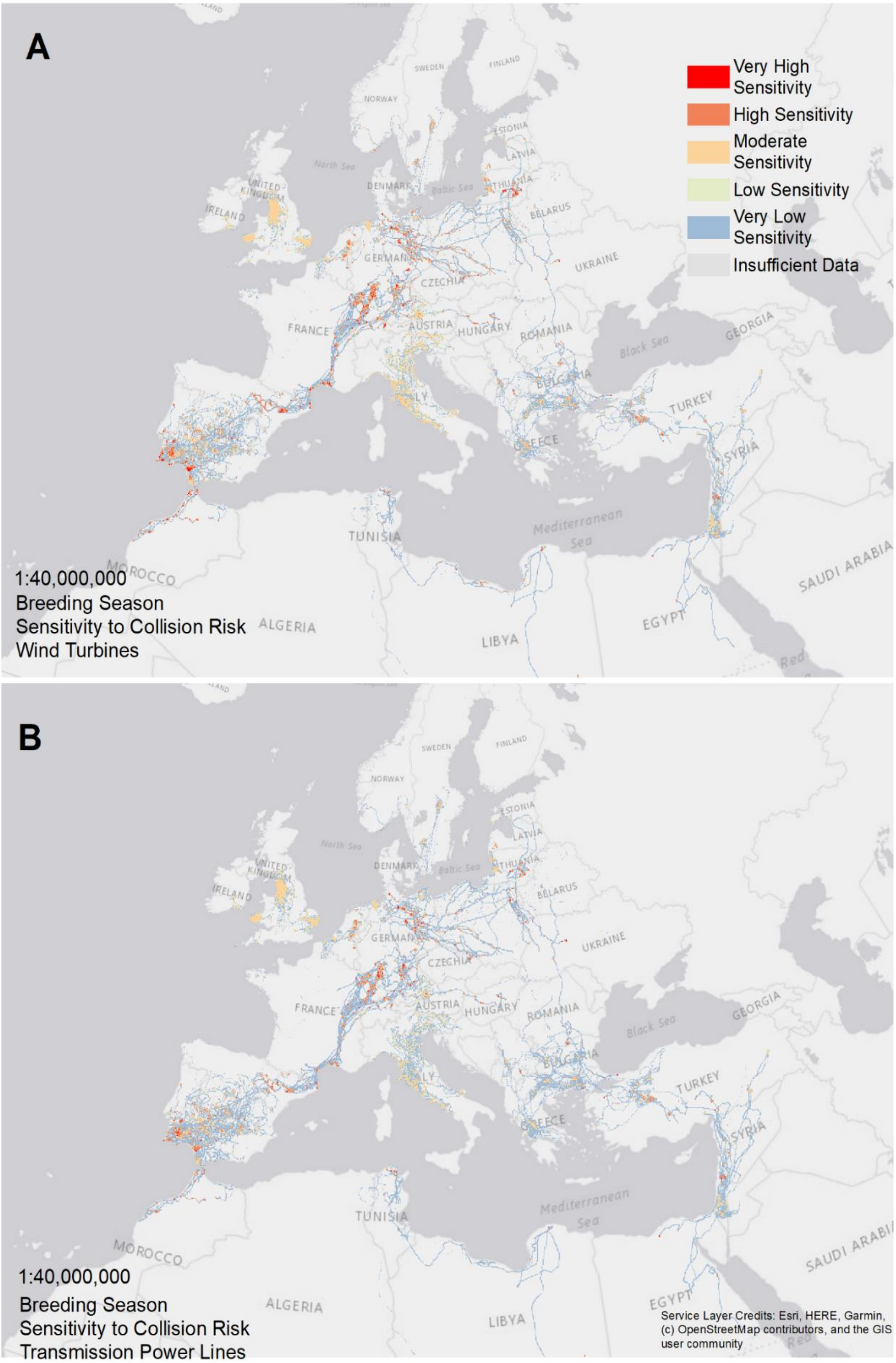

Supporting Information Figure 16: A. plots the distribution of sensitivity to wind turbines across the study region for individuals from all 27 species within the breeding season. B. plots the sensitivity to transmission power lines. Sensitivity categories represent quantiles whereby "Very High Sensitivity" are the grid cells in the top 2.5% of observations, "high sensitivity" are those grid cells in the upper quartile of sensitivity scores, "Moderate sensitivity" describes those grid cells within the interquartile range of sensitivity scores, "low sensitivity" are those grid cells in the lower quartile of sensitivity scores and "Very Low Sensitivity" grid cells represent grid cells with sensitivity approaching *or equal to zero. "Insufficient Data" indicates grid cells where data is present, but an insufficient number of GPS records are available to assess sensitivity.*

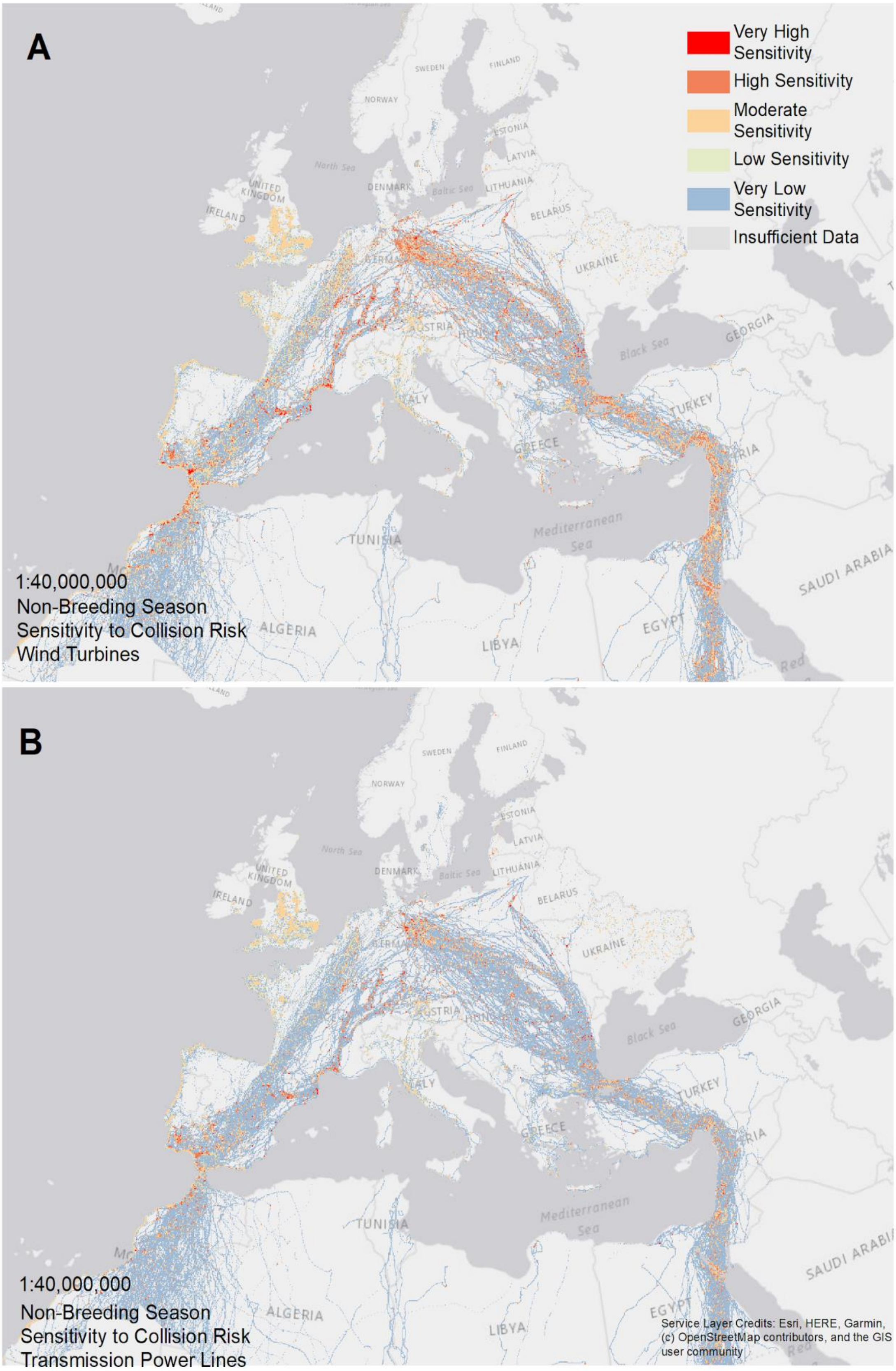

Supporting Information Figure 17: A. plots the distribution of sensitivity to wind turbines across the study region for individuals from all 27 species within the non-breeding season. B. plots the sensitivity to transmission power lines. Sensitivity categories represent quantiles whereby "Very High Sensitivity" are the grid cells in the top 2.5% of *observations, "high sensitivity" are those grid cells in the upper quartile of sensitivity scores, "Moderate sensitivity" describes those grid cells within the interquartile range of sensitivity scores, "low sensitivity" are those grid cells in the lower quartile of sensitivity scores and "Very Low Sensitivity" grid cells represent grid cells with sensitivity approaching or equal to zero. "Insufficient Data" indicates grid cells where data is present but an insufficient number of GPS records are available to assess sensitivity. Areas with no symbology represent regions for which no tracking data could be obtained.*

SECTION 1 REFERENCES

Birdlife International (2019) *Bird Life Data Zone*. Available at: http://datazone.birdlife.org/species (Accessed: 7 June 2019).

Svensson, L., Mullarney, K., Zetterström, D., 2016. Collins Bird Guide, 2nd ed. Harper Collins Publishers.

Tikkanen, H., Rytkönen, S., Karlin, O.P., Ollila, T., Pakanen, V.M., Tuohimaa, H., Orell, M., 2018. Modelling golden eagle habitat selection and flight activity in their home ranges for safer wind farm planning. Environ. Impact Assess. Rev. 71, 120–131. https://doi.org/10.1016/j.eiar.2018.04.006

SECTION 2: FAMILY SPECIFIC SENSITIVITY TO WIND TURBINES AND POWER LINES

These maps display sensitivity to wind farms and powerlines for each family of bird species included in the analysis. Grid cells are symbolised as quantiles of sensitivity within the range of sensitivity values for each taxonomic group. The map scale is also adjusted to match the extent of available tracking data for each family.

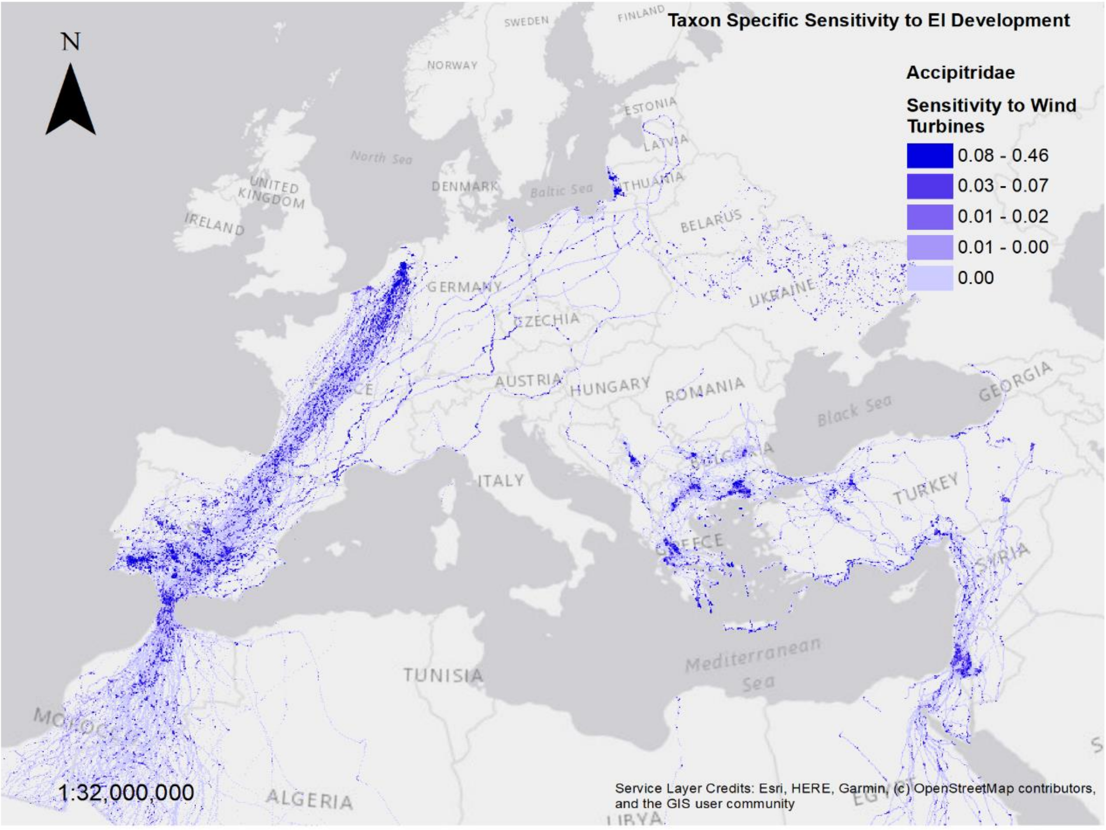

Supporting Information Figure 18: sensitivity to collision risk at danger height for wind turbines (15 - 135m) symbolised as quantiles. Map derived from GPS tracking data of raptor species within the Accipitridae family. Areas with no symbology represent regions for which no tracking data could be obtained.

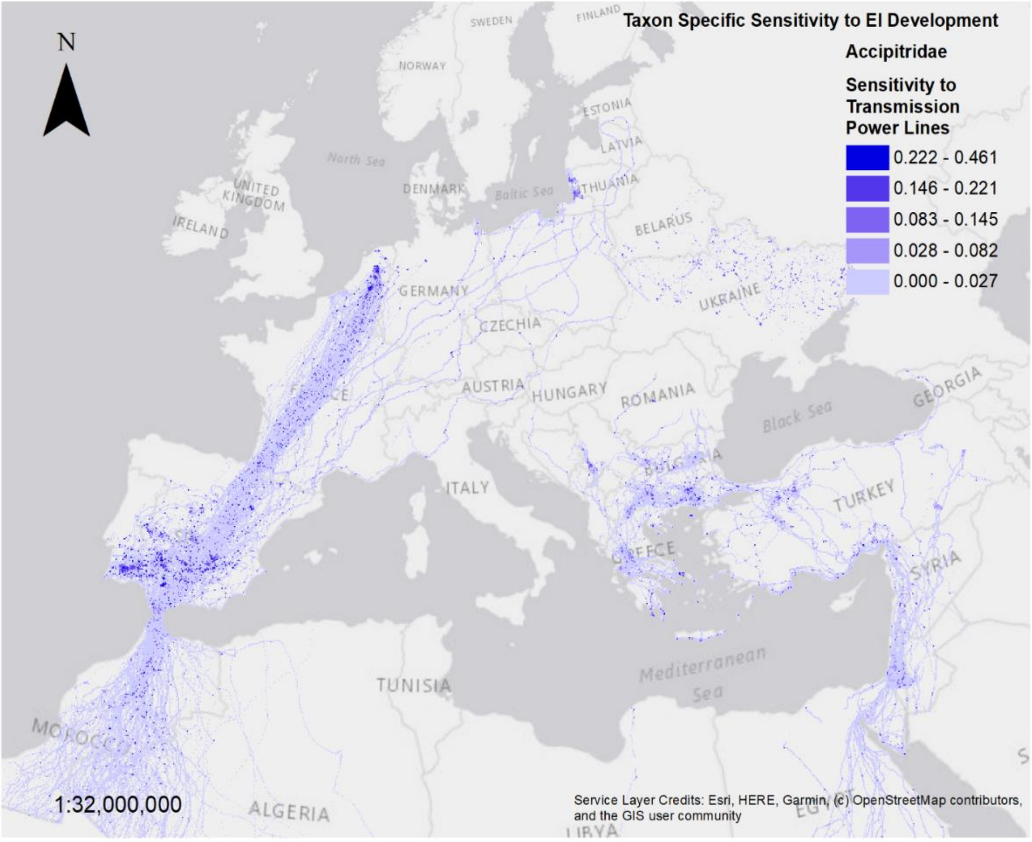

7412

7413 *Supporting Information Figure 19: sensitivity to collision risk at danger height for transmission power lines (10 - 60m)*
7414 *symbolised as quantiles. Map derived from GPS tracking data of raptor species within the Accipitridae family. Areas*
7415 *with no symbology represent regions for which no tracking data could be obtained.*

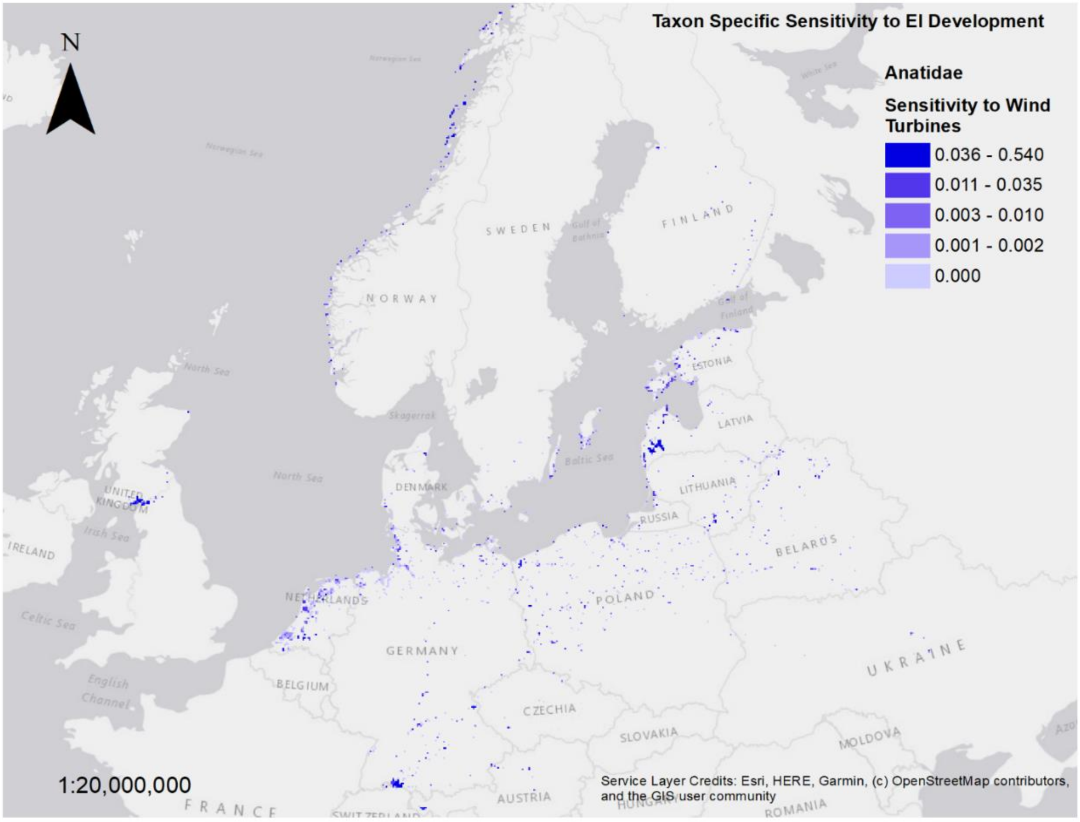

Supporting Information Figure 20: sensitivity to collision risk at danger height for wind turbines (15 - 135m) symbolised as quantiles. Map derived from GPS tracking data of waterfowl species within the Anatidae family. Areas with no symbology represent regions for which no tracking data could be obtained.

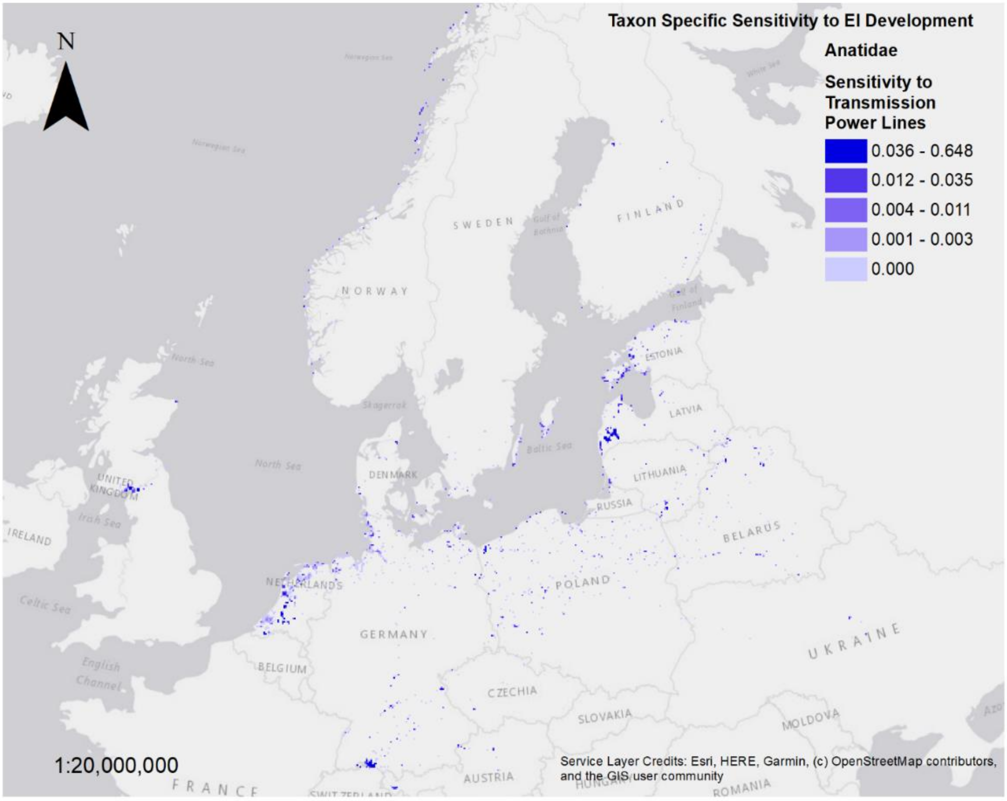

Supporting Information Figure 21: sensitivity to collision risk at danger height for transmission power lines (10 - 60m) symbolised as quantiles. Map derived from GPS tracking data of waterfowl species within the Anatidae family. Areas with no symbology represent regions for which no tracking data could be obtained.

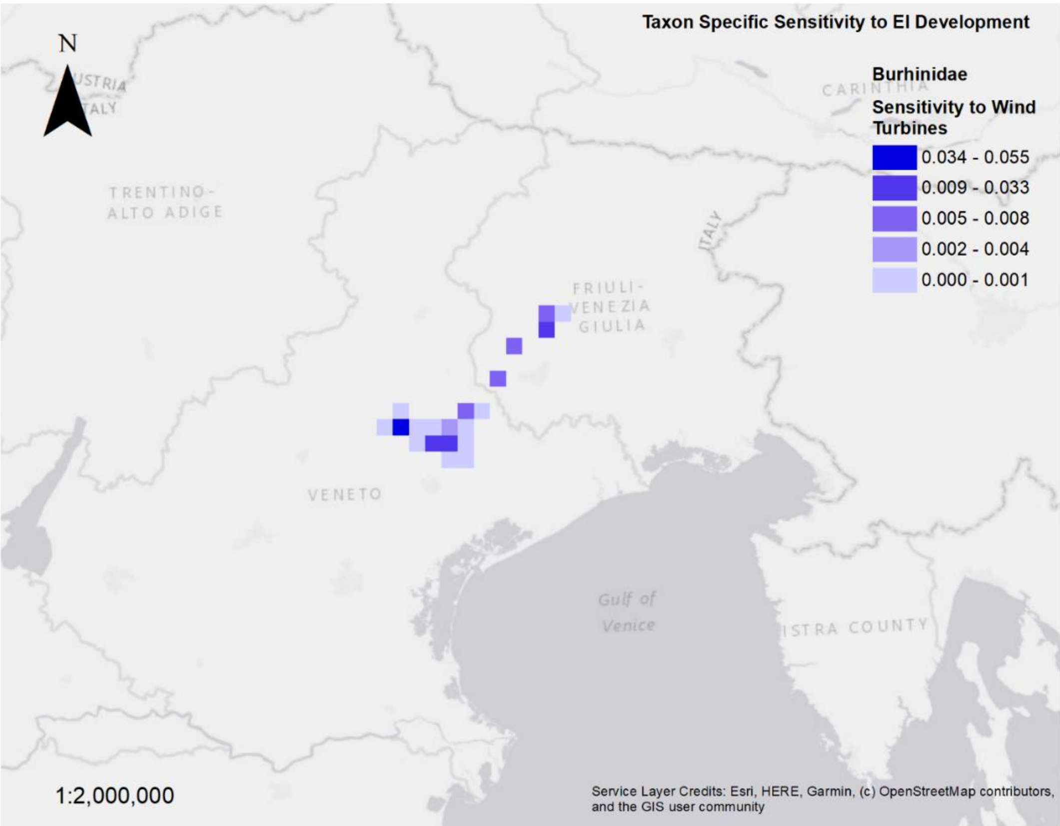

7424

7425 *Supporting Information Figure 22: sensitivity to collision risk at danger height for wind turbines (15 - 135m) symbolised*
7426 *as quantiles. Map derived from GPS tracking data of stone curlew Burhinus oedicnemus. Areas with no symbology*
7427 *represent regions for which no tracking data could be obtained.*

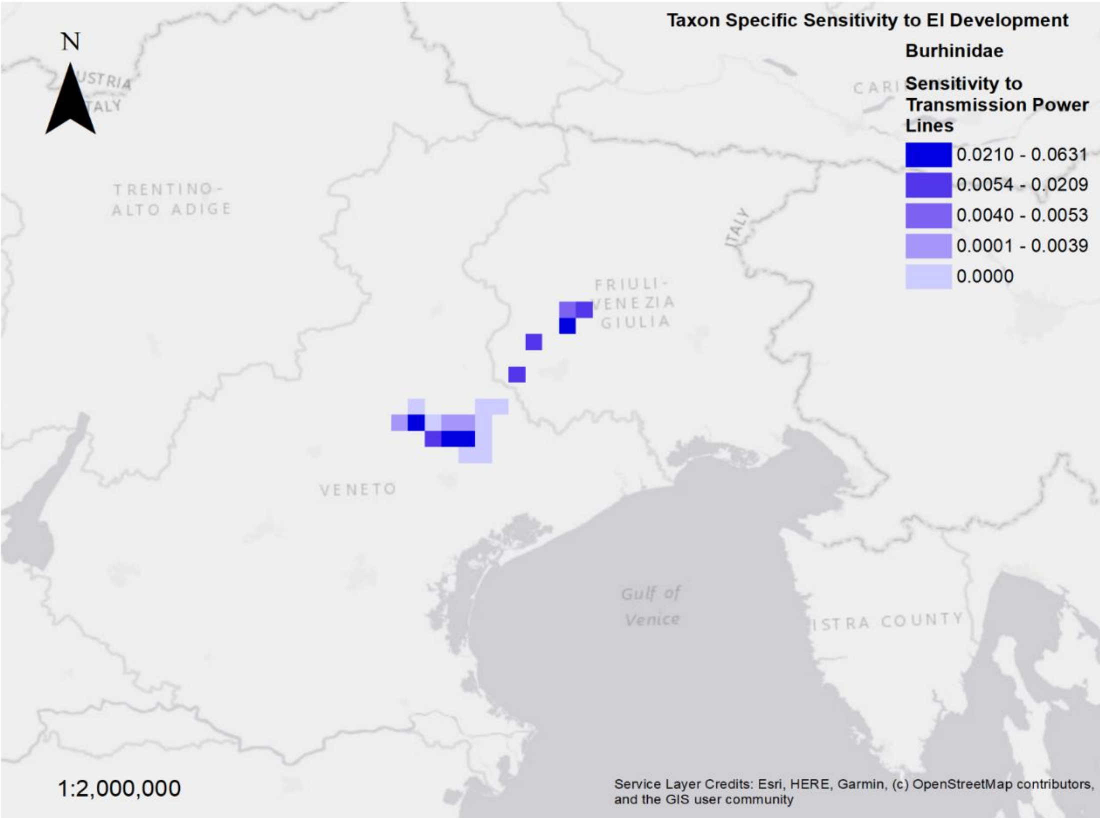

Supporting Information Figure 23: sensitivity to collision risk at danger height for transmission power lines (10 - 60m) symbolised as quantiles. Map derived from GPS tracking data of stone curlew Burhinus oedicnemus. Areas with no symbology represent regions for which no tracking data could be obtained.

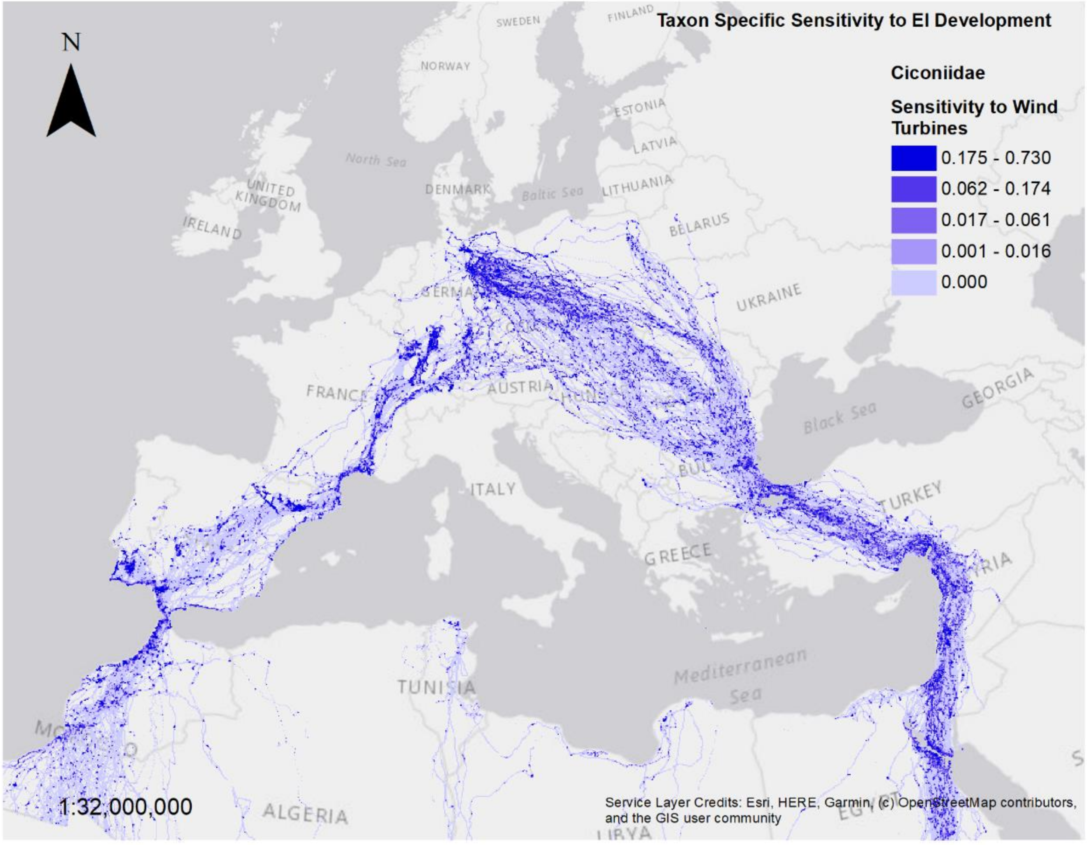

Supporting Information Figure 24: sensitivity to collision risk at danger height for wind turbines (15 - 135m) symbolised as quantiles. Map derived from GPS tracking data of white stork Ciconia ciconia and black stork Ciconia nigra. Areas with no symbology represent regions for which no tracking data could be obtained.

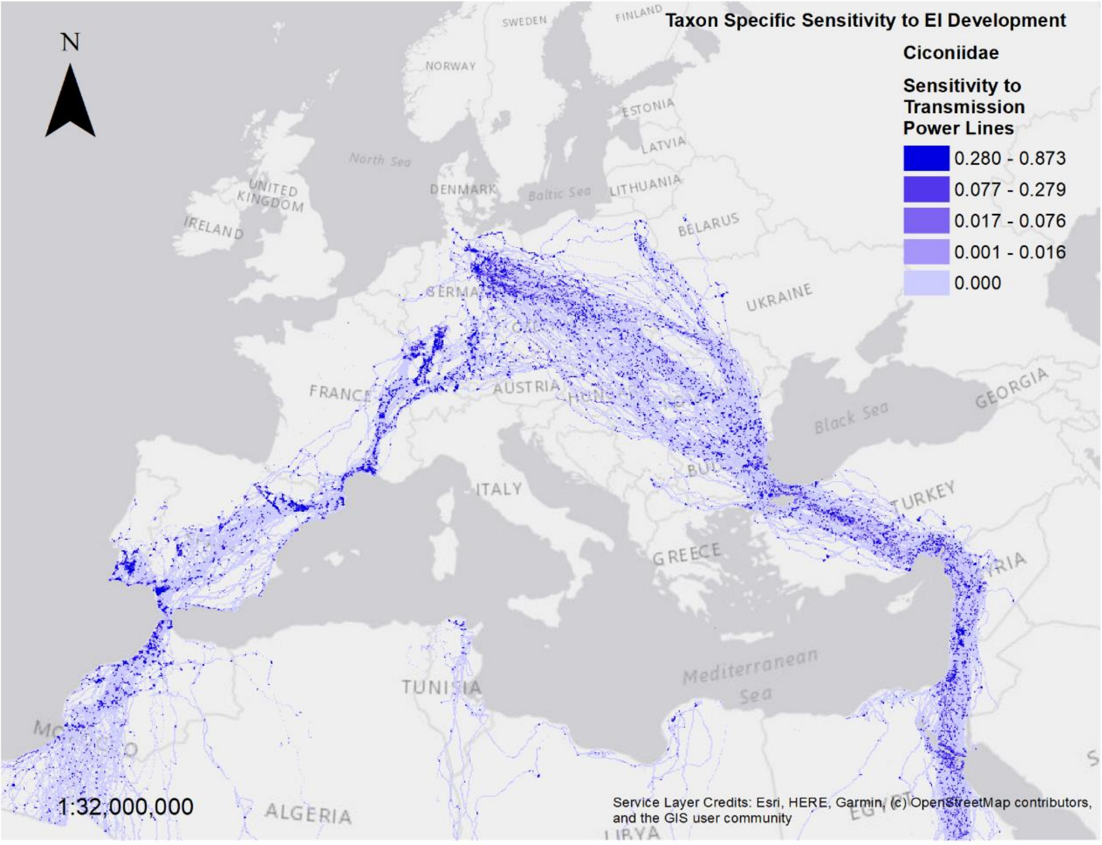

Supporting Information Figure 25: sensitivity to collision risk at danger height for transmission power lines (10 - 60m) symbolised as quantiles. Map derived from GPS tracking data of white stork Ciconia ciconia and black stork Ciconia nigra. Areas with no symbology represent regions for which no tracking data could be obtained.

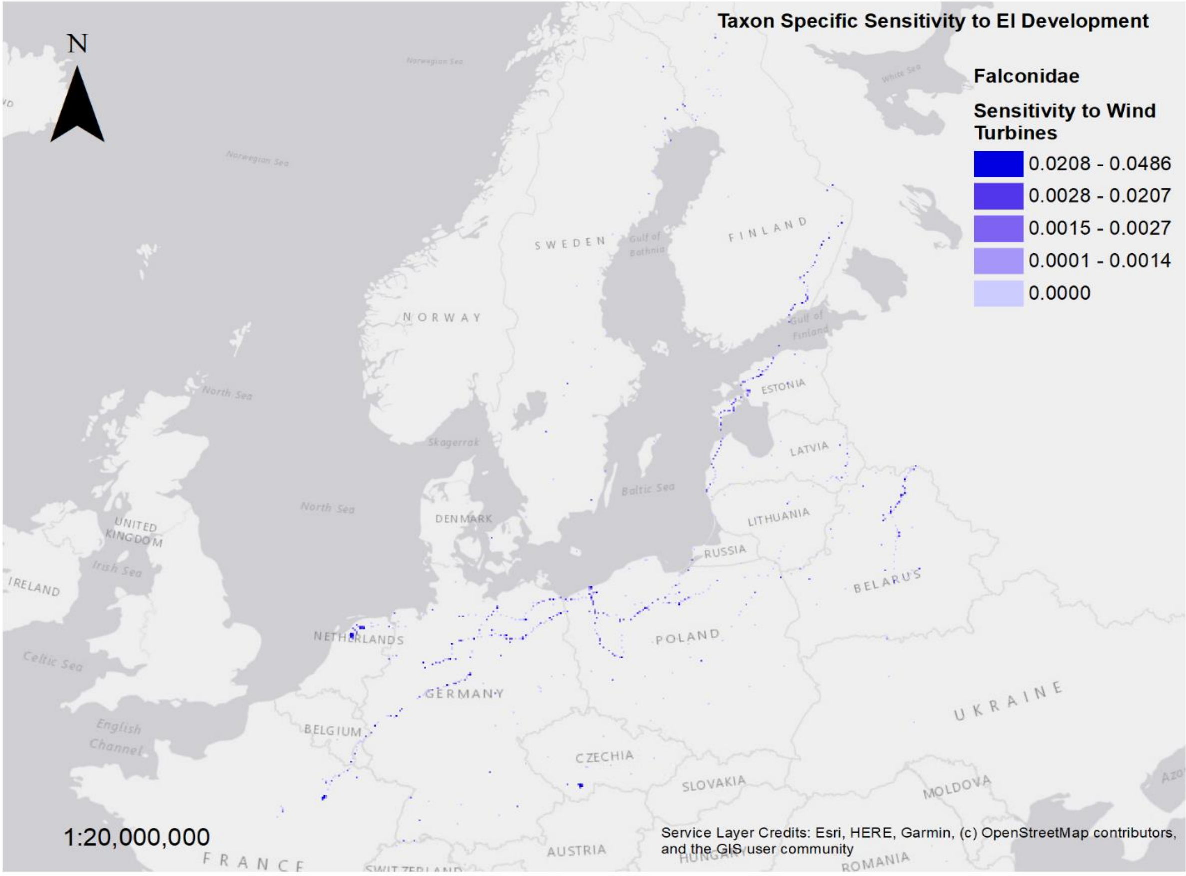

Supporting Information Figure 26: sensitivity to collision risk at danger height for wind turbines (15 - 135m) symbolised as quantiles. Map derived from GPS tracking data of peregrine falcon Falco peregrinus. Areas with no symbology represent regions for which no tracking data could be obtained.

7447 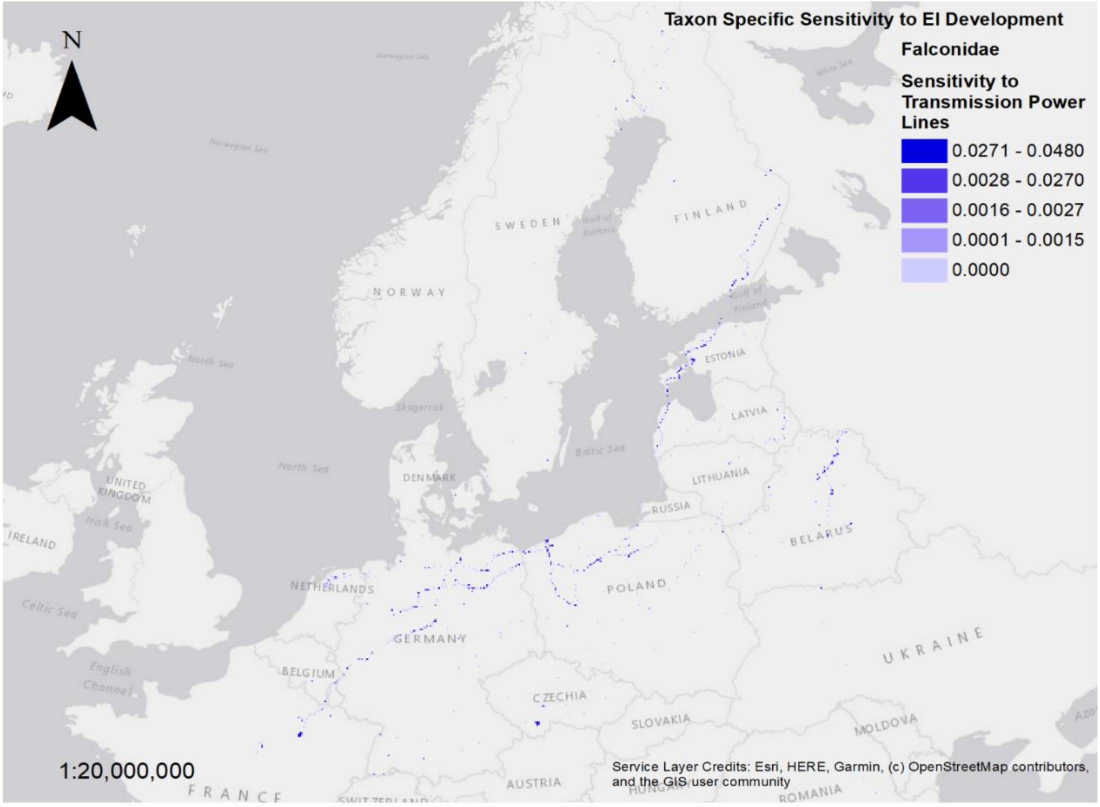

7448 *Supporting Information Figure 27: sensitivity to collision risk at danger height for transmission power lines (10 - 60m)*
7449 *symbolised as quantiles. Map derived from GPS tracking data of peregrine falcon Falco peregrinus. Areas with no*
7450 *symbology represent regions for which no tracking data could be obtained.*

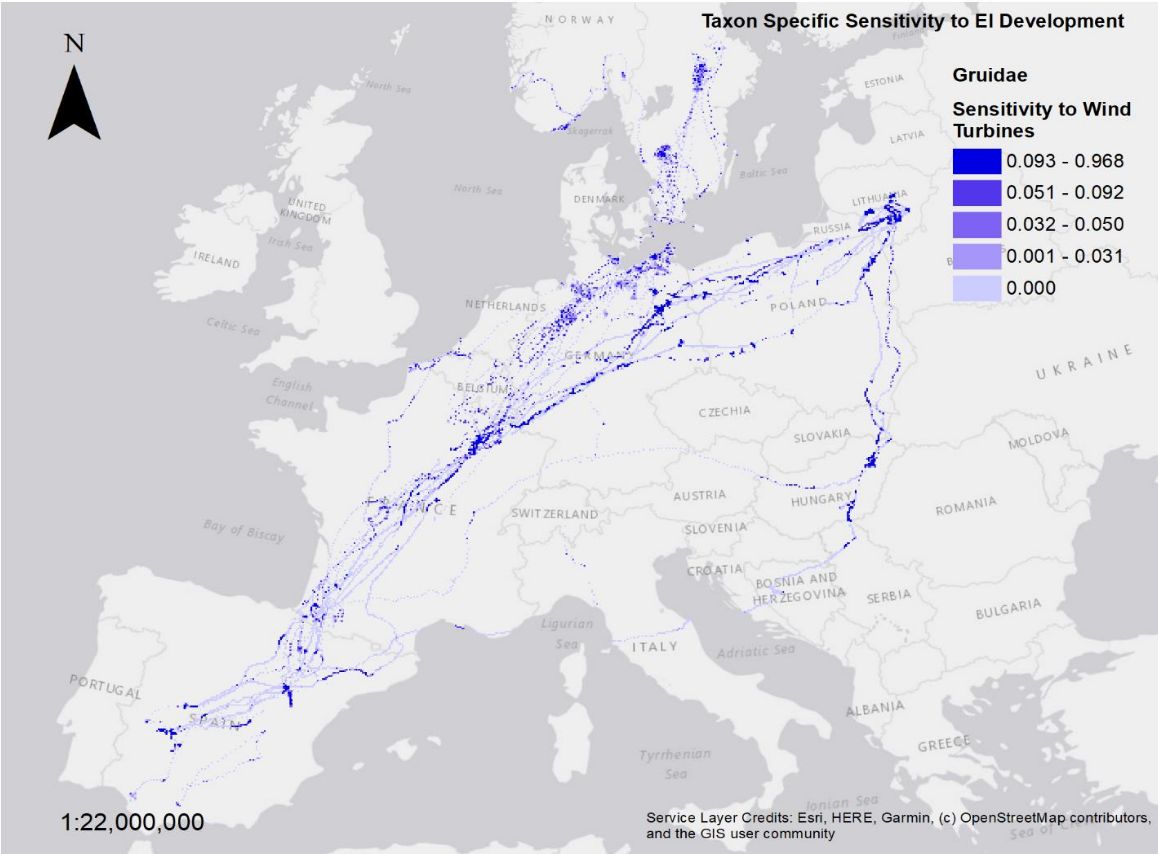

Supporting Information Figure 28: sensitivity to collision risk at danger height for wind turbines (15 - 135m) symbolised as quantiles. Map derived from GPS tracking data of common crane Grus grus. Areas with no symbology represent regions for which no tracking data could be obtained.

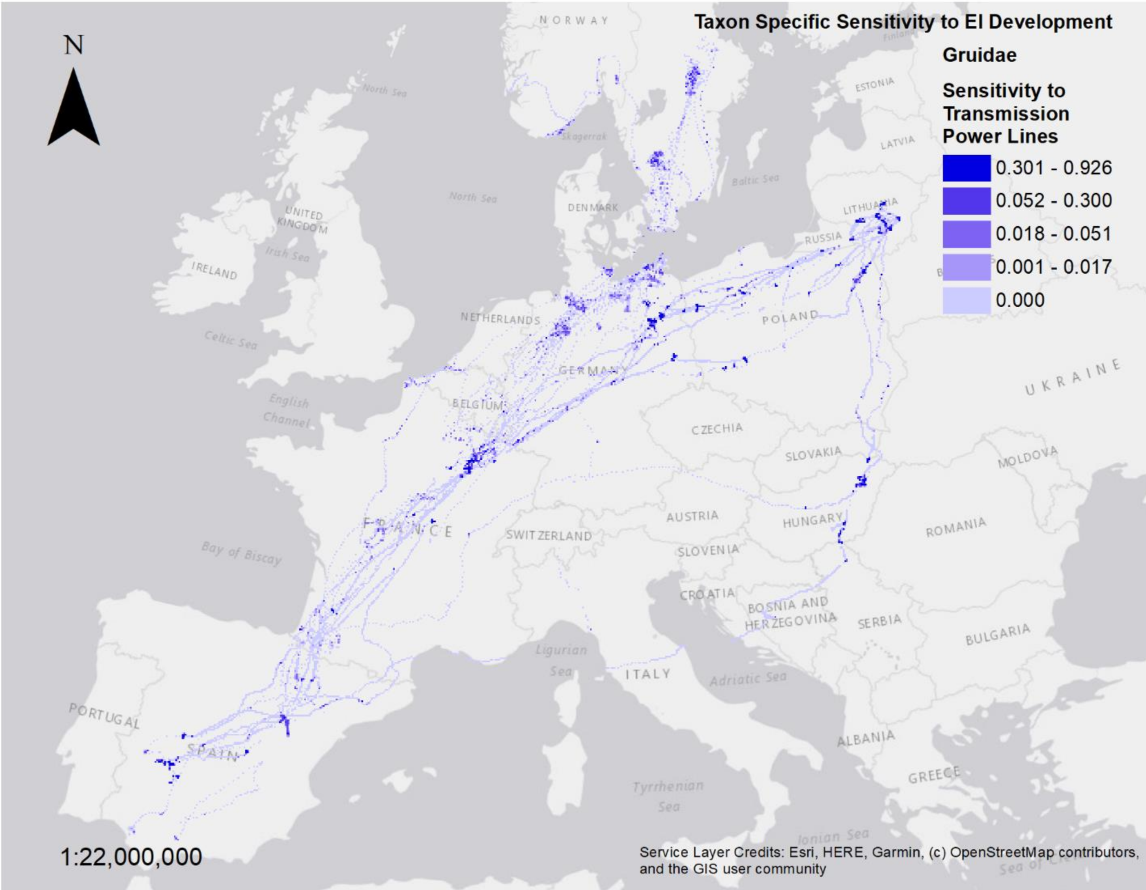

Supporting Information Figure 29: sensitivity to collision risk at danger height for transmission power lines (10 - 60m) symbolised as quantiles. Map derived from GPS tracking data of common crane Grus grus. Areas with no symbology represent regions for which no tracking data could be obtained.

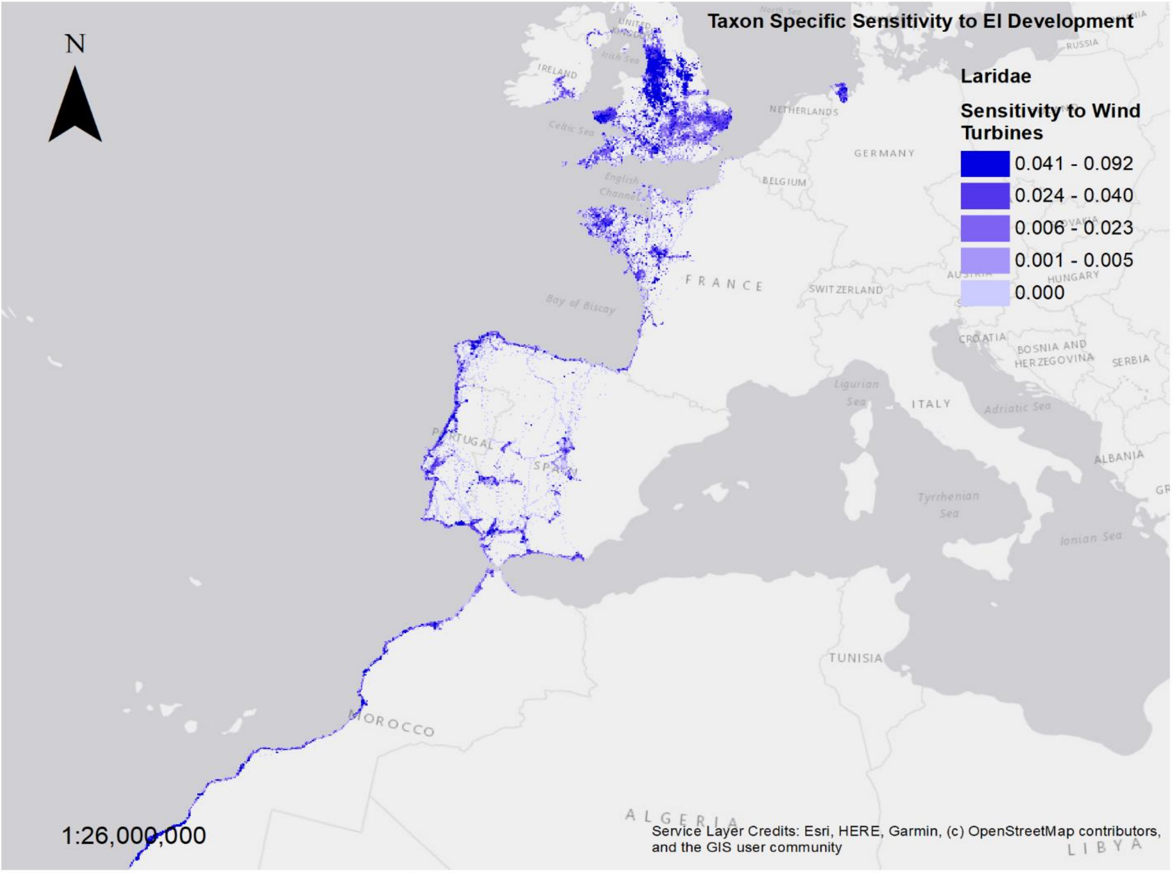

Supporting Information Figure 30: sensitivity to collision risk at danger height for wind turbines (15 - 135m) symbolised as quantiles. Map derived from GPS tracking data of lesser black-backed gulls Larus fuscus. Areas with no symbology represent regions for which no tracking data could be obtained.

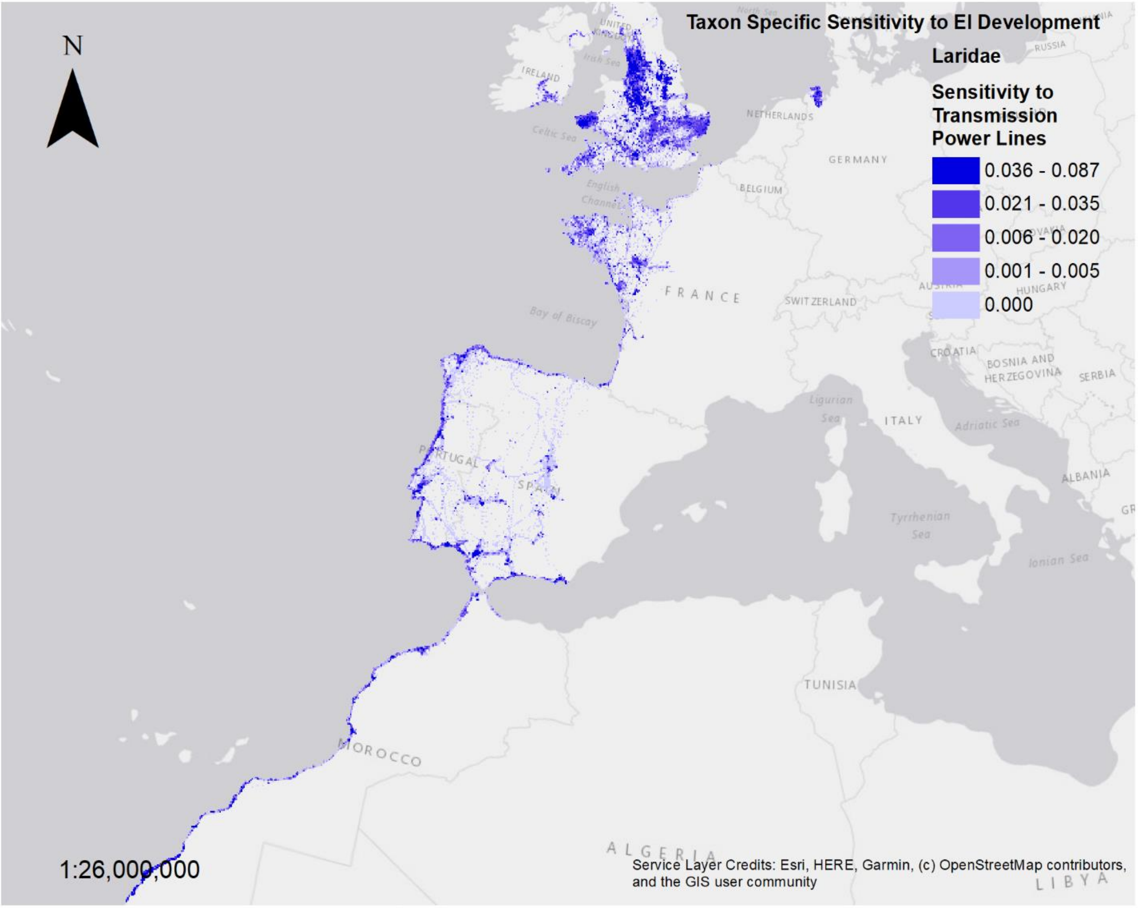

Supporting Information Figure 31: sensitivity to collision risk at danger height for transmission power lines (10 - 60m) symbolised as quantiles. Map derived from GPS tracking data of lesser black-backed gulls Larus fuscus. Areas with no symbology represent regions for which no tracking data could be obtained.

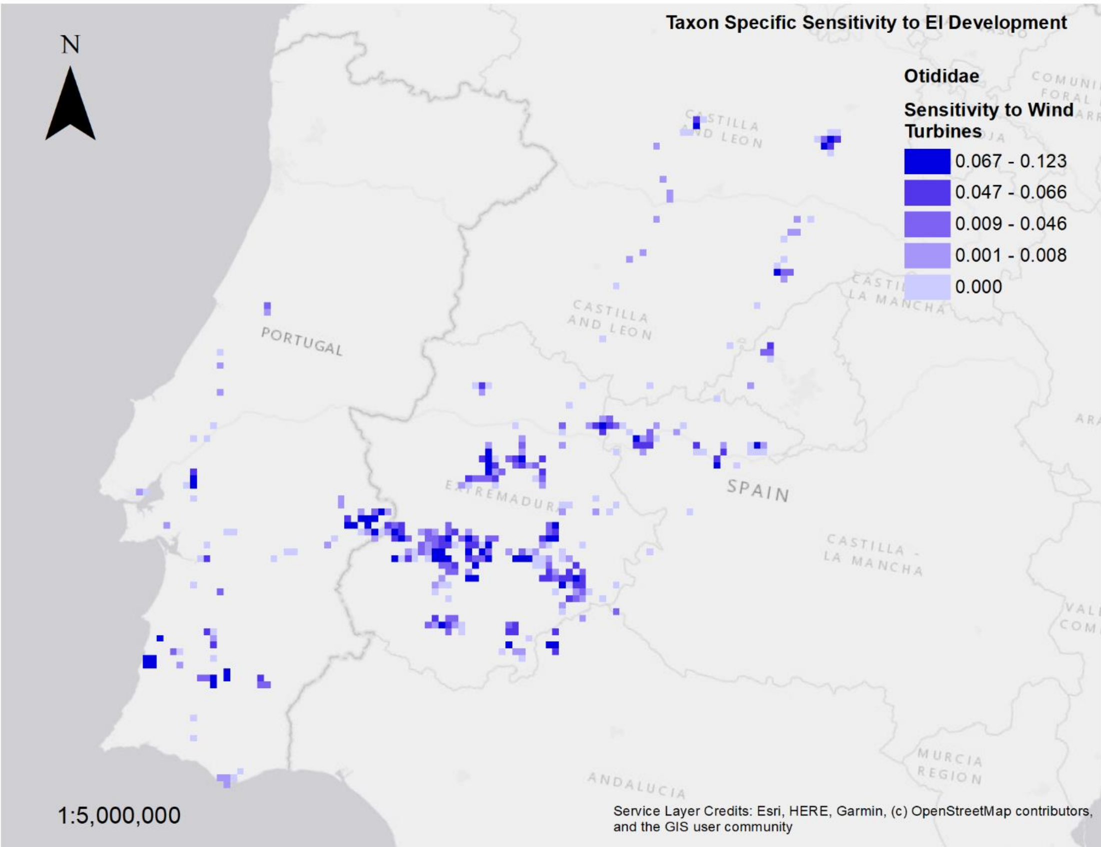

Supporting Information Figure 32: sensitivity to collision risk at danger height for wind turbines (15 - 135m) symbolised as quantiles. Map derived from GPS tracking data of little bustard Tetrax tetrax. Areas with no symbology represent regions for which no tracking data could be obtained.

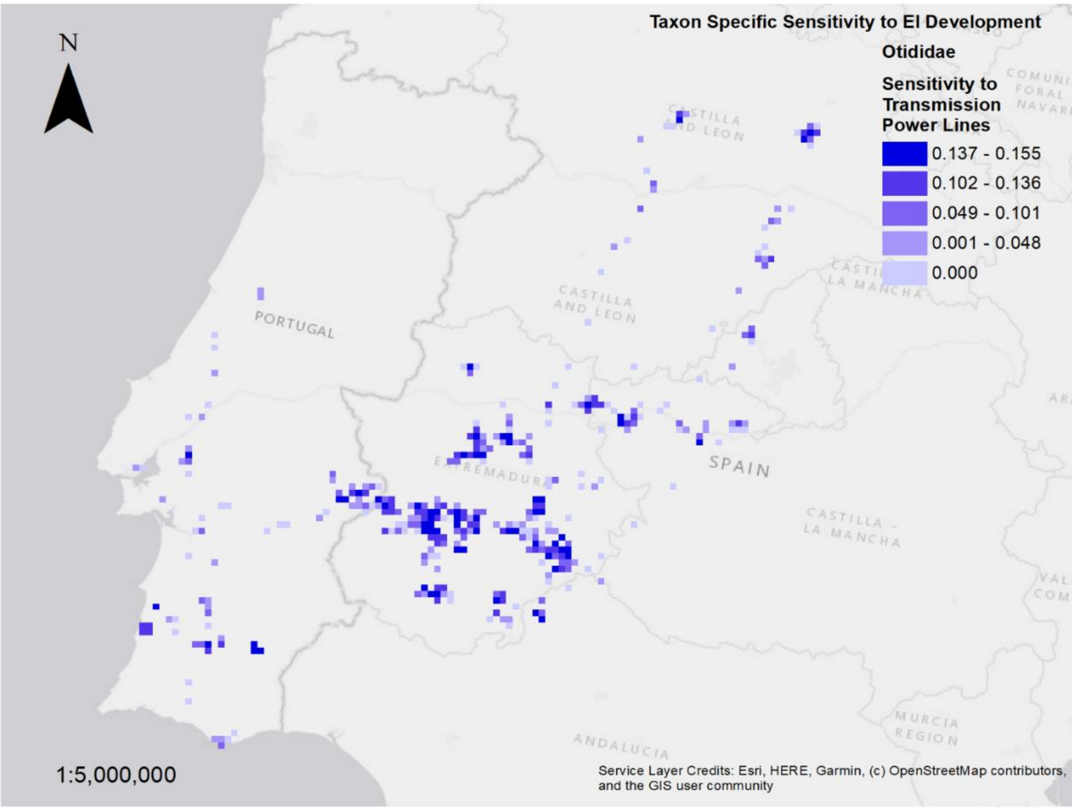

Supporting Information Figure 33: sensitivity to collision risk at danger height for transmission power lines (10 - 60m) symbolised as quantiles. Map derived from GPS tracking data of little bustard Tetrax tetrax. Areas with no symbology represent regions for which no tracking data could be obtained.

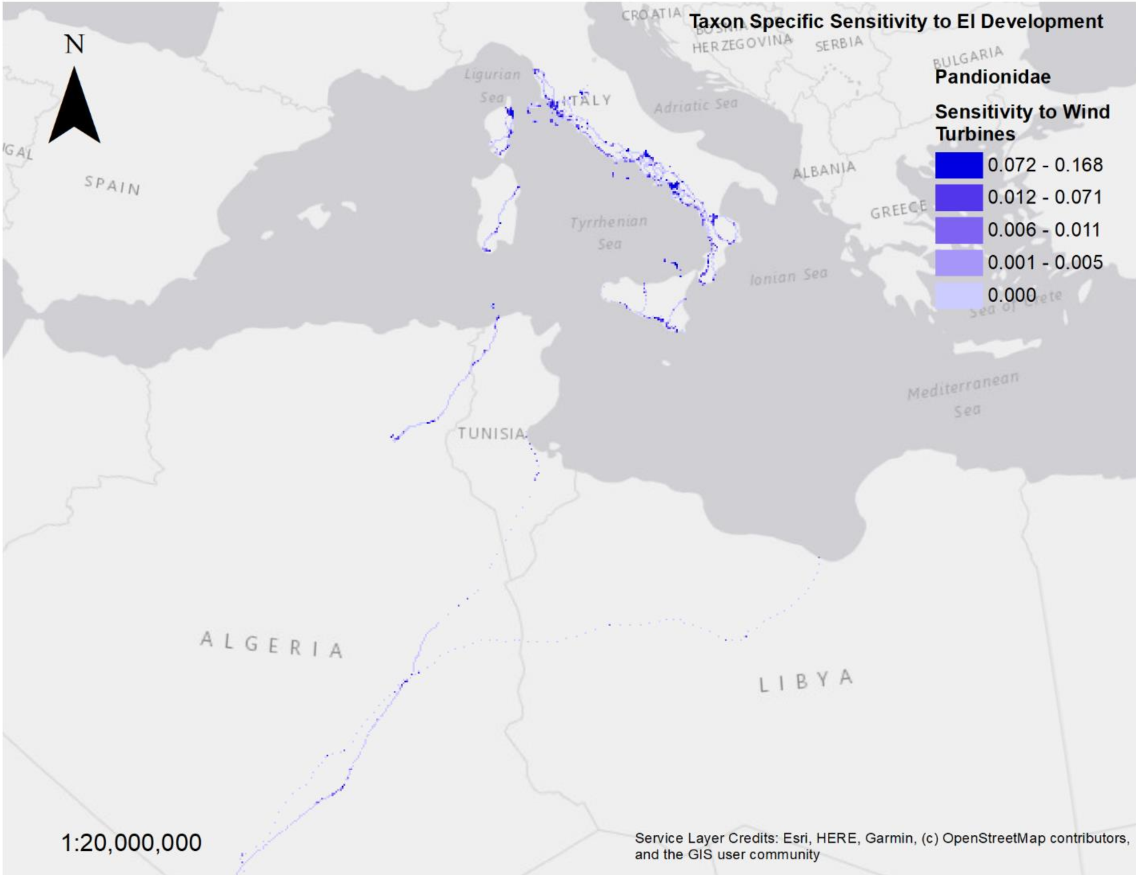

7476

7477 *Supporting Information Figure 34: sensitivity to collision risk at danger height for wind turbines (15 - 135m) symbolised*
7478 *as quantiles. Map derived from GPS tracking data of osprey Pandion haliaetus. Areas with no symbology represent*
7479 *regions for which no tracking data could be obtained.*

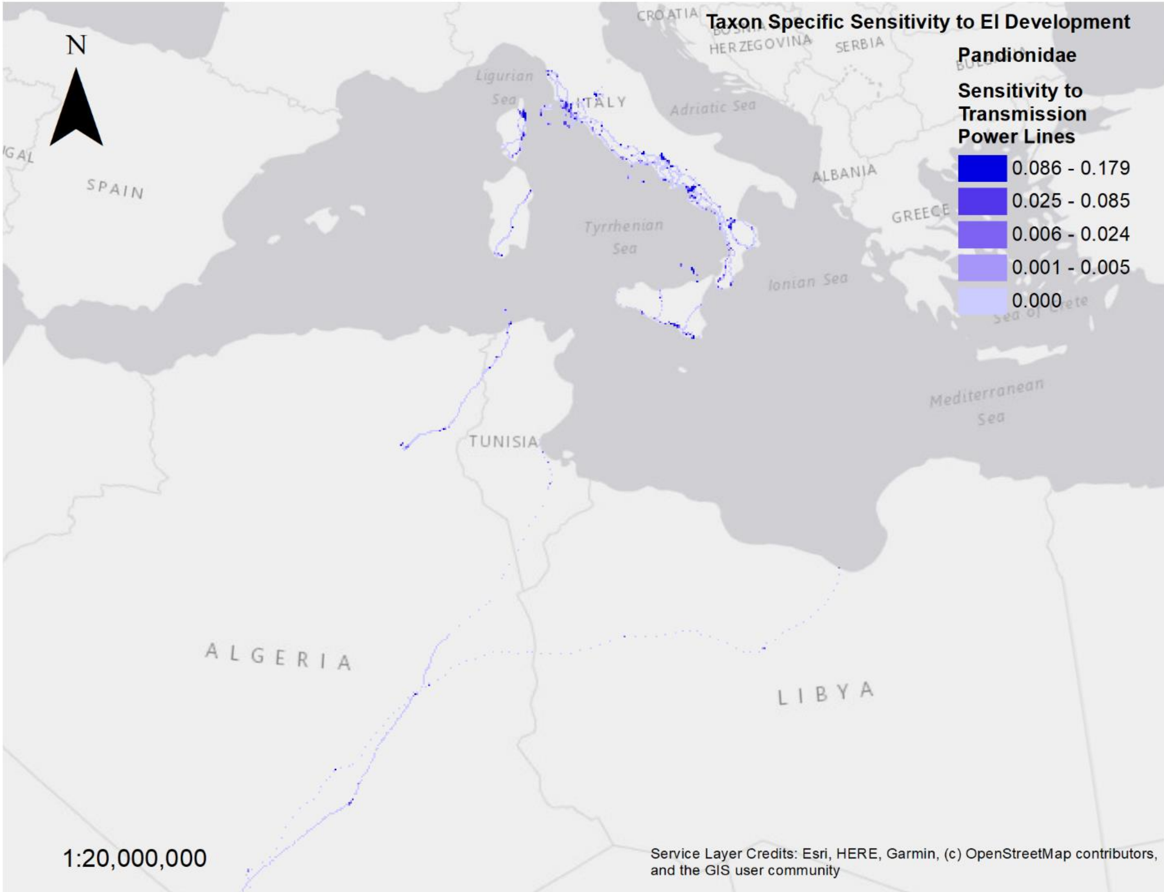

Supporting Information Figure 35: sensitivity to collision risk at danger height for transmission power lines (10 - 60m) symbolised as quantiles. Map derived from GPS tracking data of osprey Pandion haliaetus. Areas with no symbology represent regions for which no tracking data could be obtained.

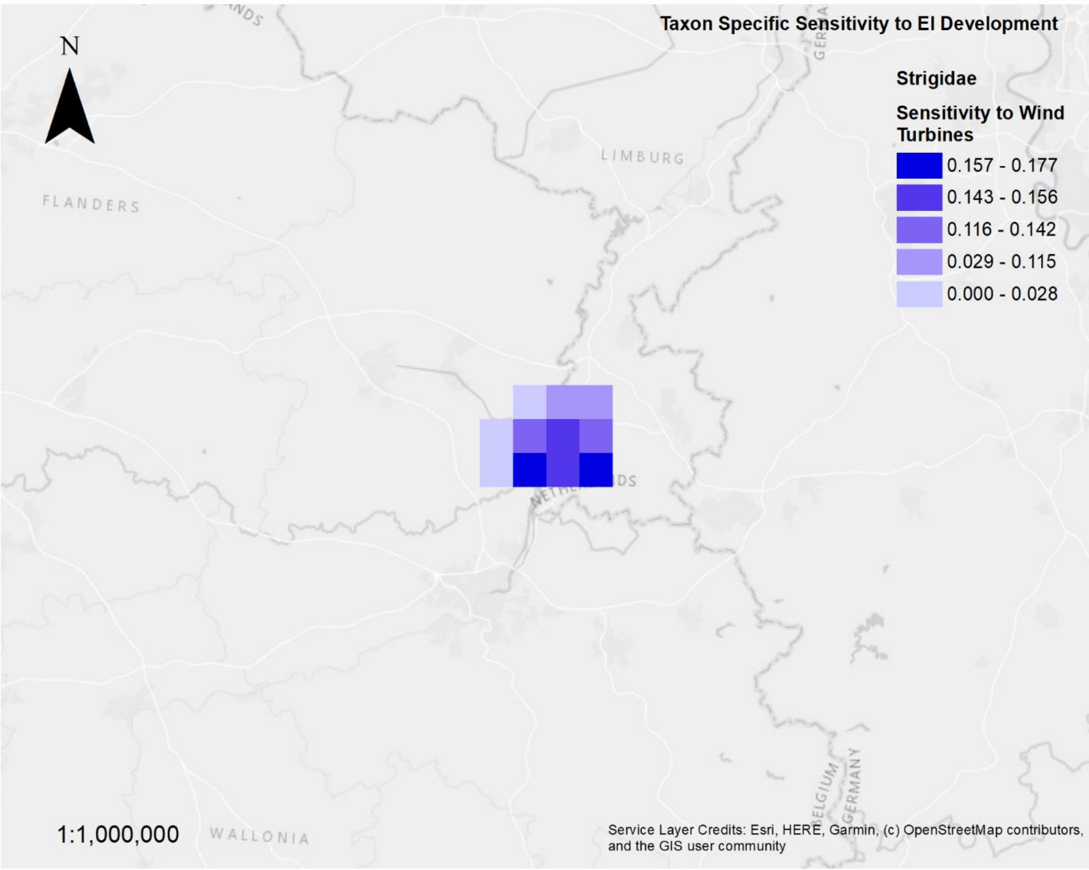

Supporting Information Figure 36: sensitivity to collision risk at danger height for wind turbines (15 - 135m) symbolised as quantiles. Map derived from GPS tracking data of Eurasian Eagle Owl Bubo bubo. Areas with no symbology represent regions for which no tracking data could be obtained.

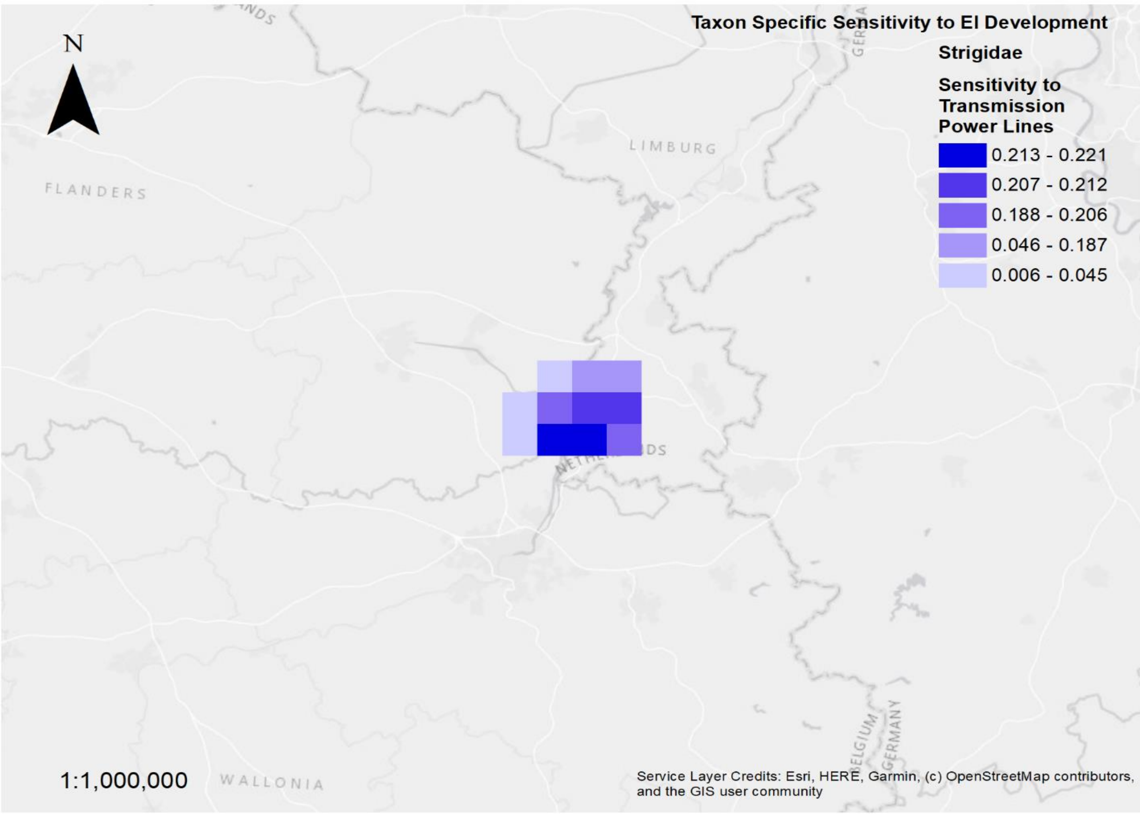

Supporting Information Figure 37: sensitivity to collision risk at danger height for transmission power lines (10 - 60m) symbolised as quantiles. Map derived from GPS tracking data of Eurasian eagle owl Bubo bubo. Areas with no symbology represent regions for which no tracking data could be obtained.

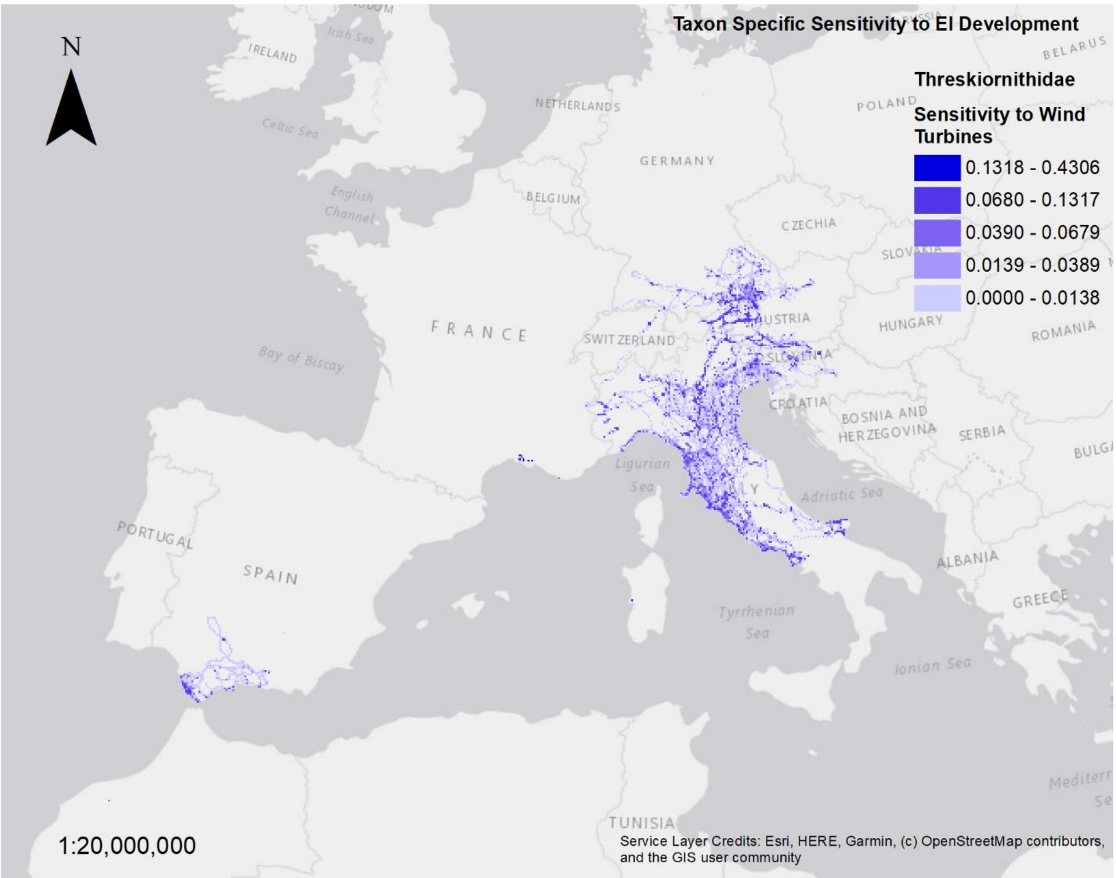

Supporting Information Figure 38: sensitivity to collision risk at danger height for wind turbines (15 - 135m) symbolised as quantiles. Map derived from GPS tracking data of northern bald ibis Geronticus eremita. Areas with no symbology represent regions for which no tracking data could be obtained.

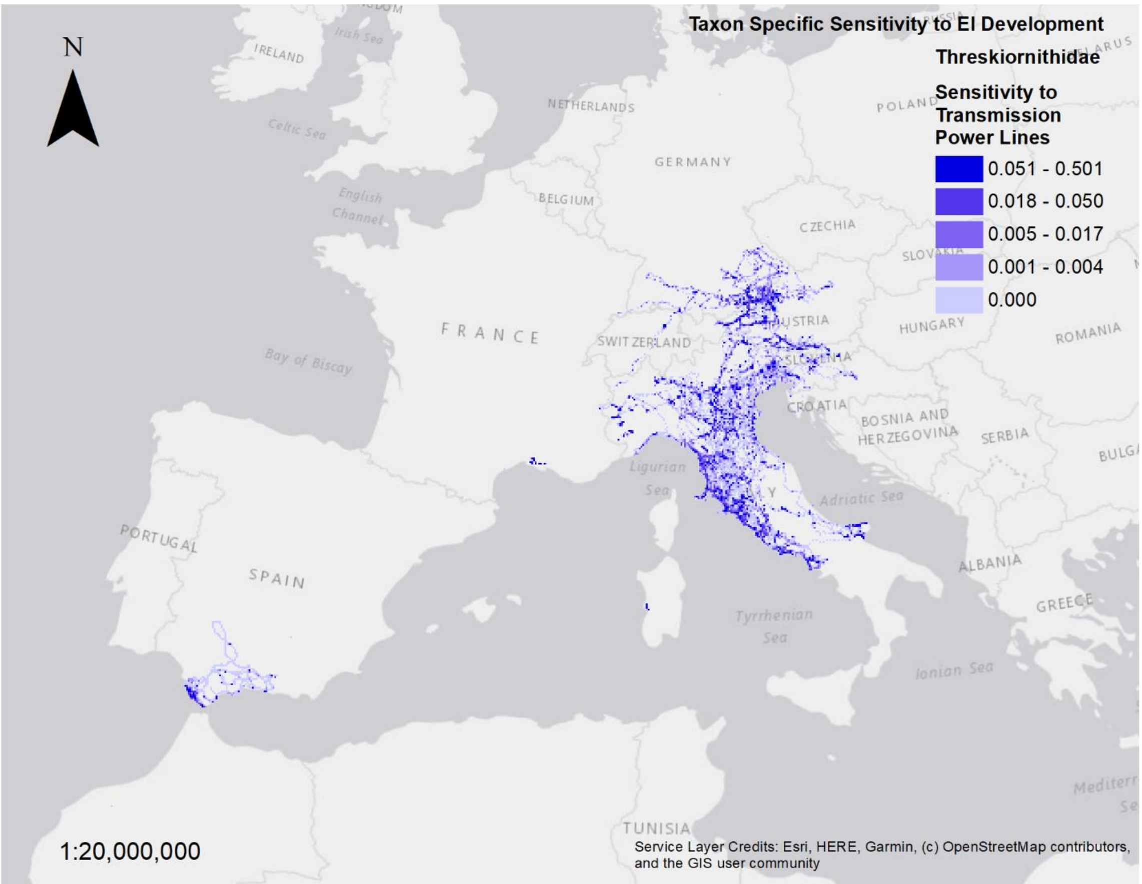

Supporting Information Figure 39: sensitivity to collision risk at danger height for transmission power lines (10 - 60m) symbolised as quantiles. Map derived from GPS tracking data of northern bald ibis Geronticus eremita. Areas with no symbology represent regions for which no tracking data could be obtained.

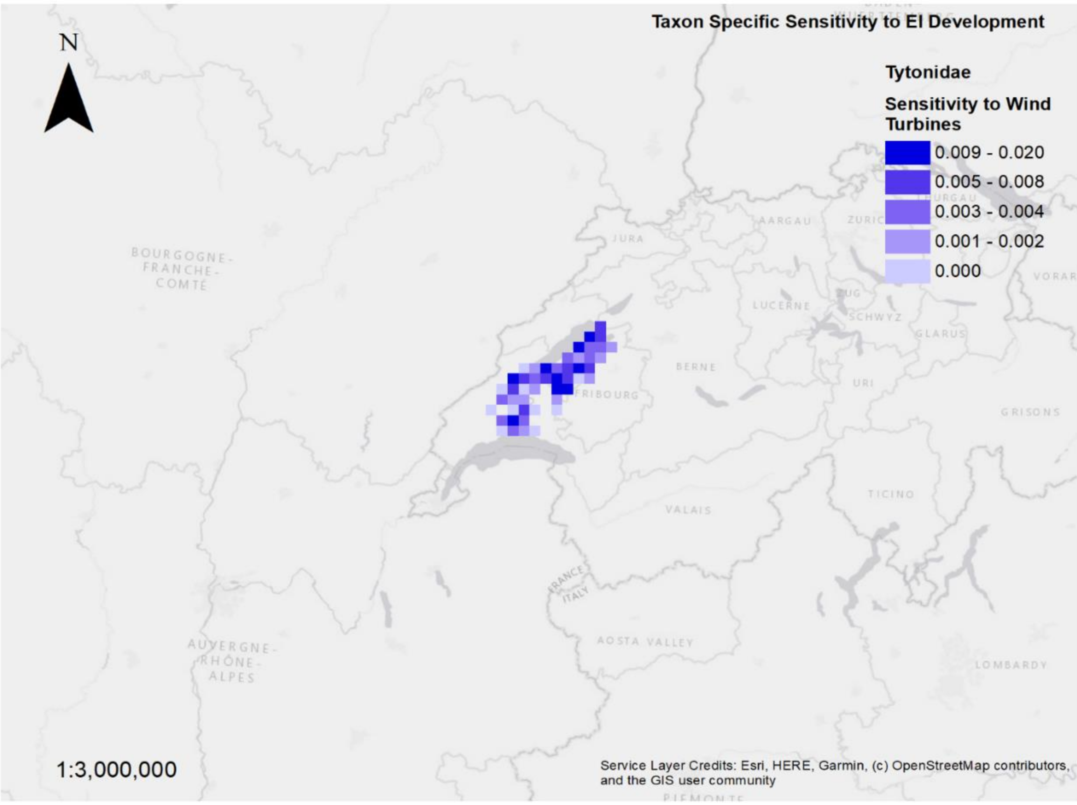

Supporting Information Figure 40: sensitivity to collision risk at danger height for wind turbines (15 - 135m) symbolised as quantiles. Map derived from GPS tracking data of barn owl Tyto alba. Areas with no symbology represent regions for which no tracking data could be obtained.

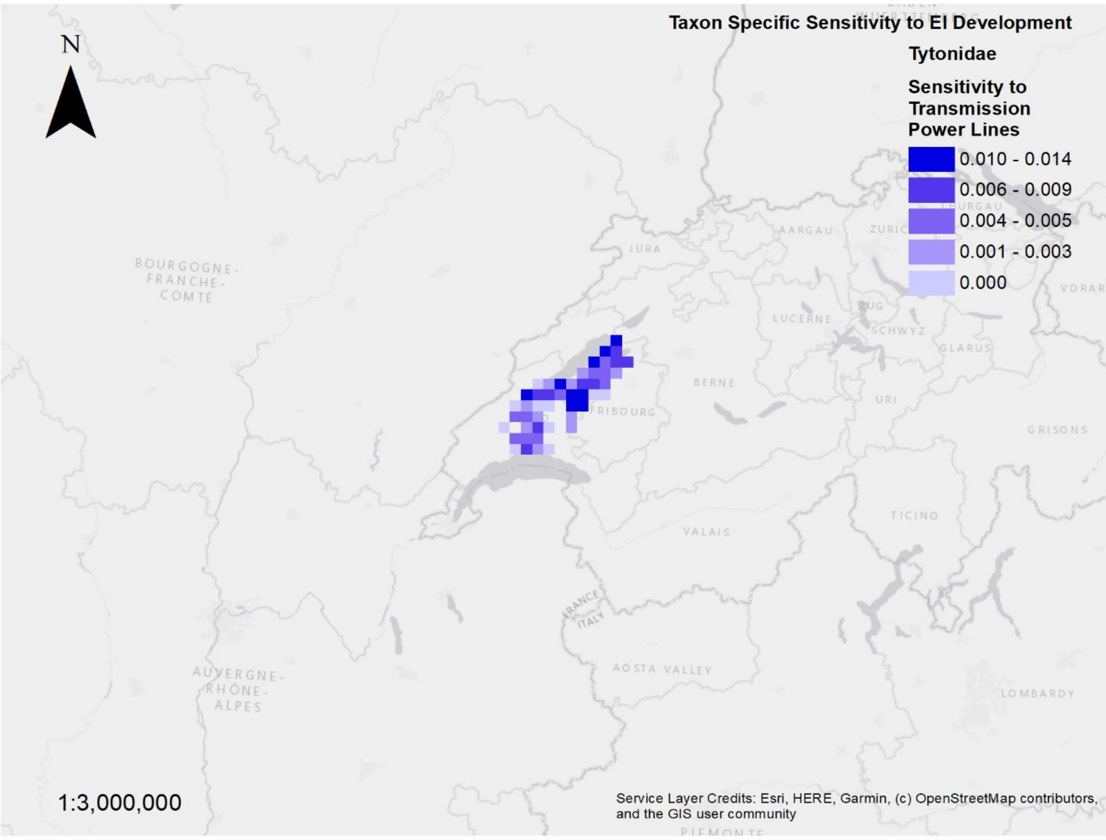

Supporting Information Figure 41: sensitivity to collision risk at danger height for transmission power lines (10 - 60m) symbolised as quantiles. Map derived from GPS tracking data of barn owl Tyto alba. Areas with no symbology represent regions for which no tracking data could be obtained.

SECTION 3: DISTRIBUTION OF VULNERABILITY BY COUNTRY

Here we summarise the number of grid cells classified as moderate, high or very high vulnerability by country. This highlights regional differences in the distribution of high vulnerability areas where mitigation to reduce risks to the tagged birds should be prioritised.

Country	Country Area (km^2)	Number of Very High Vulnerability Grid Cells	Number GPS Locations in Flight	Percentage of Country Area Occupied by Very High Vulnerability Grid Cells
Algeria	2317467.402	2	26	0.002
Austria	83944.89152	20	37580	0.596
Bulgaria	111022.8567	18	870	0.405
Czech Republic	78754.4619	17	1605	0.54
Egypt	998378.8671	16	1338	0.04
France	548056.5146	103	54769	0.47
Germany	357220.7897	134	222167	0.938
Greece	130010.4042	1	24871	0.019
Hungary	92994.77704	13	802	0.349
Israel	20705.88471	2	927	0.241
Jordan	89213.71876	2	1077	0.056
Lebanon	10214.09936	1	36	0.245
Libya	1617518.862	11	2457	0.017
Liechtenstein	176.4070574	3	3433	42.515
Lithuania	65010.18783	7	1221	0.269
Morocco	403062.1396	62	117562	0.385
Netherlands	35567.87678	1	1170	0.07
Poland	311667.8762	51	6767	0.409
Portugal	88567.32567	21	154023	0.593
Romania	237376.1567	49	5594	0.516
Serbia	88135.69057	6	25284	0.17
Slovakia	48926.5853	15	550	0.766
Spain	506153.9183	74	382089	0.366

Switzerland	41489.23198	31	40480	1.868
Syria	187960.279	9	396	0.12
Tunisia	155363.4113	7	1089	0.113
Turkey	779937.2425	34	29965	0.109
Ukraine	597502.2114	10	794	0.042
Western Sahara	269148.6809	3	1057	0.028

Supporting Information Table 5: Summary of the distribution of very high vulnerability grid cells by country.

Country	Country Area (km²)	Number of High Vulnerability Grid Cells	Number GPS Locations in Flight	Percentage of Country Area Occupied by High Vulnerability Grid Cells
Algeria	2317467.402	2	26	0.002
Austria	83944.89152	20	37580	0.596
Bulgaria	111022.8567	18	870	0.405
Czech Republic	78754.4619	17	1605	0.54
Egypt	998378.8671	16	1338	0.04
France	548056.5146	103	54769	0.47
Germany	357220.7897	134	222167	0.938
Greece	130010.4042	1	24871	0.019
Hungary	92994.77704	13	802	0.349
Israel	20705.88471	2	927	0.241
Jordan	89213.71876	2	1077	0.056
Lebanon	10214.09936	1	36	0.245
Libya	1617518.862	11	2457	0.017
Liechtenstein	176.4070574	3	3433	42.515
Lithuania	65010.18783	7	1221	0.269
Morocco	403062.1396	62	117562	0.385
Netherlands	35567.87678	1	1170	0.07
Poland	311667.8762	51	6767	0.409
Portugal	88567.32567	21	154023	0.593
Romania	237376.1567	49	5594	0.516
Serbia	88135.69057	6	25284	0.17
Slovakia	48926.5853	15	550	0.766
Spain	506153.9183	74	382089	0.366
Switzerland	41489.23198	31	40480	1.868
Syria	187960.279	9	396	0.12
Tunisia	155363.4113	7	1089	0.113
Turkey	779937.2425	34	29965	0.109
Ukraine	597502.2114	10	794	0.042
Western Sahara	269148.6809	3	1057	0.028

Supporting Information Table 6:Summary of the distribution of high vulnerability grid cells by country.

7520

7521

Country	Country Area (km²)	Number of Moderate Vulnerability Grid Cells	Number GPS Locations in Flight	Percentage of Country Area Occupied by Moderate Vulnerability Grid Cells
Albania	28654.7817	8	69	0.698
Algeria	2317467.4	22	92	0.024
Austria	83944.8915	295	47567	8.786
Belarus	207720.91	67	555	0.806
Belgium	30651.4194	201	77683	16.394
Bosnia and Herzegovina	51527.1396	7	57	0.34
Bulgaria	111022.857	265	94591	5.967
Croatia	55888.8379	23	190	1.029
Czech Republic	78754.4619	184	2257	5.841
Denmark	42710.2691	10	134	0.585
Egypt	998378.867	325	26339	0.814
Estonia	45932.0815	33	468	1.796
Finland	335279.996	12	51	0.089
France	548056.515	1590	47560	7.253
Germany	357220.79	1680	67388	11.757
Greece	130010.404	195	11437	3.75
Guernsey (UK)	72.7768437	1	2	34.352
Hungary	92994.777	169	2315	4.543
Ireland	69638.3935	55	1117	1.974
Israel	20705.8847	99	62639	11.953
Italy	299990.134	1213	126787	10.109
Jordan	89213.7188	32	2306	0.897
Latvia	64643.0295	32	265	1.238
Lebanon	10214.0994	38	968	9.301
Libya	1617518.86	35	205	0.054
Lithuania	65010.1878	108	12998	4.153
Luxembourg	2580.64061	6	16	5.813
Macedonia	25462.4392	32	4646	3.142
Moldova	33687.5854	7	35	0.519
Montenegro	13796.1116	3	11	0.544
Morocco	403062.14	510	22287	3.163

Netherlands	35567.8768	236	130373	16.588
Norway	320866.067	19	291	0.148
Palestine	6252.62103	10	7606	3.998
Poland	311667.876	726	8287	5.824
Portugal	88567.3257	328	33290	9.258
Romania	237376.157	428	5675	4.508
San Marino	59.864964	1	5	41.761
Saudi Arabia	1954166.93	1	4	0.001
Serbia	88135.6906	62	2112	1.759
Slovakia	48926.5853	102	1348	5.212
Slovenia	20421.0517	42	736	5.142
Spain	506153.918	1438	113969	7.103
Sweden	446013.828	108	2972	0.605
Switzerland	41489.232	94	7177	5.664
Syria	187960.279	209	5019	2.78
Tunisia	155363.411	18	291	0.29
Turkey	779937.242	820	24135	2.628
Ukraine	597502.211	558	3966	2.335
United Kingdom	244349.423	1625	397251	16.626
Western Sahara	269148.681	30	489	0.279

Supporting Information Table 7:Summary of the distribution of moderate vulnerability grid cells by country.

SECTION 4: VULNERABILITY TO ENERGY INFRASTRUCTURE BY FAMILY

Maps of combined vulnerability to wind farms and power lines are displayed in this section for each family of birds included in this analysis. Most families in the data set are represented by single species (*Pandonidae, Theskiornidae, Laridae, Strigidae, Otidae, Gruidae, Tytonidae, Burhinidae* and *Falconidae*). These groups could be prioritised for future tracking studies. *Ciconiidae* and *Accipitridae* are the two best represented groups in the data set. These maps highlight where each group experiences the highest vulnerability to collision risk in relation to wind turbines and power lines.

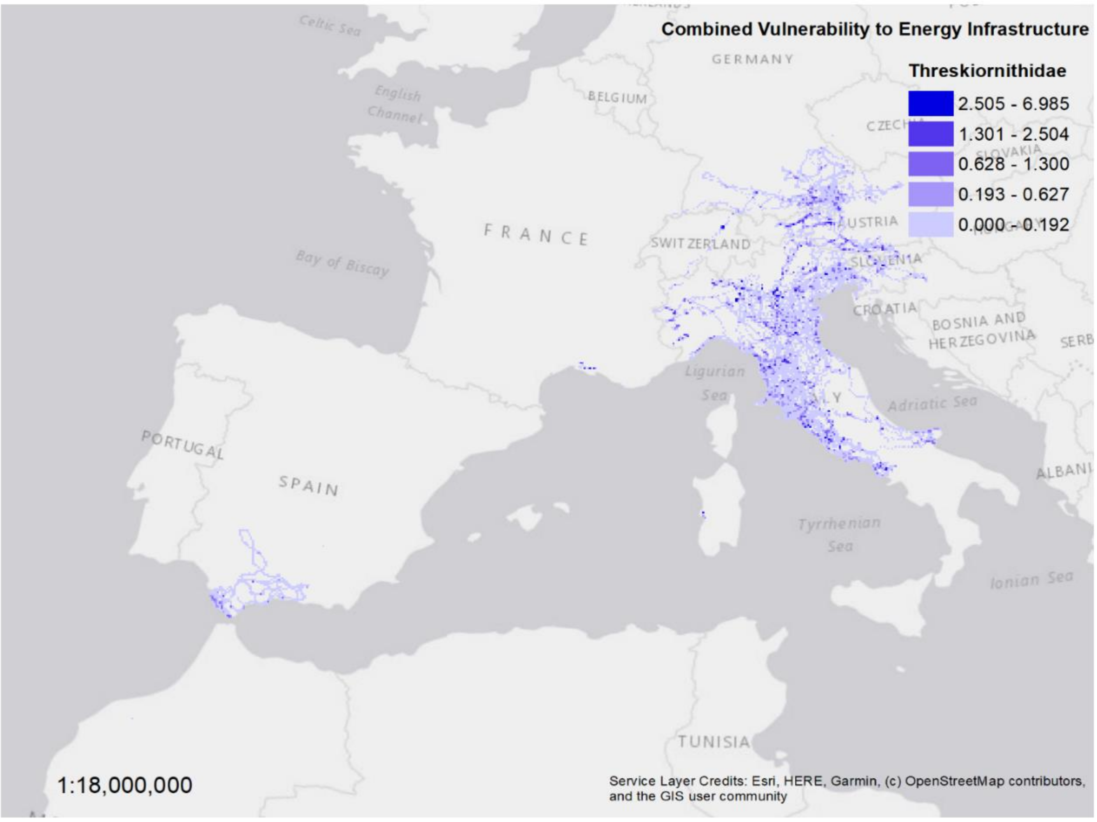

Supporting Information Figure 42: Vulnerability for all grid cells within the study area with sufficient GPS locations in flight to assess vulnerability for Theskiornithidae. Vulnerability is symbolised in quantiles from 0 – 6.9 which is the highest vulnerability score for this taxa. Areas with no symbology represent regions for which no tracking data could be obtained.

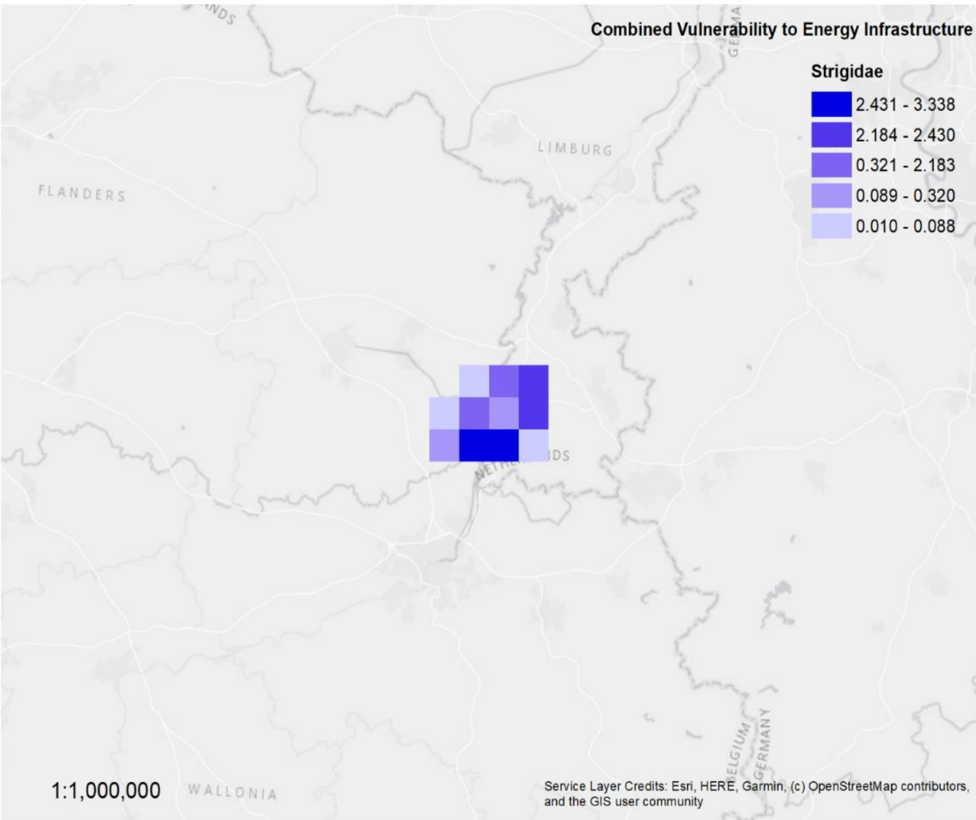

Supporting Information Figure 43: Vulnerability for all grid cells within the study area with sufficient GPS locations in flight to assess vulnerability for Strigidae. Vulnerability is symbolised in quantiles from 0 – 3.34 which is the highest vulnerability score for this taxa. Areas with no symbology represent regions for which no tracking data could be obtained.

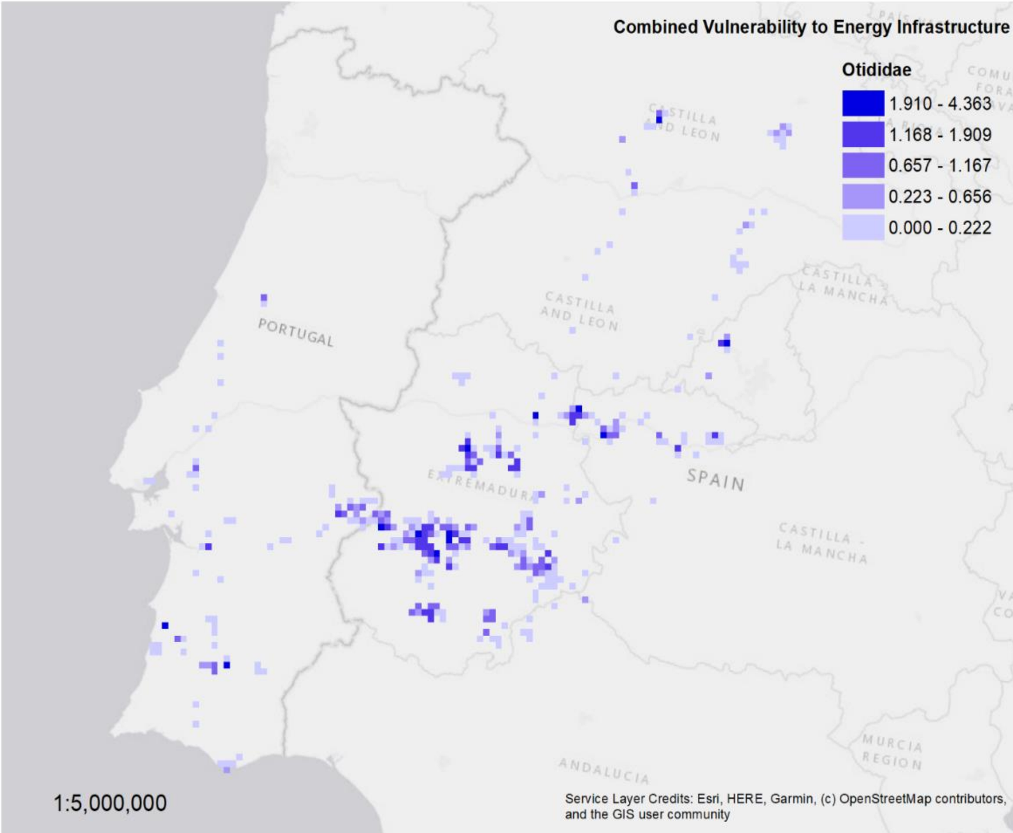

Supporting Information Figure 44: Vulnerability for all grid cells within the study area with sufficient GPS locations in flight to assess vulnerability for Otididae. Vulnerability is symbolised in quantiles from 0 – 4.36 which is the highest vulnerability score for this taxa. Areas with no symbology represent regions for which no tracking data could be obtained.

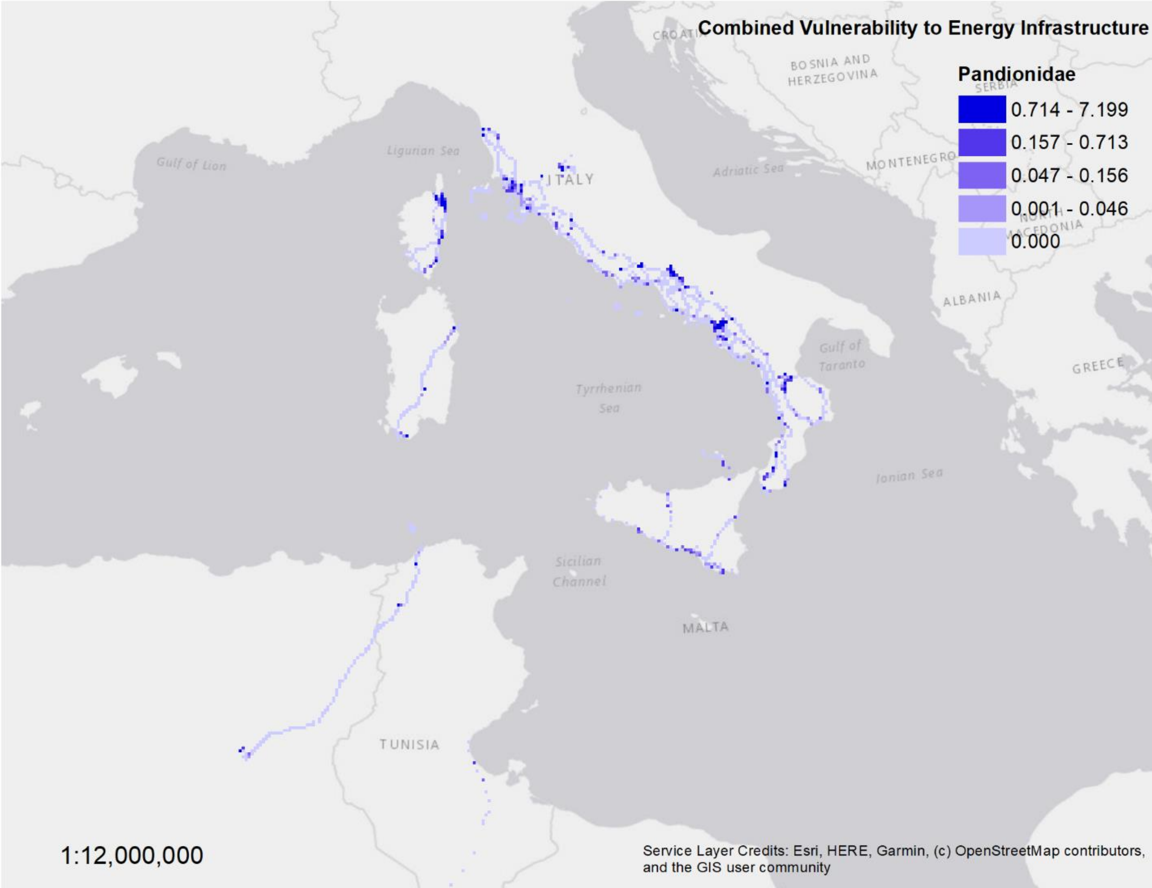

Supporting Information Figure 45: Vulnerability for all grid cells within the study area with sufficient GPS locations in flight to assess vulnerability for Pandionidae. Vulnerability is symbolised in quantiles from 0 – 7.2 which is the highest vulnerability score for this taxa. Areas with no symbology represent regions for which no tracking data could be obtained.

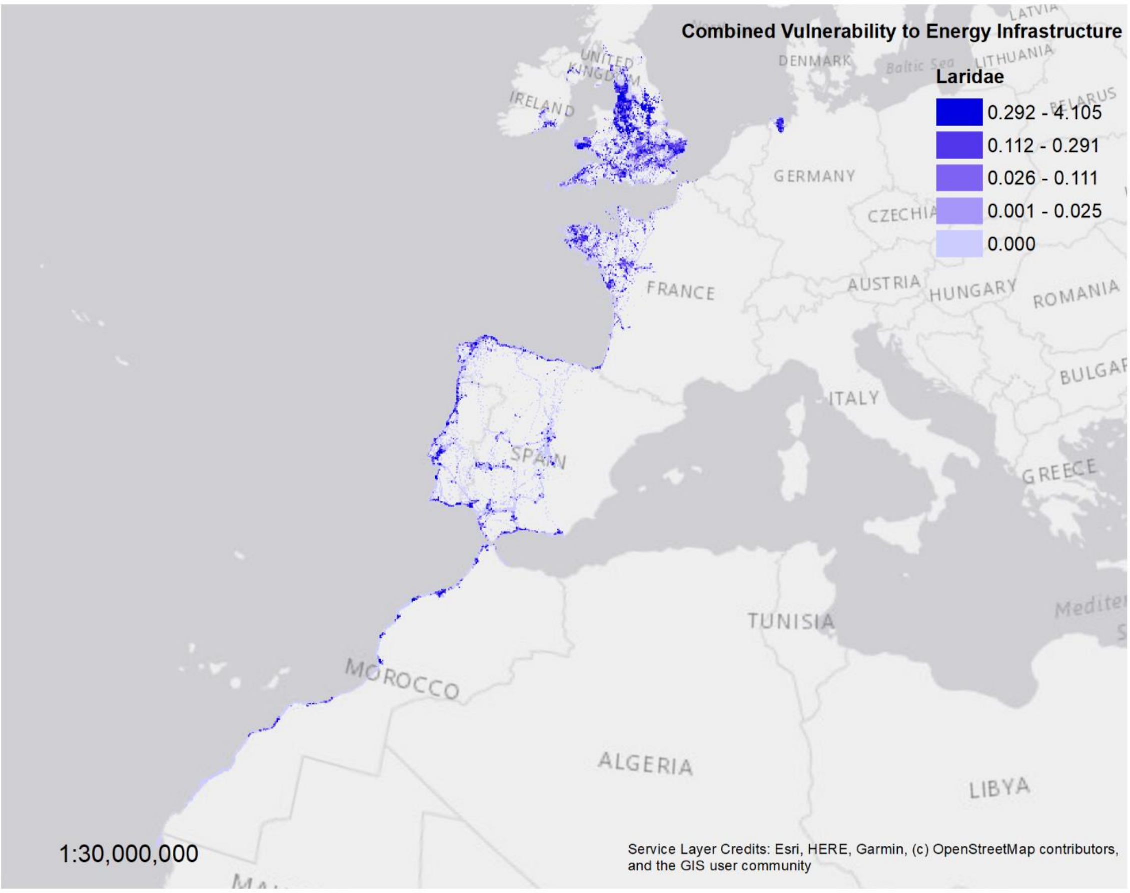

Supporting Information Figure 46: Vulnerability for all grid cells within the study area with sufficient GPS locations in flight to assess vulnerability for Laridae. Vulnerability is symbolised in quantiles from 0 – 4.12 which is the highest vulnerability score for this taxa. Areas with no symbology represent regions for which no tracking data could be obtained.

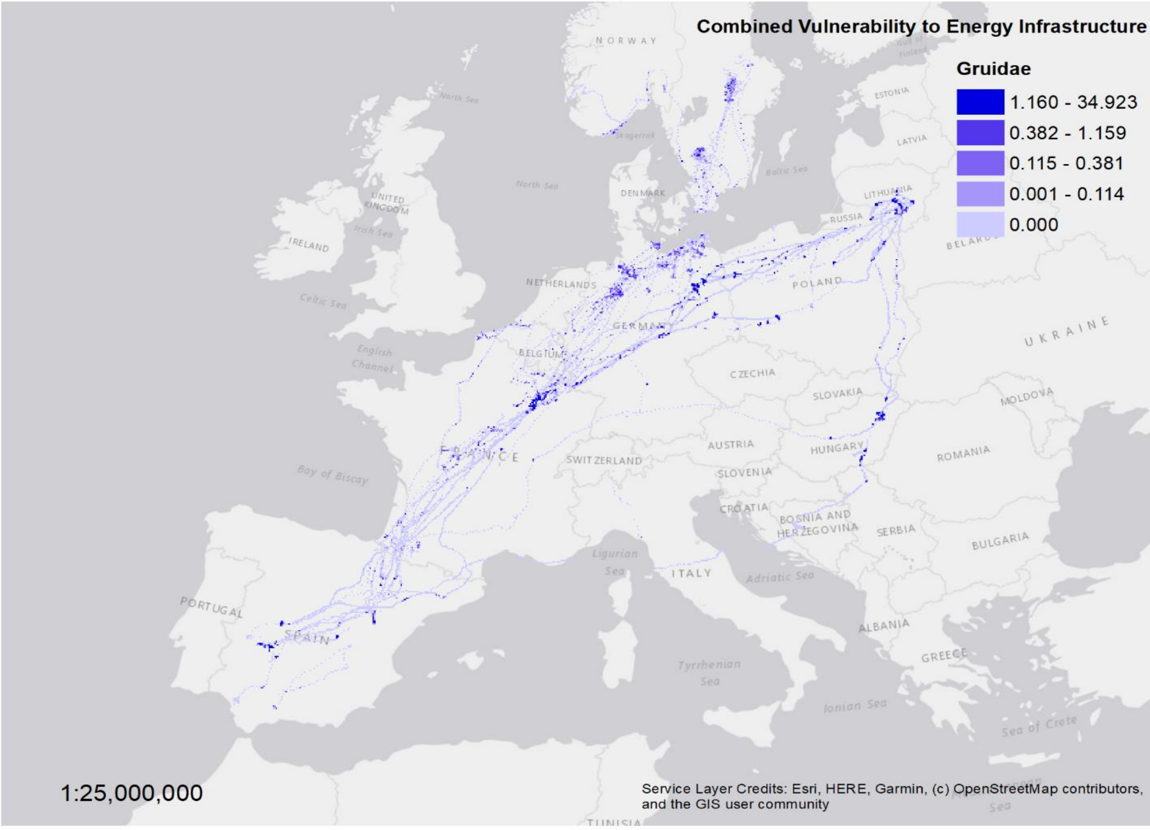

Supporting Information Figure 47: Vulnerability for all grid cells within the study area with sufficient GPS locations in flight to assess vulnerability for Gruidae. Vulnerability is symbolised in quantiles from 0 – 34.92 which is the highest vulnerability score for this taxa. Areas with no symbology represent regions for which no tracking data could be obtained.

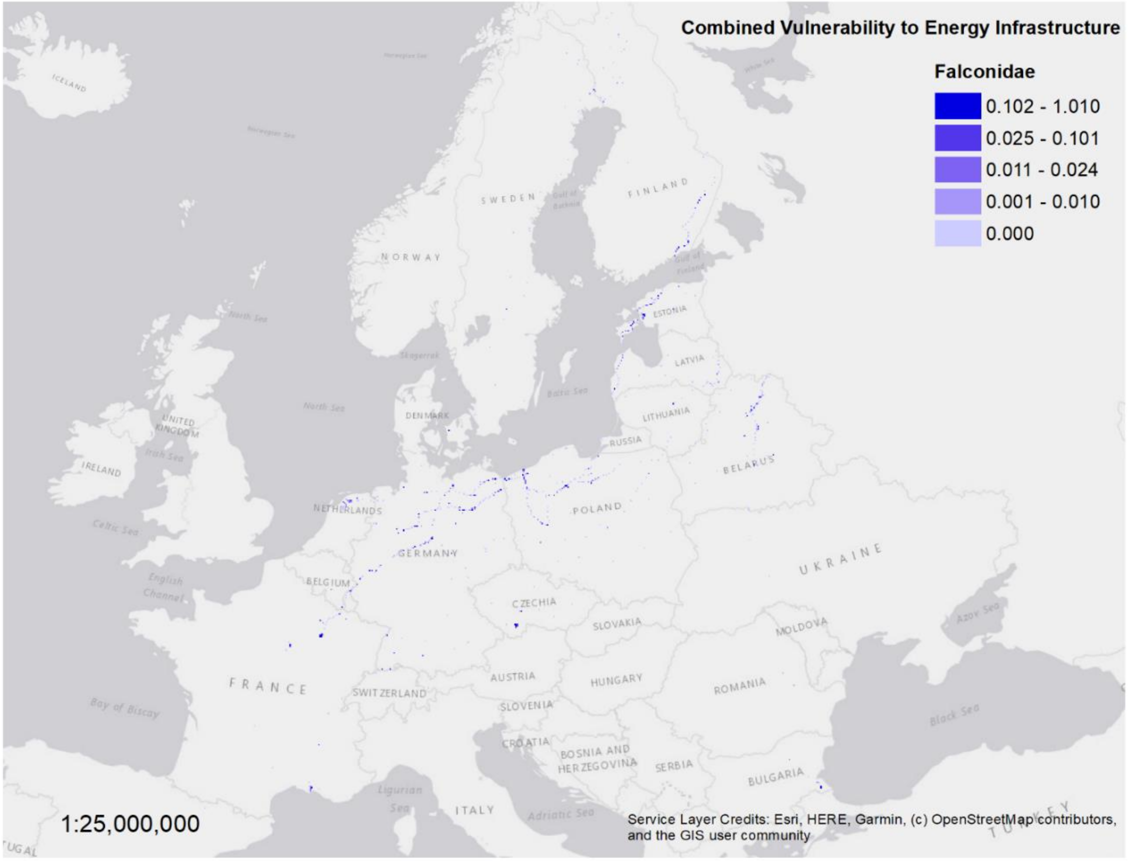

Supporting Information Figure 48: Vulnerability for all grid cells within the study area with sufficient GPS locations in flight to assess vulnerability for Falconidae represented by the peregrine falcon Falco peregrinus. Vulnerability is symbolised in quantiles from 0 – 1.01 which is the highest vulnerability score for this taxa. Areas with no symbology represent regions for which no tracking data could be obtained.

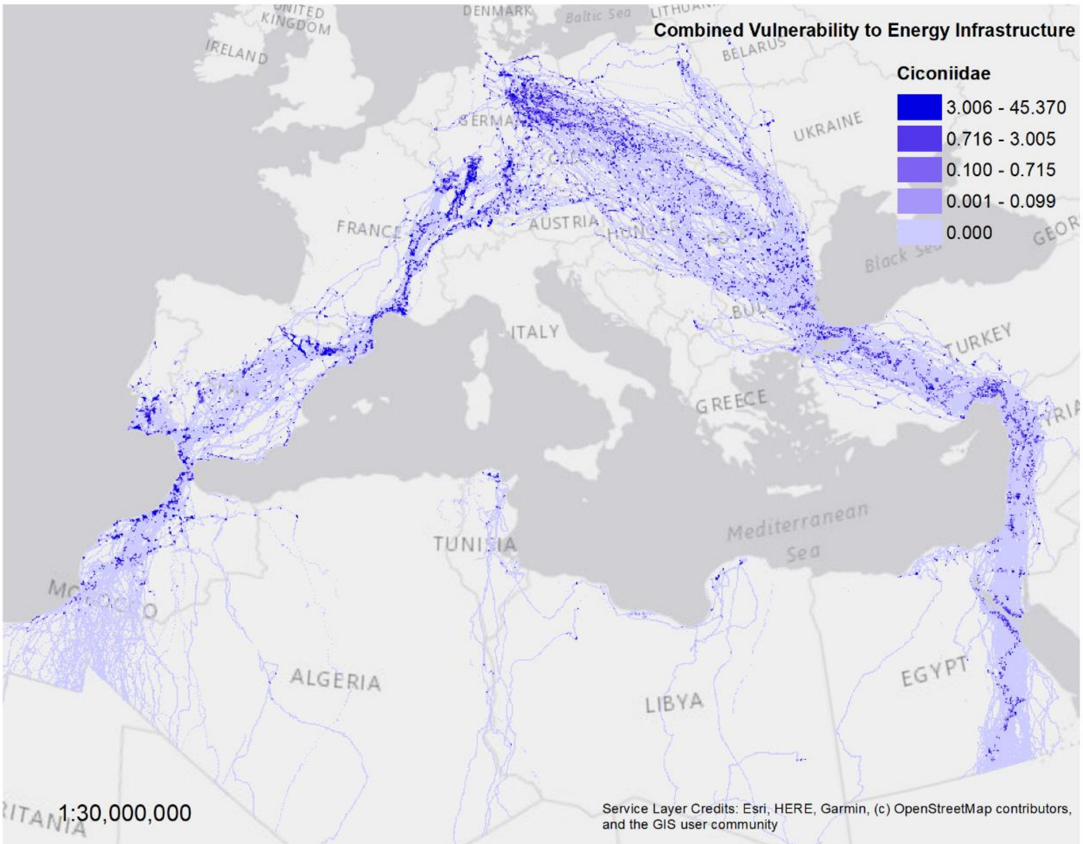

Supporting Information Figure 49: Vulnerability for all grid cells within the study area with sufficient GPS locations in flight to assess vulnerability for 45.37. Vulnerability is symbolised in quantiles from 0 – 45.37 which is the highest vulnerability score for this taxa represented by C. cicnonia and C. nigra. Areas with no symbology represent regions for which no tracking data could be obtained.

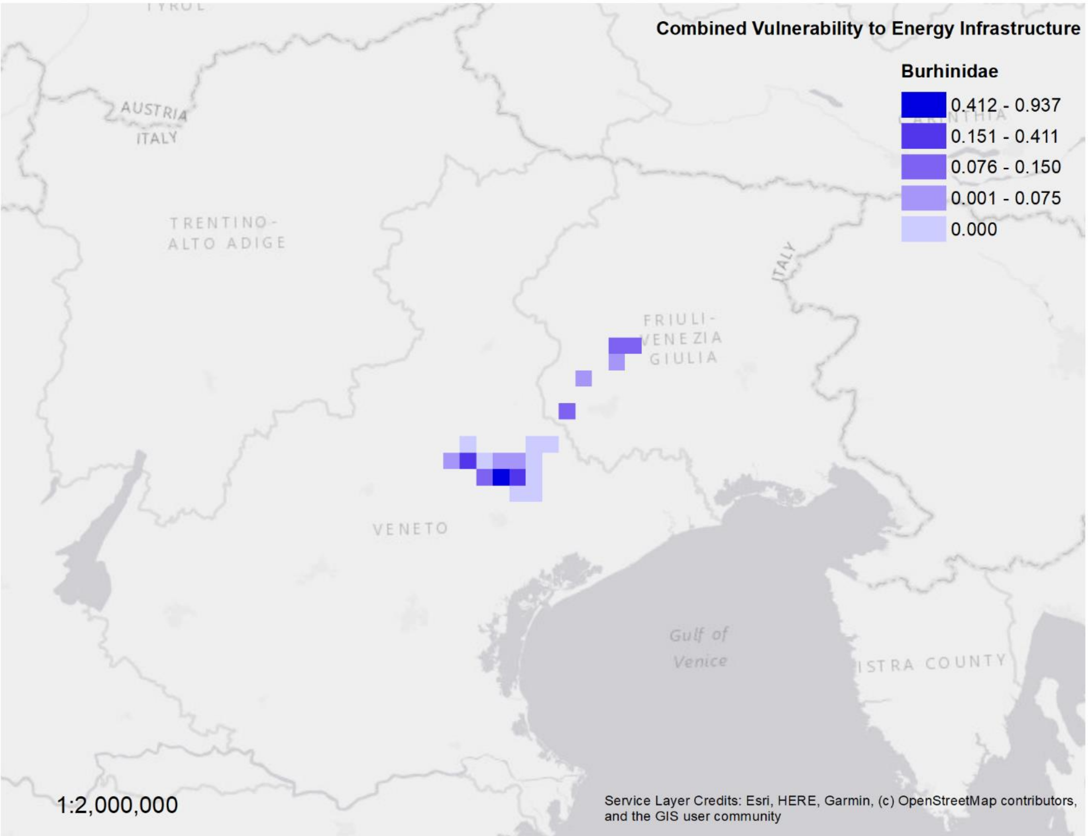

Supporting Information Figure 50: Vulnerability for all grid cells within the study area with sufficient GPS locations in flight to assess vulnerability for Burhinidae. Vulnerability is symbolised in quantiles from 0 – 0.94 which is the highest vulnerability score for this taxa represented by Burhinus oedicnemus. Areas with no symbology represent regions for which no tracking data could be obtained.

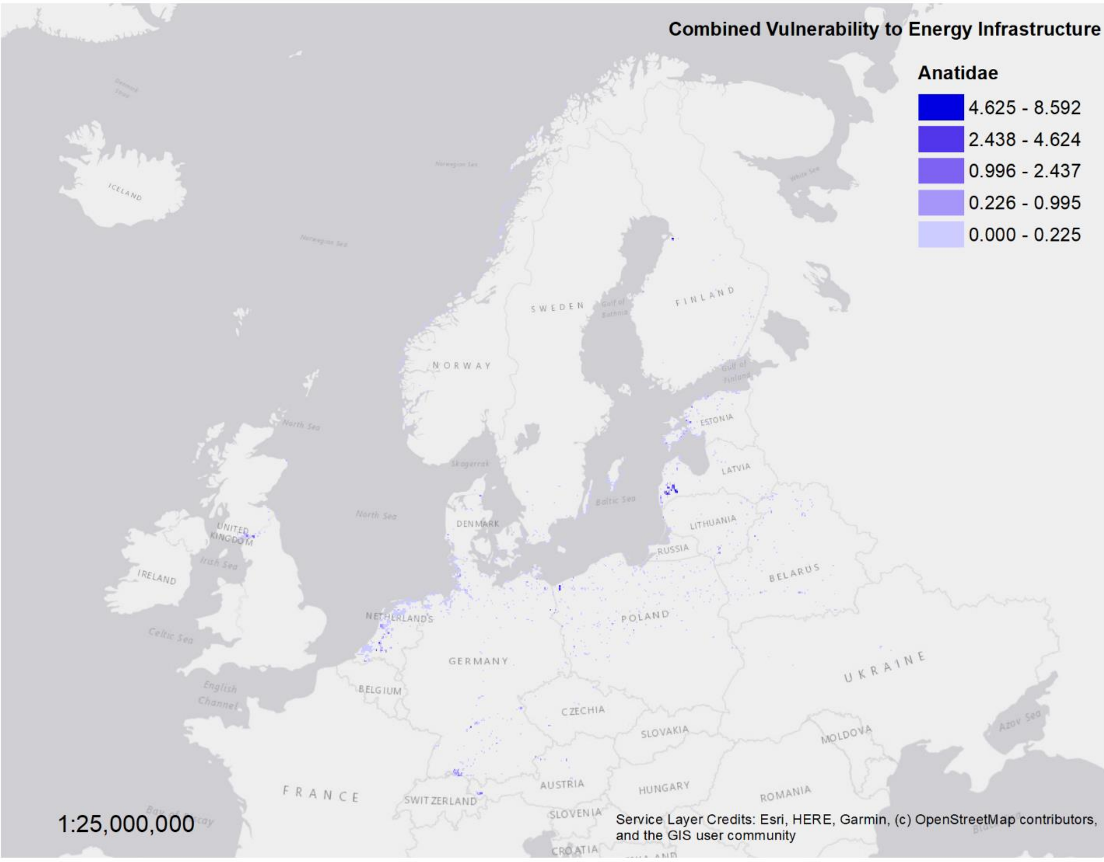

Supporting Information Figure 51: Vulnerability for all grid cells within the study area with sufficient GPS locations in flight to assess vulnerability for Anatidae. Vulnerability is symbolised in quantiles from 0 – 8.59 which is the highest vulnerability score for this taxa. Areas with no symbology represent regions for which no tracking data could be obtained.

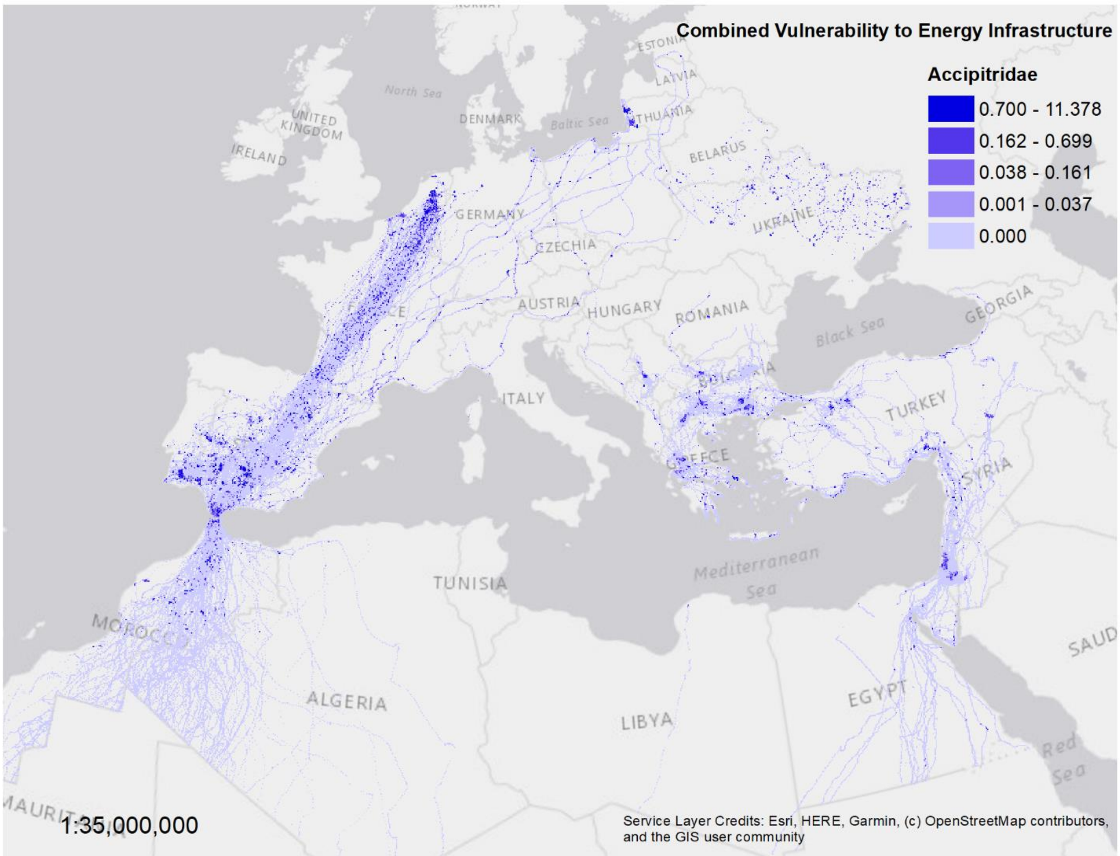

Supporting Information Figure 52: Vulnerability for all grid cells within the study area with sufficient GPS locations in flight to assess vulnerability for Accipitridae. Vulnerability is symbolised in quantiles from 0 – 11.38 which is the highest vulnerability score for this taxa. Areas with no symbology represent regions for which no tracking data could be obtained.

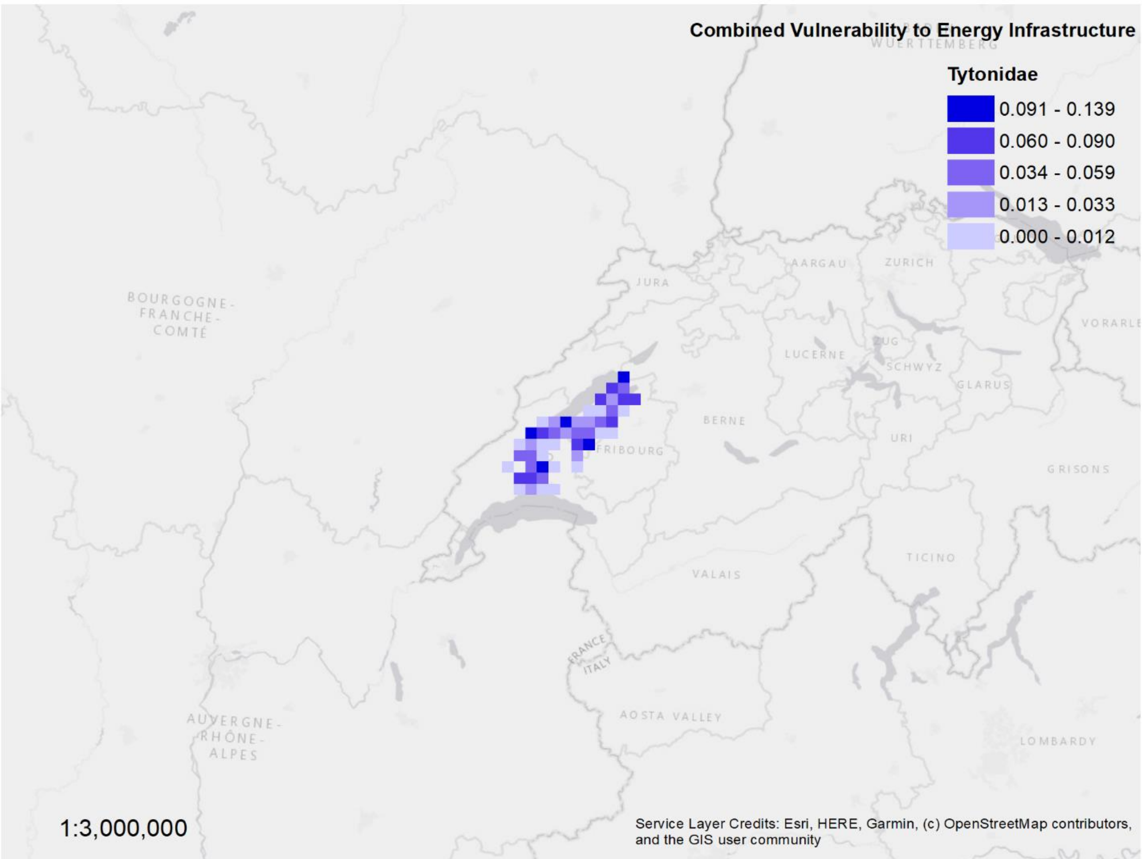

Supporting Information Figure 53: Vulnerability for all grid cells within the study area with sufficient GPS locations in flight to assess vulnerability for Tytonidae. Vulnerability is symbolised in quantiles from 0 – 0.14 which is the highest vulnerability score for this taxa represented by Barn Owl Tyto alba. Areas with no symbology represent regions for which no tracking

APPENDIX D: SUPPORTING INFORMATION FOR CHAPTER 3

Study Name	Common Name	Species	Individuals (n = 328)	Start Year	Number of GPS Points	Number of GPS Points In Flight	Country	Authors	DOI (If available) or Movebank Study ID
Eastern flyway spring migration of adult white storks (data from Rotics et al. 2018)	White Stork	*Ciconia ciconia*	36	2012	420737	192036	Germany	Ran Nathan & Shay Rotics	560041066
Fall migration of white storks in 2014	White Stork	*Ciconia ciconia*	60	2014	279127	29110	Germany	Andrea Flack	doi:10.5441/001/1.bj96m274
Lifetrack White Stork Armenia	White Stork	*Ciconia ciconia*	4	2014	903027	443	Armenia	Wolfgang Fiedler	10236270
LifeTrack White Stork Bavaria	White Stork	*Ciconia ciconia*	38	2014	114719	3298	Germany	Wolfgang Fiedler	24442409
LifeTrack White Stork Greece Evros Delta	White Stork	*Ciconia ciconia*	10	2013	61261	1489	Greece	Wolfgang Fiedler	10449535
LifeTrack White Stork Poland	White Stork	*Ciconia ciconia*	4	2013	65685	11679	Poland	Martin Wilkelski & Wolfgang Fiedler	10763606
LifeTrack White Stork Spain Donana	White Stork	*Ciconia ciconia*	2	2013	3991	5	Spain	Martin Wilkelski & Julio Blas	2988357
LifeTrack White Stork Tunisia	White Stork	*Ciconia ciconia*	9	2013	47879	4017	Tunisia	Andrea Flack	10157679
LifeTrack White Stork Vorarlberg	White Stork	*Ciconia ciconia*	4	2016	33918	1304	Switzerland	Wolfgang Fiedler	173641633
White Stork Adults 2018	White Stork	*Ciconia ciconia*	8	2018	280034	3181	Portugal	Aldina Franco & Marta Serra Acacio	451464940
White Stork Adults 2020	White Stork	*Ciconia ciconia*	4	2020	37290	2402	Portugal	Aldina Franco & Marta Serra Acacio	
White Stork Adults 2021	White Stork	*Ciconia ciconia*	5	2021	46799	1912	Portugal	Aldina Franco & Marta Serra Acacio	
White Stork	White Stork	*Ciconia ciconia*	41	2016	825214	56832	Portugal	Aldina Franco	159302811

Adults and Juveniles 2016									
White Stork Juveniles 2017	White Stork	*Ciconia ciconia*	34	2017	256252	21470	Portugal	Aldina Franco	279646867
White Stork Juveniles 2018	White Stork	*Ciconia ciconia*	2	2018	24482	3181	Portugal	Aldina Franco & Marta Serra Acacio	495405707
White Stork Juveniles 2019	White Stork	*Ciconia ciconia*	30	2019	231863	19084	Portugal	Aldina Franco & Marta Serra Acacio	
White Stork Juveniles 2020	White Stork	*Ciconia ciconia*	19	2020	72023	2402	Portugal	Aldina Franco & Marta Serra Acacio	
White Stork Juveniles 2021	White Stork	*Ciconia ciconia*	18	2021	89632	1912	Portugal	Aldina Franco & Marta Serra Acacio	

Study Name	Common Name	Species	Individuals (n = 39)	Start Year	Number of GPS Points	Number of GPS Points In Flight	Country	Authors	DOI (If available) or Movebank Study ID
Little Bustard Movement Ecology 2015 - 2016	Little Bustard	*Tetrax tetrax*	7	2015	68979	309	Portugal	João P Silva	56464970
Little Bustard Movement Ecology 2017 - 2018	Little Bustard	*Tetrax tetrax*	11	2017	111845	599	Portugal	João P Silva	253940991
Little Bustard Movement Ecology 2018 - 2019	Little Bustard	*Tetrax tetrax*	8	2018	32839	346	Portugal	João P Silva	461568973
Little Bustard Movement Ecology 2019 – 2020	Little Bustard	*Tetrax tetrax*	6	2019	81661	692	Portugal	João P Silva	769933377
Little Bustard Movement Ecology 2020 – 2021	Little Bustard	*Tetrax tetrax*	5	2020	127305	6733	Portugal	João P Silva	1083249254
Little Bustard Movement Ecology 2021 – 2022	Little Bustard	*Tetrax tetrax*	2	2021	37044	2066	Portugal	João P Silva	1471129898

Supporting Information Table 8: Movebank GNSS bird tracking studies included in the analysis for White Stork Ciconia ciconia and Little Bustard Tetrax tetrax.

	ERA5.Land.Surface.Pressure	ERA5.Total.Cloud.Cover	ERA5.Total.Precipitation	ERA5.Land.2m.Temperature	TRI	slope	Wind_Speed	Therm_Uplift	Oro_Uplift	Updraft_Coef
ERA5.Land.Surface.Pressure										
ERA5.Total.Cloud.Cover	-0.03****									
ERA5.Total.Precipitation	-0.04****	0.21****								
ERA5.Land.2m.Temperature	0.22****	-0.24****	-0.23****							
TRI	-0.09****	-0.03****	0.01****	-0.11****						
slope	-0.19****	0.02****	0.05****	-0.24****	0.61****					
Wind_Speed	-0.27****	-0.13****	-0.06****	-0.15****	0.01****	-0.08****				
Therm_Uplift	-0.07****	-0.16****	-0.17****	0.29****	0.01****	-0.02****	0.33****			
Oro_Uplift	-0.12****	-0.05****	-0.01****	-0.12****	0.07****	0.10****	0.38****	0.11****		
Updraft_Coef	-0.03****	0.00*	0.02****	-0.09****	0.10****	0.19****	-0.02****	-0.03****	0.76****	
elev_ortho	-0.80****	0.00	0.02****	-0.05****	0.13****	0.28****	-0.10****	0.09****	-0.02****	0.05****

Supporting Information Figure 54: Pearson rank correlation matrix constructed using the corstars function in R (STHDA, 2017) *to check for correlation between potential input variables to the GLMM.*

	Migration	Migration Period	Mean Start Day	Mean End Day	SD Start Day	SD End Day
			White Stork			
1	Migration	Autumn migration	226	261	27.8	41.6
2	Migration	Spring migration	55	88	25.5	26.2
3	Non-migration	Summer-Non-Migration	137	209	56	52
4	Non-migration	Winter-Non-Migration	261	55	117.8	131.9
			Little Bustard			
1	Migration	Autumn migration	200	270	47.3	68.9
2	Migration	Spring migration	96	121	50	35.2
3	Non-migration	Summer-Non-Migration	94	222	28.7	41
4	Non-migration	Winter-Non-Migration	121	269	123.6	134.3

Supporting Information Table 9: Mean migration period for each species derived from the migration start and end dates for each individual. For little bustard, where an overlap was present the migration periods were classified using the migration start and end days. For example, in little bustards, the data suggested an overlap between the end of the summer non migratory period (breeding) and the beginning of the autumn migration. As such day 200 was used as the cut off as this represented the start of migration.

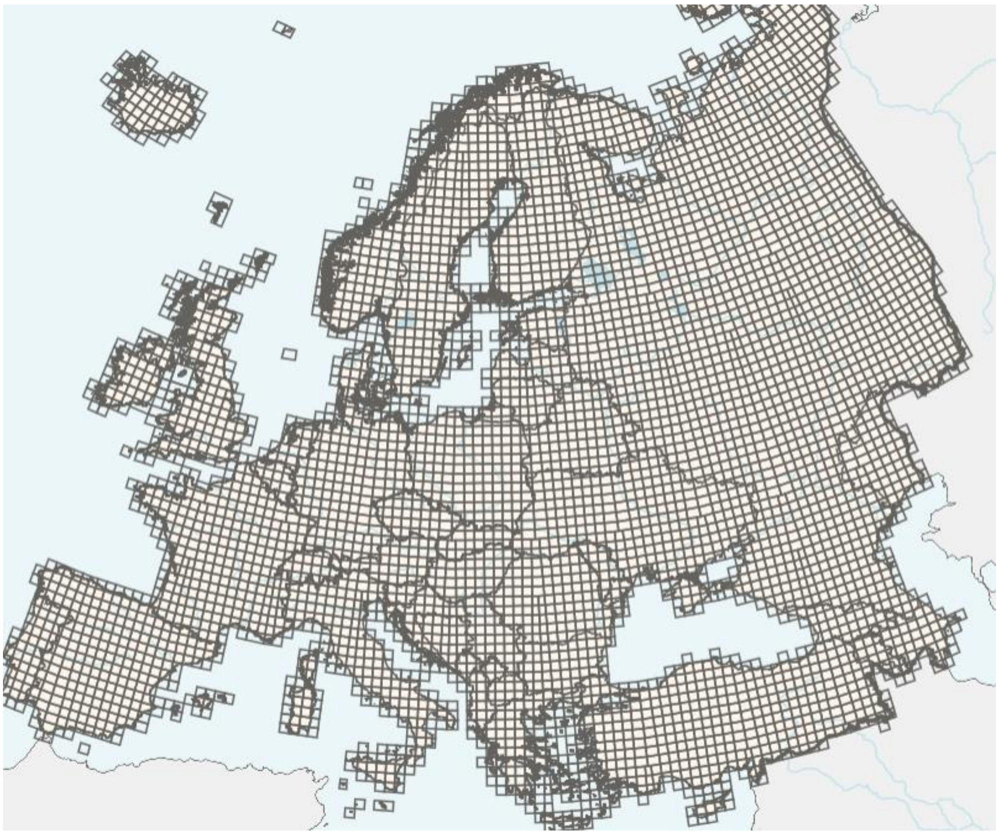

Supporting Information Figure 55: EBBA2 grid covering mainland Europe and Iceland. For the purposes of the little bustard analysis the final points surface was clipped to Iberia and France.

APPENDIX E: SUPPORTING INFORMATION FOR CHAPTER 5

COMMON NAME	SPECIES	FLIGHT STYLE	ACC AXIS	BODY_MASS_G	ACC MIN	ACC 2.5^TH	ACC MEAN	ACC 97.5^TH	ACC 1^TH	ACC 99^TH	RAW ACC MEDIAN	ACC MAX	RAW ACC 1^TH	RAW ACC 99^TH	COUNT EXCEEDANCE OF 99
COMMON CRANE	Grus grus	soaring	ACC X	6055	-1.659	-0.29	0.002	0.266	-0.408	0.357	-0.087	2.134	-0.495	0.27	998
EURASIAN EAGLE OWL	Bubo bubo	flapping	ACC X	2288	-1.736	-0.126	0.014	0.202	-0.156	0.245	1.736	2.296	1.58	1.981	63859
EURASIAN SPOONBILL	Platalea leucorodia	flapping	ACC X	1868	-2.001	-0.295	0.027	0.405	-0.397	0.48	-0.047	2.094	-0.444	0.433	676
EUROPEAN WIGEON	Mareca penelope	flapping	ACC X	725	-2.059	-0.349	0	0.358	-0.472	0.484	0.011	2.036	-0.461	0.495	5486
GREYLAG GOOSE	Anser anser	flapping	ACC X	3347	-2.139	-0.82	0.002	0.896	-0.879	0.973	-0.059	3.768	-0.938	0.914	NA
GRIFFON VULTURE	Gyps fulvus	soaring	ACC X	9250	-2.38	-0.661	-0.046	0.155	-0.725	0.156	2.38	1.715	1.655	2.536	2039
IBERIAN IMPERIAL EAGLE	Aquila adalberti	soaring	ACC X	3000	-2.742	-0.188	0.104	0.902	-0.252	0.943	-0.012	2.754	-0.264	0.932	NA
LITTLE BUSTARD	Tetrax tetrax	flapping	ACC X	900	-2.514	-0.34	-0.028	0.281	-0.387	0.322	-0.023	2.789	-0.41	0.299	2048
NORTHERN_HARRIER	Circus cyaneus	soaring	ACC X	436.5	-1.064	-0.251	-0.004	0.214	-0.351	0.292	0.091	0.959	-0.26	0.383	441
WHITE STORK	Ciconia ciconia	soaring	ACC X	3245.5	-2.025	-0.195	-0.008	0.181	-0.256	0.244	-0.023	2.07	-0.279	0.221	NA
WHOOPER_SWAN	Cygnus cygnus	flapping	ACC X	9400	-2.038	-0.398	0.002	0.424	-0.441	0.459	2.038	1.971	1.597	2.497	1677
COMMON CRANE	Grus grus	soaring	ACC Y	6055	-1.852	-0.571	0.184	1.221	-0.669	1.246	-0.196	2.243	-0.865	1.05	998
EURASIAN EAGLE OWL	Bubo bubo	flapping	ACC Y	2288	-2.145	-0.216	-0.03	0.04	-0.323	0.044	2.148	1.884	1.825	2.192	83092
EURASIAN SPOONBILL	Platalea leucorodia	flapping	ACC Y	1868	-1.85	-0.37	0.039	0.573	-0.45	0.697	-0.198	2.245	-0.648	0.499	676
EUROPEAN WIGEON	Mareca penelope	flapping	ACC Y	725	-2.228	-0.709	-0.054	0.349	-0.999	0.453	0.18	1.867	-0.819	0.633	5461
GREYLAG GOOSE	Anser anser	flapping	ACC Y	3347	-1.916	-0.299	0.13	1.377	-0.352	1.664	-0.744	3.076	-1.096	0.92	NA
GRIFFON VULTURE	Gyps fulvus	soaring	ACC Y	9250	-1.664	-0.009	0.089	0.517	-0.014	0.627	1.664	2.375	1.65	2.291	1676
IBERIAN IMPERIAL EAGLE	Aquila adalberti	soaring	ACC Y	3000	-1.553	-0.486	0.214	0.914	-0.504	0.926	0.006	1.875	-0.498	0.932	NA

LITTLE BUSTARD	Tetrax tetrax	flapping	ACC Y	900	-1.928	-0.398	0.036	0.521	-0.451	0.557	0.229	3.521	-0.223	0.785	1931
NORTHERN_HARRIER	Circus cyaneus	soaring	ACC Y	436.5	-1.203	-0.243	0.146	0.927	-0.281	1.135	-0.604	2.163	-0.885	0.531	440
WHITE STORK	Ciconia ciconia	soaring	ACC Y	3245.5	-1.604	-0.403	0.053	0.572	-0.443	0.715	-0.444	12.78	-0.887	0.271	NA
WHOOPER_SWAN	Cygnus cygnus	flapping	ACC Y	9400	-1.996	-0.431	0.02	0.519	-0.495	0.56	1.996	2.02	1.501	2.556	1683
COMMON CRANE	Grus grus	soaring	ACC Z	6055	-2.992	-1.895	-0.32	0.531	-1.972	0.671	0.944	4.48	-1.028	1.615	994
EURASIAN EAGLE OWL	Bubo bubo	flapping	ACC Z	2288	-1.874	-0.172	-0.005	0.308	-0.198	0.346	1.874	2.158	1.676	2.22	67336
EURASIAN SPOONBILL	Platalea leucorodia	flapping	ACC Z	1868	-3.058	-0.24	-0.012	0.229	-1.01	0.701	1.01	1.037	0	1.711	676
EUROPEAN WIGEON	Mareca penelope	flapping	ACC Z	725	-3.049	-1.381	-0.053	0.158	-1.952	0.824	1.001	1.046	-0.951	1.825	5457
GREYLAG GOOSE	Anser anser	flapping	ACC Z	3347	-2.074	-0.809	0.071	0.973	-0.914	1.09	0.059	4.758	-0.855	1.148	NA
GRIFFON VULTURE	Gyps fulvus	soaring	ACC Z	9250	-1.955	-0.02	0.066	0.469	-0.021	0.493	2.008	2.087	1.987	2.501	1683
IBERIAN IMPERIAL EAGLE	Aquila adalberti	soaring	ACC Z	3000	-3.305	-0.27	0.093	0.539	-0.398	0.586	-0.844	3.469	-1.242	-0.258	NA
LITTLE BUSTARD	Tetrax tetrax	flapping	ACC Z	900	-4.406	-0.094	0.037	0.305	-0.129	0.363	-0.938	3.75	-1.066	-0.574	1956
NORTHERN_HARRIER	Circus cyaneus	soaring	ACC Z	436.5	-1.813	-0.307	0.028	0.599	-0.568	0.838	0.785	1.254	0.217	1.623	441
WHITE STORK	Ciconia ciconia	soaring	ACC Z	3245.5	-2.941	-0.892	-0.076	0.326	-0.892	0.533	0.893	1.154	0.001	1.426	NA
WHOOPER_SWAN	Cygnus cygnus	flapping	ACC Z	9400	-1.976	-0.433	-0.006	0.359	-0.475	0.393	1.977	2.039	1.502	2.37	1645

Supporting Information Table 10: Summary of raw forces experienced by wild birds in three axes.

Species	Difference	Lower Bound	Upper Bound	P Value (adj)
Aquila adalberti-Anser anser	-0.07	-0.07	-0.06	0.00
Bubo bubo-Anser anser	-0.51	-0.51	-0.50	0.00
Ciconia ciconia-Anser anser	-0.29	-0.29	-0.28	0.00
Circus cyaneus-Anser anser	-0.32	-0.33	-0.32	0.00
Cygnus cygnus-Anser anser	-0.23	-0.24	-0.23	0.00
Grus grus-Anser anser	-0.02	-0.02	-0.01	0.00
Gyps fulvus-Anser anser	-0.47	-0.48	-0.47	0.00
Mareca penelope-Anser anser	-0.31	-0.32	-0.31	0.00
Platalea leucorodia-Anser anser	-0.35	-0.35	-0.34	0.00
Tetrax tetrax-Anser anser	-0.34	-0.34	-0.33	0.00
Bubo bubo-Aquila adalberti	-0.44	-0.44	-0.44	0.00
Ciconia ciconia-Aquila adalberti	-0.22	-0.22	-0.21	0.00
Circus cyaneus-Aquila adalberti	-0.25	-0.25	-0.25	0.00
Cygnus cygnus-Aquila adalberti	-0.16	-0.17	-0.16	0.00
Grus grus-Aquila adalberti	0.05	0.05	0.06	0.00
Gyps fulvus-Aquila adalberti	-0.40	-0.40	-0.40	0.00
Mareca penelope-Aquila adalberti	-0.25	-0.25	-0.24	0.00
Platalea leucorodia-Aquila adalberti	-0.28	-0.28	-0.27	0.00
Tetrax tetrax-Aquila adalberti	-0.27	-0.27	-0.27	0.00
Ciconia ciconia-Bubo bubo	0.22	0.22	0.22	0.00
Circus cyaneus-Bubo bubo	0.19	0.18	0.19	0.00
Cygnus cygnus-Bubo bubo	0.27	0.27	0.28	0.00
Grus grus-Bubo bubo	0.49	0.49	0.49	0.00
Gyps fulvus-Bubo bubo	0.04	0.03	0.04	0.00
Mareca penelope-Bubo bubo	0.19	0.19	0.19	0.00
Platalea leucorodia-Bubo bubo	0.16	0.16	0.16	0.00
Tetrax tetrax-Bubo bubo	0.17	0.17	0.17	0.00
Circus cyaneus-Ciconia ciconia	-0.04	-0.04	-0.03	0.00
Cygnus cygnus-Ciconia ciconia	0.05	0.05	0.05	0.00
Grus grus-Ciconia ciconia	0.27	0.27	0.27	0.00
Gyps fulvus-Ciconia ciconia	-0.19	-0.19	-0.19	0.00
Mareca penelope-Ciconia ciconia	-0.03	-0.03	-0.03	0.00
Platalea leucorodia-Ciconia ciconia	-0.06	-0.06	-0.06	0.00
Tetrax tetrax-Ciconia ciconia	-0.05	-0.06	-0.05	0.00
Cygnus cygnus-Circus cyaneus	0.09	0.08	0.09	0.00
Grus grus-Circus cyaneus	0.30	0.30	0.31	0.00
Gyps fulvus-Circus cyaneus	-0.15	-0.15	-0.15	0.00
Mareca penelope-Circus cyaneus	0.01	0.00	0.01	0.00
Platalea leucorodia-Circus cyaneus	-0.03	-0.03	-0.02	0.00
Tetrax tetrax-Circus cyaneus	-0.02	-0.02	-0.02	0.00
Grus grus-Cygnus cygnus	0.22	0.21	0.22	0.00
Gyps fulvus-Cygnus cygnus	-0.24	-0.24	-0.24	0.00
Mareca penelope-Cygnus cygnus	-0.08	-0.08	-0.08	0.00
Platalea leucorodia-Cygnus cygnus	-0.11	-0.12	-0.11	0.00
Tetrax tetrax-Cygnus cygnus	-0.11	-0.11	-0.10	0.00
Gyps fulvus-Grus grus	-0.45	-0.46	-0.45	0.00
Mareca penelope-Grus grus	-0.30	-0.30	-0.30	0.00
Platalea leucorodia-Grus grus	-0.33	-0.33	-0.33	0.00
Tetrax tetrax-Grus grus	-0.32	-0.33	-0.32	0.00
Mareca penelope-Gyps fulvus	0.16	0.16	0.16	0.00

Platalea leucorodia-Gyps fulvus	0.13	0.12	0.13	0.00
Tetrax tetrax-Gyps fulvus	0.13	0.13	0.13	0.00
Platalea leucorodia-Mareca penelope	-0.03	-0.03	-0.03	0.00
Tetrax tetrax-Mareca penelope	-0.02	-0.03	-0.02	0.00
Tetrax tetrax-Platalea leucorodia	0.01	0.00	0.01	0.00

Supporting Information Table 11: TUKEY-HSD Table of differences between the maximum forces experience by the wild birds. Tukey multiple comparisons of means, 95% family-wise confidence level. Fit: aov(formula = adj_acc_max ~ Species, data = Species_ACC)

A3: Collision Testing Lab Set Ups

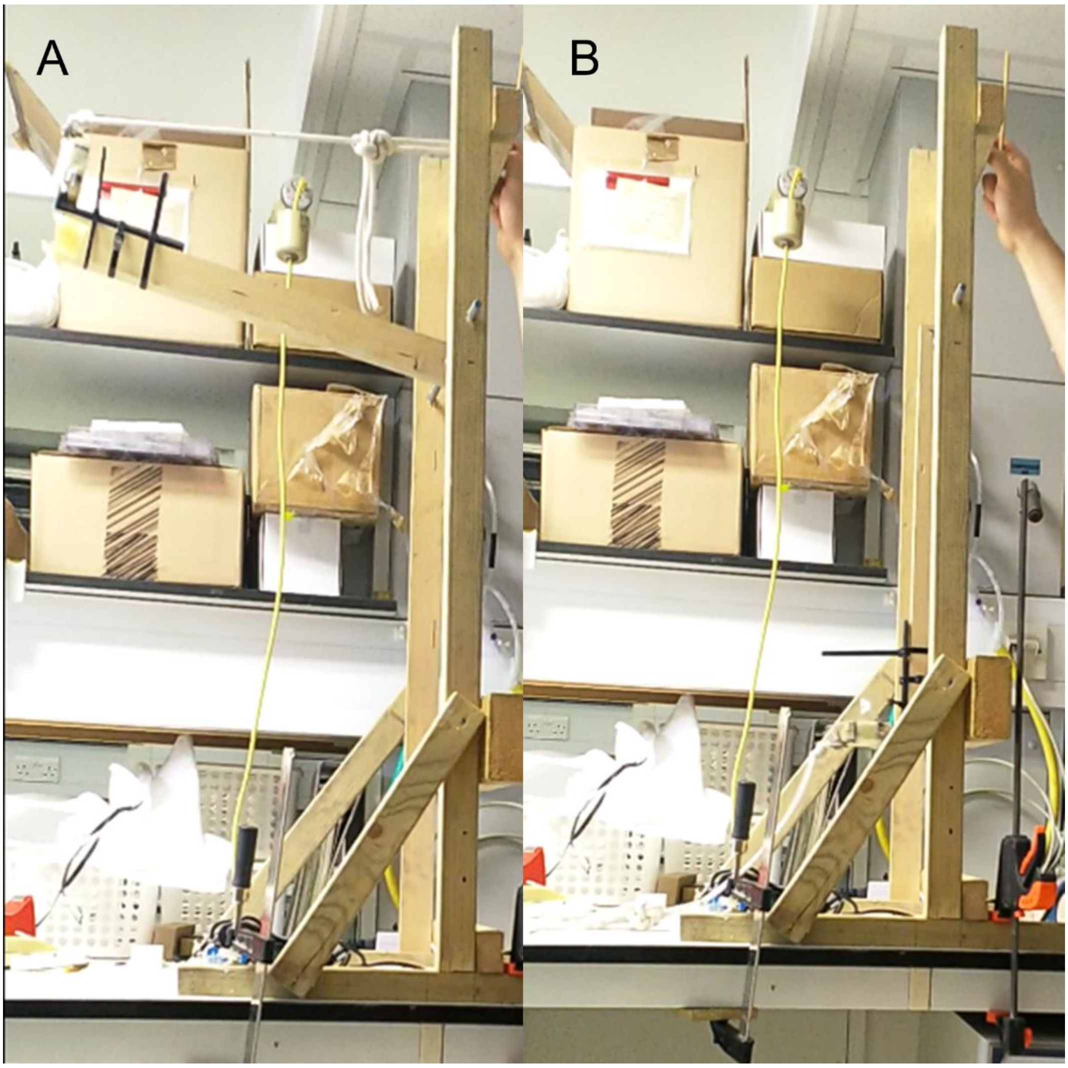

Supporting Information Figure 56: Pendulum set up for testing the effect of accelerometer sampling frequency.

Supporting Information Figure 57: Zipline set up for understanding the force signature of a collision as observed by the tag.

LIST OF FIGURES AND TABLES

1